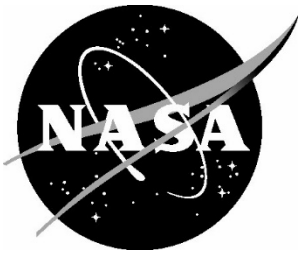
NASA/TP–20260003140



State-of-the-Art Small Spacecraft Technology

Bruce D. Yost
Brian C. Kempa
Craig D. Burkhard
NASA Ames Research Center, Moffett Field, CA

Luis Santos Soto
David E. Steinfeld
NASA Goddard Space Flight Center, Greenbelt, MD

Samuel M. Pedrotty
NASA Johnson Space Center, Houston, TX

Gabriel F. Benavides
NASA Glen Research Center, Cleveland, OH

Sasha V. Weston
MEI, subsidiary of Astrion, Moffett Field, CA

May 2026

NASA STI Program Report Series

NASA STI Program Report Series

Since its founding, NASA has been dedicated to the advancement of aeronautics and space science. The NASA scientific and technical information (STI) program plays a key part in helping NASA maintain this important role.

The NASA STI program operates under the auspices of the Agency Chief Information Officer. It collects, organizes, provides for archiving, and disseminates NASA's STI. The NASA STI program provides access to the NTRS Registered and its public interface, the NASA Technical Reports Server, thus providing one of the largest collections of aeronautical and space science STI in the world. Results are published in both non-NASA channels and by NASA in the NASA STI Report Series, which includes the following report types:

- TECHNICAL PUBLICATION. Reports of completed research or a major significant phase of research that present the results of NASA Programs and include extensive data or theoretical analysis. Includes compilations of significant scientific and technical data and information deemed to be of continuing reference value. NASA counterpart of peer-reviewed formal professional papers but has less stringent limitations on manuscript length and extent of graphic presentations.

- TECHNICAL MEMORANDUM. Scientific and technical findings that are preliminary or of specialized interest, e.g., quick release reports, working papers, and bibliographies that contain minimal annotation. Does not contain extensive analysis.

- CONTRACTOR REPORT. Scientific and technical findings by NASA-sponsored contractors and grantees.

- CONFERENCE PUBLICATION. Collected papers from scientific and technical conferences, symposia, seminars, or other meetings sponsored or co-sponsored by NASA.

- SPECIAL PUBLICATION. Scientific, technical, or historical information from NASA programs, projects, and missions, often concerned with subjects having substantial public interest.

- TECHNICAL TRANSLATION. English-language translations of foreign scientific and technical material pertinent to NASA's mission.

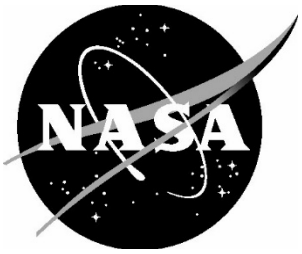
Specialized services also include organizing and publishing research results, distributing specialized research announcements and feeds, providing information desk and personal search support, and enabling data exchange services.

For more information about the NASA STI program, see the following:

- Access the NASA STI program home page at http://www.sti.nasa.gov

.

NASA/TP–20260003140



State-of-the-Art Small Spacecraft Technology

Bruce D. Yost
Brian C. Kempa
Craig D. Burkhard
NASA Ames Research Center, Moffett Field, CA

Luis Santos Soto
David E. Steinfeld
NASA Goddard Space Flight Center, Greenbelt, MD

Samuel M. Pedrotty
NASA Johnson Space Center, Houston, TX

Gabriel F. Benavides
NASA Glen Research Center, Cleveland, OH

Sasha V. Weston
MEI, subsidiary of Astrion, Moffett Field, CA

National Aeronautics and
Space Administration

Enter NASA Ames Research Center
Moffett Field, CA

May 2026

National Aeronautics and
Space Administration

Enter NASA Ames Research Center
Moffett Field, CA

May 2026

The use of trademarks or names of manufacturers in this report is for accurate reporting and does not constitute an official endorsement, either expressed or implied, of such products or manufacturers by the National Aeronautics and Space Administration.

Available from: https://www.nasa.gov/smallsat-institute/sst-soa/

NASA STI Program / Mail Stop 050
NASA Langley Research Center
Hampton, VA 23681-2199

National Aeronautics and Space Administration

SMALL SPACECRAFT SYSTEMS VIRTUAL INSTITUTE (S3VI)

Small Spacecraft Technology State of the Art Report 2026



2026 Cover Page Image Credits

Top Vehicle

NASA's Small Spacecraft Propulsion and Inspection Capability (SSPICY) mission is the agency's first commercial technology demonstration for in-space satellite servicing and inspection. The mission, led by Starfish Space of Seattle, Washington, advances an innovative approach to enabling commercial inspection of defunct, or inoperable, satellites in low Earth orbit, a precursor to capturing and repairing or removing the satellites. The spacecraft is expected to launch in late 2026 and will begin performing inspections in 2027.

Credit: Starfish Space.

Middle Four Spacecraft

NASA's Polarimeter to Unify the Corona and Heliosphere (PUNCH) mission, led by the Southwest Research Institute of Boulder, Colorado, is a constellation of four small satellites in low Earth orbit that is making global, 3D observations of the Sun's corona to better understand how the mass and energy there become the solar wind that fills the solar system. Three of the PUNCH satellites are equipped with wide field imagers and one with a narrow field imager that, working together, are creating a combined field of view and mapping the region where the Sun's corona transitions to the solar wind. The PUNCH satellites launched on March 11, 2025 aboard a SpaceX Falcon 9 rocket from Vandenberg Space Force Base in California.

Credit: Southwest Research Institute.

Lower Spacecraft

DiskSat is an innovative approach to small satellite architecture, developed in partnership with NASA and the US Space Force's Space Systems Command. The DiskSat technology demonstration mission is composed of four DiskSats to verify the performance of this new small spacecraft platform and demonstrate the launch dispenser mechanism. DiskSat's compact, plate-shaped design could offer more power and surface area for instruments and provide more opportunities for NASA to expand mission objectives for small spacecraft. The first DiskSat demonstration mission launched on December 18, 2025 on STP-S30, a Rocket Lab Electron rocket from Launch Complex 2 on Wallops Island, Virginia.

Credit: The Aerospace Corporation.

Change Summary

Published Date	Edition	Chapter	Description of Changes
May 2026	2026	Complete Spacecraft Platforms	Entire chapter updated.
		Power	Entire chapter updated.
		In-space Propulsion	Entire chapter updated.
		Guidance Navigation & Control	Updates to Rendezvous, Proximity, Operations, and Docking section.
		Structures, Materials, and Mechanisms	Minor edits throughout chapter.
		Thermal Control	Minor edits throughout chapter.
		SmallSat Avionics	Entire chapter updated.
		Communications	Free Space Optical Communications and Future Communications Technology Sections updated.
		Launch, Integration, Deployment, and Orbital Transport	Updates to Launch Paradigm; Included hardware tables; Orbital Maneuvering Vehicle section updated.
		Ground Data Systems and Mission Operations	Updated content in Ground Segment Services, Ground Station Components, Ground Data and Supporting Systems sections.
		ID and Tracking	Minor edits throughout chapter.
		Deorbit Systems	Minor edits throughout chapter.

Preface

NASA's *Small Spacecraft Technology State-of-the-art* report is updated annually to capture new information on publicly available small spacecraft systems from NASA and other sources. Each chapter captures the development status of current state-of-the-art SmallSat technologies, along with design considerations for readers when identifying components for a mission. The organizational approach for each chapter includes an introduction to the technology, the current development status of procurable systems, and summary tables of the technologies surveyed. In this way, each chapter presents a stand-alone report on the given spacecraft subsystem, with updated information on new and maturing technologies and reference missions as applicable.

When the first edition of this report was published in 2013, 247 CubeSats and 105 other non-CubeSat small spacecraft under 50 kilograms (kg) had been launched worldwide representing less than 2% of the total mass launched into orbit over multiple years. Small satellite flight heritage has greatly increased since then, with small spacecraft becoming the primary means for commercial, government, private, and academic institutions to access space. Since 2023, there has been an influx of mini-class small spacecraft constellations with a mass of 201–600 kg, as well as a new generation of larger small spacecraft constellations weighing 600–1,200 kg (1). While updates in all chapters reflect this growth in the small spacecraft market, a focused effort was made to update areas reflecting recent technology developments that may ultimately bridge existing technology gaps.

This edition features updates that reflect the next generation of small spacecraft missions. Demands for larger platforms are discussed in the *Complete Spacecraft Platforms* chapter and expanded upon in the *Integration, Launch, Deployment, and Orbital Transport* chapter. This new launch paradigm indicates an increase in Orbital Maneuvering/Transport Vehicle (OMV/OTV) services as well as in autonomous spacecraft capabilities to support higher payload data throughput. The *SmallSat Avionics* chapter received a complete rewrite that expands on the increasing onboard processing capabilities of SmallSats and CubeSats. Future RF and Optical Communications technologies and missions are highlighted in the *Communications* chapter, and in the *Guidance, Navigation, and Control* chapter, the RPOD section was updated to reflect recent interest and developments. All content in the *Power Systems* and *In-Space Propulsion* chapters was updated to reflect continued progression toward more capable SmallSats.

This report should not be considered a comprehensive overview of all technologies, but rather a general overview of current state-of-the-art SmallSat technologies and their development status. It should be noted that technology maturity designations may vary with changes to payload, mission requirements, reliability considerations, and/or the environment in which performance was demonstrated. Readers are highly encouraged to contact companies for further information regarding the performance and maturity of the described technology. Any companies mentioned in this report are for informational purposes only and do not constitute an endorsement by NASA.

References

(1) Bryce and Space Technology. "SmallSat by the Numbers, 2025." Accessed March 14, 2026. [Online] Available at: https://brycetech.com/reports/report-documents/Bryce_Smallsats_2025.pdf

Chapter Glossary

(EELV)	Evolved Expendable Launch Vehicle
(ESPA)	EELV Secondary Payload Adapter
(FASTSAT)	Fast, Affordable, Science and Technology Satellite
(LADEE)	Lunar Atmosphere and Dust Environment Explorer
(LCROSS)	Lunar Crater Observation and Sensing Satellite
(NODIS)	NASA Online Directives Information System
(SSDS)	Small Spacecraft & Distributed Systems
(SST)	Small Spacecraft Technology
(STMD)	Space Technology Mission Directorate
(TMA)	Technology Maturity Assessment
(TRL)	Technology Readiness Level
(U)	Unit

1.0 Introduction

1.1 Objective

The objective of this report is to assess and provide an overview of the state of the art in small spacecraft technologies for use by mission designers, project managers, technologists, and students, connecting current small spacecraft missions to available technologies. This report focuses on the spacecraft system in its entirety, provides current best practices for integration and key considerations for the reader where possible, and presents devices from publicly available sources for each specific spacecraft subsystem.

This report is a survey of small spacecraft technologies sourced from open literature; it is not an original source. In addition, this report only considers literature in the public domain. Information presented in this report is limited to SmallSat technology that is publicly available as of April 1, 2026. It does not include information on instrumentation, science payloads, or advances or developments that have not been publicly disclosed. Commonly used sources for data include manufacturer datasheets, press releases, conference papers, journal papers, public filings with government agencies, news articles, presentations, the compendium of databases accessed via NASA's Small Spacecraft Systems Virtual Institute (S3VI) Information Search, and engagement with companies. Data not appropriate for public dissemination, such as proprietary, export controlled, or otherwise restricted data, are not considered. We encourage the SmallSat community to publish mission outcomes and technology development milestones in publicly available conference papers, press releases, or company websites so they can be reflected in future editions of this report.

This report is funded by NASA's Space Technology Mission Directorate (STMD). It was first commissioned by the Small Spacecraft & Distributed Systems (SSDS, formally Small Spacecraft Technology (SST) program) capability within STMD in mid-2012 in response to the rapid growth in interest in using small spacecraft for low-Earth orbit, low-cost missions. The report was subsequently updated in 2015, 2018, 2020, 2021, 2022, 2023, 2024, and 2026 to capture SmallSat technology growth and maturation. In addition to reporting currently available state-of-the-art technologies that have achieved Technology Readiness Level (TRL) 5 or above, a prognosis is provided describing technologies as "on the horizon" if they are being considered for future application.

1.2 Scope

The NASA-SmallSat era began at NASA Ames Research Center with the launch of Pioneer 10 and 11 in March 1972 and April 1973, respectively, where both spacecraft weighed < 600 kg. The NASA SmallSat mission gained momentum when NASA initiated the Small Explorer (SMEX) program in 1988 to encourage the development of small spacecraft with masses in the range of ~60–350 kg to reduce cost. In 1998 NASA Ames focused its SmallSat program on lunar exploration and launched Lunar Prospector (< 700 kg), followed by the Lunar Crater Observation and Sensing Satellite (LCROSS), (< 630 kg) in 2009, and the Lunar Atmosphere and Dust Environment Explorer (LADEE), (~380 kg) which was launched in September 2013. In late 2010, NASA launched its first minisatellite called Fast, Affordable, Science and Technology Satellite (FASTSAT), which had a launch mass ~180 kg. This decrease in spacecraft mass, reduced overall cost, and increase in science capabilities ignited interest in miniaturization and maturity of aerospace technologies which have proven to be capable of producing more complex missions for less cost.

Early efforts for this report began in 2012, when the adoption of the Evolved Expendable Launch Vehicle (**E**ELV) Secondary Payload Adapter (ESPA) as a launch strategy for small spacecraft became regular use. The ESPA provided a modular packaging approach for six payload slots of

up to 180 kg mass allocation and was implemented by the U.S. Air Force for launching its secondary payload. To supplement the rising small spacecraft awareness and cost-effective launch mechanisms, this report focused on spacecraft technology where “180 kg mass limit” served as a convenient metric to classify the maximum “SmallSat” mass. SmallSats are generally categorized by their mass, and this report adopts the following five small spacecraft mass categories (1):

- minisatellites are spacecraft with a total mass of 100 – 180 kg;
- microsatellites have a total spacecraft mass of 10-100 kg;
- nanosatellites have a total mass of 1 – 10 kg;
- picosatellites have a mass of 0.1 –1 kg; and
- femtosatellites have a total spacecraft mass 0.01 – 0.09 kg.

Figure 1.1 offers examples of spacecraft categorized by mass. On the lower mass end, there are projects such as KickSat-2, which deployed 100-centimeter (cm) scale “ChipSat” spacecraft, or Sprites, from a 2U femtosatellite deployer in March 2019. These femtosatellite ChipSats are the size of a large postage stamp and have a mass below 10 grams.

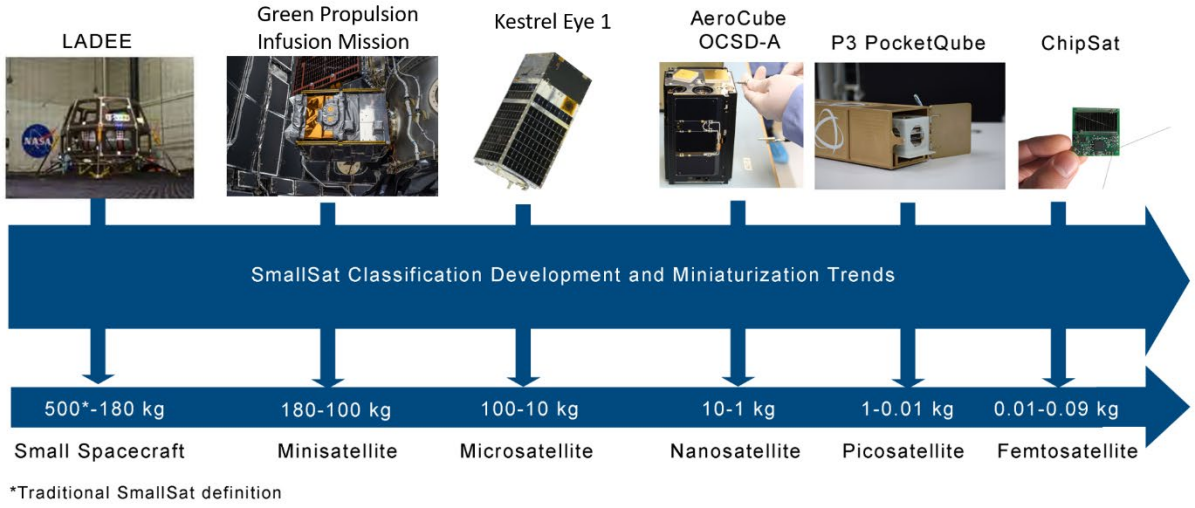


Figure 1.1: Overview of small spacecraft categories. Credit: NASA, SpaceX, Redwire Space, and Alba Orbital.

In 1999, a collaboration between California Polytechnic State University in San Luis Obispo and Stanford University in Stanford, California, developed a small educational platform called a "CubeSat" which was designed for academic space exploration and research. CubeSats are now a common form of small spacecraft that can weigh only a few kilograms and are based on a form factor of a 10 cm square cube, or unit (U) (1). While the original CubeSat was composed of a single 1U cube, in 2014 the CubeSat form factor expanded to 6U, and it is now common to combine multiple cubes to form larger units, as shown in Figure 1.3. These larger CubeSat sizes have become more standardized and popular in the past few years as much more science can be achieved at less cost with the additional volume, power, and overall increase in capability.

It is common to interchange the terms “CubeSat” and “NanoSat” (short for nanosatellite) as the original 1-3U CubeSat platforms fell under the nanosatellite category. Since the physical expansion of CubeSats now goes beyond the 6U form factor, CubeSats fall into both nanosatellite and microsatellite categories. Certain chapters of this report have a particular emphasis on CubeSat platforms as nanosatellite applications have expanded in recent years.

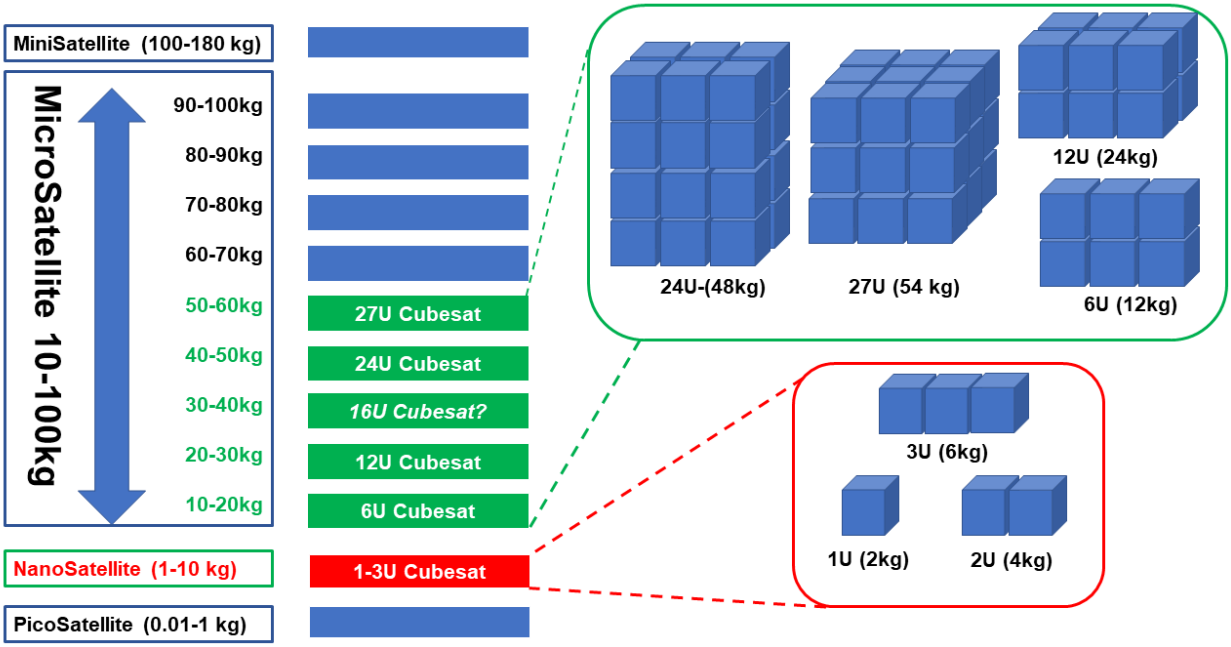


Figure 1.2: CubeSats are a class of nano- and microsatellites that use a standard size and form factor. Nanosatellite sizes compared to CubeSat containerized sizes. Credit: NASA.

1.3 Assessment

A central element of this report is to list state-of-the-art technologies by NASA standard Technology Readiness Level (TRL) as defined in NASA System Engineering Handbook. The authors have endeavored to independently verify the TRL value of each technology by reviewing and citing published test results or publicly available data to the best of their ability. Where test results and data disagree with vendors’ own advertised TRL, the authors have attempted to engage the vendors to discuss the discrepancy. Readers are strongly encouraged to follow the references cited in the literature describing the full performance range and capabilities of each technology. Readers of this report should contact individual companies to further clarify information. It is important to note that this report takes a broad system-level view. To attain a high TRL, the subsystem must be in a flight-ready configuration with all supporting infrastructure—such as mounting points, power conversion, and control algorithms—in an integrated unit.

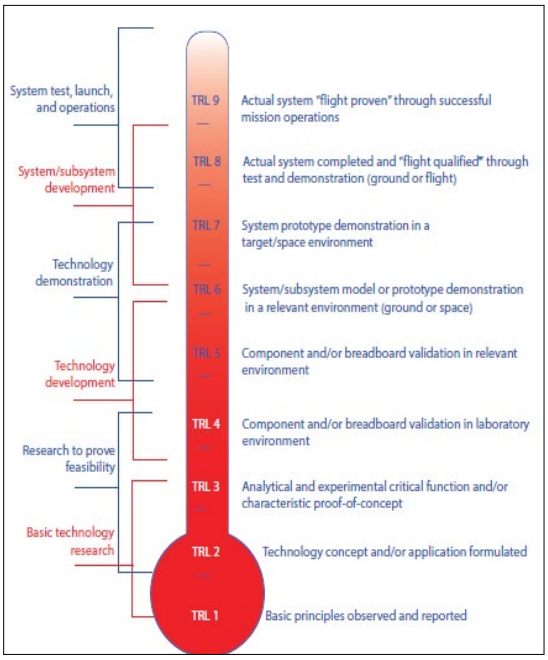


Figure 1.3: NASA’s standard Technology Readiness Level scale. Credit: NASA.

While “state-of-the-art” may be defined as the most recent development stage of technology, this report defines “state-of-the-art” in the context of NASA’s TRL scale (Figure 1.3) when assessing SmallSat technology. A technology may be deemed state-of-the-art whenever its TRL is larger than or equal to 5. A TRL of 5 indicates that the component and/or brassboard with realistic support elements was built and operated for validation in a relevant environment to demonstrate overall performance in critical areas. Success criteria include documented test performance demonstrating agreement with analytical predictions and documented definition of scaling requirements. Performance predictions are made for subsequent development phases (2).

An accurate TRL assessment requires a high degree of technical knowledge on a subject device, and an in-depth understanding of the mission (including interfaces and environment) on which the device was flown. TRL values vary depending on design factors for a specific technology. For example, differences in TRL assessment based on the operating environment may result from mechanical loads, mission duration, the thermal environment, or radiation exposure. The authors believe TRLs are most accurately determined when assessed within the context of a program’s unique requirements. If a technology has flown on a mission without success, or without providing valid confirmation to the operator, such claimed “flight heritage” is discounted. Some older technologies may still be well suited to certain mission needs and still be regarded as “state-of-the-art.” For a technology to be considered obsolete, “retired”, or no longer “state-of-the-art”, it’s performance must have been surpassed by newer technology such that it is no longer used.

While a technology with a TRL value lower than or equal to 4 may not be state of the art, in some cases these technologies may considered “on the horizon.” A TRL of 4 is defined as a component and/or breadboard validated in a laboratory environment with documented test performance demonstrating agreement with analytical predictions and a documented definition of the relevant environment. These promising technologies may soon be considered state-of-the-art for small spacecraft.

NASA standard TRL requirements for this report edition are stated in NPR 7123.1D, Appendix E, which is effective through July 05, 2028. The criteria for selection of appropriate TRL are described in the NASA Systems Engineering Handbook 6105 Rev 2 Appendix G: Technology Assessment/Insertion. Please refer to the NASA Online Directives Information System (NODIS) website https://nodis3.gsfc.nasa.gov/ for NPR documentation. The following paragraphs in sections 1.3.1 and 1.3.2 of this Introduction are excerpts from the NASA Engineering Handbook 6105 Rev 2 (pp. 252 – 254). They highlight important aspects of NASA TRL guidelines in hopes of eliminating confusion on terminology and heritage systems.

1.3.1 Terminology

“At first glance, the TRL descriptions in Figure 1.3 appear to be straightforward. It is in the process of trying to assign levels that problems arise. A primary cause of difficulty is in terminology, e.g., everyone knows what a breadboard is, but not everyone has the same definition. Also, what is a “relevant environment?” What is relevant to one application may or may not be relevant to another. Many of these terms originated in various branches of engineering and had, at the time, very specific meanings to that particular field. They have since become commonly used throughout the engineering field and often acquire differences in meaning from discipline to discipline, some differences subtle, some not so subtle. “Breadboard,” for example, comes from electrical engineering where the original use referred to checking out the functional design of an electrical circuit by populating a “breadboard” with components to verify that the design operated as anticipated. Other terms come from mechanical engineering, referring primarily to units that are subjected to different levels of stress under testing, e.g., qualification, protoflight, and flight units. The first step in developing a uniform TRL assessment (see Figure 1.4) is to define the terms

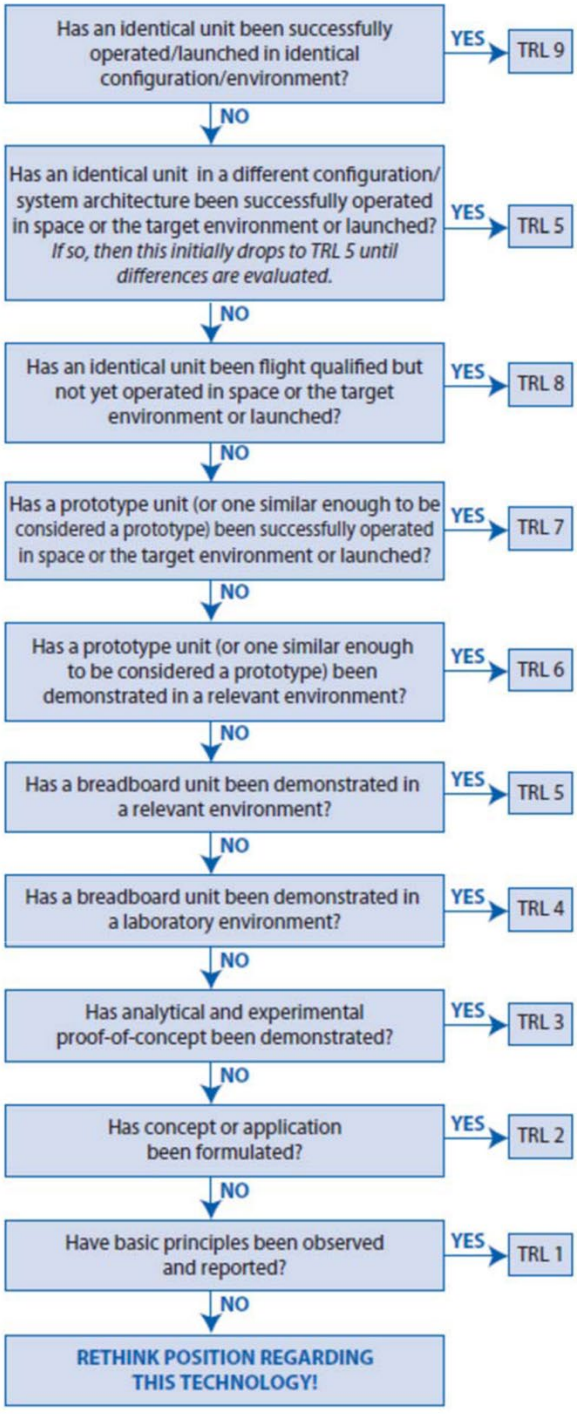


Figure 1.4: Technology Maturity Assessment thought process. Credit: NASA.

used. It is extremely important to develop and use a consistent set of definitions over the course of the program/project."

1.3.2 Heritage Systems

"Note the second box particularly refers to heritage systems (Figure 1.4). If the architecture and the environment have changed, then the TRL decreases to TRL 5—at least initially. Additional testing may need to be done for heritage systems for the new use or new environment. If in subsequent analysis the new environment is sufficiently close to the old environment or the new architecture is sufficiently close to the old architecture, then the resulting evaluation could be TRL 6 or 7, but the most important thing to realize is that it is no longer at TRL 9. Applying this process at the system level and then proceeding to lower levels of subsystems and components identifies those elements that require development and sets the stage for the subsequent phase, determining the new TRL."

References

(1) NASA. What are SmallSats and CubeSats? February 26, 2015. Revised August 6, 2017. https://www.nasa.gov/content/what-are-smallsats-and-cubesats

(2) NASA Systems Engineering Handbook. NASA/SP-2016 6105 Rev. 2.

Table of Contents

Chapter Glossary ii
2.0 Complete Spacecraft Platforms 6
2.1 Introduction 6
2.2 State-of-the-Art – Spacecraft Platforms 6
2.2.1 Hosted Orbital Services 6
2.2.2 Spacecraft Bus Procurement 10
2.3 Other Complete Spacecraft Platforms Providers 23
2.4 Programmatic and Systems Engineering Considerations 23
2.5 Summary 24
2.6 References 24



Chapter Glossary

(COTS)	Commercial-off-the-Shelf
(EELV)	Evolved Expendable Launch Vehicle
(ESPA)	EELV Secondary Payload Adapter
(GEO)	Geostationary Equatorial Orbit
(I&T)	Integration and Test
(kg)	Kilogram
(LEO)	Low Earth Orbit
(MEO)	Medium Earth Orbit
(MTBF)	Mean Time Between Failures
(NASA)	National Aeronautics and Space Administration
(SHF)	Super High Frequency
(SPA)	Secondary Payload Adapter
(STMD)	Space Technology Mission Directorate
(TRL)	Technology Readiness Level
(UHF)	Ultra High Frequency
(UK)	United Kingdom
(Unk)	Unknown
(USA)	United States of America
(VLEO)	Very Low Earth Orbit
(VHF)	Very High Frequency
(W)	Watts
(xGEO)	Beyond Geostationary Equatorial Orbit

2.0 Complete Spacecraft Platforms

2.1 Introduction

Small spacecraft continue to enable a broad range of science missions, technology demonstrations, and operational services. Regardless of mission type, each spacecraft relies on a bus, which provides essential services to the payload. These services typically include power generation and storage, thermal control, attitude determination and control, navigation and timing, communications, propulsion, and command and data handling. While this report examines the state of the art for individual subsystems, this chapter focuses on complete, readily available spacecraft platforms that practitioners can procure or access as services.

To reflect how teams make acquisition decisions, the chapter is organized into two main categories: hosted orbital services and spacecraft bus procurement. Hosted orbital services offer end-to-end mission support by integrating customer payloads onto provider-managed spacecraft and conducting system-level integration, test, commissioning, and operations. Spacecraft bus procurement focuses on purchasing a flight-proven or development-stage bus and, depending on the provider, optionally leveraging their system-level integration and test support while the customer leads mission operations. The procurement section is further subdivided by platform class: PocketQube, CubeSat, and ESPA-class.

Procuring a complete platform—whether as a hosted service or as a bus—can reduce technical and programmatic risk by leveraging proven hardware and established processes. It does not eliminate the need for mission-level trades and responsibilities, which typically include payload-to-bus interface definition and verification, environmental qualification, regulatory and spectrum licensing, concept of operations development, commissioning, and on-orbit data handling. Hosted services can shift many of these responsibilities to the provider, allowing investigators to focus on payload development and data ground processing; purchasing a bus can provide greater control over mission tailoring and operations, at the cost of increased integration effort.

Inclusion in this chapter is non-exhaustive and intended as a snapshot of the market as of January 2026; offerings evolve rapidly, and readers should confirm details directly with providers.

To use this chapter, start by clarifying your mission needs and payload envelope (mass, volume, power). If you seek end-to-end support and faster access to space, review hosted orbital services first. If you plan to own and operate the spacecraft, proceed to the bus procurement section, selecting among PocketQube, CubeSat, and ESPA-class platforms based on size and capability. Each subsection includes summary tables to help compare offerings, and Section 2.4 outlines systems engineering considerations and links to relevant guidance documents for the development of small spacecraft.

2.2 State-of-the-Art – Spacecraft Platforms

2.2.1 Hosted Orbital Services

Hosted orbital services provide end-to-end mission support by integrating customer payloads onto provider-managed spacecraft and conducting system-level integration and test, launch accommodations, commissioning, and on-orbit operations with data return. Providers differ in vehicle type, business model, and the degree of transparency and control they offer to customers, but the common objective is to reduce barriers to flight and streamline the path from payload development to scientifically or operationally useful data. This section focuses on hosted orbital services using small spacecraft platforms; other space-based hosting opportunities—such as hosting on the International Space Station, on launch vehicle structures, or on returnable capsules—exist but are beyond the scope of this chapter. Hosted orbital services can be

implemented in several ways. The choice among these models depends on payload needs, desired control and customization, as well as schedule, and budget.

- **Dedicated spacecraft**: a single customer's payload flies on its own spacecraft, with the full bus resources reserved for that mission.
- **Shared hosted capacity on provider missions**: unused mass, power, and data margins on the provider's internally funded mission are allocated to one or more customer payloads.
- **Multi-payload missions**: multiple customer payloads share a single spacecraft bus with partitioned resources and interfaces.
- **Virtual or software-only hosting**: payload functionality is implemented as software on an existing spacecraft, leveraging onboard processing and data links without dedicated hardware.

The benefits of hosted orbital services are centered on speed, cost, risk reduction, flexibility, and focus. Standardized interfaces and recurring flight campaigns can shorten the timeline from payload delivery to on-orbit operations, accelerating technology maturation and science return. Shared spacecraft resources and established processes reduce non-recurring engineering and programmatic overhead relative to building and launching a bespoke spacecraft. Providers typically leverage flight-proven buses, deployers, ground networks, and mission assurance practices, which can improve the probability of mission success. Services can be tailored to payload needs and scaled across flights or constellations, allowing adjustments to bandwidth, coverage, and mission duration as needed. Importantly, hosted services enable investigators to concentrate on instrument development and data ground processing while the provider handles spacecraft integration, commissioning, and routine operations.

Although offerings vary, hosted orbital services generally articulate clear payload acceptance envelopes and interface requirements. Customers should expect specifications for mass, volume, mounting constraints, keep-out zones, and center-of-gravity limits; power budgets, including average and peak draw, duty cycles, inrush limits, and electrical interfaces; thermal interfaces, allowable temperature ranges, and heat rejection capability; data interfaces, protocols, expected throughput, onboard storage, and downlink schedules; and attitude determination and control performance available to the payload, including pointing knowledge, control/accuracy, and stability/jitter. Providers typically define environmental qualification expectations (random vibration, shock, thermal vacuum, electromagnetic compatibility/interference), radiation environment assumptions and component-level tolerance, and software integration approaches, including flight software architectures, command/telemetry schemas, and on-orbit authority. Ground segment provisions—data formats, latency, delivery mechanisms, security measures, and archiving—are also defined as part of the interface.

Several considerations warrant careful attention during selection and contracting. Data rights and access should be explicitly defined, including ownership, latency, formats, and any restrictions on redistribution or publication. Operational authority and autonomy must be clear: who can command payload modes, update software, and respond to anomalies on orbit, and what safeguards or approval workflows apply. Regulatory and licensing responsibilities—such as spectrum coordination and remote sensing approvals—require planning; customers should confirm what support the provider offers and which tasks remain with the payload team. Cybersecurity posture across command and data links and ground systems should address authentication, encryption, monitoring, and incident response. In multi-payload missions, resource partitioning and contention management are central to predictable operations; customers should understand how power, data, pointing, and schedules are allocated and prioritized. Lead times and manifests must be realistic, and should include contingency plans for integration delays or launch slips. Mission assurance practices and flight heritage should be

reviewed for relevance to the target orbit and environment, while end-of-life planning should ensure deorbit or passivation meets applicable guidelines. Finally, export controls may affect certain providers or payload components; early planning for compliance can help mitigate delays.

To compare hosted orbital services effectively, customers can frame their selection around mission outcomes and constraints. Begin with the target orbit, coverage, and revisit rates the provider can offer, and assess whether these meet science or operational objectives. Examine payload envelopes—mass, volume, power, and thermal—and verify interface compatibility against provider standards. Evaluate the attitude control performance available to the payload and the vibration/jitter environment relative to pointing or imaging requirements. Communications capacity, downlink latency, and ground network architecture should align with data volumes and cadence; confirm that onboard storage and scheduling flexibility support high-duty-cycle payloads. Propulsion capabilities, if relevant, should cover orbit changes, collision avoidance, and disposal. Flight heritage and reliability metrics provide insight into expected performance; preference may be given to providers with demonstrated performance in similar missions. Integration and test services, facilities, and verification approaches should be commensurate with payload complexity, and data services—including processing, storage, and delivery guarantees—should meet analysis workflows. Regulatory and licensing support, cybersecurity features, schedule and production cadence, and cost structure (including any per-bit or per-pass fees) round out the comparison. Terms governing data rights, on-orbit authority, and change control should be negotiated early and documented.

Procurement of hosted orbital services typically proceeds through commercial agreements that include a statement of work, interface control documents, verification and validation plans, acceptance test procedures, project lifecycle reviews, and service-level agreements for operations and data delivery. Clear definition of deliverables and decision gates—such as project lifecycle review entrance/exit criteria, payload acceptance review, environmental test reports, mission operations plan, commissioning report, and data handover specifications—helps reduce ambiguity. Roles and responsibilities for licensing, launch integration, anomaly response, and end-of-life disposition should be explicitly assigned. If you intend to use government procurement mechanisms or programs, confirm current eligibility, terms, and contracting pathways through official documentation and appropriate contracting office.

Not all hosted service providers sell their spacecraft buses. If owning the bus is required, refer to the Spacecraft Bus Procurement section of this chapter. Offerings evolve rapidly; treat provider lists and capabilities as a snapshot as of January 2026 and confirm details directly with providers.

Table 2-1: Hosted Orbital Service Providers
(The fields indicate maximum capability; organizations may offer multiple options including smaller capabilities within the Hosted Orbital Services category)

Organization	Largest Platform	Peak Power (W)	3-σ Pointing Control/ Knowledge	Destination	US Office
2NDSpace Italy	CubeSat	>100	0.1°/0.02°	VLEO, LEO, MEO	No
AAC Clyde Space Sweden	CubeSat	400	<0.01°/<0.0075°	LEO	Yes
Aerospacelab Belgium	ESPA	300	<0.005°/ <0.005°	LEO, GEO	Yes
Alba Orbital UK	PocketQube	15	5°/2°	LEO	Yes
Alén Space Spain	CubeSat	180	0.2°/0.1°	LEO	No
Apex USA	ESPA	4,000	0.005°/ 0.0025°	LEO, MEO, GEO	Yes
Argotec Italy	ESPA	440	<0.01°/<0.008°	LEO, MEO, GEO, Deep Space	Yes
Artemis Space Technologies UK	ESPA	1,500	0.01°/0.01°	LEO, MEO, GEO, Lunar and Deep Space	No
Astranis Space Technologies Corp. USA	ESPA	300	<0.1°/ <0.09°	GEO	Yes
Astro Digital USA	ESPA	3,000	<0.03°/ <0.02°	LEO, GTO, GEO	Yes
Axelspace Japan	ESPA	1,800	<0.05°/ <0.04°	LEO	No
BAE Systems SMS USA	ESPA	2,500	<0.006°/<0.003°	LEO, MEO, GEO, Cislunar, Deep Space	Yes
Berlin Space Technologies Germany	ESPA	2,500	<0.017°/< 0.017°	LEO	Yes
Blue Canyon Technologies USA	ESPA	1,082	0.002°/0.002°	LEO, GEO, Deep Space	Yes
C3S Electronics Development Hungary	CubeSat	505	0.4°/ 0.6°	LEO, MEO	No
CesiumAstro USA	ESPA	4,500	<0.1°/<0.01°	LEO	Yes
CREOTECH Poland	ESPA	600	<0.02°/< 0.015°	LEO, MEO, GEO, Lunar, Deep Space	No
D-Orbit Italy	ESPA	300	0.1°/ 0.05°	LEO	No
D-Orbit USA	ESPA	2,000	0.1°/ 0.05°	LEO, GEO	Yes
EnduroSat Bulgaria	ESPA	6,800	0.1°/0.006°	LEO	Yes
Exobotics UK	ESPA	3,600	0.1°/ 0.008°	LEO, MEO, HEO, GEO, Lunar	No
FOSSA Systems Spain	CubeSat	60	<0.1°/<0.1°	LEO	No
German Orbital Systems Germany	CubeSat	150	<1°/< 1°	LEO	No
GomSpace Denmark	CubeSat	150	0.070°/ 0.056°	LEO, MEO, GEO, Lunar, Deep Space	Yes
Harpy Aerospace India	ESPA	2,100	0.35°/0.35°	LEO, GEO, Lunar, ISS	Yes
Hemeria France	ESPA	250	<0.03°/<0.01°	LEO, GTO, GEO	No
HEX20 India	CubeSat	150	0.008°/ 0.008°	LEO, MEO, Lunar	Yes
Hydra Space Systems Spain	CubeSat	30	<1°/< 1°	LEO	No
Innova Space Argentina	CubeSat	4	<15°/< 15°	LEO	Yes
Loft Orbital USA	ESPA	4,000	<0.01°/<0.007°	LEO	Yes
Magellan Aerospace Canada	ESPA	200	0.01°/0.01°	LEO	No
Malin Science Space Systems USA	ESPA	918	<0.015°/<0.015°	Mars	Yes
Momentus Space USA	ESPA	3,000	0.008°/ 0.008°	LEO, MEO, GEO, Lunar, Deep Space	Yes

Table 2-1: Hosted Orbital Service Providers
(The fields indicate maximum capability; organizations may offer multiple options including smaller capabilities within the Hosted Orbital Services category)

Organization	Largest Platform	Peak Power (W)	3-σ Pointing Control/ Knowledge	Destination	US Office
Moog USA	ESPA	2,000	<0.050°/<0.033°	LEO, GEO	Yes
Muon Space USA	ESPA	4,000	0.01°/0.004°	LEO	Yes
NanoAvionics Lithuania	ESPA	378	0.15°/ 0.03°	LEO	Yes
Nara Space South Korea	CubeSat	120	0.05°/ 0.03°	LEO	No
NearSpace Launch USA	CubeSat	160	0.5°/ 0.2°	LEO	Yes
Northrop Grumman USA	ESPA	420	<4°/<1°	LEO	Yes
NovaWurks USA	ESPA	>5,000	0.002°/0.0004°	LEO, GEO, xGEO	Yes
NPC SPACEMIND Italy	CubeSat	100	<0.1°/<0.1°	LEO, MEO	Yes
OHB LuxSpace Luxembourg	ESPA	600	<0.022°/ 0.01°	LEO	No
OHB Sweden Sweden	ESPA	1,500	0.008°/ 0.008°	LEO, MEO	No
Orbital Astronautics UK	ESPA	5,000	<0.05°/<0.01°	LEO, MEO, GEO, Deep Space	No
Orion Space Solutions USA	CubeSat	400	<1°/<1°	VLEO, LEO, GEO, Lunar	Yes
Pumpkin Space USA	CubeSat	400	0.05°/<0.05°	LEO, Lunar	Yes
Quantum Space USA	ESPA	400	0.006°/0.006°	LEO, GEO, Cislunar, Lunar, Deep Space	Yes
Quub, Inc.USA	CubeSat	50	5°/2°	LEO, Lunar	Yes
Redwire Space USA	ESPA	500	0.005°/0.0017°	LEO, MEO, GEO and Deep Space	Yes
Reflex Aerospace Germany	ESPA	3,000	<0.01°/<0.005°	LEO	No
SatRev Poland	CubeSat	150	1°/1°	LEO	No
SFL Missions Inc.Canada	ESPA	1,500	0.009°/0.004°	LEO, GEO, Lunar	No
Sierra Space USA	ESPA	500	0.001°/ <0.001°	LEO, MEO, GEO	Yes
SITAEL Italy	ESPA	2,000	0.0017°/ 0.001°	LEO	No
Southwest Research Institute USA	ESPA	1,550	0.015°/0.002°	LEO, GEO	Yes
Space Dynamics Laboratory USA	ESPA	2,000	0.021°/0.021°	LEO, GEO, GTO, Cislunar, Deep Space	Yes
Space Inventor Denmark	ESPA	1,500	<0.008°/<0.008°	LEO, GEO, MEO, Lunar	No
Spacemanic Czech Republic	CubeSat	216	1°/ 0.5°	LEO, MEO, GEO, Lunar	No
Spire Global USA	CubeSat	300	0.1°/ 0.05°	LEO	Yes
Surrey Satellite Technology Ltd. UK	ESPA	2,000	<0.01°/ <0.01°	LEO, MEO, GEO, Lunar	No
Terran Orbital USA	ESPA	1,500	0.014°/0.002°	LEO, GEO, Lunar	Yes
U-Space France	ESPA	250	0.007°/0.005°	LEO	No
Varda Space Industries USA	ESPA	500	2.25°/ 0.40°	LEO with Re-entry Recovery	Yes
York Space Systems USA	ESPA	2,200	0.002°/ 0.0004°	LEO, GEO, Lunar	Yes

2.2.2 Spacecraft Bus Procurement

The SmallSat market includes providers of complete spacecraft bus solutions, encompassing system-level integration and test (I&T) and operations capabilities. Providers that deliver end-to-end services are addressed in Section 2.2.1. The providers profiled here offer bus procurement

and possibly provide system-level I&T. Readers should use this document to narrow candidate options; refer to Table 2-9 for providers websites and contact information.

2.2.2.1 PocketQubes

PocketQubes are very small satellites built around a 5 cm cube unit, denoted “P.” A 1P spacecraft occupies a single 5 cm cube, and larger configurations combine units (for example, 2P, 3P, and beyond where deployers permit). Figure 2.3 illustrates the standard dimensions of a 1P unit, providing a visual reference for the geometry used across PocketQube designs. Figure 2.5 shows an example of a PocketQube. The PocketQube ecosystem has matured in recent years, and multiple providers offer off-the-shelf buses that integrate power, command and data handling, communications, and basic attitude sensing within extremely constrained mass and volume envelopes. These platforms are well suited to tightly focused technology demonstrations and compact instruments that can tolerate limited power and modest attitude control.

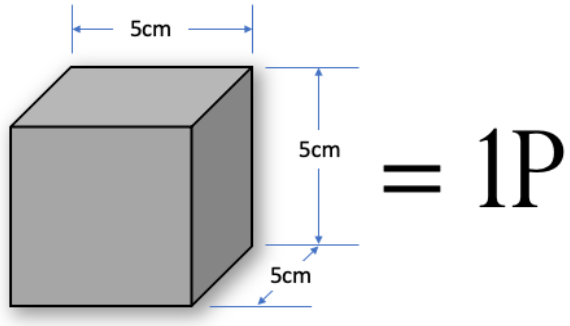


Figure 2.3: PocketQube Dimensions.



Figure 2.4: Alba Orbital Integration of PocketQubes into the Deployers. Credit: Alba Orbital.

Selecting a PocketQube bus centers on a clear understanding of payload constraints and mission requirements. Mechanical considerations include strict keep-out zones, mounting features compatible with the chosen deployer, and center-of-gravity placement to meet deployment requirements. Figure 2.4 shows PocketQubes and deployers for integration. Electrical power budgets are typically low, with tight limits on average and peak draw, duty cycles, and inrush currents; payload modes must align with available storage and generation. Communication subsystems generally offer lower data rates relative to larger classes, so data volume, latency, and downlink scheduling should be planned accordingly. Attitude determination and control capabilities vary, but pointing performance is often limited by scale; payloads that demand fine pointing or low jitter may require tailored solutions or selection of a larger platform class. Environmental qualification—random vibration, shock, thermal vacuum, and electromagnetic compatibility—should match the launch and orbit, and radiation tolerance assumptions should be confirmed with the provider.

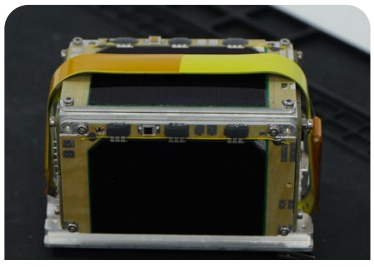


Figure 2.5: Hydra Space Systems PocketQube. Credit: Hydra Space Systems.

PocketQube deployers define the mechanical interface and envelope for flight. While a typical deployer accommodates up to 3P, larger systems may exist; specific dimensions, clamp features, and external volume allowances are determined by the deployer and launch integration configuration. As shown in Figure 2.4, understanding the deployer integration early helps ensure mechanical compatibility and proper verification of separation mechanisms. Prospective buyers should coordinate with their

sponsoring organization or launch provider to identify the deployer that will be used and verify bus compatibility. The summary table in this subsection lists representative PocketQube buses, including power availability, communications options, and any optional integration services.

Table 2-2: PocketQubes Market Solutions
(The fields indicate maximum capability; organizations may offer multiple options including smaller capabilities within the PocketQube category)

Organization	Peak Power (W)	3-σ Pointing Control/ Knowledge	Comm Options	Intended Destination	Maturity	US Office
Alba Orbital UK	15	5°/2°	UHF, S	LEO	Flown LEO	Yes
DIYSATELLITE Argentina	9	<5°/<5°	VHF, UHF, SHF	LEO, GEO, Lunar	Flown LEO	No
FOSSA Systems Spain	10	<5°/<5°	UHF, S	LEO	Flown LEO	No
Hydra Space Systems Spain	8	5°/5°	VHF, UHF	LEO	Flown LEO	No
Innova Space Argentina	3.9	N/A -Magnetic Passive	UHF	LEO	Flown LEO	Yes
Quub, Inc. USA	26	5°/2°	UHF, S	LEO, Lunar	Flown LEO	Yes

2.2.2.2 CubeSats

CubeSats are modular small satellites built from 10 cm cube units, denoted “U.” The standard—originally developed to facilitate access to space for educational missions and now widely adopted—supports a range of sizes from sub-unit form factors up to multi-unit configurations (e.g., from sub-1U form factors up to 27U-class configurations). The market offers a broad spectrum of

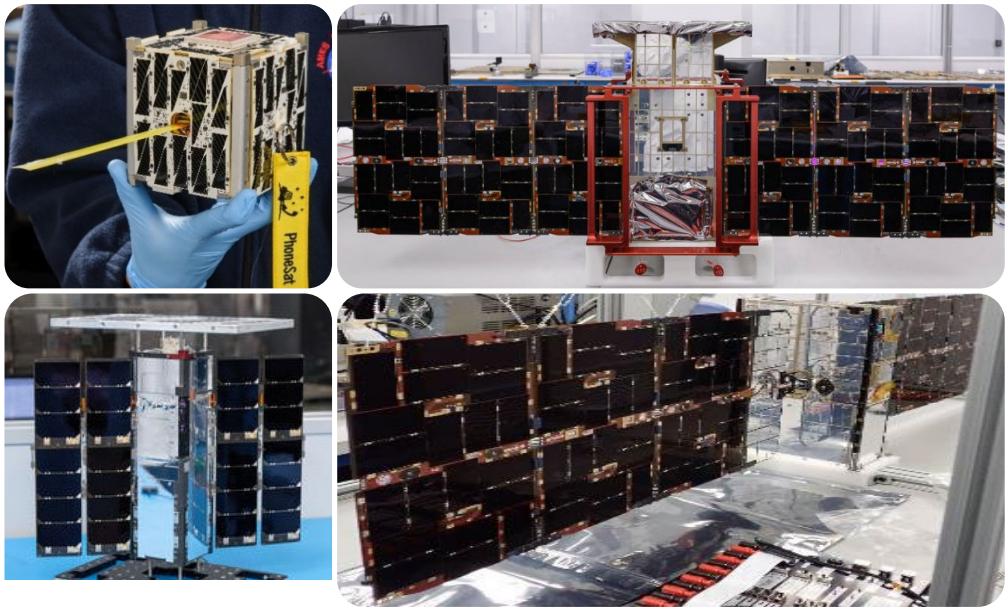


Figure 2.6: Examples of flown CubeSats. (Top left) 1U PhoneSat spacecraft, (top right) 12U CAPSTONE spacecraft, (lower left) 3U CLICK spacecraft, (lower right) 6U PTD-3 spacecraft. Credits: NASA and Terrain Orbital.

CubeSat buses spanning basic platforms for rapid technology demonstrations to highly capable systems with precise pointing, increased power generation, redundant subsystems, and

integrated propulsion. Examples of flown CubeSats at multiple sizes are shown in Figure 2.6, illustrating the diversity of implementations.

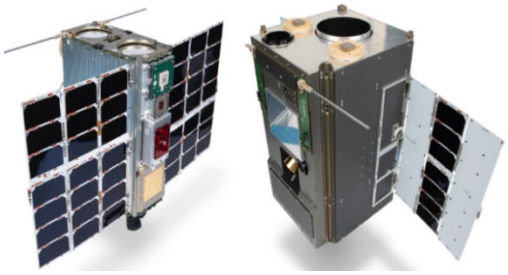


Figure 2.7: Examples of a 6U and 16U CubeSat. Credit: Spire Global.

Selecting a CubeSat bus typically begins by mapping mission requirements to size and capability. Smaller buses (e.g., 1U–3U) often suit low-power payloads and missions with relaxed pointing or data demands, while mid-size platforms (e.g., 6U) provide more power and volume, enabling more capable ADCS, communications, and propulsion subsystems. Larger configurations (e.g., 12U, 16U and above) support higher duty cycles, larger instruments, and more stringent pointing and stability requirements. Figure 2.7 provides visual examples of 6U and 16U CubeSat form factors. Across sizes, common trade factors include average and peak power availability, battery capacity and array configuration, ADCS performance (pointing accuracy, knowledge, stability, and jitter), communications bands and data rates, onboard storage, and optional propulsion (including propellant type and expected delta-V). Heritage in similar orbits and environments and the provider's test and quality practices are important indicators of reliability.

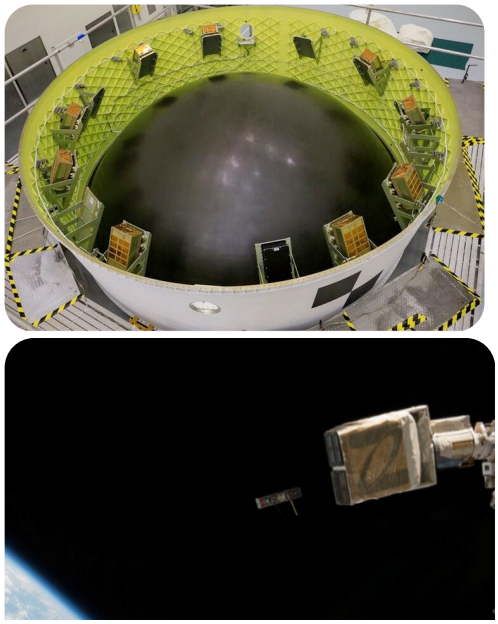


Figure 2.8: (top) Location of Artemis CubeSat deployers in between the Orion Crew Vehicle and the Interim Cryogenic Propulsion Stage (ICPS); (lower) NASA Nodes mission deployment from ISS. Credit: NASA.

Mechanical interface compliance is fundamental. CubeSat deployers enforce strict keep-out zones, surface features, and load paths. Two primary interface families are in use: classic corner rails and tab-based systems (clamped and unclamped variants). Most bus providers offer adaptations to support both, but buyers should verify the specific deployer used by their launch provider and ensure the bus meets the corresponding mechanical and environmental requirements. Differences in deployer location on the launch vehicle can affect shock, vibration, and thermal environments; qualification plans should account for these conditions. Figure 2.8 illustrates this variability, showing the location of Artemis CubeSat deployers between the Orion Crew Vehicle and the Interim Cryogenic Propulsion Stage (left), and the NASA Nodes mission deployment from the International Space Station (right). Payload teams should also confirm electrical interfaces and protocols, data handling and downlink scheduling, and any software integration requirements, including flight software hooks and command/telemetry schemas.

This report organizes CubeSat buses by size to streamline comparison. The summary tables for 0.25U–3U, 6U, 12U, and 16U+ list representative platforms. Offerings evolve quickly; readers should treat the tables as a starting point and engage providers to obtain current details.

Table 2-3: 0.25U-3U Market Solutions
(The fields indicate maximum capability; organizations may offer multiple options including smaller capabilities within the 0.25U-3U category)

Organization	Peak Power (W)	3-σ Pointing Control/ Knowledge	Comm Options	Intended Destination	Maturity	US Office
2NDSpace Italy	>100	0.1°/0.02°	VHF, UHF, S, X	VLEO, LEO, MEO	Flown LEO	No
AAC Clyde Space Sweden	90	<0.1°/<0.01°	VHF, UHF, S, X	LEO	Flown LEO	Yes
Blue Canyon Technologies USA	27	0.003°/0.003°	L, S, X	LEO, GEO, Deep Space	Flown LEO Qualified GEO and Deep Space	Yes
Deimos Space Spain	35	0.2°/0.2°	UHF, X	LEO	Flown LEO	No
EnduroSat Bulgaria	84	<1°/<0.6°	UHF, S, X	LEO	Flown LEO	Yes
Exobotics UK	75	0.1°/ 0.05°	VHF, UHF, S, X	LEO	Under Development	No
FOSSA Systems Spain	30	1°/1°	UHF, S	LEO	Flown LEO	No
German Orbital Systems Germany	35	<1°/<1°	UHF, VHF, S, X	LEO	Flown LEO	No
GomSpace Denmark	35	0.139°/0.056°	S, X	LEO	Flown LEO	Yes
Gran Systems Taiwan	50	2°/ 2°	VHF, UHF, S	LEO	Flown LEO	Yes
GUMUSH AeroSpace Turkey	80	<1°/ <0.1°	VHF, UHF, S, X	LEO	Flown LEO	No
Harpy Aerospace India	72	<0.1°/<0.01°	VHF, UHF, S, X	LEO, GEO, Lunar	Qualified LEO and Lunar	Yes
HEX20 India	30	0.003°/ 0.003°	VHF, UHF, S	LEO	Flown LEO	Yes
Hydra Space Systems Spain	30	<1°/ <1°	VHF, UHF, Ka	LEO	Under Development	No
Innova Space Argentina	7.5	<15°/<15°	UHF	LEO	Flown LEO	Yes
ISISPACE The Netherlands	50	<15°/<15°	VHF, UHF, S	LEO	Flown LEO	No
NanoAvionics Lithuania	175	13.20°/12.93°	UHF, S, X	LEO	Flown LEO	Yes
NearSpace Launch USA	100	0.5°/0.2°	L, UHF, S, X	VLEO, LEO	Flown LEO	Yes
NPC SPACEMIND Italy	51.6	<0.1°/<0.1°	UHF, S, X, Ka	LEO, MEO, GEO, Lunar	Flown LEO and MEO	Yes
Orbital Astronautics UK	400	0.1°/ 0.01°	S, X, K, Ka, Optical	LEO, MEO	Flown LEO Qualified MEO and GEO	No
Orion Space Solutions USA	8	1°/1°	L, S, X	LEO	Qualified LEO	Yes
Pumpkin Space Systems USA	200	0.05°/<0.05°	UHF, S, X, Ka	LEO	Flown LEO	Yes
Quub, Inc. USA	44	5°/2°	UHF, S	LEO, Lunar	Flown LEO	Yes
SatRev Poland	150	0.01°/0.01°	UHF, S, X	LEO	Flown LEO	No
SFL Missions Inc. Canada	100	0.009°/0.004°	UHF, S, X, Ka	LEO, GEO, Lunar	Flown LEO Qualified GEO and Lunar	No
Space Inventor Denmark	100	0.01° / 0.01°	VHF, UHF, S, X, L	LEO	Flown LEO	No
Spacemanic Czech Republic	48	1°/0.5°	VHF, UHF, S	LEO, GEO, Lunar	Flown LEO	No
U-Space France	35	10°/10°	S, X	LEO	Flown LEO	No

Table 2-4: 6U Market Solutions
(The fields indicate maximum capability; organizations may offer multiple options including smaller capabilities within the 6U category)

Organization	Peak Power (W)	3-σ Pointing Control/ Knowledge	Comm Options	Intended Destination	Maturity	US Office
2NDSpace Italy	>100	0.1°/0.02°	VHF, UHF, S, X	VLEO, LEO, MEO	Flown LEO	No
AAC Clyde Space Sweden	150	<0.1°/<0.01°	VHF, UHF, S, X	LEO	Flown LEO	Yes
Argotec Italy	80	<0.02°/<0.01°	UHF, S, X	Deep Space	Flown Deep Space	Yes
Astro Digital USA	240	<0.1°/<0.05°	UHF, S, X, Ka	LEO	Flown LEO	Yes
Blue Canyon Technologies USA	108	0.003°/0.003°	L, S, X	LEO, GEO, Deep Space	Flown LEO and Lunar Qualified GEO and Deep Space	Yes
Deimos Space Spain	40	0.05°/0.05°	UHF, S, X	LEO	Under Development	No
EnduroSat Bulgaria	172	0.08°/0.04°	UHF, S, X	LEO	Flown LEO	Yes
Exobotics UK	400	0.1°/ 0.008°	VHF, UHF, S, X, Optical	LEO	Flown LEO	No
FOSSA Systems Spain	60	<0.1°/<0.1°	UHF, S	LEO	Under Development	No
German Orbital Systems Germany	70	<1°/<1°	UHF, VHF, S, X	LEO	Flown LEO	No
GomSpace Denmark	103	0.070°/0.056°	S, X	LEO, Deep Space	Flown LEO and Deep Space	Yes
GUMUSH AeroSpace Turkey	160	<0.1°/<0.05°	VHF, UHF, S, X	LEO	Under Development	No
Harpy Aerospace India	160	<0.1°/<0.01°	VHF, UHF, S, X	LEO	Qualified LEO	Yes
HEX20 India	100	0.003°/0.003°	UHF, S, X	LEO, MEO, Lunar	Under Development	Yes
ISISPACE The Netherlands	100	<0.3°/<0.3°	UHF, S, X	LEO, Lunar	Flown LEO Qualified for Lunar	No
NanoAvionics Lithuania	175	0.18°/0.12°	UHF, S, X	LEO	Flown LEO	Yes
Nara Space South Korea	120	0.05°/0.03°	VHF, UHF, S	LEO	Flown LEO	No
NearSpace Launch USA	160	0.5°/0.2°	L, UHF, S, X	LEO	Flown LEO	Yes
NPC SPACEMIND Italy	85.2	<0.1°/<0.1°	UHF, S, X, Ka	LEO, MEO, GEO, Lunar	Flown LEO	Yes
Orbital Astronautics UK	1,000	0.1°/0.01°	S, X, K, Ka, Optical	LEO, MEO	Flown LEO Qualified MEO and GEO	No
Orion Space Solutions USA	15	1°/1°	L, S, X	LEO	Flown LEO	Yes
Pumpkin Space USA	200	0.05°/<0.05°	UHF, S, X, Ka	LEO, Lunar	Flown LEO Qualified Lunar	Yes
Quub, Inc.USA	50	5°/2°	UHF, S, Ku	LEO, Lunar	Under Development	Yes
SatRev Poland	150	0.01°/0.01°	UHF, S, X	LEO	Flown LEO	No
Space Dynamics Laboratory USA	400	0.021°/0.021°	UHF, S, X, Ka	LEO, GEO, GTO,	Flown LEO	Yes

Table 2-4: 6U Market Solutions
(The fields indicate maximum capability; organizations may offer multiple options including smaller capabilities within the 6U category)

Organization	Peak Power (W)	3-σ Pointing Control/ Knowledge	Comm Options	Intended Destination	Maturity	US Office
				Cislunar, Deep Space	Qualified GEO, GTO, Lunar and Deep Space	
SFL Missions Inc. Canada	240	0.009°/0.004°	UHF, S, X, Ka	LEO, GEO, Lunar	Flown LEO Qualified GEO and Lunar	No
Space Inventor Denmark	200	<0.008°/<0.008°	VHF, UHF, S, X	LEO	Flown LEO	No
Spacemanic Czech Republic	432	1°/0.5°	VHF, UHF, S, X	LEO, GEO, Lunar	Qualified LEO	No
Terran Orbital USA	180	0.021°/0.007°	UHF, S, X	LEO, GEO, Lunar	Flown LEO and Lunar	Yes

Table 2-5: 12U Market Solutions
(The fields indicate maximum capability; organizations may offer multiple options including smaller capabilities within the 12U category)

Organization	Peak Power (W)	3-σ Pointing Control/ Knowledge	Comm Options	Intended Destination	Maturity	US Office
2NDSpace Italy	>100	0.1°/0.02°	VHF, UHF, S, X	VLEO, LEO, MEO	Flown LEO	No
AAC Clyde Space Sweden	400	<0.01°/<0.0075°	VHF, UHF, S, X, K, Ka, Ku, Optical	LEO	Qualified LEO	Yes
Argotec Italy	100	<0.02°/<0.01°	UHF, S, X	LEO	Under Development	Yes
Blue Canyon Technologies USA	108	0.002°/0.002°	L, S, X	LEO, GEO, Deep Space	Flown LEO and GEO Qualified Deep Space	Yes
EnduroSat Bulgaria	346	0.08°/0.04°	UHF, S, X, K/Ka	LEO	Flown LEO	Yes
Exobotics UK	400	0.1°/ 0.008°	VHF, UHF, S, X, Optical	LEO, HEO, Lunar	Flown LEO and HEO	No
German Orbital Systems Germany	144	<0.1°/<0.1°	UHF, VHF, S, X	LEO	Qualified LEO	No
GomSpace Denmark	108	0.070°/0.056°	S, X	LEO	Flown LEO	Yes
GUMUSH AeroSpace Turkey	240	<0.05°/<0.05°	VHF, UHF, S, X	LEO	Under Development	No
Harpy Aerospace India	420	<0.1°/<0.01°	VHF, UHF, S, X, K, Ka, Ku, Optical	LEO	Qualified LEO	Yes
HEX20 India	125	0.008°/0.008°	UHF, S, X, Optical	LEO, MEO, Lunar	Under Development	Yes
ISISPACE The Netherlands	190	<0.03°/<0.03°	UHF, S, X, Ka	LEO	Under Development	No
NanoAvionics Lithuania	175	0.18°/0.09°	UHF, S, X	LEO	Flown LEO	Yes
Nara Space South Korea	120	0.05°/0.03°	S, X	LEO	Qualified LEO	No
NearSpace Launch USA	500	0.5°/0.2°	L, UHF, S, X	LEO, MEO	Under Development	Yes
NPC SPACEMIND Italy	96	<0.1°/<0.1°	UHF, S, X, Ka	LEO, MEO, GEO, Lunar	Flown LEO	Yes
Orbital Astronautics UK	2,000	0.05°/0.01°	S, X, K, Ka, Optical	LEO, MEO, GEO	Flown LEO Qualified MEO and GEO	No
Orion Space Solutions USA	40	<1°/<1°	L, S, X, Ka	LEO, GEO	Flown LEO	Yes
Pumpkin Space USA	400	0.05°/<0.05°	UHF, S, X, Ka	LEO, Lunar	Qualified LEO	Yes
Space Dynamics Laboratory USA	400	0.021°/0.021°	UHF, S, X, Ka	LEO, GEO, GTO, Cislunar, Deep Space	Flown LEO Qualified GEO, GTO, Lunar and Deep Space	Yes
SFL Missions Inc.Canada	322	0.009°/0.004°	UHF, S, X, Ka	LEO, GEO, Lunar	Flown LEO Qualified GEO and Lunar	No
Space Inventor Denmark	200	<0.008°/<0.008°	VHF, UHF, S, X	LEO	Flown LEO	No
Spacemanic Czech Republic	432	1°/0.5°	VHF, UHF, S, X	LEO, GEO, Lunar	Under Development	No
Terran Orbital USA	100	0.021°/0.007°	UHF, S, X	LEO, GEO, Lunar	Flown LEO and Lunar	Yes
U-Space France	150	0.009°/0.008°	S, X	LEO	Flown LEO	No

Table 2-6: 16U+ Market Solutions
(The fields indicate maximum capability; organizations may offer multiple options including smaller capabilities within the 16U+ category)

Organization	Format	Peak Power (W)	3-σ Pointing Control/ Knowledge	Comm Options	Intended Destination	Maturity	US Office
2NDSpace Italy	16U	>100	0.1°/0.02°	VHF, UHF, S, X	VLEO, LEO, MEO	Qualified LEO	No
AAC Clyde Space Sweden	16U	400	<0.01°/<0.0075°	VHF, UHF, S, X, K, Ka, Ku, Optical	LEO	Qualified LEO	Yes
Argotec Italy	16U+	220	<0.02°/<0.01°	UHF, S, X, K, Ka	GEO, Deep Space	Under Development	Yes
Astro Digital USA	16U+	500	<0.05°/<0.01°	UHF, S, X, Ku, Ka, V, W, Optical	LEO	Flown LEO	Yes
Blue Canyon Technologies USA	16U	108	0.002°/0.002°	L, S, X	LEO, GEO, Deep Space	Qualified LEO, GEO and Deep Space	Yes
Deimos Space Spain	16U+	100	0.025°/0.025°	UHF, S, X	LEO, Lunar, Deep Space	Under Development	No
EnduroSat Bulgaria	16U	346	0.08°/0.04°	UHF, S, X, K/Ka	LEO	Flown LEO	Yes
Exobotics UK	16U	400	0.1°/ 0.008°	VHF, UHF, S, X, Optical	LEO	Under Development	No
German Orbital Systems Germany	16U+	164	<1°/<1°	UHF, VHF, S, X	LEO	Qualified LEO	No
GomSpace Denmark	16U	116	0.070°/0.056°	S, X	LEO	Flown LEO	Yes
GUMUSH AeroSpace Turkey	16U	240	<0.05°/<0.05°	VHF, UHF, S, X	LEO	Under Development	No
Harpy Aerospace India	16U, 27U	420	<0.1°/<0.01°	VHF, UHF, S, X, K, Ka, Ku, Optical	LEO	Qualified LEO	Yes
HEX20 India	16U, 27U+	200	0.008°/0.008°	UHF, S, X, Optical	LEO, MEO, Lunar	Under Development	Yes
ISISPACE The Netherlands	16U	190	<0.03°/<0.03°	UHF, S, X, Ka	LEO	Under Development	No
NanoAvionics Lithuania	16U	175	0.18°/0.09°	UHF, S, X	LEO	Flown LEO	Yes
Nara Space South Korea	16U	120	0.05°/0.03°	S, X	LEO	Flown LEO	No
NPC SPACEMIND Italy	16U	120	<0.1°/<0.1°	UHF, S, X, Ka	LEO, MEO, GEO, Lunar	Under Development	Yes
Orbital Astronautics UK	16U, 27U	2,000	0.05°/0.01°	S, X, K, Ka, Optical	LEO, GEO, Lunar	Qualified LEO and GEO	No
Orion Space Solutions USA	16U+	400	<1°/<1°	L, S, X, Ka	VLEO, LEO, GEO	Qualified VLEO, LEO	Yes
Pumpkin Space USA	16U, 27U	400	0.05°/<0.05°	UHF, S, X, Ka	LEO, Lunar	Qualified LEO	Yes

SatRev Poland	16U	150	0.01°/<0.01°	UHF, S, X	LEO	Under Development	No
Space Dynamics Laboratory USA	16U+	1,600	0.021°/0.021°	UHF, S, X, Ka, Optical	LEO, GEO, GTO, Cislunar, Deep Space	Flown LEO Qualified GEO, GTO, Lunar and Deep Space	Yes
SFL Missions Inc. Canada	16U+	500	0.009°/0.004°	UHF, S, X, Ka	LEO, GEO, Lunar	Flown LEO Qualified GEO and Lunar	No
Space Inventor Denmark	16U	200	<0.008°/<0.008°	VHF, UHF, S, X, L, Ka, Ku, QV	LEO, GEO, MEO	Flown LEO and GEO	No
Spacemanic Czech Republic	16U	432	1°/0.5°	VHF, UHF, S, X	LEO, GEO, Lunar	Under Development	No
Terran Orbital USA	16U	100	0.021°/0.007°	UHF, S, X	LEO, GEO, Lunar	Flown LEO and Lunar	Yes
U-Space France	16U	150	0.009°/0.008°	S, X	LEO	Under Development	No

2.2.2.3 ESPA-Class



Figure 2.9: LandSat-9 ESPA Ring populated with payloads and mass ballasts. Credit: NASA/Randy Beaudoin.

ESPA-class spacecraft are designed to fly as secondary payloads on launch vehicles using the Evolved Expendable Launch Vehicle Secondary Payload Adapter (ESPA) or similar structures. The ESPA ring separates the primary payload from the upper stage and provides multiple mounting locations for secondary spacecraft. Rings can be stacked to accommodate additional payloads. Figure 2.9 illustrates a populated ESPA ring on the Landsat-9 mission, showing a practical arrangement of payloads and mass ballasts and providing context for available mounting configurations. For the purposes of this chapter, ESPA-class refers to platforms with mass typically under 500 kg that can be adapted to rideshare opportunities on ESPA or analogous interfaces. While some ESPA-class missions exceed this mass, the focus here aligns with SmallSat taxonomy and common rideshare constraints.

Procuring an ESPA-class bus introduces considerations distinct from PocketQubes and CubeSats. For example, requirements for safety compliance will be more stringent as an ESPA spacecraft is not encased by a deployer. Mechanical compatibility with the ring or equivalent adapter must be confirmed, including the choice of separation system, envelope constraints, and interface loads. Shock and vibration environments at the ring can differ from other locations in the stack, and qualification plans should reflect these specifics. Rideshare accommodations can also be implemented via plate-based adapters rather than direct ring ports, as depicted in Figure 2.10.

Larger buses typically offer significantly higher power generation and storage, enhanced attitude determination and control with precision pointing and jitter control, multiple communications bands and high data rates, robust thermal control, and propulsion systems capable of meaningful orbit changes and end-of-life disposal. These capabilities support a wider range of mission types, including more demanding remote sensing, communications, and technology demonstrations, potentially beyond low Earth orbit depending on the bus design and heritage.

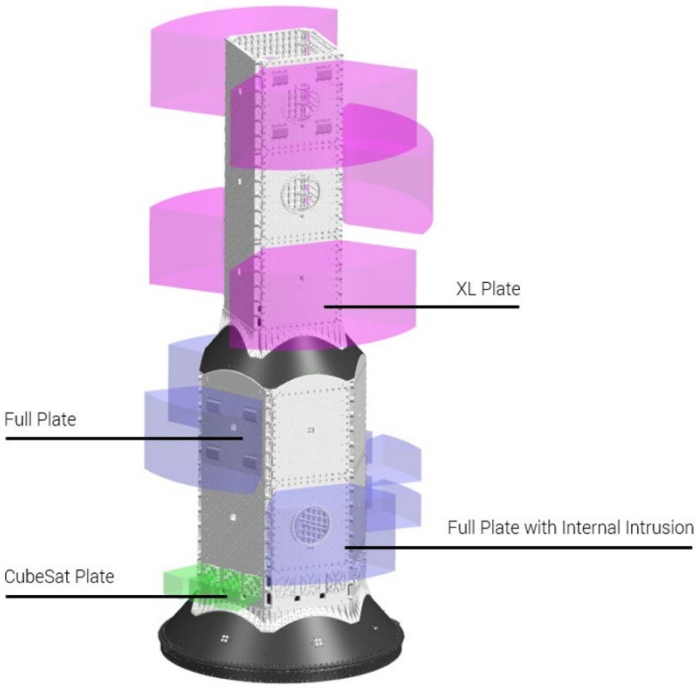


Figure 2.10: Example Payload Plate and Volume Configurations using Rideshare Plates. Credit: SpaceX.

Selection should balance capability with integration complexity and schedule. Understanding the provider's flight heritage in the target orbit and environment, mission assurance practices, and production cadence helps assess programmatic and technical risk. Payload envelope and interfaces—mechanical, electrical, thermal, data, and software—must be specified in detail, and ground segment accommodations for data delivery, latency, and security must be confirmed. Regulatory and licensing responsibilities, including spectrum and remote sensing approvals where applicable, should be planned early. End-of-life and disposal must meet applicable guidelines, and passivation requirements should be incorporated into bus design and operations. Figure 2.11 depicts an ESPA-class satellite bus from Muon Space during integration at a SpaceX facility for the Transporter-14 rideshare mission.

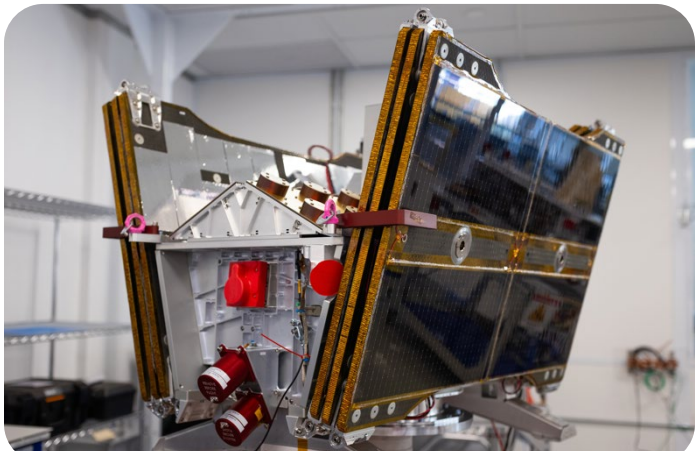


Figure 2.11: ESPA-Class satellite bus from Muon Space launched on SpaceX Transporter-14 rideshare mission in June 2025. Credit: Muon Space.

The ESPA-class summary table in this subsection presents representative commercially available platforms. As with other classes, readers should verify current specifications and lead times with providers and ensure compatibility with the specific rideshare opportunity and adapter that will be used.

Table 2-7: ESPA-Class Market Solutions
(The fields indicate maximum capability; organizations may offer multiple options including smaller capabilities within the ESPA-Class category)

Organization	Peak Power (W)	3-σ Pointing Control/ Knowledge	Comm Options	Intended Destination	Maturity	US Office
Aerospacelab Belgium	1,000	<0.003°/<0.003°	S, X, Ka, Optical	LEO, GEO	Flown LEO Under Development GEO	Yes
Airbus US Space & Defense USA	2,200	<0.006°/<0.006°	S, X, Ka, Optical	LEO	Flown LEO	Yes
Apex USA	4,000	0.005°/0.0025°	UHF, S, X, Ka	LEO, MEO, GEO	Flown LEO Under Development GEO	Yes
Argotec Italy	440	<0.01°/<0.008°	UHF, S, X, K, Ka	LEO	Qualified LEO Under Development MEO, GEO, Deep Space	Yes
Astro Digital USA	3,000	<0.03°/<0.02°	UHF, S, X, Ku, Ka, V, W, Optical	LEO, GTO, GEO	Flown LEO	Yes
Astroscale USA	3,530	0.05°/0.025°	S, X, C	LEO, GEO	Under Development	Yes
Axelspace Japan	1,800	<0.05°/<0.04°	S, X, Ka	LEO	Under Development	No
BAE Systems SMS USA	2,500	<0.006°/<0.003°	L, S, X, Ka	LEO, MEO, GEO, Cislunar, Deep Space	Flown LEO and Deep Space	Yes
Berlin Space Technologies Germany	2,500	<0.017°/<0.017°	S, X	LEO	Flown LEO	Yes
BlackSky USA	2,000	0.013°/0.009°	UHF, S, X	LEO	Flown LEO	Yes
Blue Canyon Technologies USA	1,082	0.002°/0.002°	L, S, X	LEO, GEO, Deep Space	Flown LEO and GEO Qualified Deep Space	Yes
CREOTECH Poland	600	<0.02°/<0.015°	S, X, Optical	LEO, Lunar	Flown LEO	No
Deimos Space Spain	300	<0.005°/<0.005°	S, X, iDRS	LEO	Under Development	No
EnduroSat Bulgaria	3,500/ 7,000	0.1°/0.006°	S, X, K/Ka, L, Optical	LEO	Qualified LEO (3,500W) Under Development (7,000W)	Yes
Exobotics UK	3600	0.08°/ 0.008°	VHF, UHF, S, X, Optical	LEO	Under Development	No
Harpy Aerospace India	2,100	0.35°/0.35°	S, Ka, Optical	LEO	Qualified LEO	Yes
Hemeria France	>1,000	<0.03°/<0.01°	S, X	LEO, GEO, GTO	Flown LEO Qualified GEO and GTO	No
Lockheed Martin USA	500+	<0.1°/<0.1°	S, X, Ka	LEO, GEO, Lunar, Deep Space	Flown LEO Qualified GEO, Lunar and Deep Space	Yes
Magellan Aerospace Canada	200	0.01°/0.01°	S, X	LEO	Flown LEO	No
Malin Science Space Systems USA	918	<0.015°/<0.015°	UHF, X, Ka	Mars	Under Development	Yes
Moog USA	2,000	<0.050°/<0.033°	S, X, Ka, Optical	LEO, GEO	Flown LEO Under development GEO	Yes
Momentus Space USA	3,000	0.008°/0.008°	S, X, Ka, Optical	LEO, MEO, GEO, Lunar, Deep Space	Flown LEO	Yes

Table 2-7: ESPA-Class Market Solutions
(The fields indicate maximum capability; organizations may offer multiple options including smaller capabilities within the ESPA-Class category)

Organization	Peak Power (W)	3-σ Pointing Control/ Knowledge	Comm Options	Intended Destination	Maturity	US Office
Muon Space USA	4,000	0.01°/0.004°	S, X, Optical	LEO	Flown LEO	Yes
NanoAvionics Lithuania	660	0.24°/0.09°	UHF, S, X	LEO	Flown LEO	Yes
Northrop Grumman USA	400	<0.01°/<0.008°	S, X, Ka	LEO, GEO, HEO	Flown LEO, GEO, and HEO	Yes
NovaWurks USA	>5,000	0.002°/0.0004°	UHF, S, L, X, Ka, Ku and Optical	LEO, MEO, GEO, GTO, HEO, Lunar and Deep Space	Flown LEO and GTO	Yes
OHB LuxSpace Luxembourg	834	<0.022°/ 0.01°	S, X	LEO	Qualified LEO	No
OHB Sweden Sweden	1,500	0.008°/0.008°	S, X, L	LEO, MEO	Flown LEO	No
Orbital Astronautics UK	5,000	0.05°/0.01°	S, X, K, Ka, Optical	VLEO, LEO, MEO, GEO, Deep Space	Qualified LEO	No
Quantum Space USA	1,000	0.006°/0.006°	S, X, Ka	LEO, GEO, Cislunar, Lunar, Deep Space	Under Qualified Development	Yes
Reflex Aerospace Germany	3,000	<0.01°/<0.005°	S, X, Ka, Ku, Optical	LEO	Flown LEO	No
Redwire Space USA	600	0.005°/0.0017°	UHF, S, X	VLEO, LEO, GEO	Flown LEO Under Development VLEO and GEO	Yes
SFL Missions Inc. Canada	1,500	0.009°/0.004°	UHF, S, X, Ka	LEO, GEO, Lunar	Flown LEO Qualified GEO and Lunar	No
Sierra Space USA	500	0.001°/ <0.001°	UHF, S, X	LEO, MEO, GEO	Flown LEO	Yes
SITAEL Italy	2,000	0.0017°/0.001°	S, X	LEO	Qualified LEO	No
Southwest Research Institute USA	1,550	0.015°/0.002°	S, X, Ka	LEO, GEO	Flown LEO Under Development GEO	Yes
Space Dynamics Laboratory USA	2,000	0.021°/0.021°	UHF, S, X, Ka, Optical	LEO, GEO, GTO, Cislunar, Deep Space	Flown LEO	Yes
Space Inventor Denmark	1,500	<0.008°/<0.008°	VHF, UHF, S, X, Ka, Ku, Q	LEO, GEO, MEO, Lunar	Flown LEO	No
Surrey Satellite Technology Ltd. UK	2,000	<0.01°/<0.01°	S, X, Ka, Ku, ISL	LEO, Lunar	Flown LEO Under Development Lunar	No
Terran Orbital USA	1,500	0.014°/0.002°	UHF, S, X	LEO, GEO, Lunar	Flown LEO	Yes

2.3 Other Complete Spacecraft Platforms Providers

The Small Spacecraft State of the Art team attempts to reach out to companies and organizations to obtain information directly, but the team is not always successful in receiving responses. To keep the information as updated as possible, Section 2.6 indicates if the team received a response for this edition, the previous edition or other. For companies in previous editions with older data, they have been removed from the main tables and are summarized in this section as potential providers since we have been unable to confirm their input for 2 years or more. This table also includes newly added companies from which the team has not received responses but which appear to offer spacecraft buses and/or hosted orbital services.

Table 2-8: List of other companies that may offer spacecraft buses and/or Hosted Orbital Services

Organization	PocketQubes	CubeSats	ESPA-Class
Berlin Nanospacecraft Alliance		X	
General Atomics EMS		X	X
IMT		X	
In-Space Missions		X	X
Open Cosmos		X	X
Quantum Galactics		X	
Rocket Lab			X
Satellogic			X
Space Information Laboratories		X	
XDLINX Space Lab		X	X

2.4 Programmatic and Systems Engineering Considerations

When determining the optimal mission design approach, small satellite mission developers should carefully evaluate the programmatic and systems engineering considerations that align most with their specific objectives and constraints. This assessment is crucial for making informed decisions that best serve the mission's goals and requirements. Examples of these considerations include:

- Environments the system will endure during development and in flight
- Concept of operations, including desired orbit and mission duration
- Functional and performance requirements
- Key performance parameters with appropriate margins (e.g., mass, volume, power, data link, data budget, pointing)
- Software considerations such as development environment and re-use
- Technology development considerations such as flight heritage, Technology Readiness Level (TRL), and reliability
- Risk posture for development and performance
- Trades between performance, cost, and schedule
- Procurement considerations such as production/lead time and contractual mechanisms
- Licensing requirements, as-applicable (e.g., RF licensing, remote sensing, export control, re-entry)

In addition to the considerations listed above, hosted orbital service missions should also consider:

- Payload priority/mission lifetime for multi-customer/multi-manifest missions
- Balance costs vs payload usage of platform resources (e.g., mass, volume, power, data link, data budget, pointing)

Before finalizing any mission design decisions, it is essential to thoroughly analyze and consider these factors for each potential option within the trade space. Given mission system performance requirements for key performance parameters like mass, volume, power, data link, data budget, and pointing, a functional importance rating and risk-based trade study should be used to screen the many options available. In addition to functional performance, relevant flight heritage or TRL, production lead time, and any available reliability data should be included in the trades. These, as well as cost, could drive the design to be done via COTS or commercial support.

Mission developers may want to consider the following guides to help them in their selection and design process:

- NASA CubeSat 101 Book
  https://www.nasa.gov/content/cubesat-launch-initiative-resources
- NASA CubeSat 201 Small spacecraft process, lessons learned, and reference database
  https://s3vi.ndc.nasa.gov/cubesat201/
- NASA Systems Engineering Handbook
  https://www.nasa.gov/connect/ebooks/nasa-systems-engineering-handbook
- NASA Small Spacecraft Technology Program Guidebook for Technology Development Projects
  https://www.nasa.gov/sites/default/files/atoms/files/smallsattechdevguidebook_rev-508d1.pdf

2.5 Summary

Several vendors have pre-designed fully integrated small spacecraft buses that are space-rated and available for purchase. The market ranges from companies that are willing to heavily modify their systems to fit the customer's needs to companies that standardize their systems with minimal customization to achieve lower cost. This chapter consolidated a long list of providers with key characteristics to facilitate the research and down-selection process for SmallSat practitioners.

For feedback about this chapter, email: arc-sst-soa@mail.nasa.gov. Please include a business email in case of follow up questions.

2.6 References

The references in this section are provided to facilitate the process in which practitioners can obtain information from the providers. The source indicates how the information provided in this chapter was obtained.

Source definition:

Current = organization provided the information through direct communication with the State-of-the-Art team for the **current edition** of the document.

Previous = organization provided the information through direct communication with the State-of-the-Art team on the **previous edition** of the document, and the team was unable to communicate with the organization to update the current edition of the document.

New = the inclusion of the organization is **new** for the document, but the SOA team was unable to communicate with the organization to obtain information. Organizations are encouraged to contact the SOA team to include information on corresponding tables or be removed from the chapter completely.

Obsolete = the information obtained by the State-of-the-Art team is **obsolete** since the team has been unable to communicate with the organization for more than 2 editions in a row. Organizations are encouraged to contact the SOA team to restore their place at the corresponding tables or to be removed from the chapter completely.

Table 2-9: List of Contact Information for Organizations in this Chapter

Organization	Source	Contact Email	Website
2NDSpace	Current	giulio@2ndspace.eu	2ndspace.eu
AAC Clyde Space	Current	enquiries@aac-clydespace.com	aac-clyde.space
Aerospacelab	Previous	gerry.jansson@aerospacelab.com	aerospacelab.com
Airbus US Space & Defense	Current	deborah.horn@airbusus.com	airbusus.com
Alba Orbital	Current	contact@albaorbital.com	albaorbital.com
Alén Space	Current	sales@alen.space	alen.space
Apex	Current	General Inquiries Page	apexspace.com
Argotec	Current	info@argotecgroup.com	argotecgroup.com
Artemis Space Technologies	Current	info@spaceartemis.com	spaceartemis.com
Astranis Space Technologies Corp.	Current	scott@astranis.com	astranis.com
Astro Digital	Current	brian@astrodigital.com	astrodigital.com
Astroscale	Previous	k.shahady@astroscale-us.com	astroscale-us.com
Axelspace	Current	Contact Page	axelspace.com
BAE Systems, Inc. SMS	Current	Contact Form	baesystems.com
Berlin Nanospacecraft Alliance	New	info@bna-space.de	bna-space.de
Berlin Space Technologies	Previous	info@berlin-space-tech.com	berlin-space-tech.com
BlackSky	Previous	Contact Form	blacksky.com
Blue Canyon Technologies	Current	info@bluecanyontech.com	bluecanyontech.com
C3S Electronics Development	Current	info@c3s.hu	c3s.hu
CesiumAstro	Current	info@cesiumastro.com	cesiumastro.com
CREOTECH	Current	space@creotech.pl	creotech.pl/space
D-Orbit- Italy	Current	eleonora.luraschi@dorbit.space	dorbit.space
D-Orbit- USA	Current	mike.kaplan@dorbit.com	dorbit.com
Deimos Space	Previous	cmentrena@deimos-space.com	elecnor-deimos.com
DIYSATELLITE	Previous	gus@diysatellite.com	diysatellite.com
EnduroSat	Current	Contact Page	endurosat.com
Exobotics	New	Contact Page	exobotics.space
FOSSA Systems	Current	contact@fossa.systems	fossa.systems
General Atomics EMS	Obsolete	Chris.white@ga.com	ga.com/EMS
German Orbital Systems	Current	info@orbitalsystems.de	orbitalsystems.de

Table 2-9: List of Contact Information for Organizations in this Chapter			
Organization	**Source**	**Contact Email**	**Website**
GomSpace	Current	info@gomspace.com	gomspace.com
Gran Systems	Current	info@gransystems.com	gransystems.com
GUMUSH AeroSpace	Previous	gumush@gumush.com.tr	gumush.com.tr
Harpy Aerospace	Current	jayakumar@harpyaerospace.in	harpyaerospace.in
Hemeria	Previous	Contact Form	hemeria-group.com/en
HEX20	Current	info@hex20.space	Hex20.space
Hydra Space Systems	Current	contacto@hydra-space.com	hydra-space.com
IMT	Obsolete	giovanni.cucinella@imtsrl.it	imtsrl.it
In-Space Missions	Obsolete	info@inspace.co.uk	in-space.co.uk
Innova Space	Previous	info@innova-space.com	innova-space.com/en
ISISPACE	Previous	sales@isispace.nl	isispace.nl
Lockheed Martin	Previous	timothy.m.linn@lmco.com	-
Loft Orbital	Current	justin.tilman@loftorbital.com	loftorbital.com
Magellan Aerospace	Current	rushi.ghadawala@magellan.aero	magellan.aero
Malin Space Science Systems	Current	yee@msss.com	msss.com
Momentus Space	Current	sales@momentus.space	momentus.space
Moog	Current	ddusza@moog.com	moog.com/markets/space
Muon Space	Current	info@muonspace.com	muonspace.com
NanoAvionics	Previous	info@nanoavionics.com	nanoavionics.com
Nara Space	Current	sales@naraspace.com	naraspace.com
NearSpace Launch	Previous	nsl@nearspacelaunch.com	nearspacelaunch.com
Northrop Grumman	Previous	John.Dyster@ngc.com	-
NovaWurks	Current	info@NovaWurks.com	novawurks.com
NPC SPACEMIND	Current	info@npcspacemind.com	npcspacemind.com
OHB LuxSpace	Previous	info@luxspace.lu	luxspace.lu
OHB Sweden	Current	spacesales@ohb-sweden.se	ohb-sweden.se
Open Cosmos	Obsolete	partnerships@open-cosmos.com	open-cosmos.com
Orbital Astronautics	Current	hello@orbastro.com	orbastro.com
Orion Space Solutions	Current	orioncontact@arcfield.com	orionspace.com
Pumpkin Space Systems	Current	sales@pumpkininc.com	pumpkinspace.com
Quantum Galactics	New	info@quantumgalactics.com	quantumgalactics.com
Quantum Space	Previous	sales@quantumspace.us	quantumspace.us
Quub, Inc.	Current	info@quub.space	quub.space
Redwire Space	Current	sales@rdw.com	rdw.com
Reflex Aerospace	Current	sales@reflexaerospace.com	reflexaerospace.com
Rocket Lab	New	enquiries@rocketlabusa.com	rocketlabusa.com
Satellogic	New	info@satellogic.com	satellogic.com
SatRev	Current	contact@satrev.space	satrev.space

Table 2-9: List of Contact Information for Organizations in this Chapter			
Organization	**Source**	**Contact Email**	**Website**
SFL Missions Inc.	Current	info@sflmissions.com	sflmissions.com
Sierra Space	Previous	spaceapps@sierraspace.com	sierraspace.com
SITAEL	Previous	sales.space@sitael.com	sitael.com
Southwest Research Institute	Current	spacecraft-info@swri.org	-
Space Dynamics Laboratory	Current	info@sdl.usu.edu	sdl.usu.edu
Space Information Laboratories	Obsolete	sales@spaceinformationlabs.com	spaceinformationlabs.com
Space Inventor	Current	sales@space-inventor.com	space-inventor.com
Spacemanic	Current	sales@spacemanic.com	spacemanic.com
Spire Global	Current	sales@spire.com	spire.com
Surrey Satellite Technology Ltd.	Previous	info@sstl.co.uk	sstl.co.uk
Terran Orbital	Current	info@terranorbital.com	terranorbital.com
U-Space	Current	contact@u-space.fr	u-space.fr
Varda Space Industries	Current	john.boyer@varda.com	varda.com
XDLINX Space Lab	New	info@xdlinx.space	xdlinx.space
York Space Systems	Current	BD@yorkspacesystems.com	yorkspacesystems.com

Table of Contents

Chapter Glossary ii
3.0 Power 28
3.1 Introduction 28
3.2 State-of-the-Art – Power Generation 29
3.2.1 Solar Cells 30
3.2.2 Solar Panels & Arrays 31
3.3 On the Horizon – Power Generation 38
3.3.1 Multi-junction Solar Cells 38
3.3.2 Unitized Regenerative Fuel Cells 40
3.4 State-of-the-Art – Energy Storage 41
3.4.1 Secondary Li-ion Batteries 41
3.5 On the Horizon – Energy Storage 46
3.5.1 Nanomaterials 46
3.5.2 Supercapacitors 47
3.5.3 Solid-State Batteries 48
3.5.4 Energy Storage Systems 49
3.6 State-of-the-Art – Power Management and Distribution 50
3.6.1 PMAD Selection Considerations 50
3.7 On the Horizon – Power Management and Distribution 55
3.8 Summary 55
References 55

Chapter Glossary

(AFRL)	Air Force Research Laboratory
(BMS)	Battery Management System
(BOL)	Beginning-of-Life
(CFRPs)	Composite Fiber Reinforced Panels
(CIGS)	Cu(In,Ga)Se2
(COTS)	Commercial-off-the-Shelf
(EOL)	End-of-Life
(EPS)	Electrical Power System
(ESA)	European Space Agency
(GaN)	Galium Nitride
(GRC)	NASA Glenn Research Center
(KSC)	Kennedy Space Center
(Li-ion)	Lithium-ion
($LiCF_x$)	Lithium carbon monofluoride
(LiPo)	Lithium polymer
($LiSO_2$)	Lithium sulfur dioxide
($LiSOCl_2$)	Lithium thionyl chloride
(MIL)	Military
(QML)	Qualified Manufacturers List
(NiCd)	Nickel-cadmium
(NiH_2)	Nickel-hydrogen
(OPV)	Organic Photovoltaic
(OSCAR)	Optical Sensors based on carbon materials
(PCB)	Printed Circuit Board
(PEASSS)	Piezoelectric Assisted Smart Satellite Structure
(PET)	polyethylene terephthalate
(PMAD)	Power management and distribution
(PV)	Photovoltaic
(RHUs)	Radioisotopic Heater Units
(RPS)	Radioisotope Power System
(RTGs)	Radioisotope Thermoelectric Generators
(SABER)	Solid-state Architecture Batteries for Enhanced Rechargeability and Safety
(SP)	Specific Power
(SWaP)	Size, Weight, and Power
(TPV)	Thermophotovoltaic
(TR)	Thermoradiative
(TRL)	Technology Readiness Level
(Wh/kg)	Watt hours per kilogram

3.0 Power

3.1 Introduction

The electrical power system (EPS) is a major, fundamental subsystem that encompasses electrical power generation, storage, and distribution, and typically accounts for a significant portion of spacecraft volume and mass. Power generation technologies include photovoltaic cells, panels, and arrays, and radioisotope or other radioisotope thermoelectric generators (RTGs) . Power storage is typically applied through batteries; either single-use primary batteries or rechargeable secondary batteries. Power management and distribution (PMAD) systems facilitate power control to spacecraft electrical loads and take a variety of forms that are often custom designed to meet specific mission requirements. EPS engineers frequently target a high specific power or power-to-mass ratio (Wh kg^{-1}) when selecting power generation and storage technologies to minimize system mass. For nanosatellites, EPS volume is often the primary design constraint.

Microsatellites (<200 kg) in low-Earth orbit (LEO) operate in relatively mild thermal and radiation environments, and therefore typically do not require extreme qualification standards or high Technology Readiness Levels (TRLs associated with deep-space missions). Engineers must carefully balance the differences between space-qualified parts (MIL/QML) and less stringent commercial off-the-shelf (COTS) components with mission-specific spacecraft requirements. Military or space-qualified components undergo rigorous testing—often certified for extreme temperatures (e.g., –55 °C to +125 °C), radiation tolerance, and long-term reliability—while COTS parts are usually rated for narrower ranges (–40 °C to +85 °C) and receive less comprehensive screening. While QML-qualified parts generally offer higher reliability, they are often limited in availability and subject to slow revision cycles. In contrast, COTS components typically provide better performance, quicker availability, and lower cost, making them well-suited for many small spacecraft applications.

CubeSat missions commonly use COTS parts due to their nearly exclusive operation in LEO, shorter mission durations, and more favorable environmental conditions, reducing the need for stringent qualification standards. Differences in EPS design between a ~150 kg spacecraft and a 10 kg CubeSat lie in priorities and constraints: CubeSats, with limited surface area, typically use fixed body-mounted solar cells, small batteries, and a single low-voltage bus. Conversely, a 150 kg microsatellite can support deployable solar panels, larger battery capacity with redundancy, and multiple regulated buses for power distribution. Both architectures can incorporate COTS components where mission risk permits.

This chapter reviews the following categories:

- Sections 3.2 & 3.3: Power Generation, including solar cells, panels, and arrays;
- Sections 3.4 & 3.5: Energy Storage, including Li-ion, supercapacitors, and solid-state batteries;
- Sections 3.6 & 3.7: Power Management, including modular architectures and wireless power transfer and telemetry.

The list of organizations/companies in this chapter is not all-encompassing and does not constitute an endorsement from NASA. The inclusion or omission of specific companies is not intended to reflect their technologies or relationship with NASA. The performance advertised may differ from actual performance as the information has not been independently verified by NASA subject matter experts and is based on manufacturer-provided or publicly available data. It should be noted that TRL designations may vary with changes specific to the payload, mission

requirements, reliability considerations, and/or the environment in which performance was demonstrated. Readers are highly encouraged to reach out to companies for further information regarding the performance and TRL of the technology described.

3.2 State-of-the-Art – Power Generation

Power generation on microsatellites is typically governed by a common solar power architecture (solar cells + solar panels + solar arrays). As the SmallSat industry drives demand for lower cost and increased production rates, the photovoltaics industry is adapting to meet these needs. The standardization of solar array and panel designs, deployment mechanisms, and power integration will be critical to meet the desire for large, proliferated constellations.

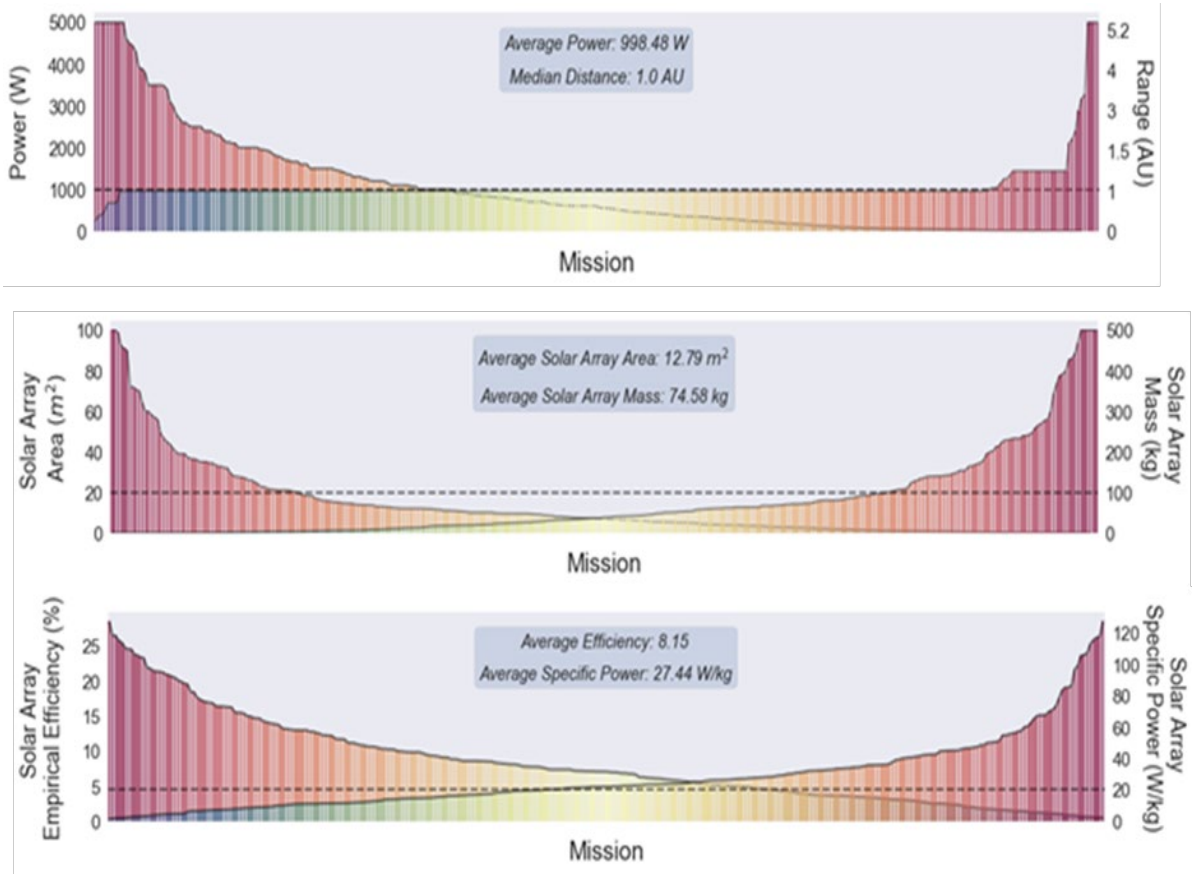


Figure 3.1: (Top) Distribution of mission range, or the furthest point from the sun that the spacecraft reaches, and mission power levels [power capped at 5 KW]. (Middle) Distribution of solar array surface area and solar array mass [mass capped at 500 Kg]. (Bottom) Distribution of solar array empirical efficiency (calculated at Earth) and specific power (for the entire array measured at the destination of the mission). X axis represents 389 missions and color scheme represents highest to lowest values (red to blue). Credit: NASA.

EPS engineers should note beginning-of-life (BOL) vs end-of-life (EOL) performance of the systems, as well as planned ground testing duration prior to operations. EPS for SmallSats is

often overdesigned to accommodate dynamic thermal environments, eclipse durations in LEO, and varying sun-angles. Figure 3.1 captures actual space system performances given such wide varying operational conditions for 389 space missions (not only SmallSats) launched since 1989 to 2021 (1). The dotted horizontal line indicated where more of the 389 missions surveyed fall under.

When possible, choosing a pre-designed and qualified panel is preferred over designing unique solar panels to reduce the cost and schedule as well as unforeseen design and manufacturing issues. Companies that have the capacity for mass production and automation are rare because space solar arrays, cells, and panels have always been a 'boutique' business; however, standardized designs like the OneWeb and Starlink constellations have been appearing more often to meet the demands of highly proliferated constellations.

The following subsections aim to capture the current state of the art and assist EPS engineers, mission designers, system engineers, etc., in designing, reviewing and ultimately constructing and operating power flight systems.

3.2.1 Solar Cells

Solar power generation is the predominant energy source for small spacecraft, with more than 90% of all nanosatellite/SmallSat form factors equipped with solar panels and rechargeable batteries (1). Photovoltaic (PV) cells, or solar cells, are made from thin semiconductor wafers that produce an electric current when exposed to light. The amount of light available to a spacecraft solar array— also called solar intensity—varies with the inverse square of the distance from the Sun. Power generation is predicated primarily by the angle of incidence to the sun. Perpendicular orientation provides maximum generation which then drops off by the cosine of the angle as the solar array is tilted away from the sun.

A basic solar cell is made from a single layer of semiconductor material (most commonly Silicon, Si) that has been doped with boron and phosphorus to create a bandgap to convert sunlight into electricity. These single-junction cells are inexpensive to manufacture but have relatively low efficiencies, around 20%. Single-junction cells are best at converting light within a narrow wavelength range and are primarily used in missions with short lifetimes or are cost sensitive and are not covered here.

By contrast, multi-junction solar cells are constructed by stacking multiple semiconductor layers, each with an optimized bandgap tuned to absorb a specific portion of the solar spectrum. This layered structure enables the cell to convert a broader range of sunlight into electricity more efficiently (minimal heat loss), achieving spectral efficiencies of 30-34% (2)(3). While the theoretical efficiency limit for an infinite-junction cell under concentrated sunlight is 86.6%, real-world performance is constrained by optical and thermal losses, semiconductor material imperfections, and electrical and thermal effects within the materials. A multi-junction cell that (4) contains only two different semiconductor materials is known as a tandem-junction cell, and there has been high interest in a hybrid-tandem cell where two different solar cell technologies are combined so energy can be more efficiently generated by separate devices (5).

The current state-of-the-art for space solar cells includes 3- to 5- junction architectures based on Group III-V semiconductor elements (like GaAs, InGaP, and Ge) with a nominal efficiency of 30% and a high of 34%. While this concept is well-established, research seeks to optimize power conversion efficiency with different combination of materials and adjusting the manufacturing process. Some modern designs include 4- to 5- junctions by adding materials like InGaAs, AlGaAs, or GaInNAs; tandem layers of perovskite on the III-V stacks are also being investigated (see Section 3.3).

Despite their advantages, solar cells face several limitations for space applications. These include reduced effectiveness in deep-space environments, lack of power generation during eclipse periods, and performance degradation over the mission lifetime (due to aging, radiation, and contamination). Solar cells also contribute significantly to spacecraft mass, surface area, and cost. To increase power generation within the limited volume of microsatellites, deployable solar panels are often used, though this increases spacecraft design complexity, reliability, and risk. Ultimately for a small spacecraft, the size, weight, and volume constraints may drive the choice of solar cell technology rather than solar cell efficiency. Since solar arrays are life-limiting components, their EOL performance at operating temperature is a critical metric. Common degradation factors include radiation exposure, coverglass or adhesive darkening, surface contamination, and mechanical or electrical failures.

Table 3-1 itemizes small spacecraft solar cell efficiency per the available manufacturers. Note the efficiency may vary depending on the solar cells chosen.

Table 3-1: Solar Cells

Manufacturer Headquarters	Cell Name	BOL Efficiency	Voc (V)	Vmp (V)	Jsc (mA/ cm^2)	Jmp (mA/ cm^2)	Pmp (W/m^2)
AZUR Space Germany	Silicon S 32	16.8	0.628	0.528	45.8	43.4	229.2
	3G30-Adv	29.5	2.7	2.411	17.2	16.71	403
	4G32-Adv	31.5	3.426	2.999	15.2	14.37	431
	TJ 3G28C	28	2.667	2.37	16.77	16.14	1367
Rocket Lab USA	ZTJ	29.5	2.726	2.41	17.4	16.5	397.7
	ZTJ+	29.4	2.69	2.39	17.1	16.65	397.9
	ZTJ Omega	30.2	2.73	2.43	17.4	16.8	408.2
	Z4J	31.3	3.95	3.54	12	11.5	407.1
	IMMα	32.0	4.78	4.28	10.7	10.12	433.1
	ZTJM	29.5	2.72	2.38	17.1	16.5	392
Boeing-SpectroLab USA	XTJ	29.5	2.633	2.348	17.76	17.02	399.6
	XTJ-Prime	30.7	2.715	2.39	18.1	17.4	415.9
	XTE-SF	32.2	2.75	2.435	18.6	17.8	433.4
	XTE-HF	32.1	2.782	2.49	18	17.4	427.9
	XTE-LILT	31.6	2.755	2.459	18.1	17.4	427.9
	UTJ	28.4	2.66	2.35	17.14	16.38	384.93
	TASC	27	2.52	2.19	32	28	270
	ITJ	26.8	2.565	2.27	16.9	16	1353

3.2.2 Solar Panels & Arrays

Solar panels and arrays are constructed from individual solar cells connected in series to form strings and in parallel to form circuits mounted on a substrate backing. Figure 3.2 has a few examples of 6U spacecraft with solar panels. While very low-power CubeSats and SmallSats may only need body-mounted solar panels, most will require more power from deployed solar arrays. The deployed solar arrays for CubeSats and SmallSats are mostly on rigid substrates made of either a printed circuit board (PCB), composite fiber reinforced panels (CFRPs), or an aluminum honeycomb panel.

Deployed solar arrays are often the largest structure on a satellite. The ratio of deployed solar array size to spacecraft size is often significantly higher than for traditional spacecraft. The size and fundamental frequency of the solar arrays impact spacecraft pointing, propulsion, and delta-

V needed for station keeping. Important considerations for SmallSat solar arrays are deployment mechanisms, deployed frequency, panel specific power, and power density, as well as stowed volume. Most of these metrics are not listed on manufacturer datasheets.

Solar array comparison can be challenging because manufacturers who make solar arrays specific to their bus and payload designs often do not report solar array power using the same metrics. Reported "power" can refer to multiple metrics: power available to the payload, peak power provided by a combination of solar array and battery, or an orbital-specific average power. Reported solar array power (Peak BOL) mainly refers to the peak power of the solar array at the beginning of life at standard test conditions (e.g., ~28°C), which is mission independent. Panel stiffness and moment of inertia usually need to be calculated for a specific spacecraft because they are dependent on multiple factors such as the size and mass of the panel, as well as spacecraft size and weight distribution. Examples of commercial solar array and panel products are shown in Table 3-2; information is from company websites and technology datasheets.

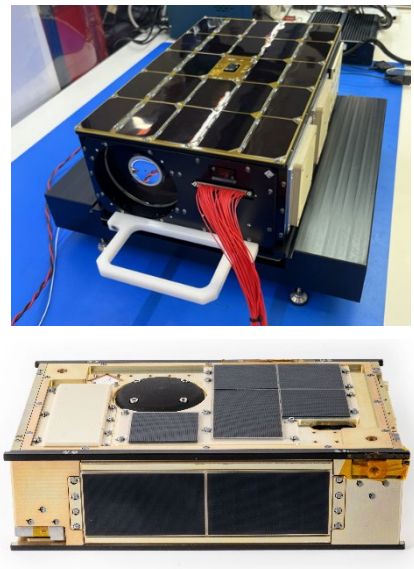


Figure 3.2: {top} XO-BUS 6U, XCUBE-1 Mission. Credit: Exobotics; and {lower} NASA JSC's R5-S10 6U spacecraft. Credit: NASA.

Table 3-2: Solar Array/Panel Products

Company Headquarters	**Product**	**Panel Type**	**Specific Power (W/kg)**	**Peak BOL Solar Array Power (W)**
AAC Clyde Space Sweden	Photon	*	*	9.25 / 3U-12 Face
2NDSpace Italy	DROP-03X	Double Deployable	62.5	22.5
	DROP-04X	Double Deployable	62.5	30
	DROP-12	Deployable	70	40
	DROP-03XL	Triple Deployable	67.5	30
	CORE-01Z	Body Mounted	65	2.45
	CORE-01	Body Mounted	70	2.45
	CORE-02	Body Mounted	65	4.88
	CORE-03	Body Mounted	72.5	8.54
	CORE-04	Body Mounted	75	11
	CORE-06Z	Body Mounted	55	4.88
	CORE-12	Body Mounted	67.5	19.52
	CORE-12Z	Body Mounted	50	9.76
	CORE-16	Body Mounted	62.5	24.4
Agencia Espacial Civil Ecuatoriana Italy	Deployable Multifunction Solar Array	Deployed Rigid	-	-
Airbus Netherlands The Netherlands	Sparkwing Solar Panel 600x570mm 36V	Body Mounted, 1-3 deployed panels, Rigid	18	88 per panel
	Sparkwing Solar Panel 600x700mm 36V	Body Mounted, 1-3 deployed panels, Rigid	21	111 per panel
	Sparkwing Solar Panel 600x820mm 36V	Body Mounted, 1-3 deployed panels, Rigid	24	133 per panel

Table 3-2: Solar Array/Panel Products				
Company Headquarters	**Product**	**Panel Type**	**Specific Power (W/kg)**	**Peak BOL Solar Array Power (W)**
	Sparkwing Solar Panel 600x965mm 36V	Body Mounted, 1-3 deployed panels, Rigid	25	155 per panel
	Sparkwing Solar Panel 750x820mm 36V	Body Mounted, 1-3 deployed panels, Rigid	29	177 per panel
	Sparkwing Solar Panel 750x965mm 36V	Body Mounted, 1-3 deployed panels, Rigid	30	199 per panel
	Sparkwing Solar Panel 750x1100mm 36V	Body Mounted, 1-3 deployed panels, Rigid	34	243 per panel
	Sparkwing Solar Panel 910x820mm 36V	Body Mounted, 1-3 deployed panels, Rigid	33	221 per panel
	Sparkwing Solar Panel 910x965mm 36V	Body Mounted, 1-3 deployed panels, Rigid	37	265 per panel
	Sparkwing Solar Panel 1000x570mm 36V	Body Mounted, 1-3 deployed panels, Rigid	29	176 per panel
	Sparkwing Solar Panel 1000x1100mm 36V	Body Mounted, 1-3 deployed panels, Rigid	39	309 per panel
	Sparkwing Solar Panel 1070x820mm 36V	Body Mounted, 1-3 deployed panels, Rigid	37	265 per panel
	Sparkwing Solar Panel 600x570mm 50V	Body Mounted, 1-3 deployed panels, Rigid	19	92 per panel
	Sparkwing Solar Panel 600x800mm 50V	Body Mounted, 1-3 deployed panels, Rigid	22	122 per panel
	Sparkwing Solar Panel 600x965mm 50V	Body Mounted, 1-3 deployed panels, Rigid	25	153 per panel
	Sparkwing Solar Panel 600x1100mm 50V	Body Mounted, 1-3 deployed panels, Rigid	28	183 per panel
Airbus Netherlands The Netherlands	Sparkwing Solar Panel 750x570mm 50V	Body Mounted, 1-3 deployed panels, Rigid	23	122 per panel
	Sparkwing Solar Panel 750x800mm 50V	Body Mounted, 1-3 deployed panels, Rigid	25	153 per panel
	Sparkwing Solar Panel 750x965mm 50V	Body Mounted, 1-3 deployed panels, Rigid	36	241 per panel
	Sparkwing Solar Panel 750x1100mm 50V	Body Mounted, 1-3 deployed panels, Rigid	34	244 per panel
	Sparkwing Solar Panel 910x570mm 50V	Body Mounted, 1-3 deployed panels, Rigid	26	153 per panel
	Sparkwing Solar Panel 910x800mm 50V	Body Mounted, 1-3 deployed panels, Rigid	32	214 per panel
	Sparkwing Solar Panel 910x965mm 50V	Body Mounted, 1-3 deployed panels, Rigid	34	244 per panel
	Sparkwing Solar Panel 910x1100mm 50V	Body Mounted, 1-3 deployed panels, Rigid	40	305 per panel
	Sparkwing Solar Panel 1070x570mm 50V	Body Mounted, 1-3 deployed panels, Rigid	29	183 per panel
	Sparkwing Solar Panel 1070x800mm 50V	Body Mounted, 1-3 deployed panels, Rigid	34	244 per panel
	Sparkwing Solar Panel 1070x965mm 50V	Body Mounted, 1-3 deployed panels, Rigid	39	305 per panel
	Sparkwing Solar Panel 1070x1100mm 50V	Body Mounted, 1-3 deployed panels, Rigid	45	366 per panel

Table 3-2: Solar Array/Panel Products				
Company Headquarters	**Product**	**Panel Type**	**Specific Power (W/kg)**	**Peak BOL Solar Array Power (W)**
	Sparkwing Solar Panel 1230x570mm 50V	Body Mounted, 1-3 deployed panels, Rigid	31	214 per panel
	Sparkwing Solar Panel 1230x800mm 50V	Body Mounted, 1-3 deployed panels, Rigid	36	275 per panel
Blue Canyon Technologies USA	BCT Solar Array	Body Mount + Deployed Rigid	*	28 – 42 for 3U / 48-118 for 6U-12U
DHV Technologies Spain	DSA-042W	Simple Deployable Wing	36	42
	BMSA-066W	Body Mounted	68	66
	DSA-079W	Simple Deployable Wing	43	80
	BMSA-050W	Body Mounted	65	50
	DSA-079W	Simple Deployable Wing	44	95
	DSA-108W	Simple Deployable Wing	50	109
	BMSA-087W	Body Mounted	68	87
	DSA-183W	Double Deployable Wing	50	183
	DSA-185W	Simple Deployable Wing	56	185
	DSA-255W	Double Deployable Wing	60	256
	BMSA-366W	Body Mounted	52	366
	DSA-373W	Double Deployable Wing	41	373
	DSA-555W	Triple Deployable Wing	60	556
	DSA-686W	Quadruple Deployable Wing	34	676
	DSA-898W	Quintuple Deployable Wing	34	889
	DSA-1268W	Sextuple Deployable Wing	46	1268
	DHV-1U Series (Body Mounted)	PCB Substrate (Polyimide)	41	2
	DHV-2U Series (Body Mounted)	PCB Substrate (Polyimide)	44	4
	DHV-3U Series (Body Mounted)	PCB Substrate (Polyimide)	56	8
	DHV-6U Series (Body Mounted)	PCB Substrate (Polyimide)	60	18
	DSA-3U-1D-L (Simple Deployable Wing)	PCB Substrate (Polyimide)	33	7
	DSA-3U-2D-L (Double Deployable Wing)	PCB Substrate (Polyimide)	35	11
	DSA-3U-3D-L (Triple Deployable Wing)	PCB Substrate (Polyimide)	46	21
	DSA-6U-1D-L (Simple Deployable Wing)	PCB Substrate (Polyimide)	67	28
	DSA-6U-1D-S (Simple Deployable Wing)	PCB Substrate (Polyimide)	35	19
	DSA-6U-2D-S (Double Deployable Wing)	PCB Substrate (Polyimide)	67	55
	DSA-6U-2D-L (Double Deployable Wing)	PCB Substrate (Polyimide)	66	41
Emxys Spain	3U Solar panel:	Body Mounted	66.6	8.2

Table 3-2: Solar Array/Panel Products				
Company Headquarters	**Product**	**Panel Type**	**Specific Power (W/kg)**	**Peak BOL Solar Array Power (W)**
	327.5x83x 2.2mm, 14.7V	(Rigid Polyimide)		
	6U Solar panel: 226.3x366x2.2mm, 33.6V	Body Mounted (Rigid Polyimide)	53.3	17.6
EnduroSat Bulgaria	3U Solar Panel/Array	Deployed Rigid	66	14.4
	6U Solar Panel/Array	Deployed Rigid	64	19.2
	8U Solar Panel/Array	Deployed Rigid	65	24.0
Exobotics United Kingdom	XO-PANEL 1U	Body Mounted	46	2.3
	XO-PANEL 2U	Body Mounted	46	4.6
	XO-PANEL 3U	Body Mounted	54	8.1
	XO-PANEL 6U	Body Mounted	62	27.8
ExoTerra Resource USA	Fold Out Solar Arrays (FOSA)	Deployed Flexible	140	150
GomSpace Denmark	Nanopower DSP	Deployed Rigid	*	1.2
	NanoPower P110	Fixed	36.9 – 92	1.2 / cell 2.4
	NanoPower MSP 16 cell	Fixed	42	1.2 /cell 19.2
	NanoPower TSP Per wing	Deployed Rigid	60	45
ISISPACE The Netherlands	Smallsat Solar Panels	Body Mount + Deployed Rigid	46	2.3 / U
Lockheed Martin USA	SmallSat Solar Array	Deployed Rigid with Additively Manufactured Substrate	53.6	170 / panel BOL at 28C
MMA Design USA	Hawk	Deployed Rigid (PCB)	121	36-112
	zHawk	Deployed Rigid (PCB)	95	36
	Next-Gen HaWK	Deployed Rigid (PCB)	100	45 - 310
NPC Spacemind Italy	SP1X	Body Mounted 1U	68	2.4
	SP1Z	Body Mounted 1U Top	68	2.4
	SP2X	Body Mounted 2U	64	4.8
	SP2Z	Body Mounted 2U Top	64	4.8
	SP3X	Body Mounted 3U	76	8.4
	SP4X	Body Mounted 4U	75	10.8
	SP4Z	Body Mounted 4U Top	58	9.6
	SP6X	Body Mounted 6U	74	19.2
	SP8X	Body Mounted 8U	68	24
	SP3X Deployable	Double wing Deployable 3U	75	21.6
	SP4X Deployable	Double wing Deployable 4U	58	28.8
	SP6X Deployable	Double wing Deployable 6U	74	57.6
	SP8X Deployable	Double wing Deployable 8U	68	72
Pumpkin Space Systems USA	Dual Articulated Deployable Solar Array	Deployed Rigid	31	135
	Dual-Quad Articulated Deployable Solar Array	Deployed Rigid	30	240
	Deployable Clamshell Solar Array (DCSA)	Deployed Rigid	44	220
	Deployable Clamshell Solar Array (DCSA)	Deployed Rigid	38	350

Table 3-2: Solar Array/Panel Products				
Company **Headquarters**	**Product**	**Panel Type**	**Specific Power (W/kg)**	**Peak BOL Solar Array Power (W)**
Redwire Space USA	ROSA	Flexible PV blanket	100	1000
	Aladdin SmallSat Array	Hybrid Array: Flex Rigid	80	300
SatRev S.A. Poland	Deployable panel	Custom size deployable 3U – 6U	40	36 for a typical 6U deployment
Sierra Space Corp USA	Surface Mount Technology Solar Panel	Composite	-	2500
Space Dynamics Laboratory USA	SDL Modular Solar Panels	Deployed Rigid	84.5	180 / panel
Spacemanic Czech Republic	RA Solar Panels	Triple Junction GaAs	38.55	19.2

* Available with inquiry to manufacturer

** For SmallSat use

While solar efficiency has been the prevailing way to characterize solar array performance, discrepancies between theoretical and empirical data indicate that specific power (SP) of the solar array fundamentally governs space mission feasibility and flexibility. Figure 3.3 visualizes the landscape of mission architectures, parameterized by power (adjusted by a factor of squared distance) and mass; the relation between these axes is the SP.

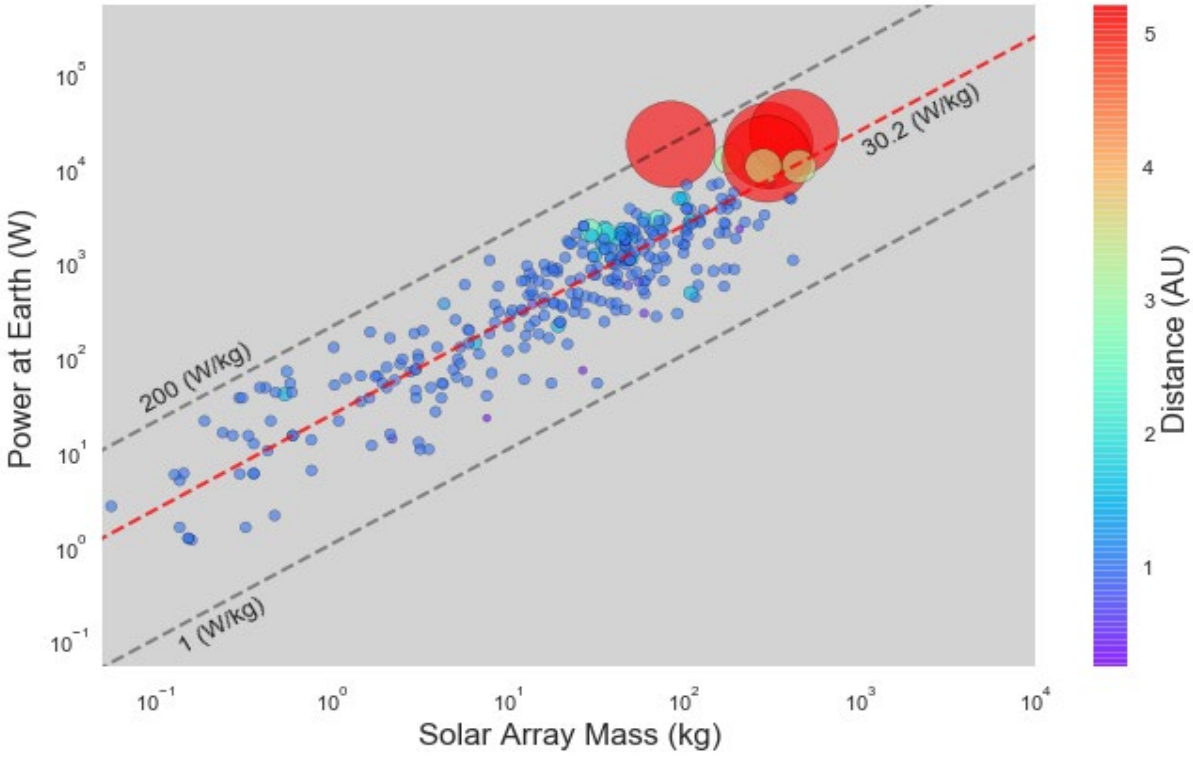


Figure 3.3: Specific power of a solar array at Earth. A minimum of 1 W/kg is plotted as a dashed black line, showing that no missions fly with any smaller specific power. The larger red circles represent the missions farther from Earth corresponding to the red color on the distance scale. Peretz et al (2024). Credit: NASA.

Space missions using solar arrays, regardless of spacecraft mass, are strongly clustered around ~30 W/kg (red dashed line) and are strongly bounded: no missions fly with SP lower than 1 W/kg (lower dashed line), and the maximum empirical SP of this dataset is 200 W/kg (upper dashed line). There are two clearly unoccupied regions: the empty region of high-mass and low-power is of little interest since this is not generally desirable; however, it is interesting that the high-power low-mass regime is empty, indicating that while this is a highly desirable region, it is technologically inaccessible.

With the average mission power consumption of 1000 W and a medium value of 600 W, Figure 3.4 shows what maximal ranges can be achieved with three hypothetical solar array technologies with specific power levels of 10, 100 and 1600 W/kg (the lines show how the Empirical Specific power changes as a function of range until it reaches the lower limit of 1 W/kg). The color-coded regions are where maximal surface area of 100 m^2 could be contained for power levels of 100, 300, and 1000 W. The areas under the line and within the colored region indicate where current (empirical evidence) and future (theoretical) missions could exist.

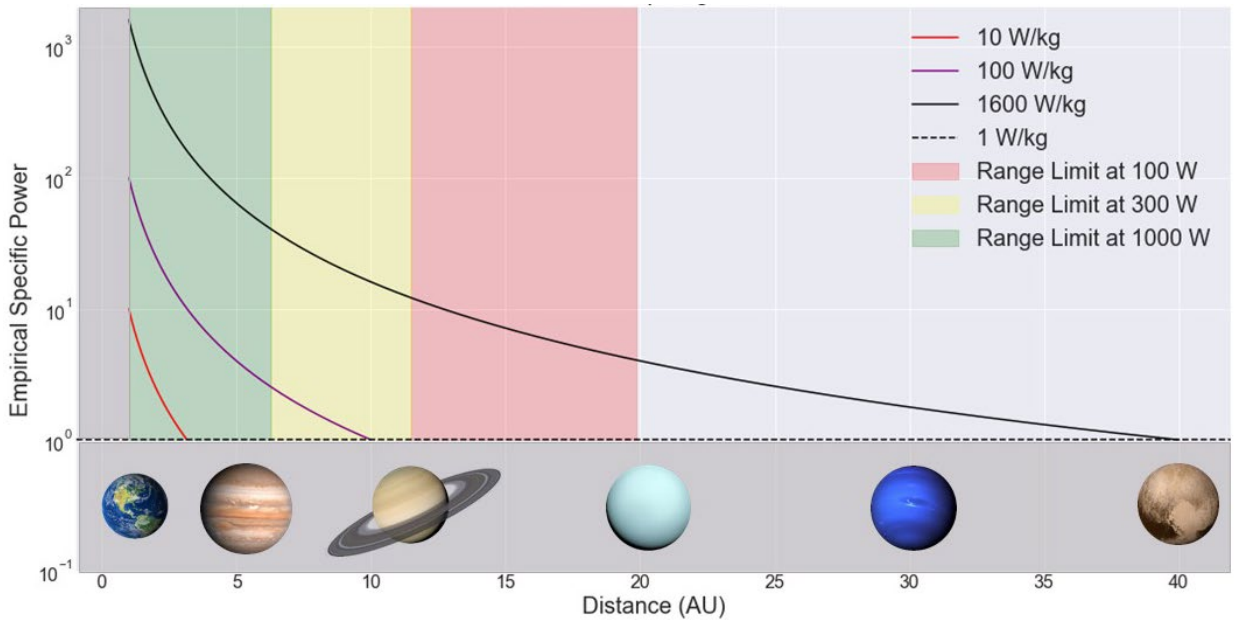


Figure 3.4: Practical power operation limit for spacecraft. Horizontal Axis is range in AU, Vertical is Specific Power in W/kg. Lines represent a hypothetical solar array Specific Power. Colored regions show where a solar array with surface area smaller than 100 m^2 could exist (green is more spacecraft power and red is less spacecraft power). Peretz et al (2024). Credit: NASA.

There are two possible approaches to improving solar array specific power: increase generated power or decrease array mass. The former has been the focus of the community for the past 40 years through improving efficiencies. However, even if triple-junction solar cell efficiency improves to the theoretical limit of approximately 40%, the surface area, mass, and storage volume required to support median power requirements for exploration of deep space are beyond the point of feasibility. The mass required from such solar array structures would be measured in thousands of kilograms; clearly a reduction in solar array mass is needed for deep space exploration missions to be feasible.

Future work is needed to reduce solar array mass; deployment mechanism mass could be reduced with light-weight components or alternate configurations (for example, using a tension-based deployment instead of a motor-driven system) to eliminate the requirement for a motor and

many spacecraft integration components. Mass reduction for the solar cells themselves can come by reducing cell thickness or increasing flexibility to increase launch vehicle stowage volume. Creating highly foldable arrays may be a desirable solution, with mass decreases possible in both deployment mechanisms and in the design of solar cells.

3.3 On the Horizon – Power Generation

The global surge in renewable energy research has significantly advanced materials science, particularly in the development of next generation power systems for small spacecraft. Innovations like advanced single-junction, multi-junction, flexible and organic solar cells are at the forefront of this progress. These technologies are poised to surpass the current state of the art in aerospace solar power, especially as their high efficiencies—demonstrated under terrestrial sunlight—are adapted for space environments. Other promising power sources such as hydrogen fuel cells, thermonuclear systems, and atomic batteries are beyond the scope of this chapter and are not discussed here.

3.3.1 Multi-junction Solar Cells

There is ongoing research and development to improve aerospace use of multi-junction solar cell technology, and recent progress within terrestrial photovoltaic applications indicates significant progress. Advancements for multi-junction cells include enhanced crystal growth techniques, studying the geometric orientation in nanostructures, improved matching the layers electrical currents, and better radiation tolerance and thermal stability.

Fraunhofer Institute for Solar Energy Systems contributed to the development a four-junction solar cell that achieved a significant 47.6% efficiency under concentrated sunlight (ideal case) using an advanced antireflection coating and optimized contact layers; and the demonstration of Si-based multi-junction solar cells with 36.1% efficiency. Future investigations are needed to solve current challenges of the complex inner structure of the layers (6).

The National Laboratory of the Rockies (NRL, previously National Renewable Energy Laboratory, NREL) has actively advanced photovoltaic technology with their suite of characterization tools for analyzing proton and electron radiation effects. Figure 3.5 below shows a cross section of a IMM solar cell by NRL. They have advanced modern photovoltaic technology, with 4- and 6-junction cells achieving or exceeding 35–38% in the lab and even reaching 47.1% under concentrated illumination for a 6-junction III-V device (8). NRL's latest developments with their dual chamber Dynamic Hydride Vapor Epitaxy (D-HVPE) growth reactor for manufacturing scalable III-V cells achieved 27% efficiency GaAs single-junction under terrestrial sunlight, which is exciting since its very likely the efficiency in space will be only a slightly lower though much higher than the current 20% nominal (9).

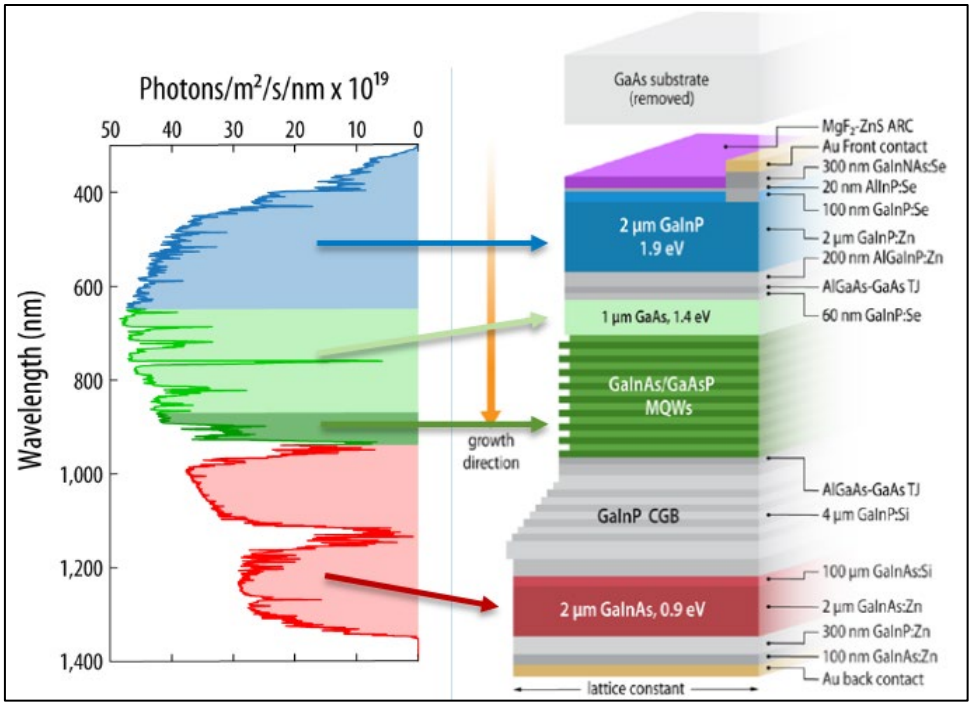


Figure 3.5: Cross section of IMM solar cell. Credit: NRL and Alfred Hicks.

Perovskite Cells

Emerging progress of perovskite technology solar cells is happening across the globe in academic institutions, R&D labs, and industry. Known for its exceptional photo-electric properties (high power-to-mass ratio, high efficiency potential, and high optical absorption) and flexibility, perovskite solar cells can convert more sunlight into energy. Major limitations are degradation, insufficient long-term stability, and durability when exposed to harsh space radiation over longer periods of time.

Perovskite materials are ideal for creating multi-junction solar cells since their electronic properties can be adjusted by altering their composition (10). Currently, the University of Science and Technology of China achieved 26.7% efficiency of a single-junction perovskite solar cell under terrestrial sunlight (11). Researchers have found that when used in tandem with other materials, Silicon being the most common, perovskite cells achieve significantly increased efficiency. LONGi company developed a crystalline silicon-perovskite tandem solar cell with 34.85% efficiency (terrestrial) and is inching closer to space demonstration.

In a collaboration with JAXA, the Ricoh Company aims to achieve practical applications of perovskite solar cells. In October 2025, Ricoh perovskite solar cells were installed on the unmanned cargo transfer spacecraft1, HTV-X1, onboard the ISS, where they are exposed for two months (12). On the same launch, Aegis Aerospace's MISSE-21 mission were halide perovskite-based cells from Georgia Institute of Technology. Instead of using silicon, researchers from Georgia Tech's School of Materials Science and Engineering develop ways to prevent the degradation of perovskite cell and promote resiliency by mixing chemistries of the materials (13)(14).

Flexible Solar Cells

Flexible and thin-film solar cells have an extremely thin layer of photovoltaic material placed on a substrate of glass or plastic; flexible substrates now also include advanced polymers and ultra-thin glass. The thickness of photovoltaic layers using modern crystalline silicon wafers are typically 100–200 microns and the thin-film layers range from <1 to a few microns depending on the material. This allows the cells to be flexible, lightweight, and cheaper to manufacture because they use less raw material. Limitations with implementing thin-film solar technology in space are the manufacturing complexity, temperature sensitivity, and reduced durability and overall power efficiency.

Recent research in thin-film solar technology is being conducted by institutions like the Korea Institute of Energy Research (KIER), Uppsala University, and Helmholtz-Zentrum Berlin often in tandem with perovskite cells for better efficiency. Researchers at KIER combined copper indium gallium selenide (CIGS) and perovskite cells and achieved a power conversion efficiency of 23.64% (16)(15). CIGS semiconductor material is a highly efficient light absorber, and active research at Uppsala University in Sweden is investigating a variety of implementation and manufacturing techniques to maximize the solar cell efficiency (17).

Organic Solar Cells

Carbon-based organic photovoltaic technology is another outlet for the next generation aerospace power generation. Organic electronics, polymers, or molecules absorb light and create a corresponding charge. A small quantity of these materials can absorb a large amount of light making them cheap, flexible, and lightweight. Improvements to organic solar cells' durability and lifespan for aerospace use are actively being developed and tested. Currently at the laboratory level, organic solar cells achieve ~20% power conversion efficiency and there are promising advancements in organic semiconducting materials and improved manufacturing strategies (18).

Researchers at the University of Michigan are studying how radiation affects different organic solar cell designs, with the goal of identifying potential approaches to mitigate degradation in complex polymer-based cells. The team identified a "trap effect" where proton exposure can damage organic solar cells by breaking side chains and creating electron traps, capturing electrons that would otherwise generate electricity. The team found that heating the cells (thermal annealing) can repair cell damage, and they believe sun-facing solar cells in space could potentially self-heal through natural heating (19).

No standardized stability tests are yet available for organic-based solar cell technology, and challenges remain in creating simultaneous environmental influences that would permit an in-depth understanding of organic photovoltaic behavior, but these achievements are enabling progress in organic-based solar cell use.

3.3.2 Unitized Regenerative Fuel Cells

A primary fuel cell can be seen as an energy generation system in that it takes consumable products, typically H2 and O2, to create electricity and water. This reaction is in a single direction, complete when all reactants are consumed. Fuel cells for energy storage are appealing for their lightweight, reliable qualities, and high energy conversion efficiency capabilities. They also allow missions to launch with a safe, storable, low-pressure, and non-toxic fuel source, making them more ideal for interplanetary missions and during eclipse periods. Primary hydrogen fuel cells cannot be recharged and are not feasible for small spacecraft, though there is active development for secondary regenerative fuel cells with promising applications in aerospace and military systems.

Like a rechargeable battery, unitized regenerative fuel cells (URFCs) is a single device that can store and generate energy by transitioning between fuel cell (discharging) and electrolysis (charging) modes. Researchers have experimented with different proton exchange membranes to separate the hydrogen and electrolyzer finding that polymer electrolyte membrane fuel cells could be well suited for space applications (20). The round-trip efficiency is a combination of the electrolysis and fuel cell processes and varies depending on the specific material technology and operating conditions.

Main limitations include designing the electrocatalyst to perform well under extreme operating conditions (i.e., high voltage) in water electrolysis and self-regenerate; achieving appropriate thermal management for the two different operating temperatures; and proper management of water during each operation (electrolysis and fuel cell).

3.4 State-of-the-Art – Energy Storage

Solar energy is not always available during spacecraft operations due to orbital dynamics, mission duration, distance from the Sun, and peak load demands, so spacecraft require onboard energy storage usually via batteries. Batteries are classified by electrochemistry; primary (non-rechargeable) and secondary (rechargeable) batteries, are each suited to different mission needs. Today, lithium-based primary batteries such as lithium sulfur dioxide ($LiSO_2$), lithium carbon monofluoride ($LiCF_x$), and lithium thionyl chloride $LiSOCl_2$ are preferred for their high energy density; silver-zinc batteries are now considered legacy systems. Since their lifespan is low, primary batteries are commonly applied in short mission durations and are not currently considered state-of-the-art energy storage systems. Therefore, the rest of this section will focus on secondary batteries only, with some exceptions.

Secondary-type batteries such as lithium-ion (Li-ion) and lithium polymer (LiPo) are now the standard for modern aerospace and commercial applications, replacing older nickel-based chemistries like nickel-cadmium (NiCd) and nickel-hydrogen (NiH_2). Li-ion batteries use organic liquid electrolytes and can reversibly convert electrical energy to chemical energy, making them rechargeable, lightweight, and energy-dense—ideal for portable electronic devices, small tools, and in spacecraft missions. In space missions, these batteries are often paired with a primary energy source (e.g., solar arrays) to provide reliable, rechargeable power. For missions requiring short, intense energy bursts, secondary batteries may also be preferred since they can reduce overall system weight and still provide high power.

The primary limitation of high-power cells is safety. The manufacturing process of Li-based batteries use flammable, liquid electrolytes that can trigger thermal runaway, potentially leading to fire or explosion. This can occur due to several causes: damage, overheating, overcharging, water exposure, or manufacturing defects. In space, the onboard energy storage must endure extreme temperature fluctuations and high charge voltages, which accelerates degradation. Over time, repeated charge/discharge cycles reduce total energy output (measured in Watt-hours). Variables influencing this aging include temperature, charge/discharge rate, depth of discharge, and storage conditions. These factors make life testing under mission-specific conditions essential before launch to ensure the battery will meet the specific mission life requirements.

3.4.1 Secondary Li-ion Batteries

Rechargeable batteries are ubiquitous in small spacecraft, and the space industry has seen incremental improvements in energy density over time. A high gravimetric energy density (energy per unit mass) enables lighter batteries with equal or greater capacity, helping to minimize launch

costs. Although battery selection for small spacecraft must consider more than just energy density—safety, cycle life, power output, and environmental resilience are all equally vital.

Recent advancements include the incorporation of silicon in anodes, high-voltage cathodes, novel electrolyte additives, and improved cell designs. This section reviews individual cell chemistries and pre-assembled batteries from various manufacturers, each leveraging different lithium-based chemistries to optimize weight and energy density. Table 3-3 lists battery pack products, organized by specific energy to align with mass and volume constraints of the spacecraft.

Li-ion battery manufacturing is concentrated among a relatively small number of companies. Listed in Table 3-3 are companies at the forefront of their respective sectors. While China has some of the largest consumer electronics and EV battery manufacturers, their products are less established in the space industry and are not included here.

Table 3-3: Commercial and Space Li-ion Manufacturers

Commercial Li-ion Manufacturing		**Space Li-ion Manufacturing**	
Company	**Headquarters**	**Company**	**Headquarters**
Panasonic	Japan	EaglePicher Technologies	USA
LG Chem	South Korea	Enersys	USA
Samsung	South Korea	GS Yuasa	Japan
E-one Moli	Taiwan	Saft	France
Sony	Japan	Tesla	USA

The chemistry and design of Li-based cells directly influence their volumetric and specific energy densities—stored energy per unit volume or weight. Current commercial Li-ion energy cells typically provide 150-270 Wh/kg and an average voltage of 3.6 V while advanced designs in laboratory and high-altitude applications have approached or exceeded practical limits for Li-ion systems at 450-500 Wh/kg (22). Amprius' silicon anode batteries powered a high-altitude pseudo satellite for 67 days in the stratosphere, delivering 450 Wh/kg (23). Lithium polymer (LiPo) cells deliver a lower energy density (150-200 Wh/kg) and have a gel-like or solid electrolyte instead of liquid, offering more flexibility in spacecraft form factor and slightly less weight. LiPo batteries may have comparable performance to Li-ion batteries, however, their lifetime is typically shorter.

Secondary battery cells are often optimized for either high energy or high power, though hybrid designs are emerging that aim to balance both, especially for electric aviation or drone applications. High-power cells typically feature low-resistance designs, such as increased coating surface area or multiple current collector contact points, enabling higher discharge rates. In contrast, high-energy cells focus on maximizing gravimetric energy density to extract the most energy per unit mass. To improve energy density, reduce safety risks, and lessen reliance on traditional Li-ion chemistries, manufacturers incorporate additives to the anodes and cathodes that enhance the electrochemical performance.

For space applications, both COTS and space-grade Li-based batteries are widely used. Unlike consumer electronics, where shorter battery life may align with product turnover, space-grade cells prioritize longevity. These cells often sacrifice energy density for better lifecycle to be able to support missions lasting 5 to 15 years or more. However, degradation trends are not always linear, and early test results may not predict long-term performance accurately.

COTS batteries have been successfully used in several CubeSat and nanosatellite missions due to their low cost, while the specialized space-grade cells from dedicated aerospace manufactures are designed specifically to operate reliably in extreme space environments. Emerging technologies like lithium-sulfur (Li-S) batteries are under evaluation for future space missions due

to their potential for even greater energy density. Environmental factors such as ambient pressure, fluid exposure, and illumination further influence battery selection. Additional variables that play a role in space are distance from energy source, relative location, and orbital gravity (24)(25).

18650 Cells

The well-known COTS 18650 (18 x 65 mm) cylindrical cells are cost-effective, offer widespread availability and proven performance. The 18650 battery is the industry standard for Li-ion and numerous manufacturers have high-performance 18650 battery packs, most of which have flown on multiple spacecraft and are documented in Table 3-4 below. 18650s have become the most used building blocks for many SmallSats, although prismatic and pouch formats are also available.

Another type of cylindrical cell is 21700 (21 x 70 mm) that has been more widely used in the automotive industry. The 21700 cells are slightly larger than 18650 cells and have some of the highest energy densities and could offer some mechanical packaging benefits with fewer cells for certain missions. While there has been some implementation of 21700 batteries on SmallSats, there is ongoing effort to improve the scalability of battery packs for space use with testing of 21700 cells (26).

Table 3-4: 18650 Cylindrical Cells

Cell	Specific Energy (Wh/kg)	Flight Heritage
Sony SE US18650 VTC4	250	Ingenuity Mars Helicopter
LG Chem ICR18650 B3 (2600 mAh)	191-205	NASA's PhoneSat, NoDES, Europa Clipper
Panasonic NCR18650B (3350 mAh)	243	MarCO, ADAPT, BioSentinel, Lunar Flashlight, NeaScout
Molicel ICR18650H (2200 mAh)	182	NASA's EDSN mission
Canon BP-930s (3000 mAh)	112	NASA's TechEdSat missions
LG Chem INR18650-MJ1 (3500 mAh)	260	NASA's PACE mission
Samsung SDI INR18650-25R (2500 mAh)	210	UNION/Lian-Hé mission

Table 3-5: Battery (Pack) Product Table						
Company Headquarters	**Product**	**Volumetric Energy Density [Wh L^{-1}]**	**Specific Energy [Wh/kg]**	**Typical Capacity [Ah]**	**Max Discharge Rate [A]**	**Cells Used**
AAC Clyde Space Sweden	Optimus	169.5	119.4	4.84	2.6	Clyde Space Li-Polymer
Aerospacelab Belgium	BM	380	-	14	12 (in / out)	4 independent battery packs of 8 lithium-ion cells each
Astro Digital USA	Direct Energy Pack	187	144	10	50	21700 Li-Ion
Argotech Italy	ELEKTRA	243.5	152.5	3.4	4	Li-Ion
Berlin Space Technologies Germany	BAT-110 Modular Battery (Nominal 3 strings)	69.73	57.75	7.5	3	Li-Fe
Dragonfly Aerospace South Africa	28-300-Battery Module	68.4	62	10	40	LiFePO4
EaglePicher Technologies USA	NPD-002271	271	153.5	14.5	15	EaglePicher Li-ion
EnduroSat Bulgaria	EPS IV (BMS)	222.9	178.1	33.5	100	Li-Ion
GomSpace Denmark	Nanopower BPX 3000mAh (e.g., 4S-2P)	262.2	172	6.0	4	GomSpace NanoPower Li-ion
	Nanopower BP4 3000mAh (e.g., 2S-2P)	239.8	168.8	6.0	4	GomSpace NanoPower Li-ion
	Nanopower BP8 (8S-1P)	227.36	177.3	3.0	4	GomSpace NanoPower Li-ion
GUMUSH AeroSpace Istanbul	n-ART BAT	184.5	155.1	6.01	8	Li-Ion
Ibeos USA	28V Modular Battery	151.1	109.8	8 - 30+	20	*
ISISPACE The Netherlands	PBP-2S1P	129.1	156.5	6.4	4	Li-Ion
	PBP-2S2P	327.85	160	12.8	8	Li-Ion
	PBP-4S1P	327.85	160	12.8	4	Li-Ion
NPC SPACEMIND Italy	KANON	167	250	13.6	6	Li-Ion
Saft France	VES16 4S1P	109.2	91	4.5	4.5 – Cont. 9 – Pulse	SAFT Li-ion
SatRev S.A. Poland	1U battery pack	--	161	360 W	15	30
SkyLabs Slovenia	SKY-NANOeps-BMM	103	89	up to 18	up to 54	LiFePO4
Space Dynamics Laboratory USA	SDL 12V Battery Pack	144	75	12.0	96	EaglePicher LP32975
Space Inventor Denmark	Bat-28-P4	100	141.8	3.4	7.5A	Space Inventor Li-Ion
	Bat-14-P4	50	123.5	3.4	7.5A	Space Inventor Li-Ion

Table 3-5: Battery (Pack) Product Table						
Company Headquarters	**Product**	**Volumetric Energy Density [Wh L^{-1}]**	**Specific Energy [Wh/kg]**	**Typical Capacity [Ah]**	**Max Discharge Rate [A]**	**Cells Used**
Vectronic Aerospace GmbH Germany	VLB-X	101.96	74.6	12	10 – Cont. 20 – Pulse	SAFT Li-Ion

* Available with Inquiry to Manufacture

3.5 On the Horizon – Energy Storage

Efforts to improve energy storage capability, power, and energy density continue as aerospace systems expand beyond Earth environments. A way for researchers to characterize energy storage is using a Ragone plot to show the non-linear relationship between the energy that can be extracted from the storage and the discharge power (27). For energy storage systems, the overall hierarchy is fundamentally the same since the last decade in terms of tradeoffs. Figure 3.6 is by researchers from the Chemical Society of Japan to illustrate the advancements in Li-based technology, supercapacitors, and solid-state battery formats.

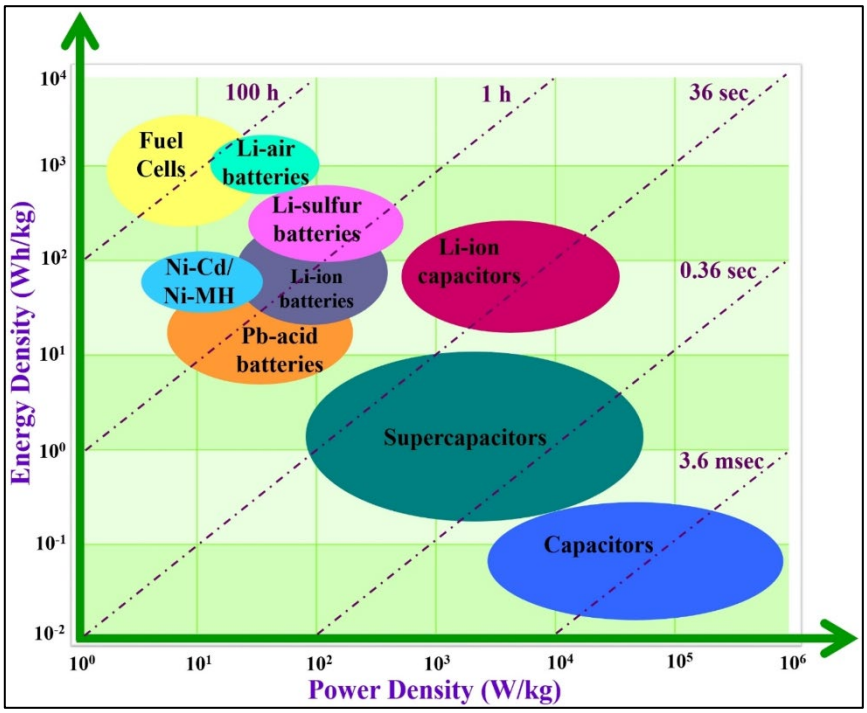


Figure 3.6 Relative power and energy densities of different energy devices. Ragone chart illustration reprinted with permission from Mateen et al. (2023) Chemical Society of Japan (29).

Ongoing research of energy storage systems indicate the successors of Li-ion cells include Li-metal, Li-Sulfur, silicon-rich anodes, high-voltage cathodes, solid-state configurations, and hybrid systems of a rechargeable battery and capacitor. While these methods have promising energy densities, they often involve trade-offs in cycle life and stability (28).

As demand grows for higher energy output in smaller volumes, several challenges remain for long-term use in space. While system-level energy density in Li-ion batteries is reduced by components like battery management systems (BMS) and thermal controls, research continues to push the performance boundaries.

3.5.1 Nanomaterials

There has been sustained focus on renewable energy sources, and the accumulated research on nanomaterial development and testing shows next-generation power (and thermal) systems will incorporate nanomaterials. Fueled by the adoption of electric automotives, research using nanomaterials as a main conductive additive for energy storage is rapidly emerging. There has been tremendous development and testing of nanomaterials, and ongoing research— now showing promising laboratory results—suggests next-generation power systems will include them. A power system with integrated carbon nanotubes into Li-ion batteries can significantly increase energy density (30); and recently researchers found that twisting ropes of single-walled carbon nanotubes can significantly increase nanomechanical energy while retaining stability across a wide temperature range (31).

Graphene is being explored for space applications for its unique electrical properties that result in enhanced durability and performance. A single layer of carbon, graphene is lightweight with high electrical conductivity, flexibility, and mechanical strength, and is also impermeable to gas and liquid (32). These qualities make graphene ideal for several uses on spacecraft power and thermal management, and as a coating for spacecraft graphene can greatly enhance the heat transport in conductive materials. Researchers have high interest in understanding how to implement graphene-based batteries and supercapacitors for space applications.

The electrical properties of conducting polymer materials can improve battery performance and are being examined for next generation additives or coatings for battery systems. Conductive polymers have high structural flexibility that can accommodate the volume changes during battery cycling when the doping type and concentration are modified (33). There exists a multitude of research on the characterization of conducting polymers in various battery chemistries with advantageous potential for space operations.

Electrolytic carbon fiber materials are emerging for spacecraft as multifunctional “structural” battery systems that can bear mechanical loads while simultaneously storing energy. Being integrated into the primary structure, this novel battery system significantly reduces mass, and benefits from the electrical characteristics of carbon fiber-based electrodes. There has been extensive research that supports the increased electrochemical performance and accuracy of the computational models (34), though further development and testing of individual components is needed to implement in space.

The manufacturing of nanomaterials for aerospace applications is a complicated process. Due to the nature of nanomaterials, there are often inconsistencies during manufacturing where attributes like uniformity, purity, and size distribution of individual nanoparticles are not uniform to achieve desired properties/performances. Scaling up from lab to production requires precise control over nanoparticle morphology, alignment, and integration into large-scale structures like spacecraft bodies and satellites. Additionally, the current performance of nanomaterial technology cannot withstand radiation-induced degradation during long term spaceflight (36).

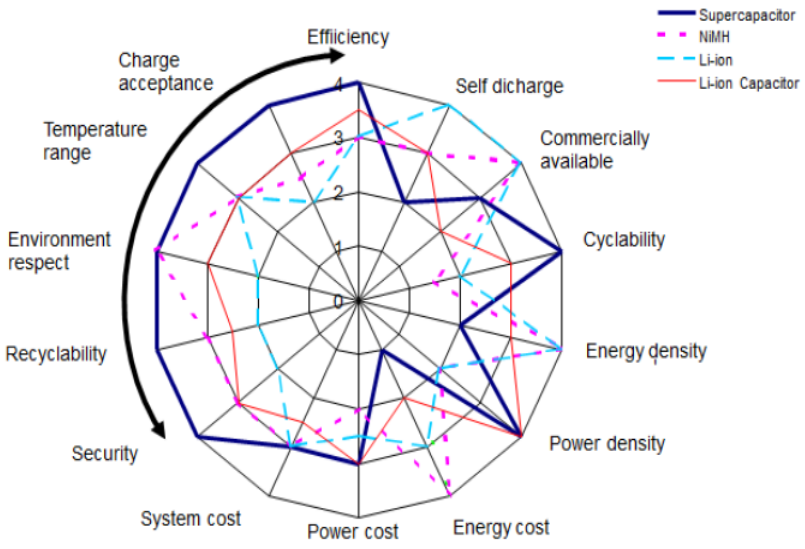


Figure 3.9: Supercapacitor comparison chart. Credit: Airbus Defense and Space and ESA (2016).

3.5.2 Supercapacitors

While traditional supercapacitors (also called ultracapacitors) have limited energy densities (~7 Wh/kg), recent advancements leveraging nanostructured carbon materials have achieved 60 Wh/kg (51). The very high power densities (10–100 kW/kg) of supercapacitors are ideal for space operations requiring rapid power transients (i.e., ADCS control, propulsion, or radar systems). Their fast charge/discharge capabilities, exceptional cycle life (over 1 million cycles), and broad operational temperature range make them well-suited for spacecraft. While

early ESA studies such as the 2010 “High Power Battery Supercapacitor Study” (54) and the 2020 qualification of the Nesscap 10F component laid the groundwork, recent ESA-backed research (e.g., Swistor SA, 2024) has demonstrated next-generation supercapacitors with enhanced energy density, thermal resilience, and environmental sustainability.

Although not likely to replace Li-ion batteries completely, supercapacitors could drastically minimize the need for a battery and help reduce weight while improving performance in some applications. Figure 3.9 shows a comparison chart (55), and Table 3-6 lists differences in Li-ion batteries and supercapacitors (56). A hybrid energy storage system combining a Li-ion battery and supercapacitor has been a niche area of research for over a decade. They provide a middle ground between power density and energy density but suffer from limited life-cycles. Some lithium-ion capacitors have demonstrated specific energies up to ~200 Wh/kg but are limited by a maximum specific power of <350 Wh/kg (58).

Table 3-6: Battery-vs-Supercapacitor Specifications

Feature	Li-Ion Battery	Supercapacitor
Gravimetric energy (Wh/kg)	150 – 265+	5 – 20
Volumetric energy (Wh L^{-1})	220 – 450	4 – 14
Power density (W kg^{-1})	1,500	3,000 – 40,000
Voltage of a cell (V)	3.6	2.7 – 3
ESR (mΩ)	500	40 - 300
Efficiency (%)	80 – 95	>98
Cyclability (nb charges)	2,000 – 70,000	500,000 – 20, 000,000
Life (years)	5 – 10	10 – 15
Self-discharge (% per month)	2	40 – 50 (descending)
Charge temperature (°C)	0 to 45	-40 to 65
Discharge temperature	-20 to 60	-40 to 85
Deep discharge pb	yes	no
Overload pb	yes	no
Risk of explosion	yes	no
Charging 1 cell	complex	easy
Charging cells in series	complex	complex
Voltage on discharge	stable	decreasing
cost ($) per kW h	235 – 1,179	11,792

3.5.3 Solid-State Batteries

The flammable nature of the liquid electrolyte in conventional Li-ion configurations presents an inherent risk of combustion, particularly in the event of physical damage or thermal runaway caused by overcharging. To mitigate these risks, spacecraft often require additional weight for thermal management and protective housings, which adds parasitic weight and complexity. In contrast, solid-state batteries replace liquid electrolytes with non-flammable solid electrolytes that maintain high ionic conductivity (42). These electrolytes, usually polymer-based, inorganic, and polymer-inorganic composites, offer several benefits over traditional Li-based batteries like improved safety, high energy and power density, greater thermal stability, mechanical flexibility, and long-life cycle. For deep-space applications, solid-state batteries are being engineered for radiation tolerance, vacuum compatibility, and mechanical robustness, often requiring trade-offs in electrolyte composition or packaging design (42).

Researchers across the globe have developed various configurations like all-solid-state lithium-ion batteries (ASSLBs), which replace both electrolyte and separator with a solid material. Solid-

state lithium–sulfur batteries (SSLSBs) combines a lithium metal anode with a sulfur cathode and solid electrolyte to achieve theoretical energy densities over 500 Wh/kg (43); and lithium metal solid-state batteries with lithium metal as the anode for higher energy density, though this requires careful engineering to prevent dendrite formation (45). Researchers at JAXA successfully characterized ASSLB on the ISS for 434 days that confirms their potential application to space exploration (44).

Despite the advantages of solid-state batteries, several challenges that must be addressed before they can be reliably adopted in space. A primary concern is thermal management of the solid electrolyte material under extreme conditions, which significantly impacts their electrochemical performance. Solid electrolytes typically have lower thermal conductivity, making it difficult to dissipate heat effectively. This can lead to localized hotspots, which degrade battery materials over time. Additionally, the mismatch in thermal expansion coefficients of the various materials in a solid-state-battery introduces mechanical stress during temperature fluctuations potentially compromising structural integrity and performance (46). See Table 3-7 for examples of solid-state batteries.

Table 3-7: Solid-State Batteries

Manufacturer	Product	Wh/kg	Wh/L
Solid Power	Silicon EV Cell	390	930
Solid Power	Lithium Metal	440	930
Solid Power	Conversion Reaction Cell	560	785
QuantumScape	LFP (projected)	230	600
QuantumScape	NMC (projected)	300	1000

3.5.4 Energy Storage Systems

A single energy storage unit that can store excess energy generated during periods of high production and make it available during low production intervals is highly advantageous for both terrestrial and space applications. A hybrid energy storage system (HESS) combines the high energy density of batteries (usually Li-ion-based) with the high-power density and longer life cycle of supercapacitors. The batteries provide primary energy storage, while the supercapacitor handles peak power demands. This reduces stress on the battery, prevents degradation, and improves power dissipation. Researchers from California State University, Northridge in collaboration with JPL developed a passive HESS that was successfully operated on nanosatellite CSUNSat-1 in 2017 (47). While the only HESS technology in space, the advancements in HESS technology have increased though mainly due to renewable energy sources for terrestrial applications.

Designing a HESS for a space mission presents several technical challenges, including the need to improve energy density and efficiency of storage technologies, ensure compatibility between different power systems within a single unit, and manage high development cost (48). Critical considerations include maintaining voltage compatibility and precisely controlling the charge and discharge rate of the storage components to ensure system stability and performance (49). For more detailed insights into ongoing development, interested readers are highly encouraged to consult references (51)(52).

3.6 State-of-the-Art – Power Management and Distribution

Power management and distribution (PMAD) systems—also called power conditioning and distribution units (PDCUs)— regulate and distribute electricity to spacecraft subsystems and instruments. PMAD systems are typically comprised of converters, power transfer circuitry, and fault management functions. These systems are most often customized per mission with specific power requirements to efficiently manage and distribute electrical power. From generation through consumption, the PMAD unit delivers energy from energy sources—such as solar arrays or batteries— and detects and isolates faults, protecting downstream components from transient disturbances. Other core functions of the PMAD system are voltage regulation from the bus to the different voltage requirements of the subsystems; load switching that enables/disables the power to subsystems; and interfaces with the onboard computer to monitor temperature and current.

An optimal PMAD architecture is fault-tolerant with high reliability and a small footprint. Traditional small spacecraft EPS operate with a main battery bus voltage of 8.2 V and provide regulated outputs at 5.0 V and 3.3 V to various subsystems via the PMAD system. However, modern small spacecraft with high-power payloads (i.e., inter-satellite cross laser links, multispectral imaging, synthetic aperture radars, IoT constellations) have more than doubled the power requirement the PMAD must handle(53). Newer converter designs with Gallium Nitride (GaN)-based power converters can support a broader range of voltages, including 12V, 28V, and 50V (54).

To further support high-performance or deep space SmallSat missions, PMAD systems are designed with enhanced shielding and fault-tolerant architectures. Aided by the rise of modular and software defined architectures, scalable PMAD designs can provide commonality across all the components in a spacecraft.

Modular Architecture

Modular architecture is ideal as it reduces mass and increases power. Shifting from fixed EPS units to flexible, mission customizable PMAD systems drives more powerful and scalable SmallSat capabilities.

Within NASA's Mars Campaign Office, the Advanced Modular Power Systems (AMPS) project—led by NASA Glenn Research Center—is developing a standardized space power system architecture at the electronics-module level. This includes defining the form and function of electronic modules (circuit cards) and modular electronic units that make up power system components. The goals include reducing power-system maintenance operations, improving system availability by minimizing outage and restoration times, and decreasing the number of unique spare parts. Together, these advances help lower sparing mass and volume requirements, which are essential for enabling sustainable exploration missions (55).

3.6.1 PMAD Selection Considerations

Key considerations in determining PMAD device selection often include conversion efficiency, input/output voltage range, output power capabilities, and size, weight, and power (SWaP). These metrics are critical to consider for good SmallSat PMAD designs, but it is important to note that PMAD devices should be selected to match the specific application of the SmallSat mission. SmallSat missions are often short and more flexible in terms of risk management than larger satellites, and therefore lend themselves to greater flexibility in design choices. One must leverage the benefits and risks to the mission at hand when choosing COTS PMAD systems, which may include the following:

- COTS PMAD may require less intensive integration and testing but may have drawbacks to be addressed in a custom PMAD build
- Unnecessary features and peripherals (e.g., excess switching, fusing, current capability) can greatly increase SWaP metrics on a SmallSat
- Variability in designs of COTS PMAD devices means that important features and protections are not available in all devices (MPPT, Dead-bus protections, redundancy mechanisms, etc.)

Due to the variability of COTS PMAD options, many choice considerations, from internal power management topologies/materials to telemetry and protection options, are either included or omitted from products depending on the manufacturer. Internal power regulation topologies have traditionally been silicon-based, but relatively recent research into the performance improvements of Gallium Nitride (GaN) topologies has increased the number of GaN-based PMAD options in the consumer market with the following benefits over their silicon counterparts:

- Ability to achieve high switching rates and lower switching losses, allowing for the downsizing of inductors and capacitors, and improving SWaP metrics
- Lack of gate oxide layer in GaN-based field-effect transistors yields improvements in overall efficiency

It must also be noted that GaN-based PMAD options are not to be considered as drop-in replacements for silicon-based PMAD options. Despite the number of performance improvements, GaN architectures come with a variety of drawbacks including high complexity of control circuitry and lack of flight heritage.

Additional considerations when selecting a PMAD device for small spacecraft include radiation tolerance, especially for missions beyond LEO, and telemetry capabilities for real-time health monitoring. As mission complexity increases, modular PMAD architectures are gaining popularity for their scalability and ease of integration. Furthermore, thermal performance remains a critical factor, particularly in high-density CubeSat designs where heat dissipation is limited.

Table 3-8 lists PMAD system manufacturers; it should be noted that this list is not exhaustive and all information is taken from company websites and datasheets. Manufacturers tend to provide a variety of PMAD devices for inclusion in small spacecraft missions. In looking at the table below, one must note that there is no single COTS PMAD solution that can fit all needs of a mission at hand. In appealing to a broad range of applications, most COTS PMAD devices make sacrifices that can impact important metrics for SmallSats, including SWaP as well as the efficiency and quality of the power being managed. In choosing to use COTS PMAD devices, designers and system architects should be aware of, and try to minimize, unnecessary features not beneficial to the mission.

Table 3-8: Power Management and Distribution System Products							
Company	**Product**	**Mass (kg)**	**Volume (cm^3)**	**Peak Power Output (W)**	**Input Voltages (VDC)**	**Output Voltages (VDC)**	**Max Efficiency (%)**
2NDSpace Italy	SOLO-EPS 4	0.465	428	104	16.8	3.3V; 5V; 12V; 16.8V	92
	SOLO-EPS 8	0.67	606	160	16.8	3.3, 5, 12, 16.8	92
AAC Clyde Space Sweden	Starbuck Micro	2.45	3968	80.4	28	28 / 5	97
	Starbuck Mini	5.9	13133	1200	*	22-34/5/8/12/15	*
	Starbuck Nano	0.086	140	*	*	3.3/5/12	*
Aerospacelab Belgium	PCDU	1.635	1715.5	960	[0; 65] V	5V [4.75, 5.25] V 12V [11.4, 12.6]	>97
Argotec Italy	PCDU VOLTA	0.97	600	100	18-22	1x 3.3 V, 1x 5 V, and 2x 12 V	75
	PCDU ZEUS	0.56	532	220 (Solar + battery power)	8.5-24 V	3.3 V; 5 V; 12 V; 28 V (unregulated)	85
	PCDU PHOENIX	1.5	1400	250	31-55 V	3.3 V; 5 V; 12 V; 28 V (unregulated)	85
Berlin Space Technologies Germany	PCU-110	1.08	1190	180	standard: 20-28 optional: 12, 15, 18	standard: 2x 12, 12x 5, 5x 3.8 optional: 1.8 – 28	*
Bradford Space Luxembourg	SuperNova modular PCDU	2.9	3045	1500	22 - 34	3.3/5/12/unreg. batt	95
C3S Electronics Development LLC Budapest	EPS1000	0.811	748.5	70	6-25V SA	9.9-12.3V, 3.3V, 5.1V	90
	EPS2000	5.8	7000	2kW	6V-25V or 30-70V (SA)	28V unregulated	97
DHV Technologies Spain	MicroEPS	1.250~2.850*	392~1045*	592 in eclipse / 693 in sunlight	9-40	3.3/5/12 Batt	>90
	NanoEPS	0.175~0.540*	283~600*	59 in eclipse / 124 in sunlight	9-28 (X/Y) / 3-18 (Z)	3.3/5/12 Batt	>93
	PicoEPS	0.110~0.315*	140~197*	29 in eclipse / 74 in sunlight	3-18	3.3/5/12 Batt	>93
	Battery Module	~3.1	~2200	~930	24	33.6	-
	PCDU	3.4~3.9	4704~5720	~900	20~70	3.3/5/12 Batt	>90
Dragonfly Aerospace South Africa	EPS-LP-1k5 (PCDU)	3.3 (Cfg: EPS-LP-12333)	5650 (Cfg: EPS-LP-12333)	1500	29.7 (22 to 36)	Battery Bus: 29.7 Regulated: 12 / 5	98
	EPS-LP-1k5 + HPIU-28V	7	10170	4200	29.7 (22 to 36)	Battery Bus: 29.7 Regulated: 12 / 5	95

Table 3-8: Power Management and Distribution System Products							
Company	**Product**	**Mass (kg)**	**Volume (cm^3)**	**Peak Power Output (W)**	**Input Voltages (VDC)**	**Output Voltages (VDC)**	**Max Efficiency (%)**
	EPS-LP-1k5 + HPIU-48V	10	11187	7200	49.5 (42 to 60)	Regulated: 28 / 12 / 5 Battery Bus: 49.5	92
Ecarver GmBH Germany	PCU-SB7	1.5	1800	250	0-24	0-24	85
Emxys Spain	ODALISS PDCU	0.36	416.3	36	14-36	Main 7.6V unreg/ Redundant 7.7V unreg/ Regulated 3.3V/ Regulated 5.0V	95
EnduroSat Bulgaria	EPS II	1.28	742	250	10-36	3.3/5/6-12/Batt	89
	CubeSat EPS	1-6	860-4000	500	0-45	3.3/5/12/Batt	87
	EPS IV	4.5	7208	7200	0 -70	12/28/Batt	90
GomSpace Denmark	P31U	0.1	127	30	0-8	3.3/5	96
	P60	**	**	100	16/32 V	3.3/5/8/12/18/ 24	-
	P80	360-610g ¥	350–586	300	0-25	3.3/5/12/18V & Vbat	-
GUMUSH AeroSpace Istanbul	n-ART EPS	0.098	160	100	4.5-30	3.3/5/8-36/Batt	94
Ibeos USA	150 W CubeSat EPS	0.14	124	150	18-42	3.3/5/12/Unreg Batt	95
Ibeos USA	200 W CubeSat EPS	0.14	124	200	12-34	3.3/5/12/Unreg Batt	96
	Modular EPS	Starting at <1	Starting at 1150	500 – 2,000	12-26	5/12/Unreg Batt	98
ISISPACE The Netherlands	ICEPS2 Type A	0.184¥	223	39.2	--	3.3/5/Unreg	96
	ICEPS2 Type B	0.31	275	78.4	--	3.3/5/Unreg	95
	ICEPS2 Type C	0.36	317	78.4	--	3.3/5/28.2/Unreg	95
Nanoavionics Lithuania	CubeSat EPS (EPS 1.0)	*	*	175	2.6-12	3.3 / 5 / 3-12	96
NPC SPACEMIND Italy	GEMINI	0.3	215	200	10 to 24	1 or 2 X 3.3 1 or 2X 5.0 2X 12V Reg up to 24V	88
Pumpkin Space Systems USA	EPSM 1	0.3	180	300	4-32	3.3-28	99
	AMPS	1.3	360	1200	5-32	--	99
SatRev S.A Poland	EPS 3S1P	0.483	397	80 W	4.5 – 20	Unreg 9.6-12.6	> 95
	EPS 3S2P	0.751	630	160 W	4.5 - 20	Unreg 9.6-12.6	> 95
	EPS 3S3P	0.989	865	240 W	4.5 - 20	Unreg 9.6-12.6	> 95

Table 3-8: Power Management and Distribution System Products							
Company	**Product**	**Mass (kg)**	**Volume (cm^3)**	**Peak Power Output (W)**	**Input Voltages (VDC)**	**Output Voltages (VDC)**	**Max Efficiency (%)**
SkyLabs Slovenia	SKY-NANOeps-PCDU-23c-5d	0.2	216.125	72	10V Unreg	3.3, 5, 12, 10 Unreg	99
Spacemanic Czech Republic	Amun 1U	0.2	175	20	~ 2.5 - 5.5	3.3 / 5 / Batt	~ 90
Space Inventor Denmark	PDU-3V3	0.104	69	80W	12 to 33.6V	3.3V	95
	PDU-5V	0.104	69	120W	12V to 33.6V	5.0V	95
	PDU-12V	0.104	69	290 W	14V to 33.6V	12V	95
	PDU-VBAT	0.104	69	1000W	12V to 33.6V	12V to 33.6V	99

* Available with inquiry to manufacturer
** Configuration dependent
† Standard Configuration
‡ Optional radiation shielding case
¥Flexible stacking options Standard options

3.7 On the Horizon – Power Management and Distribution

Power management and distribution have been steadily improving each year due to improvements in technology and the different investigative approaches to maximizing the potential of PMAD systems. This includes modular architectures, wireless telemetry, and power transmission options. However, as multi-satellite missions— such as constellations or swarms— become more common, reliability concerns of PMAD systems are shifted from a single spacecraft-level redundancy to constellation-level redundancy.

Wireless Power Transfer and Telemetry

In the commercial world, the technology already exists for wireless sensing and power transmission from the order of microwatts, all the way up to kilowatts. In the realm of SmallSats, wireless power transfer/detection would be useful as redundant options in dusty environments where physical connectors can be contaminated, or in situations where hardware needs to be swapped around and powered (battery swaps). While wireless power transfer/detection is highly inefficient when compared to conventional means, research and development in this technology for use in space applications has a lot of potential to increase the reliability and robustness of SmallSat power management and distribution.

3.8 Summary

Driven by weight and mostly size limitations, small spacecraft are using advanced power generation and storage technology such as >34% efficient solar cells and lithium-ion batteries. The higher risk tolerance of the small spacecraft community has allowed both the early adoption of technologies like flat lithium-polymer cells, as well as COTS products not specifically designed for spaceflight. This can dramatically reduce cost and increase mission-design flexibility. In this way, power subsystems are benefiting from the current trend of miniaturization in the commercial electronics market, as well as from improvements in photovoltaic and battery technology.

Despite these developments, the small spacecraft community has been unable to use other, more complex technologies. This is largely because the small spacecraft market is not yet large enough to encourage the research and development of technologies like miniaturized nuclear energy sources. Small spacecraft power subsystems would also benefit from greater availability of flexible, standardized power management and distribution systems so that every mission need not be designed from scratch. In short, today's power systems engineers are eagerly adopting certain innovative Earth-based technology (like lithium polymer batteries) while, at the same time, patiently waiting for important heritage space technology (like fuel cells) to be adapted and miniaturized. Despite the physical limitations and technical challenges these power generation technologies have, most small nanosatellites in the foreseeable future will still likely carry batteries to support transient loads.

For feedback solicitation, please email: arc-sst-soa@mail.nasa.gov. Please include a business email so someone may contact you further.

References

(1) E. Peretz et al. "The Importance of Solar Power Technology Adaptations to Space Exploration", 2024

(2) Sectrolab. "XTE-HF (High Fluence): Space Qualified Triple Junction Solar Cell," [Online] Accessed February 16, 2026. Available at: https://www.spectrolab.com/photovoltaics/XTE-HF%20Data%20Sheet%20_12.23.19.pdf

(3) Rocket Lab. “z4j+ Space Solar Cell,” [Online] Accessed February 16, 2026. Available at: https://rocketlabcorp.com/assets/Uploads/RL-SolAero-Data-Sheet-Z4J+-v8.pdf
(4) M. Alia-Novobilski. "Advanced Multi-junction Solar Cells Deliver High Efficiency, Reduced Costs for Space." January 4, 2018. [Online] Accessed February 16, 2026. Available at: https://phys.org/news/2018-01-advanced-multi-junction-solar-cells-high.html#jCp
(5) National Laboratory of the Rockies. “Hybrid Tandem Solar Cells,” December 6, 2025 [Online] Accessed February 16, 2026. Available at: https://www.nrel.gov/pv/hybrid-tandem-solar-cells
(6) Fraunhofer Institute for Solar Energy Systems ISE. "Fraunhofer ISE Develops the World's Most Efficient Solar Cell with 47.6 Percent Efficiency,” May 30, 2022. [Online] Accessed February 16, 2026. Available at: https://www.pv-magazine.com/2018/04/04/fraunhofer-ise-announces-33-efficiency-for-multi-junction-solar-cell/
(7) “Indoor photovoltaics with over 40 percent efficiency developed,” July 16, 2025. [Online] Accessed July 16, 2021. Available at: https://www.ise.fraunhofer.de/en/press-media/news/2025/indoor-photovoltaics-with-over-40-percent-efficiency-developed.html
(8) National Laboratory of the Rockies. “Photovoltaic Applications,” January 12, 2026 [Online] Accessed February 16, 2026. Available at: https://www.nlr.gov/pv/applications
(9) National Lab Discovery Series: Dynamic Hydride Vapor Phase Epitaxy – High-Performance III-V,” NREL, September 29, 2025
(10) T. CJ Yang, P. Fiala, Q. Jeangros, and C. Ballif, “High-Bandgap Perovskite Materials for Multijunction Solar Cells,” Joule 2, 1421–1436, August 15, 2018
(11) M.A. Green, E.D. Dunlop, M. Yoshita, et al. Solar cell efficiency tables (Version 64). Prog Photovolt Res Appl. 2024;32(7):425-441. doi:10.1002/pip.3831
(12) Ricoh. “Ricoh perovskite solar cells installed on Japan Aerospace Exploration Agency cargo transfer spacecraft1 HTV-X1,” Press release. October 27, 2025 [Online] Accessed February 16, 2026. Available at: https://www.ricoh.com/release/2025/1027_1
(13) J. Toon. “Space Station Testing Will Evaluate Photovoltaic Materials,” June 24, 2025. Georgia Tech Research Institute. [Online] Accessed February 16, 2026. Available at: https://www.gtri.gatech.edu/newsroom/space-station-testing-will-evaluate-photovoltaic-materials,
(14) P. A. Makode, S. P. Muduli, P. Kale. “A perspective of GaAs//Si tandem photovoltaic cell: Architecture, fabrication, and performance,” February 20, 2025. Materials Research Bulletin (190), https://doi.org/10.1016/j.materresbull.2025.113504
(15) Helmholtz-Zentrum Berlin. “Photovoltaics: Generating electricity from sunlight,” Division Solar Energy [Online] Accessed February 16, 2026. Available at: https://www.helmholtz-berlin.de/forschung/unsere-forschung/photovoltaik/index_en.html
(16) National Research Council of Science and Technology. “Lighter and More Flexible Solar Cells Achieve World’s Highest Efficiency,” newswise. April 9, 2025. [Online] Accessed February 16, 2026. Available at: https://www.newswise.com/articles/lighter-and-more-flexible-solar-cells-achieve-world-s-highest-efficiency
(17) Uppsala University. “CIGS-Based Thin Film Solar Cells,” Department of Materials Science and Engineering: Research: Solar Cell Technology. February 12, 2026. [Online] Accessed February 16, 2026. Available at: https://www.uu.se/en/department/materials-science-and-engineering/research/divisions/solar-cell-technology/cigs-based-thin-film-solar-cells
(18) Julio C. Carrillo-Sendejas, José-Luis Maldonado; Progress in organic solar cells: Materials, challenges, and novel strategies for niche applications. APL Energy 1 June 2025; 3 (2): 021501. https://doi.org/10.1063/5.0267160
(19) R. Kennedy. “Organic solar cells for space demonstrate radiation resistance, self-healing,” January 10, 2025, [Online] Accessed February 16, 2026, Available at: https://pv-magazine-

usa.com/2025/01/10/organic-solar-cells-for-space-demonstrate-radiation-resistance-self-healing/

(20) A. Shahzad, H.J Jiang, K.F Aguey-Zinsou. “Unitized regenerative fuel cells: Fundamental challenges and advancements,” Renewable and Sustainable Energy Reviews, Volume 215, 2025, 115631, ISSN 1364-0321, https://doi.org/10.1016/j.rser.2025.115631

(21) B.V Kumar, K. Kentaro, and N.C Orger. “A review on design challenges and future opportunities of battery management system for low earth orbit nanosatellites.” Discov Appl Sci 8, 470 (2026). https://doi.org/10.1007/s42452-026-08369-8

(22) H. Fan. “Exploring the Relationship Between Lithium-ion Battery Mass and Energy Density,” September 17, 2025, [Online] Accessed February 16, 2026, Available at: https://www.large-battery.com/blog/lithium-ion-battery-weight-and-density-explained-guide/

(23) Amprius Technologies. “AALTO Zephyr Achieves World-Record 67-Day Flight Powered by Amprius Ultra-High-Energy Batteries,” Announcements. [Online] Accessed February 16, 2026, Available at: https://amprius.com/aalto-zephyr-achieves-world-record-67-day-flight-powered-by-amprius-ultra-high-energy-batteries/

(24) K. Sharma and A. Santasalo-Aarnio, “Energy storage systems for space applications,” Journal of Energy Storage, Volume 128, 2025, 117131, ISSN 2352-152X, https://doi.org/10.1016/j.est.2025.117131.

(25) P. Casado, J.M. Blanes, A. Garrigós, D. Marroquí, C. Torres, “Evaluation of commercial Li-Ion 18650 battery cells for deep space applications,” Journal of Power Sources, Volume 638, 2025, 236552, ISSN 0378-7753, https://doi.org/10.1016/j.jpowsour.2025.236552.

(26) D. Petrushenko, P. Coman, et al. “Scale-Up of PPR Battery Design for 21700 Format Cells,” NASA Aerospace Battery Workshop, November 14-16, 2023.

(27) I. Beyers, A. Bensmann, R. Hanke-Rauschenbach, “Ragone plots revisited: A review of methodology and application across energy storage technologies,” Journal of Energy Storage, Volume 73, Part D, 2023, 109097, ISSN 2352-152X, https://doi.org/10.1016/j.est.2023.109097.

(28) A. Rose, “Unlocking the potential of lithium-sulfur batteries,” Argonne National Laboratory Press release, January 13, 2025, [Online] Accessed February 16, 2026, Available at: https://www.anl.gov/article/unlocking-the-potential-of-lithiumsulfur-batteries

(29) A. Mateen, M. Suneetha, S. S. Ahmad Shah, M. Usman, T. Ahmad, I. Hussain, S. Khan, M. A. Assiri, A. M. Hassan, M. S. Javed, S. S. Han, R. H. Althomali, M. M. Rahman, Chem. Rec. 2024, 24, e202300235. https://doi.org/10.1002/tcr.202300235.

(30) R. Raffaelle. "Demonstration of a Nano-Enabled Space." 2018. [Online] Available at: https://ntrs.nasa.gov/archive/nasa/casi.ntrs.nasa.gov/20170011060.pdf

(31) S. Utsumi, S.K. Ujjain, S. Takahashi, et al. “Giant nanomechanical energy storage capacity in twisted single-walled carbon nanotube ropes,” National Nanotechnology 19, 1007–1015 (2024). https://doi.org/10.1038/s41565-024-01645-x

(32) P. Kumar Kanti, P. Kumar H G, V. Wanatasanappan, A. Kumar, M. B. Regasa, “Graphene's Frontier in aerospace: current applications, challenges, and future directions for space engineering,” Nanoscale Advances, Volume 7, Issue 12, 2025, Pages 3603-3618, ISSN 2516-0230, https://doi.org/10.1039/d4na00934g.

(33) K. B. M. Ismail, M. A. Kumar, S. Mahalingam, R. Jayavel, M. Arivanandhan, J. Kim, “Conducting polymer based electrodes in metal-ion batteries: A state-of-the-art review,” Renewable and Sustainable Energy Reviews, Volume 222, 2025, 115982, ISSN 1364-0321, https://doi.org/10.1016/j.rser.2025.115982.

(34) R.L. Karkkainen. "Development of Lightweight CubeSat with Multi-Functional Structural Battery Systems." 2018. [Online] Available at: https://ntrs.nasa.gov/archive/nasa/casi.ntrs.nasa.gov/20170011078.pdf
(35) C. Larsson, F. Larsson, J. Xu, et al. Electro-chemo-mechanical modelling of structural battery composite full cells. npj Computer Materials 11, 141 (2025). https://doi.org/10.1038/s41524-025-01646-x
(36) E. Martinez, "Nanomaterials for Space Exploration: Challenges and Opportunities," American Journal of Nano Science and Technology. VOL 06 ISSUE 03 2025
(37) V. Manzi-Orezzoli and C. Moldovan, "High Energy Density Supercapacitors for Space Applications," April 28, 2025, [Online] Accessed February 16, 2026, Available at: https://passive-components.eu/high-energy-density-supercapacitors-for-space-applications/
(38) B. Faure, L. Cosqueric, and V. Gineste. "Evaluation and Qualification of Commercial Off-The-Shelf Supercapacitors for Space." 2nd Space Passive Component Days (SPCD) International Symposium. Noordwijk, The Netherlands: s.n., 2016.
(39) SupercapTech. SupercapTech. May 21, 2016. [Online] Available at: https://www.supercaptech.com/battery-vs-supercapacitor
(40) POWERBOX. "The Silent Power of Supercapacitors." White paper 017. 2019.
(41) M. Soltani and S. H. Beheshti. "A comprehensive review of lithium -ion capacitor: development, modelling, thermal management and applications," Journal of Energy Storage, Volume 34, 2021.
(42) Y. Gupta, B. Shao, and F. Han, "Solid State Batteries Volume 1: Emerging Materials and Applications ACS Symposium Series; American Chemical Society: Washington, DC, 2022.
(43) Y.Lin, L. G.Somervill, R.Rashid, R. I.Ledesma, J. H.Kang, A. R.Kavanagh, J. S.Packard, C. H.Scrudder, A. L.Durgin, V. I.Yamakov, J.Su, D. A.Dornbusch, R. P.Viggiano, J. W.Connell, Toward 500 Wh Kg−1 in Specific Energy with Ultrahigh Areal Capacity All-Solid-State Lithium–Sulfur Batteries. Small2025, 21, 2409536. https://doi.org/10.1002/smll.202409536
(44) Miyazawa, Yu, Takanobu Shimada, Tetsuhito Fuse, Shuhei Shimada, Sousuke Nishiura, Hidetake Okamoto, Tetsuya Okawa, Takeshi Hoshino, Osamu Kawasaki, and Hitoshi Naito. 2025. "Space Demonstration of All-Solid-State Lithium-Ion Batteries Aboard the International Space Station" Aerospace 12, no. 6: 514. https://doi.org/10.3390/aerospace12060514.\
(45) Liu, H., Chen, Y., Chien, PH. *et al.* Dendrite formation in solid-state batteries arising from lithium plating and electrolyte reduction. *Nat. Mater.* **24**, 581–588 (2025). https://doi.org/10.1038/s41563-024-02094-6
(46) F.A. Sima, A. Ghafari, and S. Akbari, "Enhancing Solid-State Battery Performance through Advanced Thermal Management Techniques," NanoScience Technology, Volume 14 (2024), pp: 1-19.
(47) K. B. Chin *et al*., "Flight Demonstration of a Hybrid Battery/Supercapacitor Energy Storage System in an Earth Orbiting CubeSat," in *IEEE Aerospace and Electronic Systems Magazine*, vol. 36, no. 5, pp. 24-36, 1 May 2021, doi: 10.1109/MAES.2021.3052309.
(48) Adeyinka, A.M., Esan, O.C., Ijaola, A.O. et al. Advancements in hybrid energy storage systems for enhancing renewable energy-to-grid integration. Sustainable Energy res. 11, 26 (2024). https://doi.org/10.1186/s40807-024-00120-4.
(49) R. Bugga, C. Krause, K. Billings, J.P Ruiz, et al. "NASA Battery Workshop." November 19, 2019. Accessed May 16, 2020. [Online] Available at: https://www.nasa.gov/sites/default/files/atoms/files/3-nasa_battery_workshop_nov_2019_high_power_li-ion_cells_final.pdf

(50) S Marín-Coca, E Roibás-Millán, S Pindado, M A de Miguel and H Valente, “Hybrid energy storage systems for high power spacecraft missions,” Published under license by IOP Publishing Ltd, Journal of Physics: Conference Series, Volume 2716, 012097, DOI 10.1088/1742-6596/2716/1/012097

(51) Amina Daghouri, Soumia El Hani, Youssef El Hachimi, Hamza Mediouni, Enhanced hybrid energy storage system combining battery and supercapacitor to extend nanosatellite lifespan, Results in Engineering, Volume 23, 2024, 102634, ISSN 2590-1230, https://doi.org/10.1016/j.rineng.2024.102634

(52) https://passive-components.eu/wp-content/uploads/2025/04/ORAL_Day-2_20_Algerian-Space-Agency_Hybrid-Energy-Storage-Supercapacitors.pdf

(53) https://pmarketresearch.com/auto/power-conditioning-and-distribution-unit-pcdu-for-small-satellite-market/

(54) “Comprehensive analysis of Cubesat electrical power systems for efficient energy management,” Usama Shakoor 1 · Mohanad Alayedi2 · Ebrahim E. Elsayed, | https://doi.org/10.1007/s43937-025-00069-5

(55) NASA’s Mars Campaign Office, “Advanced Modular Power Systems (AMPS),” TechPort, December 15, 2025, https://techport.nasa.gov/projects/10759



Chapter Contents

Chapter Glossary ii
4.0 In-Space Propulsion 60
4.1 Introduction 60
4.1.1 Document Organization 60
4.2 Public Data Sources and Disclaimers 60
4.3 Definitions 61
4.4 Technology Maturity 61
4.4.1 Application of the TRL Scale to Small Spacecraft Propulsion Systems 61
4.4.2 Progress Toward Mission Infusion (PMI) 62
4.5 Overview of In-Space Propulsion Technology Types 65
4.6 State-of-the-Art in Small Spacecraft Propulsion 67
4.6.1 In-Space Chemical Propulsion 67
4.6.2 In-Space Electric Propulsion 80
4.6.3 In-Space Propellant-less Propulsion 101
References 118

Chapter Glossary

(ABS)	Acrylonitrile Butadiene Styrene
(AC)	Alternating Current
(ACO)	Announcement for Collaborative Opportunity
(ACS)	Attitude Control System
(ADN)	Ammonium Dinitramide
(AFRL)	Air Force Research Laboratory
(AIS)	Applied Ion Systems
(AOCS)	Attitude and Orbit Control System
(AR)	Aerojet Rocketdyne
(ARC)	Ames Research Center
(ACE)	Astra Spacecraft Engine
(BOL)	Beginning of Life
(CHIPS)	CubeSat High Impulse Propulsion System
(CMNT)	Colloid MicroNewton Thrusters
(CNAPS)	Canadian Nanosatellite Advanced Propulsion System
(CNES)	French National Center for Space Studies
(CPOD)	CubeSat Proximity Operations Demonstration
(CUA)	CU Aerospace LLC
(DFMR)	Design for Minimum Risk
(DRM)	Design Reference Mission
(DSSP)	Digital Solid State Propulsion LLC
(EOL)	End of Life
(EMC)	Electromagnetic Compatibility
(EMI)	Electromagnetic Interference
(EP)	Electric Propulsion
(EPL)	Electric Propulsion Laboratory, Inc.
(EPSS)	Enabling Propulsion System for Small Satellites
(ESA)	European Space Agency
(ESP)	Electrically Controlled Solid Propellant
(FASTSAT)	Fast, Affordable, Science and Technology Satellite
(FEEP)	Field Emission Electric Propulsion
(FPPT)	Fiber-Fed Pulsed Plasma Thruster



(GEO)	Geostationary Equatorial Orbit
(GIT)	Gridded-ion Thrusters
(GOCE)	Gravity Field and Steady-State Ocean Circulation Explorer
(GOX)	Gaseous Oxygen
(GPIM)	Green Propellant Infusion Mission
(GPS)	Global Positioning System
(GRC)	Glenn Research Center
(GSFC)	Goddard Space Flight Center
(HAN)	Hydroxylammonium Nitrate
(HET)	Hall-effect Thruster
(HTP)	High Test Peroxide
(HTPB)	Hydroxyl-terminated Polybutadiene
(IPS)	Integrated Propulsion System
(ISS)	International Space Station
(JANNAF)	Joint Army Navy NASA Air Force
(JHU ERG)	Johns Hopkins University Energetics Research Group
(JPL)	Jet Propulsion Laboratory
(LFPS)	Lunar Flashlight Propulsion System
(LISA)	Laser Interferometer Space Antenna
(MAPS)	Modular Architecture Propulsion System
(MarCO)	Mars Cube One
(MCD)	Micro-Cavity Discharge
(MEMS)	Microelectromechanical System
(MEO)	Medium Earth Orbit
(MMH)	Monomethyl Hydrazine
(MPUC)	Monopropellant Propulsion Unit for CubeSats
(MSFC)	Marshall Space Flight Center
(MVP)	Monofilament Vaporization Propulsion
(N_2O)	Nitrous Oxide
(NEA)	Near-Earth Asteroid
(NODIS)	NASA Online Directives Information System
(NSTT)	Nanosat Terminator Tape
(OTV)	Orbital Transfer Vehicle
(PacSci EMC)	Pacific Scientific Energetic Materials Company

(PBM)	Plasma Brake Module
(PMD)	Propellant Management Device
(PMI)	Progress toward Mission Infusion
(PMMA)	Polymethyl Methacrylate
(PPT)	Pulsed Plasma Thrusters
(PPU)	Power Processing Unit
(PTD)	Pathfinder Technology Demonstration
(PTFE)	Polytetrafluoroethylene
(PUC)	Propulsion Unit for CubeSats
(ROMBUS)	Rapid Orbital Mobility Bus
(SAA)	Space Act Agreement
(SBIR)	Small Business Innovation Research
(SCAPE)	Self-Contained Atmospheric Protective Ensemble
(SEP)	Solar Electric Propulsion
(SMAP)	Soil Moisture Active Passive
(SMART-1)	Small Missions for Advanced Research in Technology
(SME)	Subject Matter Experts
(SSTP)	Small Spacecraft Technologies Program
(TCMs)	Trajectory Correction Maneuvers
(TMA)	Technology Maturity Assessment
(TRL)	Technology Readiness Level
(UTIAS)	University of Toronto Institute for Aerospace Research
(VAT)	Vacuum arc thrusters
(VENuS)	Vegetation and Environment monitoring on a New Microsatellite
(WFF)	Wallops Flight Facility

4.0 In-Space Propulsion

4.1 Introduction

In-space propulsion devices for small spacecraft are rapidly increasing in number and variety. A surge in public and private investments in small spacecraft propulsion technologies, combined with the immaturity of the overall small spacecraft market, has resulted in an abundance of confusing, unverified, sometimes conflicting, and otherwise incomplete technical literature. Furthermore, the rush by many device developers to secure market share has resulted in uncertainty regarding the true readiness of these devices for mission infusion. As third parties independently verify device performance, and end-users demonstrate these new devices in their target environments, the true maturity, capability, and flight readiness of these devices will become clearer. In the meantime, this report will attempt to reduce confusion by compiling publicly described small spacecraft propulsion devices, identifying publicly available technical literature, highlighting missions of potential interest, and organizing the data to improve comprehension.

4.1.1 Document Organization

This chapter organizes the state-of-the-art in small spacecraft propulsion into the following categories:

1. In-Space Chemical Propulsion (4.6.1)
2. In-Space Electric Propulsion (4.6.2)
3. In-Space Propellant-less Propulsion (4.6.3)

Each of these categories is further subdivided by prevailing technology types. These subsections organize each technology type as follows:

a. Technology Description
b. Key Integration and Operational Considerations
c. Current & Planned Missions
d. Summary Table of Devices
e. Notable Advancements

The organizational approach introduces each technology, outlines key integration and operational considerations, highlights recent or planned missions that may advance flight readiness, and tabulates procurable devices. Some sections also include an incomplete list of notable advancements. While the key integration and operational considerations are not comprehensive, they provide insights that may influence propulsion system decisions.

4.2 Public Data Sources and Disclaimers

This chapter is a survey of small spacecraft propulsion technologies discussed in open literature and does not serve as an original source. As such, this chapter only considers literature found in the public domain to identify and classify propulsion devices. Commonly used sources for public data include manufacturer datasheets, press releases, conference papers, journal papers, public filings with government agencies, and news articles.

This chapter summarizes device performance, capabilities, and flight history, as presented in publicly available literature. Data not appropriate for public dissemination, such as proprietary, export controlled, or otherwise restricted data, are not considered. Actual device maturity and flight history may differ from what is documented herein. Device manufacturers should be consulted for the most up-to-date and relevant data.

This chapter's primary data source is literature produced by device manufacturers. Unless otherwise stated, do not assume independent verification of device performance. Performance and capabilities described may be speculative or otherwise based on limited data.

The information presented is not intended to be exhaustive but rather to provide an overview of the current state-of-the-art technologies and their development status. It should be noted that technology maturity designations may vary with changes to payload, mission requirements, reliability considerations, and/or the environment in which performance was demonstrated. Readers are highly encouraged to reach out to companies for further information regarding the performance and maturity of these products. There is no intention of mentioning certain companies and omitting others based on their technologies or relationship with NASA.

The propulsion market is rapidly evolving, and the authors have limited time to thoroughly scour public databases. We increasingly depend on device manufacturers to provide corrections to NASA. Suggestions or corrections for this document should be submitted to the NASA Small Spacecraft Virtual Institute Agency-SmallSat-Institute@mail.nasa.gov for consideration prior to the publication of future issues.

4.3 Definitions

- *Device* refers to a component, subsystem, or system, depending on the context.
- *Technology* refers to a broad category of devices or intangible materials, such as processes.

4.4 Technology Maturity

4.4.1 Application of the TRL Scale to Small Spacecraft Propulsion Systems

NASA has a well-established guideline for performing Technology Maturity Assessment (TMA), described in detail in the NASA Systems Engineering Handbook (1). A TMA determines a device's technological maturity, which is usually communicated according to the NASA Technology Readiness Level (TRL) scale. The TRL scale is defined in NASA Procedural Requirements (NPR) 7123 (2). The NASA Systems Engineering Handbook and NPR 7123 can be accessed through the NASA Online Directives Information System (NODIS) library. Assessment of TRLs for components, systems, or software allows for clear communication between technologists, program managers, and other stakeholders regarding the maturity of a technology. Furthermore, TRL is a valuable tool to communicate the risk associated with the infusing technologies into programs. For TRLs to be applied across all technology categories, the NASA TRL definitions are written broadly and rely on subject matter experts (SME) in each discipline to interpret appropriately.

Recently, U.S. Government propulsion SMEs proposed an interpretation of the TRL scale specifically for micro-propulsion. The Micro-Propulsion Panel of the JANNAF Spacecraft Propulsion Subcommittee in 2019 published the *JANNAF Guidelines for the Application of Technology Readiness Levels (TRLs) to Micro-Propulsion Systems* (3). The guideline was updated in 2022 to reflect the latest community input (4). This guideline suggests an interpretation of TRL for micro-propulsion and reflects both NASA and DoD definitions. The JANNAF panel consisted of participants from the Air Force Research Laboratory (AFRL), Glenn Research Center (GRC), Jet Propulsion Laboratory (JPL), and Goddard Space Flight Center (GSFC). The panel received further feedback from the non-Government propulsion community. While this JANNAF guideline focuses on micro-propulsion (e.g., CubeSats), it remains relevant for rigorously assessing TRLs across the broader category of small spacecraft in-space propulsion. By establishing a common interpretation of TRL for small spacecraft propulsion, technology maturity

can be communicated more coherently and consistently between providers and stakeholders. The JANNAF guideline is open to unlimited distribution and may be requested from the Johns Hopkins University Energetics Research Group (JHU ERG). Ensure the use of the latest JANNAF guideline, as the guideline may continue to evolve with further community input.

A fundamental limitation of the JANNAF guideline for TRL assessment, and TMA in general, is the assumption of in-depth technical knowledge of the subject device. In the absence of detailed technical knowledge, especially in a broad technology survey as presented herein, a TMA may be conducted inaccurately or inconsistently. Furthermore, TRL assessment assumes an understanding of the end-user application. The same device may be assessed as being at different TRLs for infusion into different missions. For example, a device may be assessed at a high TRL for application to low-cost small spacecraft in low-Earth orbits, while it may be assessed at a lower TRL for application to geosynchronous communication satellites or NASA interplanetary missions due to differences in mission requirements. Differences in TRL assessment based on the operating environment may result from considerations such as thermal environment, mechanical loads, mission duration, or radiation exposure. Propulsion-specific variances between missions might include propellant type, total propellant throughput, throttle set-points, burn durations, and the total number of on/off cycles. As such, an accurate TRL assessment not only requires an in-depth technical understanding of a device's development history, including specifics on past flight qualification activities, but also an understanding of mission-specific environments and interfaces. The challenge of assessing an accurate TRL in a broad technology survey poses a significant burden on data collection, organization, and presentation. Such activities are better suited for programs seeking to infuse new technologies into their missions.

Given the rapid evolution of small spacecraft propulsion technologies and the variety of mission environments, as well as generally limited technical details on devices in open literature, the propulsion chapter implements a novel system to classify technical maturity according to Progress toward Mission Infusion (PMI). This novel classification system is not intended to replace TRL but serves as a complementary tool to provide initial insight into device maturity when the TRL scale cannot yet be applied accurately and consistently. This novel classification system is discussed in detail below.

Readers are strongly encouraged to perform more in-depth technical research on candidate devices based on the most up-to-date information available, as well as to assess risk within the context of their specific mission(s). A thoughtful TMA based on the examination of detailed technical data through consultation with device manufacturers can reduce program risk and increase the likelihood of mission success. This survey is not intended to replace the readers' own due diligence. Rather, this survey and PMI seek to provide early insights that may assist in down-selecting propulsion systems to a smaller set of candidate devices where an in-depth TMA becomes feasible.

4.4.2 Progress Toward Mission Infusion (PMI)

Rather than directly assessing a device's technical maturity via TRL, propulsion devices described herein are classified according to evidence of progress toward mission infusion. This is a novel classification system first introduced in this survey. Assessing the PMI of devices in a broad survey, where minimal technical insight is available, may assist with down-selecting propulsion devices early in mission concept development. Once a handful of devices are identified as possible solutions for a specific mission concept, a detailed TMA and rigorous TRL assessment should be conducted. The PMI classification system sorts devices into one of four broad technology development categories: Concept, In-Development, Engineering-to-Flight, and Flight-

Demonstrated. The following sections describe the PMI classification system in detail. Furthermore, Figure 4.1 summarizes the PMI classifications.

Concept, 'C'

The *Concept* classification reflects devices in an early stage of development, characterized by feasibility studies and the demonstration of fundamental physics. Concept devices typically align with the NASA TRL range of 1 to 3. At a minimum, these devices are established as scientifically feasible, perhaps through a review of relevant literature and/or analysis. These devices may even include experimental verification that supports the validity of the underlying physics and notional designs. While Concept devices are generally not reviewed herein, noteworthy concept devices will be classified in tables with a 'C'.

In-Development, 'D'

The *In-Development* classification reflects most devices being actively matured by industry, where only a modest number of devices may progress to spaceflight. In-Development devices typically align with the NASA TRL range of 4 to 5. While In-Development devices may have specific applications identified by their developers, no selection for a specific mission has been publicly announced. In the absence of a specific mission, device development activities typically lack rigorous system requirements and independent requirement validation. Furthermore, qualification activities conducted in the absence of a specific mission typically require delta-qualification to address mission-specific requirements. At a minimum, In-Development devices are low-fidelity devices that have been operated in an appropriate environment to demonstrate basic functionality and support prediction of the device's ultimate capabilities. They may even be medium- or high-fidelity devices operated in a simulated final environment, but lacking a specific mission pull to refine requirements and develop a robust qualification program. They may even be medium- or high-fidelity devices operated in a spaceflight demonstration but lack sufficient fidelity or demonstrated capability to reflect the anticipated final product. These devices are typically described as a technology push, rather than a mission pull. In-Development devices will be classified in tables with a 'D'.

Engineering-to-Flight, 'E'

The *Engineering-to-Flight* classification reflects devices with a publicly announced spaceflight opportunity. This classification does not necessarily imply greater technical maturity than the In-Development classification, but it does assume the propulsion device developer receives mission-specific requirements to guide final development and qualification activities. Furthermore, the Engineering-to-Flight classification assumes a mission team performed due diligence in the selection of a propulsion device, and the mission team regularly validates that the propulsion system requirements are met. Thus, while the PMI classification system does not directly assess technical maturity, there is an underlying assumption of independent validation of mission-specific requirements, where a mission team directly considers technical maturity in the process of device selection and mission infusion. Engineering-to-Flight devices typically align with the NASA TRL range of 5 to 6. At a minimum, these are medium-fidelity devices that have been operated in a simulated final environment and demonstrate key capabilities relative to the requirements of a specific mission. These devices may even be actively undergoing or have completed a flight qualification program. These devices may even include a spaceflight, but in which key capabilities were not demonstrated or further engineering is required. These devices may even include successful spaceflights, but the devices are now being applied in new environments or platforms

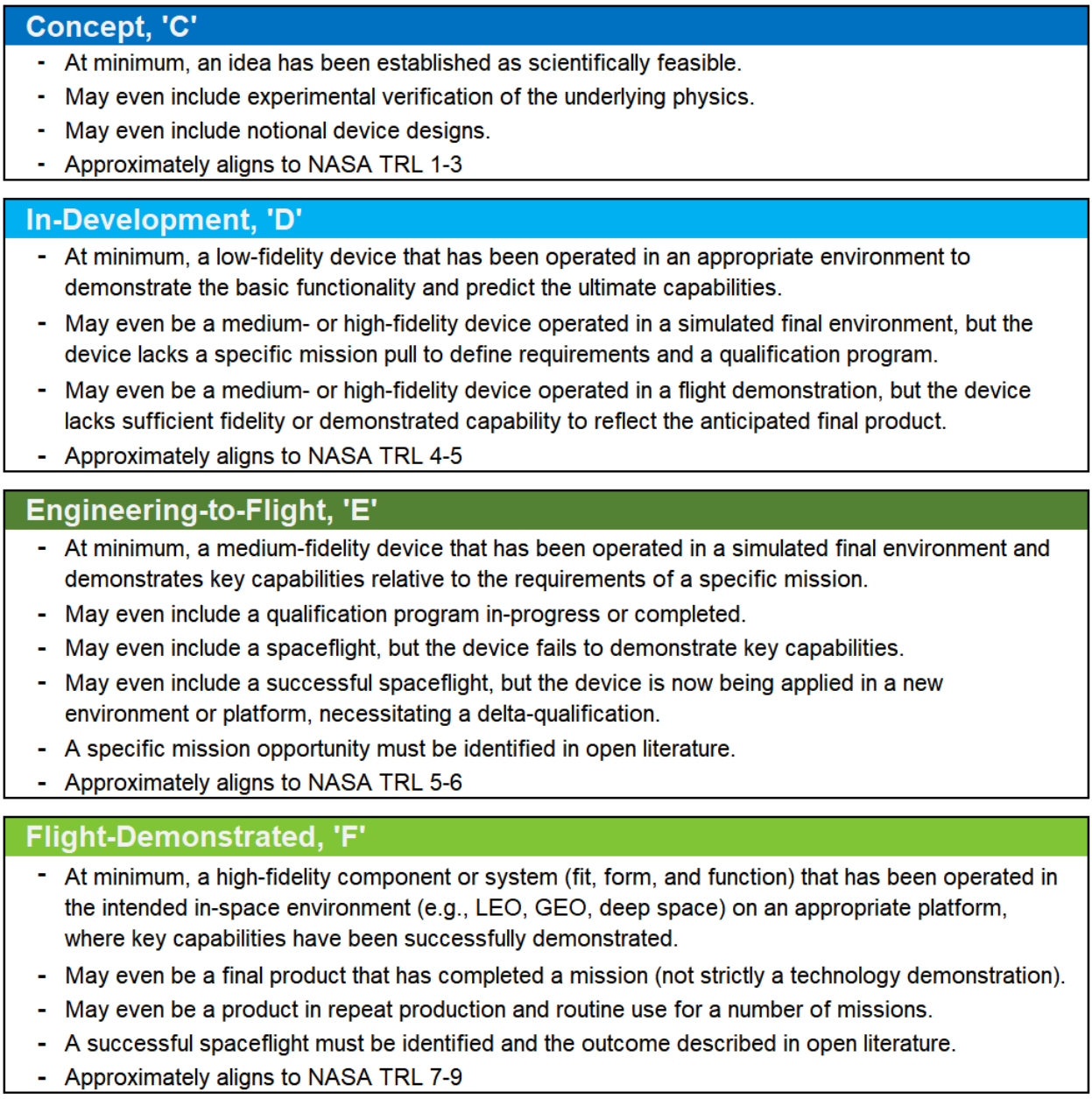


Figure 4.1: Progress toward mission infusion (PMI) device classifications. Credit: NASA.

that necessitate design modifications and/or delta-qualification. These devices must have one or more mission documented in open literature. Engineering-to-Flight devices will be classified in tables with an ‘E’.

Flight-Demonstrated, ‘F’

The *Flight-Demonstrated* classification reflects devices where a successful technology demonstration or genuine mission has been conducted and described in open literature. Flight-Demonstrated devices typically align with the NASA TRL range of 7 to 9. These devices are high-fidelity components or systems (in fit, form, and function) that have been operated in the target in-space environment (e.g., low-Earth orbit, GEO, deep space) on an appropriate platform, where all key capabilities were successfully demonstrated. These devices may even be final products,

that have completed genuine missions (not flight demonstrations). These devices may even be in repeat production and routine use for several missions. The devices must be described in open literature as successfully demonstrating key capabilities in the target environment to be considered Flight-Demonstrated. If a device has flown, but the outcome is not publicly known, the classification will remain Engineering-to-Flight. Flight-Demonstrated devices will be classified in tables with an 'F'.

4.5 Overview of In-Space Propulsion Technology Types

In-space small spacecraft propulsion technologies are generally categorized as (i) chemical, (ii) electric, or (iii) propellant-less. This chapter surveys propulsion devices within each technology category. Additionally, liquid-propellant acquisition and management devices are reviewed as an important component of in-space propulsion systems. Although other key subsystems have not yet been reviewed, such as power processing units, they may be included in future updates of this publication. Table 4-1 lists the in-space propulsion technologies reviewed. Figure 4.2 graphically illustrates the range of thrust and specific impulse for these small spacecraft propulsion devices. The thrust and specific impulse ranges provided in Table 4-1 and Figure 4.2 only summarize the performance of small spacecraft devices covered in this survey and may not reflect the broader capability of the technologies beyond small spacecraft or the limits of what is physically possible with further advancement. Furthermore, propulsion systems are often highly throttleable, and the devices surveyed herein may in many cases be capable of offering performance beyond the ranges presented in Table 4-1.

Chemical systems have enabled in-space maneuvering since the onset of the space age, proving highly capable and reliable. These include hydrazine-based systems, other mono- or bipropellant systems, hybrids, cold gas systems, and solid propellants. Typically, these systems are used when high thrust or rapid maneuvers are required. As such, chemical systems continue to be the in-space propulsion technology of choice when their total impulse capability is sufficient to meet mission requirements.

On the other hand, the application of electric propulsion devices has been historically more limited. While electric propulsion can provide an order of magnitude greater total impulse than chemical systems, research and development costs have typically eclipsed those of comparable chemical systems. Furthermore, electric propulsion generally provides thrust-to-power levels below 75 mN/kW. Thus, a small spacecraft capable of delivering 500 W to an electric propulsion system may generate no more than 38 mN of thrust. Therefore, while the total impulse capability of electric propulsion is generally considerable, these systems may need to operate for hundreds or thousands of hours, compared to the seconds or minutes required by chemical systems to achieve a similar impulse. That said, the high total impulse and low thrust requirements of many applications, such as station keeping, have maintained steady investment in electric propulsion over the decades. Only in recent years has the mission pull for electric propulsion reached a tipping point where it has overtaken chemical for specific in-space applications. Electric propulsion system types considered herein include electrothermal, electrospray, gridded ion, Hall-effect, pulsed plasma and vacuum arc, and ambipolar.

Propellant-less propulsion technologies such as solar sails, tethers, electric sails (and plasma brakes), and aerodynamic drag devices have long been investigated, but they have yet to move beyond small-scale demonstrations. However, growing needs such as orbital debris removal may offer compelling future applications.

Some notable categories are not covered in this survey, such as nuclear in-space propulsion technologies. While substantial investment continues in such areas for deep space science and

human exploration, such technologies are generally at lower TRL and typically aim to propel spacecraft substantially larger than the 180 kg wet mass limit considered in this report.

Whenever possible, this survey considers complete propulsion systems, which are composed of thrusters, feed systems, pressurization systems, propellant management and storage, and power processing units, but not the electric power supply. However, for some categories, components (e.g., thruster heads) are mentioned without consideration of the remaining subsystems necessary for full implementation. Depending on the device's intended platform (i.e., NanoSat, MicroSat, SmallSat), the propulsion system may be either highly integrated or distributed within the spacecraft. As such, it is logical to describe highly integrated propulsion units at the system level, whereas components of distributed propulsion systems may be logically treated at the sub-system level, where components from a multitude of manufacturers may be mixed and matched to create a unique mission-appropriate propulsion solution.

Table 4-1: Summary of Propulsion Technologies Surveyed

Technology	Thrust Range	Specific Impulse Range [sec]
4.6.1 CHEMICAL PROPULSION TECHNOLOGIES		
Hydrazine Monopropellant	0.25 – 28 N	180 – 285
Alternative Mono- and Bipropellants	50 mN – 22 N	150 – 310
Hybrids	8 – 222 N	215 – 300
Cold Gas	10 μN – 3.6 N	40 – 110
Solid Motors	37 – 461 N	187 – 269
Propellant Management Devices	-	-
4.6.2 ELECTRIC PROPULSION TECHNOLOGIES		
Electrothermal	0.1 mN – 1 N	20 – 350
Electrosprays	20 μN – 20 mN	225 – 3,000
Gridded Ion	0.1 – 20 mN	500 – 3,000
Hall-Effect	0.25 – 55 mN	200 – 1,920
Pulsed Plasma and Vacuum Arc Thrusters	4 – 500 μN	87 – 3,200
Ambipolar	0.5 – 17 mN	400 – 1,100
4.6.3 PROPELLANTLESS PROPULSION TECHNOLOGIES		
Solar Sails	TBD	-
Tethers	TBD	-
Electric Sails	TBD	-
Aerodynamic Drag	TBD	-

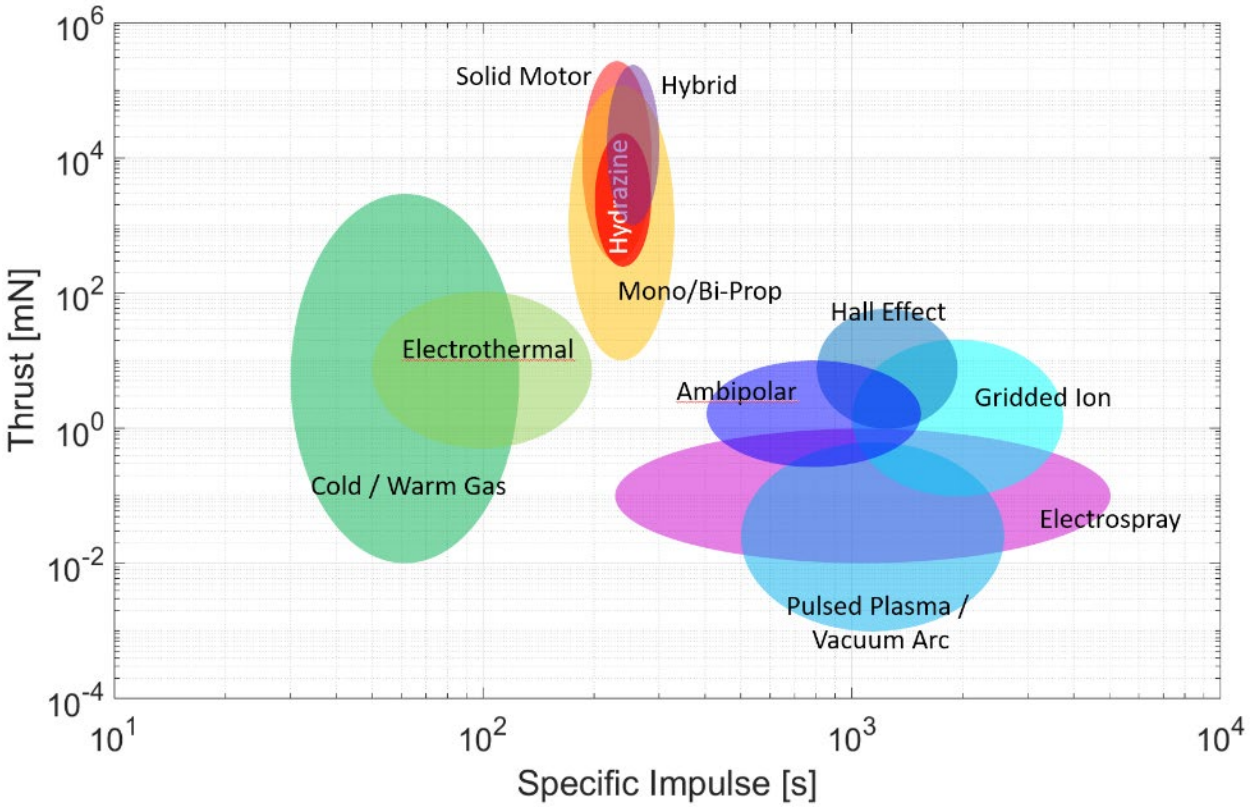


Figure 4.2: Typical small spacecraft in-space propulsion trade space (thrust vs. specific impulse). Credit: NASA.

4.6 State-of-the-Art in Small Spacecraft Propulsion

4.6.1 In-Space Chemical Propulsion

In-space chemical propulsion systems represent the most well-established of the space propulsion technologies. Chemical propulsion systems generate thrust by accelerating high-pressure gas, created by combustion or propellant decomposition and accelerated through a nozzle to supersonic speeds. Chemical propulsion systems are designed to satisfy high-thrust impulsive maneuvers. They offer lower specific impulse compared to their electric propulsion counterparts but have significantly higher thrust-to-power ratios.

Hydrazine Monopropellant

a. Technology Description

Hydrazine monopropellant systems use catalyst structures (such as S-405 granular catalyst) to decompose hydrazine to produce hot gases. Hydrazine thrusters and systems have been in extensive use since the 1960s. The low mass and volume of many heritage hydrazine propulsion systems make them suitable for small spacecraft buses, and some hydrazine thrusters used on large spacecraft may be appropriate as the main propulsion system for small spacecraft. Hydrazine thrusters typically achieve a specific impulse between 200–235 seconds for 1-N class or larger thrusters.

b. Key Integration and Operational Considerations

- **Extensive Flight Heritage:** Since hydrazine has been used extensively in spaceflight applications, the technology's traits are well understood (5).
- **Extensive Component Ecosystem:** A robust ecosystem of components and experience exists because hydrazine systems are widely used. As such, hydrazine propulsion systems are frequently customized for specific applications using the available components.
- **Multiple Cold Restarts:** These systems have typically been qualified for multiple cold starts.
- **Extensive Safety and Handling Requirements:** Hydrazine and its derivatives are corrosive, toxic, and potentially carcinogenic. Its vapor requires the use of Self-Contained Atmospheric Protective Ensemble (SCAPE) suits. This overhead must be considered when planning ground-processing workflows for spacecraft and may impose undesirable constraints on the spacecraft, the launch provider, or other spacecraft participating in the same launch opportunity. Hydrazine propulsion systems typically incorporate redundant serial valves to prevent spills or vapor leaks, which might harm ground personnel or hardware.

c. Current & Planned Missions

ArianeGroup has developed a 1-N class hydrazine thruster that has extensive flight heritage, including use on the ALSAT-2 small spacecraft (6) (7). The company also offers a 20-N hydrazine thruster with extensive flight history, although not with small spacecraft.

Aerojet-Rocketdyne (L3Harris company) has several small hydrazine thrusters with extensive flight histories. The 0.09-N MR-401, 1-N MR-103 series, 4-N MR-111G, and the 22-N MR-106L hydrazine thrusters are flight proven (8) (9) (10). In addition to four MR-107S 222-N thrusters, the OSIRIS-Rex spacecraft propulsion system has six MR-106L, sixteen MR-111G, and two MR-401 thrusters (11).

Moog has the 1-N MONARC-1, 5-N MONARC-5, and 22-N MONARC-22 series hydrazine thrusters (12). These thrusters have decades-long flight histories, although primarily as attitude control thrusters in larger satellites. NASA JPL's Soil Moisture Active/Passive (SMAP) spacecraft used eight MONARC-5 thrusters (13).

Northrop Grumman has a line of hydrazine thrusters with long flight histories as attitude control thrusters for larger satellites. The thruster line includes the 0.4-N MRE-0.1, 4.4-N MRE-1.0, and 18-N MRE 4.0 (14).

Rafael offers 1-N, 5-N, and 25-N flight proven hydrazine thrusters (15).

IHI Aerospace offers the 1-N MT-9, 4-N MT-8A, and 20-N MT-2 flight proven hydrazine thrusters (16).

Stellar Exploration Inc. developed a customizable propulsion system for small satellites. A pump-fed hydrazine monopropellant version was supplied for the EchoStar EG3 spacecraft and the Cislunar Autonomous Positioning System Technology Operations and Navigation Experiment (CAPSTONE) spacecraft. The EchoStar nanosatellite built by Tyvak has been successfully commissioned and placed in orbit (17). The CAPSTONE spacecraft was similarly built by Tyvak and launched on a Rocket Lab Electron from New Zealand on 28 June 2022. The CAPSTONE spacecraft is a 12U, 25 kg CubeSat that will help reduce risk for future lunar spacecraft by validating navigation technologies and verifying the dynamics of a halo orbit. Although

CAPSTONE experienced communication and propulsion challenges during the mission, the spacecraft achieved the expected lunar orbit (18) (19) (20).

d. Summary Table of Devices

See Table 4-2 for current state-of-the-art hydrazine monopropellant devices applicable to small spacecraft.

Alternative Monopropellants and Bipropellants

a. Technology Description

For the past several decades, Earth-storable propellants (i.e., storable at room temperature) have dominated in-space chemical propulsion systems, hydrazine for monopropellants and nitrogen tetroxide with either monomethylhydrazine or hydrazine for bipropellants. These propellants have the advantages of being ambient-temperature liquids (thus not requiring extensive thermal management) and easy to ignite (catalyst for hydrazine, hypergolic for bipropellants). However, due to the extensive handling and toxicity concerns of conventional chemical propellants, more propulsion systems using alternate propellants have been developed and adopted. Often described as “green” propellants, these alternative propellants are not necessarily benign but are not vapor hazards like conventional Earth-storable propellants and thus do not require specialized suits and breathing apparatus for handling.

Alternative monopropellants based on ionic liquids have received extensive technological development in recent years and have matured to flight-ready status. Ionic liquid monopropellants are ionic salts dissolved in water and blended with a fuel. Catalysts react the aqueous ionic salt and fuel blend for combustion. Thus, these formulations are not true monopropellants, since they have fuel and oxidizer components, but they are functionally no different than monopropellants.

The two mature ionic liquid monopropellant blends are LMP-103S, which is based on ammonium dinitramide (ADN) and ASCENT (Advanced Spacecraft Energetic Non-Toxic), formally referred to as AF-M315E, which is based on Hydroxylammonium Nitrate (HAN). These monopropellants do not present a vapor hazard and can be handled with conventional personal protection equipment (gloves, face shield). Depending on the formulations, they can also offer higher specific impulse and higher density-specific impulse than monopropellant hydrazine. The challenges with ionic liquid monopropellants are that their catalysts require more preheating than hydrazine and their higher combustion temperatures require higher temperature, more expensive catalyst and chamber materials. The ionic liquid monopropellants are not drop-in replacements for hydrazine, although their propulsion system components are similar.

Hydrogen peroxide is a high-density liquid that can be catalytically decomposed exothermically like hydrazine. Hydrogen peroxide does not present a vapor hazard, although high concentrations (>90%) can rapidly react with impurities in storage containers. Hydrogen peroxide was used extensively in the early days of space propulsion before losing favor to higher-performing hydrazine. It is now being examined again as a nontoxic alternative to hydrazine. Development efforts have focused on high-test peroxide (HTP), which has concentrations from 85–98%.

Green bipropellant combinations have also been developed, particularly for small spacecraft propulsion. For example, hydrogen peroxide and nitrous oxide have been explored as an oxidizer with alcohol as the fuel. Another example is an electrolysis system that breaks down liquid water into gaseous hydrogen and oxygen, which serve as fuel and oxidizer, respectively.

b. Key Integration and Operational Considerations

- **Improved Hazard Safety Classifications:** Air Force Range Safety AFSPCMAN91-710 (21) requirements state that if a propellant is less prone to external leakage, which is often seen with the ionic liquid "green" propellant systems due to higher viscosity, then the hazardous classification is reduced. External hydrazine leakage is considered "catastrophic," whereas using ionic liquid green propellants reduces the hazard severity classification to "critical" and possibly "marginal" per MIL-STD-882E (Standard Practice for System Safety) (22). A classification of "critical" or less only requires two seals to inhibit external leakage, meaning no additional latch valves or other isolation devices are required in the feed system (22). While these propellants are not safe for consumption, they have been shown to be less toxic compared to hydrazine. This is primarily due to green propellants having lower vapor pressures, being less flammable, and producing more benign gases (such as water vapor, hydrogen, and carbon dioxide) when combusted.
- **Simplified Safety and Handling Requirements:** Fueling spacecraft with green propellants, generally permitted as a parallel operation, may require a smaller exclusion zone, allowing for accelerated launch readiness operations (23). These green propellants are also generally less likely to undergo exothermic decomposition at room temperature due to higher ignition thresholds. Therefore, they require fewer inhibit requirements, fewer valve seats for power, and less stringent storage temperature requirements. The reduced hazard associated with some of these propellants may enable projects to take a Design for Minimum Risk (DFMR) approach to address propulsion system safety concerns, but only with the support of associated range and payload safety entities.
- **Immature Component Ecosystem:** While there are thrusters that are relatively mature, incorporating them into integrated propulsion systems is challenging, and the maturity of standalone propulsion systems has lagged the pace of component development. Historically, research and development efforts, such as Small Business Innovation Research (SBIR) efforts, have focused on component development, and not the entire system. Efforts are now being made to focus on the development of system solutions. Most of these non-toxic propellants are still in some phase of development. Additionally, data on the propellants are widely restricted. Therefore, a comprehensive, public, peer-reviewed database of compatible materials does not currently exist, and prospective system developers using these propellants may have difficulty accessing such data to guide their efforts.
- **Other Considerations for Green Propellants:** Other "green" propellants such as Hydrogen Peroxide, High Test Peroxide (HTP), and HTP/Alcohol bipropellants also have their own unique handling considerations. For instance, HTP is a strong oxidizer and can exothermically decompose rapidly if improperly stored or handled. Hydrogen Peroxide, however, has been used as a rocket propellant for many decades, and there is extensive information on safe handling, materials selection, and best practices. Electrolyzed water is another propellant option, wherein water is decomposed into hydrogen and oxygen and combusted as a traditional bipropellant thruster. However, generating and managing the power required to electrolyze the water in a compact spacecraft presents unique challenges. Yet it does provide a safe-to-launch system with very benign constituents.

c. Current & Planned Missions

ECAPS offers a range of High-Performance Green Propulsion (HPGP) thrusters, including the LMP-103S (Figure 4.3), at 100-mN, 1-N, 5-N, and 22-N thrust levels. The 1-N HPGP thrusters were first demonstrated on orbit in the Prototype Research Instruments and Space Mission technology Advancement (PRISMA) mission completed in June 2011. PRISMA consisted of two small satellites, each carrying hydrazine and HPGP systems to enable a side-by-side comparison of their performance (24).



Figure 4.3: ECAPS HPGP thruster. Credit: Bradford ECAPS.

ECAPS developed an LMP-103S based propulsion system for a constellation of Earth observing satellites, called SkySat. SkySat has a propulsion system that uses four 1-N HPGP thrusters. As of 2018, thirteen SkySat satellites with the ECAPS propulsion system had been launched and were fully operational (25).

The ECAPS LMP-103S propulsion system is also used on the Autoscale demonstration of rendezvous technologies called ELSA-d, which launched in March 2021. ELSA-d has eight 1-N ECAPS HPGP thrusters to provide re-orbiting and de-orbiting capability. A system issue impacted three of the eight ECAPS thrusters and an unresolved root cause resulted in the loss of a fourth thruster. Nevertheless, many mission goals were successfully accomplished, improving the provider's readiness for offering a commercial deorbit service (26).

VACCO provided a hybrid Micro Propulsion System (MiPS) for the ArgoMoon 6U CubeSat built for the Italian Space Agency. The ArgoMoon MiPS, Figure 4.4, has an ECAPS 100mN LMP-103S thruster with four VACCO 25-mN R134a cold gas thrusters. ArgoMoon was successfully deployed in the Artemis I mission in November 2022 (27) (28) (29).

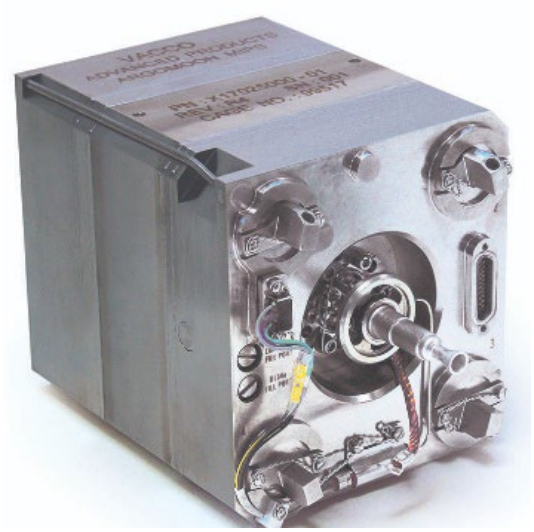


Figure 4.4: ArgoMoon hybrid Micro Propulsion System. Credit: VACCO.

Aerojet-Rocketdyne built the ASCENT-based propulsion system for the NASA Green Propellant Infusion Mission (GPIM). GPIM was an on-orbit demonstration of the ASCENT (then called AF-M315E) propulsion system, using five 1-N thrusters (Figure 4.5) for small attitude control maneuvers (30). GPIM was integrated into a small spacecraft bus (Ball Aerospace's BCP-100) and launched in June 2019 as a secondary payload on a Falcon Heavy. The five thrusters were successfully fired in space, across a range of operating modes, demonstrating attitude control and orbital inclination change capability (31).



Figure 4.5: GR1 thruster. Credit: Aerojet.

The Lunar Flashlight Propulsion System (LFPS), an ASCENT based propulsion system, was developed for the JPL Lunar Flashlight mission (32). Lunar Flashlight (Figure 4.6) was launched as a secondary payload in a December 2022 Falcon 9 launch, to map the lunar south pole for volatiles. LFPS was a pump-fed monopropellant system, using four 0.1-N ASCENT thrusters (Figure 4.7) built by Rubicon Space Systems (a division of Plasma Processes) and a micro-pump built by Flight Works Inc. The propellant management system was fabricated using additive manufacturing. During the first few days of flight, it was found that three of the four thrusters were underperforming. Based on ground testing, it was thought the underperformance might have been caused by obstructions in the propellant lines that limited propellant flow to the thrusters. Improvements were seen by increasing fuel pump pressure to clear the suspected obstructions. However, the effort was not sufficient to keep the spacecraft in the vicinity of the Moon, and the mission was terminated in May 2023 (33).

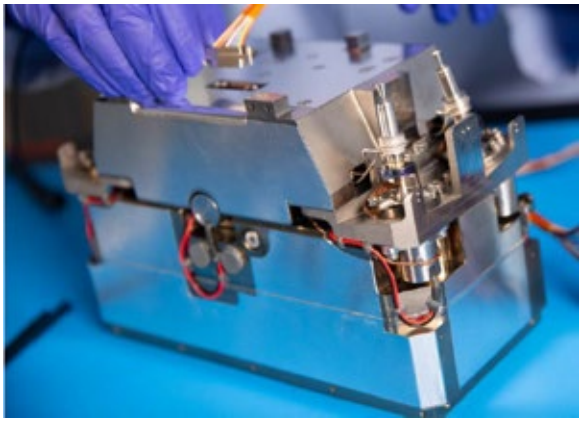


Figure 4.6: Lunar Flashlight Propulsion System. Credit: NASA.



Figure 4.7: Rubicon 0.1N ASCENT thruster. Credit: NASA MSFC.

Benchmark Space Systems offers thrusters that can be used with High Test Peroxide (HTP) as a monopropellant or as an oxidizer in a bipropellant combination with fuel. Benchmark provided a bipropellant Halcyon Avant propulsion system (Figure 4.8) that uses four 22-N thrusters using HTP and isopropyl alcohol for the Sherpa-LTC2 orbital transfer vehicle (OTV) (34). The Sherpa-LTC2 was launched on a Falcon 9 in September 2022. The OTV was used to elevate the orbit of the Varuna Technology Demonstration Mission satellite (35). In June 2021, three monopropellant HTP Halcyon systems were launched aboard the SpaceX Transporter 2 rideshare mission. One of the systems debuted Orbit Fab's RAFTI refueling kit as part of their Tenzing mission. The other two missions supported an undisclosed mission partner (36).

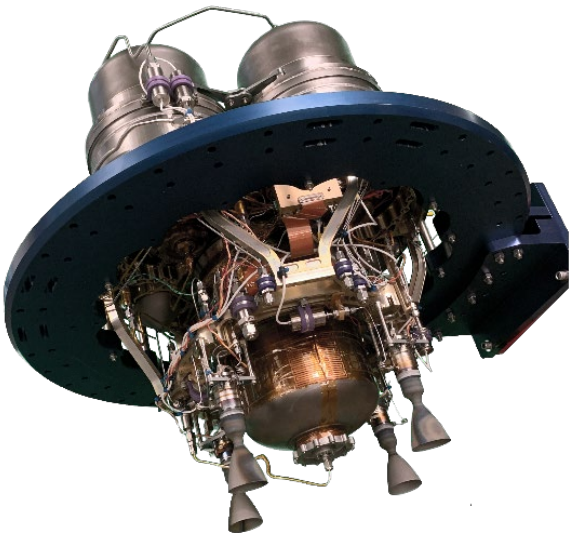


Figure 4.8: Halcyon Avant (Sherpa-LTC2 Configuration). Credit Benchmark Space Systems.

CisLunar Explorer, part of a NASA Centennial Challenges program, will use a water electrolysis propulsion system developed by Cornell University's Space Systems Design Studio on a pair of 3U CubeSats. In this system, the water is electrolyzed in the propellant tank. The gaseous hydrogen/gaseous oxygen mixture is flowed through a flame arrestor into the combustion chamber, where it is ignited by a glow plug (37). The

CubeSat was originally intended to be launched on Artemis I, but difficulties during integration bumped it from the mission (38) (39).

NASA's Small Spacecraft Technology (SST) program at Ames Research Center (ARC) launched the first Pathfinder Technology Demonstration (PTD) mission in January 2021 (40) (41). PTD-1 (Figure 4.9) tested the HYDROS-C water electrolysis propulsion system, developed by Tethers Unlimited Inc. With a volume less than 2.4U, the HYDROS-C uses water as propellant. In-orbit, water was electrolyzed into oxygen and hydrogen, then combusted like a traditional bipropellant thruster. Limited performance data has been evaluated and made public (42). The system requires 10–15 minutes of recharge time between pulses. A variant of the HYDROS-C system is the HYDROS-M system, which is intended to be sized for MicroSats. Tethers Unlimited became a subsidiary of ARKA Group LP in 2020.

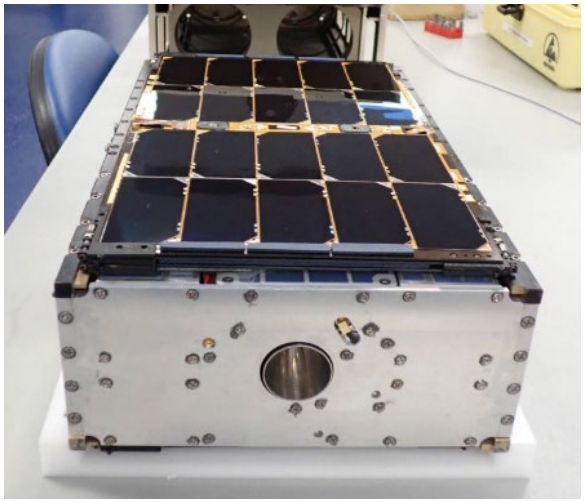


Figure 4.9: PTD-1 HYDROS-C. Credit: NASA.

NanoAvionics developed an ADN-based monopropellant propulsion system under the Enabling Propulsion System for Small Satellites (EPSS) program. The EPSS monopropellant system was demonstrated on LituanicaSAT-2, a 3U CubeSat, to correct orientation and attitude, avoid collisions, and extend orbital lifetime. LituanicaSAT-2 was launched in June 2017 and successfully separated from the primary payload (Cartosat-2) as part of the European QB50 initiative. According to product literature, multiple missions have since launched (43) (44).



Figure 4.10: CubeDrive. Credit: Dawn Aerospace.

Dawn Aerospace has developed the CubeDrive bipropellant (nitrous oxide and propylene) system that consists of a single B1 thruster, propellant tank, valves, and electronics. The thruster can also be operated in cold gas mode (for smaller impulse bits) by not engaging the spark igniter. The 0.8U (Figure 4.10) to 4U configurations provide 425 to 3,500 N-s of total impulse, respectively (45).

d. Summary Table of Devices

See Table 4-3 for the current state-of-the-art in other mono- and bipropellant devices applicable to small spacecraft.

e. Notable Advances

CU Aerospace (CUA) has developed the Monopropellant Propulsion Unit for CubeSats (MPUC) system, Figure 4.11 (46). The monopropellant is an H_2O_2-ethanol blend denoted as CMP-X. Tests on a thrust stand with a bladder-fed propellant tank demonstrated continuous thrust for greater than 50 minutes at a thrust level of 250 mN and specific impulse of 179 s with an average input power of ~6 W during catalyst warmup. 1.5U and 2U system designs have an estimated 1400 N-s and 2120 N-s total impulse, respectively. A ~900°C flame temperature allows the thrust chamber to use nonrefractory construction materials. CMP-X has low toxicity and was subjected to UN Series 1, 2, 3, and 6 testing; CMP-X demonstrated no detonation propagation when confined under a charge of high explosive, it exhibited thermal stability with no explosion or detonation during bonfire testing, and was not sensitive to drop impact or friction. CMP-X passed the criteria for either a 1.4S or a “Not Class 1” determination and may be excluded from the explosive class. Long-term storage testing shows no degradation over >1,200 days. This additively manufactured thruster passed environmental (vibration and thermal vacuum) testing and post-environmental thrust data were within experimental error of the pre-environmental data (47).

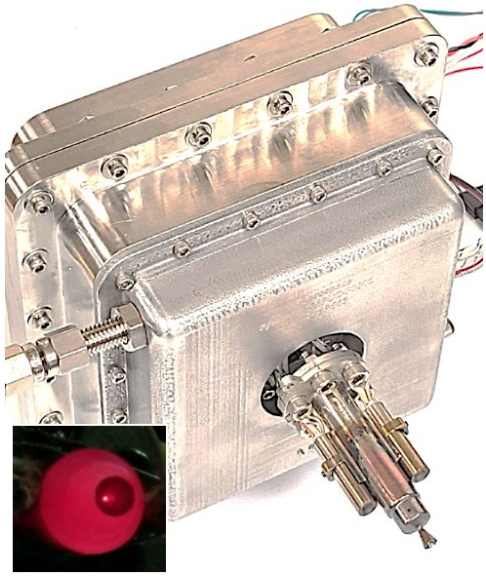


Figure 4.11: MPUC System. Credit: CU Aerospace.

VACCO has integrated four ECAPS 1-N LMP-103S thrusters into their Integrated Propulsion System (IPS) (Figure 4.12), a bolt-on propulsion module for delta-V and attitude control applications (48) (49).



Figure 4.12: VACCO Industries IPS. Credit: VACCO Industries.

Hybrids

a. Technology Description

Hybrid propulsion is a mix of solid and liquid/gas forms of propulsion. In a hybrid rocket, the fuel is typically a solid grain, and the oxidizer (often gaseous oxygen) is stored separately. The rocket is then ignited by injecting the oxidizer into the solid motor and igniting it with a spark or torch system. Since combustion can only occur while the oxidizer is flowing, these systems can readily be started or shut down by controlling oxidizer flow.

b. Key Integration and Operational Considerations

- **Improved Safety and Handling:** Hybrid systems are inherently safer to handle than solid motor systems because there is no oxidizer pre-mixed into the solid motor, which reduces the risk of premature ignition.
- **Integrates Attributes of Solids and Liquids:** Hybrids achieve many positive attributes of both solid motors (storability and handling) and liquid engines (restart and throttling).
- **Combustion Efficiency:** Combustion efficiency tends to be lower than either solid motors or liquid engines.

- **Other Drawbacks:** Regression rate control and fuel residuals tend to be more problematic in hybrid designs.

c. Current & Planned Missions

An arc-ignition “green” CubeSat hybrid thruster system prototype was developed at Utah State University and demonstrated in flight under the Undergraduate Student Instrument Project (USIP). The hybrid rocket design used a 3D-printed acrylonitrile butadiene styrene (ABS) plastic as the fuel and high-pressure gaseous oxygen (GOX) as the oxidizer. For safety considerations, the oxidizer was diluted to 60% nitrogen and 40% oxygen for the demonstration. On March 25, 2018, the system was successfully tested aboard a sounding rocket launched from NASA Wallops Flight Facility (WFF) into space and the motor was successfully re-fired five times. During the tests, 8 N of thrust and a specific impulse of 215 s were achieved as predicted (50) (51). The Space Dynamics Lab has miniaturized this technology to be better suited for CubeSat applications (0.25-0.5 N).

d. Summary Table of Devices

See Table 4-4 for current state-of-the-art hybrid devices applicable to small spacecraft.

e. Notable Advances

Utah State University has tested Nytrox, a blend of nitrous oxide and oxygen, and ABS. The testing was focused on a 25–50 N system for a 12U sized vehicle. Investigating different nozzle materials for low erosion in long duration burns is a key concern (52) (53).

JPL developed a hybrid propulsion system for a 12U CubeSat and a 100 kg SmallSat. Testing included regression rate characterization of clear and black polymethyl methacrylate fuels with GOX to be included in propulsion system sizing. Vacuum testing included an improvement of the ignition system to a laser-operated system that eliminates the need for a separate ignition fuel gas (54) (55) (56) (57).

NASA ARC developed a polymethyl methacrylate (PMMA) and nitrous oxide hybrid system that used ethylene and nitrous oxide thrusters. The ethylene and nitrous oxide also function as the hybrid ignition source. The hybrid system had a demonstrated efficiency of 91% and calculated specific impulse of 247 s, making it competitive with current small satellite propulsion systems (58) (59).

Aerospace Corporation and Penn State University developed an “Advanced Hybrid Rocket Motor Propulsion Unit for CubeSats (PUC)”. The design used additive manufacturing techniques for the carbon filled polyamide structure including the nitrous oxide tank and a paraffin grain within an acrylic shell, with acrylic diaphragms 3D printed in-situ in the grain for enhanced performance. This design fits in a 1U space, for a 3U or 6U spacecraft (60).

Parabilis Space Technologies developed two small satellite propulsion systems. Rapid Orbital Mobility Bus (ROMBUS) is a hybrid rocket-based system with nitrous oxide as the oxidizer and PMMA or hydroxyl-terminated polybutadiene (HTPB) as the fuel. It provides high-impulse thrust for satellite translational maneuvers which can be used for initial orbit insertion, rapid orbit rephasing, threat/collision avoidance, and targeted re-entry at the satellite’s mission end of life (61). Nano Orbital Transfer System (OTS) is a HTPB and nitrous oxide (N_2O) hybrid system, with N_2O-based ACS thrusters. Nano OTS leverages Parabilis’ proven hybrid engine and small satellite technologies for low-cost, high-performance maneuvers using non-toxic green propellants. The OTS has a modular design, enabling rapid and low-cost configuration of stages to accommodate 3U size NanoSats up to >50 kg MicroSat-size vehicles (62).

Cold Gas

a. Technology Description

Cold gas propulsion systems are simple, mature, and safe, although they provide relatively limited total impulse. There is no combustion in cold gas systems, with thrust produced by expelling gaseous propellant through a diverging nozzle. Propellants can be stored as compressed gases, saturated liquids, or solids. Gaseous nitrogen is a commonly used propellant for cold gas systems, although many other gases have been used in the long history of cold gas propulsion. For gases, the tradeoff is between performance and storage; lower molecular weight gases offer higher specific impulse but require more voluminous storage. Saturated liquids are stored at low pressure and vaporized when introduced into a low-pressure chamber. The dense storage of saturated liquids and their property of self-pressurization has made them popular as a propellant for CubeSat missions. The liquid propellants may require a pressurant or are self-pressurized, if stored in a two-phase liquid-gas state. Solid propellants can be used in a cold gas system by subliming solid propellants with adequate heat.

A derivative of cold gas systems is electrothermal or “warm gas” systems, in which the propellant is somewhat heated without chemical reaction and accelerated through a nozzle. The additional heating results in a modest improvement in thrust and specific impulse compared to a pure cold gas system, but typically burdens the spacecraft with increased power consumption. Electrothermal systems are described in more detail in the Electric Propulsion section.

b. Key Integration and Operational Considerations

- **Low Cost and Complexity:** Cold gas thrusters are often attractive and suitable for small buses due to their relatively low cost and complexity.
- **Safe:** Most cold gas thrusters use inert, non-toxic propellants, which is advantageous for secondary payloads that must adopt “do no harm” approaches to primary payloads.
- **Small Impulse Bit:** Cold gas systems are often well suited to provide attitude control since they can provide very small minimum impulse bits for precise maneuvering.
- **Small Total Impulse:** The low specific impulse of these systems limits their ability to provide large orbital correction maneuvers.
- **Integrated Systems Optimized for CubeSats:** Designs optimized around the limited resources of a CubeSat have improved the capability of these systems for small buses.

c. Missions

The Micro-Electromechanical-based PICOSAT Satellite Inspector, or MEPSI, built by the Aerospace Corporation, flew aboard STS-113 in 2002 and STS-116 in 2006. The spacecraft included both target and imaging/inspector vehicles connected via a tether. The two vehicles were each 4 x 4 x 5 in^3 in volume and had five cold-gas thrusters, producing approximately 20 mN. The MEPSI propulsion system was produced using stereo-lithography. It was suited as a propulsion research unit for PicoSats (63).

Marotta developed a cold gas micro-thruster, CGMT-000-9, for fine attitude adjustment maneuvers that flew on the NASA ST-5 mission in 2006. The thruster operated in blowdown mode with gaseous nitrogen, starting at 2.4 N and ending at 0.05 N (64) (65).

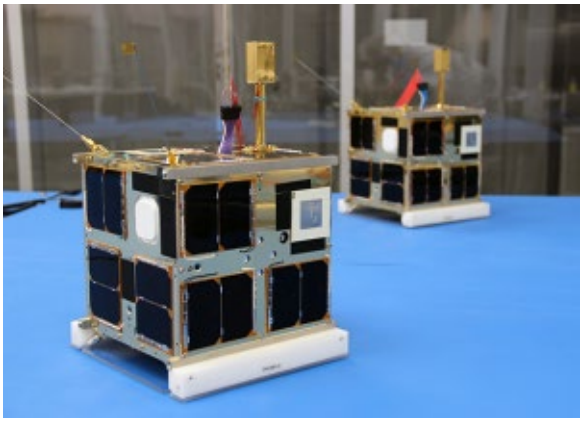


Figure 4.13: CanX-4 and CanX-5 formation flying nanosatellites with CNAPS propulsion systems. Credit: UTIAS SFL.

In June 2014, Space Flight Laboratory at the University of Toronto Institute for Aerospace Research (UTIAS) launched two 15 kg small spacecraft (CanX-4 and CanX-5) to demonstrate formation flying. The Canadian Nanosatellite Advanced Propulsion System (CNAPS), shown in Figure 4.13, consisted of four thrusters fueled with liquid sulfur hexafluoride. This propulsion module is a novel version of the previous NanoPS that flew on the CanX-2 mission in 2008. The non-toxic sulfur hexafluoride propellant was selected because it has a high vapor pressure and density, which are important properties for making a compact self-pressurizing system. The propulsion system was successfully used for drift recovery and autonomously maintaining a formation from 1-km range down to 50-m separation (66) (67) (68) (69).

Microspace Rapid Pte Ltd of Singapore developed a cold gas propulsion system for the POPSAT-HIP1 CubeSat demonstration mission that launched June 2014. It consists of eight micro-nozzles that provide control for three rotational axes with a single thrust axis for translational applications. The total delta-v was estimated from laboratory data to between 2.25 and 3.05 ms^{-1}. Each thruster has 1 mN of nominal thrust using argon. An electromagnetic microvalve with a very short opening time of 1 m-s operates each thruster (70).

GomSpace (acquired NanoSpace in 2016) has developed two related propulsion systems called the NanoProp CGP3 and NanoProp 6U. Both use proportional thrust control of four nozzles to control spacecraft attitude and provide delta-v. The CGP3 was flown on the TW-1 3U CubeSat launched in 2015. The 6U configuration was flown on GOMX-4B in 2018 as a formation flight demonstration (71) (72) (73) (74).

An ACS cold gas propulsion system using R-236fa was produced and tested by Lightsey Space Research for the NASA ARC BioSentinel mission, a 6U CubeSat that launched on Artemis I in November 2022. The propulsion system enables detumbling and pointing for communication back to Earth. The propulsion system uses a 3D-printed propellant tank to reduce part count and make efficient use of the available volume. The system contains six RCS thrusters and one delta-v thruster. The delta-v thruster was included to allow for collision avoidance but was ultimately not needed. One of the RCS thruster valves failed in the closed position during RCS checkout. Rather than further attempting to actuate the valve, and risk the valve failing open, a workaround was identified to perform momentum unloading with the remaining five RCS thrusters. As of May 2023, the propulsion system had accumulated 408 firings and continued to operate as expected. The initial phase of the mission was completed in April 2023. NASA extended the mission by up to an additional 28 months, or as late as September 2025 (75) (76) (77) (78).

The ThrustMe I2T5 subliming iodine cold gas module, Figure 4.14, was the first iodine propulsion system to be spaceflight tested, flown on the Xiaoxiang 1-08 satellite in 2019 (79) (80). Since then, the system was also launched on RTAF's NAPA-2 in June 2021 and on Spire's L3C in January 2023. Additional I2T5 launched on the Robusta-3A satellite in 2024, developed by CSUM, which carries various scientific payloads related to meteorology and technology demonstration (81) (82).

The CubeSat Proximity Operations Demonstration (CPOD) is a mission led by Terra Orbital (83) to demonstrate autonomous on-orbit rendezvous and proximity operations using two identical 3U CubeSats. Each spacecraft incorporates a cold gas propulsion system built by VACCO Industries that provides up to 186 N-s of total impulse. This module uses the self-pressurizing refrigerant R236fa propellant, which is exhausted through a total of eight thrusters distributed in pairs at the four corners of the module. CPOD launched in May 2022 as part of SpaceX's Transporter-5 mission. The CPOD mission demonstrated rendezvous of the CubeSats with intersatellite distances closing from 997 km to a minimum of 0.36 km. On-orbit limitations on experimentation were attributed to multiple factors as the launch date slipped due to many years of delay, including obsolete hardware, partial failure in the solar panels, and a propulsion system anomaly suspected to be a plenum leak (84) (85).



Figure 4.14: I2T5 Iodine Cold Gas Module. Credit: ThrustMe.

The Mars Cube One (MarCO) technology demonstration mission consisted of two identical CubeSats that followed the InSight spacecraft to Mars in loose formation in 2018. The MarCO spacecraft performed five trajectory correction maneuvers (TCMs) during the mission to Mars. The TCMs were conducted using an R236fa cold gas propulsion system developed by VACCO Industries, which contains four thrusters for attitude control and another four for TCMs. MarCO-B developed a propulsion system leak, which required constant maintenance. A tank to plenum leak was identified prior to launch, which the mission accepted. However, a second leak through a MarCO-B thruster valve developed during flight. The combination of both leaks resulted in a continuous moment on the MarCO-B spacecraft. The MarCO spacecraft succeeded in their mission to relay telemetry from the InSight lander during its descent to Mars (86) (87) (88) (89).

Near-Earth Asteroid Scout (NEA Scout) was a joint MSFC and JPL mission that had a VACCO cold gas MiPS (R236FA propellant), with six 25-mN thrusters, to assist the main propulsion system, a solar sail. However, after deployment from Artemis I in November 2022, the project team was not able to communicate with the spacecraft (90) (91) (92).

d. Summary Table of Devices

See Table 4-5 for the current state-of-the-art cold gas devices applicable to small spacecraft.

Solid Motors

a. Technology Description

Solid rocket motors have an oxidizer and fuel mechanical mixture stored in solid form (propellant grain). For small satellites, solid rocket motors may be used for impulsive maneuvers such as orbit insertion or quick deorbiting. They achieve moderate specific impulses and high thrust magnitudes. There are some electrically controlled solid thrusters that operate in the millinewton range that are restartable and have steering capabilities. Solid rocket arrays can be compact and suitable for small buses. Composed of several miniature solid rockets, individual units can be fired alone or together, as needed.

b. Key Integration and Operational Considerations

- **Thrust Vector Control:** Thrust vector control systems can be coupled with existing solid rocket motors to provide controllable high delta-v maneuvering.
- **Usually Single-Burn:** In general, solid motors are considered a single-burn event system. To achieve multiple burns, the system must be either electrically restartable (a.k.a. electric solid propellants), or several small units must be matrixed into an array configuration. Because electrically controlled solid propellants (ESPs) are electrically ignited, they are considered safer than traditional solid energetic propellants.

c. Current & Planned Missions

Northrop Grumman offers the STAR 3 motor, which has a maximum thrust of 2050 N. The STAR 3 motor was used as the Transverse Impulse Rocket System for the Mars Exploration Rover (MER) program and was used in 2004 to reduce the lateral velocity of the MER Spirit lander. The STAR 4G motor was developed and tested by NASA GSFC as an orbit-adjust motor for deploying nanosatellite constellations but was not flown, although it is still offered by Northrop Grumman along with other, higher total impulse motors in the STAR line (93).

The Pacific Scientific Energetic Materials Company (PacSci EMC) Modular Architecture Propulsion System (MAPS) array (Figure 4.15) has a 10-plus year in-orbit lifespan. The MAPS system provides three-axes capability to control attitude, deorbit, drag makeup, and plane and attitude changes with a delta-v greater than 50 m s^{-1}. The capability of the MAPS “plug-and-play” bolt-on design and clean-burning propellant array is scalable and can be custom-fit for a range of interfaces. MAPS was flown in 2017 aboard PacSciSat, which successfully completed all mission objectives (94) (95).

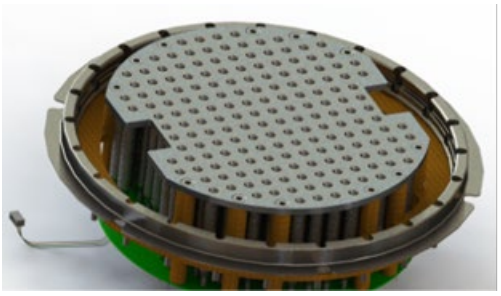


Figure 4.15: PacSci EMC MAPS sealed solid propellant rocket motor array. Credit: PacSci.

d. Summary Table of Devices

See Table 4-6 for the current state-of-the-art solid motor devices applicable to small spacecraft.

Propellant Management Devices

a. Technology Description

While not directly a thrust-producing device, propellant management devices (PMDs) are frequently used in liquid propulsion systems to reliably deliver propellant to thruster units. PMDs are commonly a critical part of in-space liquid propulsion systems that do not use bellows or membrane-type tanks. As small spacecraft look toward more complex propulsion system requirements, PMDs will undoubtedly play an integral role. Historically, small spacecraft have used bellows or membrane tanks to ensure propellant delivery and expulsion. However, there is the potential to incorporate PMD structures into additively manufactured tanks and propulsion systems, permitting more conformal structures to be created and optimized for small spacecraft missions. As such, PMDs are briefly covered here for awareness. A more detailed treatment and explanation can be found in the literature. A comprehensive, up-to-date list of the types of PMDs, as well as missions employing PMDs, is available in Hartwig (96).

b. Key Integration and Operational Considerations

The purpose of PMDs is to separate liquid and vapor phases within the propellant storage tank upstream of the thruster and to transfer vapor-free propellant in any gravitational or thermal

environment. PMDs have flight heritage with all classical storage systems, have been flown with LMP-103S, have no flight heritage with cryogenic propellants, and have been implemented in electric propulsion systems. Multiple PMDs are often required to meet the demands of a particular mission, whether using storable or cryogenic propellants.

c. Current & Planned Missions

The Lunar Flashlight Propulsion System used a PMD sponge and ribbon vane. The sponge was additively manufactured, while the ribbon vane was cut from sheet metal and bent to conform to the required dimensions. Surface tension properties, a necessary parameter for PMD sizing, were determined for the ASCENT propellant by Kent State University, funded and managed by NASA. The design and modelling were a joint effort between MSFC and GRC.

d. Summary Table of Devices

No summary table is included for propellant management devices.

e. Notable Advances

Northrop Grumman has made advances in the development of SmallSat- and CubeSat-scale diaphragm propellant tanks using materials that are compatible with hydrazine and some green monopropellant fuels (97), and demonstrated the utility of additive manufacturing in producing tank shells.

4.6.2 In-Space Electric Propulsion

In-space electric propulsion (EP) is any in-space propulsion technology wherein a propellant is accelerated through the conversion of electrical energy into kinetic energy. The electrical energy source powering in-space EP is historically solar, therefore these technologies are often referred to as solar electric propulsion (SEP), although other energy sources such as nuclear reactors or beamed energy are conceivable. The energy conversion occurs by one of three mechanisms: electrothermal, electrostatic, or electromagnetic acceleration (132) (133). Each of these technologies is covered herein.

This survey of the state-of-the-art in EP does not attempt to review all known devices but focuses on those that can be commercially procured or devices that appear on a path toward commercial availability. The intent is to aid mission design groups and other in-space propulsion end-users by improving their awareness of the full breadth of potentially procurable EP devices that may meet their mission requirements.

Instead of detailing the complete operating range for each propulsion device, the authors provide only the metrics associated with the nominal operating condition to improve comprehension of the data and make initial device comparisons more straightforward. When a manufacturer does not specifically state a nominal operating condition in the literature, the manufacturer may have been contacted to determine a preferred nominal operating condition; otherwise, a nominal operating condition was assumed based on similarity to other devices. For those metrics not specifically found in published literature, approximations have been made when determinable from the available data. Readers are strongly encouraged to follow the references cited to the literature describing each device's full performance range and capabilities.

Electrothermal

a. Technology Description

Electrothermal technologies use electrical energy to increase the enthalpy of a propellant, whereas chemical technologies rely on exothermal chemical reactions. Once heated, the

propellant is accelerated and expelled through a conventional converging-diverging nozzle to convert the acquired energy into kinetic energy, like chemical propulsion systems. The specific impulse achieved with electrothermal devices is typically of similar magnitude to chemical devices given that both electrothermal and chemical devices are fundamentally limited by the working temperature limits of materials. However, electrothermal technologies can achieve a somewhat higher specific impulse than chemical systems since they are not subject to the limits of chemical energy storage.

Electrothermal devices are typically subclassified into one of the following three categories:

1. *Resistojet devices* employ an electrical heater to raise the temperature of a surface that in turn increases the temperature of a gaseous propellant.
2. *Arcjet devices* sustain an electrical arc through an ionized gaseous propellant, resulting in ohmic heating.
3. *Electrodeless* thrusters heat a gaseous propellant through an inductively or capacitively coupled discharge or by radiation.

b. Key Integration and Operational Considerations

- **Propellant Selection:** Electrothermal technologies offer some of the most lenient restrictions on propellant selection for in-space propulsion. Whereas chemical systems require propellants with both the right chemical and physical properties to achieve the desired performance, electrothermal systems primarily depend on acceptable physical properties. For example, electrothermal devices can often employ inert gases or even waste products such as water and carbon dioxide. They also allow use of novel propellants such as high storage density refrigerants or in-situ resources. That said, not all propellants can be electrothermally heated without negative consequences. Thermal decomposition of complex molecules may result in the formation of polymers and other inconvenient byproducts. These byproducts may result in clogging of the propulsion system and/or spacecraft contamination.
- **Propellant Storage:** Electrothermal devices may require that propellants be maintained at a high plenum pressure to operate efficiently. This may require a high-pressure propellant storage and delivery system.
- **High Temperature Materials:** The working temperature limit of propellant-wetted surfaces in the thruster head is a key limitation on the performance of electrothermal devices. As such, very high temperature materials, such as tungsten and molybdenum alloys, are often employed to maximize performance. The total mass and shape of these high temperature materials are a safety consideration during spacecraft disposal. While most spacecraft materials burn up on re-entry, the re-entry behavior of devices using these high temperature materials will be scrutinized when assessing the danger of debris to life and property.
- **Power Processing:** While some simple resistojet devices may operate directly from spacecraft bus power, other electrothermal devices may require a relatively complex power processing unit (PPU). For example, a radio-frequency electrodeless thruster requires circuitry to convert the direct-current bus power to a high-frequency alternating current. In some cases, the cost and integration challenges of the PPU can greatly exceed those of the thruster.
- **Thermal Soak-back:** Given the high operating temperatures of electrothermal devices, any reliance on the spacecraft for thermal management of the thruster head should be assessed. While the ideal propulsion system would apply no thermal load on the

spacecraft, some thermal soak-back to the spacecraft is inevitable, whether through the mounting structure, propellant lines, cable harness, or radiation.

c. Missions

The Bradford (formerly Deep Space Industries) Comet water-based electrothermal propulsion system (Figure 4.16) has been implemented by multiple customers operating in low-Earth orbit, including HawkEye 360, Capella Space, and BlackSky Global (134). All missions use the same Comet thruster head, while the BlackSky Global satellites use a larger tank to provide a greater total impulse capability. The HawkEye 360 Pathfinder mission is a constellation of three small microsatellites built by Space Flight Laboratory (SFL) based on its 15-kg NEMO platform; each spacecraft measures 20 x 20 x 44 cm^3 with a mass of 13.4 kg (135) (136). The Comet provides each HawkEye 360 pathfinder a total delta-v capability of 96 ms^{-1}. The approximate dimensions of the BlackSky Global spacecraft are 55 x 67 x 86 cm^3 with a mass of 56 kg (138).

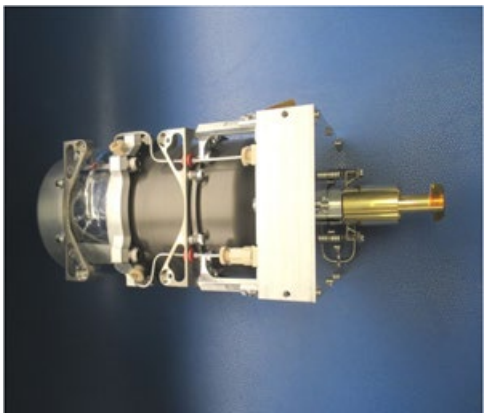


Figure 4.16: Comet-1000. Credit: Bradford Space.

The Propulsion Unit for CubeSats (PUC) system (139), Figure 4.17, was designed and fabricated by CU Aerospace LLC (Champaign, IL) and VACCO Industries under contract with the U.S. Air Force to supply two government missions (140). The system was acquired for drag makeup capability to extend asset lifetime in low-Earth orbit. The system uses SO_2 as a self-pressurizing liquid propellant. The propulsion system electrothermally heats the propellant using a micro-cavity discharge (MCD) and expels the propellant through a single nozzle (141). It can alternatively use R134a or R236fa propellants, but only in cold-gas mode with reduced performance. Eight flight units were delivered to the Air Force in 2014, although it remains unknown if any have flown.



Figure 4.17: PUC module. Credit: CU Aerospace.

In 2019, CU Aerospace was selected for a NASA STMD Tipping Point award to design, fabricate, integrate, and perform mission operations for the Dual Propulsion Experiment (DUPLEX) 6U CubeSat. DUPLEX has two of CU Aerospace's micro-propulsion systems onboard: one Monofilament Vaporization Propulsion (MVP) system (142) (143) (144), Figure 4.18, and one Fiber-Fed Pulsed Plasma Thruster (FPPT) system (148) (149) (150) (151) (152), Figure 4.45. The MVP is an electrothermal device that vaporizes and heats an inert solid polymer propellant fiber to 725 K. The coiled solid filament approach for propellant storage and delivery addresses common propellant safety concerns, which often limit the application of propulsion on low-cost CubeSats. In-orbit operations will demonstrate multiple mission capabilities including inclination change, orbit

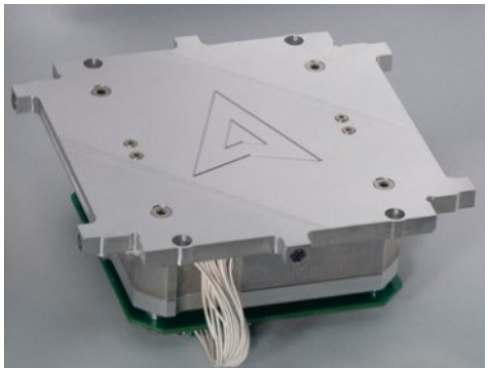


Figure 4.18: MVP module. Credit: CU Aerospace.

raising and lowering, drag makeup, and deorbit burns. DUPLEX was delivered to the International Space Station on a Cygnus cargo ship in September 2025 (154) (155).

AuroraSat-1 is a technology demonstration 1.5U CubeSat that is demonstrating multiple propulsion devices by Aurora Propulsion Technologies. AuroraSat-1 carries Aurora's smallest version of Aurora Resistojet Module for Attitude control (ARM-A) (156), Figure 4.19, and a demonstration unit of their Plasma Brake Module (PBM) (157). The ARM-A system integrated into AuroraSat-1 has six resistojet thrusters for full 3-axis attitude control and 70 grams of water propellant, providing a total impulse of 70 N-s. AuroraSat-1 is built by SatRevolution, with Aurora providing the payloads. The satellite was launched by Rocket Lab in May 2022. (158) (159). See section 4.6.3 for discussion of the PBM module.



Figure 4.19: Aurora Resistojet Module for Attitude Control. Credit: Aurora Propulsion Technologies.

The OPTIMAL-1 technology demonstration 3U nanosatellite by ArkEdge Space Inc. launched in late 2022 and was deployed from the International Space Station in early 2023. Among other technology demonstration devices, OPTIMAL-1 contains a Pale Blue water resistojet thruster (160).

SPHERE-1 EYE, a 6U CubeSat developed by Sony Group Corporation, includes a Pale Blue Water Resistojet Thruster. The satellite was launched aboard a SpaceX Falcon 9 on January 3rd, 2023, and has been orbiting Earth at an altitude between 500 km to 600 km. The water propulsion system is expected to prolong the satellite's life by 2.5 years. The propulsion system operated for approximately 2 minutes on March 3rd, 2023, and the company confirmed the successful generation of thrust from flight telemetry (161).

d. Summary Table of Devices

See Table 4-7 for current state-of-the-art electrothermal devices applicable to small spacecraft.

Electrosprays

a. Technology Description

Electrospray propulsion systems generate thrust by electrostatically extracting and accelerating ions or droplets from a low-vapor-pressure, electrically conductive, liquid propellant (Figure 4.20). This technology can generally be classified into the following types according to the propellant used:

Ionic-Liquid Electrosprays: These technologies use ionic liquids (i.e., salts in a liquid phase at room conditions) as propellant. The propellant is stored as a liquid, and onboard heaters may be present to maintain propellant properties within the desired operational temperature range. Commonly used propellants include 1-ethyl-3-methylimidazolium tetrafluoroborate (EMI-BF4) and bis(trifluoromethylsulfonyl)imide (EMI-Im). Thrusters that principally emit droplets are also referred to as colloid thrusters.

Field Emission Electric Propulsion (FEEP): These technologies use low-melting-point metals as propellant. The propellant is typically stored as a solid, and onboard heaters are used to liquefy the propellant prior to thruster operations. Common propellants include indium and gallium.

Feed systems for electrospray technologies can be actively fed via pressurant gas or passively fed via capillary forces. The ion (high-I_{SP}) or droplet (moderate-I_{SP}) emission can be controlled by modulation of the high-voltage (i.e., >1 kV) input in a closed-loop feedback system with current measurements. Stable operations in either emission mode can provide precise impulse bits.

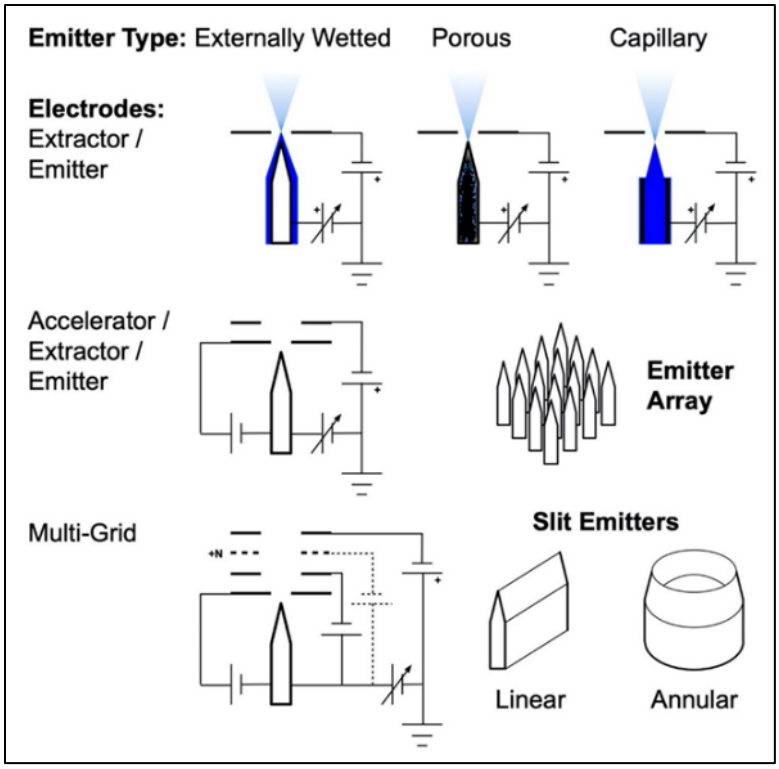


Figure 4.20: Schematic of typical electrospray emitter and electrode configurations. Credit: NASA.

b. Key Integration and Operational Considerations

- **Charge Balance**: Ionic liquid propellants can support electrospray operations with just cation (i.e., positively charged) emission or bi-polar emission (i.e., both anions and cations). For cation-only emission, as with FEEP thrusters, a separate cathode neutralizer is needed to maintain overall charge balance; such neutralizers do not necessarily need to be tightly integrated with the thruster heads. As such, the additional mass, volume, and power impacts must be considered in spacecraft integration. For electrospray technologies using bi-polar emission, reliable high-voltage switching in the power electronics becomes a critical consideration.
- **Plume Contamination**: Because propellants for electrospray propulsion systems are electrically conductive and condensable as liquids or solids, impingement of the thruster plume on spacecraft surfaces may lead to electrical shorting and surface contamination of solar panels and sensitive spacecraft components. Consideration of only the primary beam plume may not be sufficient, as droplet emission and molecular fragmentation within the plume can generate off-axis species. Plume shields are frequently employed on spacecraft to protect sensitive surfaces in the absence of high-fidelity electrospray plume models or characterization data.
- **Propellant Handling and Thruster Contamination**: Ionic liquids and metallic propellants can be sensitive to humidity and oxidation, so care is needed if extended storage is required prior to flight. Electrospray technologies can also be sensitive to contamination of the thruster head during propellant loading, ground testing (e.g., backsputter or outgassed materials from the test facility), and handling (i.e., foreign object debris). Precautions should be taken to minimize contamination risks from manufacturing, through test and launch. Post-launch, ionic liquids can outgas (e.g., water vapor) when exposed to the space environment, and such behavior should be accounted for in the mission operations. Due to environmental factors such as spacecraft outgassing and atomic oxygen levels, thruster operations following spacecraft deployment may need a conditioning or burn-in period before achieving full propulsive performance.

- **Performance Stability and Lifetime**: As an electrospray propulsion system operates over time, the propulsive performance can degrade as the plume impinges upon and deposits condensable propellant on thruster head surfaces; in time, sufficiently deposited propellant buildup can electrically short out the thruster electrodes and terminate thruster operation. Especially for missions with large total impulse requirements, lifetime testing or validated life models of the electrospray propulsion system in a relevant environment are important for understanding end-of-life behavior.
- **Specific Impulse**: Even for electrosprays that principally emit ions, operational thruster modes and instabilities can result in droplet emission that degrade the specific impulse and thrust efficiency. Caution is advised when considering claimed specific impulse or other propulsive properties (e.g., thrust vector and beam divergence) derived from plume characteristics; verification test data in a relevant environment are important for properly assessing these claims.
- **Precision Thrust**: Electrospray devices have the potential to provide very precise thrust during continuous operations. For devices that can operate in pulsed mode via pulsed modulation of the high-voltage input, fine impulse bits (i.e., <10 μN-s) may be achievable. Such operations can permit precise control over spacecraft attitude and maneuvering. Verification test data in a relevant environment should be used to properly assess the degree of thrust precision.

c. Missions

The ESA Laser Interferometer Space Antenna (LISA) Pathfinder spacecraft was launched in December 2015 on Vega flight VV06. Onboard were two integrated propulsion modules associated with the NASA Space Technology 7 Disturbance Reduction System (ST7 DRS). Each propulsion module contained four independent Busek Colloid MicroNewton Thrusters (CMNT), propellant-less cathode neutralizers, power processing units, digital control electronics, and low-pressure propellant tanks. The propulsion system was successfully commissioned in-orbit in January 2016 after having been fully fueled and stored for almost eight years. The electrospray modules (Figure 4.21) were operated at the Earth-Sun Lagrange Point 1 for 90 days to counteract solar disturbance forces on the spacecraft; seven of the eight thrusters demonstrated performance consistent with ground test results, and the full propulsion system met mission-level performance requirements (163).

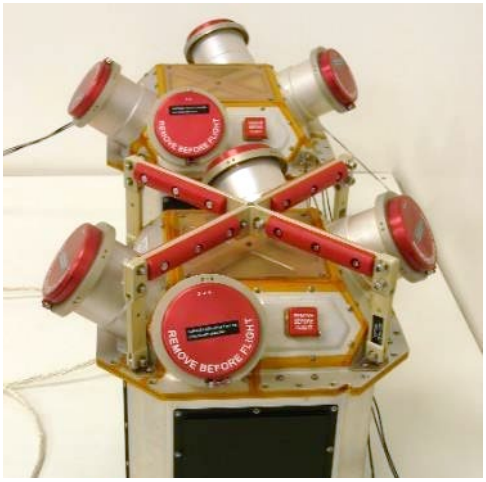


Figure 4.21: Flight CMNT modules for LISA Pathfinder. Credit: Busek.

The Enpulsion Nano FEEP (Figure 4.22), formerly the IFM Nano, was first integrated onboard a 3U Planet Labs Flock 3P CubeSat and launched via PSLV-C40 in January 2018. The indium-propellant propulsion system (with integrated thruster head, propellant storage, and power processing unit) was demonstrated in a 491-km by 510-km orbit. Two thruster firing sequences were reported, with the first a 15-minute firing in non-eclipse and the second a 30-minute firing in eclipse. Global Positioning System (GPS) telemetry data onboard the spacecraft indicated good



Figure 4.22: Nano. Credit: Enpulsion.

agreement with the ~220 μN commanded thrust (164). Since this initial demonstration, the Enpulsion Nano has flown onboard other spacecraft, but limited on-orbit data is publicly available. These missions include the ICEYE-X2 (launched onboard Falcon-9 flight F9-64 in December 2018) to provide low-Earth orbit interferometric synthetic aperture radar observations (165) (166) and the DOD-funded Harbinger technology demonstrator (launched onboard Electron flight STP-27RD in May 2019) (167) (168). The Enpulsion Nano was also integrated onboard the Zentrum für Telematik (Würzburg) NetSat formation-flying demonstrator mission, which launched as a Soyuz-2 rideshare in September 2020 (169) (170). A summary of available on-orbit statistics, anomalies, and lessons learned for the Enpulsion Nano family (Nano, Nano R^3, and Nano AR^3) is available (171).



Figure 4.23: Micro R^3. Credit: Enpulsion.

An Enpulsion Micro R^3 (Figure 4.23) was housed onboard the GMS-T mission, which launched in January 2021 onboard a Rocket Lab Electron. The telecommunications satellite uses an OHB Sweden Innosat platform with propulsive capability for collision avoidance. Inaugural on-orbit commissioning of the propulsion system was confirmed in March 2021 (173).

The University Würzburg Experimental Satellite 4 (UWE-4) was launched as a secondary payload onboard the Soyuz Kanopus-V 5 and 6 mission in December 2018. This 1U spacecraft housed two Morpheus Space NanoFEEP systems, with each system consisting of two gallium-propellant thrusters, a power processing unit board for the UNISEC Europe bus, and a propellant-less cathode neutralizer. An experiment using one thruster as an attitude control actuator was reported, with the increased spacecraft rotation rate corresponding to a derived thrust magnitude of ~5 μN; anomalous torque was attributed to unexpected impingement of the thruster plume upon the spacecraft antenna (174) (175). Orbit lowering capability was demonstrated in 2020; of the four individual thrusters, three experienced anomalous behavior during the UWE-4 mission (176). A 3U-Cubsat implementation of the same NanoFEEP technology is shown in Figure 4.24.



Figure 4.24: Eight NanoFEEP thrusters integrated on 3U-Cubesat bus. Credit: Morpheus Space.

d. Summary Table of Devices

See Table 4-8 for current state-of-the-art electrospray devices applicable to small spacecraft.

Gridded-Ion

a. Technology Description

Gridded-ion propulsion systems ionize gaseous propellants via a plasma discharge, and the resultant ions are subsequently accelerated via electrostatic grids (i.e., ion optics). This technology can generally be classified according to the type of plasma discharge employed:

- **Direct-Current (DC) Discharge**: The propellant is ionized via electron bombardment from an internal discharge cathode (Figure 4.25).

- **Radio-Frequency (RF) Discharge**: No internal discharge cathode is present. Instead, the propellant is ionized via RF or microwave excitation from an RF generator (Figure 4.26).

Gridded-ion thrusters typically operate at high voltages and include an external neutralizer cathode to maintain plume charge neutrality. High specific impulse can be achieved, but the thrust density is fundamentally limited by space-charge effects. While the earliest thruster technologies used metallic propellants (i.e., mercury and cesium), modern gridded-ion thrusters use noble gases (e.g., xenon, krypton) or iodine.

b. Key Integration and Operational Considerations

- **Performance Prediction:** Due to the enclosed region of ion generation and acceleration, gridded ion thrusters tend to be less sensitive to test-facility backpressure effects than other devices such as Hall thrusters. This allows for more reliable prediction of in-flight performance based on ground measurements. Furthermore, the separation between ion generation and acceleration mechanisms within the device tends to make calculations of thrust and ion velocity (or I_{SP}) more straightforward.
- **Grid Erosion**: Charge-exchange ions formed between and downstream of the ion optics can impinge upon and erode the grids. Over time, this erosion can lead to a variety of failure modes, including grid structural failure, an inability to prevent electrons from back streaming into the discharge chamber, or the generation of an inter-grid electrical short due to the deposition of electrically conductive grid material. Proper grid alignment must be maintained during thruster assembly, transport, launch, and operations to minimize grid erosion. Random vibration tests at the proto-flight level should be conducted to verify the survivability of the ion optics against launch loads. Validated thermal modeling may be needed to assess the impact of grid thermal expansion during operation.
- **Foreign Object Debris**: The grids are separated by a small gap, typically less than 1 mm, to maximize the electric field and thrust capability of the device. As a result, gridded-ion thrusters tend to be sensitive to foreign object debris, which can bridge the inter-grid gap and cause electrical shorting. Precautions should be taken to minimize such contamination risks from manufacturing, through test, and to launch.
- **Cathode Lifetime**: Cathodes for plasma discharge or plume neutralization may be sensitive to propellant purity and pre-launch environmental exposure. Feed system cleanliness, bake-out, and use of a high-purity propellant are key factors in maximizing cathode lifetime. The technology provider may recommend maximum cumulative atmospheric exposure and humidity to reduce risk.
- **Roll Torque**: Misalignments in the ion optics can lead to disturbances in the thrust vector, resulting in a torque around the roll axis that cannot be addressed by the mounting gimbal. For missions requiring extended thruster operations, a secondary propulsion system or reaction wheels may be needed to counter the torque buildup (177).
- **Electromagnetic Interactions**: For RF-discharge thrusters, electromagnetic interference and compatibility (EMI/EMC) testing may be critical to assess the impact of thruster operations on spacecraft communications and payload functions.
- **Power Electronics:** Operation of gridded-ion thrusters requires multiple high-voltage power supplies for discharge operation (ion generation), ion acceleration, and neutralization, leading to potentially complex and expensive power electronics.
- **Iodine Propellant:** To address the volume constraints of small spacecraft, iodine is an interesting propellant. Compared to xenon, iodine's storage density is three times greater. Furthermore, iodine stores as a solid with low vapor pressure. However, iodine is a strong oxidizer, and the long-duration impact on the thruster and spacecraft remain largely unknown. Recent and upcoming flights will provide insight into potential spacecraft

interactions and the long-term reliability of feed system and thruster components exposed to iodine.

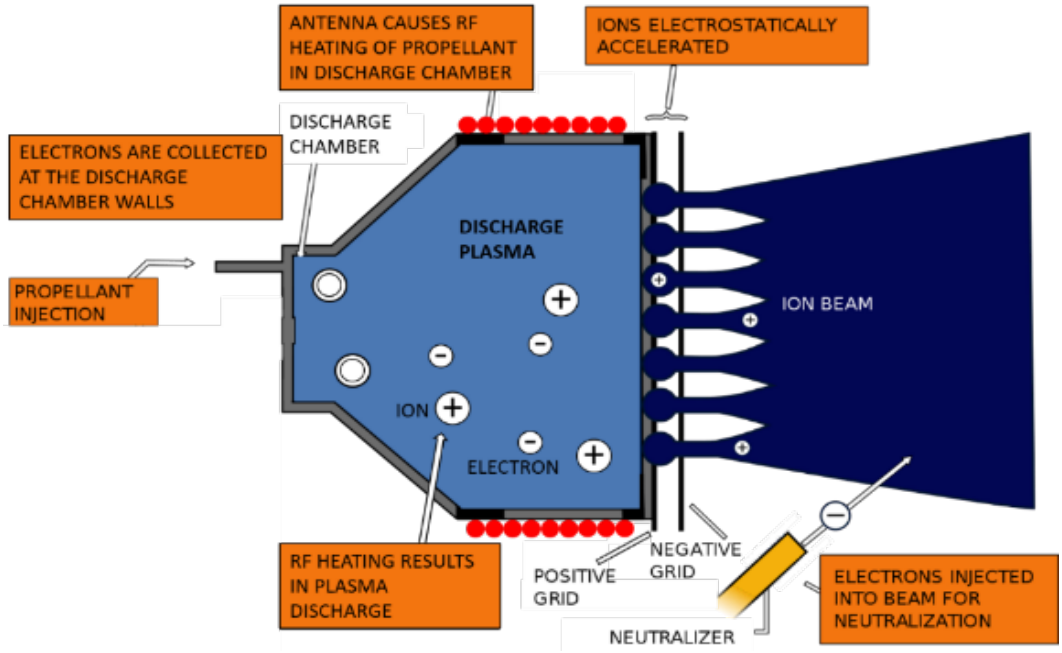


Figure 4.25: Schematic of typical DC-discharge gridded-ion thruster. Credit: NASA.

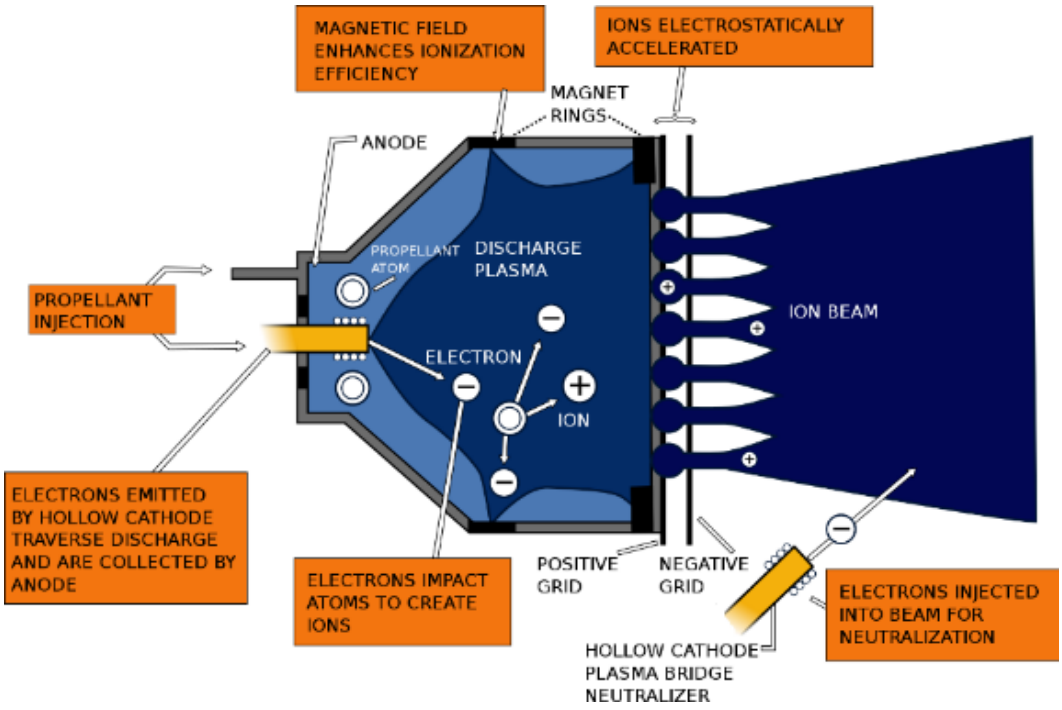


Figure 4.26: Schematic of typical RF-discharge gridded-ion thruster. Credit: NASA.

c. Missions

The ESA Gravity Field and Steady-State Ocean Circulation Explorer (GOCE) was launched in March 2009 onboard a Rokot / Briz-KM to provide detailed mapping of Earth's gravitational field and ocean dynamics from an altitude of ~220-260 km. Two QinetiQ T5 DC-discharge gridded-ion thrusters (Figure 4.27), with one serving as a redundant backup, successfully provided drag make-up for the 1000-kg satellite until the xenon propellant was exhausted in October 2013 (178) (179) (180) (181).



Figure 4.27: T5 gridded-ion thruster for GOCE mission. Credit: QinetiQ.

ThrustMe's NPT30-I2 1U or 1.5U (Figure 4.28), an integrated, RF-discharge gridded-ion propulsion system, has at least two units in space as of July 2023. The Beihangkongshi-1 satellite was launched in November 2020 onboard a Long March 6 rocket. As part of the first on-orbit demonstration of iodine-propellant electric propulsion, two 90-minute burns provided an orbital altitude change of 700 m (182) as described in a Nature publication (183). In April 2023, the 1.5U flew onboard a Space Flight Laboratory of the University of Toronto Institute for Aerospace Studies (UTIAS) 35-kg DEFIANT bus for the Norwegian Space Agency's NorSat-TD mission (184), which included a demonstration of satellite collision avoidance maneuvers (185). As of July 2023, ThrustMe reported more than 100 systems on order (186) (187).



Figure 4.28: NPT30-I2-1U. Credit: ThrustMe.

The Lunar IceCube and LunarH-Map missions both included a Busek BIT-3 propulsion system (Figure 4.29) with solid iodine propellant. The BIT-3 system was the primary propulsion for each spacecraft's lunar transfer, orbit capture, orbit lowering, and spacecraft disposal. Each integrated BIT-3 system includes a low-pressure propellant tank with heated propellant-feed system components, a power processing unit to control the RF thruster and RF cathode, and a two-axis gimbal assembly.

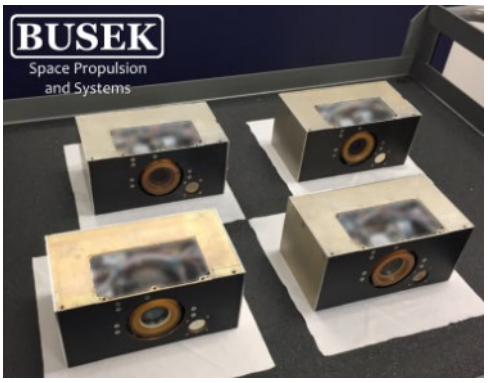


Figure 4.29: BIT-3 thruster. Credit: Busek.

The Lunar IceCube mission, led by Morehead State University, aimed to characterize the distribution of water and other volatiles on the Moon from a highly inclined lunar orbit with a perilune less than 100 km. The 6U spacecraft was launched as a secondary payload onboard Artemis I (188) (189). Communication issues with the CubeSat were reported shortly after launch (190).

The Lunar Polar Hydrogen Mapper (LunaH-Map) mission, led by Arizona State University, aimed to map hydrogen distributions at the lunar south pole from a lunar orbit with a perilune less than 20 km. The 6U spacecraft was launched as a secondary payload onboard Artemis I (191). The mission ended in late 2023 as the BIT-3 was inoperable and unable to perform the required

mission maneuvers. The mission team concluded that the propulsion system's tank valve was stuck closed (192) (193). As of April 2026, Busek indicates that several BIT-3 systems are operational in commercial missions, although mission details have not been publicly disclosed.

d. Summary Table of Devices

See Table 4-9 for current state-of-the-art gridded-ion devices applicable to small spacecraft.

Hall-Effect

a. Technology Description

The Hall-effect thruster (HET) is arguably the most successful in-space EP technology by quantity of units flown. The Soviet Union first flew a pair of EDB Fakel SPT-60 HETs on the Meteor-1-10 spacecraft in 1971. Between 1971 and 2018, over 300 additional HETs flew internationally, although EDB Fakel produced the vast majority. The first flight of a non-Russian HET was on board the European Space Agency (ESA) Small Missions for Advanced Research in Technology (SMART-1) spacecraft in 2003. SMART-1 employed the French PPS-1350 HET, produced by Safran (194). The first flight of a U.S. manufactured HET, the Busek BHT-200, was onboard the TacSat-2 spacecraft (195), a U.S. Air Force Research Laboratory (AFRL) experimental satellite in 2006. In 2010, Aerojet, another U.S. entity, began commercially delivering their 4.5 kW XR5 HET (196), formerly BPT-4000. Launches of HETs greatly accelerated in 2019 with the launch of 120 SpaceX Starlink and 6 OneWeb spacecraft (197), each using an HET. As of April 2026, SpaceX has launched over 11,500 Starlink satellites, and OneWeb has launched over 650 satellites. Suffice to say that HETs have become a mainstream in-space propulsion technology.

The rapid growth in demand for HETs can be attributed to their simple design, historically well-demonstrated reliability, good efficiency, high specific impulse, and high thrust-to-power ratio. Although gridded-ion thrusters (GIT) can achieve a higher specific impulse than HETs, HETs can achieve higher thrust-to-power ratios because HETs have a higher density quasi-neutral plasma, which is not subject to space-charge limitations. The HETs' higher thrust-to-power ratio will typically shorten spacecraft transit time. On the other end of the spectrum, arcjets provide significantly higher thrust than HETs, however material limitations prevent arcjets from matching the HETs' electrical efficiency and specific impulse. For many missions, HETs provide a good balance of specific impulse, thrust, cost, and reliability.

HETs are a form of ion propulsion, ionizing and electrostatically accelerating the propellant. Historically, HETs flown in space have relied on xenon propellant, given its high molecular weight, low ionization energy, and ease of handling. One recent exception is the SpaceX Starlink spacecraft using krypton propellant. While HETs typically operate less efficiently with krypton propellant, and krypton has more challenging storage requirements, krypton gas is considerably lower in cost than xenon gas. Lower cost is a compelling attribute, especially when the number of spacecraft are in the thousands, as with the Starlink constellation. While xenon is generally a superior propellant, krypton-fed Hall thrusters will likely become more common. SpaceX's 2nd Generation Starlink spacecraft made another first using argon as a Hall thruster propellant. While argon has been commonly tested with laboratory HETs due to its low cost and good availability, argon is not generally considered a good choice for spaceflight due to its challenging storage requirements. However, given SpaceX's need for such large volumes of propellant for thousands of satellites, overcoming supply chain limitations provides a justification for this generally non-ideal propellant. Many other propellants have been considered and ground tested for Hall-effect thrusters, but to date Hall-effect thrusters have flown using primarily xenon, krypton, or argon.

As schematically shown in Figure 4.30, HETs apply a strong axial electric field and radial magnetic field near the discharge chamber exit plane. The **ExB** force greatly slows the mean axial velocity of electrons and results in an azimuthal electron current many times greater than the beam current. This azimuthal current provides the means by which the incoming neutral propellant is collisionally ionized. These ions are electrostatically accelerated and only weakly affected by the magnetic field. The electron source is a low-work-function material typically housed in a refractory metal structure (i.e., hollow cathode), historically located external to the HET body. Many recent thruster designs have begun centrally mounting the cathode in the HET body as shown in Figure 4.30. The cathode feeds electrons to the HET plasma and neutralizes the plasma plume ejected from the thruster. The high voltage annular anode sits at the rear of the discharge chamber and typically functions as the propellant distribution manifold.

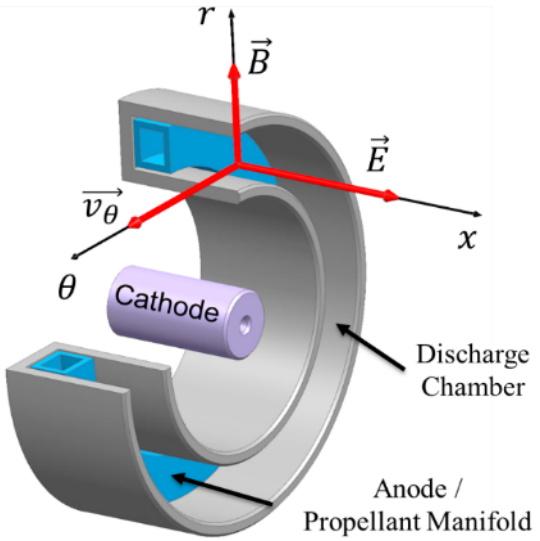


Figure 4.30: Hall-effect Thruster schematic. Credit: NASA.

b. Key Integration and Operational Considerations

- **Ground Facility Effects:** Ground facility effects may result in inconsistencies between ground and flight performance. The significance of the inconsistencies depends on factors such as test facility scale, pumping speed, intrusiveness of diagnostics, and thruster electrical configuration.
- **Contamination:** Plume ions of an HET can affect spacecraft surfaces by erosion or contamination, even at large plume angles. Ground facility measurement of ion density at large angles may underpredict flight conditions.
- **Thermal Soak-Back:** HET core temperature may exceed 400°C with the cathode exceeding 1000°C. Most HET waste heat radiates directly from the HET surfaces. However, some thermal soak-back to the spacecraft will occur through the mounting structure, propellant feed lines, electrical harness, and radiation.
- **Survival Heaters:** Given the thermal isolation between the HET and spacecraft, the HET may require a survival heater depending on the qualification temperature and flight environments.
- **Performance:** HET performance may vary over the life of the device due to erosion and contamination of the plasma wetted HET surfaces. Magnetically shielded thrusters demonstrate less time dependence in performance than classical HETs.
- **Thruster Lifetime:** Classical HETs are primarily life-limited by erosion of the discharge chamber wall. Magnetically shielded HETs are primarily life-limited by erosion of the front pole covers.
- **Cathode Lifetime:** Cathode lifetime may be sensitive to propellant purity and pre-launch environmental exposure. Feed system cleanliness, bake-out, and use of a high-purity propellant are key factors in maximizing cathode lifetime. The HET manufacturer may recommend a maximum cumulative atmospheric exposure and humidity. Some cathode emitter formulations are less sensitive to propellant impurities and atmospheric exposure, but these formulations may require other trades such as a higher operating temperature.

- **Roll Torque**: The **ExB** force results in a slight swirl torque. For missions requiring extended thruster operations, a secondary propulsion system or reaction wheels may be needed to counter the torque buildup. The roll torque may largely be countered by periodically reversing the direction of the magnetic field. Field reversal requires switching the polarity of the current to the magnet coils. Field reversal is only possible with HETs using electromagnets.
- **Thrust Vector**: Non-uniformity of the azimuthal plasma, magnetic field, or propellant flow may result in slight variations of the thrust vector relative to the HET physical centerline. Temperature variation of the HET, such as during startup, may result in a slight drifting of the thrust vector.
- **Heaterless Cathodes:** Heaterless cathode technologies continue to mature. The benefit of a heaterless cathode is elimination of the cathode heater, typically an expensive component due to rigorous manufacturing and acceptance processes. However, the physics of heaterless cathode life-limiting processes requires further understanding. Nevertheless, heaterless cathode demonstrations have empirically shown significant promise. Heaterless cathode requirements on the EP system differ from an HET with a cathode heater. Impacts on the power processing unit and feed system should be well understood when trading a heaterless versus heated cathode.
- **Throttling Range:** HETs typically throttle stably over a wide range of power and discharge voltage. This makes an HET attractive for missions requiring multiple throttle set-points. However, an HET operates most efficiently at specific throttle conditions. Operating at off-nominal conditions may result in decreased specific impulse and/or electrical efficiency.

c. Missions

Canopus-V (or Kanopus-V) is a Russian Space Agency spacecraft for Earth observation with a design life of 5 years. The 450 kg spacecraft launched in 2012 employed a pair of EDB Fakel SPT-50 thrusters. Similarly, the Canopus-V-IK (Kanopus-V-IK) launched in 2017 with a pair of SPT-50 thrusters. The SPT-50 thrusters have a long history of spaceflight dating back to the late 1970s. Although the Canopus bus exceeds 450 kg, the power class and physical scale of the SPT-50 are appropriate for smaller spacecraft. The SPT-50 is nominally a 220 W thruster operated on xenon propellant (198) (199) (200).

The KazSat-1 and KazSat-2 spacecraft produced by Khrunichev Space Center in cooperation with Thales Alenia Space launched in 2006 and 2011, respectively. The KazSat spacecraft are geosynchronous communication satellites. These spacecraft employ the EDB Fakel SPT-70BR thruster. The SPT-70BR is Fakel's latest version of the SPT-70 product line. EDB Fakel optimized the SPT-70 for operation between 600 and 700 W, but no more than 900 W. Experiments demonstrate a lifetime of 3,100 hours, equating to about 450 kNs. The SPT-70 thrusters have a long history of spaceflight dating back to the early 1980s. Control of KazSat-1 was lost in 2008 (201) (202).

The Busek BHT-200 (Figure 4.31) has the distinction of being the first U.S.-made HET to operate in space. The BHT-200 has flight heritage from demonstrations on the TacSat-2 mission launched in 2006, FalconSat-5 mission launched in 2010, and FalconSat-6 mission launched in 2018. A Busek PPU powered the 200 W HET for each of the FalconSat missions (203) (204) (205). Ground testing of the BHT-200 includes multiple propellants, although all



Figure 4.31: BHT-200 thruster. Credit: Busek.

spaceflights of the BHT-200 have used xenon. Busek developed an iodine compatible derivative of the BHT-200 for the NASA iSat mission. It was determined during the course of the iSat project that additional development related to iodine compatible cathodes was required before conducting an in-space demonstration of the technology (206) (207).

The Israel Space Agency and the French National Center for Space Studies (CNES) jointly developed the Vegetation and Environment monitoring on a New Microsatellite (VENuS) spacecraft launched in 2017. The 268 kg VENuS spacecraft includes a pair of Rafael IHET-300 thrusters (Figure 4.32) and 16 kg of xenon propellant. In-flight operations have demonstrated operation between 250 and 600 W. Rafael developed the IHET-300, nominally operating at 300 W, specifically for small spacecraft (208) (209) (210) (211) (212).



Figure 4.32: IHET-300 thruster. Credit: Rafael.

The European and Italian space agencies selected the SITAEL HT100 (Figure 4.33) for an in-orbit validation program to evaluate the device's capabilities for orbital maintenance and accelerated reentry of a small spacecraft. The uHETSat mission is the first in-orbit demonstration of the HT100. The mission uses the thruster to raise and lower its orbit over a series of verification tests conducted during a planned two-year lifespan. The mission seeks to conduct at least one thousand ignition cycles. The HT100 is nominally a 175 W device operating on xenon propellant. The uHETSat uses the SITAEL S-75 microsatellite platform that is 75 kg with dimensions of 60 x 40 x 36 cm^3. The spacecraft launched on December 1, 2023 (213) (214) (215) (216). The HT100 is also baselined for the Italian Space Agency Platino-1 and Platino-2 spacecraft (217).

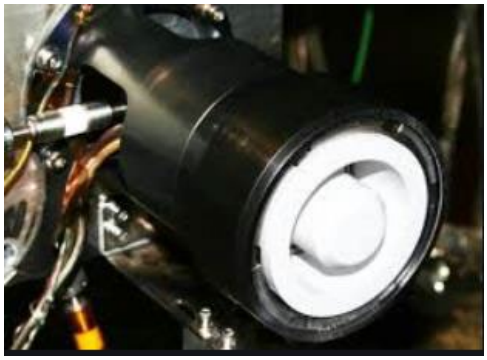


Figure 4.33: HT100 thruster. Credit: SITAEL.

The Astra Spacecraft Engine (ASE), Figure 4.34, successfully achieved orbital ignition onboard the Spaceflight Sherpa-LTE1 orbital transfer vehicle, which launched on SpaceX's Transporter-2 mission on June 30, 2021 (218). This single-string system is sized to achieve a controlled de-orbit of Sherpa-LTE1 (219). On-orbit performance was demonstrated by operating the system for 5-minute durations. The first 54 maneuvers have been reported (220). After outgassing, performance metrics were nominal within one standard deviation of ground test data. On-orbit thrust averaged 22.4 mN, and specific impulse for each 5-minute thrust maneuver averaged 1108 seconds. Total propulsion system power processing efficiency averaged 94%, including feed system power, circuit efficiency, and housekeeping loads (221). As of November 2023, the ASE aboard the Sherpa-LTE1 had operated for more than 800 five-minute maneuvers (i.e., accumulated total duration of ~70 hours) (218). On July 7, 2024, Sherpa-LTE1 safely deorbited

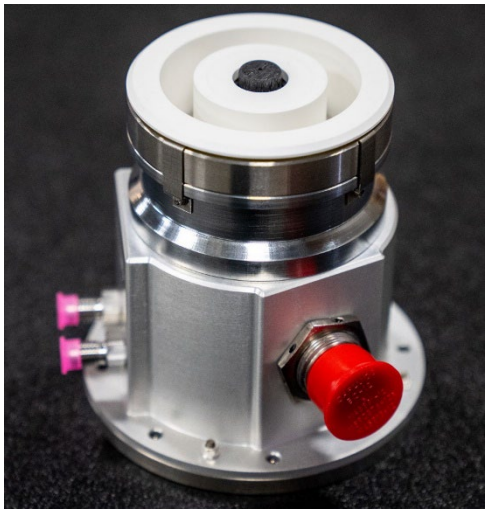


Figure 4.34: Astra Spacecraft Engine (ASE). Credit: Astra.

(222). The ASE is designed for operation with xenon and krypton propellants and sized to fit ESPA-class missions. The propulsion system includes several key technologies, including permanent magnets, a heatless instant start cathode, and a radiation hardened PPU. Astra has also reportedly sold ASE units to LeoStella (223), Apex (224), and Astroscale (225). As of March 2023, Astra had reported nine ASE units in orbit (224).

Exotrail's first in-orbit propulsion demonstration was in November 2020. NanoAvionics and Exotrail partnered to integrate Exotrail's spaceware-nano (Figure 4.35) into a NanoAvionics M6P nanosatellite 6U bus, which was built, integrated, and qualified in 10 months. Following this, Exotrail signed a contract with AAC Clyde Space to provide propulsion for the Eutelsat ELO 3 (2022) and ELO4 (2023) 6U CubeSats (226) (227) (228) (229) (230), and a contract with Aerospace Lab to provide its spaceware-nano for Aerospace Lab's Risk Reduction Flight (RRF) mission. The Aerospace Lab spacecraft, known as "Arthur," was launched in 2021 (231) (232). Blue Canyon Technologies (BCT) selected the Exotrail's spaceware system for its Venus-class microsatellite platform, which will be used for the NASA's INCUS mission, which is expected to launch in 2027 (233) (234).



Figure 4.35: spaceware-nano thruster. Credit: Exotrail.

A spaceware-micro (Figure 4.36) was reported to be integrated onboard a York Space Systems S-Class platform for a satellite mission scheduled for launch in late 2023, aiming to orbit the Moon and deliver Earth-to-Moon telecommunication services in support of Intuitive Machines' lunar south pole mission (235). Exotrail also has agreements to provide the spaceware-micro for missions by OHB Luxspace (236), Satrec Initiative (237), Astro Digital (238), and Muon Space (239).

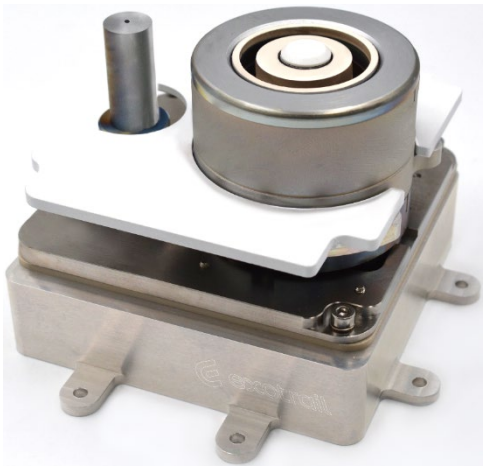


Figure 4.36: spaceware-micro thruster. Credit: Exotrail.

Exotrail launched its spacevan In-Orbit Demonstration (IOD) mission in November 2023. The spacevan uses Exotrail's spaceware-micro to demonstrate its capabilities (e.g., plane change and altitude change) (240) (241).

Airbus will integrate Exotrail's spaceware - mini thruster, Exotrail's 300W–600W class electric propulsion system, onto Airbus' Earth Observation satellite platform portfolio. Exotrail anticipated completion of the thruster's qualification activities in 2024 (242).

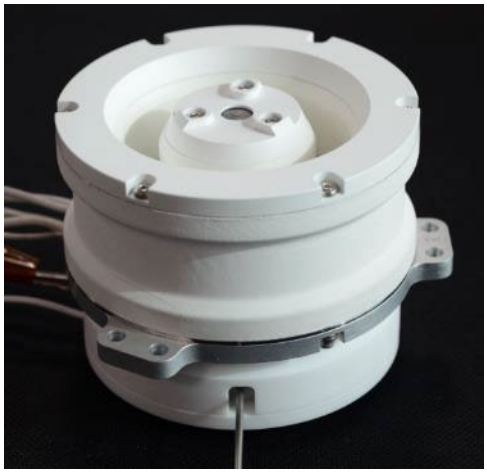


Figure 4.37: Halo thruster. Credit: ExoTerra Resource.

Blue Canyon, a Raytheon subsidiary, produced satellites for the DARPA Blackjack program. Blue Canyon selected ExoTerra's Halo thruster (Figure 4.37), for its Phase 2 and Phase 3 satellites (243). ExoTerra has demonstrated Halo on three Blackjack satellites that launched in June 2023 on the SpaceX

Transporter-8 rideshare. These are the first flights of ExoTerra's Halo electric propulsion system (244). Additionally, ExoTerra received a NASA Tipping Point award to perform an in-orbit demonstration of their 12U Courier SEP spacecraft bus. The bus includes ExoTerra's Halo thruster, xenon flow control system (XFC), power processing unit (PPU), and deployable solar arrays. The Courier spacecraft provides up to 1 km/s of delta-v, while hosting a 2U, 4 kg payload. The Tipping Point mission objective is to demonstrate the SEP system by spiraling to 800 km from a drop-off orbit of 400 km and then deorbiting. Primary mission objectives include demonstration of the solar array deployment and power generation, PPU efficiency, and 2 kg of thruster propellant throughput. For the Tipping Point mission, the 0.85 kg, 1/3U thruster will nominally operate at 135 W discharge power and produce ~8 mN of thrust (245) (246) (247) (248) (249).

ExoTerra reported in May 2025 delivering 21 Halo propulsion modules to York Space Systems for the Space Development Agency (SDA) Transport Layer (250). ExoTerra was acquired by Voyager Technologies in late 2025 (251).

ExoTerra Resource is commercializing as Halo12 (Figure 4.38) a version of JPL's Magnetically Shielded Miniature (MaSMi) Hall thruster technology for multiple unnamed flight opportunities. JPL performed extensive development of the technology between 2011 and 2021, culminating in a 7,205-hour wear test of JPL's engineering model thruster. The life test processed over 100 kg of xenon propellant and produced a total impulse of approximately 1.55 MN-s. Exoterra's unnamed flight programs (252) require additional life time, beyond JPL's demonstration, so the same JPL engineering model thruster was recently installed in JPL's high-bay vacuum facility to extend the demonstration to 8187 hours and 1.73 MN-s. Other qualification tests conducted by JPL include a 25,000 ignition cycle heaterless cathode demonstration, a 3000-cycle coil TVAC test, and dynamic testing of the thruster (253). It is important to note that the thruster tested by JPL was not produced by Exoterra. However, given that the JPL produced thruster continues to be operated in support of Exoterra's commercialization activities, it is plausable that Exoterra has retained the key life limiting features of the JPL design (252) (254).

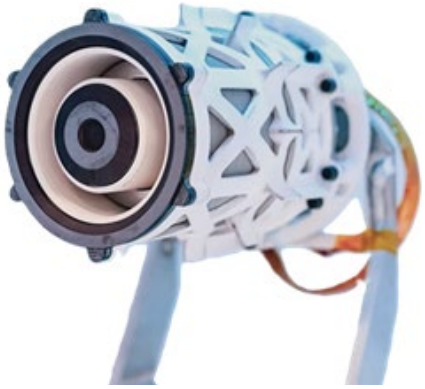


Figure 4.38: Halo12. Credit: ExoTerra Resource, LLC

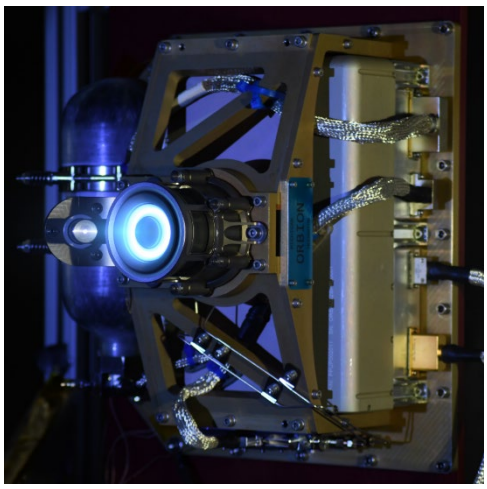


Figure 4.39: Aurora HET, PPU and XFC. Credit: Orbion Space.

Orbion's Aurora Hall-effect thruster system (Figure 4.39) is flying on Capella Space's synthetic aperture radar satellites (255), and will fly on a U.S. Space Force weather satellite under contract with General Atomics Electromagnetic Systems (GA-EMS) (256). Orbion also delivered 33 Aurora propulsion modules to York Space Systems for a military constellation (257). The Aurora propulsion system consists of the Hall-effect thruster and cathode, power processing unit, propellant flow system, and cable harnessing. The system is used for orbit raising, orbit maintenance, and de-orbit. In ground qualification testing, Aurora has demonstrated 400 kN-s total impulse (258). In 2026, Orbion became a wholly owned U.S. subsidiary of York Space (259).

Busek has supplied its BHT-350, Figure 4.40, Hall-effect thruster to Airbus OneWeb Satellites (AOS) for a range of missions. Busek engineered and qualified the thrusters for orbit raising, orbit maintenance, and end-of-life de-orbit. Eighty OneWeb satellites with BHT-350s launched in December 2022 and January 2023. More than 100 units were operating on OneWeb satellites as of August 2023 with all thrusters reported as operational (260) (261) (262) (263).



Figure 4.40: BHT-350 Flight Units. Credit: Busek Co.

Busek shipped its first flight BHT-600 Hall-effect thruster system to a U.S. Government customer in early 2021. The BHT-600 previously demonstrated a 7,000-hour ground test performed at NASA GRC as part of a NASA Announcement for Collaborative Opportunity (ACO) Space Act Agreement (SAA), Figure 4.41. The thruster successfully demonstrated 70 kilograms of xenon propellant throughput before the ground test was terminated (264) (265).



Figure 4.41: BHT-600 Installed in NASA GRC Vacuum Test Facility. Credit: Busek Co.

Northrop Grumman's (NG) Space Systems Sector has developed the NGHT-1X (Figure 4.42) thruster for its next generation satellite servicing vehicle known as the Mission Extension Pod (MEP). MEP carries power and propulsion for self-propelled orbit raising as well as station keeping and momentum management when docked to a client vehicle. MEP is designed for a 6-year mission life but can carry a propellant load that permits even longer lifetimes. The thruster is designed to generate a minimum total impulse of 2.1 MN-s, not including margin, to enable the MEP mission. NG partnered with the NASA Glenn Research Center (GRC) to develop the NGHT-1X, licensing NASA's technology for a high propellant throughput, sub-kilowatt Hall-effect thruster. NG's SpaceLogistics has sold all three MEPs that are on the manifest for the first launch on a Falcon 9 rocket planned for 2026 (266) (267) (268) (269) (270) (271) (272).

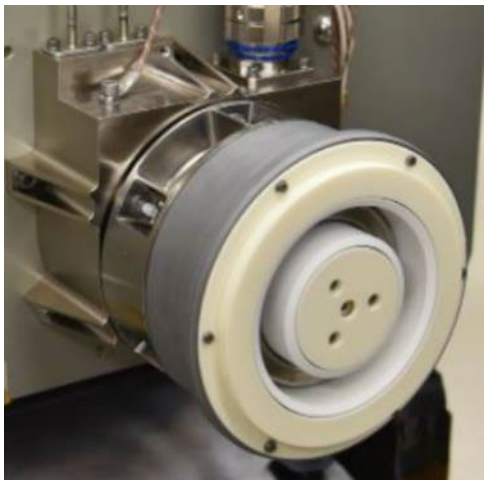


Figure 4.42: NGHT-1X Engineering Model Hall-Effect Thruster. Credit: Northrop Grumman.

The EOS SAT-1 developed by Dragonfly Aerospace for the EOS Data Analytics space mission successfully tested its SETS SPS-25 propulsion system. The EOS SAT-1 launched on a Falcon 9 rocket on January 3, 2023 (273) (274).

The Aliena Pte Ltd MUSIC-SI Hall thruster (figure 4.43) was integrated on the NuX-1 3U nanosatellite in July 2021. In-orbit deployment was achieved in January 2022 during SpaceX Transport 3 Mission. Aliena's Hall thruster became the first to operate on board such a small satellite, featuring the lowest power consumption for a commercial Hall thruster at 20W (275) (276) (277) (278) (279).

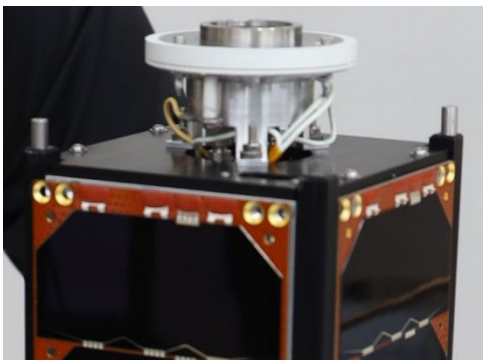


Figure 4.43: NuX-1 satellite with MUSIC-SI Hall Thruster. Credit: Aliena Pte Ltd

The MUSIC-HM Hall thruster from Aliena and four ARM-A resistojets from Aurora Propulsion Technologies form the Multi-modal Electric Propulsion Engine (MEPE). MEPE was deployed on an Orbital Astronautics 12U satellite (ORB-12 Strider) in July 2023 by a PSLV rocket (PSLV C-56 DS-SAR mission). The mission will demonstrate the capability of these propulsion systems to support a small satellite constellation. MEPE's dual electric propulsion technologies allow both the high thrust, low specific impulse of resistojets and low thrust, high specific impulse of Hall thrusters. Both systems share a common propellant, electronics, and fluidics (275) (279) (280).

d. Summary Table of Devices

See Table 4-10 for current state-of-the-art HET devices applicable to small spacecraft.

Pulsed Plasma and Vacuum Arc Thrusters

a. Technology Description

Pulsed Plasma Thrusters (PPT) produce thrust by triggering an electric arc between a pair of electrodes that typically ablates a solid-state propellant like polytetrafluoroethylene (PTFE) or ionizes a gaseous propellant. The plasma may be accelerated by either electrothermal or electromagnetic forces. Whether the mechanism of acceleration is electrothermal, electromagnetic, or often some combination thereof, is determined by the device topology (281).

Electrothermal PPTs characteristically include a chamber formed by a pair of electrodes and solid propellant, wherein propellant ablation and heating occur. During and immediately following each electric discharge, pressure accumulates and accelerates the propellant through a single opening. Electromagnetic PPTs characteristically do not highly confine the propellant as plasma forms. The current pulse, which may exceed tens of thousands of amps, highly ionizes the ablated material or gas. The current pulse further establishes a magnetic field, where the **jxB** force accelerates the plasma. PPT devices that are predominantly electrothermal typically offer higher thrust, while devices that are predominantly electromagnetic offer higher specific impulse.

The simplest PPTs have no moving parts, which may provide a high degree of reliability. However, as the solid propellant is consumed, the profile of the propellant surfaces constantly change. Thus, PPTs with static solid propellant demonstrate a change in performance over their life and inherently have a relatively limited lifetime. More complex solid propellant PPTs include a propellant feed mechanism. Typically, the propellant surface profile changes during an initial burn-in period but then settles into a steady-state behavior where the propellant advancement is balanced by the propellant ablation.

PPT devices are suitable for attitude control and precision pointing applications. PPTs offer small and repeatable impulse bits, which allow for very high precision maneuvering. The complete propulsion system consists of a thruster, an ignitor, and a power processing unit (PPU). Energy to form the pulsed discharge is stored in a high voltage capacitor bank, which often accounts for

a significant portion of the system mass. Once the capacitors are charged, resulting in a large differential voltage between the electrodes, the ignitor provides seed material that allows the discharge between the electrodes to form. Various materials and gases (including water vapor) have been tested with PPTs; however, PTFE remains most common.

Vacuum arc thrusters (VAT) are another type of pulsed plasma propulsion (282). This technology consists of two metallic electrodes separated by a dielectric insulator. Unlike PPTs, one VAT electrode is sacrificial, providing the propellant source. The mechanism for propellant acceleration is predominantly electromagnetic, resulting in a characteristically high specific impulse and low thrust. One variant of the VAT is predominantly electrostatic, through the inclusion of a downstream electrostatic grid.

b. Key Integration and Operational Considerations

- **Safety**: PPT capacitor banks often store tens of joules of energy at potentially a couple thousand volts. Follow good electrical safety practices when operating and storing PPTs in a laboratory environment.
- **Input Power Range**: PPTs and VATs are pulsed devices, which operate by discharging energy stored in capacitors with each pulse. Thus, the propulsion system's average power draw from the spacecraft bus can be quite low or high depending on capacitor energy storage and pulse frequency. This flexibility allows PPTs to be applied to spacecraft with limited power budgets of just a few watts, or ample power budgets of hundreds of watts.
- **Minimum Impulse Bit:** A compelling capability of pulsed devices is the ability to generate small, precise, and well-timed impulse bits for precise spacecraft maneuvering. By controlling the discharge voltage, very small impulse bits on the order of micronewton-seconds are easily achieved.
- **Compact and Simple Designs:** PPTs and VATs are typically very simple and compact devices. While the total impulse capability is small compared to other forms of EP, these devices offer a particularly attractive solution for CubeSats, where low cost may be a more significant consideration than total impulse. The systems are also attractive for learning environments where propulsion expertise such as high-pressure feed systems and propellant management may be lacking.
- **Late-Time Ablation**: Although pulsed devices allow for operation over a wide range of pulse frequency, thruster efficiency typically improves with higher pulse rate. Late-time ablation is a key inefficiency of solid propellant pulsed devices, where material continues to ablate from the propellant surface well after the discharge pulse. The amount of material accelerated may be maximized through higher frequency pulsing.
- **Thrust-to-Power:** Pulsed devices suffer from several inefficiencies including late time ablation, frozen flow, and wall heating. Propulsion system efficiency is typically below 20%, and may be as low as a few percent. Thus, although pulsed devices may have high specific impulse, the thrust-to-power is low. Small spacecraft with limited power for propulsion may find that large propellant loads provide little benefit as there is inherently a limitation to the number of pulses achievable over the life of the power-limited spacecraft.
- **Thermal Soak-back:** The low thruster efficiencies may result in large thermal loads on the spacecraft due to thermal soak-back, especially at high rates of pulsing. The spacecraft's ability to radiate this energy to limit heating may set an upper bound on the pulse frequency.
- **Ignitor:** Pulsed devices usually require some form of ignitor to provide seed material to lower the impedance between the electrodes and initiate the discharge pulse. As such, the lifetime of the ignitor may drive the lifetime of the thruster. Ignitors may fail due to

erosion or fouling that prevents sparking. Some devices may include multiple redundant ignitors to increase system lifetime.

- **Shorting:** The electrodes of pulsed devices are separated by isolating elements. Shadow shielding or other physical features are typically necessary to avoid shorting between electrodes as conductive material ejected by the thruster accumulates. While PTFE is an insulator, the PTFE is reduced to carbon and fluorine when ablated, where carbon accumulation provides a potentially conductive path. VATs employ metal propellants that can similarly result in unintended shorting.
- **Spacecraft Contamination:** As with any conductive propellant, spacecraft contamination is a concern. Plume interaction with the spacecraft must be understood to assess the impact of the plume on the operation of critical surfaces such as solar panels, antennas, and radiators.

c. Missions

In 2019, CU Aerospace was selected for a NASA STMD Tipping Point award to design, fabricate, integrate, and perform mission operations for the DUPLEX 6U CubeSat having two of CU Aerospace's micro-propulsion systems onboard, one Monofilament Vaporization Propulsion (MVP) system (142) (143) (144), shown in figure 4.18, and one Fiber-Fed Pulsed Plasma Thruster (FPPT) system (148) (149) (150) (151) (152), shown in figure 4.45. The FPPT can provide a large total impulse primary propulsion for micro-satellites through implementation of a novel PTFE fiber propellant storage and delivery mechanism. A major enhancement of the FPPT technology over classical PPTs is the ability to control both the propellant feed rate and pulse energy, thereby providing control of both the specific impulse and thrust. The FPPT can also provide precision control capability for small spacecraft requiring capabilities such as precision pointing or formation flying. Thrust-vectoring capability of ±10° in the yaw and pitch axes (also with the potential for roll control authority) has been incorporated into the system, allowing for limited ACS capability and wheel desaturation for deep space missions. In-orbit operations will demonstrate multiple mission capabilities including inclination change, orbit raising and lowering, drag makeup, and deorbit burns. DUPLEX was delivered to the International Space Station on a Cygnus cargo ship in September 2025 (154) (155).



Figure 4.45: FPPT 1.7U module. Credit: CU Aerospace.

The Benchmark Space Systems' Xantus thruster (figure 4.44) is a millinewton-class non-toxic metal plasma thruster that is compatible with multiple solid metal propellants (283). The baseline molybdenum propellant has a measured specific impulse of 1774 seconds. The Xantus thruster first launched in January 2023 on board the USSF Rapid Revisit Optical Cloud Imager (RROCI) 12U CubeSat demonstration mission. However, the RROCI spacecraft failed to deploy after launch. Xantus was successfully deployed on board an Orion Space Solutions' 12U CubeSat in low-Earth orbit in March 2024 (284) (285).

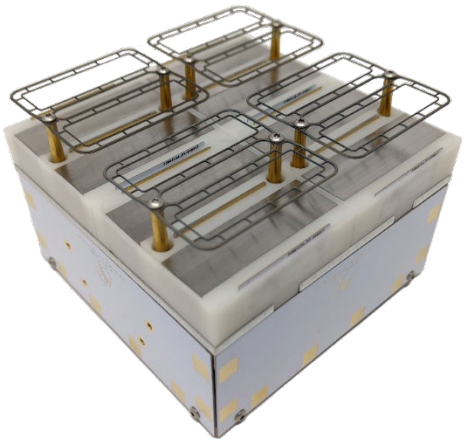


Figure 4.44: Xantus Thruster. Credit: Benchmark Space Systems.

Comat's Plasma Jet Pack (PJP) vacuum arc thruster can be configured with up to four nozzles operating on a solid/inert propellant to provide vectorized thrust (286). The PJP has launched as part of the Vega VV23 mission on the ∑yndeo-2 6U CubeSat. At the time of this publication, no details have yet been reported on the commissioning of the propulsion system (287).

The Neumann Drive is a center-triggered pulsed cathodic arc propulsion technology developed by Neumann Space using molybdenum propellant. The Neumann Drive is offered in multiple configurations offering a range of propulsive performance depending on available spacecraft power (288). The ND-15 thruster, designed for nanosatellites, was demonstrated on Australia's Skykraft satellite (289) (290) (291), and another ND-15 was flown in late 2023 on the University of Melbourne's SpIRIT nanosatellite (292) (295). The ND-50, a more compact system, was deployed in January 2025 on the 6U EDISON satellite (296) and in January 2026 on the 150 kg CarbSAR satellite (297) (298).

d. Summary Table of Devices

See Table 4-11 for current state-of-the-art pulsed plasma and vacuum arc devices applicable to small spacecraft.

Ambipolar

a. Technology Description

Ambipolar thrusters ionize gaseous propellant within a discharge cavity via various means, including DC breakdown or RF excitation. The escape of high-mobility electrons from the discharge cavity creates a charge imbalance in the plasma discharge, and the subsequent ambipolar diffusion accelerates ions out of the cavity to generate thrust.

Because the thruster plume is charge-neutral, no neutralizer assembly is necessary. A variety of propellants are theoretically usable due to the absence of exposed electrodes (and their associated material compatibility concerns).

b. Key Integration and Operational Considerations

- **Propellant Agnostic**: While ambipolar thrusters may be operable on a variety of propellants thanks to the devices' lack of exposed electrodes, different propellants will have different ionization costs (i.e., impact on thruster efficiency), plume behavior, and propellant storage requirements that should be considered during propellant selection.
- **Electromagnetic Interactions**: For RF-discharge thrusters, electromagnetic interference and compatibility (EMI/EMC) testing may be critical to assess the impact of thruster operations on spacecraft communications and payload functionality.
- **Thermal Soak-back**: Low thruster efficiencies may result in large thermal loads on the spacecraft due to thermal soak-back. Validated thermal modeling should be considered to assess impacts to the host spacecraft.

c. Missions

The SpaceX Falcon 9 Transporter-1 launch in January 2021 included two small satellites with the Phase Four Maxwell Block 1 onboard. This integrated propulsion system (Figure 4.46) includes the RF thruster and power electronics along with a xenon propellant tank and feed



Figure 4.46: Maxwell Block 1. Credit Phase Four.

system (299). Phase Four has further reported in 2023 that its Maxwell Block 2, with improved modularity and performance compared to Block 1, has been demonstrated on orbit (300).

The UniSat-7 mission, led by GAUSS, is a 36-kg microsatellite that launched via Soyuz-2-1a Fregat in March 2021. This technology demonstration mission included a T4i iodine-propellant REGULUS (50-I2-Small) module (Figure 4.47), an integrated propulsion system that includes thruster, power processing unit, and heated propellant-feed components. The propulsion demonstration is expected to include orbit raising and lowering around the 600-km orbit (302) (303) (304).

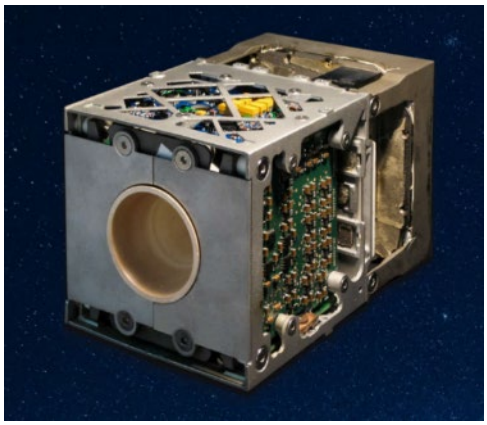


Figure 4.47: REGULUS propulsion module. Credit: T4i.

A 6U CubeSat from Team Miles was awarded a rideshare slot onboard Artemis I, as one of the winning teams in NASA's Cube Quest Challenge. The objective of the mission was to demonstrate deep space communications from beyond a 2.5-million mile range. Twelve ConstantQ water-propellant thrusters (Figure 4.48), an earlier version of Team Miles' current M1.4 system, were integrated onboard the CubeSat to provide primary propulsion as well as 3-axis control (305) (306). While the spacecraft was deployed in November 2022, communications contact was not established (424).

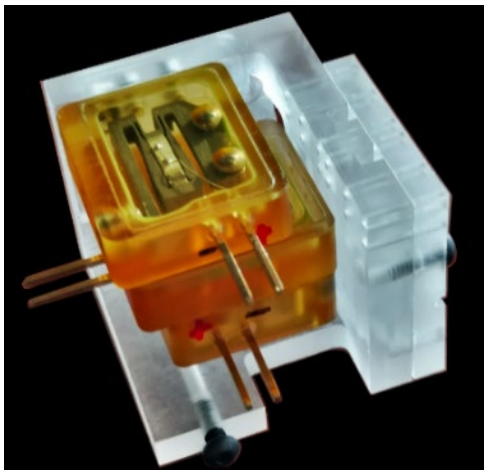


Figure 4.48: ConstantQ thruster head. Credit: Miles Space.

d. Summary Table of Devices

See Table 4-12 for current state-of-the-art ambipolar devices applicable to small spacecraft.

4.6.3 In-Space Propellant-less Propulsion

Propellantless propulsion systems generate thrust via interaction with the surrounding environment (e.g., solar photon pressure, planetary magnetic fields, solar wind and ionospheric plasma pressures, and planetary atmospheres). By contrast, chemical and electric propulsion systems generate thrust by expulsion of reaction mass (i.e., propellant). Four propellant-less propulsion technologies have undergone in-space demonstrations to date, including solar sails, tethers, electric sails (and plasma brakes), and aerodynamic drag devices.

Solar Sails

a. Technology Description

Solar sails use solar radiation pressure to generate thrust by reflecting photons via lightweight, highly reflective membranes. While no commercial products are presently available, a handful of missions have sought to demonstrate the technology using small spacecraft.

b. Missions

NASA's NanoSail-D2, Figure 4.49, launched as a 3U CubeSat secondary payload onboard the Fast, Affordable, Science and Technology Satellite (FASTSAT) bus in November 2010. The 10-m^2 sail made of CP-1 deployed from a 650 km circular orbit and deorbited the spacecraft after 240 days in orbit (307).

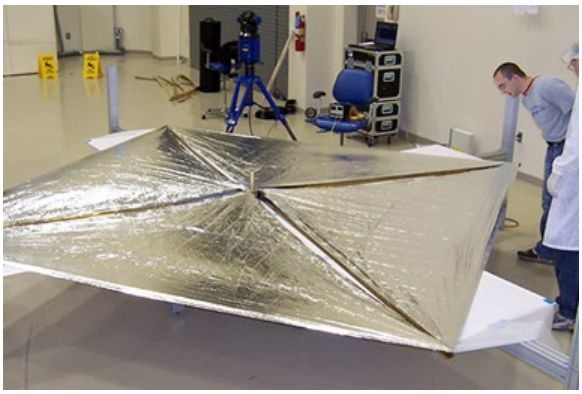


Figure 4.49: Deployment test of the NanoSail solar sail. Credit: NASA.

The Planetary Society's LightSail 2 mission launched as a 3U CubeSat secondary payload on the Department of Defense's Space Test Program (STP-2) in June 2019. The 32-m^2 mylar solar sail was deployed at 720 km altitude and demonstrated apogee raising of ~10 km. Its mission was still ongoing as of September 2022 (308).

NASA's Near-Earth Asteroid (NEA) Scout (Figure 4.50) mission launched as a secondary payload onboard Artemis I in November 2022. Unfortunately, contact was never made with the spacecraft, and the sail could not be tested. The 6U CubeSat was to deploy an 85-m^2 solar sail and conduct a flyby of an asteroid within two years of launch (309) (310).

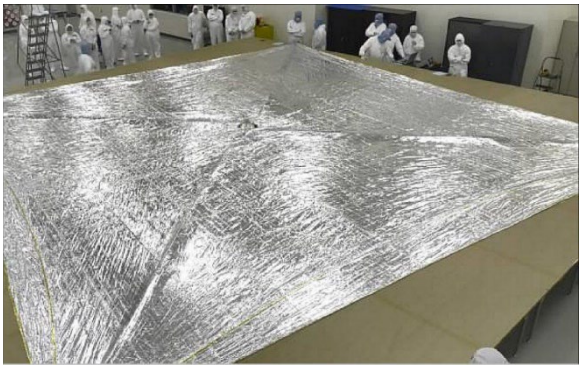


Figure 4.50: Deployment test of the Near-Earth Asteroid Scout solar sail. Credit: NASA.

NASA's Advanced Composite Solar Sail System (ACS3) technology demonstration uses composite materials for solar sail propulsion. The unfurled sail, approximately 9-m^2, was deployed from a 12U CubeSat that launched in 2024 (311).

Tethers

a. Technology Description

NASA has developed tether technology for space applications since the 1960s. A tether is nothing more than a long wire, conducting or nonconducting, deployed from a spacecraft in orbit. Two types of tethers and systems can be used for space transportation, with both having had their fundamental physical principles demonstrated in space:

- **Electrodynamic Tethers (EDT)**: A propulsive force of $F=ILxB$ (Lorentz force) is generated on a spacecraft-tether system when a current I from an onboard power supply is fed into a tether of length L against the electromotive force (emf) induced in it by the geomagnetic field B. This concept will work near any planet with a magnetosphere (Earth, Jupiter, etc.). The resulting force may be used to accelerate the deorbit of a spacecraft, boost a spacecraft's orbital altitude (by reversing the direction of current flow using an onboard power supply), or change its orbital inclination.
- **Momentum Exchange Tethers**: Using completely different physical principles, long nonconducting tethers can exchange momentum between two masses in orbit to place one body into a higher orbit or a transfer orbit for lunar and planetary missions. Recently completed system studies of this concept indicate that it would be a relatively low-cost in-space asset with long-term, multi-mission capability.

b. Missions

Important milestones include retrieval of a tether in space on the Tethered Satellite System (TSS) mission (TSS-1, 1992), the accidental momentum-exchange boost of the TSS-1R satellite when the tether broke during flight (TSS-1R, 1996), successful deployment of a 20 km-long tether in space (SEDS-1, 1993), closed-loop control of tether deployment (SEDS-2, 1994), and operation of an electrodynamic tether with tether current driven in both directions (i.e., power and thrust modes) (PMG, 1993).

More recently, Georgia Institute of Technology's Prox-1 mission was launched as a secondary payload on the Department of Defense's Space Test Program (STP-2) in June 2019. The 70 kg spacecraft served as the host and deployer for the LightSail 2 mission. The Prox-1 spacecraft housed a Tethers Unlimited Nanosat Terminator Tape (NSTT), shown in Figure 4.51, which deployed a 70-m tether in September 2019 to lower the orbit from 717 km. Data from the Space Surveillance Network indicate that the NSTT caused Prox-1 to deorbit more than 24 times faster than otherwise expected. This rate of orbital decay will enable Prox-1 to meet its 25-year deorbit requirement (312) (313) (314).



Figure 4.51: Nanosat Terminator Tape (NSTT). Credit: Tethers Unlimited.

The Naval Postgraduate School's NPSat-1 was launched as a secondary payload on STP-2 and deployed its NSTT in late 2020 (314). TriSept's DragRacer technology demonstration mission, launched as a rideshare onboard an Electron rocket in November 2020, sought to conduct a direct comparison of the deorbiting rates of two Millennium Space Systems satellites, one of which used a 250-m NSTT (314) (315). A comparison of flight data for operation of the NSTT from each of these three missions has been publicly released (316).

Electric Sails

a. Technology Description

An electric sail (also known as an electric solar wind sail or an E-sail) uses the dynamic pressure of the solar wind as a source of thrust. By using positively charged wires deployed from a spacecraft to create electric fields around each wire, a large "virtual" sail is created that deflects solar wind protons and extracts their momentum. Unlike EDTs, they do not derive thrust using the Lorentz force. Electric sails must be used outside the Earth's magnetosphere.

A closely related concept to the electric sail is the plasma brake, an electrostatic deorbit propulsion system that, like the electric sail, uses Coulomb collisions between the charged wire and the ions in the surrounding environment (e.g., the Earth's ionosphere) to generate an electrostatic force orthogonal to the tether direction, which lowers the spacecraft's orbital altitude.

These technologies are relatively immature, but researchers in Europe and the U.S. have been making incremental progress on their development.

b. Missions

The AuroraSat-1 satellite was launched on an Electron rocket on May 5, 2022 (158) (159). The spacecraft was built by SatRevolution with Aurora Propulsion Technologies providing the payloads. The mission serves as a technology demonstration for a Plasma Brake module (157) (Figure 4.52) and an Aurora Resistojet Module for Attitude control (ARM-A) (156) (Figure 4.19), both produced by Aurora. The Plasma Brake module on AuroraSat-1 is a dual-redundant system for demonstration purposes. A 50-m tether will be deployed to demonstrate its deorbiting capability.

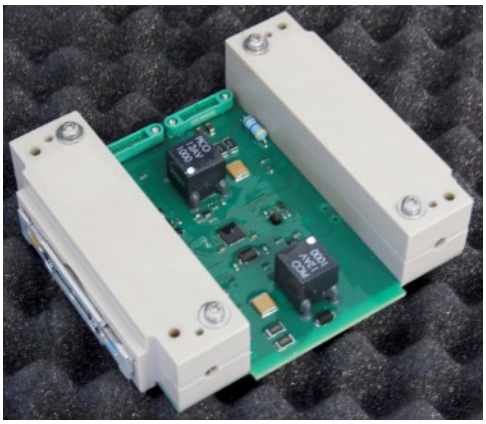


Figure 4.52: Plasma Brake Module (PBM) demo unit. Credit: Aurora Propulsion Technologies.

Aerodynamic Drag

a. Technology Description

Satellites have historically deorbited from low-Earth orbits with the aid of thrusters or passive atmospheric drag. Given the increasing rate of new spacecraft launched and the associated potential for new orbital debris following completion of missions, orbital debris management has gained increasing attention. Space debris poses a growing threat to active satellites and human activity in space. Allowing decades for defunct spacecraft to decay naturally from low-Earth orbit is no longer sufficient, as the Federal Communications Commission in late 2022 adopted a draft rule that requires <2,000 km altitude spacecraft to deorbit within 5 years of mission completion (318). Aerodynamic drag devices may provide one method to rapidly remove spacecraft from low-Earth orbits upon mission completion.

Below about 1,000 km altitude, the atmosphere exerts a measurable drag force opposite the relative motion of any spacecraft, which results in a slow orbital decay. The intensity of the drag force exerted on the spacecraft depends on numerous factors such as local atmospheric density, the spacecraft forward facing area, the spacecraft velocity, and a drag coefficient. The drag coefficient accounts for the drag force's dependence on an object's unique geometric profile. While the spacecraft velocity and local atmospheric density are largely mission dependent, a spacecraft's forward-facing area and drag coefficient can be altered by introducing aerodynamic drag devices such as exo-brakes and ballutes. These deployable or inflatable parachutes and balloons can greatly increase the drag force exerted on spacecraft by an order of magnitude or more and significantly increase the rate of orbital decay.

Furthermore, aerodynamic drag devices may be useful to reduce the spacecraft propellant mass required for orbit capture and disposal at other planetary bodies, given sufficient atmospheric density exists.

For further details on these devices, see the Deorbit Systems chapter.

Table 4-2: Hydrazine Chemical Propulsion												
Manufacturer	**Product**	**Propellant**	**Thrust per Thruster (Quantity)**	**Specific Impulse**	**Total Impulse**	**Mass**	**Envelope**	**Power**	**ACS**	**PMI Status**	**Missions**	**References**
---	**---**	**---**	**[N]**	**[s]**	**[kN-s]**	**[kg]**	**[cm³ or U]**	**[W]**	**Y/N**	**C,D,E,F**	**---**	**---**
Integrated Propulsion Systems												
Aerojet Rocketdyne USA	MPS-120	Hydrazine	0.25 – 1.0 (4)	-	2 (2U) 0.8 (1U)	2.5† (2U) 1.6† (1U)	2U 1U	-	Y	D	-	(99)
Aerojet Rocketdyne USA	MPS-125	Hydrazine	0.25 – 1.0 (4)	-	14 (8U) 9.9 (6U) 5.2 (4U)	12.1† (8U) 9.3† (6U) 6.2† (4U)	8U 6U 4U	-	Y	D	-	(99)
Stellar Exploration USA	Monopropellant CubeSat System	Hydrazine	-	200s	-	-	-	-	Y	F	Echostar Global 3, NASA Capstone	(17) (18) (19) (20) (100)
Stellar Exploration USA	Bipropellant CubeSat system	Hydrazine/ NTO	-	285	-	-	-	-	Y	D	-	(100)
Thruster												
Aerojet Rocketdyne USA	MR-103	Hydrazine	1	202 - 224	183	0.33 - 0.37	-	< 16	-	F	numerous	(8)
Aerojet Rocketdyne USA	MR-106	Hydrazine	22	228 - 235	561	0.59	-	< 36	-	F	numerous	(8)
Aerojet Rocketdyne USA	MR-111	Hydrazine	4	219 - 229	262	0.37	-	< 16	-	F	numerous	(8)
Aerojet Rocketdyne USA	MR-401	Hydrazine	0.08	182	200	0.60	-	-	-	F	Numerous	(8)
ArianeGroup France	1 N	Hydrazine	1	200 - 223	135	0.29	-	-	-	F	ALSAT-2, numerous	(6) (7)
ArianeGroup France	20 N	Hydrazine	20	222 - 230	517	0.65	-	-	-	F	Numerous	(7)
IHI Aerospace Japan	MT-9	Hydrazine	1	208 - 215	(100 kg)*	-	-	-	-	F	Numerous	(16)
IHI Aerospace Japan	MT-8A	Hydrazine	5	212 - 225	(190 kg)*	-	-	-	-	F	Numerous	(16)
IHI Aerospace Japan	MT-2	Hydrazine	20	210 - 226	(115 kg)*	-	-	-	-	F	Numerous	(16)
Moog USA	MONARC-1	Hydrazine	1	227	111	0.38	113x50 mm	18 (valve)	-	F	numerous	(12)
Moog USA	MONARC-5	Hydrazine	4.5	226	613	0.49	203x380 mm	18 (valve)	-	F	NASA SMAP, numerous	(12) (13)
Moog USA	MONARC-22-6	Hydrazine	22	228	533	0.72	203x380 mm	30 (valve)	-	F	numerous	(12)
Moog USA	MONARC-22-12	Hydrazine	22	228	1,173	0.69	229x530 mm	30 (valve)	-	F	numerous	(12)
Northrop Grumman USA	MRE-0.1	Hydrazine	1	216	(34 kg)*	0.5	114x175 mm	15	-	F	numerous	(14)
Northrop Grumman USA	MRE-1.0	Hydrazine	5	218	(544 kg)*	0.5	114x188 mm	15	-	F	numerous	(14)
Northrop Grumman USA	MRE-4.0	Hydrazine	18	217	(249 kg)*	0.5	61x206 mm	30	-	F	numerous	(14)
Rafael Israel	1N	Hydrazine	1	205 - 214	100	0.31	-	9 (valve)		F	numerous	(15)
Rafael Israel	5N	Hydrazine	6	210 - 220	74	0.31	-	9 (valve)		F	numerous	(15)
Rafael Israel	25N	Hydrazine	28	205 - 220	100	0.53	-	15 (valve)		F	numerous	(15)

Note that all data is documented as provided in the references. Unless otherwise published, do not assume the data has been independently verified.
† denotes a wet mass, ‡ denotes a dry mass, "-" = denotes data not available or applicable, * denotes mass of propellant throughput, rather than total impulse

Table 4-3: Alternative Monopropellant and Bipropellant Propulsion												
Manufacturer	**Product**	**Propellant**	**Thrust per Thruster (Quantity)**	**Specific Impulse**	**Total Impulse**	**Mass**	**Envelope**	**Power**	**ACS**	**PMI Status**	**Missions**	**References**
---	---	---	**[N]**	**[s]**	**[kN-s]**	**[kg]**	**[cm³ or U]**	**[W]**	**Y/N**	**C,D,E,F**	---	---
Integrated Propulsion Systems												
Aerojet Rocketdyne USA	MPS-130	ASCENT	0.25 – 1.0 (4)	-	2.7 (2U) 1.1 (1U)	2.8† (2U) 1.7† (1U)	2U 1U	-	Y	D	-	(98) (99)
Aerojet Rocketdyne USA	MPS-135	ASCENT	0.25 – 1.0 (4)	-	19.4 (8U) 13.7 (6U) 7.3 (4U)	14.7† (8U) 11.2† (6U) 7.2† (4U)	8U 6U 4U	-	Y	D	-	(99)
Aerospace Corp. USA	HyPer	H_2O_2	-	-	-	-	0.25U	-	-	D	-	(101)
Benchmark Space Systems USA	Halcyon	HTP	0.25 1 5 10	150 - 170	(1.56 kg)* (6.6 kg)* (32.5 kg)* (65 kg)*	-	-	< 4	Y	E	Transporter 2 (Undisclosed missions)	(36) (102) (103) (104)
Benchmark Space Systems USA	Halcyon Avant	HTP + Fuel	2 10 22	290 - 310	(6.8 kg)* (34 kg)* (74.8 kg)*	-	-	< 15	Y	F	Sherpa-TLC2	(34) (35) (104)
Benchmark Space Systems USA	Peregrine	HTP & Alcohol	0.1 - 22 (1-8)	270 - 300	5 - 150	-	-	-	-	D	-	(104)
ECAPS Sweden	SkySat 1N HPGP Propulsion System	LMP-103S	1.0 (4)	> 200	21	22†	55 x 55 x 15	10	Y	F	Skysat, PRISMA, Astroscale ELSA-d	(24) (25) (26) (27) (105) (106) (107) (108)
Busek USA	BGT-X5 System	ASCENT	0.5	220 - 225	0.57	1.5†	1U	20	N	D	-	(112) (113) (114)
Cornell University USA	Cislunar Explorer	Water (Electrolysis)	-	-	-	-	6U total (2-units)	-	-	E	CubeQuest Challenge (removed from Artemis 1)	(37) (38) (39)
CU Aerospace USA	MPUC	(CMP-X) Peroxide/ Ethanol blend	0.23	178	1.4 (1.5U) 2.1 (2U)	2.5† (1.5U) 3.3† (2U)	1.5U 2U	3	N	D	-	(46) (47)
Dawn Aerospace New Zealand	CubeDrive	Nitrous Oxide & Propylene	0.5	-	0.425 1.450	1.17† 2.70†	0.8U 2U	-	N	F	Multiple	(45) (115)
Dawn Aerospace New Zealand	SatDrive	Nitrous Oxide & Propylene	0.5 – 16.7	250 - 280	5 – 500	-	-	-	N	F	Multiple	(45) (115)
Moog USA	Monopropellant Propulsion Module	Green or 'Traditional'	0.5	224	0.5	1.0†	1U	2 x 22.5 W/Thruster	N	D	-	(116)
Rubicon Space Systems USA	Sprite	ASCENT	0.05 - 0.15	>195	> 1	< 2.2†	1.5U	2 - 16	N	E	GPDM	(110) (111) (117)
NASA MSFC USA	LFPS	ASCENT	0.1 (4)	> 200s	> 3.5	< 5.5†	~2.4U	15 - 47	Y	E	Lunar Flashlight	(32) (33)
NanoAvionics Lithuania	EPSS C1K	IADN-blend	1.0 BOL 0.22 EOL	213	> 0.4	1.2†	1.3U	9.6 (preheat) 1.7 (firing)	N	F	Lituanica-2	(43) (44)
NanoAvionics Lithuania	EPSS C2	IADN-blend	1.0 BOL 0.25 EOL	220	> 1.7	2.6†	2U	-	N	D	-	(43)

Note that all data is documented as provided in the references. Unless otherwise published, do not assume the data has been independently verified.
† denotes a wet mass, ‡ denotes a dry mass, "-" = denotes data not available or applicable, * denotes mass of propellant throughput, rather than total impulse, BOL = Beginning of Life, EOL = End of Life

Table 4-3 (cont.): Other Monopropellant and Bipropellant Propulsion												
Manufacturer	**Product**	**Propellant**	**Thrust per Thruster (Quantity)**	**Specific Impulse**	**Total Impulse**	**Mass**	**Envelope**	**Power**	**ACS**	**PMI Status**	**Missions**	**References**
---	---	---	**[N]**	**[s]**	**[kN-s]**	**[kg]**	**[cm³ or U]**	**[W]**	**Y/N**	**C,D,E,F**	---	---
Integrated Propulsion Systems (cont.)												
Tethers Unlimited USA (Subsidiary of ARKA Group LP)	HYDROS-C	Water (Electrolysis)	> 1.2	> 310	> 2.1	2.7†	19 x 13 x 9.2	5 - 25	N	F	Pathfinder Technology Demonstration	(41) (42) (118) (119)
Tethers Unlimited USA (Subsidiary of ARKA Group LP)	HYDROS-M	Water (Electrolysis)	> 1.2 (1)	> 310	> 18	13.7†	38.1 dia. x 19.1	7 - 40	N	D	-	(120)
VACCO USA	ArgoMoon Hybrid MiPS	LMP-103S/ R134a	0.1 (1)	190	0.78	2.07†	1.3U	4.3 20 (max)	Y	F	ArgoMoon (Artemis I)	(27) (28) (29)
VACCO USA	Green Propulsion System (MiPS)	LMP-103S	0.1 (4)	190	3.3	5†	3U	15 (max)	Y	D	-	(121)
VACCO USA	Integrated Propulsion System	LMP-103S	1 (4)	200	12	14.7†	11U	50 (max)	Y	D	-	(48) (49)
Thruster Heads												
Aerojet Rocketdyne USA	GR-1	ASCENT	0.3 - 1.4	231	(12 kg)*	-	-	18 (max)	-	F	GPIM	(8) (30) (31)
Aerojet Rocketdyne USA	GR-22	ASCENT	8 - 25	250	74	-	-	28	-	F	GPIM	(8) (30) (31)
Benchmark Space Systems USA	Felicette	HTP	0.4 - 1.2	161	> 10	-	-	-	-	E	Transporter 2 (Undisclosed missions)	(36) (104)
Benchmark Space Systems USA	Lynx	HTP	2 - 2.5	295	> 20	-	-	-	-	D	-	(104)
Benchmark Space Systems USA	Ocelot	HTP	18 - 22	302	> 240	-	-	-	-	F	Sherpa-TLC2	(34) (35) (104)
ECAPS Sweden	0.1 N HPGP	LMP-103S	0.03 - 0.1	196 - 209	(1 kg)*	0.04 excl. FCV	-	6.3 - 8	-	F	ArgoMoon	(24) (27) (107)
ECAPS Sweden	1 N HPGP	LMP-103S	0.25 - 1	204 - 235	(24 kg)*	0.38	-	8 - 10	-	F	PRISMA, SkySat, ELSA-d	(24) (25) (26) (27) (107) (108)
ECAPS Sweden	1 N GP	LMP-103S/LT	0.25 - 1	194 - 227	(5 - 8 kg)*	0.38	-	8 - 10	-	D		(108)
ECAPS Sweden	5 N HPGP	LMP-103S	1.5 - 5.5	239 - 253	-	0.48	-	15 - 25	-	D	-	(107)
ECAPS Sweden	22 N HPGP	LMP-103S	5.5 - 22	243 - 255	(150 kg)*	1.1	-	25 - 50	-	D	-	(107)
Dawn Aerospace New Zealand	B20 Thruster	Nitrous Oxide & Propylene	6.1 - 16.7	-	-	0.6	17.6 x 8.0 x 7.9	-	-	F	numerous	(45)
Dawn Aerospace New Zealand	B1 Thruster	Nitrous Oxide & Propylene	0.46 - 1.28	-	-	0.26	10.8 x 7.9 x 4.0	-	-	F	numerous	(45)
Rubicon Space Systems USA	0.1N	ASCENT	0.1	>195	5.7	0.06	2.5 dia x 4	8	-	E	Lunar Flashlight, GPDM	(32) (33) (109) (110) (111)
Rubicon Space Systems USA	1N LT (HT)	ASCENT	1	>250	12 (33)	0.25	6 dia x 16	15 (25)	-	D	-	(109)
Rubicon Space Systems USA	5N LT (HT)	ASCENT	5	>250	12 (118)	0.30	6 dia x 16	25	-	D	-	(109)

Note that all data is documented as provided in the references. Unless otherwise published, do not assume the data has been independently verified.
† denotes a wet mass, ‡ denotes a dry mass, "-" = denotes data not available or applicable, * denotes mass of propellant throughput, rather than total impulse

Table 4-4: Hybrid Chemical Propulsion												
Manufacturer	**Product**	**Propellant**	**Thrust (Quantity)**	**Specific Impulse**	**Total Impulse**	**Mass**	**Envelope**	**Power**	**ACS**	**PMI Status**	**Missions**	**References**
---	**---**	**---**	**[N]**	**[s]**	**[kN-s]**	**[kg]**	**[cm^3 or U]**	**[W]**	**Y/N**	**C,D,E,F**	**---**	**---**
Aerospace Corp. USA	Propulsion Unit for CubeSats	Paraffin/Nitrous Oxide	-	-	-	-	1U	-	-	D		(60)
JPL USA	Hybrid Rocket	PMMA/GOX	-	> 300	-	-	-	-	-	D	-	(54) (55) (56) (57)
NASA Ames USA	Hybrid Rocket	PMMA/ Nitrous Oxide	25	247	-	-	-	-	-	D		(58) (59)
Parabilis Space Technologies USA	ROMBUS	Various/N2O	222	260	44.6	49	55 dia. x 46	-	Y	D		(61)
Parabilis Space Technologies USA	NanoSat Obrital Transfer System	HTPB/N2O	9.4	245	-	-	-	-	Y	C		(62)
Utah State Univ. USA	Green Hybrid Rocket	ABS/Nytrox	25 - 50	220 - 300	-	-	-	< 30 for 1-2 seconds	-	D		(52) (53)
Utah State Univ. USA	Green Hybrid Rocket	ABS/GOX	8	215	-	-	-	-	-	D	-	(50) (51)

Note that all data is documented as provided in the references. Unless otherwise published, do not assume the data has been independently verified.
† denotes a wet mass, ‡ denotes a dry mass, "-" = denotes data not available or applicable

Table 4-5: Cold Gas Propulsion												
Manufacturer	**Product**	**Propellant**	**Thrust (Quantity)**	**Specific Impulse**	**Total Impulse**	**Mass**	**Envelope**	**Power**	**ACS**	**PMI Status**	**Missions**	**References**
---	---	---	**[mN]**	**[s]**	**[N-s]**	**[kg]**	**[cm^3 or U]**	**[W]**	**Y/N**	**C,D,E,F**	---	---
Integrated Propulsion Systems												
Aerospace Corp. USA	MEPSI	R236fa	20	-	-	0.188†	-	-	Y	E	STS-113 and STS-116	(63)
Benchmark Space Systems USA	Starling	Nitrogen	10 - 1000	70	-	0.75†	0.5U	< 4	Y	D	-	(104)
GomSpace Sweden	NanoProp CGP3	Butane	0.01 – 1 (4)	60 - 110	40	0.35†	5 x 10 x 10	< 2	Y	E	TW-1	(71) (73) (74) (124)
GomSpace Sweden	NanoProp 6U	Butane	0.1 – 10 (4)	60 - 110	80	0.900†	2 x 10 x 20	< 2	Y	F	GOMX-4B	(71) (72) (125)
Lightsey Space Research USA	BioSentinel Propulsion System	R236fa	20	47	79.8	1.28†	4 x 10 x 20	< 1 idle, < 4 operating	Y	E	BioSentinel	(75) (76) (77) (78)
Microspace Rapid Pte Ltd Singapore	POPSAT-HIP1	Argon	0.083 – 1.1 (8)	43	-	-	-	-	-	E	POPSAT-HIP1	(70)
T4i Italy	IANUS	R134a	6.8/10.6/26.2 (x/y/z)	40	38	0.5‡	0.5	<40	Y	E	Hera Milani	(126)
T4i Italy	PERSEUS	R134a	27/9/9 (x/y/z)	40	450	2.5‡	2.5	<20	Y	F	Iperdrone.0	(126)
ThrustMe France	I2T5	Iodine	0.35	-	75	0.9†	0.5U	5	N	F	Xiaoxiang 1-08, NAPA-2, Spire L3C Demo, Robusta-3A (2024**)	(79) (80) (81) (82)
UTIAS/SFL Canada	CNAPS	Sulfur Hexafluoride	12.5 - 50	40	100	-	-	-	N	F	CanX-4/CanX-5	(66) (67) (68) (69)
VACCO USA	NEA Scout	R236fa	25 (6)	-	500	2.54†	2U	< 55 warmup < 9 operating	Y	E	NEA Scout	(90) (91) (92)
VACCO USA	MiPS Standard	R236fa	25 (4)	-	82 - 515	0.85 – 2.46†	0.4 – 1.5U	< 12	Y	D	-	(127)
VACCO USA	MarCO-A and -B MiPS	R236fa	25 (8)	-	755	3.49†	8 x 15 x 20	-	Y	E	MarCO-A & -B	(86) (87) (88) (89)
VACCO USA	C-POD	R236fa	10 (8)	40	186	1.25†	1U	5	Y	E	CPOD	(83) (84) (85)
Thruster Heads												
Marotta USA	CGMT	Nitrogen	105 - 2360	-	-	< 0.06	-	< 7	-	F	NMP ST5	(64) (65)
Moog USA	058E143-146	Nitrogen	10 - 40	60	-	0.04	1.4 x 5.7	< 10	-	F	CHAMP, GRACE	(128)
Moog USA	058E142A	Nitrogen	120	57	-	0.016	1.4 x 2.0	< 35	-	F	Spitzer Space Telescope	(128)
Moog USA	058E151	Nitrogen	120	65	-	0.07	1.9 x 4.1	< 10.5	-	F	Spitzer Space Telescope	(128)
Moog USA	058-118	Nitrogen	3600	57	-	0.023	0.7 x 2.5	< 30	-	F	SAFER, Pluto Fast Flyby	(128)
Moog USA	58E163A	Nitrogen, Xenon, Argon	1300	70 N2, 21 Xe, 54 Ar	-	0.115	2.4 x 5.3	< 10.5	-	F	GEO applications	(128)

Note that all data is documented as provided in the references. Unless otherwise published, do not assume the data has been independently verified.
† denotes a wet mass, ‡ denotes a dry mass, "-" = denotes data not available or applicable, ** anticipated launch date

Table 4-6: Solid Motor Chemical Propulsion												
Manufacturer	**Product**	**Propellant**	**Thrust (Quantity)**	**Specific Impulse**	**Total Impulse**	**Mass**	**Envelope**	**Power**	**ACS**	**PMI Status**	**Missions**	**References**
---	**---**	**---**	**[N]**	**[s]**	**[N-s]**	**[kg]**	**[cm^3 or U]**	**[W]**	**Y/N**	**C,D,E,F**	**---**	**---**
Integrated Propulsion Systems												
PacSci EMC USA	MAPS	-	-	-	-	-	-	-	-	E	PacSciSat	(94) (95)
Thruster Heads												
Industrial Solid Propulsion USA	ISP 30 sec. Motor	80% Solids HTPB/AP	37	187	996	0.95†	5.7	-	-	D	Optical target at Kirtland AFB	(130)
Northrop Grumman USA	STAR 3	TP-H-3498	461	266	1,250	1.16†	8 dia. x 29	-	-	E	Mars Exploration Rover Spirit lander	(131)
Northrop Grumman USA	STAR 4G	TP-H-3399	258	269	2,650	1.5†	11.3 dia. x 13.8	-	-	D	-	(131)

Note that all data is documented as provided in the references. Unless otherwise published, do not assume the data has been independently verified.
† denotes a wet mass, ‡ denotes a dry mass, "-" = denotes data not available or applicable

Table 4-7: Electrothermal Electric Propulsion												
Manufacturer	**Product**	**Propellant**	**Thrust***	**Specific Impulse***	**Total Impulse***	**Mass**	**Envelope**	**Power**	**ACS**	**PMI Status**	**Missions**	**References**
---	**---**	**---**	**[mN]**	**[s]**	**[N-s]**	**[kg]**	**[cm³ or U]**	**[W]**	**Y/N**	**C,D,E,F**	**---**	**---**
Integrated Propulsion Systems												
AIS USA	AIS-SWAG1-PQ	Adamantane	0.12	20	3	0.224†	4.2 x 4.2 x 5.4	5	N	D	-	(317)
AIS USA	AIS-SWAG1-DUO	Adamantane	0.24	20	6	0.449†	8.6 x 4.2 x 5.4	10	N	D	-	(317)
AIS USA	AIS-SWAG1-QUAD	Adamantane	0.48	20	12	0.898†	8.6 x 8.6 x 5.4	20	N	D	-	(317)
Aurora Finland	ARM-A	Water	0.5	100	70	0.280†	0.3U	10£	Y	E	AuroraSat-1 (2022), ORB-12 STRIDER	(156) (158) (159) (280)
Aurora Finland	ARM-C	Water	1	-	-	0.050†	45	12 (max)	N	D	-	(162)
Benchmark Space Systems USA	Starling Ardent	Nitrogen	10 - 1000	70 – 140	-	1.15	1U	10 – 100	Y	D	-	(104)
Bradford Space Netherlands	Comet-1000	H_2O	17	175	1,150	1.55†	2,300	50 (max)	N	F	HawkEye 360, Capella Space, Transporter 7	(134) (135) (136) (137)
Bradford Space Netherlands	Comet-8000	H_2O	17	175	8,348	6.68†	23,760	55 (max)	N	F	BlackSky	(134) (137) (138)
CU Aerospace USA	CHIPS-180	R134a	15	67	176	1.03†	540	20	Y	D	-	(319) (320) (321) (322)
CU Aerospace USA	CHIPS-500	R134a	25	69	505	1.84†	1300	25	Y	D	-	(319) (320) (321) (322)
CU Aerospace USA	CHIPS-1000	R134a	31	70	1,030	3.13†	2500	30	Y	D	-	(319) (320) (321) (322)
CU Aerospace and VACCO USA	PUC	SO_2	4.5	70	184	0.72†	0.35U	15	N	E	8 flight units delivered to AFRL	(139) (140) (141)
CU Aerospace USA	MVP	Delrin Fiber	4.5	66	280	1.06†	0.93U	45	N	E	DUPLEX (2025)	(142) (143) (144) (145) (154) (155)
EPL USA	APS 100	Ammonia	28	280	2,200	2.63†	2.5U	100	N	D	-	(323)
EPL USA	APS 500	Ammonia	150	350	25,200	13.4†	27,300	450	N	E	Atomos Space (2024**)	(323) (324)
Pale Blue Japan	PBR-10	Water	1.0	-	55	0.6†	0.5U	6	N	E	ArkEdge AE1c	(325) (326)
Pale Blue Japan	PBR-20	Water	1.0	-	220	1.5†	1U	20	N	E	ArkEdge OPTIMAL-1; SPHERE-1 EYE	(160) (161) (325)
Pale Blue Japan	PBR-30	Water	12	-	400	2.1†	2U	35	N	D	-	(325)
SteamJet Space Systems UK	Steam TunaCan Thruster	Water	6	172	219	0.54†	402	< 19.9	N	D	-	(146)
SteamJet Space Systems UK	Steam Thruster One	Water	6	172	-	-	-	19.9	N	D	-	(147)
Thruster Heads												
SITAEL Italy	XR-50	Ar, Xe, N_2	100	55-85	≤ 72,000	0.22‡	45.8	≤ 50	-	D	-	(327) (328)
SITAEL Italy	XR-100	Ar, Xe, N_2	125	63-105	≤ 90,000	0.22‡	45.8	≤ 80	-	D	-	(327) (328)
SITAEL Italy	XR-150	Ar, Xe, N_2	250 (Ar) 100 (Xe)	58-110	≤ 180,000	0.22‡	45.8	≤ 95	-	D	-	(327) (328)

Note that all data is documented as provided in the references. Unless otherwise published, do not assume the data has been independently verified.

*nominal values (see references for full performance ranges), ** anticipated launch date, † denotes a wet mass, ‡ denotes a dry mass, £ per active thruster, "-" = denotes data not available or applicable

Table 4-8: Electrospray Electric Propulsion												
Manufacturer	**Product**	**Propellant**	**Thrust***	**Specific Impulse***	**Total Impulse***	**Mass**	**Envelope**	**Power**	**Neutralizer**	**PMI Status**	**Missions**	**References**
---	**---**	**---**	**[μN]**	**[s]**	**[N-s]**	**[kg]**	**[cm³ or U]**	**[W]**	**---**	**C,D,E,F**	**---**	**---**
Integrated Propulsion Systems												
Busek USA	CMNT (4x heads)	EMI-Im (ionic)	4 x 20	225	980	14.8†	29U	16.5	Carbon Nanotube	F	LISA Pathfinder	(163)
Busek USA	BET-MAX (Config. A)	EMI-Im (ionic)	4 x 55	850	4 x 92§	0.8†	1250	12	Carbon Nanotube	E	US Government	(329) (330) (331) (332) (333) (334) (335)
Busek USA	BET-MAX (Config. B)	EMI-Im (ionic)	4 x 40	2300	4 x 250	0.8†	1250	14	Carbon Nanotube	D	-	(335)
Enpulsion Austria	Nano	Indium (FEEP)	330	1,500 (alpha); 3,000 (gamma)	> 3,000 (alpha); > 5,000 (gamma)	0.90†	10 x 10 x 8.3	40	Thermionic	F	Flock 3p', ICEYE X2, Harbinger, NetSat, and others	(164) (165) (166) (167) (168) (169) (170) (171) (336) (337) (338)
Enpulsion Austria	Nano R³	Indium (FEEP)	350	1,500 (alpha); 2,700 (gamma)	> 3,000 (alpha); > 5,000 (gamma)	1.4†	9.8 x 9.9 x 9.5	45	Thermionic	E	(Evolution of Nano design)	(171) (172) (339)
Enpulsion Austria	Micro R³	Indium (FEEP)	1,000	2,100 (alpha); 2,750 (gamma)	> 25,000 (alpha); > 35,000 (gamma)	3.9†	14 x 12 x 13.3	105	Thermionic	F	GMS-T	(172) (173) (340) (341)
Enpulsion Austria	Neo	Indium (FEEP)	20,000	1,500	> 550,000	30†	34 x 34 x 15	800	Thermionic	D	-	(342)
Morpheus Space Germany	NanoFEEP (2x heads)	Gallium (FEEP)	< 40	-	-	0.16‡	9 x 2.5 x 4.3	< 3	Propellant-less	E	UWE-4	(174) (175) (343) (344)
Morpheus Space Germany	MultiFEEP (2x heads)	Gallium (FEEP)	< 140	-	-	0.28‡	9 x 4.5 x 4.5	< 19	Propellant-less	D	-	(343)

Note that all data is documented as provided in the references. Unless otherwise published, do not assume the data has been independently verified.
*nominal values (see references for full performance ranges), ** anticipated launch date, † denotes a wet mass, ‡ denotes a dry mass, § demonstrated, "-" = denotes data not available or applicable

Table 4-9: Gridded-Ion Electric Propulsion													
Manufacturer	**Product**	**Type**	**Propellant**	**Thrust***	**Specific Impulse***	**Total Impulse***	**Mass**	**Envelope**	**Power**	**Cathode Type**	**PMI Status**	**Missions**	**References**
---	---		---	**[mN]**	**[s]**	**[kN-s]**	**[kg]**	**[cm^3 or U]**	**[W]**	---	**C,D,E,F**	---	---
Integrated Propulsion Systems													
Avant Space Russia	GT-50	RF Ion	Xenon	< 7	-	-	< 8†	< 4U	< 240	Hollow	D	-	(345) (346)
Busek USA	BIT-3	RF Ion	Iodine	1.0	1,960	31.7	2.9†	18 x 8.8 x 10.2	70	RF	E	Lunar IceCube; LunaH-Map	(188) (189) (190) (191) (192) (193) (347) (348) (349) (350) (351) (352)
Pale Blue Japan	PBI	RF Ion	Water	0.35	2000	7	1.6†	10 x 10 x 11	60	RF	E	ON-SCV 018; ON-SCV 021	(353) (354) (355) (356) (357)
ThrustMe France	NPT30-I2	RF Ion	Iodine	< 1.3	2,400	5.5 (1U) 14 (1.5U)	1.2† (1U) 1.85† (1.5U)	1U 1.5U	< 81	Thermionic	F	Beihangkongshi-1; NORSAT-TD	(182) (183) (184) (185) (186) (187) (358) (359) (360)
Thruster Heads													
Ariane Group Germany	RIT µX	RF Ion	Xenon	< 0.5	-	-	0.44‡	7.8 x 7.8 x 7.6	< 50	RF	D	-	(361) (362) (363) (364) (365) (366)
Ariane Group Germany	RIT 10 EVO	RF Ion	Xenon	< 15	-	-	1.8‡	18.6 x 18.6 x 13.4	< 435	Hollow	E	(Identical to flight-heritage RIT-10 with contemporary grid design)	(361) (363) (367)
QinetiQ UK	T5	DC Ion	Xenon	< 20	< 3,000	-	2‡	19 x 19 x 24.2	< 600	Hollow	F	GOCE	(178) (179) (180) (181)

Note that all data is documented as provided in the references. Unless otherwise published, do not assume the data has been independently verified.

*nominal values (see references for full performance ranges), ** anticipated launch date, † denotes a wet mass, ‡ denotes a dry mass, "-" = denotes data not available or applicable, RF = Radio Frequency, DC = Direct Current, DDL = Destroyed During Launch

Table 4-10: Hall-Effect Electric Propulsion Thrusters												
Manufacturer	**Product**	**Propellant**	**Thrust***	**Specific Impulse***	**Total Impulse***	**Mass**	**Envelope**	**Thruster Power***	**Cathode Type**	**PMI Status**	**Missions**	**References**
---	---	---	**[mN]**	**[s]**	**[kN-s]**	**[kg]**	**[cm^3 or U]**	**[W]**	**Notes**	**C,D,E,F**	---	---
Aliena Pte Ltd Singapore	MUSIC-SI	Xenon	< 0.25	< 200	1	2†	1.5U	20	None	E	NuX-1	(275) (276) (277) (278) (279)
Aliena Pte Ltd Singapore	MUSIC-HM	Xenon	3	1,000	15	5†	4U	100	EM-HL	E	ORB-12 STRIDER	(275) (279) (280)
Astra USA	ASE	Xenon	25	1,400	300	1.0	-	400‡	CM-HL	F	Sherpa-LTE	(218) (220) (219) (220) (221) (223) (224)
Astra USA	ASE	Krypton	18	1,300	300	1.0	-	400‡	CM-HL	D	-	(218)
Busek USA	BHT-100	Xenon	6.3	1,086	150	1.2	275 wo cath.	105	EM-SH	D	-	(203) (368)
Busek USA	BHT-200	Xenon	13	1,390	84§	1.2	675 wo cath.	250‡	EM-SH	F	TacSat-2, FalconSat-5, -6	(203) (204) (205) (206)
Busek USA	BHT-200-I	Iodine	14	1390	-	1.2	675 wo cath.	250	EM-SH	E	NASA iSat (Cancelled)	(204) (206) (207)
Busek USA	BHT-350	Xenon	17	1,244	212§	1.9	-	350	EM-SH	F	OneWeb Satellites	(260) (261) (262) (263)
Busek USA	BHT-600	Xenon	39	1,500	1000§	2.8	1,470 wo cath.	680‡	EM-SH	E	US Government	(203) (264) (265) (369) (370)
Busek USA	BHT-600-I	Iodine	39	-	-	2.8	1,470 wo cath.	600	EM-SH	D	-	(206) (369) (370) (371)
EDB Fakel Russia	SPT-50	Xenon	14	860	126§	1.2	1,092	220	EM-SH	F	Canopus-V	(198) (199) (200) (201) (372)
EDB Fakel Russia	SPT-50M	Xenon	14.8	930	266	1.3	---	220	EM-SH	D	-	(372)
EDB Fakel Russia	SPT-70BR	Xenon	39	1,470	435§	2.0	1,453	660	EM-SH	F	KazSat-1, KazSat-2	(201) (202)
EDB Fakel Russia	SPT-70M	Xenon	41.3	1,580	-	-	-	660	EM-SH	D	-	(202)
EDB Fakel Russia	SPT-70M	Krypton	31.3	1,460	-	-	-	660	EM-SH	D	-	(202)
ExoTerra USA	Halo	Xenon	19.6	1,294	>375	0.83	375	400‡	CM-HL	F	Blackjack	(243) (244) (245) (246) (247) (248) (249) (250) (251)
ExoTerra USA	Halo	Krypton	12	900	>175	0.83	375	300‡	CM-HL	D	-	(373)
ExoTerra USA	Halo12	Xenon	50	1,900	> 2,000	3.4	1,700	1,000‡	CM-HL	E[1]	Undisclosed mission	(252) (253) (254) (374)
ExoTerra USA	Halo12	Krypton	55	1,575	> 2,000	3.4	1,700	1,000‡	CM-HL	D[1]	-	(375)
Exotrail France	spaceware nano	Xenon	2.5	800	6	-	2.5U	60	EM-SH	F	M6P Demo, Arthur, ELO3 and ELO4, Otter Pup, INCUS (2027)	(226) (227) (228) (229) (230) (231) (232) (233) (234)
Exotrail France	spaceware micro	Xenon	7	1,000	60	-	960	150	EM-SH	F	York Space (2023**), SpaceVan, Astro Digital (2024**), Satrec Initiative (2025**), Muon Space (2026**)	(226) (229) (235) (236) (237) (238) (239) (240) (241)
Exotrail France	spaceware mini	Xenon	23	1,300	300	-	-	400	EM-SH	E	Airbus' Earth Observation satellite platform portfolio	(226) (242)

Note that all data is documented as provided in the references. Unless otherwise published, do not assume the data has been independently verified.

*nominal values (see references for full performance ranges), ** anticipated launch date, ‡ PPU input power, § demonstrated, CM = Center Mounted, EM = Externally Mounted, SH = Swaged Heater, HL = Heater-less, JPL = Jet Propulsion Laboratory, SETS = Space Electric Thruster Systems, EDB = Experimental Design Bureau, [1]ExoTerra is commercializing the JPL developed MaSMi thruster, "-" = denotes data not available or applicable

Table 4-10 (cont.): Hall-Effect Electric Propulsion Thrusters												
Manufacturer	**Product**	**Propellant**	**Thrust***	**Specific Impulse***	**Total Impulse***	**Mass**	**Envelope**	**Thruster Power***	**Cathode Type**	**PMI Status**	**Missions**	**References**
---	---	---	**[mN]**	**[s]**	**[kN-s]**	**[kg]**	**[cm^3]**	**[W]**	**Notes**	**C,D,E,F**	---	---
JPL [USA]	MaSMi	Xenon	55	1,920	> 1,550[§]	3.4	1,700	1,000	CM-HL	D	-	(252) (253) (376) (377) (378) (379) (380) (381) (382) (383) (384) (385) (386) (387)
Northrop Grumman [USA]	NGHT-1X	Xenon	55	1,700	> 2,000	3.1	-	900	CM-SH	E	MEP (2026)	(266) (267) (268) (269) (270) (271) (272)
Orbion [USA]	Aurora	Xenon	15.6	1,280	400	1.5	-	300	EM-SH	F	Capella-17, GA-EMS, York Space Constellation	(256) (257) (258) (259) (388) (389) (390) (391) (392) (393)
Pale Blue [Japan]	PBH-100	Xenon	8	-	50	-	-	190	μwave	D	-	(394)
Pulsar Fusion [UK]	LeoBear	Xenon	-	-	-	3.0	13 x 13 x 15	500	EM-SH	D	-	(395) (396)
Rafael [Israel]	R-200	Xenon	13	1,160	200	-	-	250	EM-HL	D	-	(208) (397) (398)
Rafael [Israel]	IHET-300	Xenon	> 14.3	> 1,210	> 135	1.5	1,836	300	EM-SH	F	VENuS	(208) (209) (210) (211) (212)
Rafael [Israel]	R-800	Xenon	-	-	> 600	-	-	800	EM-HL	D	-	(208) (399)
Safran [France]	PPS-X00	Xenon	43	1,530	1,000	< 3.2	22 x 17 x 14	650	EM-SH	E	Vestri (2026**)	(400) (401) (402) (403) (404)
SITAEL [Italy]	HT100	Xenon	9	1,300	73	-	407 wo cath.	175	EM-SH	E	uHETSat, Platino-1 (2026**), Platino-2 (2026**)	(213) (214) (215) (216) (217)
SITAEL [Italy]	HT400	Xenon	27.5	1230	1,000	2.77	1,330	615	EM-SH	D	-	(405) (406) (407)
SETS [Ukraine]	ST25	Xenon	7.6	1,000	115	0.95 (with 2 cathodes)	12 x 10 x 7.3	140	EM-SH	F	EOS SAT-1	(273) (274) (408) (409)
SETS [Ukraine]	ST40	Xenon	25	1,450	350	1.5 (with 2 cathodes)	18 x 11 x 13	450	EM-SH	D	-	(410)

Note that all data is documented as provided in the references. Unless otherwise published, do not assume the data has been independently verified.
*nominal values (see references for full performance ranges), ** anticipated launch date, ‡ PPU input power, § demonstrated, CM = Center Mounted, EM = Externally Mounted, SH = Swaged Heater, HL = Heater-less, JPL = Jet Propulsion Laboratory, SETS = Space Electric Thruster Systems, EDB = Experimental Design Bureau, [1]ExoTerra is commercializing the JPL developed MaSMi thruster, "-" = denotes data not available or applicable

Table 4-11: Pulsed Plasma and Vacuum Arc Electric Propulsion													
Manufacturer	**Product**	**Propellant**	**Thrust***	**Impulse Bit**	**Specific Impulse***	**Total Impulse***	**Mass**	**Envelope**	**Power***	**ACS**	**PMI Status**	**Missions**	**References**
---	---	---	**[μN]**	**[μNs]**	**[s]**	**[N-s]**	**[kg]**	**[cm³ or U]**	**[W]**	**Y/N**	**C,D,E,F**	---	---
Integrated Propulsion Systems													
AIS USA	AIS-VAT1-PQ	Bismuth	26	-	87	0.13	0.056†	37	5	N	D	---	(317)
AIS USA	AIS-VAT1-DUO	Bismuth	52	-	87	0.26	0.084†	74	10	N	D	---	(317)
AIS USA	AIS-VAT1-QUAD	Bismuth	104	-	87	0.52	0.177†	148	20	N	D	---	(317)
Benchmark Space Systems USA	Xantus Metal Plasma Thruster	Molybdenum	400	1	1,774	5,000	1.2†	0.53U	40	N	E	USSF RROCI (not deployed), USSF EWS	(411) (283) (284) (285)
Comat France	Plasma Jet Pack	Metal	150	20	2,000	120£	1.2†£	0.66U£	30	N	E	∑yndeo-2	(286) (287) (412)
CU Aerospace USA	FPPT-1.7	PTFE Fiber	500	165	3,200	24,000	3.0†	1.7U	96	Y	E	DUPLEX (2025)	(148) (149) (150) (151) (152) (153) (154) (155)
Hypernova Space Technologies South Africa	NanoThruster A, Size XS	Solid-state fuel	80	-	≥500	-	0.8†	0.5	10	N	D	---	(413)
Mars Space Ltd UK Clyde Space Sweden	PPTCUP	PTFE	40	40	600	44	0.28†	0.33U	2	N	D	---	(414) (415)
Neumann Space Australia	ND-15	Molybdenum	3.75	45	2,000	880	1.9†	1.5U	15	N	F	Skyride, Apogee	(288) (289) (290) (291) (292) (293) (294) (295)
Neumann Space Australia	ND-50	Molybdenum	100	150	2,000	1,800	1.3†	1U	50	N	F	Edison, CarbSAR	(288) (296) (297) (298)

Note that all data is documented as provided in the references. Unless otherwise published, do not assume the data has been independently verified.

*nominal values (see references for full performance ranges), ** anticipated launch date, † denotes a wet mass, ‡ denotes a dry mass, "-" = denotes data not available or applicable, ESV = Ejector Spring Volume, £ assumes power unit and 2 nozzles

Table 4-12: Ambipolar Electric Propulsion												
Manufacturer	**Product**	**Propellant**	**Thrust***	**Specific Impulse***	**Total Impulse***	**Mass**	**Envelope**	**Power**	**ACS**	**PMI Status**	**Missions**	**References**
---	**---**	**---**	**[mN]**	**[s]**	**[kN-s]**	**[kg]**	**[cm^3]**	**[W]**	**Y/N**	**C,D,E,F**	**---**	**---**
Integrated Propulsion Systems												
Phase Four [USA]	Maxwell (Block 1)[RF]	Xenon	7	400	5	5.9‡	19 x 13.5 x 19	450	N	F	Capella	(299) (301) (416) (417) (418) (419)
Phase Four [USA]	Maxwell (Block 2)[RF]	Xenon	13	700	-	5.0 (without tank)	22 x 12 x 24 (without tank)	450	N	E	(Mission Not Specified)	(419) (420) (300)
Phase Four [USA]	Maxwell (Kr)[RF]	Krypton	13.6	1,110	-	-	-	550	N	D	-	(300) (421)
T4i [Italy]	REGULUS-50-I2[RF]	Iodine	0.55	550	3 (Small); 7 (Medium); 11 (Large)	2.5† (Small); 4† (Medium); 5.1† (Large)	9.4 x 9.5 x {15, 18, 20} {Small, Medium, Large}	50	N	E	UniSat-7	(302) (303) (422) (304) (423)
T4i [Italy]	REGULUS-150-I2[RF]	Iodine	2	1000	11	6.1†	12 x 12 x 27	150	N	D	-	(423)
Miles Space [USA]	M1.4	Water	17.2	-	-	1.0†	9.5 x 9.5 x 9.5	6	N	E	Team Miles	(305) (306) (424) (424)

Note that all data is documented as provided in the references. Unless otherwise published, do not assume the data has been independently verified.
*nominal values (see references for full performance ranges), ** anticipated launch date, † denotes a wet mass, ‡ denotes a dry mass, "-" = denotes data not available or applicable, RF = Radio Frequency

Table 4-13: Propellant-less Propulsion												
Manufacturer	**Product**	**Propellant**	**Thrust***	**Specific Impulse***	**Total Impulse***	**Mass**	**Envelope**	**Power**	**ACS**	**PMI Status**	**Missions**	**References**
---	**---**	**---**	**[mN]**	**[s]**	**[kN-s]**	**[kg]**	**[cm^3]**	**[W]**	**Y/N**	**C,D,E,F**	**---**	**---**
Aurora Propulsion Technologies [Finland]	Plasma Brake	-	< 100 mN/m	-	-	< 2	1U	< 4	N	E	AuroraSat-1	(157) (158) (159)
Tethers Unlimited [USA]	NSTT	-	-	-	-	0.81	18 x 18 x 1.8	-	N	F	Prox-1, NPSat-1, DragRacer	(312) (313) (314) (315) (316) (426)

Note that all data is documented as provided in the references. Unless otherwise published, do not assume the data has been independently verified.
*nominal values (see references for full performance ranges), ** anticipated launch date, † denotes a wet mass, ‡ denotes a dry mass, "-" = denotes data not available or applicable
See Chapter on Passive Deorbit Systems for review of aerodynamic drag devices.

References

(1) "NASA Systems Engineering Handbook." NASA/SP-2016-6105, Rev2.
(2) "NASA Systems Engineering Processes and Requirements." NPR 7123.1C, Effective 14 February 2020, Expiration 14 February 2025.
(3) JANNAF Spacecraft Propulsion Subcommittee, Micro-Propulsion Panel, "JANNAF Guidelines for the Application of Technology Readiness Levels (TRLs) to Micro-Propulsion Systems." JANNAF 2019, Tampa, FL, Distribution Unlimited
(4) JANNAF Spacecraft Propulsion Subcommittee, Micro-Propulsion Panel, "JANNAF Guidelines for the Application of Technology Readiness Levels (TRLs) to Micro-Propulsion Systems. 2022 Edition" JANNAF 2022, Huntsville, AL, Distribution Unlimited
(5) Marshall, W. M. and M. Deans. "Recommended Figures of Merit for Green Monopropellants." NASA TM-2013-216560. National Aeronautics & Space Administration. Cleveland, OH. August, 2013.
(6) "AlSat-2". URL:https://directory.eoportal.org/web/eoportal/satellite-missions/a/alsat-2
(7) Arianegroup. "Chemical Monopropellant Thruster Family." Product Brochure. URL:http://www.space-propulsion.com/brochures/hydrazine-thrusters/hydrazine-thrusters.pdf
(8) Aerojet Rocketdyne an L3Harris Technology Company "Monopropellant Rocket Engines Spec Sheet" Product Brochure. URL:https://www.l3harris.com/resources/monopropellant-rocket-engines-data-sheet
(9) Stratton, J. 2004. "The use of the aerojet MR-103H thruster on the New Horizons mission to Pluto." 55th International Astronautical Congress.
(10) Press Release, "Aerojet Rocketdyne Propulsion Guides Cassini to its Grand Finale at Saturn," September 15, 2017.
(11) Press Release, "Aerojet Rocketdyne Propulsion Powers OSIRIS-REx's Approach of Asteroid Bennu", August 24, 2018.
(12) Moog Space and Defense Group. "Monopropellant Thrusters Datasheet", URL: https://www.moog.com/products/propulsion/space-propulsion/spacecraft-propulsion/thrusters/monopropellant-thrusters.html
(13) "Moog Supports ULA Delta II Launch with NASA Spacecraft for Enhanced Understanding of Weather and Climate," Space News, January 31, 2015.
(14) Northrop Grumman Website, "Propulsion Products and Services," URL: https://www.northropgrumman.com/space/propulsion-products-and-services/
(15) Rafael, "Rafael Space Propulsion Catalogue," 2024, URL: https://www.rafael.co.il/system/space-propulsion-systems-components/
(16) IHI datasheet, URL:https://www.ihi.co.jp/ia/en/products/space/satprop/index.html
(17) Werner, D., "Stellar Exploration propels EchoStar nanosatellite to valuable slot," SpaceNews, August 10, 2021, URL: https://spacenews.com/stellar-exploration-propels-echostar-nanosatellite/
(18) "CAPSTONE Launches to Test New Orbit for NASA's Artemis Moon Missions," NASA Press Release, June 28, 2022.
(19) "What is CAPSTONE," NASA website, Accessed 22 November 2023, URL: https://www.nasa.gov/smallspacecraft/capstone/
(20) Foust, J., "CAPSTONE working well more than a year after launch," SpaceNews, 24 July 2023, URL: https://spacenews.com/capstone-working-well-more-than-a-year-after-launch/
(21) United States Air Force – Air Force Space Command. AFSPCMAN 91-710. "Range Safety User Requirements." 1 July 2004. Certified Current 17 September, 2013.
(22) Spores, R., Masses, R., Kimbrel, S., McLean, C. AIAA-2013-3849. "GPIM AF-M315E Propulsion System." 49th AIAA/ASME/SAE/ASEE Joint Propulsion Conference & Exhibit. San Jose.

(23) Mulkey, H., J. Miller, and C. Bacha. “Green Propellant Loading Demonstration at U.S. Range.” AIAA-2016-4576. AIAA Propulsion and Energy Forum. Salt Lake City, UT. July 25-27, 2016.
(24) Dinardi, A. and Persson, M., “High Performance Green Propulsion (HPGP): A Flight-Proven Capability and Cost Game-Changer for Small and Secondary Satellites,” 26th Annual AIAA/USU Conference on Small Satellites, August 2023.
(25) Friedhoff, P., K. Anflo, M. Persson, and P. Thormahlen. “Growing Constellation of Ammonium Dinitramide (ADN) Based High Performance Green Propulsion (HPGP) Systems." AIAA-2018-4754. AIAA Propulsion and Energy Forum, Cincinnati, OH, July 9-11, 2018.
(26) “Astroscale Debris-Removal Demo Makes Close Approach Despite Thruster Issues,” SpaceNews, May 4, 2022.
(27) “Bradford ECAPS Thrusts Out the Firm’s Successes,” Satnews, 12 June 2020, URL: https://news.satnews.com/2020/06/12/bradford-ecaps-thrusts-out-the-firms-successes/
(28) VACCO Indurstries, “ArgoMoon Propulsion System,” Product Brochure, URL: https://cubesat-propulsion.com/wp-content/uploads/2017/08/X17025000-data-sheet-080217.pdf
(29) eoPortal, “ArgoMoon CubeSat,” Accessed 22 November 2023, URL: https://www.eoportal.org/satellite-missions/argomoon
(30) McLean, C H, W D Deininger, B M Marotta et al. AIAA-2015-3751. "Green Propellant Infusion Mission Program Overview, Status, and Flight Operations." 51st AIAA/ASME/SAE/ASEE Joint Propulsion Conference, July 2015
(31) “NASA Satellite Set to Conclude Successful Green Propellant Demo Mission,” Spaceflight Now, August 17, 2020.
(32) Smith, C., Cheek, N., Burnside, C., et. al., “The Journey of the Lunar Flashlight Propulsion System from Launch through End of Mission,” 37th Annual Small Satellite Conference, August 2023.
(33) “NASA Ends Lunar Flashlight Mission Because of Thruster Problems, Space News, May 15, 2023.
(34) “Benchmark Green Propellant Thrusters Installed on Sherpa Tug,” Space News, December 21, 2021.
(35) “Sherpa Tug Starts Raising Orit More Than a Month After Launch,” Space News, October, 2022.
(36) “Benchmark Space Systems triples propulsion production capacity and doubles personnel to meet demand,” Satellite Evolution, 5 April 2022.
(37) Zucherman, A., et. al., “Cislunar Explorers: Lessons Learned from the Development of an Interplanetary CubeSat,” 2020 Small Satellite Conference, Logan, UT, SSC20-WP2-23.
(38) Muhlberger, C., “Cislunar Explorers: A Student Cubesat Demonstrating low-Cost Technology for Lunar Exploration,” Lunar Exploration Analysis Group (2021).
(39) NASA Space Science Data Coordinated Archive, “Cislunar Explorers,” Accessed 22 Nov 2023, URL: https://nssdc.gsfc.nasa.gov/nmc/spacecraft/display.action?id=CISLUNEXP
(40) “Pathfinder Technology Demonstrator, Demonstrating Novel CubeSat Technologies in Low-Earth Orbit”, February 2,2021, URL: https://www.nasa.gov/smallspacecraft/pathfinder-technology-demonstrator/
(41) Satnews, “Rocket Fuel You Can Drink?” 26 January 2021.
(42) Porter, A., Freedman, M., Grist, R., Wesson, C., and Hanson, M., “Flight Qualification of a Water Electrolysis Propulsion System,” 35th Small Satellite Conference, Logan, UT, Paper No: SSC21-XI-06, 2021.
(43) NanoAvionics. “CubeSat Propulsion System EPSS.” https://nanoavionics.com/CubeSat-components/CubeSat-propulsion-system-epss/

(44) NanoAvionics, “A Successful In-Orbit Test of the First Ever Chemical Propulsion System Running On-Board a CubeSat Was Performed,” Press Release, 21 July 2017.
(45) Dawn Aerospace Website, “Green Propulsion,” URL: https://www.dawnaerospace.com/green-propulsion
(46) CU Aerospace. “Monopropellant Propulsion Unit for CubeSats (MPUC) System”, Company Website, Datasheet, July 2023, https://cuaerospace.com/products-services/space-propulsion-systems/monopropellant-propulsion-unit-mpuc
(47) King, D., Woodruff, C., Camp, J., and Carroll, D. “Development and Testing of a Low Flame Temperature, Peroxide-Alcohol-Based Monopropellant Thruster.” 35th Small Satellite Conf., Paper # SSC21-S1-41, Logan, UT, Aug. 6-9, 2021.
(48) VACCO Industries, “Integrated Propulsion System,” Product Brochure, URL: https://www.CubeSat-propulsion.com/wp-content/uploads/2019/08/Integrated-Propulsion-System-datasheet-080519.pdf
(49) Cardin, J., Schappell, T., and Day, C., “Testing of a Green Monopropellant Integrated Propulsion System,” 34th Annual Small Satellite Conference, SSC20-IX-02, Logan, UT, Aug 2020.
(50) Whitmore , S A, S L Merkley, Z S Spurrier, and S D Walker. 2015. "Development of a Power Efficient, Restartable, 'Green' Propellant Thruster for Small Spacecraft and Satellites." 29th Annual AIAA/USU Conference on Small Satellites.
(51) Bulcher, A. M. and S. A. Whitmore. “A Green Hybrid Thruster Using Moderately Enriched Compressed Air as the Oxidizer.” AIAA-2018-4841. AIAA Propulsion and Energy Forum. Cincinnati, OH. July 9-11, 2018. doi: 10.2514/6.2018-4841
(52) Whitmore, S., Babb, R., Gardner, T., Lloyd, K., Stephens, J.,” Pyrolytic Graphite and Boron Nitride as Low-Erosion Nozzle Materials for Long-Duration Hybrid Rocket Testing”. AIAA-2020-3740, AIAA Propulsion and Energy Forum, 2020.
(53) Whitmore, S., Babb, R., Stephens, J.,Horlacher, J., “Further Development of Low-Erosion Nozzle Materials for Long-Duration Hybrid Rocket Burns”. AIAA Propulsion and Energy Forum, 2021.
(54) Jens, E., Karp, A., Williams, K., Nakazono, B., Rabinovitch, J., Dyrda, D., and Mechentel, F. “Low Pressure Ignition Testing of a Hybrid SmallSat Motor.” AIAA-2019-4009, AIAA Propulsion and Energy Forum, 2019. https://doi.org/10.2514/6.2019-4009.
(55) Rabinovitch, J., Jens, E, Karp, A, Nakazono, N, Conte, A, Vaughan, D., “Characterization of PolyMethylMethAcrylate as a Fuel for Hybrid Rocket Motors”. AIAA-2018-4530, AIAA Propulsion and Energy Forum, 2018.
(56) Jens, E., Karp, A., Rabinovitch, J., Nakazono, B., Conte, A., Vaughan, D.” Design of Interplanetary Hybrid CubeSat and SmallSat Propulsion Systems.” AIAA-2018-4668, AIAA Propulsion and Energy Forum, 2018.
(57) Dyrda, D., Mechentel, F., Cantwell, B., Karp, A., Rabinovitch, J., Jens, E., “Diode Laser Ignition Testing for PMMA/GOX Hybrid Motors.” AIAA-2019-4095, AIAA Propulsion and Energy Forum, 2019.
(58) Simurda, L., Zilliac, G. and Zaseck, C., "High Performance Hybrid Propulsion System for Small Satellites," AIAA-2013-3635, 49th AIAA/ASME/SAE/ASEE Joint Propulsion Conference, 2013.
(59) Simurda, L, Zilliac, G., “Continued Testing of a High Performance Hybrid Propulsion System for Small Satellites”, AIAA-2015-4201, AIAA Propulsion and Energy Forum, 2015.
(60) Desain, J., Brady, B., Curtiss, T., Hsu-Schouten, A., Fuller, J., Boyer, J.E., McKnight, B., Cortopassi, A., “Advanced Hybrid Rocket Motor Propulsion Unit for CubeSats(PUC)”. Aerospace Report No. TOR-2015-03522.
(61) ROMBUS Rapid Orbital Mobility Bus.” Parabilis Space Technologies, datasheet
(62) Nano OTS Nanosatellite Orbital Transfer System”, Parabilis Space Technologies, datasheet

(63) Hinkley, D. “A Novel Cold Gas Propulsion System for Nanosatellites and Picosatellites.” AIAA, 22nd Annual Conference on Small Satellites, SSC08-VII-7.
(64) Schappell, D T, E Scarduffa, P Smith, and N Solway. AIAA-2005-4055. "Advances in Marotta Electric and Satellite Propulsion Fluid Control Activities." 41st AIAA/ASME/SAE/ASEE Joint Propulsion Conference.
(65) Marotta, “Cold Gas Microthruster,” Datasheet, Accessed 23 Nov 2023, URL: https://marotta.com/products/flow-controls/satellite-propulsion-controls/cold-gas-microthruster/
(66) Pauliukonis, R S. 2017. "Fuel system comprising sulfur hexafluoride and lithium containing fuel." https://patents.google.com/patent/US3325318.
(67) Bonin, G, N Roth, S Armitage, J Newman, B. Risi, and R. Zee., "CanX-4 and CanX-5 Precision Formation Flight: Mission Accomplished!" 29th Annual AIAA/USU Conference on Small Satellites, 2015.
(68) Newman, J and Zee, R. E. “Drift Recovery and Station Keeping Results for the Historic CanX-4/CanX-5 Formation Flying Mission.” 29th Annual AIAA/USU Conference on Small Satellites, Logan, UT, 2015.
(69) Risi, B.W. “Propulsion System Development for the CanX-4 and CanX-5 Dual Nanosatellite Formation Flying Mission.” Master of Applied Science Thesis, University of Toronto, 2014.
(70) Manzoni, G, and Y L Brama. 2015. "CubeSat Micropropulsion Characterization in Low Earth Orbit." 29th Annual AIAA/USU Conference on Small Satellites.
(71) GOMSpace. “Attitude and Orbit Control Systems,” Company Website
(72) “GomX-4,” https://directory.eoportal.org/web/eoportal/satellite-missions/g/gomx-4.
(73) Kvell, U, M Puusepp, F Kaminski, and et al. 2014. "Nanosatellite orbit control using MEMS cold gas thrusters." Proceedings of the Estonian Academy of Sciences, 63, 2S, 279–285.
(74) Palmer, K., Sundqvist, J., Salaverri, A., Gronland, T., Li, Z., and Wu, S.. “In-Orbit Demonstration of a MEMS-based Micropropulsion System for CubeSats.” Small Satellite Conference, August 2016.
(75) National Aeronautics & Space Administration. “BioSentinel.” Fact Sheet. https://www.nasa.gov/sites/default/files/atoms/files/biosentinel_fact_sheet-16apr2019_508.pdf
(76) Lightsey, E. G., T. Stevenson, and M. Sorgenfrei. “Development and Testing of a 3-D-Printed Cold Gas Thruster for an Interplanetary CubeSat.” Proceedings of the IEEE, Vol. 106, No. 3, March, 2018. doi: 10.1109/JPROC.2018.2799898
(77) Napoli, M., et al, “BioSentinel: Mission summary and lessons learned from the first deep space biology CubeSat mission,” 37th Small Satellite Conference, Logan, UT, Aug 2023, SSC23-I-02.
(78) Rutter, D., “NASA Extends BioSentinel’s Mission to Measure Deep Space Radiation,” NASA Website, 7 Aug 2023, URL: https://www.nasa.gov/image-article/nasa-extends-biosentinels-mission-to-measure-deep-space-radiation/
(79) Editorial, “Iodine Impulse for SmallSats Demo’d On-Orbit by ThrustMe and Spacety,” SmallSat News, 25 November 2019.
(80) Werner, D., “Thrustme, Spacety report initial success of cold gas thruster,” SpaceNews, 23 November, 2019.
(81) Martinez, J., Rafalskyi, D., Aanesland, A., Laurand, X., Martinez, S., and Quinsac, G., “An off-axis iodine propulsion system for the Robusta-3A mission, 34th Small Satellite Conference, SSC20-IX-03, 2020.
(82) ThrustMe, “I2T5 Cold Iodine Thruster,” Company Datasheet, Version 02/21, 2021.

(83) Bowen, J, M Villa, and A Williams. 2015. "CubeSat based Rendezvous, Proximity Operations, and Docking in the CPOD Mission." 29th Annual AIAA/USU Conference on Small Satellites.
(84) VACCO Industries. “NASA C-POD Micro CubeSat Propulsion System.” Product Brochure. URL: https://cubesat-propulsion.com/reaction-control-propulsion-module/
(85) Spiegel, I., Zhou, B., Goodloe, R., Fox, B., and DiMateo, J., “CubeSat Proximity Operations Demonstration (CPOD) Mission Results,” 37th Annual Small Satellite Conference, Logan, UT, Aug 2023, SSC23-XI-01.
(86) Klesh, A, and J Krajewski. 2015. "MarCO: CubeSats to Mars in 2016." 29th Annual AIAA/USU Conference on Small Satellites.
(87) Jet Propulsion Laboratory, National Aeronautics and Space Administration. “Mars Cube One (MarCO).” URL: https://www.jpl.nasa.gov/news/press_kits/insight/launch/appendix/mars-cube-one/
(88) VACCO Industries. “JPL MarCO – Micro CubeSat Propulsion System.” Product Brochure. URL: https://cubesat-propulsion.com/jpl-marco-micro-propulsion-system/
(89) Klesh, A., Baker, J., and Krajewski, J., “MarCO: Flight Review and Lessons Learned,” 33rd Annual Small Satellite Conference, Logan, UT, 2019, SSC19-III-04.
(90) NEA Scout Propulsion System, Datasheet, VACCO Industries, July 2017
(91) Lockett, T., Castillo-Rogez, J., Johnson, L., Lightholder, J., and Few, A., “Near-Earth Asteroid Scout Flight Mission,” IEEE A&E Systems Magazine, March 2020, DOI. No. 10.1109/MAES.2019.2958729
(92) “NEA Scout,” NASA website, Accessed 24 Nov 2023, URL: https://science.nasa.gov/mission/nea-scout/
(93) Northrup Grumman Propulsion Product Catalog, April 2016.
(94) BusinessWire.com. 2017. “PacSci EMC Demonstrates First Ever Successful Orbital Maneuvers and Orbit Raising of a CubeSat Using a Commercial Solid Rocket Motor Array.”
(95) Terran Orbital Mission Summary, “PACSCISAT,” Accessed 24 Nov 2023, URL: https://terranorbital.com/missions/pacscisat/
(96) Hartwig, J.W. “Propellant Management Devices for Low Gravity Fluid Management: Past, Present, and Future Applications.” AIAA Journal of Spacecraft and Rockets Vol. 54, No. 4, 808 – 824. 2017.
(97) W. Tam, G. Kawahara, K. Wlodarczyk, “Review of ATK Diaphragm Tanks-An Update”, Space Propulsion 2018, SP2018_00024.
(98) Carpenter, C, D Schmuland, J Overly, and R Masse. 2014. "Test Results for the MPS-120 and MPS-130 CubeSat Propulsion Systems." 28th Annual AIAA/USU Conference on Small Satellites. Logan.
(99) Aerojet Rocketdyne. “Modular Propulsion Systems.” Product Brochure.
(100) Stellar Exploration, “Propulsion for Small Spacecraft.” Product Brochure.
(101) Aerospace Corporation. “Propelling the Field of SmallSats Forward.” https://aerospace.org/article/propelling-field-small-sats-forward
(102) Rainbow, J., “Benchmark Space Systems unveils in-space mobility-as-a-service business,” SpaceNews, 23, June, 2021.
(103) Gagne, K. R., M. R. McDevitt, and D. L. Hitt. "A Dual Mode Propulsion System for Small Satellite Applications." Aerospace. Vol. 5, No. 52. 2018. doi: 10.3390/aerospace5020052
(104) Benchmark Space Systems. “Products.” Product Datasheets, URL: https://www.benchmarkspacesystems.com/products
(105) Anflo, K. and B. Crowe. “In-Space Demonstration of an ADN-based Propulsion System.” AIAA-2011-5832. 47th AIAA/ASME/SAE/ASEE Joint Propulsion Conference & Exhibit. San Diego, CA. July 31 – August 3, 2011.
(106) “SkySat: Quick Facts,” eoPortal, July 26, 2016.

(107) Bradford ECAPS. “High Performance Green Propulsion.” Product Brochure.
(108) Bradford ECAPS. “1N GP Thruster.” https://www.ecaps.space/products-1ngp.php
(109) Rubicon Space Systems., “Thrusters,” Product Brochure, URL: https://www.rubicon.space/products-cat/1/thrusters
(110) Williams, N.J., et al., “A Green Propulsion Dual Mode (GPDM) In-Space Technology Demonstration on a 6U CubeSat,” 36th Small Satellite Conference, Logan, UT, 2024.
(111) Werner, D., “Rubicon delivers propulsion for NASA dual-mode mission,” Space News, 9 January 2025.
(112) Busek Co., Inc. “BGT-X5 Green Monopropellant Thruster.” Product Brochure.
(113) Busek Co., Inc. “Green Monopropellant Thrusters.” http://busek.com/technologies__greenmonoprop.htm
(114) Tsay, M., C. Feng, and J. Zwahlen. “System-Level Demonstration of Busek’s 1U CubeSat Green Propulsion Module ‘AMAC’.” AIAA-2017-4946. 53rd AIAA/SAE/ASEE Joint Propulsion Conference. Atlanta, GA. 10-12 July, 2017.
(115) Dawn Aerospace, “Customers and Missions,” Company Website, Accessed April 2026, URL: https://www.dawnaerospace.com/heritage-and-missions
(116) Moog, Inc. “Monopropellant Propulsion Module.” Product Brochure. https://www.moog.com/content/dam/moog/literature/sdg/space/propulsion/moog-monopropellant-propulsion-module-datasheet.pdf
(117) Rubicon Space Systems., “Sprite Propulsion System,” Product Brochure
(118) Tethers Unlimited. “Hydros-C” Product Brochure.
(119) NASA, 2015, “Pathfinder Technology Demonstrator.” National Aeronautics & Space Administration.
(120) Tethers Unlimited. “Hydros-M” Product Brochure.
(121) VACCO Industries. “Green Propulsion System.” Product Brochure. https://www.CubeSat-propulsion.com/wp-content/uploads/2019/08/X19041000-Green-Propulsion-System-data-sheet-073019.pdf
(122) Benchmark Space Systems., “Products”., Accessed Sept 2023. URL: https://www.benchmarkspacesystems.com/products#slide-1-6
(123) Jens, E., Karp, A., Rabinovitch, J., Nakazono, B., Conte, A., Vaughan, D.” Design of Interplanetary Hybrid CubeSat and SmallSat Propulsion Systems.” AIAA-2018-4668, AIAA Propulsion and Energy Forum, 2018.
(124) GOMspace. “NanoProp CGP-3.” Product Brochure.
(125) GOMspace. “NanoProp 6U.” Product Brochure.https://gomspace.com/UserFiles/Subsystems/flyer/gomspace_nanoprop_cgp6_flyer.pdf
(126) T4i, “Products”, Accessed March 2026, URL: https://www.t4innovation.com/ianus-perseus-cold-gas/
(127) VACCO Industries. “Standard Propulsion System.” Product Brochure. URL: https://cubesat-propulsion.com/standard-propulsion-system/
(128) Moog, “Cold Gas Thrursters,” Moog Datasheet, 2021
(129) Thrasher, J. and M. McPherson. “Design and Qualification of DSSP’s CubeSat Delta-V Motor (CDM-1).” Digital Solid State Propulsion, Inc. Poster presented at Small Satellites Conference. Logan, UT. 2015. https://digitalcommons.usu.edu/cgi/viewcontent.cgi?article=3261&context=smallsat
(130) Industrial Solid Propellant, Inc. “Product Portfolio.” Product Brochure. http://www.specificimpulse.com/
(131) Northrop Grumman, “Propulsion Products Catalog.” Product Brochure. 2016, URL: https://cdn.prd.ngc.agencyq.site/-/media/wp-content/uploads/NG-Propulsion-Products-Catalog.pdf

(132) Jahn, R. G. and Choueiri, E. Y. “Electric Propulsion.” Academic Press, Encyclopedia of Physical Science and Technology, Third Edition, Volume 5, 2002.
(133) Goebel, D. M. and Katz, I. “Fundamentals of Electric Propulsion: Ion and Hall Thrusters.” California Institute of Technology, Jet Propulsion Laboratory, JPL Space Science and Technology Series, 2008.
(134) Bradford Space, “Comet: Water-based Propulsion for Small Satellites.” Company Website, Datasheet, Copyright 2019.
(135) Sarda, K., Roth, N., Zee, R. E., Cajacob, D., and Orr, N. G. “Making the Invisible Visible: Precision RF-Emitter Geolocation from Space by the HawkEye 360 Pathfinder Mission.” 32nd AIAA/USU Conference on Small Satellites, Logan, UT, 2018.
(136) eoPortal, “HawkEye 360 Pathfinder Cluster Mission to identify RFI locations.” June, 2020. URL: https://directory.eoportal.org/web/eoportal/satellite-missions/h/hawkeye
(137) Bradford Space, “Missions,” Company website, Accessed Sept. 2023.
(138) BlackSky Global, “Global-4 Orbital Debris Assessment Report (ODAR).” FCC Licensing, 18 December, 2018.
(139) CU Aerospace, “Propulsion Unit for CubeSats.” Company Website, URL: https://cuaerospace.com/products-services/space-propulsion-systems/propulsion-unit-for-cubesats-puc, Datasheet, 2020.
(140) Carroll, D. L., Cardin, J. M., Burton, R. L., Benavides, G. F., Hejmanowski, N., Woodruff, C., Bassett, K., King, D., Laystrom-Woodard, J., Richardson, L., Day, C., Hageman, K., and Bhandari, R. "Propulsion Unit for CubeSats (PUC)." 62nd JANNAF Propulsion Meeting, Nashville, TN, 1-5 June, 2015, Paper Tracking # 4059, 2015, Dist. A.
(141) Burton, R.L., Benavides, G.F., and Carroll, D.L. “Space Thruster using Robust Microcavity Discharge.” U.S. Patent No. 9,242,747 B1, 2016.
(142) Woodruff, C., Carroll, D., King, D., Burton, R., and Hejmanowski, N. “Monofilament Vaporization Propulsion (MVP) – CubeSat propulsion system with inert polymer propellant.” Small Satellite Conf., Paper # SSX18-III-09, Logan, UT, Aug. 6-9, 2018.
(143) CU Aerospace, “Monofilament Vaporization Propulsion System Solid Inert Polymer Propellant.” Company Website, URL: https://cuaerospace.com/products-services/space-propulsion-systems/monofilament-vaporization-propulsion-mvp, Datasheet, 2020.
(144) Woodruff, C., Parta, M., King, D., Woodruff, A., Burton, R., and Carroll, D. "Monofilament Vaporization Propulsion (MVP) Flight-like System Performance." 37th International Electric Propulsion Conference (IEPC) 2022, Boston, Massachusetts, Paper # IEPC 2022-575, 2022.
(145) CU Aerospace, “Space Systems Hardware: Hardware for the Future,” Company website, Accessed Sept. 2023, URL: https://cuaerospace.com/technologies/space-systems-hardware
(146) Steam TunaCan Thruster," SteamJet company website, Accessed Sept. 2023, URL: https://steamjet.space/
(147) Steam Thruster One," SteamJet company website, Accessed Sept. 2023, URL: https://steamjet.space/
(148) Woodruff, C., King, D., Burton, R., Bowman, J., and Carroll, D. "Development of a Fiber-Fed Pulsed Plasma Thruster for Small Satellites." Small Satellite Conference, Logan, UT, Paper # SSC19-WKVIII-06, 2019.
(149) Woodruff, C., King, D., Burton, R., and Carroll, D. "Fiber-fed Pulsed Plasma Thruster for Small Satellites." 36th International Electric Propulsion Conference (IEPC) 2019, Vienna, Austria, Paper # IEPC 2019-A899, 2019.
(150) Woodruff, C., King, D., Burton, R., and Carroll, D. “Fiber-Fed Advanced Pulsed Plasma Thruster (FPPT).” U.S. Patent # 10,570,892, Feb. 25, 2020, and 11,242,844, Feb. 8, 2022.

(151) Woodruff, C., Parta, M., King, D., Burton, R., and Carroll, D. "Fiber-Fed Pulsed Plasma Thruster (FPPT) with Multi-axis Thrust Vectoring." 37th International Electric Propulsion Conference (IEPC) 2022, Boston, Massachusetts, Paper # IEPC 2022-558, 2022.
(152) CU Aerospace, “Fiber-Fed Pulsed Plasma Thruster System Solid Inert Polymer Propellant.” Company Website, URL: URL: https://cuaerospace.com/products-services/space-propulsion-systems/fiber-fed-pulsed-plasma-thruster-fppt, Datasheet, 2022.
(153) CU Aerospace, “Space Systems Hardware: Hardware for the Future”, Accessed Nov. 2023. URL: https://cuaerospace.com/technologies/space-systems-hardware
(154) “NASA Funds Long-Standing Partners in CubeSat Development.” Press Release, University of Illinois at Urbana/Champaign, Aerospace Engineering, 9 Oct., 2019.
(155) CU Aerospace, “CU Aerospace DUPLEX Satellite headed to the ISS on SpaceX NG-23 Mission“, Press Release, 16 September 2025. https://www.prlog.org/13099711-cu-aerospace-duplex-satellite-headed-to-the-iss-on-spacex-ng-23-mission.html
(156) Aurora Propulsion Technologies, “ARM-A Datasheet.” Company Website, URL: https://auroraptfi/thrusters/, Datasheet, Copyright May, 2021.
(157) Aurora Propulsion Technologies, “Deorbiting Old Satellites & Used Rockets with Aurora Plasma Brake.” Company Website, URL: https://auroraptfi/deorbiting/#plasmabrake, Brochure, Copyright March, 2022
(158) “Aurora Successfully Launches First Sustainable Propulsion Tech Demonstration,“ Aurura Propulsion Technologies, Press Release, May 3, 2022.
(159) “The Flying Object (AuroraSat-1, Aurora CubeSat),” Nanosats Database, URL: https://www.nanosats.eu/sat/aurorasat-1, Updated July 23, 2022.
(160) Spacewatch.Global, “Space BD Successfully Deploys OPTIMAL-1 into Orbit,” Feb. 3, 2023, URL: https://spacewatch.global/2023/02/space-bd-successfully-deploys-optimal-1-into-orbit/
(161) Nakagawa, Y., Iwakawa, A., Kameyama, and S., Kikuchi, T., “On-orbit Demonstration of the Water Resistojet Propulsion System on Commercial 6U-Sat Sphere-1 EYE,” 37th Annual Small Satellite Conference, Logan, UT, August 2023, SSC23-VI-02.
(162) “Collision Avoidance for CubeSats and SmallSats with ARM-C,” Aurora Brochure, Company Website, Dated March 21, 2022.
(163) Ziemer, J., Marrese-Reading, Colleen, Cutler, C., Dunn, C., Romero-Wolf, A., Javidnia, S., Le, T., Li, I., Barela, P., Demmons, N., Hruby, V., Slutsky, J., Thorpe, J., Maghami, P., Hsu, O., and O’Donnell, J. “In-Flight Verification and Validation of Colloid Microthruster Performance.” AIAA Propulsion and Energy Forum, Cincinnati, OH, AIAA-2018-4643.
(164) Krejci, D., Reissner, A., Seifert, B., Jelem, D., Horbe, T., Plesescu, F., Friedhoff, P., and Lai, S. “Demonstration of the IFM Nano FEEP Thruster in Low Earth Orbit.” 4S Symposium, 2018.
(165) Krejci, D., Reissner, A., Schonherr, T., Seifert, B., Saleem, Z., and Alejos, R. “Recent Flight Data from IFM Nano Thrusters in a Low Earth Orbit.” 36th IEPC, Vienna, Austria, IEPC-2019-A724.
(166) Amos, J. “ICEYE’s Small Radar Satellites Achieve Big Capability.” BBC News, 6 May, 2020, URL: https://www.bbc.com/news/science-environment-52560809
(167) Werner, D. “Key Hurdle Cleared for York Space Systems and U.S. Army Small Satellite Launch.” SpaceNews, 22 February, 2018, URL: https://spacenews.com/key-hurdle-cleared-for-york-space-systems-and-u-s-army-small-satellite-launch/
(168) Clark, S. “Rocket Lab Deploys Experimental U.S. Military SmallSats on First Night Launch.” Spaceflight Now, 5 May, 2019. URL: https://spaceflightnow.com/2019/05/05/rocket-labs-deploys-experimental-u-s-military-SmallSats-on-first-night-launch/

(169) Wörner, N. “Sensor Networks of Satellites.” ElektronikNet, 26 May, 2020. URL: https://www.elektroniknet.de/international/sensor-networks-of-satellites-176831.html
(170) “NetSat – Pioneering Research in Formation Control”, website accessed June 2021, https://www.telematik-zentrum.de/en/projects/netsat/
(171) D. Krejci and A. Reissner, “The First 100 FEEP Propulsion Systems in Space: A Statistical View and Lessons Learnt of 4 Years of ENPULSION”, IEPC-2022-199, 37th International Electric Propulsion Conference, Cambridge, MA, 19-23 June 2022.
(172) Grimaud, L., Schonherr, T., Vasiljevich, I., Reissner, A., Krejci, D., and Seifert, B., “Qualification status update of the MICRO R3 and NANO R3 FEEP thrusters,” IEPC-2022-200, 37th International Electric Propulsion Conference, Cambridge, MA, 19-23 June 2022.
(173) “First Use of the Enpulsion Micro R3 Thruster in the GMS-T Mission”, Space Daily, 18 March 2021.
(174) Bangert, P., Kramer, A., and Schilling, K. “UWE-4: Integration State of the First Electrically Propelled 1U CubeSat.” 31st Annual AIAA/USU Conference on Small Satellites, SSC17-WK-47, 2017.
(175) Kramer, A., Bangert, P., and Schilling, K. “Hybrid Attitude Control On-Board UWE-4 Using Magnetorquers and the Electric Propulsion System NanoFEEP.” 33rd Annual AIAA/USU Conference on Small Satellites, SSC19-WKI-02, 2019.
(176) D. Werner, “Miniature Thruster Propels Single CubeSat to Lower Orbit”, SpaceNews, 22 July 2020, https://spacenews.com/uwe-4-lowers-altitude/
(177) N. Arthur. “Ion Thruster Produced Roll Torque.” AIAA-2019-4166.
(178) N. Wallace et al., “The GOCE Ion Propulsion Assembly – Lessons Learnt from the First 22 Months of Flight Operations”, IEPC-2011-327.
(179) “ESA’s GOCE Mission Comes to an End”, ESA press release #33-2013, 21 Oct 2013, https://www.esa.int/Newsroom/Press_Releases/ESA_s_GOCE_mission_comes_to_an_end
(180) C.H. Edwards et al., “The T5 Ion Propulsion Assembly for Drag Compensation on GOCE”, 2nd International GOCE User Workshop, ESA-ESRIN Frascati Italy, 8-10 March 2004.
(181) P.N. Randall et al., “T5 Performance, Industrialization and Future Applications”, IEPC-2019-688.
(182) A. Jones, “French Startup Demonstrates Iodine Propulsion in Potential Boost for Space Debris Mitigation Efforts”, SpaceNews, 22 January 2021, https://spacenews.com/french-startup-demonstrates-iodine-propulsion-in-potential-boost-for-space-debris-mitigation-efforts/
(183) Rafalskyi, D., Martínez, J.M., Habl, L. et al. In-orbit demonstration of an iodine electric propulsion system. Nature 599, 411–415 (2021). https://doi.org/10.1038/s41586-021-04015-y
(184) “ThrustMe NPT30-I2 iodine electric propulsion system launched on board the NorSat-TD satellite”, TURUSTME web post,17 April 2023, URL: https://www.thrustme.fr/post/89-thrustme-npt30-i2-iodine-electric-propulsion-system-launched-on-board-the-norsat-td-satellite
(185) “Trial Integration Completed By Norwegian Space Agency Of ThrustMe’s Propulsion System For NorSat-TD”, SatNews, 27 April 2021, https://news.satnews.com/2021/04/27/trial-integration-completed-by-norwegian-space-agency-of-thrustmes-propulsion-system-for-norsat-td/
(186) “TrustMe exceeds 100 orders for propulsion systems”, TURUSTME web post, 25 May 2023, URL: https://www.thrustme.fr/post/91-thrustme-exceeds-100-orders-for-propulsion-systems

(187) "ThrustMe selected to provide Turion Space with vital propulsion capacities", TURUSTME web post, 4 May, 2023, URL: https://www.thrustme.fr/post/90-thrustme-selected-to-provide-turion-space-with-vital-propulsion-capacities
(188) Malphrus, B. "The Lunar IceCube EM-1 Mission: Prospecting the Moon for Water Ice." IEEE Aerospace and Electronic Systems Magazine, Vol 34, Issue 4, DOI: 10.1109/MAES.2019.2909384.
(189) Clark, P. "Lunar Ice Cube Mission: Determining Lunar Water Dynamics with a First Generation Deep Space CubeSat." 47th Lunar and Planetary Science Conference, 2016.
(190) Foust, J., "Deep space smallsats face big challenges," Spacenews, 17 February 2023, URL: https://spacenews.com/deep-space-smallsats-face-big-challenges/
(191) Hardgrove, C. "The Lunar Polar Hydrogen Mapper CubeSat Mission." IEEE Aerospace and Electronic Systems Magazine, Vol 35, Issue 3, DOI: 10.1109/MAES.2019.2950747.
(192) Morton, Erin, "NASA's LunaH-Map Mission Ends, Validates Science Instrument Performance," NASA blog, 3 August 2023, URL: https://blogs.nasa.gov/lunah-map/2023/08/03/nasas-lunah-map-mission-ends-validates-science-instrument-performance/
(193) Foust, J., "Artemis 1 cubesate nearing end of mission," SpaceNews, 2 May 2023, URL: https://spacenews.com/artemis-1-cubesat-nearing-end-of-mission/
(194) eoPortal, "SMART-1 (Small Mission for Advanced Research in Technology." June, 2020. URL: https://directory.eoportal.org/web/eoportal/satellite-missions/s/smart-1
(195) eoPortal, "TacSat-2 / Roadrunner." June 2020. URL: https://earth.esa.int/web/eoportal/satellite-missions/content/-/article/tacsat2
(196) de Grys, K., Mathers, A., Welander, B., and Khayms, V. "Demonstration of 10,400 Hours of Operation on a 4.5 kW Qualification Model Hall Thruster." 46th AIAA Joint Propulsion Conference, Nashville, TN, July, 2010.
(197) Sheetz, M. and Petrova, M. "Why in the next decade companies will launch thousands more satellites than in all of history." CNBC, 15 December, 2019. URL: https://www.cnbc.com/2019/12/14/spacex-oneweb-and-amazon-to-launch-thousands-more-satellites-in-2020s.html
(198) Gorbunov, A., Khodnenko, V., Khromov, A., Murashko, V., Koryakin, A., Zhosan, V., and Grikhin, G. "Vernier Propulsion System for Small Earth Remote Sensing Satellite "Canopus-V." 32nd IEPC, Wiesbaden, Germany, 2011.
(199) eoPortal, "Kanopus-V 1 (Kanous-Vulkan N1, Environmental Satellite)." June, 2020. URL: https://directory.eoportal.org/web/eoportal/satellite-missions/k/kanopus-v-1
(200) eoPortal, "Kanopus-V-IK 1 (Kanous-Vulkan-Infra-Krasny-1)." June, 2020. URL: https://directory.eoportal.org/web/eoportal/satellite-missions/k/kanopus-v-ik-1
(201) EDB Fakel, "Stationary Plasma Thrusters." Company Website, Datasheet, 2020.
(202) Gnizdor, R., Markov, A., Mitrofanova, O., and Semenenko, D. "The research of the modified SPT-70 thruster parameters and characteristics." 36th IEPC, Vienna, Austria, 2019.
(203) Hruby, P., Demmons, N., Courtney, D., Tsay, M., Szabo, J., and Hruby, V. "Overview of Busek Electric Propulsion." 36th IEPC, Vienna, Austria, 2019.
(204) Busek, "BHT-200 Busek Hall Effect Thruster." Company Website, Datasheet, 2019.
(205) Hruby, V., Monheiser, J., Pote, B., Freeman, C., and Connolly, W. "Low Power, Hall Thruster Propulsion System." IEPC-99-092, Kitakyushu, Japan, 1999.
(206) Kamhawi, H., Haag, T., Benavides, G., Hickman, T., Smith, T., Williams, G., Myers, J., Polzin, K., Dankanich, J., Byrne, L., Szabo, J., and Lee, L. "Overview of Iodine Propellant Hall Thruster Development Activities at NASA Glenn Research Center." 52nd AIAA Joint Propulsion Conference, Salt Lake City, Utah, 2016.
(207) NASA TechPort, "Iodine Satellite (iSAT)." June, 2020. URL: https://techport.nasa.gov/view/91492

(208) Lev, D., Zimmerman, R., Shoor, B., Appel, L., Ben-Ephraim, M., Herscovitz, J., and Epstein, O. “Electric Propulsion Activities at Rafael in 2019.” 36th IEPC, Vienna, Austria, 2019.
(209) Herscovitz, J., and Karnieli, A. “VENuS Program: Broad and New Horizons for Super-Spectral Imaging and Electric Propulsion Missions for a Small Satellite.” 22nd AIAA/USU Conference on Small Satellites, Logan, Utah, 2008.
(210) Herscovitz, J., Appel, L., Barnett, D., Baron, D., Davidson, A., Gontmacher, P., Kedem, M., Lev, D., Merenstein, A., Rbinovich, L., Reiner, D., Salama, O., Amit-Shapira, Y., Shechter, Y., Shoor, B., Warshavsky, A., and Zhuravel, N. “VENuS – A Novel Technological Mission Using Electric Propulsion.” 35th IEPC, Atlanta, Georgia, 2017.
(211) Herscovitz, J., Lev, D., Shoor, B., Katz-Franco, D., Berkman, S., Baron, D, and Adler, S. “VENuS – Updates on Technological Mission using the Israeli Hall Effect Thruster (IHET).” 36th IEPC, Vienna, Austria, 2019.
(212) eoPortal “VENuS (Vegetation and Environment monitoring on a New Microsatellite).” June, 2020. URL: https://directory.eoportal.org/web/eoportal/satellite-missions/v-w-x-y-z/venus
(213) Misuri, T., Ducci, C., Gregucci, S., Pedrini, D., Cannelli, F., Cesari, U., Nania, F., Vicini, A., Pace, G., Magistro, F., Cenni, J., Dignani, D., Farauanu, C., Quaranta, V., Tiseo, B., Orefice, M., and Bruno, G. “SITAEL HT100 Thruster Unit, Full Ground Qualification.” 36th IEPC, Vienna, Austria, 2019.
(214) Tambini, A., Antonini, F., Melega, N., Mariotti, G., Centonze, V., and Gabriele, A. “uHETsat small Power System for high demanding payloads.” European Space Power Conference, 2019.
(215) SITAEL “Electric Propulsion – HT100 Hall Effect Thruster Product Sheet.” Company Website, Datasheet, 2020.
(216) ESA, “Compact electric thruster cleared for space firing,” ESA website, Press release, 27 June 2023, URL: https://www.esa.int/Enabling_Support/Space_Engineering_Technology/Compact_electric_thruster_cleared_for_space_firing
(217) SITAEL, “Earth Observation,” Company website, Accessed 26 Nov 2023, URL: https://www.sitael.com/space/references-and-customers/earth-observation/
(218) Astra, “Astra Spacecraft Engine.” Company Website, Accessed Nov 2023.
(219) Spaceflight, “Sherpa Program: New Orbital Transfer Vehicles Launch Smallsats to Custom Orbital Destination,” Spaceflight Website, URL: https://spaceflight.com/sherpa/#sherpalte, Accessed October 2022.
(220) Gill, M., Martinez, R., Zannos, A., Bailey, T., Cassidy, M., Cooney, J., Crawford, A., Cuadra, J., Delgado, J., Fuller, J., Haverty, M., Hopkins, M., Keyes, E., Lee, L, Massey, D., McClellan, K., Pittman, J., Schmidt, M., Shiyani, D., and Sorel, T., “On-Orbit Data and Validation of Astra’s ACE Electric Propulsion System,” 36th Annual Small Spacecraft Conference, Logan, UT, Paper No.: SSC22-S2-08, 2022.
(221) Astra, “On-Orbit Validation of the Astra Spacecraft Engine,” Press Release, 22 Aug 2022, URL: https://astra.com/news/on-orbit-validation-of-the-astra-spacecraft-engine/
(222) Kayhan Space Satcat, SHERPA-LTE1, 48941 (Decayed), Orbit data source: Space-Track, https://www.satcat.com/sats/48941
(223) Foust, J., “Astra wins order for electric thrusters from LeoStella,” SpaceNews, April 12, 2022.
(224) Foust, J., “Astra, Exotrail win satellite propulsion orders,” SpaceNews, 28 April 2023, URL: https://spacenews.com/astra-exotrail-win-satellite-propulsion-orders/
(225) Astra, “Astra Announces Spacecraft Engine Contract with Astroscale,” Press Release, 13 Oct 2022, URL: https://astra.com/news/spacecraft-engine-contract-with-astroscale/

(226) Exotrail, “Hall effect thruster for small satellites.” Company Website, Online Datasheet, May, 2022.
(227) Exotrail Press Release, “Exotrail delivers its first Hall Effect Propulsion system prototype for In-Orbit Demonstration mission.” 02 October, 2019.
(228) Exotrail Press Release, “Exotrail secures contract with AAC Clyde Space to equip their spacecrafts for Eutelsat’s ELO 3 and 4.” 18 February, 2020.
(229) Gurciullo, A., Jarrige, J., Lascombes, P., and Packan, D. “Experimental performance and plume characterization of a miniaturized 50W Hall thruster.” 36th IEPC, Vienna, Austria, 2019.
(230) ExoTrail Press Release, “Exotrail paves the way for new space mobility with first of its kind successful in-orbit demonstration mission,” 01 January 2021.
(231) Moriconi, B., Hallouin, T., Gurciullo, A., “Hall Thruster ExoMG™ - micro, ExoMG™ - nano and low current cathode development at Exotrail: cyclic life testing results.” 37th IEPC, Cambridge,USA, 2022.
(232) Aerospacelab Press Release, “Press release – Arthur, Aerospacelab launched the first Belgianprivate commercial satellite”, 30 June 2021.
(233) NASA, “NASA Selects New Mission to Study Storms, Impacts on Climate Models,” NASA website, 5 Nov 2023, URL: https://www.nasa.gov/news-release/nasa-selects-new-mission-to-study-storms-impacts-on-climate-models/
(234) Exotrail, “Exotrail will provide Blue Canyon Technologies with electric propulsion systems for NASA’s INCUS mission,” Press Release, 22 June 2023, URL: https://www.exotrail.com/blog/exotrail-blue-canyon-technologies
(235) Exotrail, “York Space Systems tackled Exotrail electric propulsion system for its Cislunar mission”, Press Release, 08 September 2021.
(236) Exotrail, “OHB LUXSPACE inks contract with exotrail for ExoMG™ electric propulsion system onboard triton-x heavy platform.”, Press Release, 23 November 2021.
(237) Exotrail, “Exotrail electric propulsion systems selected by Korean satellite manufacturer Satrec Initiative,” Press Release, 26 April 2023, URL: https://www.exotrail.com/blog/satrec-initiative
(238) “Exotrail to provide Astro Digital with electric propulsion systems,” Spacewatch, 4 April 2023, URL: https://spacewatch.global/2023/04/exotrail-to-provide-astro-digital-with-electric-propulsion-systems/
(239) Exotrail, “Exotrail’s electric propulsion systems to be used in Muon Space’s climate monitoring constellation,” Press Release, 24 Aug 2023, URL: https://www.exotrail.com/blog/exotrail-muon-contract-for-climate-monitoring
(240) Exotrail Press Release, “Exotrail to debut its SpaceVan™ in-space mobility service on October2023 SpaceX Falcon 9 mission”, 12 April 2022.
(241) Foust, J. “Exotrail deploys first satellite from orbital transfer vehicle,” Space News, March 6, 2024, URL: https://spacenews.com/exotrail-deploys-first-satellite-from-orbital-transfer-vehicle/
(242) Exotrail, “Exotrail and Airbus to partner on small Earth Observation satellites propulsion,” Press Release, 20 Sept 2023, URL: https://www.exotrail.com/blog/exotrail-and-airbus-to-partner-on-small-earth-observation-satellites-propulsion
(243) Werner, D., “ExoTerra to provide Blackjack Satellite thrusters,” SpaceNews, 30 August, 2021.
(244) Werner D., “ExoTerra gains flight heritage for Halo thrusters,” SpaceNews, 8 Aug 2023, URL: https://spacenews.com/exoterra-gains-flight-heritage-for-halo-thrusters/
(245) ExoTerra Resource, “Halo Hall-Effect Thruster - Xenon.” Company Website, Datasheet.
(246) VanWoerkom, M., Gorokhovsky, V., Pulido, G., Pettigrew, R., and Seidcheck, A. “Test Results of ExoTerra’s Halo Micro Electric Propulsion System.” 36th IEPC, Vienna, Austria, 2019.

(247) NASA Press Release, “NASA Announces New Tipping Point Partnerships for Moon and Mars Technologies.” 27 September, 2019.
(248) Glascock, M. S., Kiefer, E., and VanWoerkom, M.; “Performance and Capability Overview of the Halo Electric Propulsion System”, International Electric Propulsion Conference, IEPC-2022-301, 2022.
(249) Glascock, M. S. and VanWoerkom, M., “Channel Erosion Measurements and Predictions in a 400 W Hall Thruster,” International Electric Propulsion Conference, IEPC-2022-300, 2022.
(250) Werner, D., “ExoTerra delivers 21 propulsion modules for SDA satellites,” Space News, May 27, 2025, URL: https://spacenews.com/exoterra-delivers-21-propulsion-modules-for-sda-satellites/
(251) Werner, D., “Voyager Technologies acquires ExoTerra Resources,” Space News, October 27, 2025, URL: https://spacenews.com/voyager-technologies-acquires-exoterra-resources/
(252) Simmonds, J., Chaplin, V., Byrne, M., Goebel, D., Lobbia, R., Hofer, R., Conversano, R., “Magnetically Shielded Miniature Hall Thruster: Flight Qualification, LIF, and Krypton Performance,” AIAA SciTech Forum, 8-12 January 2024, Orlando, FL.
(253) Chaplin, V., Simmonds, J., Bryne, M., Goebel, D., Ortega, A., Lobbia, R., Mikellides, I., Hofer, R., Zhu, B., Ratliff, J., and Conversano, R., “Extended Life Qualification of the Magnetically Shielded Miniature (MaSMi) Hall Thruster,” 37th Small Satellite Conference, Logan, UT, Aug 2023, SSC23-VI-01.
(254) Exoterra Resource, “Halo12 Electric Propulsion System - Xenon,” Company Datasheet, Dated 16 December 2022.
(255) Capella Space, "Capella Space Reveals First Light Imagery from Capella-17 "No Cloudy Days" Mission, July 8, 2025.
(256) Werner, D., “Orbion to supply propulsion for General Atomics weather satellite,” SpaceNews, 24 June, 2022.
(257) Erwin, S., “Orbion delivers 33 electric thrusters to York Space Systems for U.S. military constellation,” Space News, 13 January, 2026, URL: https://spacenews.com/orbion-delivers-33-electric-thrusters-to-york-space-for-u-s-military-constellation/
(258) Hall, S. J., Fruncek, C. E., Dahl, P. N., Baxendale, S. E., Armstrong, M. M., Dickey, A., Washeleski, R. L., Makela, J. M., Sommerville, J. D., and King, L. B., “Flight Qualification of the Orbion Aurora Electric Propulsion System,” In Space Propulsion Conference, Vol. SP2024_303, Glasgow, Scotland, UK, 2024.
(259) York Space Systems, “York Space Systems Acquires Orbion Space Technology, Further Strengthening Supply Chain with Flight-Proven Spacecraft Capability,” Business Wire, 12 March 2026.
(260) Busek, “BHT-350 Hall Effect Thruster,” Company Datasheet, Copyright 2021.
(261) Busek, “Busek Scales Thruster Production for Airbus OneWeb Satellites,” Company Press Release, June 22, 2022.
(262) Werner, D., "Busek ramps up production for OneWeb constellation,” SpaceNews, 6 Feb 2023, URL: https://spacenews.com/busek-ramps-up-production-for-oneweb-constellation/
(263) Werner, D., “Busek lauds on-orbit performance of OneWeb’s Hall-effect thrusters,” SpaceNews, 8 Aug 2023, URL: https://spacenews.com/busek-lauds-on-orbit-performance-of-onewebs-hall-effect-thrusters/
(264) Busek Co Press Release, “Busek Ships First LEO to GEO Capable Electric Propulsion System – Design Demonstrated One Million Newton-Seconds in NASA-Led Test,” PR Newswire, 23 February 2021.
(265) Szabo, J., Byrne, L., Strain, M., Paintal, S., Sawyer, S., Yu, T., Kolencik, G., and Hruby, V., “One Million Newton-Second Duration Test of a 600 Watt Hall Effect Thruster Fueled By Xenon,” 2020 AIAA Propulsion and Energy Forum, Virtual Event, August 24-28, 2020.

(266) Nikrant, A., Glogowski, M., Cochran, D., Moquin, T., Choi, Y., Benavides, G., Kamhawi, H., Sarver-Verhey, T., Baird, M., Rhodes, C., and Mackey, J., "Overview and Performance Characterization of Northrop Grumman's 1kW Hall Thruster String," 37th IEPC, Boston, MA, Paper No. IEPC-2022-303, 19-23 June, 2022.
(267) Nikrant, A., Switzer, Z., Glogowski, M., Benavides, G., Baird, M., and Makey, J., "NGHT-1X Pole Cover Erosion Measurements on Xenon and Krypton," AIAA SCITECH 2024 Forum, 8-12 January 2024, Orlando, FL.
(268) Switzer, Z., Nikrant, A., Martinez, L., and Glogowski, M., "NGHT-1X High Current Density Operation on Xenon and Krypton," AIAA SCITECH 2024 Forum, 8-12 January 2024, Orlando, FL.
(269) Erwin, S., "Northrop Grumman says customers are 'lined up' for on-orbit satellite servicing," SpaceNews, 24 March, 2022.
(270) Jewett, R., "Optus Orders Mission Extension Pod from Northrop Grumman's SpaceLogistics," Via Satellite Article, 22 February, 2022.
(271) NASA, "Small Spacecraft Electric Propulsion Opens New Deep Space Opportunities," NASA Press Release, 19 April, 2022.
(272) Northrop Grumman, "Northrop Grumman's SpaceLogistics Continues Revolutionary Satellite Life-Extension Work with Sale of Third Mission Extension Pod," Press Release, 20 June 2023, URL: https://news.northropgrumman.com/news/releases/northrop-grummans-spacelogistics-continues-revolutionary-satellite-life-extension-work-with-sale-of-third-mission-extension-pod
(273) SETS, "SETS' SPS-25 Propulsion System Proves Successful in Space Testing Despite Challenging Circumstances in Ukraine," Press Release, 21 June 2023, URL: https://www.prnewswire.com/news-releases/sets-sps-25-propulsion-system-proves-successful-in-space-testing-despite-challenging-circumstances-in-ukraine-301855868.html
(274) Werner, D. and Klaczynska, M., "EOS Data Analytics and Space Electric Thruster Systems demonstrate technology in orbit," SpaceNews, 5 June 2023, URL: https://spacenews.com/eos-data-analytics-and-space-electric-thruster-systems-demonstrate-technology-in-orbit/
(275) Aliena Pte Ltd, "MUSIC Electric Propulsion System," Company website, Accessed 4 December 2023, URL: https://www.aliena.sg/music
(276) Aliena and NuSpace Press Release, "Singapore's Aliena & NuSpace to launch demonstration mission for constellation management system," SpaceTechAsia, 28 September 2019, URL: https://www.spacetechasia.com/singapores-aliena-nuspace-to-launch-demonstration-mission-for-constellation-management-system/
(277) Press Release, "Lightweight engine launched into space," Nanyang Technological University – Singapore, 14 January 2022, URL: https://www.ntu.edu.sg/news/detail/ntu-singapore-startup-aliena-deploys-compact-and-fuel-efficient-satellite-engine-into-space
(278) Khoo, K. S., Laterza, M., Lim, J. W. M., and Potrivitu, G.-C., "Novel cathodeless and very low-power Hall thruster: qualification and integration on a 3U platform for an in-orbit demonstration mission," Proceedings of the 37th International Electric Propulsion Conference, IEPC-2022-326, Cambridge, MA, USA, 2022.
(279) Laterza, M., Potrivitu, G-C., Agarwal, D., Khoo, K. S., Pontianus, N., Lim, J. W. M., Eunseo, E. H., Supriyadi, S. D., Li, C., Liau, L., Ramachandran, P., Teo, C., Ng, Z. K., Tsang, S. H., and Teo, H. T. E., "MUlti-Stage Ignition Compact thruster concept and testing," Proceedings of the 37th International Electric Propulsion Conference, IEPC-2022-294, Cambridge, MA, USA, 2022.
(280) Press Release "Aliena signs contract with Orbital Astronautics for ORB-12 STRIDER mission," SatNews, 23 September 2021, URL:

https://news.satnews.com/2021/09/23/aliena-signs-contract-with-orbital-astronautics-for-orb-12-strider-mission/
(281) Burton, R. “Pulsed Plasma Thrusters.” In Encyclopedia of Aerospace Engineering (eds R. Blockley and W. Shyy). doi:10.1002/9780470686652.eae120.
(282) Kolbeck, J., Anders, A., Beilis, I., and Keidar, M. “Micro-propulsion based on vacuum arcs.” Journal of Applied Physics, June, 2019, https://doi.org/10.1063/1.5081096.
(283) Benchmark Space Systems, “Xantus.” Datasheet, June 2023, Accessed Sept. 2023, URL: https://www.benchmarkspacesystems.com/xantus-data-sheet
(284) Werner, D., “Benchmark signs contracts for metal plasma thrusters,” SpaceNews, 15 March 2023, URL: https://spacenews.com/benchmark-signs-contracts-for-metal-plasma-thrusters/
(285) Benchmark, “Benchmark Electric Propulsion Thrusters on Orbit and Poised for First Fire,” Press Release, 19 March 2024.
(286) Comat, “Plasma Jet Pack technology,” Datasheet, Accessed Sept. 2023, URL: https://comat.space/en/p/small-sat-en/en-pjp-technology/
(287) Comat, “Great news: Our PJP boards on Vega Mission VV23,” Accessed Sept. 2023, URL: https://comat.space/en/actualites/micro-propulsion/
(288) Neumann Space, “Neumann Drive Datasheet,” Datasheet, Sept. 2023.
(289) Satnews, “Neumann Drive® propulsion system now integrated onto Australia’s Skykraft satellite,” News article, 14 March 2023, URL: https://news.satnews.com/2023/03/14/neumann-drive-propulsion-system-now-integrated-onto-australias-skykraft-satellite/
(290) Foust, J., “SpaceX launches eighth dedicated smallsat rideshare mission,” SpaceNews, 12 June 2023, URL: https://spacenews.com/spacex-launches-eighth-dedicated-smallsat-rideshare-mission/
(291) Neumann Space, “Australia’s world leading propulsion technology achieves first space launch,” Press Release, 13 June 2023, URL: https://neumannspace.com/wp-content/uploads/2023/06/2023-06-13_Media-Release-Neumann-Space-First-Launch.pdf
(292) Australian Space Agency, “Ground-breaking nanosatellite showcases Australian technology,” 2 March 2023, URL:https://www.industry.gov.au/news/ground-breaking-nanosatellite-showcases-australian-technology
(293) Dalton, Angus, “How do you break Australia’s satellite drought? Hitch a ride with Elon Musk,” The Sydney Morning Herald, Oct. 9, 2023, Accessed Nov. 2023, URL: https://www.smh.com.au/national/how-do-you-break-australia-s-satellite-drought-hitch-a-ride-with-elon-musk-20231003-p5e9bs.html
(294) University of Melbourne, “SpIRIT of science: University of Melbourne-led satellite mission launch countdown begins,” News article, Oct. 9, 2023, Accessed Nov. 2023, URL: https://www.unimelb.edu.au/newsroom/news/2023/october/spirit-of-science-university-of-melbourne-led-satellite-mission-launch-countdown-begins
(295) EX2, “Avalon 2023: Inovor Technologies prepares for busy 2023,” 14 March 2023, URL:https://www.ex2.com.au/news/avalon-2023-inovor-technologies-prepares-for-busy-2023/
(296) Garman, L., “Neumann Space to test electric propulsion system in orbit,” Space Connect, 6 June 2023, URL:https://www.spaceconnectonline.com.au/satellites/5911-neumann-space-space-inventor-partner-to-trial-propulsion-tech
(297) “SSTL+Neumann Space partner to test Australian made propulsion system on demo mission,” Satnews, 8 August 2023, URL:https://news.satnews.com/2023/08/08/sstl-neumann-space-partner-to-test-australian-made-propulsion-system-on-demo-mission/
(298) Neumann Space, “Missions,” Company Website, Accessed 11 April 2026, URL: https://neumannspace.com/missions/

(299) J. Foust, “Phase Four Launches First Plasma Propulsion Systems”, SpaceNews, 25 January 2021, https://spacenews.com/phase-four-launches-first-plasma-propulsion-systems/
(300) Werner, D., “Phase Four Demonstrates Maxwell Block 2 Thruster In Orbit,” SpaceNews, 12 September 2023, https://spacenews.com/phase-four-demonstrates-maxwell-block-2-thruster-in-orbit/
(301) Debra Werner “Capella Space and Phase Four reveal Maxwell Engine performance” SpaceNews 30 June 2021.
(302) REGULUS, 6 May 2020, URL: https://www.t4innovation.com/wp-content/uploads/2020/05/T4i-REGULUS-Magazine.pdf
(303) Bellomo, N. “Enhancement of Microsatellites’ Mission Capabilities: Integration of REGULUS Electric Propulsion Module into UniSat-7.” 70th International Astronautical Congress, Washington, D.C., October, 2019.
(304) Bellomo, N., et al., “Design and In-Orbit Demonstration of REGULUS, an Iodine Electric Propulsion System”, CEAS Space Journal, 7 June 2021.
(305) “Cube Quest Challenge NASA Facts.” NASA, FS-2019-12-073-MSFC. URL: https://www.nasa.gov/sites/default/files/atoms/files/cubequest_fs_june2020_508.pdf
(306) “Three DIY CubeSats Score Rides on NASA’s First Flight of Orion, Space Launch System.” NASA Press Release 17-055, 8 June, 2017. URL: https://www.nasa.gov/press-release/three-diy-CubeSats-score-rides-on-nasa-s-first-flight-of-orion-space-launch-system
(307) Alhorn, D., Casas, J., Agasid, E., Adams, C., Laue, G., Kitts, C., and O’Brien, S. “NanoSail-D: The Small Satellite That Could!” SmallSat Conference, 2011.
(308) Mansell, J., Spencer, D., Plante, B., Diaz, A., Fernandez, M., Bellardo, J., Betts, B., and Nye, B. “Orbit and Attitude Performance of the LightSail 2 Solar Sail Spacecraft.” AIAA 2020-2177.
(309) “NEA Scout, NASA’s solar sail mission to an asteroid,” The Planetary Society, Accessed Nov. 2023, URL: https://www.planetary.org/space-missions/nea-scout
(310) Johnson, L, et al. “Near Earth Asteroid Scout: Exploring Asteroid 1991VG Using a SmallSat.” *Proceedings of the 70th International Astronautical Congress*, IAC-19/B4/2.
(311) NASA, “Advanced Composite Solar Sail System (ACS3): Using Sunlight to Power Deep Space Exploration,” Press Release, October 16, 2023, URL: https://www.nasa.gov/smallspacecraft/what-is-acs3/
(312) “AE’s Prox-1 Satellite Launches from Kennedy Space Center.” Georgia Institute of Technology, 25 June, 2019. URL: https://ae.gatech.edu/news/2019/06/aes-prox-1-satellite-launches-kennedy-space-center
(313) C. Henry. “Tethers Unlimited Says Early Results of Deorbit Hardware Test Promising.” SpaceNews, 23 January, 2020. URL: https://spacenews.com/tethers-unlimited-says-early-results-of-deorbit-hardware-test-promising/
(314) Clark, S. “SmallSat Companies Teaming Up on Deorbit Experiment.” Spaceflight Now, 15 August, 2019. URL: https://spaceflightnow.com/2019/08/15/SmallSat-companies-teaming-up-on-deorbit-experiment/
(315) Satnews, “SmallSat Space Debris Remediation Technology Being Demo’d By Millennium Space Systems,” 7 December 2020.
(316) Stankey, H. and Hoyt, R., “In-Flight Performance of the Terminator Tape End-of-Life Deorbit Module,” 35th Small Satellite Conference, Logan, UT, Paper No: SSC21-XI-03, 2021.
(317) Applied Ion Systems, “Products,” Technical Data, Accessed: Sept. 2023. URL: https://appliedionsystems.com/products/

(318) Federal Communications Commission, “FCC Adopts New ‘5-Year Rule’ for Deorbiting Satellites to Address Growing Risk of Orbital Debris”, press release, 9 September 2022, accessible at: https://docs.fcc.gov/public/attachments/DOC-387720A1.pdf
(319) Hejmanowski, N. J., Woodruff, C. A., Burton, R. L., Carroll D. L., Palla, A. D., and Cardin J. M. “CubeSat High Impulse Propulsion System (CHIPS) Design and Performance.” 63rd JANNAF Propulsion Meeting, Paper Tracking # 4800, Phoenix, AZ, 2016, Dist. A.
(320) Hejmanowski, N. J., Woodruff, C. A., Burton, R. L., and Carroll D. L. “Electrothermal Space Thruster Heater for Decomposable Propellants.” U.S. Patent # 9,909,574 B1, 2018.
(321) Hejmanowski, N. J., Woodruff, C., Burton, R.L., Carroll, D.L., and Cardin, J. "CubeSat High Impulse Propulsion System (CHIPS)." 62nd JANNAF Propulsion Meeting, Paper Tracking # 4032, Nashville, TN, 1-5 June, 2015, Dist. A.
(322) CU Aerospace, “CubeSat High Impulse Propulsion System.” Company Website, URL: https://cuaerospace.com/products-services/space-propulsion-systems/cubesat-high-impulse-propulsion-chips, Datasheet, 2022.
(323) Electric Propulsion Laboratory, Inc, “Space-based Resistojets,” Company website, Accessed 3 December 2023, URL: https://electricpropulsionlab.com/resistojet-propulsion-systems/
(324) Alamalhodaei, Aria, “Atomos Space books launch to demonstrate rendezvous, docking and refueling in-orbit,” TechCrunch, 25 July 2023, URL: https://techcrunch.com/2023/07/25/atomos-space-books-launch-to-demonstrate-rendezvous-docking-and-refueling-in-orbit/
(325) Pale Blue, “Products,” Company Website. Accessed April 2026, URL: https://pale-blue.co.jp/product/
(326) ArkEdgeSpace, “ArkEdge Space Achieves Full Success in On-Orbit Demonstration of Space Components with Micro-satellite AE1c,” Press Release, 11 June 2025, URL: https://arkedgespace.com/en/news/2025-06-11_ae1c
(327) Cifali, G., Gregucci, S., Andreussi, T., and Andrenucci, M. “Resistojet Thrusters for Auxiliary Propulsion of Full Electric Platforms.” 35th International Electric Propulsion Conference, Atlanta, GA, IEPC-2017-371, 2017.
(328) Sitael, “XR Resistojet Product Family.” Datasheet, Company Website, Copyright 2015.
(329) Courtney, D., Wright, P., Lafko, D., Metivier, E., and Demmons, N. “Electrospray Propulsion for Precise Attitude and Position Control.” AAS 17-088, Breckenridge, CO., 2017.
(330) D. Courtney et al. “Electrospray Thrusters for Small Spacecraft Control: Pulsed and Steady State Operation.” AIAA-2018-4654.
(331) Courtney, D., Wood, Z., and Fedkiw, T. “Reconstructing Electrospray Plume Current Spatial Distributions Using Computed Tomography.” 36th IEPC, Vienna, Austria, IEPC-2019-A-787.
(332) D. Courtney et al. “High-Speed Transient Characterization of the Busek BET-300-P Electrospray Thruster.” 36th IEPC, Vienna, Austria, IEPC-2019-A-788.
(333) T. Fedkiw, Z. Wood, and N. Demmons, “Environmental and Lifetime Testing of the BET-300-P Electrospray Thruster”, AIAA 2020-3614.
(334) Demmons, N., et al., “Qualification of the BET-MAX Electrospray Propulsion System”, IEPC-2022-196, 37th International Electric Propulsion Conference, Cambridge, MA, 19-23 June 2022.
(335) Busek, “BET-MAX Electrospray Thruster System”, Company Datasheet, Dated August 2021.
(336) Enpulsion, “IFM Nano Thruster.” Company Website, Datasheet ENP2018-001.F.1, Accessed 2020.

(337) Schönherr, T., Little, B., Krejci, D., Reissner, A., and Seifert, B. “Development, Production, and Testing of the IFM Nano FEEP Thruster.” 36th IEPC, Vienna, Austria, IEPC-2019-362, 2019.
(338) Krejci, D., Hugonnaud, V., Schonherr, T., Little, B., Reissner, A., Seifert, B., Kock, Q, Borras, E., and Amo, J. “Full Performance Mapping of the IFM Nano Thruster, Including Direct Thrust Measurements.” *Journal of Small Satellites*, 2019, Vol. 8, No. 2, pp. 881-893.
(339) Enpulsion, “Enpulsion Nano R3.” Company Website, Datasheet ENP2019-086.E.1, Accessed 2022.
(340) Enpulsion, “Enpulsion Micro R3.” Company Website, Datasheet ENP2018-002.H.1, Accessed 2021.
(341) Grimaud, L., Krejci, D., and Seifert, B. “The IFM Micro FEEP Thruster: A Modular Design for SmallSat Propulsion.” 36th IEPC, Vienna, Austria, IEPC-2019-A675, 2019.
(342) Enpulsion, “Enpulsion Neo.” Company Datasheet, Accessed October 2023, URL: https://www.enpulsion.com/
(343) Morpheus Space, “nanoFEEP and multiFEEP.” Company Website, Datasheet, June, 2020.
(344) Bock, D., Spethmann, A., Trottenberg, T., Kersten, H., and Tajmar, M. “In-Plume Thrust Measurement of NanoFEEP Thruster with a Force Measuring Probe Using Laser Interferometry.” 36th IEPC, Vienna, Austria, IEPC-2017-391, 2017.
(345) Avant Space, “GT-50 RF Ion Thruster.” Company Datasheet. URL: http://www.avantspace.com/upload/iblock/dc9/Data-sheet.pdf
(346) Kralkin, E., et al. “Exploratory Testing of a Radio-Frequency Thruster for Small Satellites.” IEPC-2017-425.
(347) Busek, “BIT-3 RF Ion Thruster.” Company Website, Datasheet, Copyright 2019.
(348) “All-Electric CubeSat Propulsion Technologies for Versatile Mission Application.” 32nd International Symposium on Space Technology and Science (ISTS), Fukui, Japan, June, 2019, ISTS-2019-b-002.
(349) Tsay, M., Frongillo, J., Model, J., Zwahlen, J., Barcroft, C., Feng, C. “Neutralization Demo and Thrust Stand Measurement for BIT-3 RF Ion Thruster.” 2017 AIAA Propulsion and Energy Forum, Atlanta, GA, July, 2017, AIAA-2017-4890.
(350) Tsay, M., “3,500-Hour Wear Test Result of BIT-3 RF Ion Propulsion System”, IEPC-2022-255, 37th International Electric Propulsion Conference, Cambridge, MA, 19-23 June 2022.
(351) Tsay, M., et al., “Volume Production of Gen-2 Iodine BIT-3 Ion Propulsion System”, IEPC-2022-267, 37th International Electric Propulsion Conference, Cambridge, MA, 19-23 June 2022.
(352) Tsay, M., Terhaar, R., Emmi, K., and Barcroft, C., “Twin Ion Engine Demonstration for Small Spacecraft Applications,” 36th Annual Small Satellite Conference, Logan, UT, 2022, SSC22-X-04.
(353) Pale Blue, “Products – Ion Thruster,” Website Datasheet, Accessed October 2022.
(354) Nakagawa, Y., Yaginuma, K., Asakawa, J., and Koizumi, H., “1U+Water Ion and Resistojet Thruster Module for On-Orbit Demonstration,” IEPC-2022-276, 37th International Electric Propulsion Conference, Cambridge, MA, 19-23 June 2022.
(355) Navin, J., “JAXA Epsilon fails on sixth flight carrying RAISE-3 and others,” NASA Spaceflight.com, 11 October 2022
(356) “Development of Water Gridded Ion Thruster for Small Satellites: Toward On-Orbit Demonstration” Poster, Small Satellite Conference, 02 August 2023, Utah State University, Logan, UT, URL: https://digitalcommons.usu.edu/smallsat/2023/all2023/217/

(357) Patton, T., "ION Satellite Carrier Marks Significant Milestone with Recent Launch," The Journal of Space Commerce, 3 December 2025, URL: https://www.exterrajsc.com/p/ion-satellite-carrier-marks-significant
(358) ThrustMe, "NPT30-I2 1.5U," Company Website, Datasheet, Copyright 2020.
(359) Martinez, J., Rafalskyi, D., and Aanesland, A. "Development and Testing of the NPT30-I2 Iodine Ion Thruster." 36th IEPC, Vienna, Austria, IEPC-2019-811, 2019.
(360) ThrustMe, "NPT30-I2 1U," Company Website, Datasheet, Copyright 2021.
(361) Leiter, H., Lauer, D., Bauer, P., Berger, M., and Rath, M. "The Ariane Group Electric Propulsion Program 2019-2020." 36th IEPC, Vienna, Austria, IEPC-2019-592, 2019.
(362) Leiter, H., Altmann, C., Lauer, D., Rath, M., Becker, F., Feili, D., and Amo, J. "A Nouvelle Neutralization Concept for RIT-μX Miniaturized Radio Frequency Ion Thruster Systems." 36th IEPC, Vienna, Austria, IEPC-2019-806, 2019.
(363) Ariane Group, "Electric Propulsion Systems and Components." Company Website, Datasheet, Accessed 2020.
(364) Leiter, H., Lotz, B., Feili, D., Tartz, M., Neumann, H., and Cara, D. "Design Development and Test of the RIT-μX Mini Ion Engine System." IEPC-2009-179.
(365) Leiter, H., et al., "Recent Development of the RIT-μX Thruster and System", IEPC-2022-252, 37th International Electric Propulsion Conference, Cambridge, MA, 19-23 June 2022.
(366) Holste, K., et al., "Endurance and Coupling Test of the RIT-μX", IEPC-2022-247, 37th International Electric Propulsion Conference, Cambridge, MA, 19-23 June 2022.
(367) Leiter, H., Altmann, C., Porst, J., Lauer, D., Berger, M., and Rath, M. "Six Decades of thrust – The Ariane Group Radiofrequency Ion Thrusters and Systems Family." IEPC-2017-027.
(368) Szabo, J., Tedrake, R., Metivier, E., Paintal, S., and Taillefer, Z. "Characterization of a One Hundred Watt, Long Lifetime Hall Effect Thruster for Small Spacecraft." 53rd AIAA Joint Propulsion Conference, Atlanta, Georgia, 2017.
(369) Busek, "BHT-600 Busek Hall Effect Thruster." Company Website, Datasheet, 2016.
(370) Szabo, J., Pote, B., Tedrake, R., Paintal, S., Byrne, L., Hruby, V., Kamhawi, H., and Smith, T. "High Throughput 600 Watt Hall Effect Thruster for Space Exploration." 52nd AIAA Joint Propulsion Conference, Salt Lake City, Utah, 2016.
(371) Benavides, G., Kamhawi, H., Mackey, J., Haag, T., and Costa, G., "Iodine Hall-Effect Electric Propulsion System Research, Development, and System Durability Demonstration," 2018 Joint Propulsion Conference, Cincinnati, Ohio, July 9-11, 2018.
(372) Saevets, P., Semenenko, D., Albertoni, R., and Scremin, G. "Development of a Long-Life Low-Power Hall Thruster." 35th IEPC, Atlanta, Georgia, 2017.
(373) ExoTerra Resource, "Halo Hall-Effect Thruster - Krypton." Company Website, Datasheet.
(374) Virgin Orbit, "Exoterra, Virgin Orbit Win NASA Phase II SBIR Award for Solar Electric Propulsion Upper Stage," Company Press Release, June 1, 2021.
(375) Exoterra Resource, "Halo12 Electric Propulsion System - Krypton," Company Datasheet, Dated 16 December 2022.
(376) Conversano, R., Goebel, D., Katz, I., and Hofer, R. "Low-Power Hall Thruster with an Internally Mounted Low-Current Hollow Cathode." U.S. Patent No. 10,723,489, 2020.
(377) Conversano, R., Reilly, S., Kerber, T., Brooks, J., and Goebel, D. "Development of and Acceptance Test Preparations for the Thruster Component of the Ascendant Sub-kW Transcelestial Electric Propulsion System (ASTRAEUS)." 36th IEPC, Vienna, Austria, 2019.
(378) Conversano, R., Lobbia, R., Kerber, T., Tilley, K., Goebel, D., and Reilly, S. "Performance characterization of a low-power magnetically shielded Hall thruster with an internally-mounted hollow cathode." Plasma Sources Science and Technology, Vol. 28, No. 10, 2019.

(379) Conversano, R., Barchowsky, A., Lobbia, R., Chaplin, V., Lopez-Ortega, A., Loveland, J., Lui, A., Becatti, G., Reilly, S., Goebel, D., Snyder, J., Hofer, R., Randolph, T., Mikellides, I., Vorperian, V., Carr, G., Rapinchuk, J., Villalpando, C., and Grebow, D. “Overview of the Ascendant Sub-kW Transcelestial Electric Propulsion System (ASTRAEUS).” 36th IEPC, Vienna, Austria, 2019.
(380) Lobbia, R., Conversano, R., Ortega, A., Reilly, S., Mikellides, I. “Pole Erosion Measurements for the Development Model of the Magnetically Shielded Miniature Hall Thruster (MaSMi-DM).” 36th IEPC, Vienna, Austria, 2019.
(381) Ortega, A., Mikellides, I., Conversano, R., Lobbia, R., Chaplin, V. “Plasma Simulations for the Assessment of Pole Erosion in the Magnetically Shielded Miniature Hall Thruster (MaSMi)." 36th IEPC, Vienna, Austria, 2019.
(382) JPL Press Release, “2020 Technology Highlights, Jet Propulsion Laboratory,” CL#20-6401.
(383) Conversano, R., Barchowsky, A., Vorperian, V., Chaplin, V., Becatti, G., Carr, G., Stell, C., Loveland, J., and Goebel, D., “Cathode & Electromagnet Qualification Status and Power Processing Unit Development Update for the Ascendant Sub-kW Transcelestial Electric Propulsion System,” 34th Small Satellite Conference, 2020, SSC20-VI-10.
(384) Conversano, R., Lobbia, R., Lopez-Ortega, A., Chaplin, V., Reilly, S., Arestie, S., Goebel, D., “Long-Duration Wear Testing of the ASTRAEUS Hall Thruster, Phase 1: 50 kg Xe Total Throughput,” Space Propulsion 2020+1, 17-19 March 2021, SP2020-005.
(385) Conversano, R. W., Lobbia, R. B., Arestie, S. M., Lopez-Ortega, A., Chaplin, V. H., Reilly, S. W., and Goebel, D. M.; “Demonstration of 100 kg Xenon Propellant Throughput by a Low-Power Magnetically Shielded Hall Thruster,” Journal of Propulsion and Power, 2022.
(386) Conversano, R. W., Becatti, G., Goebel, D. M., and Chaplin, V. H.; “Demonstration of 13,011-hours of Operation of a Proto-Flight Compact Heaterless Lanthanum Hexaboride Hollow Cathode,” Acta Astronautica, Vol. 197, 2022, pp. 53-59. DOI: https://doi.org/10.1016/j.actaastro.2022.05.015.
(387) Becatti, G., Conversano, R. W, and Goebel, D. M., “Demonstration of 25,000 ignitions on a proto-flight compact heaterless lanthanum hexaboride hollow cathode,” Acta Astronautica, Vol. 178, 2021, pp. 181-191, DOI: https://doi.org/10.1016/j.actaastro.2020.09.013.
(388) Fruncek, C. E., Sommerville, J. D., Makela, J. M., Hall, S. J., Terhune, K. J., and King, L. B., “Qualification of the Aurora Low-Power Hall-Effect Thruster Part I: Environments and Performance,” presented at the 38th International Electric Propulsion Conference, IEPC-2024-392, Toulouse, France, 2024.
(389) Dahl, P. N., Hall, S. J., Sommerville, J. D., Terhune, K. J., Makela, J. M., King, L. B., and Myers, R. M., “Qualification of the Aurora Low-Power Hall-Effect Thruster Part II: Life Test Status as of 6,000 Hours,” presented at the 38th International Electric Propulsion Conference, IEPC-2024-389, Toulouse, France, 2024.
(390) Baxendale, S. E., Makela, J. M., Bartelli, B. J., Sommerville, J. D., and King, L. B., “Qualification of the Aurora Power Processing Unit,” presented at the 38th International Electric Propulsion Conference, IEPC-2024-396, Toulouse, France, 2024.
(391) Dickey, A., DeVlieg, I., Ford, N., Washeleski, R. L., Moler, J., Makela, J. M., Sommerville, J. D., and King, L. B., “Qualification of the Aurora Low-Power PMA,” presented at the 38th International Electric Propulsion Conference, IEPC-2024-394, Toulouse, France, 2024.
(392) Armstrong, M. M., Terhune, K. J., Anderson, K., Makela, J. M., Hall, S. J., Washeleski, R. L., Kari, J., Goodreau, C., Sommerville, J. D., and King, L. B., “Integrated System Testing and Software Qualification of the Aurora Electric Propulsion System,” presented at the 38th International Electric Propulsion Conference, IEPC-2024-397, Toulouse, France, 2024.

(393) Orbion, “Aurora,” Company Website, Datasheet, Accessed 26 Nov 2023.
(394) Pale Blue, “PBH-100,” Company Website, Datasheet, Accessed 11 April 2026.
(395) Pulsar Fusion, “Performance Evaluation of Pulsar Fusion's 500W Hall Effect Thruster with Integrated LaB6 Cathode Using Xenon Propellant,” Company Website, White Paper, 26 Aug 2025, URL: https://pulsarfusion.com/wp-content/uploads/2025/08/PF-LEOBEAR-KR-2025-V3-XE-_compressed.pdf
(396) Pulsar Fusion, “LeoBear,” Company Website, URL: https://pulsarfusion.com/electric-propulsion/#leobear
(397) Lev, D., Franco, D., Zimmerman, R., Tordjman, M., Auslender, B., and Epsteain, O., “96 kN-sec Endurance Test of the R-200 Low Power Hall Thruster,” 37th IEPC, Boston, MA, Paper No: IEPC-2022-399, 19-23, June 2022.
(398) Lev, D., Franco, D., Auslender, B., and Epstein, O., “Extension of the Operation Envelope of the R-200 Low Power Hall Thruster,” 37th IEPC, Boston, MA, Paper No: IEPC-2022-357, 19-23, June 2022.
(399) Appel, L., Medvinsky, G., Shoor, B., Sirota, A., Zimmerman, R., Lev, D., Epstein, O., “Integration Test of the R-800 Low Power Hall Thruster Electric Propulsion System,” 37th IEPC, Boston, MA, Paper No: IEPC-2022-358, 19-23, June 2022.
(400) Safran, “PPS-X00 Stationary Plasma Thruster,” Company Datasheet, Dated 11/09/19.
(401) Vaudolon, J., Vial, V., Cornu, N., and Habbassi, I. “PPS-X00 Thruster Development Status at Safran.” 36th IEPC, Vienna, Austria, 2019.
(402) Erwin, S., “Safran, Terran Orbital to explore joint production of satellite propulsion systems,” SpaceNews, 23 June 2023, URL: https://spacenews.com/safran-and-terran-orbital-to-explore-joint-production-of-satellite-propulsion-systems-in-the-u-s/
(403) Piragino, A., et. al.,”Safran’s EPS-X00 low power system: Latest Development and Qualification Tests,” 39th International Electric Propulsion Conference, London, UK, 14-19 Sept 2025, IEPC-2025-526, URL: https://www.electricrocket.org/IEPC_2025/London/submission_526.pdf
(404) Safran, “Safran DSI to Supply Electric Propulsion Systems for AstroForge’s Upcoming Vestri Asteroid Mission,” PR Newswire, 11 Aug 2025.
(405) SITAEL “Electric Propulsion – HT400 Hall Effect Thruster Product Sheet.” Company Website, Datasheet, 2020.
(406) Ducci, C., Raiji, H., Pedrini, D., Misuri, T., and Onida, L. “SITAEL’s HT400 Hall Effect Thruster for Constellation Applications.” 36th IEPC, Vienna, Austria, 2019.
(407) Pedrini, D., Ducci, C., Misuri, T., Paganucci, F., Andrenucci, M. “Sitael Hollow Cathodes for Low-Power Hall Effect Thrusters.” IEEE Transactions on Plasma Science, Vol. 46, No. 2, February, 2018.
(408) Space Electric Thruster Systems “ST25 Hall-Effect Thruster.” Company Website, Datasheet, 2020.
(409) Petrenko, O., Tolok, S., Maslov, V., Kulagin, S., Serbin, V., Alekseenko, O., and Shcherbak, D. “Electric propulsion system SPS-25 with Hall Thruster.” 70th International Astronautical Congress (IAC),Washington D.C., October 2019.
(410) Space Electric Thruster Systems “ST40 Hall-Effect Thruster.” Company Website, Datasheet, 2020.
(411) Krishnan, M., Velas, K., and Leemans, S. “Metal Plasma Thruster for Small Satellites.” Journal of Propulsion and Power, March, 2020, DOI: 10.2514/1.B37603.
(412) Jarrige, J., Packan, D., Blanchet, A., and Herrero, L., “Direct Thrust Measurement of a Vacuum Arc Thruster,” IEPC-2019-521, Vienna, Austria, 15-20 September 2019.
(413) Hypernova Space Technologies, “NanoThruster A,” Datasheet.
(414) Ciaralli et al. “Results of the Qualification Test Campaign of a Pulsed Plasma Thruster for CubeSat Propulsion (PPTCUP).” Acta Astronautica, Volume 121, Pages 314-322, April–May, 2016.

(415) Mars Space Ltd., “Pulsed Plasma Thruster (PPT) projects,” Company website, Accessed Sept. 2023, URL: http://mars-space.co.uk/
(416) Siddiqui, M., Cretel, C., Synowiec, J., Hsu, A., Young, J., and Spektor, R. “First Performance Measurements of the Phase Four RF Thruster.” 35th IEPC, Atlanta, GA, October, 2017.
(417) Siddiqui, M. and Cretel, C. “Updated Performance Measurements and Analysis of the Phase Four RF Thruster.” Joint Propulsion Conference, Cincinnati, OH, AIAA-2018-4817.
(418) Cretel, C., Ajamia, M., Thompson, D., and Siddiqui, M. “Torsional Balance Thrust Measurement Techniques for Small RF Thrusters.”
(419) “Meet Maxwell.” Phase Four, website, accessed 2020.
(420) Phase Four, “Maxwell Product Suite,” Website Datasheet, Accessed October 2022
(421) “The Maxwell RF Propulsion System”, Phase Four Product Brochure, Available at 2023 Small Satellite Conference, Logan, UT.
(422) “REGULUS Electrical Propulsion System for Micro-satellites.” T4i, datasheet. URL: https://www.t4innovation.com/wp-content/uploads/2019/10/T4i_REGULUS_datasheet_.pdf
(423) “T4i REGULUS Family”, Company Website, Accessed October 2023, https://www.t4innovation.com/regulus-electric-propulsion/
(424) “The M1.4 Thruster with ConstantQ Propulsion”, Company Website, Accessed October 2023.
(425) “Team Miles”, NASA Space Science Data Coordinated Archive, Accessed October 2023, https://nssdc.gsfc.nasa.gov/nmc/spacecraft/display.action?id=TEAMMILES/.
(426) “Terminator Tape.” Tethers Unlimited, datasheet, 2020.



Table of Contents

Chapter Glossary ii
5 Guidance, Navigation & Control 140
5.1 Introduction 140
5.2 State-of-the-Art – GNC Subsystems 141
5.2.1 Integrated Units 141
5.2.2 Reaction Wheels 143
5.2.3 Magnetic Torquers 145
5.2.4 Thrusters 147
5.2.5 Star Trackers 148
5.2.6 Magnetometers 150
5.2.7 Sun Sensors 151
5.2.8 Horizon Sensors 154
5.2.9 Inertial Sensing 154
5.2.10 GPS Receivers 158
5.2.11 Deep Space Navigation 159
5.2.12 Atomic Clocks 159
5.2.13 LiDAR 160
5.3 Formation Flying, Rendezvous and Proximity Operations 160
5.4 On the Horizon 163
5.5 Summary 164
5.6 References 164

Chapter Glossary

(ADCS)	Attitude Determination and Control System
(AutoNGC)	Autonomous Navigation, Guidance, and Control
(C/A)	Coarse/Acquisition (GPS civilian signal)
(COCOM)	Coordinating Committee for Multilateral Export Controls
(COTS)	Commercial Off-the-Shelf
(DOF)	Degrees of Freedom
(DSAC)	Deep Space Atomic Clock
(DSN)	Deep Space Network
(EAR)	Export Administration Regulations
(FOG)	Fiber Optic Gyro (standardized from plural usage)
(GNC)	Guidance, Navigation, and Control
(GNSS)	Global Navigation Satellite System
(GPS)	Global Positioning System
(GSO)	Geostationary Orbit
(HCI)	Horizon Crossing Indicator
(IMU)	Inertial Measurement Unit
(IRU)	Inertial Reference Unit
(ISAM)	In-Space Servicing, Assembly, and Manufacturing
(JPL)	Jet Propulsion Laboratory
(LiDAR)	Light Detection and Ranging
(LMRST)	Low Mass Radio Science Transponder
(MarCO)	Mars Cube One
(MEMS)	Microelectromechanical Systems
(PFF)	Precision Formation Flying
(PMSM)	Permanent Magnet Synchronous Motor
(PNT)	Position, Navigation, and Timing
(QUEST)	Quaternion Estimator
(RPO)	Rendezvous and Proximity Operations
(RPOD)	Rendezvous, Proximity Operations, and Docking
(SDST)	Small Deep Space Transponder
(SGP4)	Simplified General Perturbations 4
(SSA)	Space Situational Awareness
(STM)	Space Traffic Management

(SWaP)	Size, Weight, and Power
(TLE)	Two-Line Element
(TRL)	Technology Readiness Level
(TRIAD)	Tri-Axial Attitude Determination Method
(USTP)	University SmallSat Technology Partnerships

5 Guidance, Navigation & Control

5.1 Introduction

The Guidance, Navigation & Control (GNC) subsystem includes the components used for position determination and those used by the Attitude Determination and Control System (ADCS). In Earth orbit, onboard position determination can be provided by a Global Positioning System (GPS) receiver. Alternatively, ground-based radar tracking systems can also be used. If onboard knowledge is required, then these radar observations can be uploaded and paired with a suitable onboard orbit propagator. Commonly, the U.S. Air Force (USAF) publishes Two-Line Element sets (TLE) (1), which are paired with a Simplified General Perturbations 4 (SGP4) propagator (2). In deep space, position determination is performed using the Deep Space Network (DSN) and an onboard radio transponder (3). There are also technologies being developed that use optical detection of celestial bodies, such as planets and X-ray pulsars, to calculate position data (4).

Using SmallSats in cislunar space and beyond requires a slightly different approach than the GNC subsystem approach than that used in low-Earth orbit. Use of the Earth's magnetic field, for example, is not possible in these missions, and alternate ADCS designs and methods must be carefully considered. Two communication relay CubeSats (Mars Cube One, MarCO) successfully demonstrated such interplanetary capability during the 2018 InSight mission to Mars (5). This interplanetary mission demonstrated both the capability of this class of spacecraft and GNC fine-pointing design for deep-space communication.

ADCS includes sensors to determine attitude and spin rate, such as star trackers, sun sensors, horizon sensors, magnetometers, and gyros. In addition, the ADCS is often used to control the vehicle during trajectory correction maneuvers and, using accelerometers, to terminate maneuvers when the desired velocity change has been achieved. Actuators are designed to change a spacecraft's attitude and to impart velocity change during trajectory correction maneuvers. Common spacecraft actuators include magnetic torquers, reaction wheels, and thrusters. There are many attitude determination and control architectures and algorithms suitable for use in small spacecraft (6).

Miniaturization of existing technologies is a continuing trend in small spacecraft GNC. While three-axis stabilized, GPS-equipped, 100 kg class spacecraft have been flown for decades, such technologies have only recently become available for micro- and nano-class spacecraft. Table 5-1 summarizes the current state-of-the-art performance for GNC subsystems in small spacecraft. Performance greatly depends on spacecraft size, with a range of values for nano- to micro-class spacecraft.

The list of organizations/companies in this chapter is not all-encompassing and does not constitute an endorsement from NASA. There is no intention of mentioning certain companies and omitting others based on their technologies or relationship with NASA. The performance advertised may differ from actual performance, as the information has not been independently verified by NASA subject matter experts and relies on information provided directly by manufacturers or publicly available information. It should be noted that Technology Readiness Level (TRL) designations may vary with changes specific to the payload, mission requirements, reliability considerations, and/or the environment in which performance was demonstrated. Readers are highly encouraged to reach out to companies for further information regarding the performance and TRL of the described technology.

Table 5-1: State-of-the-Art GNC Subsystems		
Component	**Performance**	**TRL**
Reaction Wheels	0.00023 – 0.3 Nm peak torque, 0.0005 – 8 N m s storage	7-9
Magnetic Torquers	0.15 A m^2 – 15 A m^2	7-9
Star Trackers	8 arcsec pointing knowledge	7-9
Sun Sensors	0.1° accuracy	7-9
Earth Sensors	0.25° accuracy	7-9
Inertial Sensors	Gyros: 0.15° h^{-1} bias stability, 0.02° $h^{-1/2}$ ARW Accels: 3 µg bias stability, 0.02 (m s^{-1})/$h^{-1/2}$ VRW	7-9
GPS Receivers	1.5 m position accuracy	7-9
Integrated Units	0.002-5° pointing capability	7-9
Atomic Clocks	10 – 150 Frequency Range (MHz)	5-6
Deep Space Navigation	Bands: X, Ka, S, and UHF	7-9
Altimeters	~15 meters altitude, ~3 cm accuracy	7

5.2 State-of-the-Art – GNC Subsystems

5.2.1 Integrated Units



Figure 5.1: BCT XACT integrated ADCS unit. Credit: Blue Canyon Technologies.

Integrated units combine multiple attitude and navigation components to provide a simple, single-component solution to spacecraft GNC requirements. Typical components include reaction wheels, magnetometers, magnetic torquers, fine and/or coarse Sun sensors, GPS, and star trackers. The systems often include processors and software with attitude determination and control capabilities to support common mission profiles, including Sun tracking, inertial pointing, and Earth target tracking. In addition, providers such as Blue Canyon Technologies (BCT) and CubeSpace provide overall GNC design and simulation with their products to ensure mission objectives can be met within the desired orbit environment and hardware constraints of the integrated unit and spacecraft bus. Using these integrated units can increase overall mission success, as the included ADCS software is also high TRL. BCT's XACT (Figure 5.1) flew on the NASA-led MarCO and ASTERIA missions, which were both 6U platforms, and has also flown on 3U missions (MinXSS was deployed from NanoRacks in February 2016). Table 5-2 describes integrated systems currently available with TRL values of 7-9.

Table 5-2: Currently Available Integrated Systems						
Manufacturer	**Model**	**Mass (kg)**	**Actuators**	**Sensors**	**Processor**	**Pointing Accuracy**
AAC Clyde Space	iADCS-200	0.470	3 reaction wheels 3 magnetic torquers	1 star tracker, 1 IMU, Optionally high precision magnetometer and sun sensors	Yes	<1°
	iADCS-400	1.7	3 reaction wheels 3 magnetorquers	1 star tracker, 1 IMU, Optionally high precision magnetometer and sun sensors	Yes	<1°
Arcsec	Arcus ADC	0.715	3 reaction wheels 3 magnetic torquers	1 star tracker, 3 gyros 6 photodiodes 3 magnetometers	Yes	0.1°
Berlin Space Technologies	IADCS-100	0.4	3 reaction wheels 3 magnetic torquers	1 star tracker, 3 gyros, 1 magnetometer, 1 accelerometer	Yes	<<1 deg
Blue Canyon Technologies	XACT-15	0.885	3 reaction wheels 3 magnetorquers	1-2 Star Trackers, 1-4 Sun Sensors, IMU, Magnetometer, GPS	Yes	0.003/0.007°
	XACT-50	1.230	3 reaction wheels 3 magnetorquers	1-2 Star Trackers, 1-4 Sun Sensors, IMU, Magnetometer, GPS	Yes	0.003/0.007°
	XACT-100	1.813	3 – 4 reaction wheels 3 magnetorquers	1-2 Star Trackers, 1-4 Sun Sensors, IMU, Magnetometer, GPS	Yes	0.003/0.007°
	Flexcore	†	3 – 4 reaction wheels 3 magnetorquers	1-2 Star Trackers, 1-4 Sun Sensors, IMU, Magnetometer, GPS	Yes	0.002°
CubeSpace Satellite Systems	CubeADCS	0.26*	3/4(Pyramid) x reaction wheels, 3 x Magnetorquers distributed or integrated with ADCS core (3U/6U only)	Up to 4 x FSS, 2 x EHS, 2 x STR, 2 x MGTM. All distributed	5Hz	~70 arcsec (3 sigma) †

*Mass may vary if actuators are integrated inside CubeADCS core.
†Configuration dependent.

5.2.2 Reaction Wheels

Miniaturized reaction wheels can provide small spacecraft with three-axis precision pointing capability. Reaction wheels provide torque and momentum storage along the wheel spin axis, causing the spacecraft to counter-rotate about its center of mass due to conservation of angular momentum from the wheel spin direction. For example, the spacecraft deployment process typically results in some tipoff momentum that can be observed as induced angular rates. This tipoff momentum can be stored in the reaction wheels, reducing the angular rate of the spacecraft to near zero. Reaction wheels must be carefully selected based on factors including the moment of inertia of the spacecraft, required momentum storage capacity, and mission slew rate requirements. Once a wheel reaches its maximum speed, it becomes saturated and can no longer provide torque or store momentum along that axis. To prevent this, reaction wheels need to be periodically desaturated using an actuator that provides an external torque, such as thrusters or magnetic torquers (7). By providing an external torque in an opposing direction, the reaction wheel compensates and spins down to keep the spacecraft at its target state (8).

While one or two reaction wheels can be used for a momentum-biased spacecraft, a full three-axis controlled spacecraft requires three wheels mounted orthogonally. As reaction wheel failure is a common failure mode in many missions, it is common to include three additional wheels as a hot backup (8). On smaller spacecraft where SWaP requirements prohibit redundant reaction wheels, a four-wheel configuration is often used to provide fault tolerance (9). The multiple reaction wheels are often assembled in a “skewed” or angled configuration such that there exists cross-coupled torques across two or more reaction wheels. While this reduces the torque performance in any single axis, it allows reduced but redundant torque capability across multiple axes. The result is that should any single reaction wheel fail, one or more reaction wheels are available as a reduced-capability backup option.

Though reaction wheels are typically the primary choice for precision three-axis pointing, other important considerations must be addressed. For example, they can introduce major attitude disturbances through static and dynamic imbalances, which can generate undesired forces, torques, and moments. While placing reaction wheels near the spacecraft center-of-gravity can help minimize the force/torque effects, other disturbances are location-independent and careful design considerations must be made (8). Reaction wheels are typically not magnetically clean, whether they are in the electromagnetic controller for spinning the wheels or ferrous materials being used in the wheel rotor itself, so careful placement within the spacecraft bus is required. Wheels typically should be placed with sufficient separation from magnetometers or other sensitive instrumentation. As magnetic torquers are the primary method of preventing reaction wheel saturation for small spacecraft in Earth orbit, they require accurate measurements of the Earth’s magnetic field to determine torquer commands, making wheel placement especially critical in the spacecraft bus design (11). Another consideration is how the reaction wheel is used in orbit and the required pointing precision. Most reaction wheels have reduced performance around zero-crossings (transition between positive/negative speeds), so some missions choose to bias the momentum (e.g., wheels running at approximately half their maximum speed when at zero spacecraft angular rate) (12). This can provide finer control with less jitter at the expense of reduced overall momentum capacity (effectively half).

Table 5-3 lists a selection of high-heritage miniature reaction wheels. Except for three units, all listed reaction wheels have spaceflight heritage.

Table 5-3: High Heritage Miniature Reaction Wheels							
Manufacturer	**Model**	**Mass (kg)**	**Peak Power (W)**	**Peak Torque (Nm)**	**Momentum Capacity (Nms)**	**# Wheels**	**Rad. Tol. (krad)**
AAC Clyde Space	RW210	0.48	0.8	0.0001	0.006	1	36
	RW400	0.375	15	0.008	0.050	1	36
	Trillian-1	1.5	24	47.1	1.2	1	--
Astrofein	RW1 Type A	≤ 0.025	< 0.375 + PWDE	23e-6	5.8e-4	1	/
	RW1 Type B	≤ 0.012	< 0.3 + PWDE	4e-6	1.0e-4	1	/
	RW25	≤ 0.2	< 2.8	0.002	0.03	1	/
	RW35	≤ 0.5	≤ 9	0.005	0.1	1	20
	RW90	≤ 0.9	≤ 16.5	0.015	0.35	1	20
	RW100	≤ 0.8	≤ 25	0.02	0.4	1	20
	RW150	≤ 1.3	≤ 42	0.03	1	1	20
	RWT150	≤ 1.5	≤ 120	0.1	1	1	20
	RW250	≤ 2.75	≤ 100	0.1	4	1	20
	RWT250	≤ 2.75	≤ 200	0.3	4	1	20
Berlin Space Technologies	RWA05	1.700	23.5	0.016	0.5	1	30
Blue Canyon Technologies	RWp015	0.130	5.5	0.004	0.015	1	--
	RWp050	0.240	9	0.007	0.050	1	--
	RWp100	0.330	9	0.007	0.100	1	--
	RWp500	0.750	25	0.025	0.500	1	--
	RW1	0.950	100	0.07	1.000	1	--
	RW4	3.200	204	0.250	4.000	1	--
	RW8	4.400	204	0.250	8.000	1	--
	RW16	7.5	204	0.25	16	1	--
Comat	RW20	0.180	1	0.002	0.02	1	20*
	RW40	0.230	1	0.004	0.04	1	20*
	RW60	0.275	1	0.006	0.06	1	20*
CubeSpace Satellite Systems	CubeWheel CW0017	0.06	0.85	0.23	0.0017	1/3/4 (Pyramid)	24
	CubeWheel CW0057	0.115	2.7	2	0.0057	1/3/4 (Pyramid)	24
	CubeWheel CW0162	0.144	7.2	7	0.0162	1/3/4 (Pyramid)	24
	CubeWheel CW0500	0.310	15	16	0.05	1/3/4 (Pyramid)	24
	CubeWheel CW1200	0.450 *	32	20	0.12	1/3/4 (Pyramid)	24
	CubeWheel CW2500	0.750 *	33	27	0.25	1/3/4 (Pyramid)	24
	CubeWheel CW5000	1.084	48	37	0.5	1/3/4 (Pyramid)	24
	CubeWheel CW10K	2.1*	50	37	1	1/3/4 (Pyramid)	24
	CubeWheel CW40K	2.2*	85	37	4	1/3/4 (Pyramid)	24
GomSpace	NanoTorque GSW-600	0.940	0.3	0.0015	0.019	1	--

Table 5-3: High Heritage Miniature Reaction Wheels							
Manufacturer	**Model**	**Mass (kg)**	**Peak Power (W)**	**Peak Torque (Nm)**	**Momentum Capacity (Nms)**	**# Wheels**	**Rad. Tol. (krad)**
NanoAvionics	RWO	0.137	3.25	0.0032	0.020	1	20
	4RWO	0.665	6	0.0059	0.037	4	20
NewSpace Systems	NRWA-T6	<5	136	0.3	0.00783	1	20
	NRWA-T065	1.55	1.7	0.02	0.00094	1	10
	NRWA-T2	2.8	0.4	0.09	0.00163	1	10
Rocket Lab	RW-0.03	0.185	1.8	0.002	0.040	1	20
	RW-0.003	0.048	--	0.001	0.005	1	10
	RW-0.01	0.122	1.05	0.001	0.018	1	20
	RW3-0.06	0.235	23.4	0.020	0.180	1	20
	RW4-0.2	0.6	--	0.1	0.2	1	60
	RW4-0.4	0.77	--	0.1	0.4	1	60
	RW4-1.0	1.38	43	0.1	1	1	60
Space Inventor	WHL-100	0.35	TBD	20	100	1	--
	WHL-200	0.42	TBD	25	200	1	--
	WHL-500	0.8	TBD	50	500	1	--
	WHL-1000	1.175	180	100	1000	1	--
	WHL-12000	5.9	--	1200	12000	1	--
Vectronic Aerospace	VRW-B-02	1	45	0.02	0.2	1	20
	VRW-C-05	1.2	65	0.05	0.6	1	20
	VRW-C-1	2.3	65	0.05	1.2	1	20
	VRW-D-1	1.9	65	0.05	1.2	1	20
	VRW-D-16	1.8	65	0.05	1.6	1	20
	VRW-D-2	2	65	0.05	2.0	1	20
	VRW-D-27	2.45	65	0.05	2.7	1	20
	VRW-D-4	2.5	65/110	0.05/0.09	4.0	1	20
	VRW-D-6	3	65/110	0.05/0.09	6.0	1	20
	VRW-D-8	3.5	110	0.09	8.0	1	20
VEOWARE	WHL-100	0.35	--	0.02	0.1	1	--
	WHL-200	0.43	--	0.025	0.2	1	--
	WHL-500	0.8	--	0.5	0.5	1	--
	WHL-100	1.2	--	0.1	1	1	--

*Printed Circuit Board (PCB) level

5.2.3 Magnetic Torquers

Magnetic torquers provide control torques perpendicular to the local external magnetic field. They are divided into two categories and are usually labeled as air coils or torquer bars/rods. Both operate by applying an electric current through a coiled conductor, generating a magnetic dipole through the center of the coil that loops around itself (8). This generated magnetic dipole interacts with the local external magnetic field, generating a torque perpendicular to the dipole and the field. The strength of the dipole, and thereby the torque, is governed by the area of the coil and the number of turns in the coil. For torquer bars/rods, a ferrous core is added, which greatly amplifies



Figure 5.3: Magnetorquers for micro satellites. Credit: ZARM Technik.

the strength of the magnetic field without an increase in required power consumption. While these bars/rods typically provide volume and power savings, the ferrous material can hold a residual field even when the device is powered off, which can affect other sensitive instrumentation such as magnetometers. With air coils, however, residual magnetic fields dissipate very rapidly when powered off. Air coils typically need a larger coil radius and/or more windings with higher power consumption to provide an equivalent magnetic dipole as compared to torquer bars/rods. Many are custom designed specifically for the mission's spacecraft bus, such as being integrated into a components PCB inner layer. As such, fewer providers offer them as COTS components. Table 5-4 lists a selection of high-heritage magnetic torquers and Figure 5.3 illustrates some of ZARM Technik's product offerings.

As control torques can only be provided in the plane perpendicular to the local magnetic field and generated magnetic dipole, magnetic torquers alone cannot typically provide three-axis stabilization. A spacecraft will typically have three magnetic torquers mounted on orthogonal axes, and there is usually no need for redundant torquers because the electro-mechanical design provides internal redundancy (8). Some research shows that coarse three-axis pointing can be achieved, but this requires multiple orbits and sufficient orbit inclination to provide external magnetic field variability. Typically, magnetic torquers are used to remove excess momentum from reaction wheels. As the torque generated by magnetic torquers acts externally to the spacecraft, the reaction wheels apply an internal counter torque to compensate and reduce their stored momentum. Magnetic torquers are also used on spinner missions, where they can slowly spin up the spacecraft by applying an external torque over time.

Use of magnetic torquers beyond low-Earth orbit and in interplanetary applications needs to be carefully investigated since their successful operation is dependent on a significant local external magnetic field. This magnetic field may or may not be available in the location and environment of a given mission, and additional control methods may be required.

Table 5-4: High Heritage Magnetic Torquers

Manufacturer	Model	Mass (kg)	Power (W)	Peak Dipole (A m^2)	# Axes	Rad Tol. (krad)
AAC Clyde Space	MTQ800	0.395	3	15	1	--
CubeSpace Satellite Systems	CubeTorquer CR0002	0.0165	0.49	0.2	1	24
	CubeTorquer CR0003	0.023	0.38	0.3	1	24
	CubeTorquer CR0004	0.023	0.63	0.4	1	24
	CubeTorquer CR0006	0.031	0.56	0.6	1	24
	CubeTorquer CR0008	0.028	0.56	0.8	1	24
	CubeTorquer CR0010	0.037	0.67	1	1	24
	CubeTorquer CR0012	0.045	0.68	1.2	1	24
	CubeTorquer CR0020	0.054	0.77	2	1	24
GomSpace	Nano Torque GST-600	-	-	0.31–0.34	3	-
	NanoTorque Z-axis Internal	0.106	-	0.139	1	-
ISISPACE	Magnetorquer Board	0.196	1.2	0.20	3	-
MEISEI	Magnetic Torque Actuator for Spacecraft	0.5	1	12	1	-
NanoAvionics	MTQ3X	0.205	0.4	0.30	3	-
	MTQ MP42	0.215	2.5	5	1	
NewSpace Systems	NCTR-M003	0.030	0.25	0.29	1	-
	NCTR-M012	0.053	0.8	1.19	1	-

Table 5-4: High Heritage Magnetic Torquers						
Manufacturer	**Model**	**Mass (kg)**	**Power (W)**	**Peak Dipole (A m^2)**	**# Axes**	**Rad Tol. (krad)**
	NCTR-M016	0.053	1.2	1.6	1	-
Rocket Lab	TQ-40	0.825	-	48.00	1	-
	TQ-15	0.400	-	19.00	1	-
Space Inventor	MT-0,425	0.1	0.3	0.425	1	-
	MT-1	0.23	0.27	1	1	-
	MT-2	0.375	0.25	2	1	-
ZARM Technik**	MT0.2-1	0.012-0.014	0.135-0.25	0.2	1	NA*
	MT0.5-1	0.009	0.275	0.5	1	NA*
	MT0.7-1-01	0.035	0.5	0.7	1	NA*
	MT1-1-01	0.065	0.23	1	1	NA*
	MT1.5-1-01	0.097	0.4	1.5	1	NA*
	MT2-1-02	0.1	0.5	2	1	NA*
	MT3-1-D22042701	0.15	0.7	3	1	NA*
	MT4-1	0.15	0.6	4	1	NA*
	MT5-1	0.19-0.3	0.73-0.75	5	1	NA*
	MT5-2	0.31	0.77	5	1	NA*
	MT6-2	0.25-0.3	0.48-1.1	6	1	NA*
	MT7-2	0.4	0.9	7	1	NA*
	MT10-1	0.35-0.4	0.53-0.8	10	1	NA*
	MT10-2	0.37-0.48	0.7-1	10	1	NA*
	MT15-1	0.4-0.55	1.0-1.55	15	1	NA*

* Only EEE parts are connector and wires. Magnetorquer is not sensitive to ionizing radiation.
** ZARM Technik: Over 200 models available with design to mass/power optimization.

5.2.4 Thrusters

Thrusters can generate forces and torques, providing spacecraft with both attitude and translational control capabilities (8). As they are not dependent on external fields or dynamics, they can be used in any orbit. However, they require some type of expendable fuel source, so the thruster lifetime can be limited. While not typically employed on SmallSats for attitude control, recent advances propulsion miniaturization have enabled COTS availability. Thrusters have the advantage of providing large external torques for rapid maneuvers, quick reaction wheel desaturation, and spin stabilization. When used for attitude control, these systems can become more complex to mitigate induced translational dynamics.

When these propulsion systems are used to provide orbital and/or translational control, attitude control remains necessary to control the direction of thrust. Even with a full three degree-of-freedom thruster system, depending on the thruster configuration and the center of gravity of the spacecraft, thrusters can impart undesired torques that must be mitigated using attitude control systems such as reaction wheels or ACS thrusters.

One critical application of state-of-the-art thrusters is on proximity operations missions, an increasing area of focus for advanced mission concepts. Proximity operations require both high-precision translational and attitude control that typically cannot be achieved with other actuators. Further discussion is provided in Section 5.3.1. Translation and pointing accuracy are determined by minimum impulse bit and control authority by thruster force, with significant improvements made recently in this field. An in-depth discussion on thrusters for attitude and translational control is provided in Chapter 4: *In-Space Propulsion*.

5.2.5 Star Trackers

A star tracker can provide an accurate estimate of the absolute three-axis attitude by comparing a digital image to an onboard star catalog (9). Star trackers identify and track multiple stars and provide three-axis attitude solutions up to several times per second (8). While simple in concept, star trackers are among the most expensive small spacecraft components with a significant variance in capabilities between manufacturers. To operate, the sensor requires a clear field-of-view of a starfield such that an initial lost-in-space solution can be found. This initial acquisition depends on the FOV, magnitude of the stars, and the star tracker's internal processing capabilities. Factors such as spacecraft angular rate, external light sources, and glare can corrupt and invalidate the solution. Missions dependent on accurate attitude information typically include IMU-propagated Kalman filter to maintain an attitude solution when the star tracker may lose the solution. Mission design and star tracker integration into the spacecraft bus also require careful geometry analysis to ensure that the FOV remains clear for critical mission operations. Missions with propulsion must also worry about contaminating the optics from thruster exhaust plumes.

While all COTS star tracker suppliers can provide a full state attitude solution, it is their accuracy and capabilities in difficult situations that distinguish the components and drastically increase their cost. Most modern star trackers can provide knowledge of the sensor's boresight to within a few arcseconds, with reduced knowledge about the roll axis (8) when the spacecraft is inertially fixed. The accuracy is typically dependent on the optics' FOV, the sensor's resolution, and the processing power dictating the size of the star catalog. However, this accuracy can quickly degrade if the spacecraft has some angular rate. For example, cheaper star trackers might be able to track a solution at up to 0.3 deg/s spacecraft angular rates, whereas more expensive options may track up to 3.0 deg/s. Other factors such as stray light resilience, initial acquisition time, and precision also drive up costs. State-of-the-art developments focus on improving the speed and accuracy of the sensors, as well as decreasing their size and mass. These advancements have allowed new manufacturers to enter the field with lower-cost options, allowing missions to obtain full 3-axis attitude information with a sensor that would otherwise be cost-prohibitive. Table 5-5 lists some models suitable for use on small spacecraft. For example, Arcsec's Sagitta Star Tracker was launched on the SIMBA CubeSat in 2020.

Table 5-5: Star Trackers Suitable for Small Spacecraft							
Manufacturer	**Model**	**Mass (kg)**	**Power (W)**	**FOV**	**Cross axis Accuracy (1 or 3s)**	**Twist Accuracy (1 or 3s)**	**Rad. Tol. (krad)**
Arcsec	Sagitta	0.275	1.4	25.4°	6	30	20
	Twinkle	0.04	0.6	10.4°	30	180	-
BAE Systems Inc, Space and Mission Systems	CT-2020	3.000	8	-	1.5"	1"	-
Berlin Space Technologies / AAC Clyde Space	ST200	0.040, 0.106*	0.65	22°	30"	200"	11
	ST400	0.250, 0.270*	0.75	15°	15"	150"	11
Blue Canyon Technologies	Standard NST	0.350	<1.5(5V) or <3.5(28V)	10° x 12°	Gen 2: 6"	Gen 2: 40"	-
	Full-Extension NST	0.85	<1.5(5V) or <3.5(28V)	10° x 12°	Gen 2: 6 Gen 3: 1	Gen 2: 40 Gen 3: 10	
Creare	UST	0.840	-	-	7"	15"	-
CubeSpace Satellite Systems	CubeStar	0.047	0.271	59.4°	0.02°	0.06°	24
Danish Technical University	MicroASC	0.425	1.9	-	2”	-	-
Jena-Optronik	ASTRO CL	0.305	<1.0	25° full cone	6"	48"	50
	ASTRO APS	~2	<6 (<12 w/ TEC)	20° full cone	3"	24"	100
	ASTRO APS3	1.8	<6 (<8 w/ TEC)	20° full cone	2.4"	21"	100
Leonardo	Spacestar	1.600	6	20° x 20°	7.7"	10.6"	-
NanoAvionics	ST-1	0.108	1.2	21° full-cone	8"	50"	20
Redwire Space	Star Tracker	0.475	2.5	14x19	10/27"	51"	75
Rocket Lab	ST-16RT2	0.185	1	8° half-cone	5"	55"	-
Sodern	Auriga-CP	0.225	0.8	30°	10"	70"	35
	Hydra-M	1.4	0.7	22°	3"	30"	50
	Hydra-TC	1.6	9.5	23,6°	3"	30"	50
Solar MEMS Technologies	STNS	0.14	1	12°	40"	70"	20
Space Inventor	ASTRO CL	0.465	1.5	25°	2	12	100
Space Micro	MIST	0.520	3	14.5°	15"	105"	30
	µSTAR-100M	1.800	5	-	15"	105"	100
	µSTAR-200M	2.100	8-10	-	15"	105"	100
	µSTAR-200H	2.700	10	-	3"	21"	100
	µSTAR-400M	3.300	18	-	15"	105"	100
Terma	T1	0.637 OH	0.8 OH*, 2.5	20° circular	3.0"	21"	55†
	T3	0.45 (DPU) 0.330	2	20° circular	3.2"	22"	35
Vectronic Aerospace	VST-41MN	0.7 - 0.9	2.5	14° x 14°	27"	183"	20
	VST-68M	0.470	3	14° x 14°	7.5"	45"	20

*Mass includes Baffle. †SEE Immune

5.2.6 Magnetometers



Figure 5.4: NSS Magnetometer. Credit: NewSpace Systems.

Magnetometers provide measurements of the local magnetic field, which can be used to provide a real-time estimate of two-axis attitude information (14). This requires that a well-modeled magnetic field model is available to reference the measured magnetic field (8). With a time history of magnetometer data, algorithms exist (such as Kalman filters) that can provide full-state attitude and rate knowledge from magnetometer-only measurements. Using other sources of unit vector measurements (e.g., Sun sensor for Sun vector knowledge) can provide real-time three-axis attitude information by using algorithms such as TRIAD and QUEST. In addition to attitude information, knowledge of the local magnetic field is required to determine the necessary dipole for magnetic torquers to produce a desired external torque on the spacecraft.

As a magnetometer cannot differentiate between sources of magnetic fields, placement on the spacecraft bus must be carefully considered. Sources such as reaction wheels and magnetic torquer rods can change the local magnetic field, as well as other sources of electromagnetic fields such as power systems, cabling harnesses, and even solar cells (8). Spacecraft with critical magnetic field measurement requirements may choose to place the magnetometer on a boom extending from the spacecraft, as magnetic dipole falls off at the inverse cube of distance. In addition to careful spacecraft placement, experience has shown that magnetometers may require on-orbit recalibration, which requires orbital position and preferably attitude data. Table 5-6 provides a summary of some three-axis magnetometers available for small spacecraft, one of which is illustrated in Figure 5.4.

Table 5-6: Three-axis Magnetometers for Small Spacecraft

Manufacturer	Model	Mass (kg)	Power (W)	Resolution (nT)	Orthogonality	Rad Tolerance (krad)
AAC Clyde Space	MM200	0.012	0.01	1.18	-	30
	MAG-3	0.100	Voltage Dependent	-	1°	10
CubeSpace Satellite Systems	CubeMag Deployable	0.016	0.23	13	0.6	24
	CubeMag Compact	0.006	0.23	25	0.6	24
Exobotics	XO-SENSE-MAG	0.05	< 0.01	13	-	150
GomSpace	NanoSense M315	0.008	-	-	-	-
MEISEI	3-Axis Magnetometer for Small Satellite	0.220	1.5	-	1°	-
NewSpace Systems	NMRM-Bn25o485	0.085	0.75	8	1°	10
Space Inventor	IMU-P4	0.1	--	13 nT	--	--
ZARM Technik	Analogue High-Rel Fluxgate Magnetometer FGM-A-75	0.33	0.75 W	±75000	1°	50
	Digital AMR Magnetometer AMR-D-100-EFRS485	0.18	0.3 W	±100000	1°	-

5.2.7 Sun Sensors



Figure 5.5: Redwire coarse Sun sensor detector (cosine type). Credit: Redwire Space.

Sun sensors are used to estimate the direction of the Sun in a spacecraft body frame. Sun direction estimates can be used for attitude estimation, though to obtain a three-axis attitude estimate, at least one additional independent source of attitude information is required (e.g., the Earth nadir vector or the direction to a star). Because the Sun is easily identifiable and extremely bright, Sun sensors are often used for fault detection and recovery. However, care must be taken to ensure the Moon or Earth's albedo does not inadvertently perturb the measurement. Even glint off nearby spacecraft components can corrupt measurements for certain Sun sensors types (8). One method to limit albedo effects is to exclude measurements below a certain brightness threshold (albedo is typically measured as a fraction of solar maximum), but care must be taken with this method as it may limit the effective field-of-view of the sensor (the cutoff threshold corresponds to the solar angle yielding the same cosine loss). Commercial examples of small spacecraft Sun sensors are described in Table 5-7.

There are several types of Sun sensors that operate on different principles.

Cosine detectors are photocells. Their output is the current generated by the cell, which is (roughly) proportional to the cosine of the angle between the sensor boresight and the Sun. Typically, several cosine detectors (pointing in different directions) are used on a spacecraft for full sky coverage. These sensors are the most susceptible to albedo effects. Cosine detectors (e.g., Figure 5.5) are inexpensive, low-mass, simple, and reliable devices, but their accuracy is typically limited to a few degrees, and they require analog-to-digital converters.

Quadrant detectors. Quadrant Sun sensors typically operate by shining sunlight through a square window onto a 2 x 2 array of photodiodes. The current generated by each photodiode is a function of the direction of the Sun relative to the sensor boresight. The measured currents from all four cells are then combined mathematically to produce the angles to the Sun. While more accurate than cosine detectors, they have a similar sensitivity to albedo effects.

Digital Sun Sensor. The Sun illuminates a narrow slit with a number of photodiodes located behind a geometrically coded bit mask. Depending on the angle to the Sun, the photodiodes will be illuminated as per the geometric pattern, resulting in correspondingly different photocurrents, which are then amplified and thresholded against an average value. Given the known slit geometries, this digital bit output can then be converted to a Sun angle.

Sun Camera. Some Sun sensors are built as small cameras that image the Sun. Since the Sun is so bright, the optics include elements to decrease the throughput. A computer identifies the image of the Sun and calculate the centroid. Sun sensors can be made very accurate this way and typically have built-in albedo rejection. Sometimes, multiple apertures are included to increase accuracy.

Table 5-7: Commercial sun sensors									
Manufacturer	**Model**	**Sensor Type**	**Mass (kg)**	**Peak Power (W)**	**Analog or Digital**	**FOV**	**Accuracy (3s)**	**# Measurement Angles**	**Rad. Tol. (krad)**
AAC Clyde Space	SS200	-	0.003	0.04	Digital	110°	<1°	-	>36
Berlin Space Technologies	FSSA-110	Fine Sun Sensor	With 3x sensor: 0.102	0.185	Analog	114°	5°	?	>20
Bradford Space	CoSS	Cosine	0.024	0	Analog	160° full cone	3°	1	40000
	CoSS-R	Cosine	0.015	0	Analog	180° full cone	3°	1	120000
	CSS	Cosine	0.215	0	Analog	180°x180°	1.5°	2	70000
	FSS	Quadrant	0.375	0.25	Analog	128° x 128°	0.3°	2	100
	Mini-FSS	Quadrant	0.050	0	Analog	128° x 128°	0.2°	2	20000
CubeSpace Satellite Systems	CubeSense	Camera	0.015	0.174	Digital	0.2°	2	24	-
GomSpace	NanoSense FSS	Quadrant	0.002	-	Digital	45°, 60°	±0.5°, ±2°	2	-
Lens R&D	BiSon64-ET	Quadrant	0.023	0	Analog	±58° per axis	0.5°	2	9200
	BiSon64-ET-B	Quadrant	0.033	0	Analog	±58° per axis	0.5°	2	9200
	MAUS	Quadrant	0.014	0	Analog	±57° per axis	0.5°	2	9200
Needronix	Eagle	Fine Sun Sensor (±55°)	0.003	<0.007	Digital	110°	< ±0.15°	2 plus Irradiation and Gyro	>20
	Eagle Plus	Fine Sun Sensor (±55°)	0.005	<0.015	Digital	110°	< ±0.1°	2 plus Irradiation and Gyro	>20
	Eagle Point	Fine Sun Pointing (±5.5°)	0.006	<0.015	Digital	11°	< ±0.01°	2 plus Irradiation and Gyro	>20
	Swan	Coarse Sun Sensor Pyramid	0.070	0	Analog	170° (~ 2π Steradian)	< ±1° (Region I.)	2	>1000
NewSpace Systems	NFSS-411	-	0.035	0.150	Digital	140°	0.1°	--	20
	NCSS-SA05	-	0.005	0.05	Analog	114°	0.5°	--	-
Redwire Space	Coarse Analog Sun Sensor	Coarse Analog Sun Sensor	0.045	0	Analog	±40°	±1°	1	>100
	Coarse Sun Sensor (Cosine Type)	Coarse Sun Sensor (Cosine Type)	0.010	0	Analog	~ Cosine, Conical Symmetry	±2° to ±5°	Configuration dependent	>100
	Coarse Sun Sensor Pyramid	Coarse Sun Sensor Pyramid	0.13	0	Analog	2π steradian+	±1° to ±3°	2	>100

Table 5-7: Commercial sun sensors									
Manufacturer	**Model**	**Sensor Type**	**Mass (kg)**	**Peak Power (W)**	**Analog or Digital**	**FOV**	**Accuracy (3s)**	**# Measurement Angles**	**Rad. Tol. (krad)**
	Digital Sun Sensor (±32°)	Digital Sun Sensor (±32°)	Sensor 0.3 kg Electronics ~1	1	Digital	±32° x ±32° (each sensor)	±0.125°	2	100
	Digital Sun Sensor (±64°)	Digital Sun Sensor (±64°)	Sensor0.25 Electronics 0.29 - 1.1	0.5	Digital	128° X 128° (each sensor) Note: 4π steradians achieved with 5 sensors	±0.25°	2	100
	Fine Pointing Sun Sensor	Fine Pointing Sun Sensor	Sensor .95 Electronics 1.08	< 3	Digital	±4.25° x ±4.25° (Typical)	Better than ±0.01°	2	100
	Fine Spinning Sun Sensor (±64°)	Fine Spinning Sun Sensor (±64°)	Sensor 0.109 Electronics 0.475 – 0.725	0.5	Analog and Digital	±64° Fan Shaped (each sensor)	±0.1°	1 plus Sun Pulse	100
	Micro Sun Sensor	Micro Sun Sensor	< 0.002	< 0.02	Analog	± 85° Minimum	±5°	2	~10
	Miniature Spinning Sun Sensor (±87.5°)	Miniature Spinning Sun Sensor (±87.5°)	< 0.25	0.5	Digital	±87.5° (From normal to spin axis)	±0.1°	1 plus Sun Pulse	100
	Fine Sun Sensor (±50°)	Fine Sun Sensor (±50°)	-	-	Digital	100 X 100 Each Sensor	±0.01° TO ±0.05°	2	100, 150, or 300
Solar MEMS Technologies	nanoSSOC-A60	Orthogonal	0.004	0.007	Analog	±60° per axis	0.5°	2	100
	nanoSSOC-D60	Orthogonal	0.007	0.076	Digital	±60° per axis	0.5°	2	30
	SSOC-A60	Orthogonal	0.025	0.01	Analog	±60° per axis	0.5°	2	100
	SSOC-D60	Orthogonal	0.035	0.315	Digital	±60° per axis	0.5°	2	30
	ACSS	Quadrant & Redundant	0.035	0.072	Analog	±60° per axis	0.5°	2	200
Space Inventor	FSS	Quadrant	0.01	0.1	Digital	55° half-cone	< 3 deg	2	-
Space Micro	CSS-01, CSS-02	Cosine	0.010	0	Analog	120° full cone	5°	1	100
	MSS-01	Quadrant	0.036	0	Analog	48° full cone	1°	2	100

5.2.8 Horizon Sensors

Horizon sensors can be simple infrared horizon-crossing indicators (HCI) or more advanced thermopile sensors that can detect temperature differences between the poles and equator. The sensors are typically either static or scanning, but by characterizing horizon crossings over a series of measurements, the sensors can provide an accurate nadir vector, which can then be used for attitude determination and/or attitude control guidance (8). For terrestrial applications, these sensors are referred to as Earth sensors, but they can be used for other planets. Examples of such technologies are described in Table 5-8 and shown in Figure 5.6.



Figure 5.6: MAI-SES. Credit: Redwire Space.

In addition to the commercially available sensors listed in Table 5-8, there has been recent academic interest in horizon sensors for CubeSats with promising results (4)(15)(16).

Table 5-8: Commercially Available Horizon Sensors

Manufacturer	Model	Sensor Type	Mass (kg)	Peak Power (W)	Analog or Digital	Accuracy	# Measurement Angles	Rad. Tol. (krad)
CubeSpace Satellite Systems	CubeSense Earth	Infrared camera	0.018	0.28	Digital	1°	-	24
Servo	Mini Digital HCI	Pyroelectric	0.050	Voltage Dependent	Digital	0.75°	--	--
	RH 310 HCI	Pyroelectric	1.5	1	--	0.015°	--	20
Solar MEMS Technologies	HSNS	Infrared	0.120	0.150	Digital	1°	2	30

5.2.9 Inertial Sensing

Inertial sensors include gyroscopes for measuring angular change and accelerometers for measuring velocity change. They are packaged in different ways that range from single-axis devices (e.g., a single gyroscope or accelerometer) to packages that include three orthogonal axes of gyroscopes (Inertial Reference Unit (IRU)), to units containing three orthogonal gyros and three orthogonal accelerometers (Inertial Measurement Unit (IMU)). These sensors are frequently used to propagate the vehicle state between measurement updates from non-inertial sensors. For example, star trackers typically provide attitude updates at a few Hertz. If the control system requires accurate knowledge between star tracker updates, an IMU may be used for attitude propagation over that interval.

Gyroscope technologies typically used in modern small spacecraft are fiber optic gyros (FOGs) and MEMS gyros, with FOGs typically offering superior performance at a mass and cost penalty (18). While MEMS are smaller and can provide sufficient performance, they are more susceptible to radiation and single-event upsets, with radiation-hardened models only recently becoming available (8). Other gyroscope types exist (e.g., resonator gyros, ring laser gyros), but these are not common in the SmallSat/CubeSat world due to size, weight, and power (SWaP) and cost.

Gyro behavior is a complex topic (19), and gyro performance is typically characterized by a multitude of parameters. Table 5-9 only includes bias stability and angle random walk for gyros, and bias stability and velocity random walk for accelerometers, as these are often key performance parameters. That said, when selecting inertial sensors, it is important to consider other factors such as dynamic range, output resolution, bias, sample rate, etc. Factors such as turn-on bias and bias drift require onboard estimation of bias so that the sensor can be used in attitude determination and control systems.

Table 5-9: Gyros Available for Small Spacecraft													
Manufacturer	Model	Sensor Type	Technology	Mass (kg)	Power (W)	Gyros				Accelerometers			
							Bias Stability		ARW		Bias Stability		VRW
						# Axes	(°/hr)	stat	(°/rt(hr))	# Axes	(µg)	stat	(m/sec)/ rt(hr)
Emcore	QRS11	Gyro	MEMS	≤0.06	0.8	1	6	Typical	-	-	-	-	-
	QRS28	Gyro	MEMS	≤0.025	0.5	2	-	-	-	-	-	-	-
Honeywell	MIMU	IMU	RLG	4	34	3	0.05	-	0.01	-	100	-	-
	HG1700	IMU	RLG	0.9	5.000	3	1.000	1σ	0.125	3	1000	1σ	0.65
	HG4934SRS (68904934-BA60)	IRU	MEMS	0.145	<5.500 peak	3	< 3.0	3s	<0.20 max	None IRU only	None, IRU only	None IRU only	None, IRU only
L3	CIRUS	Gyros	FOG	15.400	40.000	3	0.000	1σ	0.100	0	-	-	-
NewSpace Systems	NSGY-001	IRU	Image-based rotation estimate	0.055	0.200	3	-		-	0	-	-	-
Northrop Grumman	LN-200S	IMU	FOG, SiAc	0.748	12	3	1.000	1σ	0.070	3	300	1σ	-
NovAtel	OEM-IMU-STIM300	IMU	MEMS	0.055	1.50	3	0.500	--	0.150	3	50	-	0.060
Safran	STIM202	IRU	MEMS	0.055	1.500	3	0.400	--	0.170	0	-	-	-
	STIM210	IRU	MEMS	0.052	1.500	3	0.300	--	0.150	0	-	-	-
	STIM300	IMU	MEMS	0.055	2.000	3	0.300	--	0.150	3	50	--	0.07
	STIM318	IMU	MEMS	0.057	2.500	3	0.300	--	0.150	3	3	--	0.015
	STIM320	IMU	MEMS	0.057	2.500	3	0.300	--	0.100	3	3	--	0.015
	STIM277H	IRU	MEMS	0.052	1.500	3	0.300	--	0.150	0	-	--	-
	STIM377H	IMU	MEMS	0.055	2.000	3	0.300	--	0.150	3	50	--	0.07
Silicon Sensing Systems	CRH03	Gyro	MEMS	0.42	0.2W	1	CRH03-010 – 0.03 CRH03-025 – 0.04 CRH03-100 – 0.04 CRH03-200 – 0.05 CRH03-400 – 0.1		CRH03-010 – 0.005 CRH03-025 – 0.006 CRH03-100 – 0.006 CRH03-200 – 0.008 CRH03-400 – 0.010	0	-	-	-

Table 5-9: Gyros Available for Small Spacecraft													
Manufacturer	**Model**	**Sensor Type**	**Technology**	**Mass (kg)**	**Power (W)**	**Gyros**				**Accelerometers**			
							Bias Stability		**ARW**		**Bias Stability**		**VRW**
						# Axes	**(°/hr)**	**stat**	**(°/rt(hr))**	**# Axes**	**(µg)**	**stat**	**(m/sec)/ rt(hr)**
	CRH03 (OEM)	Gyro	MEMS	0.18	0.2W	1	CRH03-010 – 0.03 CRH03-025 – 0.04 CRH03-100 – 0.04 CRH03-200 – 0.05 CRH03-400 – 0.1		CRH03-010 – 0.005 CRH03-025 – 0.006 CRH03-100 – 0.006 CRH03-200 – 0.008 CRH03-400 – 0.010	0	-	-	-
	RPU30	Gyro	MEMS	1.35	<0.8W	3	0.06		0.006	0	-	-	-
	DMU41	9 DoF IMU	MEMS	<2	<1.5W	3	0.1		0.015	3	15	-	0.05
	CAS	Acc	MEMS	0.004	-	0	-		-	2	CAS2X1S - 7.5 CAS2X2S - 7.5 CAS2X3S - 7.5 CAS2X4S - 25 CAS2X5S - 75		CAS2X1S - TBC CAS2X2S - TBC CAS2X3S - TBC CAS2X4S - TBC CAS2X5S - TBC
Space Inventor	IMU-P4	MEMS	--	0.15	0.2	--	0.3 deg/hr		--		0.15 mm/s^2		30 mm/ s/√(hr)
VectorNav	VN-100*	IMU + magnetometer+barometer	MEMS	0.015	0.220	3	10.000	max	0.210	3	40	max	0.082
	VN-110*	IMU + magnetometer	MEMS	0.125	2.500	3	1.000	max	0.0833	3	10	max	0.024

*Small form-factor versions of these products available.
-- Represents unknown data

5.2.10 GPS Receivers

For low-Earth orbit spacecraft, GPS receivers are now the primary method for performing orbit determination, replacing ground-based tracking methods. Onboard GPS receivers are now considered a mature technology for small spacecraft; examples are listed in Table 5-10. There are also next-generation chip-size COTS GPS solutions; for example, the NovAtel OEM 719 board has replaced the ubiquitous OEMV1.

By measuring the time of arrival of signals from multiple GPS spacecraft, the GPS receiver can determine its position to a high degree of accuracy (8). A minimum of four spacecraft must be visible to the GPS receiver, of which three provide position data and a fourth provides timing to correct the GPS receiver's clock bias. With multiple GPS antennas, a spacecraft's GPS receiver can be used for attitude determination using phase differences in GPS signals, though the accuracy of this method is limited and prone to errors. GPS accuracy is limited by propagation variability through the exosphere and the underlying precision of the civilian-use C/A code (20). GPS units are controlled under the Export Administration Regulations (EAR) and must be licensed to remove COCOM limits (21).

Although the usability of GPS is limited to LEO missions, past experiments have demonstrated the ability to use weak GPS signals at GSO, and potentially at cislunar distances (23)(22). Development and testing in this rapidly growing field may soon make onboard GPS receivers more widely available.

Table 5-10: GPS Receivers for Small Spacecraft

Manufacturer	Model	Mass (kg)	Power (W)	Accuracy (m)	Radiation Tolerance (krad)
AAC Clyde Space	GNSS-701	0.16	--	< 5	10
APL	Frontier Radio Lite	0.4	1.4	15	20
Aerospacelab	GNSS-VSP	0.394	2.4	1.5 (RMS)	-
General Dynamics	Explorer	1.2	8	15	-
	Viceroy-4	1.1	8	15	-
GomSpace	0.285	3	< 10	< 20	0.285
NovaTel	OEM 719	0.031	0.9	-	-
SkyFox Labs	piNAV-NG	0.024	0.124	10	30
SENyT	Q Series	0.14	2	< 3	-
Space Inventor	GNSS-3	0.1	0.2	2 (CEP)*	-
Spacemanic	Celeste GNSS	0.025	0.25	2 (CEP)*	-
Surrey Satellite Technology	SGR-Ligo	0.09	0.5	5	5
U-blox	ZED-F9P-05B	0.0018	0.01	1.5, 2.25	-
Septentrio	AsteRx-m3 ProBase	0.0027	1	0.0013	-
	Mosaic-T	0.0068	0.6	1.2, 1.9	-
	AsteRx SBi3 Pro+	0.49	1.5	1.2, 1.9	-

*Circular Error Probable

5.2.11 Deep Space Navigation



Figure 5.7: General Dynamics SDST. Credit: General Dynamics.

In deep space, navigation is performed using radio transponders in conjunction with the Deep Space Network (DSN). As of 2020, the only deep space transponder with flight heritage suitable for small spacecraft was the JPL-designed, and General Dynamics-manufactured Small Deep Space Transponder (SDST). JPL has also designed IRIS V2, which is a deep space transponder that is better suited to the CubeSat form factor. Table 5-11 details these two radios, and the SDST is shown in Figure 5.7. IRIS V2, derived from the Low Mass Radio Science Transponder (LMRST), has flown on the MarCO CubeSats in 2018, LICIACube, which performed an asteroid flyby in September 2022, the 12U lunar CAPSTONE spacecraft that entered a lunar orbit November 13, 2022, and on six Artemis 1 secondary CubeSat payloads (Lunar Flashlight, LunaH-Map, ArgoMoon, CubeSat for Solar Particles, Biosentinel, and NEA Scout). It is also scheduled to fly on INSPIRE (24).

Table 5-11: Deep Space Transponders for Small Spacecraft

Manufacturer	Model	Mass (kg)	Rx Power (W)	Bands	Rad. Tol. (krad)
General Dynamics	SDST	3.2	12.5	X, Ka	50
Space Dynamics Laboratory	IRIS V2.1	1.1	10.3	X, Ka, S, or UHF	25
	Iris Radio V3	0.8	10	Simultaneous Multi-band: X, Ka, S	25

5.2.12 Atomic Clocks

Atomic clocks have been used on larger spacecraft in low-Earth orbit for several years now; however, integrating them on small spacecraft is relatively new. Table 5-12 provides examples of commercially available atomic clocks and oscillators for SmallSats. The conventional method for spacecraft navigation is a two-way tracking system using ground-based antennas and atomic clocks. The time difference between a signal sent from a ground station and the spacecraft's response can be used to determine the spacecraft's location, velocity, and (using multiple signals) its trajectory. This is inefficient, as the spacecraft must wait for navigation commands from the ground station instead of making real-time decisions, and the ground station can only track one spacecraft at a time, because it must wait for the spacecraft to return a signal (25). In deep space navigation, the distances are much greater between the ground station and spacecraft, and the accuracy of the radio signals must be measured within a few nanoseconds.

More small spacecraft designers are developing their own atomic clocks and oscillators that are stable and properly synchronized for use in space. They are designed to fit small spacecraft for missions that are power- and volume-limited or require multiple radios.

Table 5-12: Atomic Clocks and Oscillators for Small Spacecraft						
Manufacturer	**Model**	**Dimensions (mm)**	**Mass (kg)**	**Power (W)**	**Frequency Range (MHz)**	**Rad. Tol. (krad)**
AccuBeat	Ultra-Stable Oscillator	131x120x105	2	6.5	57.51852	50
Bliley Technologies	Iris Series 1"x1" OCXO for LEO	19x11x19	0.016	1.5	10 -100	39
	Aether Series TCVCXO for LEO	21x14x8	-	0.056	10 - 150	37
Microchip	Chip Scale Atomic Clocks (CSACs)	41x36x12	0.035	0.12	10	20
Safran Timing Technologies SA	MO	44x54x57	0.22	3.5 Nom 5.5 Max	10	100
	mRO-50	51x51x20	0.080	0.4 Nom	10	25 Min
	miniRAFS	108x53x68	0.45	< 12 Max	60 and 10	-
	LNMO	50x50x30	0.1	1.5 Nom 2.5 Max	5 – 40	100
*Q-Tech Corporation	Class B+ Products Hybrid Crystal Clock Oscillators	5x7	-	-	-	-

- Represents unknown data
*Company offers several options viable for Smallsats

5.2.13 LiDAR

Over the last decade, Light Detection and Ranging (LiDAR) has been an emerging sensor type that matured via terrestrial applications (such as automotive systems) and is used in larger spacecraft capable of proximity operations, such as Orion. This type of sensor has applications for small spacecraft altimetry and relative navigation (e.g., Mars helicopter, rendezvous and docking, and formation flying). Table 5-13 lists examples of LiDAR systems with flight heritage.

Table 5-13: Lidar for Small Spacecraft					
Manufacturer	**Model**	**Mass (kg)**	**Power (W)**	**Max Range (m)**	**Rad. Tol. (krad)**
ASC	GSFL-4K (3D)	3	30	>1 km in altimeter mode	-
Garmin	Lidar Lite V3	0.022	0.7	40	-

- Represents unknown data

5.3 Formation Flying, Rendezvous and Proximity Operations

Other GNC advances involve research on SmallSats performing precision formation flying (PFF) and on-orbit rendezvous and proximity operations (RPO). Many research papers have discussed methods to achieve these capabilities, and extravehicular free flyer missions have demonstrated this capability in the past few decades. To enable autonomous PFF and RPO missions, spacecraft require a suite of sensors to feed onboard navigation filters to determine relative positions and attitudes, complex guidance laws to maintain formations within constraints and prevent on-orbit conjunctions, as well as advanced actuation methods to control the relative states of the

spacecraft. While some commercial sensors and actuators exist specifically for enabling PFF and RPO missions, current research and missions are leveraging novel hardware and methods to achieve these objectives using existing components.

To enable relative guidance and control, it is important to first estimate the relative position and velocity, as well as attitude, of the spacecraft. Relative navigation can be accomplished using hardware specifically designed for the task, such as LiDAR, or repurposed hardware. For example, the PY4 mission demonstrated on-orbit range measurements between two spacecraft using S-band radio modules, augmented with a GPS receiver on the anchor spacecraft, and a batch Kalman filter to determine the relative position vector of a target spacecraft to an accuracy of approximately 4 meters (28). A mission using vision-based systems was Seeker, a 3U CubeSat that was deployed in September 2019 and designed to demonstrate capabilities basic proximity operations capabilities with a path to inspection of crewed vehicles. Seeker used a COTS laser rangefinder combined with a COTS industrial camera that fed a convolutional neural network to estimate bearing to a non-cooperative client. While Seeker did not complete all of its planned maneuvers, many core technologies were successfully demonstrated (30). The CubeSat Proximity Operations Demonstration (CPOD) mission used an optics module with four imagers for relative ranging and target attitude determination but required priori knowledge and markers on the tracked spacecraft (31). Launched in 2023, NASA's Starling mission used its commercial star trackers to feed an orbit estimation algorithm known as the Starling Formation-flying Optical eXperiment (StarFOX). StarFOX provided angles-only relative navigation of an object, demonstrating on orbit relative position knowledge with only 0.5% error relative to range using one or multiple observers (32). In 2025, R5 Spacecraft 7 used a COTS industrial-grade LiDAR to perform proximity operations with a Falcon 9 upper stage. These missions illustrate the complexity of the navigation problem, especially as much of it must be done autonomously without ground-based intervention to achieve the objectives of PFF and RPO missions.

Once the navigation system has converged, guidance laws are used to determine trajectories to achieve PFF and RPO objectives, as well as avoid conjunctions with nearby objects. While this field is primarily research-based and dependent on algorithms instead of hardware, there is some development in packaged software suites to enable PFF and RPO missions. The Autonomous Navigation, Guidance, and Control Software (autoNGC) suite is being developed by NASA Goddard Space Flight Center to enable autonomous operations when ground communications are limited or unavailable, a critical need for cis-lunar and deep space missions (33). Lockheed Martin, in collaboration with government and industry partners, is developing the 12U LINUSS platform that will eventually offer spacecraft upgrade and servicing capabilities, a service heavily dependent on PFF and RPO technologies (34). The mission tested Lockheed Martin's Horizon Command & Control and Compass Mission Planning Software, which seeks to provide a software solution for various mission operations including PFF (35). It is expected that this field will grow with the continued increased interest in PFF and RPO missions and that demand for software suites with proven flight heritage will become more common.

While there have been multiple successful demonstrations of on-orbit relative navigation for missions conducting PFF and RPO objectives, many of these missions have experienced control system and actuator challenges. The Seeker mission experienced multiple failures with the thruster system likely related to a FPGA controller failure, resulting in the inability to thrust in multiple axes, causing the mission to not meet its minimum objective (30). CPOD attempted the characterization of low-power proximity operations technologies, however it was only able to demonstrate limited RPO and unable to complete the planned docking maneuvers before its mission ended June 2023. The CPOD mission experienced partial solar panel failures resulting in lower power margins that limited mission operations, and experienced a propulsion system

anomaly that was most likely related to a plenum leak. Although, the mission was able to demonstrate both far- and near-field rendezvous and ingress maneuvers, achieving most of the mission objectives. The spacecraft ran out of fuel before completing some of these objectives, preventing execution of the docking procedure which was intended to use a magnetic actuator to dock the two spacecraft. The Lockheed Martin LINUSS mission also experienced a plenum leak and required continuous ground interventions by the development team to overcome the continual challenges experienced (34). The Starling swarm, which ended its initial mission in May 2024, experienced a leak in the propellant system and initially a sticky refill valve, though both anomalies were able to be resolved through ground operations (37). The mission was ultimately able to resume its in-train formation using thrusters to lower each swarm member's altitude and let differential drag establish required separations, allowing the mission to continue conducting various experiments. Other missions had success using non-propulsive control techniques like drag separation for formation maintenance. The PY4 mission successfully used drag separation for both in-track and cross-track maneuvers by controlling each individual member's attitude to create the requisite drag differential (38). While such missions are less prone to failure by not relying on a propulsion system, they are typically limited to far-field rendezvous and cannot achieve PFF or near-field RPO objectives like docking.

The complexity of PFF and RPO missions for SmallSats continues to challenge the hardware, software, and operational design; however, these challenges will continue to be addressed as more industry, government, and university entities become involved. The recent successes of SmallSat swarms employing PFF indicate they are key contributors to the advancement of space situational awareness (SSA), space traffic management (STM), and in-space servicing and manufacturing (ISAM). In addition to distributed spacecraft autonomy (DSA) technology maturation, rendezvous, proximity operations, and docking (RPOD) is another key capability required for future space operations. These operations include inspection, refueling, repair, PFF, sample collection, or debris remediation.

A key technology to implement SSA, STM, and ISAM operations is the development of reliable docking and attachment mechanisms. For SmallSats in particular, the ability to dock, attach, or capture another object, whether a mothership, a cooperative servicing spacecraft, an asteroid, or orbital debris, is essential to perform on-orbit operations. While docking mechanisms exist on larger spacecraft, that technology is impractical for SmallSats due to SWaP-C concerns. Therefore, recent years have seen a surge in research and development focused on lightweight, low-complexity, and scalable attachment technologies for SmallSats. Additionally, docking and attachment research spans multiple disciplines such as mechanical engineering, robotics and control, materials science, and others. Commercial effort in applying docking mechanisms to assist deorbit maneuvers is described in the *Deorbit Systems* chapter, and robotic manipulation is discussed in the *Structures, Materials, and Mechanisms* chapter.

Ongoing efforts across NASA, other government agencies, industry, and academia are maturing RPOD technology. A commercial collaboration between Starfish Space and Impulse Space on the "Remora" mission that launched in December 2025 achieved fully autonomous RPO in LEO with just a single camera system and closed-loop GNC software, enabling autonomous rendezvous between two Impulse Mira LEO Express vehicles (40). University of North Dakota's Rendezvous & Operations for Autonomous Docking and Servicing (UND ROADS) is a low-cost flight demonstration of two 3U CubeSats to achieve RPO and docking with centimeter-level accuracy via RF ranging and carrier-phase GNSS, featuring magnetic docking and predictive GNC algorithms (41). The two UND ROADS CubeSats were launched June 2025 and are still operational (42).

5.4 On the Horizon

In general, technological progress in guidance, navigation, and control is advancing quickly in automotive applications but is lagging slightly in the aerospace industry. Given the high maturity of existing GNC components, future developments in traditional GNC systems are focused on incremental improvements, such as decreases in mass and power, and increases in longevity and/or accuracy. This is especially true for GNC components designed for deep space missions that have only recently been considered for small spacecraft.

Other areas of focus that enhance GNC capabilities include autonomous formation flying for SmallSat constellations such as RPOD and position, navigation, and timing (PNT) technologies. Recent advances in PNT have been driven by rapid advances in inertial sensors, atomic clocks, and emerging magnetic navigation methods tailored for near-Earth environments. Modern inertial measurement units are leveraging breakthroughs in micro- and nano-fabrication, quantum sensing, and low-drift architectures to achieve high precision independent of GNSS (43)(44). In parallel, atomic clock development—particularly compact optical and chip-scale systems—continues to improve timing stability and resilience, enabling more accurate synchronization and robust PNT solutions for both terrestrial and space applications (45)(46). Complementing these technologies, magnetic navigation is becoming a viable GNSS alternative or augmentation layer, using Earth's geomagnetic signatures and real-time field models to support navigation in GNSS-degraded or denied regions. Together, these maturing capabilities are pushing PNT resilience and autonomy to new levels for near-Earth missions and operational environments. Several projects funded via NASA's Small Spacecraft Distributed Systems (SSDS, formerly Small Spacecraft Technology) program through the University SmallSat Technology Partnerships (USTP) initiative are advancing GNC systems. Listed below in Table 5-14 are projects that focus on GNC advancements, and further information can be found at the USTP website:

https://www.nasa.gov/smallspacecraft/university-smallsat-technology-partnership-initiative/

Table 5-14: USTP Initiative GNC Projects

Project	University	Current Status	Reference
DESPINA: X-Ray spectrometer optimized for deep space PNT using pulsar and other astrophysical X-ray sources	University of Minnesota	Still in development	(47)
ODIN: OPNAV instrument for deep space navigation	Georgia Institute of Technology	Still in development	(47)
High-TRL optical frequency combs (OFC) that enable planar on-chip navigation-grade oscillators with significantly better noise performance	California Institute of Technology	Still in development	(47)
On-Orbit Demonstration of Surface Feature-Based Navigation and Timing	University of Texas, Austin	Still in development	USTP Technology Expo presentation
Autonomous Nanosatellite Swarming (ANS) using	Stanford University	Onboard Starling mission (Launched in 2023)	USTP Technology Expo presentation

Radio Frequency and Optical Navigation			
Distributed multi-GNSS Timing and Localization (DiGiTaL)	Stanford University	Leveraged technology for ANS in Starling mission	USTP Technology Expo presentation
Mems Reaction Control and Maneuvering for Picosat beyond LEO	Purdue University	Awarded a suborbital flight test through NASA's Flight Opportunities program	(29)
A Small Satellite Lunar Communications and Navigation System	University of Boulder, Colorado	Still in development	USTP Technology Expo presentation
A high-precision continuous-time PNT compact module for the LunaNet small spacecraft	University of California, Los Angeles	Still in development	USTP Technology Expo presentation

5.5 Summary

Conventional small spacecraft GNC technology is a mature area, with many high TRL components previously flown in Earth orbit and offered by several vendors. These GNC techniques are generally semi- or non-autonomous as on-board observations are collected with the assistance of ground-based support. As interest in deep space exploration with small spacecraft grows, semi- to-fully-autonomous navigation methods must advance. It is likely that future deep space navigation will rely solely on fully autonomous GNC methods that require no ground-based intervention to collect and provide navigation data. This is a desirable capability as the spacecraft's dependence on Earth-based tracking resources (such as DSN) is reduced and the demand for navigation accuracy increases at large distances from Earth. The success of the Starling mission in performing PFF reliably without external commands has paved the way for future DSN-independent solutions.

Current methods advancing deep space navigation involve both ground- and space-based tracking in conjunction with optical navigation techniques. To support this maturity, the small spacecraft industry has seen a rapid progression in PNT technologies, including inertial sensors, optical accelerometers, atomic clocks, and magnetic navigation for near-Earth environments. Advancements in RPOD technologies hold exciting implications for the future and will likely lead to growth in the SmallSat industry.

The rising popularity of SmallSats in general, and CubeSats in particular, means there is high demand for components, and engineers are often faced with high costs. The challenges that inhibited SmallSat engineers from achieving desired GNC/ADCS solutions a decade ago are less significant. There exists a multitude of best practices for assembling inexpensive and reliable attitude determination and navigation systems.

For feedback solicitation, please email: arc-sst-soa@mail.nasa.gov. Please include a valid business email so someone may contact you further.

5.6 References

(1) L.C.G Shepherd. and A.F.S.C Shepherd. "Space Surveillance Network." Shared Space Situational Awareness Conference. Colorado Springs. 2006.

(2) D. Vallado, P. Crawford, R. Hujsak and T.S. Kelso. "Revisiting Spacetrack Report #3," AIAA 2006-6753. AIAA/AAS Astrodynamics Specialist Conference and Exhibit. August 2006.

(3) Thornton, C L and Border, J S: "Radiometric Tracking Techniques for Deep-Space Navigation." s.l: John Wiley & Sons, 2003.
(4) K. Kapás, T. Bozóki, G. Dálya et al. “Attitude determination for nano-satellites – I. Spherical projections for large field of view infrasensors.” Exp Astron 51, 515–527, 2021.
(5) JPL. “MarCO,” [Online] Available at: https://www.jpl.nasa.gov/missions/mars-cube-one-marco/
(6) J.R. Wertz. "Spacecraft attitude determination and control." Springer Science & Business Media. Vol. 73. 2012.
(7) R. Kulczycki and P. Wisniewski. “Slew Maneuver Control for Spacecraft Equipped with Star Camera and Reaction Wheels.” 2005. Vol. 13, no. 3, pp. 349–356.
(8) J. L. Crassidis. "Spacecraft attitude determination." Encyclopedia of systems and control. 2021, Cham: Springer International Publishing. 2097-2104.
(9) B.B. Spratling and D. Mortari. ““A survey on star identification algorithms.” 2009.
(10) Jin, J, Ko, S and Ryoo, C K: “Fault Tolerant Control for Satellites with Four Reaction Wheels.” 2008. Vol. 16, no. 10, pp. 1250–1258.
(11) M.G. Finley, R.M. Broadfoot, S. Shekhar, and D.M. Miles. “Identification and removal of reaction wheel interference from in-situ magnetic field data using multichannel singular spectrum analysis.” 2023. Journal of Geophysical Research: Space Physics, 128, e2022JA031020. https://doi.org/10.1029/2022JA031020
(12) U. P. Sampaio, A. St-Amour, J. Lafontaine. “Zero-Speed Crossing Avoidance with Three Active Reaction Wheels using Set-Point Angular Momentum Management,.” 2016. IFAC-PapersOnLine, Volume 49, Issue 17. Pages 135-140, ISSN 2405-8963, https://doi.org/10.1016/j.ifacol.2016.09.024
(13) C.C. Liebe, "Star Trackers for Attitude Determination," IEEE Aerospace and Electronic Systems Magazine, vol. 10, no. 6, pp. 10-16, June 1995, doi: 10.1109/62.387971
(14) M.L. Psiaki, F. Martel, F and P.K. Pal. “Three-Axis Attitude Determination Via Kalman Filtering of Magnetometer Data.” Vol. 13, no. 3, pp. 506–514. 1990.
(15) J.H. Wessels. "Infrared Horizon Sensor for CubeSat Implementation." Master’s Thesis, Stellenbosch University. March 2018.
(16) A. Pelemeshko et al. "High-Precision CubeSat Sun Sensor Coupled with Infrared Earth Horizon Detector." 2020. IOP Conf. Ser.: Mater. Sci. Eng. Vol. 734. pp. 0121-8.
(17) M. M. Kobayashi et al. "The Iris Deep-Space Transponder for the SLS EM-1 Secondary Payloads." IEEE Aerospace and Electronic Systems Magazine, vol. 34, no. 9, pp. 34-44, 1 Sept. 2019.
(18) D. Greenheck et al. “Design and Testing of a Low-Cost MEMS IMU Cluster for SmallSat Applications.” 28th Annual AIAA/USU Conference on Small Satellites, 2014.
(19) S. Merhav. “Aerospace Sensor Systems and Applications.” Springer New York, 1998.
(20) O. Montenbruck et al. “Precision Spacecraft Navigation Using a Low-Cost GPS Receiver.” 2014. Vol. 16, no. 4, pp. 519–529.
(21) “Foreign Availability Determination Procedures and Criteria.” 2015. Office of the Federal Register. Title 15 Part 768.7.
(22) A. Hadhazy. "Cosmic GPS." Aerospace America. [Online] May 2020. Available at: https://aerospaceamerica.aiaa.org/features/cosmic-gps/
(23) J. Foust: "GPS in Space." MIT Technology Review. [Online] January 2002. https://www.technologyreview.com/2002/01/01/275613/gps-in-space/
(24) F.H. Aguirre. “X-Band Electronics for The INSPIRE CubeSat Deep Space Radio." 2015. IEEE Aerospace Conference.
(25) D. Baird. "NASA Tests Atomic Clock for Deep Space Navigation." [Online] 2018. Available at: https://www.jpl.nasa.gov/news/news.php?feature=7053

(26) J.W Kolar et al. "High-Speed Magnetically Levitated Reaction Wheels for Small Satellites." Anacapri, Capri: 23rd International Symposium on Power Electronics, Electrical Drives, Automation and Motion (SPEEDAM 2016), 2016.

(27) A.G. Cofer. "Film Evaporation Mems Thruster Array for Micropropulsion." Open Access Dissertations. 1106. 2014. Available at: https://core.ac.uk/download/pdf/220145833.pdf

(28) M. Holliday, R. Ticknor, R. Hunter, J. Stupl, P. Fisch, I. Sow, J. Willis, and Z. Manchester. "The PY4 Mission: A Low-Cost Demonstration of CubeSat Formation-Flying Technologies." 2024. Weekend Session VIII: Advanced Technologies - Research & Academia 2, 38th Annual AIAA/USU Small Satellite Conference, Logan UT.

(29) Jill Davis, Henry Pernicka. "Proximity operations about and identification of non-cooperative resident space objects using stereo imaging." 2019. Acta Astronautica, Volume 155, Pages 418-425, ISSN 0094-5765, https://doi.org/10.1016/j.actaastro.2018.10.033.

(30) S. M. Pedrotty, "Seeker Overview and Mission 1 Review-- A New Development Approach for In-Space Inspectors." 2021. [Online] Available at: https://www.nasa.gov/smallsat-institute/seeker-overview-and-mission-1-review--a-new-development-approach-for-in-space-inspectors

(31) J. Bowen, M. Villa, and A. Williams. "CubeSat based Rendezvous, Proximity Operations, and Docking in the CPOD Mission." 2015. Weekend Session VIII: Advanced Technologies - Research & Academia 2, 29th Annual AIAA/USU Small Satellite Conference, Logan UT.

(32) J. Kruger, S. D'Amico, and S.S. Hwang. "Starling Formation-Flying Optical Experiment: Initial Operations and Flight Results." 2024. Weekday Session 11: Advanced Technologies 2, 38th Annual AIAA/USU Small Satellite Conference, Logan UT.

(33) S. Hur-Diaz, B. Azimi, M. Romeo, A. Lionis, N. Stacey, R. Pritchett, G. Crum, and S. Semper. "Autonomous Navigation, Guidance, and Control Software in a Low SWaP Box." 2024. Weekday Poster Session 5, 29th Annual AIAA/USU Small Satellite Conference, Logan UT.

(34) D. Barnhart, D. M. Shoemaker, E. T. King, T. Logue, and M. J. Lavis. "LM LINUSS™ - Lockheed Martin In-Space Upgrade Servicing System." 2023. Weekday Session 9: Formation Flying and RPO, 37th Annual AIAA/USU Small Satellite Conference, Logan UT.

(35) Lockheed Martin. Horizon Command & Control (C2) and Compass Mission Planning Software. [Online] Available at: https://www.lockheedmartin.com/en-us/products/satellite-software.html

(36) I. A. Spiegal, B. Zhou, R. Goodloe, B. Fox, J. DiMatteo. "CubeSat Proximity Operations Demonstration (CPOD) Mission Results." 2023. Weekday Session 9: Formation Flying and RPO, 37th Annual AIAA/USU Small Satellite Conference, Logan UT.

(37) T. Stevenson. "Flight Results and Lessons Learned From the Starling Propulsion System." 2024. Weekday Session 7: Propulsion, 38th Annual AIAA/USU Small Satellite Conference, Logan UT.

(38) G. Falcone, J. B. Willis, Z. Manchester. "Propulsion-Free Cross-Track Control of a LEO Small-Satellite Constellation with Differential Drag." 2023. Systems and Control, Electrical Engineering and Systems Science, Cornell University. Available at: https://arxiv.org/abs/2306.13844

(39) D. Dickinson. "NICER and SEXTANT demonstrate XNAV pulsar navigation system that may be used on Artemis." 2020. [Online] Available at: https://skyandtelescope.org/astronomy-news/nasa-to-use-pulsar-navigation-for-deep-space-missions/

(40) Impulse Space. "Starfish Space Completes Autonomous Rendezvous and Proximity Mission in LEO with Impulse Space," December 15, 2025, [Online] Available at: https://www.impulsespace.com/updates/starfish-space-completes-autonomous-rendezvous-and-proximity-mission-in-leo-with-impulse-space

(41) University of North Dakota, “ROADS Mission,” John D. Odegard School of Aerospace Sciences, [Online] Available at: https://aero.und.edu/space/operations-group/roads-mission.html

(42) B. Dubensky, “UND in Orbit,” February 11, 2026, [Online] Available at: https://knoxradio.com/2026/02/11/und-in-orbit/

(43) “Quantum PNT Breaks Out as DIU and DARPA Make GPS-Proof Nav Real,” The Relay, October 8, 2025, [Online] Available at: https://therelaymag.com/quantum-pnt-breaks-out-as-diu-and-darpa-make-gps-proof-nav-real

(44) M. Muradoglu and M.T. Johnsson et al. “Quantum-assured magnetic navigation achieves positioning accuracy better than a strategic-grade INS in airborne and ground-based field trials”, 2025, 2504.08167, https://arxiv.org/abs/2504.08167.

(45) Z. Luo and T. C. Briles et al. “A scalable infrastructure for strontium optical clocks with integrated photonics,”2026, 2604.03229, https://arxiv.org/abs/2604.03229.

(46) Tang, Z., Li, C., Zhang, X. *et al.* 1-MHz linewidth VCSEL enabled by monolithically integrated passive cavity for high-stability chip-scale atomic clocks. *Light Sci Appl* **15**, 94 (2026). https://doi.org/10.1038/s41377-026-02192-x

(47) National Aeronautics and Space Administration, “NASA Selects Universities to Support Small Spacecraft Technologies,” December 8, 2023, https://www.nasa.gov/directorates/stmd/small-spacecraft-technology-program/nasa-selects-universities-to-support-small-spacecraft-technologies/



Table of Contents

Chapter Glossary ii
6.0 Structure, Mechanisms, and Materials 168
6.1 Introduction 168
6.2 State-of-the-Art – Primary Structures 169
6.2.1 CubeSat Standard 169
6.2.2 Custom CubeSat Primary Structures 171
6.2.3 Primary Structure Standard Dispenser 172
6.2.4 CubeSat Structures Construction Methods 172
6.3 State-of-the-Art – Mechanisms 173
6.3.1 Actuators 174
6.3.2 Deployable Structures 176
6.3.3 Robotic Manipulator 178
6.3.4 Reliability Considerations 178
6.4 State-of-the-Art – Polymeric Additive Manufacturing 179
6.4.1 Applicability of TRL to Polymer AM 179
6.4.2 Inspection and Testing 180
6.4.3 Thermoplastics and Photopolymers 180
6.4.4 AM Design Optimization 188
6.5 Radiation Effects and Mitigation Strategies 190
6.5.1 Shielding from the Space Environment 190
6.5.2 Inherent Mass Shielding 190
6.5.3 Shields-1 Mission, Radiation Shielding for CubeSat Structural Design 192
6.5.4 Ad Hoc Shielding 193
6.5.5 Charge Dissipation Coating 193
6.5.6 LUNA Innovations, Inc. XP Charge Dissipation Coating 193
6.6 Summary 194
References 194

Chapter Glossary

(ABS)	Acrylonitrile Butadiene Styrene
(ACS3)	Advanced Composite Solar Sail System
(AE)	Aerospace Corporation Electron
(AM)	Additive manufacturing
(AP)	Aerospace Corporation Proton
(CAM)	Computer Aided Manufacturing
(CFRP)	Carbon Fiber Reinforced Polymers
(CNC)	Computerized Numerical Control
(COTS)	Commercial-off-the-shelf
(CSLI)	CubeSat Launch Initiative
(CTE)	Coefficient of Thermal Expansion
(DCB)	Deployable Composite Boom
(DDD)	Displacement Damage Dose
(DLP)	Digital Light Projection
(DOF)	Degrees of Freedom
(EEE)	Electrical, Electronic and Electro-mechanical
(EELV)	Evolved Expendable Launch Vehicle
(ESD)	Electrostatic Discharge
(ESPA)	EELV Secondary Payload Adapter
(FDM)	Fused Deposition Modeling
(FFF)	Fused Filament Fabrication
(FPGAs)	Field Programmable Gate Arrays
(FST)	Flame, Smoke, and Toxicity
(GCD)	Game Changing Development
(GEVS)	General Environmental Verification Standard
(HDT)	Heat Deflection Temperature
(ISS)	International Space Station
(MOSFETs)	Metal Oxide Semiconductor Field Effect Transistors
(PAEK)	Polyaryletherketone
(PC)	Polycarbonate
(PCB)	Printed Circuit Board
(PEEK)	Polyetheretherketone
(PEI)	Polyetherimide

(PEKK)	Polyetherketoneketone
(PLA)	Polylactic Acid
(PLEO)	Polar Low-Earth Orbit
(RECS)	Robotic Experimental Construction Satellite
(ROC)	Roll Out Composite
(SADA)	Solar Array Drive Actuator
(SBIR)	Small Business Innovation Research
(SD)	Secure Digital
(SEUs)	Single Event Upsets
(SLA)	Stereolithography
(SLS)	Selective Laser Sintering
(SPEs)	Solar Particle Events
(STELOC)	Stable Tubular Extendable Lock-Out Composite
(TID)	Total Ionizing Dose
(TRL)	Technology Readiness Level

6.0 Structure, Mechanisms, and Materials

6.1 Introduction

Material selection is a primary consideration in small spacecraft structures. Requirements for both physical properties (density, thermal expansion, and radiation resistance) and mechanical properties (modulus, strength, and toughness) must be satisfied. The typical spacecraft structure incorporates both metallic and non-metallic materials, each offering distinct advantages and limitations. Metals are generally homogeneous and isotropic, meaning properties are consistent throughout the material. Non-metals, such as composites, are inherently inhomogeneous and anisotropic, enabling properties to be tailored to specific load paths. Recently, resin photopolymer-based additive manufacturing (AM) has advanced sufficiently to create near-isotropic parts in certain applications. In general, structural materials selection is governed by the spacecraft operating environment while ensuring adequate margin for launch and operational loads. Additional considerations include thermal balance and thermal stress management. Payload or instrument sensitivity to outgassing and thermal displacements must also be considered.

AM has enabled increasingly customized structural solutions for SmallSats and demonstrated high-throughput fabrication of complex structures. Materials that were once out of reach of AM are now accessible in higher-end systems. Once only for secondary structures, AM is increasingly being applied to primary structures— particularly in CubeSat and PocketQube-class spacecraft.

However, for larger SmallSats such as Evolved Expendable Launch Vehicle (EELV) Secondary Payload Adapter (ESPA)-class, conventional machined assemblies constructed from aluminum alloys remain the dominant approach for primary structures. Secondary structures, such as solar panels, thermal blankets, and subsystems, are attached to primary structures. These structures are generally self-supporting and transmit minimal critical structural loads. Failure of a primary structure typically results in catastrophic mission failure, and while failure of a secondary structure may not compromise spacecraft integrity, it can significantly impact mission performance. These structural categories serve as a good reference but can be hard to distinguish for small spacecraft that are particularly constrained by volume. This is especially true for SmallSats since their capabilities are now comparable to full size buses, but the volume afforded by dispensers or deployment rings becomes the constraining factor. Therefore, it is imperative that structural components are as volume efficient as possible. The primary structural components need to serve multiple functions to maximize volume efficiency. Such functions may include thermal management, radiation shielding, pressure containment, and even strain actuation. These are often assigned to secondary structural components in larger spacecraft.

Structural design is influenced by subsystem integration, launch environments, mission application, and operational environment. There are different configurations for spin-stabilized and 3-axis stabilized systems, and the instrumentation used places requirements on the structure. Some instruments require mechanisms, such as deployable booms, to create enough distance between a magnetometer and the spacecraft for minimal structural effects on the measurement. The spacecraft exterior and interior material and electronic subsystems need to be understood in the specific mission environment (e.g., in-space charging effects). Mitigation for charge build-up is provided in Section 6.5.

Highly configurable or modular systems are often desirable for rapid development missions, as prototyping and firmware and software development can be extended later into the design cycle with flight hardware in the loop. Card slot systems not only provide those benefits, but when paired

with certain standards, they can still fulfill the same structural, mechanical, and thermal requirements as the current CubeSat method of “stacking” electronics and payloads.

The advancement of SmallSat mechanisms, particularly in deployable structures, actuators, and switches, have increased SmallSat capabilities beyond original structural volume constraints. Deployable structures enable large structural applications with minimal volume requirements, while actuator and switch mechanisms provide motion and deployment applications.

An overview of radiation effects and some mitigation strategies is included in this chapter because radiation exposure can impact the structural design of small spacecraft. For SmallSats operating out of low-Earth orbit with increased radiation exposure, mission planners may also want to consider risk mitigation strategies associated with specific radiation environments. This includes both interplanetary missions, where solar radiation dominates, and polar low-Earth orbit (PLEO) missions, where solar radiation risk increases over the poles. In addition, the solar maximum that started in 2024 (1), which is associated with an increased number of solar particle events (SPEs), is expected to persist through 2026 and should be considered in mission planning.

The list of organizations/companies in this chapter is not all-encompassing and does not constitute an endorsement from NASA. The inclusion or omission of specific companies is not intended to reflect their technical merit or relationship with NASA. The performance advertised may differ from actual performance as the information has not been independently verified and is based on manufacturer-provided or publicly available data. It should be noted that TRL designations may vary with changes specific to the payload, mission requirements, reliability considerations, and/or the environment in which performance was demonstrated. Readers are highly encouraged to reach out to companies for further information regarding the performance and TRL of the described technology.

6.2 State-of-the-Art – Primary Structures

6.2.1 CubeSat Standard

Two general approaches are common for primary structures, often called frames or chassis, in the small spacecraft market: commercial-off-the-shelf (COTS) structures and custom-machined or additively manufactured components. Most COTS offerings are for the CubeSat market. COTS structures can simplify development, but only when mission complexity and subsystem and payload requirements fall within the design intent of a particular structure. Custom-machined structures enable greater flexibility in mission-specific system and payload design. Typical commercially available structures are designed for low-Earth orbit applications and limited mission durations, where shielding requirements are generally limited to modest radiation protection from the Van Allen belts.

Table 6-1: CubeSat Standard Structure Dimensions

Type	Dimension (mm)	Average Structure Weight (kg)
1U	100 x 100 x 113.5	0.118
1.5U	100 x 100 x 170.2	0.142-0.25
2U	100 x 100 x 227	0.220
3U	100 x 100 x 340.5	0.352
6U	100 x 226.3 x 366	0.916-1.94
12U	226.3 x 226.3 x 366	1.84

The CubeSat standard has evolved over many years of increasing use. The CubeSat standard structures, also referred to as canisterized satellites, include 1U, 1.5U, 2U, 3U, 6U, and 12U. Larger sizes exist but are less common. Table 6-1 shows the nominal weight limits and dimensions of each CubeSat structure from the CubeSat Design Specification document. There

is an extra-volume (XL) option available for 3U, 6U, and 12U CubeSats; this additional volume, commonly referred to as the “tuna can” volume, is associated with an individual dispenser type. This cylindrical additional volume allows structural extensions that can accommodate various components. Steamjet Space has developed Steam Thruster, a tuna can-sized electrothermal thruster specifically designed for CubeSats. The 3U CubeSat Elfin mission used this tuna can space for antenna deployment. The Shields mission also accommodated a radiator within its tuna can volume. Figure 6.1 shows this optional volume and location on the CubeSat.

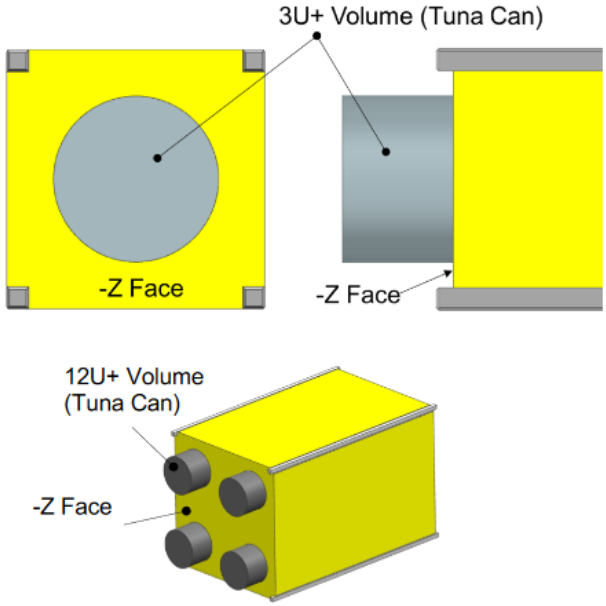


Figure 6.1: Optional extra volume shown on 3U and 12U –Z face (also known as a "Tuna Can"). Credit: Cal Poly CubeSat Laboratory.

Several companies provide CubeSat primary structures. Most are machined from aluminum alloy 6061 or 7075 and are designed with several mounting locations for components to allow flexibility in spacecraft configuration. The SmallSat community has witnessed an increase in CubeSat standard configuration over the last 10 years from 1U to 3U, to include 6U and 12U. This shift has been driven by demand for greater mission capability on smaller platforms and by the need for additional volume to support more complex CubeSats designs. Table 6-2 lists several commercial primary CubeSat structures. Of the offerings included here, 1U, 3U, and 6U frames are the most prevalent; however, 12U frames are becoming more widely available as dispenser options for the 12U form factor increase. Figure 6.2 shows some commercial examples of 3U, 6U and 12U CubeSat structures.



Figure 6.2: Various commercial CubeSat structures. Top Left: NanoAvionics 3U Structure. Credit: NanoAvionics. Top Right: 6U nanosatellite structure. Credit: GomSpace. Lower Left: 12U Structure. Credit: C3S Electronics Development, LLC. Lower Right: 16U structure. Credit: EnduroSat.

8U and 16U CubeSat Structure

Following the market trend toward larger CubeSat structures, several companies offer configurations not formally recognized by the CubeSat standard, such as the 8U and 16U. Customized dispensers are available that will host these larger volumes.

Table 6-2: Commercial Primary CubeSat Structures	
Manufacturer Headquarters	**Structure (U)**
2NDSpace Italy	VERSE 1U, 2U, 3U, 6U, 8U, 12U, 16U
AAC Clyde Space Sweden	ZAPHOD 1U, 2U, 3U, 6U, 12U
C3S Electronics Development Hungary	3U, 6U, 8U, 12U, 16U
Cervos Space Turkey	1U, 2U, 3U, 6U
EnduroSat Bulgaria	1U, 1.5U, 3U, 6UXL, 8U 12UXL, 16U
Exobotics United Kingdom	1U, 2U, 3U, 6U, 12U, 16U
German Orbital Systems Germany	1U, 2U, 3U, 6U, 12U
GomSpace Denmark	3U, 6U, 8U, 12U, 16U
Gran Systems Taiwan	1U, 1.5U, 2U, 3U, 6U, 6UXL, 8U, 12UXL, 16U, 27U, 64U
Gumush Istanbul	n-ART 1U, 2U, 3U
ISISPACE The Netherlands	1U, 2U, 2UXL, 3U, 6U, 8U, 12U, 16U
Ishitoshi Machining Japan	MBF-1U, 3U
NanoAvionics Lithuania	1U, 2U, 3U, 6U, 12U, 16U
Pumpkin Space Systems USA	Supernova 1U, 3U, 6U, 12U
NPC Spacemind Italy	SM 1U, 1.5U, 2U, 3U, 6U, 6U XL, 8U, 12U, 12U XL, 16U
Nara Space South Korea	12U, 16U
SatRev Poland	6U
Space Inventor Denmark	3U, 6U, 8U, 12U, 16U

6.2.2 Custom CubeSat Primary Structures

A growing development in building custom small satellites is the use of detailed interface requirement guidelines for payload and spacecraft integration. These guidelines focus on payload designs that account for rideshare safety considerations related to mission readiness and deployment methods. Safety considerations include safety switches such as the "remove before flight" pins and foot switches, and requirements that the spacecraft remain powered off while stowed in the deployment dispensers. Other safety requirements often entail anodized aluminum rails and specified limits on mass, center of gravity, and external dimensions to ensure successful canister or dispenser deployment.

DiskSat Structure

The Aerospace Corporation is developing a DiskSat (Figure 6.3) demonstration mission with support from NASA's Space Technology Mission Directorate (STMD). The DiskSat is a 1m diameter circular disk, 2.5 cm thick, constructed as a graphite-epoxy composite sandwich, with a structural mass of less than 3 kg/m^2. The volume is approximately 20 liters, equivalent to a hypothetical '20U' spacecraft. While the entire volume will not be filled, the increased

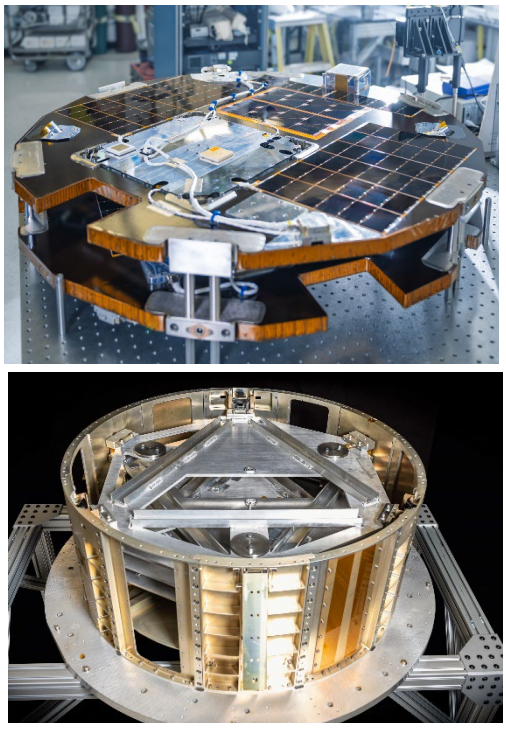


Figure 6.3: {top} Two DiskSat spacecraft during integration. {lower} DiskSat spacecraft dispenser Credit: The Aerospace Corporation.

surface area supports power generation, aperture allocation, thermal management, and manufacturing simplification. First launch for the demonstration mission occurred in December 2025, the launch dispenser functioned as designed, communications with ground network were successful, and the mission is currently in the checkout and initialization phase (2).

6.2.3 Primary Structure Standard Dispenser

The box that houses the CubeSats in the launch vehicle is called a dispenser (or deployer), and it dispenses (or deploys) the CubeSat into the desired orbit. The CubeSat uses the entire volume of the dispenser to maximize available volume. Since CubeSats adopt a standard size and form factor, CubeSat dispensers have also been standardized with two constraint systems: rail- or tab-type. This allows spacecraft designers and launch service providers to minimize launch integration costs, increase access to space, and sustain frequent launches (3). The CubeSat Design Specification document by the CubeSat Program at Cal Poly was created to provide CubeSat developers with baseline requirements compatible with as many CubeSat dispensers and launch opportunities as possible, reducing the risk of launch interface failures (4). To view the most current versions of the CubeSat Design Specification, please visit: http://www.cubesat.org. The CubeSat Design Specification document includes rail systems. The Canisterized Satellite Dispensers (CSD) tab system created by Planetary Systems Corporation (now Rocket Lab) is the most widely available tab dispenser that offers design flexibility for structures that do not require the use of rails. See the CSD datasheet for detailed information on tab dispensers (5).

A tab-style canister deployment system uses tabs that are loaded to hold the CubeSat to a wall of the canister and are released upon deployment. The vibrational load during launch passes from the launch vehicle to the canister structure with the pre-loaded CubeSat. A CubeSat using a rail dispenser is lightly loaded on the z-axis. On the x and y axes a thin gap exists between dispenser rails and the CubeSat rails, which can cause vibrational chatter. The vibrational chatter increases the mechanical load of the CubeSat during testing and launch. For more CubeSat rail vs tab dispensers and commercial launch integration hardware, please refer to *Chapter 10: Launch, Deployment, Integration, and Orbital Transport*.

The required interface documents originate with the rideshare integrator for the specific dispenser being used with the launch vehicle. The launch vehicle provider typically provides the launch vibration environment. The NASA CubeSat Launch Initiative (CSLI) requires CubeSat or SmallSat systems to withstand the General Environmental Verification Standard (GEVS) vibration environment of approximately 10 G_{rms} over a 2-minute period (6). The detailed dispenser or canister dimensional requirements provide enough information, including CAD drawings in many cases, to enable custom structural design applications.

6.2.4 CubeSat Structures Construction Methods

Monocoque Construction

Monocoque structures are load-bearing skins that have significant heritage in aircraft. On small spacecraft, the intent of this design is several-fold – maximizing internal volume, providing additional thermal mass for heat sinks or sources, enabling more mounting points, and increasing surface area to potentially reduce total ionizing dose (TID). Monocoque construction is common, and “extruded” designs are relatively easy to fabricate through computer numerical control (CNC) machining, waterjet cutting, or laser cutting.

Modular Frame Designs

Modular frames allow for a flexible internal design for rapid-development missions, while still ensuring strict adherence to external dimensions of the CubeSat standard, especially when deployment from a standardized, reusable dispenser is required. Open frames are suitable for low-Earth orbit, as radiation shielding is not provided by the structure. Care must also be taken to design for thermal mass requirements, as modular frames are inherently low in mass.

Additively Manufactured Designs

The use of additive manufacturing allows for structural designs that cannot be produced using traditional methods or would be prohibitively expensive to manufacture using conventional machining. The additive manufacturing process allows for much more design flexibility to customize structures to specific mission needs. Topology optimization methods, which generally create structures that are only feasible for additive manufacturing, can be used to minimize the amount of material and thus mass needed for the spacecraft structure. Some CubeSat missions have already flown using polymeric printed structures instead of metal, which can significantly reduce both mass and cost. Considerations need to be made regarding electrostatic discharge (ESD), grounding, and other possible electrical considerations for a polymeric frame. Additionally, fasteners for polymeric structures need to be evaluated differently than for metal, as polymers do not form threads as strong as metals and heat-set inserts may not hold well in the structure under the temperature extremes of space.

6.3 State-of-the-Art – Mechanisms

Spacecraft commonly carry onboard devices whose function is based on mechanical movement (i.e., sliding, rolling, rotating, separating, unfolding, or spinning) to either modify part of the spacecraft's geometry or to ensure operational function of a component or instrument. These devices are known as mechanisms, and as spacecraft become more sophisticated with advances in the miniaturization of electronics and systems, their reliance on mechanisms increases significantly.

The domain of spacecraft mechanisms is quite broad, encompassing many different types across the design and operational life of a spacecraft, including moving components associated with each phase:

- Deployment: dispensing spacecraft into orbit
- Beginning of mission life: deployments of solar arrays, booms, antennas, instrumentation, etc.
- Mission maintenance: sun tracking, pointing antennas and instruments, active doors or shields, gyroscopes and reaction wheels, thrusters, etc.
- End-of-life: deorbiting methods

The technology within the mechanism to perform the movement is accomplished with an actuator. Depending on the actuation method, spacecraft mechanisms are either passively or actively driven. Passive mechanisms do not consume electrical energy and provide driving power via spring loading, and active mechanisms are motorized to produce driving power for mechanism operation. Most mechanisms can use both passive and active capabilities depending on the application. Table 6-4 provides an overview of common spacecraft mechanisms and examples of technologies used.

The state-of-the-art for small spacecraft mechanisms is characterized by high reliability, low power consumption, and lightweight design, and the common mechanisms listed below are considered state-of-the-art for small spacecraft use. For the purposes of this chapter, the mechanisms focus on deployable structures, robotic manipulation, release actuation, component

pointing, and gimbal mechanisms. Reliability considerations are provided for optimal operational capabilities, as well as a brief explanation of the factors that affect mechanism performance.

Table 6-4: Type of Spacecraft Mechanisms		
Type of Mechanism	**Description**	**Technology Examples**
Separation and Release	Reliable stowage and release of spacecraft and deployable components upon an external command (active) or spring-loaded (passive).	Clamp band systems, Frangibolts, release nuts, pin pullers, bolts, burn wire, hinges, and passive spring-loaded switches
Motorized	Allows for rotatory motion of spacecraft components.	Solar Array Drive Assembly, directional antennas, combination of dampeners and absorbers
Attitude Control	Provides pointing accuracy and stability for spacecraft and components.	Reaction (momentum) wheel assembly, gimbals, component pointing, passive methods

6.3.1 Actuators

By classical definition, actuators are devices that convert electrical, thermal, hydraulic, and/or pneumatic energy into mechanical motion when energy is applied. Active, or commanded, actuators use onboard data links and electronic control systems to determine the transfer of energy; whereas passive, or reactive, actuators allow the spacecraft environment (including external launch systems) to dictate actuator energy transfer. Table 6-5 provides some commercial actuators for SmallSats.

Specifically, spacecraft actuators are used for a variety of purposes, including:

- Attitude control and gimbaling: to control the orientation of either part (gimbaling), or all (attitude control), of a spacecraft in space. This is important for pointing sensors, instruments, and/or communications antennas in a direction required for their use.
    - Attitude control general types: reaction control thrusters, momentum wheels, control moment gyros, magnetic torquers, aerodynamic control surfaces, solar sails, and gravity gradient stabilizers.
    - Gimbal general types: single-axis, dual-axis, and triple-axis systems.
- Propulsion: supporting attitude control system operations, maneuvering to a new orbit, or reducing orbital velocity to begin atmospheric reentry.
    - General types: chemical rocket engines (which can be the same as the upper stage launch vehicle engines), reaction control thrusters, and electric propulsion systems. These systems typically require actuated valves to operate.
- Deployment, docking and separation: extend and unfold solar panels, antennas, and other spacecraft components requiring unpacking to function.
    - Deployment general types: hinge-and-spring based, linear-actuator-and-scissor-frame based, roll-out systems, and inflatable structures.
    - Docking general types: probe-and-drogue, peripheral, and soft-capture systems.
    - Separation general types: spring-powered or gas-powered systems.
- Thermal control: manage all or part of the spacecraft temperature. This is important for protecting internal components from extreme temperatures.
    - General types: louvers, heat pipes, thermoelectric/Peltier devices, and pumped thermal fluid systems.

Mechanical actuation methods/techniques that are found in many of the above systems include:

- Electric and electromagnetic: AC/DC motor, piezoelectric ceramics, and push/pull & rotary solenoids (including solenoid valves), and microelectromechanical systems (MEMS).
- Thermal & thermoelectric: Shape memory alloys (SMA), phase-change liquids/solids (paraffin wax, liquid metals), thermofluidic gas systems, thermal bimorph structures, harmonic drive micro actuators (HMAs), thermal knife cutters, and magnesium alloy band systems.

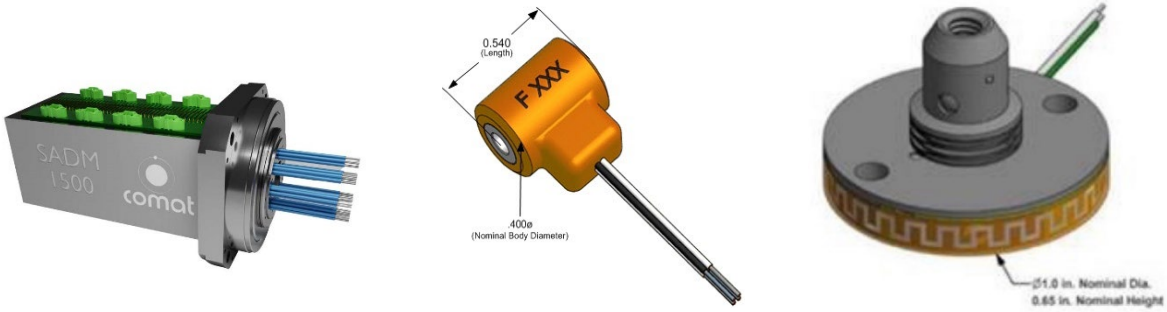


Figure 6.4: (top left) SADM 1500. Credit: Comat. (middle) TiNi Aerospace Frangibolt Actuator and (right) ML50 microlatch. Credit: Ensign-Bickford Aerospace & Defense.

Table 6-5: Commercial Actuator Mechanisms

Manufacturer Headquarters	Product	Mass (kg)	Size (mm)	Power Consumption	Actuation method
Beyond Gravity Switzerland	Separation Nut PSM 3/8B	0.23	58.5x36x56	-	-
Comat Space France	Solar Array Drive Mechanism - 400	0.465	83x62x46	4 W	Geared motor
	Solar Array Drive Mechanism - 1500	3.5	201x132	13 W	Geared motor
DCUBED Germany	Micro Pin Puller (uD3PP)	0.08	25.5x25.5x 25.5	-	SMA
	Nano Pin Puller (nD3PP)	0.025	17x17x17	-	SMA
	Micro Release Nut (uD3RN)	0.078	25x25x25	-	SMA
DHV Technology Spain	MicroSADA-10	< 0.25	100x100x10	< 6 W	Stepper Motor
	MicroSADA-18	< 0.95	226x80x18	< 10 W	Stepper Motor
	SADA-M	< 2	155x180	5W (nominal) / 10W (peak)	Stepper Motor
Ensign-Bickford Aerospace & Defense Company USA	TiNi™ Flat Pack FP50	0.033	2.3x1.3x0.24	1.25 W	SMA
	TiNi™ FD04 Frangibolt	0.007	13.72x10.16	15 W @ 9 VD	SMA
	TiNi™ ML50	0.010	25.4x16.5	2 W @ 7 VD	SMA
	TiNi™P5 Nano Pin Puller	0.015	25.4x16.5	1.5A to 3.75A	SMA
	TiNi™ P5 Pin Puller	0.018	28x26	0.5A to 2A	SMA
	NEA 9040 Mini	0.030	28x32	0.4A to 1.5A	SMA
	NEA 1120 Pin Puller	0.014	21x22	Min 3A	Split Spool
Honeybee and MMA Design USA	Solar Array Drive Actuator (SADA)	3.1	127x210	-	Stepper Motor
Nimesis Technology France	Triggy	0.004-0.271	*	*	SMA

Table 6-5: Commercial Actuator Mechanisms					
Manufacturer Headquarters	**Product**	**Mass (kg)**	**Size (mm)**	**Power Consumption**	**Actuation method**
	Gripper	<0.032	39x35x7.6	7.4 W (average)	SMA
Moog USA	Type 2 Side-Drive Solar Array Drive Mechanism (SADM)	5	234x278.6	15 W	-
Revolv Space Netherlands	Solar array drive actuator (SARA)	0.3	97x97x23	0.5 W (idle)	-
Sierra Space USA	High-Output Paraffin Actuator (HOPA)	0.35	44x14x14	5 W	Paraffin
	C14E-TC Solar Array Drive Assembly (SADA)	2.9	210x140x140	-	Stepper Motor
	C14C-TC Solar Array Drive Assembly (SADA)	2.2	172x140x140	-	Stepper Motor
	C14 Bi-Axis Gimbal	1.23	155x72x72	-	Stepper Motor
	C14E Bi-Axis Gimbal	1.72	221x112x112	-	Stepper Motor
ThermOmegaTech USA	High Output Paraffin Actuator (HOPA)	1.27	71.2x35.56	-	Paraffin
UARX Space	HADES Pico	0.095	60x62x20	1.2A @12V	Fuse Wire
	HADES Medius	0.15	70x80x25	1.2A @12V	Fuse Wire
	HELIOS Coarse Sun Sensors	0.01	32x32x11	0.05 W	5V, I2C

Data unknown is represented by -
* See reference

6.3.2 Deployable Structures

Space deployable mechanisms are structures folded into a compact configuration and deployed into a larger predetermined shape. The development of deployable structures on spacecraft is important to enable greater mission performance. Once deployed, the structures reconfigure, changing shape and size through folding and unfolding mechanisms. Common spacecraft deployables include antennas, radiators, solar panels, gravity gradient booms, and other science instruments. Small spacecraft are well-suited for deployable structures to enhance the functionality of a compact platform. However, there are limited designs for compact, lightweight, low power deployable structures that can be folded or rolled up for launch and then self-deployed in space to support such systems on small satellites.

There are different types of deployment mechanisms to ensure the deployed structure effectively expands to the desired configuration in orbit: folding, sleeve, truss, and inflatable. Deployable solar arrays are a common folded-type of passive deployment mechanism that uses spring and hinge systems to increase available solar power for the spacecraft. Please refer to the *Power* chapter for deployable solar panels and arrays. The sleeve-type deployment mechanism is implemented using a rolling or sliding screw conveyor and is commonly seen on SmallSats for various antennas (30). Inflatable deployment structures are lightweight film materials typically used for larger deployed



Figure 6.5: GPX-2 CAD image with gravity gradient boom deployed. Credit: NASA.

structures, like solar sails. Please refer to the *Deorbit Systems* chapter for deployable mechanisms used for deorbit devices.

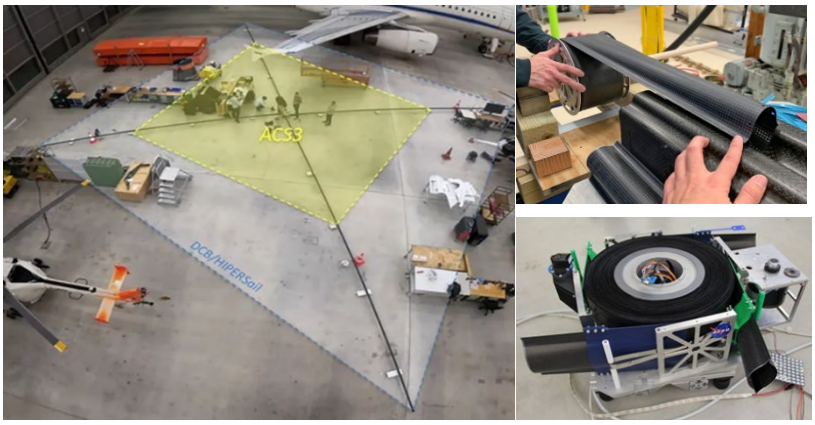


Figure 6.6: NASA Deployable Composite Boom (DCB) technology. Credit: NASA.

For SmallSat applications, it is common that deployable components are on a boom – a cantilever arm ejected from the spacecraft – that can perform various tasks once deployed. See Figure 6.5 for NASA's GPX-2 CubeSat mission with a Redwire Space deployable boom to create gravity gradient stabilization as an example. SmallSat deployable structures are common and are associated with high reliability. Engineers have started developing deployables with different materials to decrease stowage volume, mass, and power. Table 6-6 lists a selection of commercially available deployable booms.

NASA Langley Research Center (LaRC) developed Deployable Composite Booms (DCB) through the Space Technology Mission Directorate (STMD) Game Changing Development (GCD) program and a joint effort with the German Aerospace Center, see Figure 6.6. DCBs have high bending and torsional stiffness, packaging efficiency, thermal stability, and 25% less weight than metallic booms (31). The Advanced Composite Solar Sail System (ACS3) project demonstrated the DCB technology for solar sailing applications after launching April 2024. The DCB/ACS3 7-m boom technology is extensible to 16.5 m deployable boom lengths (32).

Engineers have started using origami – the art of paper folding – as a strategy of deployable structure design. Origami structures are flexible in their deployment direction so that they can be easily collapsed along the same path they are deployed. One advantage of origami-inspired mechanisms is potentially faster and cheaper prototyping. Instead of relying on laser cutting or 3D-printing, prototyping of origami-inspired mechanisms can be accomplished using inexpensive materials like paper before moving to other more expensive materials. Many resources and patterns already exist that detail how designs can be created and modified or adapted for engineering purposes (33). Solar panels and arrays, solar sails, and sunshades are examples of ongoing origami engineered SmallSat components.

Table 6-6: Commercial Deployable Booms

Manufacturer	Product
Composite Technology Development	Stable Tubular Extendable Lock-Out Composite (STELOC)
Oxford Space Systems	AstroTube deployable boom
Redwire Space	Roll Out Composite (ROC) booms
Redwire Space	CubeSat ROC Boom Deployer
Redwire Space	ROC-FALL system
Magellan Aerospace	Deployable Boom
Rolatube Technology	Deployable Composite Booms
Northrup Grumman	Coil Booms
Northrup Grumman	Telescoping Tube Masts

6.3.3 Robotic Manipulator

The need for in-space servicing is receiving more attention from the SmallSat community with the increasing demand for more complex SmallSat systems with greater capability and longer mission lifetimes. These types of challenges are being solved with robotic manipulation systems that can perform intricate actions in space. Tasks such as repairing defunct satellites, in-orbit assembly, satellite servicing, debris capture, spacecraft system upkeep, construction, and repair are important advances for future space operations; however, these activities remain expensive and high risk. Current robotic solutions for in-space construction and repair involve humans and use very large, expensive, custom-built robotic arms with limited capabilities, such as the Canadarm. As NASA's Artemis architecture prepares for astronaut presence in lunar and deep space missions on the Lunar Gateway, there is a growing need for more advanced and maneuverable space robotic systems. The use of these sophisticated robotic systems on a SmallSat is more attractive than traditional larger platforms as SmallSats present a more cost-effective and agile solution. A more agile robotic system can be stowed in a small volume and deployed to perform several tasks automatically or semi-automatically.

This section provides an overview of the ongoing efforts to further develop robotic systems on SmallSats. Table 6-7 lists a non-exhaustive set of ongoing developments. This type of SmallSat mechanism is maturing through research and development across government, academia, and commercial entities (42). For example, the Naval Academy Satellite Team for Autonomous Robotics (NSTAR) has developed an autonomous 3U CubeSat robotic arm system called the Robotic Experimental Construction Satellite (RECS) for testing on the ISS. RECS was launched in November 2022 (43).

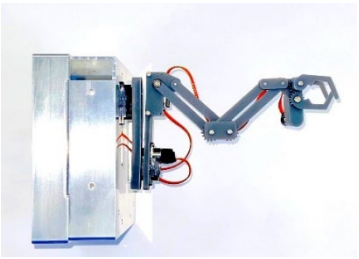


Figure 6.7: RECS robotic arm. Credits: US Naval Academy.

Table 6-7: Robotic Arms for Small Spacecraft

Manufacturer	Product	Mass (kg)	Extendable ength (mm)	Stowed Envelope (mm)	DOF	Power Consumption (W)	Actuator method	Form Factor
U.S. Naval Academy	3U CubeSat with two robotic arms	4	600	300x100x100	6 plus "claw" end-effector actuation	-	Stepper motor	RECS 3U (Nov 2022)
Redwire Space	-	-	1 to 4 m reach	-	5 to 7	8 to 65	-	ESPA class satellites
Sierra Lobo	Sierra Lobo Arm (SLAC 1)	-	100x100x100	30x50x65	3	1.5	-	-

- Represents unknown data

6.3.4 Reliability Considerations

Mechanisms add capabilities and complexities to small satellite design, and therefore additional integration and testing are required. NASA Reliability and Maintainability Standard (44) describes maintainability, and "test as you fly," along with other mitigation strategies and considerations. For

mechanisms, it is important to test the full subsystem and system integration levels for power consumption and subsystem dependencies. Mechanisms have lifetimes, so it is important to ensure maintainability and understand mechanism lifetime from test to flight. Because mechanisms add complexity and can introduce single-point failure risk in some instances, such as attitude control, solar panel pointing, directional antenna control, or one-time subsystem deployment switches, it is important to focus on reliability strategies. Mechanisms have contributed to over 10% of reported small satellite failures (45). Adding a mechanism to enable a mission generally increases risk.

The space environment adds to reliability considerations for operations in vacuum, plasma, or extreme thermal environments. For mechanism reliability, there are multiple steps that contribute to risk mitigation. Sarafin et al. describe a multi-step approach for a reliable mechanism design, including design simplicity, margin, supplier selection, and testing (46). The steps include guidance for torque margin for rotating components, such as solar panel and antenna pointing motors (46)(47)(48). During ground testing of mechanisms, it is important to understand mechanism lifetime to ensure the component performs throughout the planned mission duration. Materials considerations contribute to mechanism reliability in the space environment, including lubricant use and material coatings to avoid corrosion and welding of dissimilar materials (47)(48)(49). Because mechanisms are critical for advanced spacecraft capabilities, including power, communications, and science/research instruments, it is important to add mechanism margin and testing to spacecraft development and/or subsystem and system integration.

6.4 State-of-the-Art – Polymeric Additive Manufacturing

Additive manufacturing (AM) processes for primary spacecraft structures have long been proposed but only recently have such methodologies been adopted for flight. AM has been common for SmallSat secondary structural elements for many years. Typically, the advantage of AM is to free the designer from constraints imposed by standard manufacturing processes and to allow for monolithic structural elements with complex geometry. In practice, additive manufacturing has a separate design space and design process, which has seen tighter integration into computer-aided design (CAD), computer-aided manufacturing (CAM), and modal and structural analysis packages in the past few years. Such tools can enable quicker turnaround times for SmallSat development and have been instrumental in mass optimization, the use of AM materials for radiation shielding, and enabling high-throughput, high-quality manufacturing. As the AM field is rapidly evolving, this section makes a best attempt to cover as many materials and printers as possible that are potentially applicable to SmallSat development.

6.4.1 Applicability of TRL to Polymer AM

While AM systems and platforms might be considered mature and of high TRL, the TRL of AM parts configured for spaceflight depends on the material, the configuration of the actual part, the manufacturing process used, the postprocessing of the manufactured part, the testing and qualification process, and many other factors. For example, nylon fabricated with a fused filament fabrication (FFF) system will have different bulk structural properties from nylon fabricated with a selective laser sintering (SLS) system. Furthermore, printer and material settings (e.g., temperature) also play a role in final part properties, meaning the same part from the same material on the same machine can have different properties if the parameters vary.

In other words, a TRL might be assignable to a component created through a particular manufacturing process with a specific material. If a particular component manufactured with nylon on an FFF system was flown to LEO successfully, the TRL for this component would be Level 7. If this component was subsequently flown on another mission manufactured with Antero 840

PEEK also on an FFF system, the TRL would still be 7. Documentation of the manufacturing process is important to properly account for the TRL. This section focuses on polymer AM and does not address metal AM for SmallSats.

6.4.2 Inspection and Testing

When new materials and/or processes are used, testing must be performed to minimize risk and bridge the gap between TRL levels. In particular, the only way to validate a tailored structure, component, or material is through testing, especially if more freedom is afforded to research and development. For new material types, if there is latitude afforded in upfront research and development, mechanical, modal, and thermal tests should be performed to compare against a known, proven baseline structural design.

6.4.3 Thermoplastics and Photopolymers

With the expansion of available open-source AM platforms in the last decade, thermoplastics and photopolymer materials have rapidly gained traction and acceptance in many applications ranging from mechanical validation and fit-checking to engineering-grade, low-rate production applications. Photopolymer or “thermoset” resins and associated manufacturing processes have improved to the point where microfluidics experiments may be additively manufactured, with the microfluidics channels and growth chambers directly manufactured as one piece, as opposed to traditional approaches of machining plastic or glass blocks.

As of publication, there are three primary methods of conducting AM for plastics: FFF (also referred to as fused deposition modeling (FDM)), which uses thermoplastics in either a spool or pellet form; stereolithography (SLA), which uses photopolymer resin; and SLS, which uses a fine powder or photoset resin. Within SLA, there are two methods of curing resin: digital light projection (DLP), which uses a very high-resolution LED matrix – a monochrome display – to cure the entire layer nearly instantly; and polyjet (also known as resin jet) which deposits resin from a line array of jets, much like an inkjet printer with a large print head.

Certain thermoplastics are quickly gaining acceptance for high-reliability parts and applications on Earth, although, as of this writing, they have yet to gain widespread acceptance for space applications. One reason for this is that AM methods cannot yet produce surfaces as smooth as machined metals, which is often a requirement for parts with tight tolerances. However, some thermoplastics are machinable, such as nylon or polyetherimide (PEI). Like the manufacture of cast iron parts, machining to a final, high tolerance specification may allow these thermoplastics to gain further acceptance.

Except for some large-format AM centers, almost all thermoplastics are manufactured in spools and may or may not be packaged for proprietary solutions. For SLA, almost all resins are used specifically for commercial solutions and dedicated AM centers. Additionally, some manufacturers may mix in additives to enhance material properties or to ease the printing process. Because of this, the following sections on each material include a table of materials for both open-source and commercial solutions, along with selected properties of interest. Availability of recommended nozzle and bed temperatures is indicative of the ability to be printed on an open-source machine, unless otherwise noted in the material description. Materials are not picked according to preference but based on the availability of technical specifications and potential applicability. For various types of AM solutions, readers are encouraged to use these sections as a rough guide for currently available commercial filaments. Additionally, the material tables will be expanded as more data is obtained for these materials.

Surface discharge, or electrostatic discharge (ESD), is a result of in-space charging effects and is caused by interactions between the space plasma environment and spacecraft

materials and electronic subsystems (50). The field buildup and ESD can negatively affect the spacecraft, and there are design precautions which must be considered depending on the spacecraft's operational environment. Per ESD guidelines from NASA Spacecraft Charging Handbook 4002A, dielectric materials above 10^{12} Ohm (Ω) cm should be avoided because charge accumulation occurs regardless. Please refer to the NASA Handbook 4002A, 5.2.1.5 Material Selection for more information. Historically, ESD due to faulty grounding has been a leading cause of spacecraft or subsystem failures (50). Most ESD rated thermoplastics have a surface resistivity between 10^6 and 10^9 ohms. Increasing the extrusion temperature decreases the surface resistivity.

Polylactic Acid (PLA)

PLA is the most common filament used in AM, and Table 6-7 lists several PLA filaments. It exhibits very low shrinkage and is extremely easy to print because it does not require a high-temperature bed or a heated build chamber and requires a relatively low extruder (nozzle) temperature. It also has low off-gassing during printing, which is important in open-frame AM systems in rapid prototyping environments such as lab settings. Unless the application has a very short-term exposure to harsh conditions, and if the conditions are well characterized and controlled, it is not recommended to use PLA for an application beyond TRL 3-4. For laboratory settings in controlled environments not subject to excessive mechanical forces, ESD-compatible filaments are available.

Table 6-7: Polylactic Acid Filaments

Filament Name (Citation)	ISO 75/ASTM D648 Deflection Temp (°C)	ISO 179-1 Hardness (kJ/m^2) or Izod D256-10A (J/m)	ISO 527-1/ASTM D638 ZX Tensile strength (MPa)	ASTM D790/ISO 178 Flexural strength (MPa)	Nozzle Temp (°C)	Bed Temp (°C)	Density (g/cc)	ESD Risk* (Ω-cm)
Prusament PLA	55	12 kJ/m^2	57	N/A	215	50-60	1.24	No
Verbatim PLA	50	16 kJ/m^2	63	N/A	210	50-60	1.24	No
ColorFabb PLA-PHA (51)	N/A	30 kJ/m^2	61	89	210	50-60	1.24	No
Stratasys PLA (52)	51	27 kJ/m^2	26	84	N/A	N/A	1.264	No, 10^{15}
3DXSTAT™ ESD-PLA	55	N/A	55	95	210	23-60	1.26	Yes, 10^6-10^9

Acrylonitrile Butadiene Styrene (ABS)

ABS has traditionally been the choice for higher-strength, lightweight prints from the FDM process in the open-source community. In the early days of hobbyist 3D printing, ABS was a preferred material because there was an existing supply chain making ABS filaments for weed-whackers. It is generally temperature-resistant and UV resistant but turns yellow and eventually becomes more brittle over time when exposed to sunlight. It is a moderately difficult filament to print, especially in open-frame systems. High temperature gradients during printing may cause warping as parts get larger. Enclosed AM systems with heated chambers print ABS well. For many systems, passive chamber heating is sufficient, although active heating can provide better results. Extrusion and bed temperatures for ABS tend to be slightly higher than those for PLA. Additionally, ABS shrinks 1 to 3 percent of its printed size upon cooling; the shrinkage varies from manufacturer to manufacturer and, to a lesser extent, can also be affected by the rate of cooling. ABS has flown as the complete structure for KickSat-2, a femtosat deployer for chip-scale satellites (53). The single-use design, short mission duration, and intricate dispenser frame made a conventionally machined deployer mass- and cost-prohibitive. Table 6-8 lists some examples of ABS filaments.

Table 6-8: ABS Filaments

Filament Name	ISO 75/ASTM D648 Deflection Temp (°C)	ISO 179-1 Hardness (kJ/m^2) or Izod D256-10A (J/m)	ISO 527-1/ASTM D638 Tensile strength (MPa)	ASTM D790/ISO 178 Flexural strength (MPa)	Nozzle Temp (°C)	Bed Temp (°C)	Density (g/cc)	ESD Risk (Ω-cm)
Stratasys ABS-CF10	100	20-51 J/m	21	29-69	N/A	N/A	1.0972	Marginal 10^4-10^9
Stratasys ABS-ESD7	105	36.2 J/m	35	44	N/A	N/A	1.07	Marginal 10^4-10^9
3DXSTAT™ ESD-ABS	97	N/A	58	80	230	110	1.09	Yes, 10^6-10^9
Verbatim ABS	106 (ISO 306)	21 J/m	47	78	240-260	90	1.05	No
Kimya ABS Carbon	N/A	N/A	36.7	N/A	250-260	90-100	1.05	N/A

Nylon

Versatile and tough, there are multiple formulations for nylon that allow for a very wide range of applications and material properties. In general, nylon is more difficult to manufacture than ABS on open-source FFF systems because it requires an enclosure for thermal stability and additional bed preparation for improved adhesion. It is also extremely hygroscopic; if possible, filament should be baked out before printing and must be kept in a dedicated dry box while printing or while being stored. Nylon and composite blends are very common because they can achieve high part strength at a lower price than many of the higher-end thermoplastics. Secondary structural pieces have been flown through the TechEdSat program using Markforged Onyx carbon fiber filaments as a flight example. Table 6-9 lists some representative examples of nylon filaments.

Table 6-9: Nylon Filaments

Filament Name (Citation)	ISO 75/ASTM D648 Deflection Temp (°C)	ISO 179-1 Hardness (kJ/m^2) or Izod D256-10A (J/m)	ISO 527-1/ASTM D638 ZX Tensile strength (MPa)	ASTM D790/ISO 178 Flexural strength (MPa)	Nozzle Temp (°C)	Bed Temp (°C)	Density (g/cc)	ESD Risk (Ω-cm)
Taulman3D Alloy 910 (54)	82	N/A	56	N/A	250-255	30-65	N/A	Unk
Taulman3D Alloy 910 HDT (54)	112	N/A	56	N/A	285-300	55	N/A	Unk
Taulman3D Nylon 680 Food Grade (55)	N/A	N/A	47	N/A	250-255	30-65	N/A	No
Markforged Onyx ESD (56)	138	44 J/m	52	83	285	non-heated	1.2	Yes, 10^5-10^7
3DXTECH CARBONX™ HTN+CF (57)	240	N/A	87	95	295	130	1.24	Marginal 10^9
Stratasys Nylon 12 (58)	92-95	71-138 J/m	33-42	55-57	N/A	N/A	1.01	No, 10^{13}
Novamid 1030 PA-CF10	153-184	N/A	38	70	275	60	1.17	--

Polycarbonate (PC)

Also known as Lexan™, this thermoplastic has some of the highest impact resistance, tensile strength, and temperature resistance available for most open-source-based AM systems. After manufacturing, it is dimensionally stable and exhibits very stiff behavior. However, it is difficult to print on open-frame, open-source AM systems due to very high warping, especially when printing large components. Very high bed, chamber, and nozzle temperatures are required, and poor adhesion to the bed is a common issue. Interface adhesives are recommended to improve print-bed adhesion. It is also highly hygroscopic; if possible, the filament should be baked out before printing and kept in a dedicated dry box while printing and during storage. Certain filaments, like the Prusament PC Blend, have additives to mitigate some of the difficulties of printing PC, particularly those related to its higher temperature requirements. Table 6-10 lists some representative polycarbonate filaments.

Table 6-10: Polycarbonate Filaments

Filament Name (Citation)	ISO 75/ASTM D648 Deflection Temp (°C)	ISO 179-1 Hardness (kJ/m^2) or Izod D256-10A (J/m)	ISO 527-1/ASTM D638 ZX Tensile strength (MPa)	ASTM D790/ISO 178 Flexural strength (MPa)	Nozzle Temp (°C)	Bed Temp (°C)	Density (g/cc)	ESD Risk (Ω-cm)
Prusament PC Blend (59)	113	No break for ISO 179	63	88-94	275	110	1.22	No
Prusament PC Blend Carbon Fiber (59)	114	35 kJ/m^2	55-65	85-106	285	110	1.16	No
Stratasys PC (60)	143	27-77 J/m	60	75	N/A	N/A	1.20	No
Polymax PC	99-114	21.5 kJ/m^2	59.7	94.1	280	100	1.19	--
3DXtech ESD-PC	135	N/A	68	95	295	130	1.24	10^7 - 10^9
3DXtech CF-PC	133	N/A	70	90	300	140	1.36	--
Polymaker PC-ABS	106	25.8 kJ/m^2	39.9	66.3	250-270	90-105	1.1	--

Windform

Manufactured by CRP Technology, these proprietary materials are classified as a carbon-fiber-reinforced polymer originally designed for the automotive racing industry. They are unique in that these composites are manufactured through selective laser sintering (SLS) (61). This results in higher dimensional stability and more isotropic properties than FFF, as well as the ability to produce small features slightly better than the FFF process. Windform XT 1.0 and 2.0 have been used on CubeSat and PocketQube platforms and have flight heritage through KySat-2 (launched on ELaNa IV) and TANCREDO-1 (launched through the ISS via JEM in 2017) (62). The PACE-1 CubeSat also used Windform 3D-printed components to mount optical devices. Table 6-11 lists representative CRP Windform filaments. The NASA GPX-2 Windform XT 2.0 structure launched in July 2022 and is currently operational. Some of the printed parts in the Crew Dragon spacecraft are made from Windform SP.

Table 6-11: CRP Windform

Filament Name (Citation)	ISO 75/ASTM D648 Deflection Temp (°C)	ISO 179-1 Hardness (kJ/m^2) or Izod D256-10A (J/m)	ISO 527-1/ASTM D638 ZX Tensile strength (MPa)	ASTM D790/ISO 178 Flexural strength (MPa)	Manufacturing process	Bed Temp (°C)	Density (g/cc)	ESD Risk (Ω-cm)
Windform XT 2.0	173	4.72 kJ/m^2	84	133	N/A, SLS	N/A, SLS	1.097	Yes 10^8
Windform RS (64)	181	10.8 kJ/m^2	48-85	139	SLS	SLS	1.10	Yes 10^8
Windform SP	187	5.82 kJ/m^2	76.1	120.1	SLS	N/A	1.11	Yes $<10^8$

Polyetherimide

Polyetherimide (PEI), also known by the Saudi SABIC trade name Ultem™, is a very tough thermoplastic resin with high thermal and chemical stability. It is inherently flame-resistant and can be machined. Some formulations of PEI are FAA-approved for flame, smoke, and toxicity (FST), and may also have ESD formulations. PEI is also known for extremely low off-gassing, which is crucial for optical components and sensitive scientific packages. PEI requires high nozzle and bed temperatures. For all but the smallest of parts, a heated chamber is required, with temperatures in excess of 120°C producing the best results. Due to these factors, PEI is only reliably printable on commercial FFF systems. It is also highly hygroscopic; filament should be baked out before printing and kept in a dedicated or heated dry box while both printing and in storage. PEI has similar characteristics to polyetheretherketone (PEEK), typically with slightly lower mechanical strength. PEI is a common bed material for higher-end open-source FFF systems due to its adhesive properties with other thermoplastics at higher temperatures. Ultem 1010 tends to have better mechanical properties than Ultem 9085; however it is generally more

challenging to print due to lower bed adhesion. Table 6-12 lists some representative PEI filaments.

Table 6-12: PEI Filaments

Filament Name (Citation)	ISO 75/ASTM D648 Deflection Temp (°C)	ISO 179-1 Hardness (kJ/m^2) or Izod D256-10A (J/m)	ISO 527-1/ASTM D638 ZX Tensile strength (MPa)	ASTM D790/ISO 178 Flexural strength (MPa)	Nozzle Temp (°C)	Bed Temp (°C)	Density (g/cc)	ESD Risk
THERMAX™ Ultem™ 9085	158	N/A	63	90	275	115	1.34	No
3DXSTAT™ Ultem™ 1010 CF-ESD (65)	205	N/A	62	115	395	150	1.34	Yes, 10^7-10^9
Stratasys Ultem™ 1010 CG(66)	212	22-27 J/m	81	82-128	N/A	N/A	1.29	No, 10^{14}
Stratasys Ultem™ 9085 (67)	153	39-88 J/m	69	80-98	N/A	N/A	1.27	No, 10^{15}
Zortrax Z-PEI 9085 (68)	186	N/A	54	90	N/A	N/A	1.34	No
Sabic Ultem™ AM9085F	175	33-104 J/m	80	90	345	180	1.28	10^{15}
CarbonX CF-Ultem™ 9085	165	N/A	93	120	390	140	1.39	--
CarbonX CF-Ultem™ 1010	205	N/A	145	120	385	140	1.31	--

PAEK

Polyetheretherketone (PEEK) and polyetherketoneketone (PEKK) – in the polyaryletherketone (PAEK) family – are the highest-performing thermoplastics developed as of this writing. With certain additives and matrix materials, they can rival the strength of stainless steel and withstand over 200°C continuously in some formulations after annealing. Annealing PEEK/PEKK can cause part shrinkage up to 3% this should be accounted for in either the original design or in the part slicing software. PEEK/PEKK are naturally flame-retardant; they are widely accepted for use in aviation ducting. They also achieve extremely low off-gassing in operation, which makes these thermoplastics good candidates for compatibility with optical components in space. Due to the extreme conditions required for manufacturing and the very high filament cost, these materials are only reliably available for printing in extremely robust commercial FFF systems with sealed and heated chambers. It is also highly hygroscopic; filament should be baked out before printing and kept in a dedicated or heated dry box while both printing and in storage. PEEK has heritage on long-term, external ISS experiments and structural elements on the Juno spacecraft, making

it suitable for extreme radiation environments (69). Table 6-13 lists some representative PAEK-based filaments.

Table 6-13: PAEK-based Filaments

Filament Name (Citation)	ISO 75/ASTM D648 Deflection Temp (°C)	ISO 179-1 Hardness (kJ/m^2) or Izod D256-10A (J/m)	ISO 527-1/ASTM D638 ZX Tensile strength (MPa)	ASTM D790/ISO 178 Flexural strength (MPa)	Nozzle Temp (°C)	Bed Temp (°C)	Density (g/cc)	ESD Risk (Ω-cm)
3DXSTAT™ ESD-PEEK (70)	140	N/A	105	141	380-400	150	1.32	Yes, 10^7-10^9
3DXSTAT™ ESD-PEKK	185	N/A	109	135	375	140	1.34	Yes, 10^7-10^9
CarbonX™ CF PEKK-Aerospace	285	N/A	126	178	390	140	1.33	Yes, 10^7
Stratasys Antero 840 (71)	150	28-43 J/m	95	87-139	N/A	N/A	1.27	Yes, 10^4-10^9
Zortrax Z-PEEK (72)	160	N/A	100	130	N/A	N/A	1.30	N/A
Thermax PEKK	150 (182 post anneal)	N/A	105	95 (134 post anneal)	350-370	140	1.27	--
Kimya CF-PEKK	150	N/A	39.1	85.9	370	150	1.27	--
3DGence PEEK	N/A	5 kj/m^2	105	130	420	100	N/A	--
CarbonX PEEK-CF10	265	N/A	105	136	400	140	1.39	--
CarbonX PEEK-CF20	305	N/A	126	145	420	140	1.39	$<10^6$

Photopolymers

Otherwise known as “thermosets,” these materials are liquid polymers cured by optical and thermal processes. Compared to other AM processes, photopolymers and their manufacturing processes allow for superior isotropic material properties, very high resolution, and the ability to manufacture optical-quality parts. In general, photopolymers produce parts that are more brittle than their thermoplastic counterparts; special selection is required for more ductile properties. Some formulations, especially from 3D Systems and Stratasys, are designed for extreme temperature resistance and strength, desirable in aerospace applications. In some cases, the listed heat deflection temperature (HDT) may be superior to those of PAEK materials. As previously discussed, there are three major methods of curing photopolymers, one of which is

proprietary. Many photopolymers are specifically paired for commercial systems. As a result, Table 6-14 includes the commercial system associated with the photopolymer.

Some of the photopolymers listed below have several additional characteristics not listed in this table, including, but not limited to, elasticity, tear strength, optical clarity, water absorption, and medical grade certifications. Such characteristics may be useful for biological experiments in future SmallSat missions. Please consult the products' specific websites and datasheets for additional detailed information. Additionally, photopolymers printed via a polyjet process have the advantage of being able to be mixed, in-situ, as the object is being manufactured. This allows for continuously varying material properties throughout the object. All photopolymer printing processes require at least a two-step post-processing process consisting of a print wash and curing step. Table 6-14 lists some representative photopolymers.

Table 6-14: Photopolymers

Photopolymer Name (Citation)	ISO 75/ASTM D648 HDT (°C)	ISO 179-1/ASTM D256-10A (J/m)	ISO 527-1/ASTM D638 Tensile (MPa)	ASTM D790 Flexural (MPa)	Density (g/cc) at 25°C	ESD Risk (Ω-cm)	Manufacturing and/or Machine Type
Accura Bluestone (73)	267-284	13-17	66-68	124-154	1.78	ND	3D Systems ProX 800
VisiJet M2S-HT250 (74)	250	10	51	83	1.15	ND	3DS MJP 2500 Plus
DSM Somos® Watershed XC	50	25	50	69	1.12	ND	Stratasys V650 Flex SL
Henkel LOCTITE® IND402 A70 Flex (75)	N/A	N/A	5.5	N/A	1.068	ND	Several
Henkel LOCTITE® 3D 3843 (76)	80	54	60	81	N/A	ND	DLP SLA types only
Somos® Perform	132-268	17-20	68-80	120-146	1.61	N/A	SLA types only

6.4.4 AM Design Optimization

Design optimization is an integral part of manufacturing validation and testing. As previously discussed for AM, validation, testing, and optimization encompass all materials and manufacturing processes. Software platforms help speed up this process, especially those that integrate toolpath generation, computer-aided manufacturing (CAM), load analysis, and infill generation. The inherent advantage of AM in allowing monolithic structural elements implies a much-expanded design space compared to subtractive manufacturing. Furthermore, AM processes can create interior features and volumes that cannot be made using subtractive processes because subtractive methods need to have access from the part exterior to any feature. Software has kept up with the pace of manufacturing advances and incorporates tools to assist with AM designs.

The manufacturing ecosystem includes software ranging from simple CAM solutions generating toolpaths (G-code) to comprehensive structural analysis and high-fidelity manufacturing simulations. As of this writing, AM has gained significant traction and value in low-TRL demonstrations and physical validation, partly due to the ease of fabrication in typical AM ecosystems. It is beginning to displace traditional machining – "subtractive" manufacturing – as AM systems have matured enough to print advanced thermoplastics, resins, and metals.

Infill Patterns

Due to the flexibility that AM offers, new methods of structural lightweighting are now possible. "Lightweighting" refers to the reduction of mass in structural elements, without compromising structural integrity. The best examples of well-proven heritage methods of lightweighting are "honeycomb" sandwiched aluminum panels, subtractive machining, and truss structures. However, such methods have certain limitations. Honeycomb panels, for example, do not have uniform, or isotropic, properties as they do not exhibit the same stiffness in all directions.

Lightweighting in AM encompasses what is called "infill," or the internal structure of a typically hollow body or panel. With a minimal increase in mass, an internal structure manufactured with AM can vastly increase the strength of a body. Very recently, the AM community has renewed interest in the use of the gyroid pattern, discovered by NASA researcher Alan Schoen in 1970, due to the ease of generation in AM toolpath programs, as well as its rotational nature which minimizes any empty columns in a part. Aside from honeycomb and gyroids, several options for infill exist. Different options are offered with different AM-focused software packages. Newer software allows for variable density infills and higher pattern density (and thus strength where needed), and lower pattern density in other regions to reduce overall mass.

Multi Material Parts

Many AM platforms use more than one type of material in their part fabrication process. The use of dissimilar materials creates volumes within a part with varying strength, flexibility, chemical resistance, color, and other characteristics. Depending on the size of the volumes and their compatibility with each other, a geometric feature may be required to lock them together. FDM platforms primarily use multiple extruders with their own material feeds for multi-material printing. Tool changing printers that swap out different extruder assemblies during printing are also starting to enter the consumer market. At the time of writing, there is a small but growing number of open-source FFF printers that feed multiple different filaments through the same nozzle by automatically swapping filaments, having multi-in one out nozzles, splicing strands of different filament together, or using filaments made from multiple polymers. Methods such as these tend to be more limited than multi-tool methods because the extrusion temperature ranges of the materials used need to be similar to prevent printing issues. Multi-material printing is achieved in SLS platforms by depositing different powdered materials or binding agents on a given layer. For SLA printing, polyjet systems can use multiple materials in a single print.

The most common use of multi material printing is to use a separate polymer for the support structure. A second polymer that is chemically soluble, in a solution the model material is not, can allow for the creation of more complex part geometries that could potentially be damaged, or would be inaccessible, from mechanical removal. Low temperature FFF applications primarily use polyvinyl alcohol (PVA) or butene-diol vinyl alcohol (BVOH) as a water-soluble support structure. Higher temperature FFF support materials tend to be proprietary formulations based on acrylate polymers that dissolve in basic solutions. Alternatively, for chemically soluble supports, some FFF platforms will use a support material that has poor adhesion to the model material, so it can be mechanically removed more easily.

Digital Materials

Both honeycomb panels and AM parts with infill have a common, repetitive unit cell. By repeating this unit cell throughout the interior of a part, or as a structure on its own, a larger structure may be made. Further, by defining properties within this unit cell, information can effectively be encoded into the design, allowing for differing behavior across different parts of the structure. Digital materials can dramatically expand the design space of a structure, allowing for targeted optimization of various properties such as mass to strength ratios, flexibility, structural lightweighting, and others. As previously discussed, with certain resin polyjet AM centers, resins can be mixed in real time to form an object that has continuously varying properties. For example, a part could be made to have a gradient from a rigid to a flexible material that would facilitate bending in one axis over another.

6.5 Radiation Effects and Mitigation Strategies

6.5.1 Shielding from the Space Environment

Radiation shielding has been described as a cost-effective way of mitigating the risk of mission failure due to total ionizing dose (TID) and internal charging effects on electronic devices. In space mission analysis and design, the average historical cost for adding shielding to a mission is below 10% of the total cost of the spacecraft (77). The benefits include reducing the risk of early total ionizing dose-induced electronics failures (78). Some of the key CubeSat and SmallSat commercial electronic semiconductor parts include processors, voltage regulators, and memory devices, which are key components in delivering scientific and technology demonstration data (79).

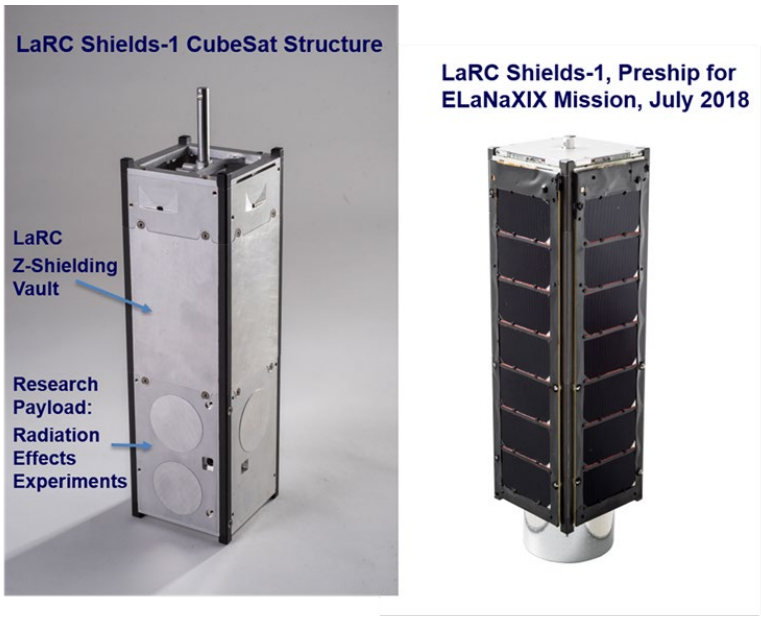
Shielding the spacecraft is often the simplest method to reduce both a spacecraft's ratio of total ionizing dose to displacement damage dose (TID/DDD) accumulation, and the rate at which single event upsets (SEUs) occur when applied appropriately. Shielding involves two basic methods: shielding with the spacecraft's pre-existing mass (including the external skin or chassis, which exists in every case whether desired or not) and spot/sector shielding. This type of shielding, known as passive shielding, is most effective against lower energy radiation and is best used against high particle flux environments, including the densest portions of the Van Allen belts, the Jovian magnetosphere, and short-lived solar particle events. In some cases, increased shielding is more detrimental than if none was used, owing to the secondary particles generated by highly penetrating energetic particles. Therefore, it is important to analyze both the thickness and type of materials used to shield all critical parts of the spacecraft. Due to the strong omnidirectionality of most forms of particle radiation, spacecraft need to be shielded from the full 4π steradian celestial sphere. This brings the notion of "shielding-per-unit-solid-angle" into the design space, where small holes or gaps in shielding are often only detrimental proportionally to the hole's solid angle as viewed by the concerned electrical, electronic and electro-mechanical (EEE) components. Essentially, completely enclosing critical components should not be considered a strict design constraint when other structural considerations exist.

6.5.2 Inherent Mass Shielding

Inherent mass shielding consists of using the entirety of the pre-existing spacecraft's mass to shield sensitive electronic components that are not heavily dependent on their location within the spacecraft. This often includes the main spacecraft bus processors, power switches, etc. Again, the notion of "shielding-per-unit-solid-angle" is invoked here, where a component could be well shielded from its "backside" (2π steradian hemisphere) and weakly shielded from the "front" due to its location near the spacecraft surface. It would only then require additional shielding from its front to meet operational requirements. The classic method employed here is to increase the

spacecraft's structural skin thickness to account for the additional shielding required. This is the classic method largely due to its simplicity, where merely a thicker extrusion of material is used for construction. The disadvantage to this method is that the material used, very often aluminum, is mass optimized for structural and surface charging concerns and not for shielding either protons/ions or electrons. Recent research has gone into optimizing structural materials for both structural and shielding concerns; currently an active area of NASA's Small Business Innovation Research (SBIR) program research and development.

The process to determine exactly how much inherent shielding exists involves using a reverse ray-tracing program on the spacecraft solid model from the specific point(s) of interest. After generating the "shielding-per-unit-solid-angle" map of the critical area(s) of the spacecraft, a trade study can be performed on how and where best to apply further shielding.



Shields-1 structure and Final Preship Picture with LaRC Z-Shielding Vault and Experiment, Solar Panels and Thermal Radiator

Figure 6.14: Shields-1 Z-shielding structure and final preship picture, ELaNaXIX Mission. Credit: NASA.

Numerous CubeSat and SmallSat systems use commercial processors, radios, regulators, memory, and SD cards. Many of these products rely on silicon diodes and metal oxide semiconductor field effect transistors (MOSFETs) in these missions. A comprehensive NASA guidance document on the use of commercial electronic parts was published for the ISS orbit, which is a low-Earth orbit where the predominant radiation source is the South Atlantic anomaly. The hardness of commercial parts was noted as having a range from 2-10 kRad (80). For typical thin CubeSat shielding of 0.20 cm (0.080 in) aluminum, yearly trapped dose is 1,383 Rad; with an additional estimated 750 Rad from solar particle events, the total dose increases to 2,133 Rad for the ELaNaXIX Mission environment at 85 degrees inclination and 500 km circular orbit (Table 6-16) (81). Adding a two-fold increase for the trapped belt radiation uncertainty brings the total radiation near the TID lifetime of many commercial parts (80), even before estimating a SPE TID contribution. The uncertainty of radiation model results of low-Earth orbit below 840 km has been estimated as at least a two-fold factor; Van Allen Belt models are empirical and rely on data in the orbital environment (82). The NASA Preferred Reliability Series "Radiation Design Margin Requirements" also recommends a radiation design margin of 2 for reliability (83). Currently, The Aerospace Corporation proton (AP) (63) and The Aerospace Corporation electron (AE) (85) models do not have radiation data below 840 km, and radiation estimates are extrapolated for the lower orbits (82). For spacecraft interplanetary trajectories near the Sun or Earth, the radiation contributions from SPEs will be higher than low-Earth orbit, where there is some limited SPE radiation protection by the magnetosphere. By reducing the total ionizing dose on commercial

parts, the mission lifetimes can be increased by reducing the risk of electronic failures on sensitive semiconductor parts.

6.5.3 Shields-1 Mission, Radiation Shielding for CubeSat Structural Design

Shields-1 launched through the ELaNaXIX Mission in December 2018, and while in LEO increased the development level of atomic-number (Z) Grade radiation shielding with an electronic enclosure (vault) and Z-grade radiation shielding slabs with aluminum baselines experiments (Figure 6.14) (86). Preliminary results in Table 6-15 show a significant reduction in total ionizing dose in comparison to typical modeled 0.20 cm (0.080 in) aluminum structures sold by commercial CubeSat providers. The 3.02 g cm^{-2} Z-shielding vault has over an 18 times reduction in total ionizing dose compared to modeled 0.20 cm aluminum shielding (81).

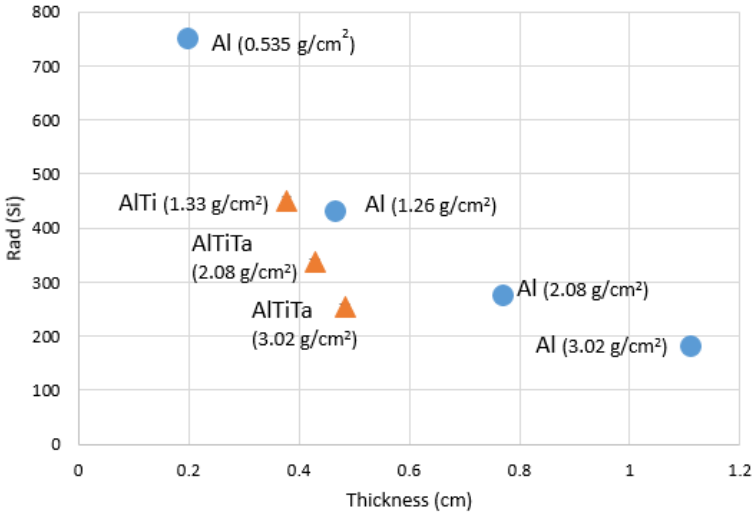


Figure 6.15: SPE Contribution to TID in PLEO, King Sphere Model, ELaNaXIX Shields-1 orbit. Credit: NASA.

Z-shielding enables a low-volume shielding solution for CubeSat and SmallSat applications where reduced volume is important. AlTiTa, Z–shielding, at 2.08 g cm^{-2} reduces the dose from a SPE by approximately half when compared to a standard 0.2 cm aluminum structure (Figure 6.15). NASA has innovated “Methods of Making Z-Shielding” with patents in preparing different structural shielding approaches (87)(88)(89)(90), from metals to hybrid metal laminates and thin structural radiation shielding, to enable low-volume integrated solutions with CubeSats and SmallSats (91).

Table 6-15: Shields-1 Experimental Total Ionizing Dose Measurements in PLEO

Shielding	Areal Density (g/cm^2)	Thickness (cm)	Trapped Belts TID Total (Rad (Si)/Year)	SPE King Sphere Model, (Rad (Si))
Al	0.535	0.198	1383+/-47 #	750+/-5
Al	1.26	0.465	**90.9 +/-2.7 (SL)**	432 +/- 7
Al	1.69	0.624	**84.3 +/-2.5 (SL)**	345 +/- 9
Al	3.02	1.11	**73.6 +/-3.2 (SL)**	183 +/- 11
AlTi	1.33	0.378	**89.7 +/-2.7 (SL)**	451 +/- 6
AlTiTa20	2.08	0.429	**84.3 +/-2.5 (SL)**	338 +/- 6
AlTiTa40	3.02	0.483	**81.9 +/-3.4 (SL) 75.6+/-3.2 (Vault)**	253 +/- 6

*Shields-1 Experimental total ionizing dose measurements in PLEO in comparison to typical 0.20 cm aluminum shielding commercially available for CubeSats and SPE additional contributions to dose. **Bold values** Shields-1 experimental results. SL = Slab, Vault = Z-Shielding electronics enclosure. # sphere Space Environment Information System (SPENVIS) Multi-layered Shielding Simulation Software (MULASSIS) AP8 Min AE8 Max modeled results. SPE King Sphere Model SPENVIS MULASSIS modeled results.*

6.5.4 Ad Hoc Shielding

There are two types of ad hoc shielding used on spacecraft: spot shielding, where a single board or component is covered in shield material (often conformally), and sector shielding, where only critical areas of the spacecraft have shielding enhancement. These two methods are often used in concert as necessary to further insulate particularly sensitive components without unnecessarily increasing the overall shield mass and/or volume. Ad hoc shielding is more efficient per unit mass than inherent mass shielding because it can be optimized for the spacecraft's intended radiation environment while relaxing the structural constraints. The most recent methods include multi-layer shields with layer-unique elemental atomic numbers, which are layered advantageously (often in a low-high-low Z scheme), known as "graded-Z" shielding, and advanced low-Z polymer or composite mixtures doped with high-Z, metallic micro-particles. Low-Z elements are particularly capable of shielding protons and ions while generating little secondary radiation, whereas high-Z elements scatter electrons and photons much more efficiently. Neutron shielding is a unique problem, where optimal shield materials often depend on the particle energies involved. Commercial options include notably Tethers Unlimited's VSRS system for small spacecraft, which was specifically designed to be manufactured under a 3D printed fused filament fabrication process for conformal coating applications (a method which optimizes volume and minimizes shield gaps).

6.5.5 Charge Dissipation Coating

The addition of conformal coatings over finished electronic boards is another method to mitigate electrostatic discharge in sensitive electronic environments. Arathane, polyurethane coating materials (92), and HumiSeal acrylic coatings (93) have been used to mitigate discharge and provide limited moisture protection for electronic boards. This simple protective coating over sensitive electronic boards helps support mission assurance and safety efforts. Charge dissipation films have decreased electrical resistances in comparison to standard electronics and have been described by NASA as coatings that have volume resistivities between 10^8 – 10^{12} ohm-cm. In comparison, typical conformal coatings have volume resistivities from 10^{12} – 10^{15} ohm-cm (50).

6.5.6 LUNA Innovations, Inc. XP Charge Dissipation Coating

The XP Charge Dissipation Coating has volume resistivities in the range of 10^8 – 10^{12} ohm-cm (Table 6-16) and is currently developing space heritage through the NASA MISSE 9 mission and Shields-1 (94). The XP Charge Dissipation Coatings were developed through the NASA SBIR program from 2010 to the present for extreme electron radiation environments, such as outer planets, medium-Earth, and geostationary orbits, to mitigate charging effects on electronic boards.

Table 6-16: XP Charge Dissipation Coating and Commercial Conformal Coating Resistivity Comparisons

Material	Volume Resistivity (Ohm-cm)
XP Charge Dissipation Coating	10^8 – 10^{12}, 4.7 x 10^9 at 25°C
Arathane 5750 A/B	9.3 X 10^{15} at 25°C, 2.0 X 10^{13} at 95°C
Humiseal 1B73	5.5 x 10^{14} Ohms (Insulation Resistance per MIL-I-46058C)

Compared to typical commercial conformal coatings, the LUNA XP Charge Dissipation Coating has reduced electrical resistance, which reduces surface charging risk on electronic boards. LUNA XP Coating (Figure 6.16) on an electronic board has transparency for visual parts inspection. For extreme radiation environments, a combination of

radiation shielding and charge dissipation coating reduces the ionizing radiation that contributes to charging and provides a surface pathway for removing charge to ground (50).

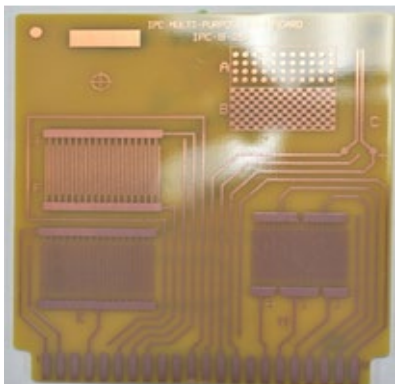


Figure 6.16: Transparent LUNA XP Charge Dissipation Coating on an electronic board. Credit: LUNA Innovations, Inc.

6.6 Summary

This chapter has been updated with the current status of structures, materials, and mechanisms for small satellite missions. Additions include custom structure references addressing the dimensional and material requirements of integrating deployment systems, new mechanisms technology to reflect the ongoing growth in SmallSat mechanical devices, and more commercially procured deployable booms and larger CubeSat primary structures (12U and 16U), as well as the upcoming DiskSat structure. The radiation environment section, state-of-the-art radiation shielding, and charge dissipation materials have been updated. Reflecting the fast pace of development in additive manufacturing, a selection of available thermoplastics and resin-based materials suitable for different TRL levels has been detailed.

There has been a high focus on deployment mechanisms with respect to lightweighting and reliability. Small spacecraft subsystems related to antenna booms, gravity gradients, stabilization, sensors, sails, and solar panels are some examples. These technologies are gaining space heritage through operations and are increasingly included in mission planning. The growth of these deployment mechanisms increases the capabilities of SmallSat technology and will be a continued focus in the next edition of this report.

For feedback solicitation, please email: arc-sst-soa@mail.nasa.gov. Please include a business email so someone may contact you further.

References

(1) Space Weather Prediction Center. Solar Cycle 25 Forecast Update. December 19, 2019. [Online] Available at: https://www.swpc.noaa.gov/news/solar-cycle-25-forecast-update

(2) R. Welle, C. Venturini, D. Hinkley, J. Gangestad, S. Grasso, A. Muszynski, R. Hunter, C. Frost, D. Mayer, and C. Baker, “DiskSat: Demonstration Mission for a Two-Dimensional Satellite Architecture,” Proceedings of the AIAA/USU Conference on Small Satellites, Out of this World!, SSC22-VIII-01, 2022.

(3) R. Hevner, W. Holemans, J. Puig-Suari, and R. Twiggs. “An Advanced Standard for CubeSat.” 2003. 25th Annual AIAA/USU Conference for Small Satellites.

(4) NASA Goddard Technical Standards, “GSFC General Environmental Verification Standard (GEVS) for GSFC Flight Programs and Projects,” GSFC-STD-7000B, 28 April 2021.

(5) Tianyuan Ye *et al.* “Review of Deployable Mechanism Test Technologies Oriented Towards Deep Space Exploration,” 2021 *IOP Conference Ser.: Material Science Engineering.* 1043 052022

(6) NASA. "Deployable Composite Booms (DCB)." August 26, 2020. [Online] Accessed May 18, 2021. Available at: https://www.nasa.gov/centers-and-facilities/langley/deployable-composite-booms-dcb/

(7) NASA. “Advanced Composite Solar Sail System: Using Sunlight to Power Deep Space Exploration.” [Online] June 23, 2021. Accessed October 2022. Available at: https://www.nasa.gov/directorates/spacetech/small_spacecraft/ACS3/

(8) Brigham Young University. “Origami-Inspired Mechanisms Explained.” 2022. Accessed October 2022. [Online] Available at: https://www.compliantmechanisms.byu.edu/about-origami-mechanisms
(9) J. Reveles et al. “In-Orbit Performance of AstroTube: AlSat Nano's Low Mass Deployable Composite Boom Payload.” Proceedings of the AIAA/USU 31st Annual AIAA/USU Conference of Small Satellites, Logan, UT, 2017.
(10) B.L. Davis, W.H. Francis, J.A. Goff, M.C. Cross, and D.J. Copel. “Big Deployables in Small Satellites,” Proceedings of the AIAA/USU Conference on Small Satellites, The Commerce of Small Satellites, SSC12-XII-1, 2014.
(11) NASA. “In-space Servicing, Assembly, and Manufacturing (ISAM) State of Play,” 2023 Edition. Available at: https://www.nasa.gov/wp-content/uploads/2023/10/isam-state-of-play-2023.pdf
(12) A. Nance and M. Thibault. “CubeSat-scale Robotic Arms in Space,” US Naval Academy. CubeSat Developer’s Workshop Conference 2023. Available at: http://mstl.atl.calpoly.edu/~workshop/archive/2023/presentations/2023_Day2_Session6_ThibaultNance.pdf
(13) NASA Reliability and Maintainability (R&M) Standard for Spaceflight and Support Systems, NASA-STD-8729.1A – 2017-06-13.
(14) Raja Pandi Perumal, Holger Voos, Florio Dalla Vedova, Hubert Moser. “Small Satellite Reliability, A Decade in Review,” SSC21-WKIII-02, 35th Annual Small Satellite Conference, Logan, UT, 2021, p.12.
(15) Thomas P. Sarafin Ed, Spacecraft Structures and Mechanisms. Damon D. Phinney and William R. Britton, Ch.19 “Developing Mechanisms,” pp.665-734.
(16) NASA Standard 5017B, “Design and Development Requirements for Mechanisms,” 12/06/2022, p. 117
(17) MIL-A-83577B (USAF), 2/1/1988, “Assemblies, Moving Mechanical, for Space and Launch Vehicles, General Specifications,” p.70.
(18) MIL-PRF-8625F w/ amendement 2, 11/23/2020, “Anodic Coatings for Aluminum and Aluminum Alloy,” p.20.
(19) NASA. Technical Handbook, “Mitigating In-Space Charging Effects – A Guideline.” NASA-HDBK-4002A. October 19, 2017.
(20) ColorFabb. “PLA/PHA.” Technical Datasheet, April 8, 2020. [Online] Available at: https://colorfabb.com/media/datasheets/tds/colorfabb/TDS_E_ColorFabb_PLA_PHA.pd
(21) Stratasys. “PLA: Economy Thermoplastic for Stratasys F123 Series Printers.” Technical Datasheet 2018. Available at: https://stratasysstorage01.file.core.windows.net/ssys-websites-files-prod/Public1/Materials/FDM/PLA/PLA%20-%20EN%20Data%20Sheet%20FDM%20Material.pdf?sv=2017-04-17&sr=f&sig=colFyWKHIkaQ9GUZsyg0%2FFwD%2FIlpuft2a2SR%2FYKqFEg%3D&st=2022-11-27T23%3A00%3A27Z&se=2023-11-28T23%3A00%3A27Z&sp=rwl
(22) NASA. “What is KickSat-2?” June 3, 2019. Accessed July 12, 2021. [Online] Available at: https://www.nasa.gov/ames/kicksat
(23) Taulman3D. “Alloy 910 Specifications.” Accessed July 12, 2021. [Online] Available at: https://taulman3d.com/alloy-910-spec.html
(24) Taulman3D. “Alloy 680 Specifications.” Accessed July 12, 2021. [Online] Available at: https://taulman3d.com/nylon-680-spec.html
(25) Markforged. “Onyx ESD™.” Technical Datasheet. Accessed July 12, 2021. [Online] Available at: https://markforged.com/materials/plastics/onyx-esd
(26) 3DXTech Additive Manufacturing. “CARBONX HTN+CF [HIGH TEMP CF NYLON].” Accessed July 12, 2021. [Online] Available at: https://www.3dxtech.com/product/carbonx-htn-cf/

(27) Statasys. “Nylon 12.” Accessed July 12, 2021. [Online] Available at: https://www.stratasys.com/materials/search/fdm-nylon-12
(28) Prusa Polymers. “Prusament PC Blend.” Technical Datasheet. [Online] Available at: https://prusament.com/media/2022/10/PCBlendCF_Prusament_TDS_2022_16_EN.pdf
(29) Stratasys. “PC (Polycarbonate): FDM Thermoplastic Filament.” Technical Datasheet, Accessed July 12, 2021. [Online] Available at: https://www.stratasys.com/-/media/files/material-spec-sheets/mds_fdm_pc_0920a.pdf
(30) CRP Technology. "High performance composite materials for SLS.” 2018. [Online] Available at: https://www.windform.com/top-line/#strength
(31) CRP Technology. “Windform 3D Printing materials launch into Orbit on KySat-2.” Accessed July 12, 2021. [Online]. Available at: https://www.crp-usa.net/windform-3d-printing-materials-launch-orbit kysat-2/
(32) CRP Technology. “Winform XT 2.0” Technical Datasheet.Accessed July 12, 2021. [Online] Available at: http://www.windform.com/windform-xt-2-0.html
(33) CRP Technology. “Winform RS” Technical Datasheet. Accessed July 12, 2021. [Online] Available at: http://www.windform.com/windform-rs.html
(34) 3DXTech Additive Manufacturing. “3DXSTAT™ ESD-Ultem™ 3D Printing Filament.” Technical Datasheet. [Online] Available at: https://www.3dxtech.com/wp-content/uploads/2020/11/ESD_Ultem_v3.pdf
(35) Stratasys. “ULTEM 1010 Resin.” Accessed July 12, 2021. [Online] Available at: https://www.stratasys.com/en/materials/materials-catalog/fdm-materials/ultem-1010/
(36) Stratasys. “ULTEM 9085 Resin.” Accessed July 12, 2021. [Online] Available at: https://www.stratasys.com/en/materials/materials-catalog/fdm-materials/ultem-9085/
(37) Zortrax. “Aerospace-Grade Flame-Retardant Filament.” Technical Datasheet, October 9, 2020, Updated June 22, 2021. [Online] Available at: https://cf.zortrax.com/wp-content/uploads/2020/10/Z-PEI_9085_Technical_Data_Sheet_eng.pdf
(38) TechBriefs. “Plastic Components Ride Juno Spacecraft to Jupiter.” August 1, 2012. [Online] Available at: https://www.techbriefs.com/component/content/article/tb/pub/features/applications/14486
(39) 3DXTech Additive Manufacturing. “3DXSTAT™ ESD-PEEK 3D Printing Filament.” [Online] Available at: https://www.3dxtech.com/product/3dxstat-esd-peek/
(40) Stratasys. “Antero 840CN03 High-Performance PEKK-Based ESD Thermoplastic.” [Online] Accessed July 12, 2021. Available at: https://www.stratasys.com/materials/search/antero-840cn03
(41) Zortrax. “Z-PEEL.” Accessed July 12, 2021. [Online] Available at: https://zortrax.com/filaments/z-peek/
(42) 3D Systems Inc. "Accura Bluestone Technical Data." September 2020. [Online] Available at: https://www.3dsystems.com/sites/default/files/2020-11/3d-systems-accura-bluestone-datasheet-usen-2020-09-15-a-print.pdf
(43) 3D Systems, Inc. “VisiJet M2S-HT250 (MJP).” Accessed June 24, 2021. [Online] Available at: https://www.3dsystems.com/materials/visijet-m2s-ht250
(44) Henkel Corporation, Loctite. “IND402TM: PhotoElastic A70 High Rebound Black.” Technical Datasheet. March 22, 2022. [Online] Available at: https://www.loctiteam.com/wp-content/uploads/2022/03/Loctite-3D-IND402-A70-High-Rebound-2022_03_22.pdf
(45) Stratasys. “LOCTITE ® 3D 3843 High Toughness by Henkel.” [Online] Available at: https://www.stratasys.com/en/materials/materials-catalog/p3-materials/loctite-3d-3843-high-toughness/
(46) J.R. Wertz and W.J. Larson. “Space Mission Analysis and Design, Third Edition.” Space Technology Library, Space Technology Series, Hawthorne, CA: Microcosm Press and New York: Springer, 1999, p.976.

(47) D. Hastings and H. Garrett, "Spacecraft Environment Interactions." New York, NY: Cambridge University Press, 1996, p.292.
(48) M. Langer and M. Boumeester. "Reliability of CubeSats – Statistical Data, Developers' Beliefs and the Way Forward," 30th Annual AIAA/USU Conference on Small Satellites, August 2016, Logan, UT, SSC16-X-2, 1-12.
(49) NASA Preferred Reliability Series PD 1258, "Space Radiation Effects on Electronic Components in Low Earth Orbit," August 1996.
(50) D.L. Thomsen. "Shields-1 Preliminary Radiation Shielding Dosimetry in Polar Low Earth Orbit," Committee on Space Research (COSPAR), Small Satellites for Sustainable Science and Development, Herzliya, Israel, 7 November 2019.
(51) Vampola, A. L. "The Space Particle Environment," NASA/SDIO Space Environmental Effects on Materials Workshop, NASA Conference Proceedings 3035, part 2, NASA Langley Research Center, Hampton, VA June 28 – July 1, 1988, pg. 367.
(52) NASA Preferred Reliability Series PD 1260, "Radiation Design Margin Requirement," May 1996.
(53) D.M. Sawyer and J.I. Vette, "AP-8 Trapped Proton Environment for Solar Maximum and Solar Minimum." NSSDC/WDC-A-R&S 76-06, 1976.
(54) J.I. Vette. "The AE-8 Trapped Electron Model Environment." NSSDC/WDC-A-R&S 91-24, 1991a.
(55) D.L. Thomsen III, W. Kim, and J.W. Cutler. "Shields-1, A SmallSat Radiation Shielding Technology Demonstration," 29th AIAA/USU Conference on Small Satellites, SSC15-XII-9, August 2015.
(56) D.L. Thomsen III, R.J. Cano, B.J. Jensen, S.J. Hales, and J.A. Alexa. "Methods of Making Z-Shielding." U.S. Patent No. 8,661,653, 4 March 2014.
(57) U.S. Patent No. 10,039,217, July 31, 2018, "Methods of Making Z-Shielding." D.L. Thomsen III, R.J. Cano, B.J. Jensen, S.J. Hales, and J.A. Alexa.
(58) D.L. Thomsen III. "Method of Making Thin Atomic (Z) Grade Shields." U.S. Patent No. 10,600,52212, March 24, 2020.
(59) D.L. Thomsen III, S.N. Sankaran, and J.A. Alexa. "Atomic Number (Z) Grade Shielding Materials and Methods of Making Atomic Number (Z) Grade Shielding." U.S. Patent No. 10,919,650, February 16, 2021.
(60) D.L. Thomsen III and W.R. Girard. "Method of Making Atomic Number (Z) Grade Small SAT Radiation Shielding Vault." U.S. Patent No. 11,043,311, June 22, 2021.
(61) Arathane. [Online] Available at: https://apps.huntsmanservice.com/WebFolder/ui/browse.do?pFileName=/opt/TDS/Huntsman%20Advanced%20Materials/English%20US/Long/Arathane%205750%20AB_LV_US_e.pdf
(62) Chase Electronic Coatings. "HumiSeal® 1B73 Acrylic Conformal Coating Technical Data Sheet." [Online] Available at: https://chasecorp.com/humiseal1/wp-content/uploads/sites/12/2018/10/1B73-TDS.pdf
(63) LUNA. "Luna coating provides radiation protection in space." [Online] February 2, 2018. Accessed June 28, 2020. Available at: https://lunainc.com/blog/luna-coating-provides-radiation-protection-space

Chapter Glossary ii
7.0 Thermal Control 198
7.1 Introduction 198
7.2 State-of-the-Art – Passive Systems 199
7.2.1 Sprayable Thermal Control Coatings, Tapes, and MLI 201
7.2.2 Thermal Straps 204
7.2.3 Thermal Contact Conductance and Bolted Joint Conductance 206
7.2.4 Thermal Interface Materials and Conductive Gaskets 206
7.2.5 Sunshields 207
7.2.6 Thermal Louvers 207
7.2.7 Deployable Radiators 208
7.2.8 Heat Pipes 209
7.2.9 Phase Change Materials and Thermal Storage Units 209
7.2.10 Thermal Switches 210
7.2.11 Multifunctional Thermal Structures 211
7.3 State-of-the-Art – Active Systems 211
7.3.1 Heaters 212
7.3.2 Cryocoolers 213
7.3.3 Thermoelectric Coolers (TECs) 214
7.3.4 Fluid Loops 215
7.4 Summary 216
References 217



Chapter Glossary

(APG)	Annealed Pyrolytic Graphite
(ATA)	Active Thermal Architecture
(BIRD)	Bi-Spectral Infrared Detection
(BOL)	Beginning of Life
(EOL)	End of Life
(ESPA)	EELV Secondary Payload Adapter
(FEP)	Fluorinated Ethylene Propylene
(FETS)	Folding Elastic Thermal Surface
(FOX)	Flat-Plate Heat Pipe On-Orbit Experiment
(GFTS)	Graphite Fiber Thermal Straps
(GSFC)	Goddard Space Flight Center
(HEC)	High Efficiency Cooler
(HX)	Heat Exchanger
(IR)	Infrared
(ISS)	International Space Station
(MLI)	Multi-Layer Insulation
(MPFL)	Mechanically Pumped Fluid Loop
(MWIR)	Midwave Infrared
(NLAS)	Nanosatellite Launch Adapter System
(OHP)	Oscillating Heat Pipe
(PCM)	Phase Change Material
(PID)	Proportional–Integral–Derivative (control algorithm)
(PFL)	Pumped Fluid Loop
(PGF)	Pyrovo Pyrolytic Graphite Film
(PGS)	Pyrolytic Graphite Sheets
(PRISM)	Portable Remote Imaging Spectrometer
(q_{albedo})	Solar heating reflected by the planet
(Q_{gen})	Heat generated by the spacecraft
($Q_{out,rad}$)	Heat emitted via radiation
($q_{planetshine}$)	IR heating from the planet
(q_{solar})	Solar heating
(Q_{stored})	Heat stored by the spacecraft
(SDL)	Space Dynamics Laboratory

(SI)	International System of Units
(SPOT)	Standard Passive Orbital Thermal-Control
(SST)	Small Satellite Technology
(TAFTS)	Two Arm Flexible Thermal Strap
(TEC)	Thermoelectric Cooler
(TMT)	Thermal Management Technologies
(TRL)	Technology Readiness Level
(TSU)	Thermal Storage Unit
(UAM)	Ultrasonic additive manufacturing
(VDA)	Vacuum Deposited Aluminum

7.0 Thermal Control

7.1 Introduction

All spacecraft components have a range of allowable temperatures that must be maintained to meet both survival and operational requirements during all mission phases. Spacecraft temperatures are determined by how much heat is absorbed, stored, generated, and dissipated by the spacecraft. Figure 7.1 shows a simplified overview of heat exchange from a satellite orbiting Earth, but the heating principles apply to any planet or body a spacecraft orbits.

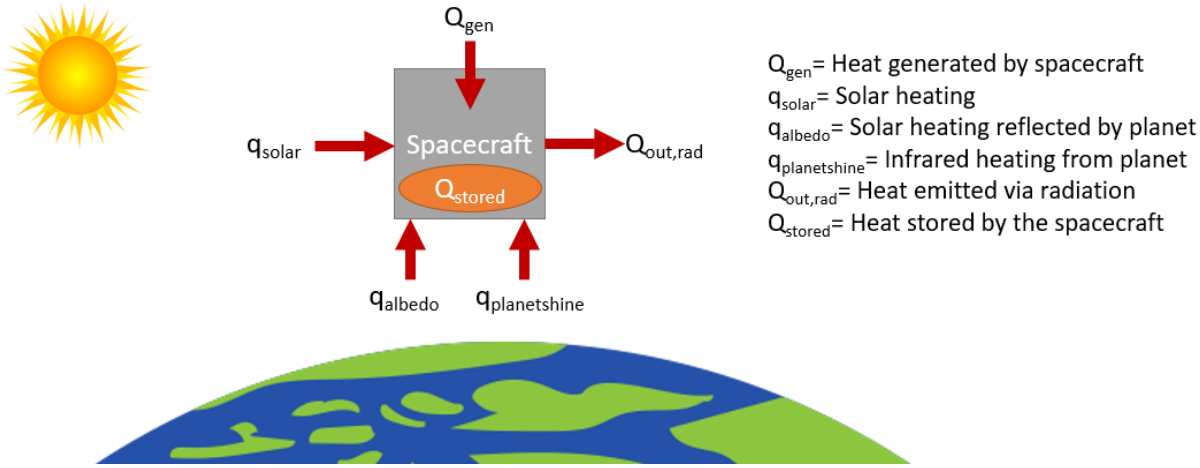


Figure 7.1: Orbiting spacecraft heating simplified overview. Q_{gen}, $Q_{out,rad}$, and Q_{stored} are represented as heat values, Watts per square meter in International System of Units (SI), whereas q_{solar}, q_{albedo}, and $q_{planetshine}$ are represented as heat fluxes. Credit: NASA.

The heat exchange depends on several factors listed below. Solar absorptivity and infrared (IR) emissivity are surface optical properties referenced below and described further in Section 7.2.1: Sprayable Thermal Control Coatings, Tapes, and MLI. Thermal control of a spacecraft is achieved by balancing the energy flows as shown in Equation 1:

$$q_{solar} + q_{albedo} + q_{planetshine} + Q_{gen} = Q_{stored} + Q_{out,rad} \quad (1)$$

- Q_{gen} (heat generated by the spacecraft) depends on the power dissipation of the spacecraft components.
- The amount of q_{solar} (solar heating) absorbed by the spacecraft depends on the solar flux, which is determined by the distance to the Sun, the surface area viewing the Sun (view factor), and the solar absorptivity of that surface.
- The amount of q_{albedo} (solar heating reflected by the planet) absorbed by the spacecraft depends on the planetary body, the surface area viewing the planet (view factor), and the solar absorptivity of that surface.
- The amount of $q_{planetshine}$ (IR heating from the planet) absorbed by the spacecraft depends on the planetary body, the surface area viewing the planet (view factor), and the IR emissivity of that surface.
- $Q_{out,rad}$ (heat emitted via radiation) includes the surface area designated as radiator space, the IR emissivity of the surface, and the difference in temperature between the spacecraft radiator and the heat sink to which it is dissipating, typically and most effectively to deep space. $Q_{out,rad}$ also includes heat lost through insulation or other surfaces not specifically intended to function as radiators (i.e., parasitic losses).

- Q_{stored} (heat stored by the spacecraft) is based on the thermal capacitance of the spacecraft.

Temperatures are regulated with passive and/or active thermal management technologies and design methods. Many of the same thermal management methods used on larger spacecraft are also applicable to SmallSats, and given the increased interest in small spacecraft over the last decade, some spacecraft thermal control technologies have been miniaturized or otherwise adapted to apply to SmallSats. Thermal control methods and technologies as applied to large spacecraft are considered state-of-the-art for the purposes of this review, but may have a Technology Readiness Level (TRL) value less than 9 for small spacecraft applications.

Challenges of designing thermal control systems for SmallSats stem from several intrinsic properties, summarized in **Table 7-1**. Due to the small size and volume limitations inside the deployer or around deployables, there is often no room for multi-layer insulation (MLI) on CubeSats. The thermal solution must be worked out as a coatings problem, exposing the CubeSat to more pronounced transient thermal behaviors.

Table 7-1: SmallSat Thermal Control Challenges

SmallSat Property	Challenge
Low thermal mass	The spacecraft is more reactive to changing thermal environments.
Limited external surface area	There is less real estate to be allocated to solar cells, designated radiator area, and/or viewports required for science instruments.
Limited volume	There is less space for electronic components, science instruments, and thermal control hardware. Components can be more thermally coupled, and it can be harder to isolate different thermal zones.
Limited power	There is less power available for powered thermal control technology.
Power Density	There is a big challenge to dissipate power as electronics are stacked close to each other, sometimes with no direct path to radiator.
MLI Edge Effects	MLI can “short” along the edges resulting in degraded performance, not specific to SmallSats but more of a general spacecraft issue.

The information described in this section is not exhaustive but instead provides an overview of current state-of-the-art thermal technologies and their level of development. The list of organizations/companies in this chapter is not all-encompassing and does not constitute an endorsement by NASA. There is no intention to mention certain companies and omit others based on their technologies or their relationship with NASA. The performance advertised may differ from actual performance because the information has not been independently verified by NASA subject matter experts and relies on information provided directly by manufacturers or from publicly available data. It should be noted that TRL designations may vary depending on the payload, mission requirements, reliability considerations, and/or the environment in which performance was demonstrated. Readers are highly encouraged to contact companies for further information regarding the performance and TRL of the described technologies.

7.2 State-of-the-Art – Passive Systems

Passive thermal control maintains component temperatures without using electrically powered equipment. Passive systems are typically associated with low cost, volume, weight, and risk, and are advantageous for spacecraft with limited mass, volume, and power, like SmallSats and especially CubeSats. MLI, coatings, surface finishes, interface conductance, heat pipes, sunshades, thermal straps, interface materials, and louvers are some examples of passive thermal control technologies.

In addition to passive thermal control technologies, structural and electrical design methods also contribute to passively managing the thermal environment. These design methods include the following:

- Material selection:
  - Structural component materials are chosen based on the needed heat transfer through the structure. A high or low thermal conductivity may be more advantageous depending on the application.
- Spacecraft orientation:
  - If orientation is not dictated by science objectives, changing the orientation of the spacecraft can help regulate temperatures.
  - Changing orientation may only be needed during certain mission phases, such as science operations, if larger amounts of heat are dissipated.
  - This method is often used in conjunction with other thermal control methods, such as orienting the spacecraft so that the radiator area can face deep space.
- Thermal interfaces:
  - Definition of the thermal contact between components through specific mounting methods can thermally isolate components or allow more heat to be transferred to a structural element (or radiator area) as needed. For example:
    - Heat transfer can be reduced by mounting a component through multiple stacked washers with low thermal conductivity (i.e., thermal isolation).
    - Heat transfer can be increased by mounting components with more fasteners (if applicable) and can be further increased by using thermal interface materials between a component and its mounting surface.
- Circuit board design considerations:
  - Copper layers within each board can be increased in number or thickness to conduct heat away from electrical components through the boards to their structural connection points.
  - Circuit boards can be mounted to increase heat transfer away from the boards to the structure, such as by mounting with wedge locks.

Table 7-2: SmallSat Passive Thermal Technologies

Passive Technology	Description
Sprayable Thermal Control Coatings	Specialized liquid coatings applied to the spacecraft surfaces to manage and regulate the ratio of absorptivity and emissivity for optimal energy balance and thermal performance.
Films, Tapes, and MLI	Materials used to modify spacecraft surface properties to manage and regulate temperature.
Thermal Straps	Provide a conductive link between a heat source and thermal sink to conductively transfer heat.
Thermal Contact Conductance and Bolted Joint Conductance	Heat transfer by “contact” conductance between two surfaces pressed together by uniform pressure can be varied by using interface filler materials and conductive gaskets.
Sunshields	Deployed material that reduces the amount of incident solar flux on a spacecraft.
Thermal Louvers	Controls heat transfer between spacecraft surfaces.
Deployable Radiators	Dedicated surface for dissipating excess heat via radiative heat transfer.

Phase Change Materials	Energy is absorbed as material within a metal compartment changes phase because of exposure to a heat source.
Mechanical Thermostat	An electromechanical device which controls the flow of electrical current in response to temperature change.

Below provides a description of current passive thermal control technology as applied to SmallSats. One key factor to consider when choosing thermal control technology, both passive and active, is the temperature limit of the technology itself. The goal is to use the appropriate technology to maintain the temperatures of spacecraft components within their limits, but the technology used to achieve this also has limits. It is recommended to verify that the technology used is applicable to the given design not only with respect to its needed function, but also with respect to the environment (temperature limits).

7.2.1 Sprayable Thermal Control Coatings, Tapes, and MLI

In a vacuum, heat is transferred only by radiation and conduction with no convection. The internal environment of a fully enclosed small satellite is usually dominated by conductive heat transfer, while heat transfer to and from the outside environment is driven via thermal radiation. Many missions with electrical surface resistivity requirements use coatings with these properties to address surface charging concerns (this also applies to MLI). For SmallSat missions where extensive use of MLI is not practical (see MLI paragraph on page 207), a combination of several different coatings is needed to achieve optimal energy balance and thermal performance. There are also coatings that better approximate the use of MLI by being relatively low emissivity (such as 0.25) with a lower alpha (0.1) so they don't overheat in the sun. These are colloquially known as tailorable emittance coatings, which involve some oxide depositions starting with a vacuum deposited aluminum (VDA) base to increase emissivity while keeping the solar absorptivity (alpha) low.

The thermal radiation band of the electromagnetic spectrum is between 0.1 and 100 μm in wavelength, as shown in Figure 7.2. Outside of the thermal radiation waveband, electromagnetic energy generally passes through objects or has very little heat energy under practical conditions. Thermal analyses are typically conducted using a two-waveband absorptance model that subdivides the thermal energy spectrum into solar (< 3 μm) and IR (> 3 μm) wavelengths. Thermal radiation heat transfer is controlled by using materials that have specific optical surface properties, namely solar absorptivity and IR emissivity. Solar absorptivity governs how much incident heating

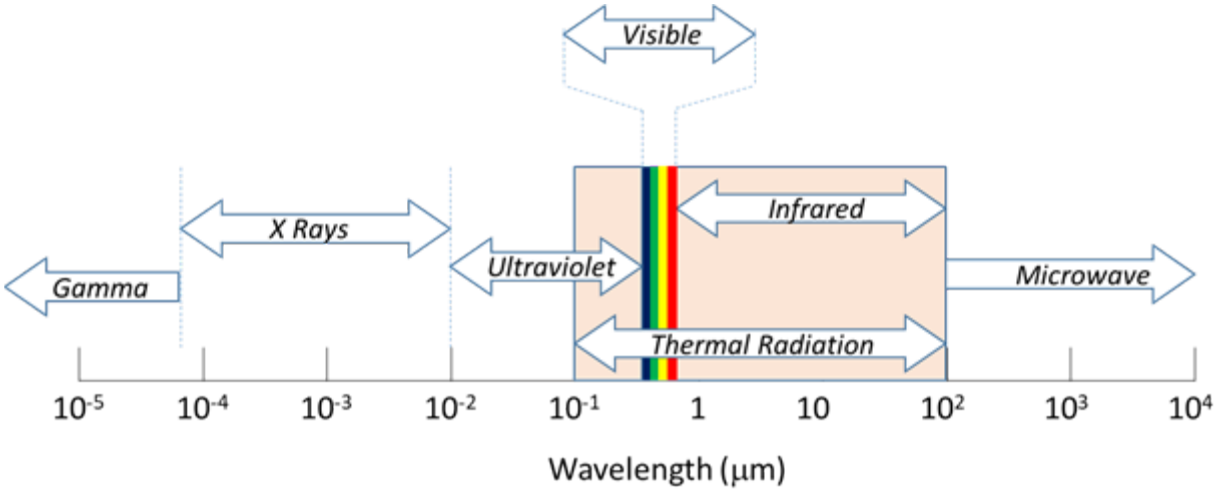


Figure 7.2: Electromagnetic spectrum showing the range of thermal radiation. Credit: NASA.

from solar radiation a spacecraft absorbs, while IR emissivity determines how much heat a spacecraft emits to space, relative to a perfect blackbody emitter, and what fraction of thermal radiation from IR sources (e.g., the Earth, Moon, or any particularly hot spacecraft components) are absorbed by that spacecraft surface.

The surface properties of a spacecraft can be modified by adding specialized paints, coatings, surface finishes, or adhesive tapes, depending on the needs of the spacecraft. For example, matte black paint has a high solar absorptivity and high IR emissivity for surfaces required to absorb a high percentage of solar heating and emit a high percentage of spacecraft heat. Alternatively, matte white paint has a low solar absorptivity and high IR emissivity (1) for surfaces required to absorb a low percentage of solar heating and emit a high percentage of spacecraft heat (e.g., radiator). Second-surface silver Fluorinated Ethylene Propylene (FEP) tapes offer excellent performance as radiator coatings, reflecting incident solar energy (low solar absorptivity) while simultaneously emitting spacecraft thermal energy efficiently (high IR emissivity). The selection between paints, coatings, and tapes depends on the specific application. Tape is typically easy to apply and remove, is comparatively inexpensive, and often has a longer usable lifetime than paint. Tape can also be added later in the assembly process if changes to thermal control are required after the spacecraft has already begun assembly. Some tapes, however, must be handled carefully to maintain optical properties and can be difficult to bond properly to curved surfaces.

While optical films and tapes may have solar absorptivities and IR emissivities very close to the datasheet values as received from the manufacturer, these two values will change throughout the mission. Coatings will darken due to atomic oxygen bombardment (low Earth orbit), UV light (high Earth orbit, GEO, and beyond), and other cosmic rays. This will increase the solar absorptance values, some quite substantially. The longer the mission duration, the more the optical coating properties will change. It is important that the thermal engineer takes this into consideration; thermal performance at the beginning-of-life (BOL) of a tape/film may not be the same at its end-of-life (EOL). Thermal analysis should take this into consideration and appropriately bias the optical property values in the thermal models to account for this degradation. BOL measurements from the datasheets (used for cold biased conditions) should not be used for EOL modeling, which represents hot-biased conditions.

Coatings and paints must often be applied earlier in the assembly process but can more easily cover non-flat surfaces. However, some paints, such as Parker-Lord's Aeroglaze 306/307, are expensive and require extensive and highly specialized processes to apply. Different options may also have different temperature limits. All these factors must be considered with respect to the application when selecting the final solution. Table 7-3 has a list of non-exhaustive sprayable thermal control coatings that include application difficulty and specific notes on some of the products.

One example, BioSentinel, a 6U spacecraft that launched as a secondary payload on the Artemis I mission in 2022, made extensive use of Sheldahl metallized tape coatings and second-surface silvered FEP tapes to control its external thermal radiative properties and overall energy balance (2). Another example, Picard, a 150 kg SmallSat, used white paint on the Sun pointing face to reduce the amount of solar flux absorbed and lower temperatures. For most small spacecraft projects to date, adhesive tapes, such as silver FEP, or other standard surface finishes (e.g., polishing, anodize, alodine) have been the preferred choices.

Table 7-3: Sprayable Thermal Control Coatings					
Manufacturer	**Product**	**Color**	**Cost**	**Difficulty to Apply***	**Notes**
Socomore	Z306 Polyurethane	Black	$	1	
	Z307 Polyurethane	Black	$$	1	
	A276 Polyurethane	White	$	1	Not UV stable
Huntington Ingalls Industries (formerly Alion and IITRI)	Z93P Silicate	White	$$	3	**
	Z93-C55 Silicate	White	$$$	4	Thickness control paramount **
	S13GP:6N/LO-1 Silicone	White	$$$	1	Dedicated equipment/cross contamination
AZ Technology	AZ-93 Silicate	White	$$	3	**
	AZ2000 Silicate	Off-white	$$$	4	May require specialty, epoxy primer **
	AZW/LA-II Silicate	White	$$$$	5	Thickness control paramount **

*1 not difficult, 5 extremely
**All silicates require temperature and RH control

A MLI blanket is typically comprised of multiple inner layers of a thin material with low IR emissivity (usually 10 to 20 layers) and a durable outer layer. The amount of radiative heat transfer allowed is limited by the many layers of reflectors. The low IR emissivity layers are either embossed or alternated with thin netting to limit conduction through the layers. Perforations may be added to allow the MLI to vent trapped gas once arriving on-orbit, although this can also be achieved via edge venting. MLI is used as a thermal radiation barrier to both protect spacecraft from incoming solar and IR flux, and to prevent undesired radiative heat dissipation to space. It is commonly used to maintain temperature ranges for components in-orbit.

MLI is delicate and performance drops drastically if compressed (causing a thermally conductive “short circuit”), so it should be used with caution or avoided altogether on the exterior of small satellites that fit into a deployer (e.g., P-POD, NLAS). MLI blankets can also pose a potential snagging hazard in these tight-fitting, pusher-spring style deployers. Additionally, MLI blankets tend to drop efficiency as size decreases because heat transfer through the blanket increases closer to the blanket edges, and the specific attachment method has a large impact on performance because attachment to the spacecraft creates a heat path. Due to these challenges, MLI generally does not perform as well on small spacecraft (more specifically CubeSat form factors) as on larger spacecraft. Surface coatings are typically less delicate and more appropriate for the exterior of a small spacecraft that will be deployed from a dispenser. Internal MLI blankets that do not receive direct solar thermal radiation can often be replaced by a variety of low emissivity tapes or coatings that perform equally well in that context, using less volume and at a potentially lower cost.

Table 7-4: Films, Tapes and MLI		
Manufacturer	**Film Product**	**Typical Solar Absorptivity BOL**
Astral Technologies Unlimited	StaMet/100XC Kapton	0.5
	StaMet/275XC Kapton	0.56

Table 7-4: Films, Tapes and MLI		
Manufacturer	**Film Product**	**Typical Solar Absorptivity BOL**
Astral Technologies Unlimited Multek/Sheldahl	0.010" FEP/Ag/Inconel	0.08
	0.005" FEP/Ag/Inconel	0.07
	ITO/0.010" FEP/Ag/Inconel, perforated	0.09
	ITO/0.005" FEP/Ag/Inconel, perforated	0.08
	Germanium/100XC Kapton	0.55
Dunmore Multek/Sheldahl	VDA/200HN/PSA	0.08
	200HN/VDA/PSA	0.41
	100HN/VDA/PSA	0.38
	VDG/200HN/PSA	0.2
NASA GSFC	GSFC Silver Composite Coating/ 200HN Kapton	0.1
	GSFC Aluminum Composite Coating/200HN Kapton	0.14
	GSFC Aluminum Composite Coating/100XC Kapton	0.2
	GSFC Aluminum Composite Coating/275XC Kapton	0.28
	GSFC Tailorable Emittance Coating/200HN Kapton	0.14
Thales	Optical Solar Reflector CMX 0.005"	0.08

7.2.2 Thermal Straps

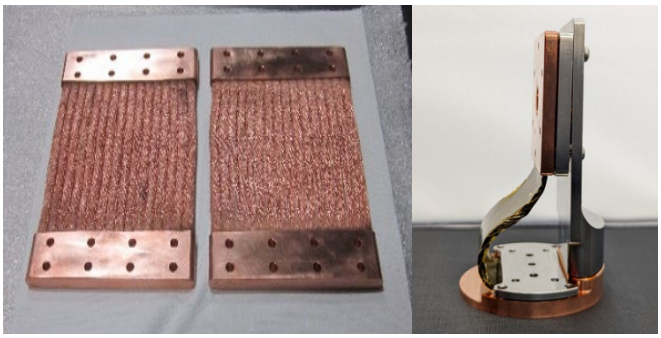


Figure 7.3: Flexible thermal straps. Credit: Thermal Management Technologies. Q-Strap. Credit: Redwire Space.

A thermal strap is a flexible, thermally conductive link added between a heat source and a sink to conductively transfer heat. They are often used between high-heat-dissipating chips or components and a chassis wall or other radiator surface. Their flexibility prevents the addition of significant structural loads. Thermal straps can be made of metal, traditionally copper or aluminum, or high-conductivity carbon materials, such as graphite. They can be formed of multiple foil sheets or wound cables (also referred to as ropes and braids), with end blocks at each end to hold the sheets/cables in place and to mount or otherwise attach to the required surfaces. Straps with more than two end blocks and multiple material combinations can also be produced and have been used on larger spacecraft. Advances in thermal straps are being developed to further increase heat transfer capability, and custom thermal straps are now commonly fabricated and tested using graphite materials due to improved thermal conductivity.

Space Dynamics Laboratory (SDL) developed solderless, flexible thermal straps without solder, epoxy, or other filler materials. Figure 7.4 shows a comparison of the as-tested conductance for

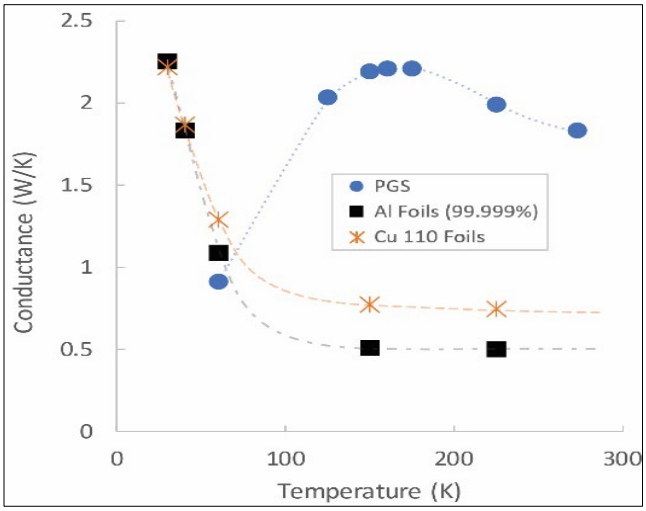




Figure 7.4: Thermal strap design with aluminum foils, copper foils, and PGS in aluminum end blocks (above), and their respective measured thermal conductance (left). The dashed lines connecting data points are based on material thermal conductivity curves. Credit: SDL.

the same strap geometry fabricated with three different foil materials: aluminum, copper, and pyrolytic graphite sheets (PGS), demonstrating that PGS increases the overall thermal conductivity. SDL supplied Utah State University with a PGS strap for the Active Thermal Architecture (ATA) project sponsored by the Small Spacecraft Technology (SST) program. A follow-on to this ATA project is referenced in the Cryocooler section. Boyd Corporation has designed thermal straps using their patented K-core technology that has an annealed pyrolytic graphite (APG) core within an encapsulating structure (4). Technology Applications, Inc. has specialized in testing and developing Graphite Fiber Thermal Straps (GFTS), with flight heritage primarily on larger spacecraft missions (Orion and SPICE) (5). The Pyrovo Pyrolytic Graphite Film (PGF) thermal straps developed by Thermotive have flown in optical cooling applications for high altitude cameras and avionics on larger spacecraft, on JPL's ASTERIA CubeSat in 2017, and on the Mars 2020 rover mission (6).

Table 7-5: Thermal Straps

Manufacturer	Product	Material
Technology Applications, Inc.	Copper Cable	Copper
	Copper Foil	Copper
	Aluminum Foil	Aluminum 1100
	PGL	Pyro Graphite
	GFTS	Graphite Fiber
Thermotive	Copper Foil	Copper
	Aluminum Foil	Aluminum 1100
	Pyrovo	Pyro Graphite Film
Space Dynamics Laboratory	PGS	Pyrolytic Graphite Sheet
	Aluminum Foil	Aluminum 99.999% and 1235
	Copper Foil	Copper 101 and 110
	Copper Braid	Copper Braid
Redwire Space	Q-Strap	High-k graphite material
Thermal Management Technologies	TMT010-200 Series	Copper Foil
	TMT010-300 Series	Copper Braid (small)
	TMT010-400 Series	Copper Braid (large)
	Customized	Copper braid or foil or using aluminum foil

Table 7-5: Thermal Straps		
Manufacturer	**Product**	**Material**
Boyd Corporation	k-Core Graphite-Encapsulated	Pyrolytic graphite

7.2.3 Thermal Contact Conductance and Bolted Joint Conductance

Two surfaces pressed together by uniform pressure will transfer heat via thermal contact conductance. This conductance value is a product of the heat transfer coefficient and the effective contact surface area. The heat transfer between such interfaces can be varied by using thermal interface filler materials and conductive gaskets (7).

Bolted joints experience non-uniform pressure, creating a more complex heat transfer scenario where the conductance depends on screw size, torque, surface properties, and other factors. The conductance can be varied by changing torque, surface properties, finishes, and materials. Table 7-6 provides the thermal contact conductance of various screws (7).

Table 7-6: Bolted Joint Thermal Conductance Design Guideline		
	Conductance [W/K]	
Screw Size	**Small Stiff Surface**	**Large Thin Surfaces**
2-56	0.21	0.105
4-40	0.26	0.132
6-32	0.42	0.176
8-32	0.80	0.264
10-32	1.32	0.527
1/4-28	3.51	1.054

7.2.4 Thermal Interface Materials and Conductive Gaskets

Thermal interface materials can be inserted between two components to increase the conductive heat transfer between them. They are often made as a sheet or pad of material sandwiched between surfaces, but there are many different types that vary in material, thickness, thermal conductivity, temperature limits, and vacuum compatibility. Thermal interface materials can also be a grease or paste.

Thinner sheets of materials are commonly used between heat-dissipating electronics boxes and mounting surfaces to thermally sink the hot components to a colder surface and reduce the temperature of the electronics. The performance of these types of materials depends on reaching

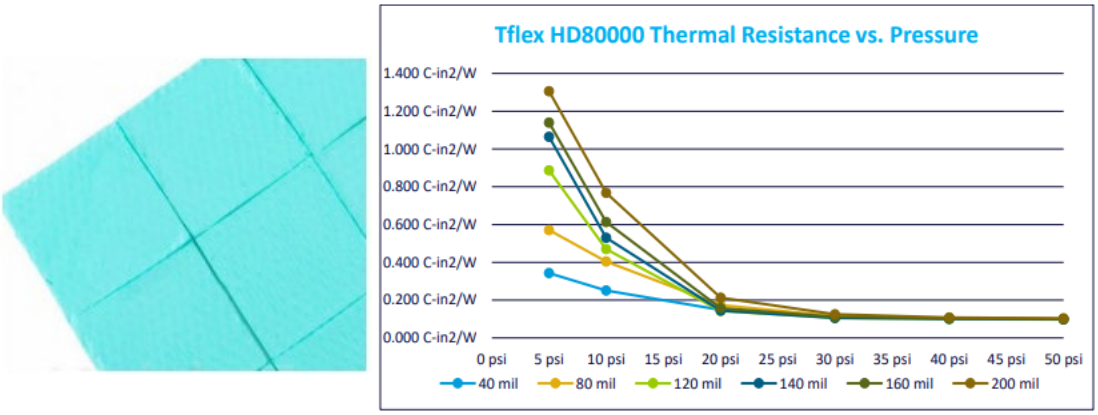


Figure 7.5: Laird Tflex HD80000 series sheets (left) and thermal resistance vs. pressure (right). Credit: Laird Performance Materials.

a certain contact pressure between components to ensure adequate heat transfer. Laird Performance Materials has developed many different types of thermal interface materials for a variety of applications. For example, their Tflex series, shown in Figure 7.5, is about 1 to 5 mm thick with a thermal conductivity of 6 W mK^{-1} (8), whereas their Tgon series of materials are about 0.13 to 0.5 mm thick with a thermal conductivity of 5 W mK^{-1} (9).

Thicker pad-like materials, such as Henkel brand GAP PADs, are often used between high-heat-dissipating chips on electronic boards and the electronics enclosure. These are also made to fit a variety of applications, with varying materials, thickness, conformability, tear resistance, electrical isolation, thermal conductivity, and more (10). Several additional thermal interface materials developed by Henkel Corporation are shown in Figure 7.6. For conductive gaskets and interface materials, see Table 7-7.

Table 7-7: Thermal Interface Materials and Conductive Gaskets

Manufacturer	Product	Recommended Conductance (W/in2-C)
Parker Chomerics	Nusil CV-2946	3.5
NeoGraf	Egraf HT-1210	2
NeoGraf	Egraf HT-C3200	2.5
Parker Chomerics	Chotherm 1671	0.75
Parker Chomerics	Therm a gap 579	0.9
Laird Performance Materials	T-PLI 220	1.5
Henkel Corporation	Gap Pad 300	1.25
Indium Corporation	Indium foil 0.005"	0.9
Carbice Corporation	Structured Space Pad	1.94

7.2.5 Sunshields

A sunshield, or sunshade, is an often-deployed device made up of a material with low solar absorptivity that reduces the amount of incident solar flux impinging on a spacecraft, by blocking the view to the Sun. Sunshields are commonly used for spacecraft thermal control, although they have only recently been designed for small spacecraft.

7.2.6 Thermal Louvers

Thermal louvers are thermally activated shutters that regulate how much heat the louvered surface can dissipate. As the louvers open, the average IR emissivity of the surface changes, changing how much heat the surface dissipates. Full-sized louvers on larger spacecraft have high efficacy for thermal control; however, integration on small spacecraft is challenging. Typical spacecraft louvers are associated with greater mass and input power, which are both limited on small spacecraft. Although commonly defined as active thermal control, in this context louvers are

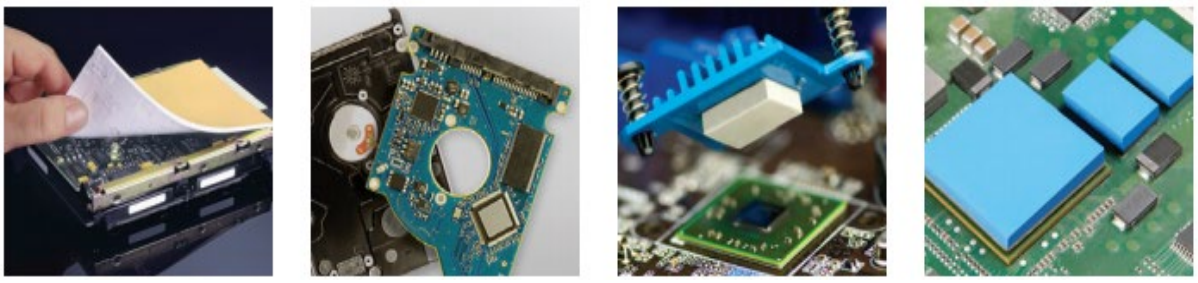


Figure 7.6: A variety of thermal interface materials. Credit: Henkel Corporation.

considered a passive thermal control component because the CubeSat-adapted design considered does not require spacecraft power.

7.2.7 Deployable Radiators

A radiator is a dedicated surface for dissipating excess heat via radiative heat transfer and has a high IR emissivity and low solar absorptivity—an optical property combination typically referred to as "radiator properties." A deployable radiator is stowed during transit or when the radiator is not needed and deployed when excess heat dissipation is required. Deployable radiators on small spacecraft can be challenging due to volume constraints. While paint has been widely used to create efficient radiator surfaces on larger spacecraft, the relatively limited available external surface area on SmallSats that already have body-mounted solar cells reduces the available potential for creating dedicated radiative surfaces. For a system that requires a large amount of heat dissipation, a passive deployable radiator would greatly enhance thermal performance by increasing the available radiative surface area. Since deployable radiators may be needed because of a lack of radiator surfaces on the spacecraft body due to body-mounted solar cells, an alternate approach (more common for CubeSats) is to use the chassis body as the radiator area and have a deployable solar array. Also, deployed solar arrays would be able to radiate from a high emissivity/low solar absorptance backside for improved thermal management of the array. Figure 7.7 shows an example of a deployable thermal dissipation technology from Redwire Space.

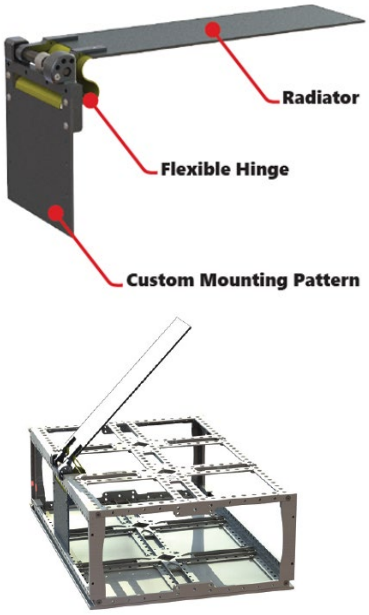


Figure 7.7: Q-Rad deployable radiator technology. Credit: Redwire Space.

A novel deployable radiator is being developed by JPL, California Polytechnic San Luis Obispo, and California State University, Los Angles. At the core of this technology is an Additively Manufactured Deployable Radiator with embedded Oscillating Heat Pipes (AMDROHP) that enables heat to be efficiently transported across moving interfaces. The current AMDROHP radiator design is shown in Figure 7.8 and consists of an evaporator and a condenser plate, and a series of flexible joints connecting the two plates. AMDROHP can be stowed within a 3U CubeSat and can be passively deployed without the use of an actuator. This AMDROHP technology is currently in the testing phase and further design optimization is ongoing. This project is funded by NASA's Small Spacecraft & Distributed Systems (SSDS, formally Small Spacecraft Technology program) in the University SmallSat Technology Partnerships initiative within the 2020 cohort.

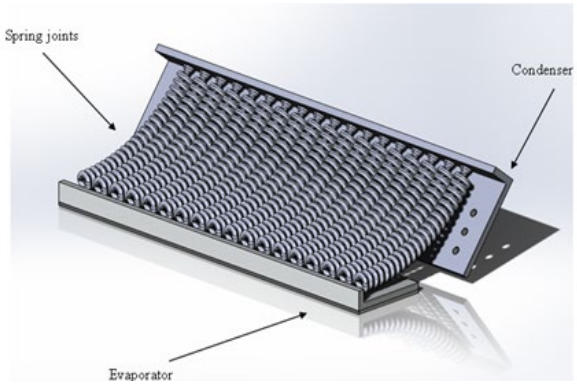


Figure 7.8: Rendering of an AMDROHP radiator design. Credits: California State Los Angles, Jet Propulsion Laboratory, and California Polytechnic San Luis Obispo.

7.2.8 Heat Pipes

A traditional heat pipe is a passive device comprised of a metal container (pipe) that holds a liquid under pressure and has a porous wick-like structure within the container. When heat is applied to one end of the tube, the liquid inside the tube near the hot end vaporizes and moves through the tube to the cooler end, where it condenses back into a liquid. The wick transports the condensed liquid back to the hot end via capillary action. There are also more complicated and non-passive types of heat pipes, such as variable conductance, diode, and loop heat pipes, which are not further explained in this document.

Heat pipes are an efficient passive thermal transfer technology, in which a closed-loop system transports excess heat via temperature gradients, typically from electrical devices to a colder surface, which is often either a radiator surface, or a heat sink that is thermally coupled to a radiator. Traditional constant conductance heat pipes are cylindrical in shape with a grooved inner wick, like those used on Bi-Spectral Infrared Detection (BIRD), a 92 kg satellite launched in 2001, to join satellite segments (13). Heat pipes can also be configured as flat plates with tubing sandwiched between two plates and charged with a working fluid. SDS-4, a 50 kg small spacecraft launched in 2012, incorporated the Flat-Plate Heat Pipe On-Orbit Experiment (FOX), developed at JAXA (14).

The FlexCool heat pipe by Redwire Space is a bent, flat heat pipe developed as a cross between a heat pipe and a thermal strap that can be customized for higher heat fluxes by increasing the thickness. This heat pipe flew on TechEdSat-10, a 6U CubeSat deployed from the ISS in 2020, to thermally manage the radio. An image of this technology in a 1U CubeSat model is shown in Figure 7.9.

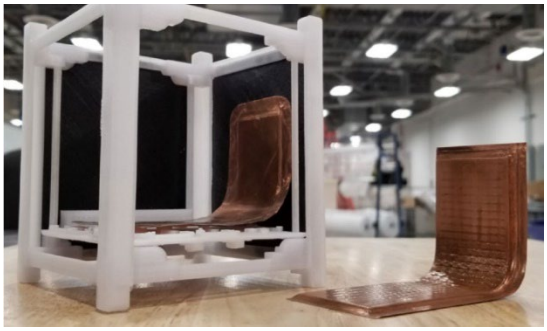


Figure 7.9: FlexCool conformable micro heat pipe before integrating with TechEdSat-10 DVB-S2 radio. Credit: Redwire Space.

7.2.9 Phase Change Materials and Thermal Storage Units

A phase change material used as a thermal storage unit is made up of a material (e.g., wax) within a metal housing with a heat source attached, so that as the source conducts heat to the enclosure, the phase change material within absorbs the energy as it changes phase (usually from solid to liquid). Then, as the heat source energy output reduces, the phase change material releases the energy as it changes back to its initial phase (usually from liquid to solid). Owing to the low thermal conductivity of the phase change material, the metal housing must conduct heat into the phase change material for efficient solidification or melting. See Table 7-8 for common phase change materials.

Table 7-8: Phase Change Materials

Material	Melting Point (°C)	Heat of Fusion (kJ/kg)
Salicylic Acid	159	199
Bee Wax	61.8	177
Paraffin	20-60	140-280
Polyethylene glycol 600	20-25	146
Glycerol	18	199
Acetic acid	17	187
Water	0	333
Isopropyl alcohol	-89	88

Table 7-8: Phase Change Materials		
Material	**Melting Point (°C)**	**Heat of Fusion (kJ/kg)**
Butane	-135	76
Ethane	-172	93
Methane	-183	59

Thermal storage units are typically used with components that will experience repeated temperature cycling, or to slow down the temperature transient caused by a high heat dissipation event, or a temporary change in the environment such an eclipse. They can be challenging to apply to CubeSats and other small satellites because of the extra mass of the required housing.

Thermal Management Technologies developed a phase-changing thermal storage unit (TSU) that accounts for desired phase-change temperatures, interfaces, temperature stability, stored energy, and heat removal methodologies. This device will allow the user to control temperature peaks, maintain stable temperatures, and/or provide energy storage (15). Redwire Space developed multiple phase-change-materials (PCM)-based thermal energy storage panels for the CubeSat form factor that can be easily stacked between critical components (16). Figure 7-10 shows two examples of thermal storage technology solutions: Q-Store and Q-Cache.

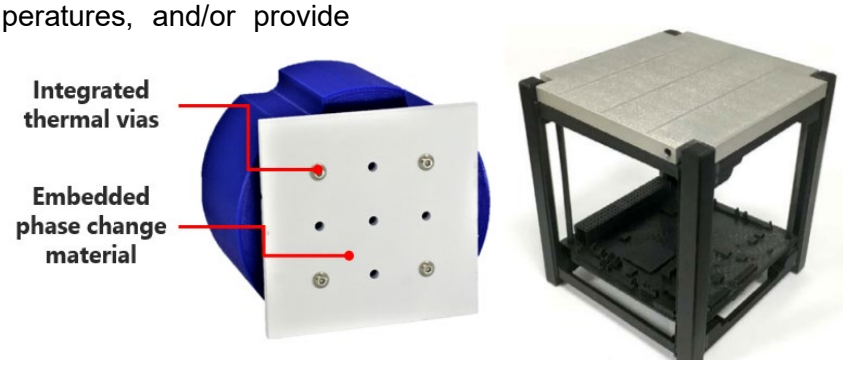


Figure 7.10: Redwire Space's thermal energy storage technologies: (left) Q-Store and (right) Q-Cache. Credit: Redwire Space.

7.2.10 Thermal Switches

A thermal switch is a device that switches a heat conduction path between either a strong thermal coupling or a weak thermal coupling (thermal isolation) as needed to control the temperature of heat-producing components. A switch typically connects a heat-producing component and a low-temperature sink, such as a radiator. Heat switches differ from thermostats in that they passively modulate thermal coupling, while thermostats modulate heater circuits (17). Part of the challenge with the integration of a thermal switch in SmallSats is that they take up additional space between a component and a heat sink. Typically, heat switches may provide a conduction ratio of 10:1, with a technology goal of 100:1 (18). See Table 7-9 for examples of commercial thermal switches.

Table 7-9: Thermal Switches							
Manufacturer	**Product**	**Type**	**Max Conductance**	**Min Conductance**	**Mass**	**Max Q**	**Notes:**
ACT	(Study)	VCHP	20 W/K	0.01 to 0.04 W/K	0.3 to 0.5 kg	--	VCHP Variable Cond. Heat Pipe)
Sierra Space	Passive Thermal Control Heat Switch	Mechanical	1 W/K	0.015 W/K	~0.110 kg	6 W	Originally designed for Martian surface ops.

Table 7-9: Thermal Switches							
Manufacturer	**Product**	**Type**	**Max Conductance**	**Min Conductance**	**Mass**	**Max Q**	**Notes:**
Sierra Space	HP Thin Plate	Mechanical	607 W/m^2/°C	7.8 W/m^2/°C	2.72 g/cm^3	12 W	Based on single "cell" design (25.4 mm x 25.4 mm)
Sierra Space	Diaphragm Thin Plate	Mechanical	607 W/m^2/°C	7.1 W/m^2/°C	2.72 g/cm^3	12 W	Based on single "cell" design (41.3 mm x 41.3 mm)

7.2.11 Multifunctional Thermal Structures

A newer development in passive thermal control for small spacecraft is multifunctional thermal structures. These integrate thermal control capabilities directly into the structure. This is particularly advantageous for small spacecraft due to their strict mass and volume constraints. Currently, Thermal Management Technologies has adapted its multifunction heat spreading structure technology, scaled it to smaller satellite configurations, and designated it Standard Passive Orbital Thermal-control (SPOT) Structures. SPOT Structures come in four standard configurations: 6U, 12U, Launch-U, and ESPA (19). Each incorporates heat-spreading technology that improves the ability to radiate waste heat. They incorporate features such as low mass, high stiffness and strength, and integrated heat pipes. This new technology is at TRL 4.

7.3 State-of-the-Art – Active Systems

Active thermal control methods rely on input power for operation and have been shown to be more effective in maintaining tighter temperature control for components with more stringent temperature requirements or higher heat loads (20). Typical active thermal devices used on large-scale spacecraft include electrical resistance heaters, cryocoolers, thermoelectric coolers, and fluid loops. Electrical heaters are usually easily integrated into SmallSat architectures as they do not typically require significant mass or volume. Heaters are frequently used in all space applications, including small and large satellites; therefore they are often included as passive thermal control technology. Other active systems are challenging to integrate into CubeSats and other small satellites because of the power, mass, and volume requirements associated with each technology. Until spacecraft designers can miniaturize existing actively controlled thermal techniques and reduce power requirements or increase available spacecraft power, most active thermal systems in small spacecraft are limited and have a TRL range of 3-6. Descriptions of SmallSat active thermal technologies are provided in Table 7-10.

Table 7-10: SmallSat Active Thermal Technologies	
Active Technology	**Description**
Electrical Heaters	Space heaters use an electrical-resistance element in between two sheets of flexible electrically insulating material.
Cryocoolers	Miniature refrigeration system designed to cool components to extremely low temperatures.
Thermoelectric Coolers (TEC)	Miniature solid-state heat pumps which provide localized cooling via the Peltier effect, which is cooling resulting from passing electric current through a junction formed by two dissimilar metals.
Fluid Loops	System that circulates a working fluid through the spacecraft to a heat sink.

7.3.1 Heaters

Electrical resistance heaters used on small spacecraft are most often Kapton heaters, which consist of a polyimide film with etched foil circuits that produce heat when electrical current is applied. Kapton heaters also often have a pressure-sensitive adhesive on one side for easy application. Heaters are usually controlled by a thermostat or temperature sensor and used in cold environments to maintain battery temperatures, typically for components with the narrowest temperature limits. The low mass of SmallSats requires little additional heater power to maintain temperature limits, and therefore heaters do not typically need to be very high power to effectively manage temperatures. The TRL values for electrical heaters on SmallSats are 7-9 in LEO environments.

The 1U CubeSats Compass-1, MASAT-1, and OUTFI-1 each required an electrical heater attached to the battery in addition to passive control for the entire spacecraft system to maintain thermal regulation during eclipse periods (21). Additionally, as biological payloads become more common on small spacecraft, their temperature limits must also be considered and maintained. NASA ARC biological nanosats (GeneSat, PharmaSat, O/OREOS, SporeSat, EcAMSat, and BioSentinel) all used actively controlled heaters for precise temperature maintenance of their biological payloads, with closed-loop temperature feedback. See Table 7-11 for examples of electrical heaters for active thermal systems.

Table 7-11: Active Thermal Systems - Electrical Heaters

Manufacturer	Product	Power (W/cm^2)	Temp Limits	Material	Notes
Omega	KHLVA, PLM-Series	0.4 to 1.56	-40°C to 149°C (w/PSA) -57°C to 232°C (w/o PSA)	Kapton (polyimide)	Various sizes, rectangular/square/round, w & w/o pressure sensitive adhesive (PSA), Low-Outgassing
Omega	Polyimide Heater Kit	0.4 to 1.56	-200°C to 200°C (w/PSA)	Kapton (polyimide)	Various shapes. 149°C for continuous ops due to PSA limits.
Tempco	SHK Series	0.8 to 6.2	-35°C to 150°C (w/ Al Foil)	Kapton (polyimide) Some w/ Al Foil	Rectangular/square/round, w/ (PSA). Some model available w/ AL foil for extended temp limits.
Tayco	Flexible Circuit Heater	Up to 3.1	-200°C to 200°C	Kapton (polyimide)	Various shapes and watt densities.
Hi-Heat Industries	Polyimide Flexible	Up to 3.1	-200°C to 200°C	Kapton (polyimide)	Quick turnaround for custom sizes and resistances
Minco	Polyimide Thermofoil HK Series	0.8 to 5.1	-200°C to 200°C -200°C to 150°C (w/ Al Foil)	Kapton (polyimide) Some w/ Al Foil	Mountings: #12 & arcrylic PSA, epoxy, shrink band, stretch tape, clamping. NASA rated for materials & vacuum.

Table 7-11: Active Thermal Systems - Electrical Heaters					
Manufacturer	**Product**	**Power (W/cm^2)**	**Temp Limits**	**Material**	**Notes**
Birk Manufacturing	Polyimide-Traditional	0.02 to 3.1	See Notes	Kapton (polyimide)	Max Temps: FEP-Bonded & All Polyimide(260°C); Acrylic Bonded(120°C).
Birk Manufacturing	Polyimide-High Temp	0.02 to 7.75	See Notes	Kapton (polyimide)	Max Temp: up to 300°C
Chromalox	KPH, KPM Series	0.4 to 1.56	-200°C to 200°C* -200°C to 121°C**	Kapton (polyimide)	* FEP Construction, Acrylic construction
All Flex Solutions	Custom Designs	--	--	--	See website for design guide, options.

7.3.2 Cryocoolers

Cryocoolers are refrigeration devices designed to cool to temperatures of approximately 100K and below. A summary of cryocooler systems is given in Figure 7.11, and a detailed review of the basic types of cryocoolers and their applications is provided by Radebaugh (22). The first two systems (a) and (b) are recuperative cycles, while (c), (d), and (e) are regenerative cycles. Cryocoolers are used on instruments or subsystems requiring cryogenic cooling, such as high-precision IR sensors. Instruments such as imaging spectrometers, interferometers, and midwave infrared (MWIR) sensors require cryocoolers to function at extremely low temperatures. The low temperature improves instrument dynamic range and extends the wavelength coverage. The use of cryocoolers is also associated with longer instrument lifetimes, low vibration, high thermodynamic efficiency, low mass, and cooling temperatures less than 50K (23). Cryocoolers on small spacecraft are still a new concept; however, there have been two CubeSats with cryocooling on board. Lunar IceCube, a 6U secondary payload launched on Artemis I in 2022 and developed by Morehead State University, used a 600 mW cryocooler for its BIRCHES point spectrometer (24). For more examples of cryocooler solutions, see Table 7-12.

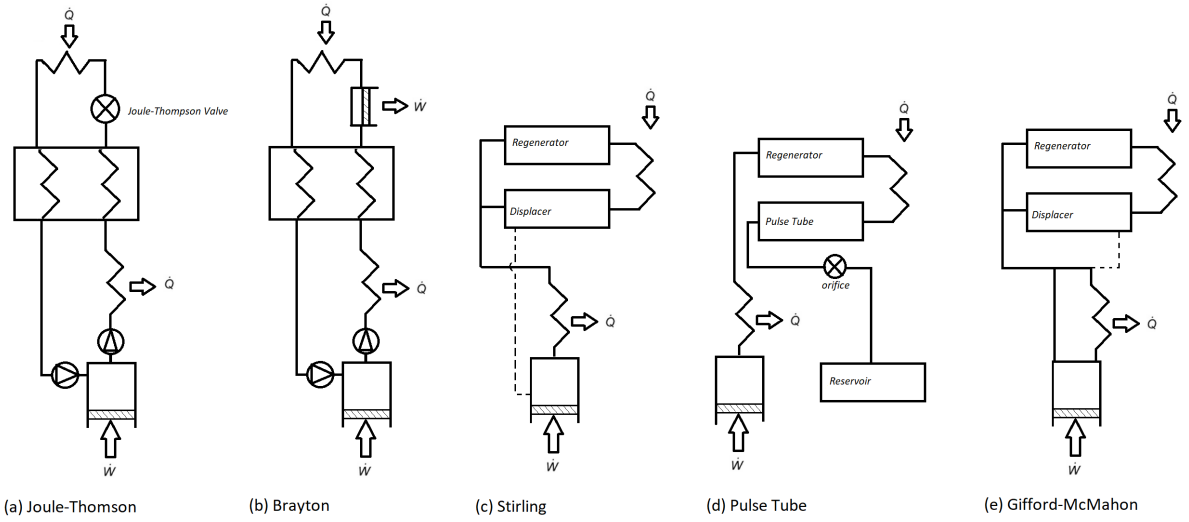


Figure 7.11: A comparison of cryocooler types. Credit: NASA.

Table 7-12: Active Thermal Systems - Cryocoolers							
Manufacturer	**Product**	**Form factor**	**Life (yrs)**	**Mass (kg)**	**Power (W)**	**TRL**	**Notes:**
Lockheed Martin Space	MICRO 1-1	~1U	10	0.350	15	7 - 9	1 W cooling @150K cold tip. Integrated on LunIR CubeSat (launcher: Artemis I).
	MICRO 1-2	~1U	10	0.475	25	6	2 W cooling @105K cold tip. Tested for MISE. Tentatively slated for integration into Europa Clipper.
	MICRO 1-3	~1U	10		40	5	Original design point: 1.4 W cooling @105K (40 W). Max Cooling: 2.9 W @200K (30 W).
AIM Infrarot-Module GmbH	SF070	~1U	>3.5 (MTTF)	0.85	24	6 - 9	0.6 W @80K cold tip. Slated from HyTi: Hyperspectral Thermal Imager (6U CubeSat).
SunPower - Ametek	CryoTel DS Mini	<2U	>14	1.20	45	6	1.8 W @77K (23°C reject). Op to 40K.
	CryoTel MT	<3U	>23	2.10	80	6	5 W @77K (23°C reject). Op to 40K.
Ricor	K508N	1U+	15	0.475	5.5	4 - 6	0.2 W @80K (23°C reject). Demo for 'Active CryoCubeSat (ACCS)' project.

TRL values provided are specific to low-Earth environments for SmallSats <180 kg.

7.3.3 Thermoelectric Coolers (TECs)

TECs are miniature solid-state heat pumps that provide localized cooling via the Peltier effect, which is cooling resulting from passing an electric current through a junction formed by two dissimilar metals. TECs have been used to cool star trackers, IR sensors, and low-noise amplifiers on large spacecraft. Advantages of TECs are that they have no moving parts and are reliable, noiseless, lightweight, and compact. Their use is limited below temperatures of 130 K due to low efficiency and reduced performance at large temperature differences. Furthermore, TECs are mechanically fragile and highly sensitive to thermal expansion stresses. External stresses can be mitigated by adding a thermally conductive strap on the cold side (25). Table 7-13 provides an overview of commercial thermoelectric coolers.

Table 7-13: Thermoelectric Coolers					
Manufacturer	**Product**	**Cooling Capacity**	**ΔT @ 27°C**	**Operating Temp**	**Notes:**
Laird Technologies	*Examples:* CP Series PolarTec PT Series UltraTEC UTX Series HighTemp ETX Series Multistage MS Series	1.8 - 118 W 18 - 71 W 69 - 299 W 7.7 - 322 W 0.3 - 38 W	68 - 74°C 68 - 74°C 68 - 74°C 68 - 74°C 81 - 129°C	< 80°C < 80°C < 80°C < 150°C < 80°C	
Custom Thermoelectric	04801-9A30-18RB	6.1 W	70°C (Max)	< 200°C	

Table 7-13: Thermoelectric Coolers					
Manufacturer	**Product**	**Cooling Capacity**	**ΔT @ 27°C**	**Operating Temp**	**Notes:**
FerroTec	9502/031/018 M	4.1 W	70°C (Max)		Values @ 50°C
Coherent (formerly Marlow)	Muti Stage SP2394-07AB	4.5 W	130°C (Max)	< 85°C	Values @27°C, Designed for zero/high G
Coherent (formerly Marlow)	Single Stage CT12-4	37.0 W	70°C (Max)	< 130°C	Values @27°C, Designed for zero/high G

7.3.4 Fluid Loops

A pumped fluid loop (PFL) consists of a circulating pump that moves a liquid through tubing connected to a heat exchanger and a heat sink. A heat source is mounted to the heat exchanger, and the pumped fluid carries the heat from the source to a heat sink, typically a radiator; the cooled fluid is returned to the heat source to continue providing cooling. A PFL is capable of cooling multiple locations via forced convective fluid cooling. Mechanically pumped fluid loops (MPFL) are not typically used on SmallSats because they are associated with higher power consumption and mass.

The Active Thermal Architecture (ATA) system is an advanced, active thermal control technology for small satellites in support of advanced missions in deep space, heliophysics, Earth science, and communications. The ATA technology is capable of high-power thermal rejection and zonal temperature control of satellite buses, payloads, and high-energy-density components. The ATA system includes integrated heaters and a PID-based control algorithm to dynamically tune the satellite's thermal rejection and zonal temperature control as a function of payload and mission parameters. The ATA project was developed by the Center for Space Engineering at Utah State University and funded by NASA SSDS in partnership with JPL with the USTP 2018 cohort. The ATA is a sub-1U two-stage active thermal control system targeted at 6U CubeSat form factors and larger. The first stage consists of an MPFL with a micro-pump that circulates a single-phase heat transfer fluid between an internal heat exchanger and a deployed tracking radiator. The second stage is composed of a miniature tactical cryocooler that directly provides cryogenic cooling to payload instrumentation. The conceptual operation of the ATA system is shown in

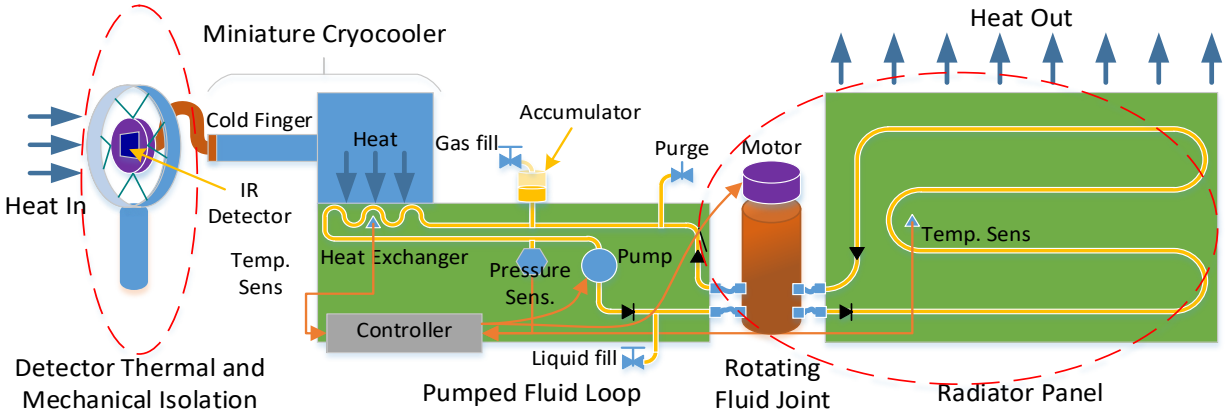


Figure 7.13: Conceptual operation of the ATA thermal control system. Credits: CSE/USU/ NASA/JPL.

Figure 7.13. The ATA system is scheduled to fly on the upcoming ACMES mission, a technology demonstration flight funded by NASA ESTO through an InVEST grant.

Ultrasonic additive manufacturing (Fabrisonics UAM) techniques were used to simplify and miniaturize the ATA system by embedding the MPFL fluid channels directly into the integrated HX, CubeSat chassis, and the external radiator, to create integrated multifunctional structures. By leveraging UAM 3D printing, the ATA system can improve baseline thermal performance by >200%, a mass savings of more than >30%, and a savings on cost and schedule of better than >50%. The ATA system also features flexible, multi-axis rotary fluid unions and an integrated geared micro-motor, which enables the two-stage deployment and solar tracking of the ATA radiator. The ATA features passive vibration isolation and jitter cancellation technologies such as a floating wire-rope isolator design, particle damping, flexible PGS thermal links, and a custom Kevlar isolated cryogenic electro-optical detector mount. Figure 7.14 shows some of the technologies developed for ATA, as well as the ground-based prototype CubeSat.

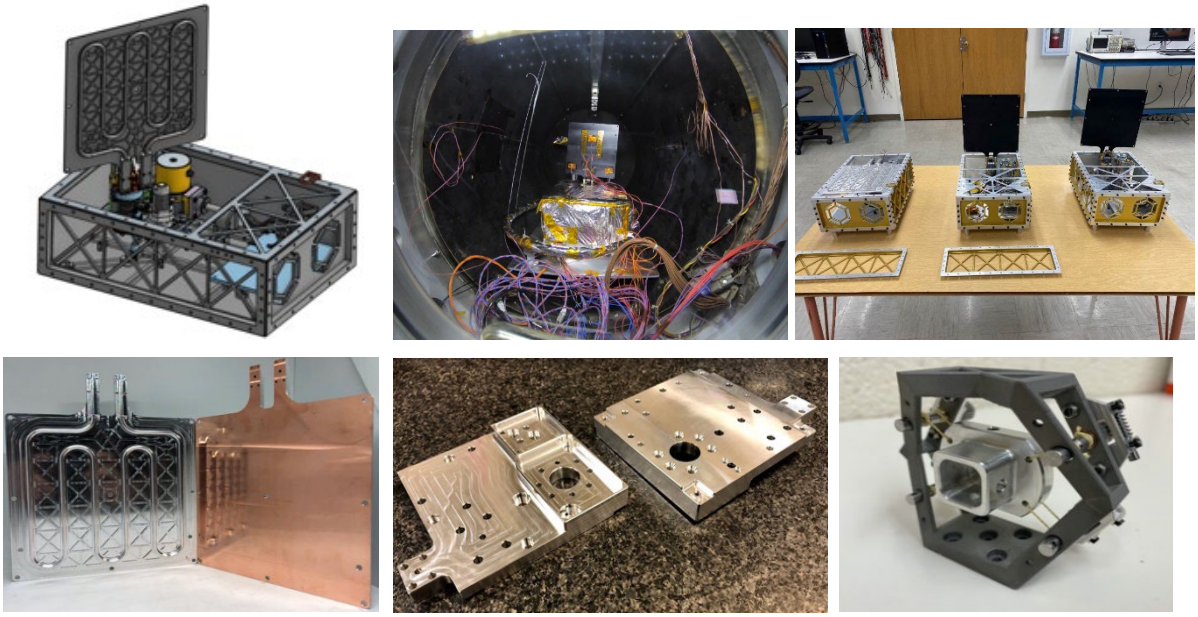


Figure 7.14: From top left: ATA CubeSat prototype, ATA subsystem testing, ATA prototypes, UAM radiator with copper backing, UAM heat exchanger, Kevlar isolated cryogenic electro-optical prototype mount. Credits: CSE/USU/NASA/JPL.

Table 7-14: Active Thermal Systems - Fluid Loops

Manufacturer	Product	Cooling Capacity	Mass	Volume	TRL	Notes
Netherlands Aerospace Centre	Mini-MPL	>20 W	-	< 1U	4 - 6	Scalable to ≤ 200W
Lockheed Martin	Joule-Thomson Microcryocooler	-	0.2 kg	< 1U (Est.)	4 - 5	

TRL values provided are specific to low-Earth environments for SmallSats <180 kg.

7.4 Summary

As thermal management on small spacecraft is limited by mass, surface area, volume, and power constraints, traditional passive technologies such as paints, coatings, tapes, MLI, and thermal

straps continue to dominate thermal design. Active technologies, such as thin, flexible resistance heaters, have also seen significant use in small spacecraft, including some with advanced closed-loop control. Many technologies that have to date only been integrated on larger spacecraft are being designed, evaluated, and tested for small spacecraft to meet the growing needs of SmallSat developers as these systems become more advanced. Deployable solar panels that have been used by many SmallSats are paving the way for deployable thermal components, while advanced deployable radiators and thermal storage units are still undergoing testing for small spacecraft.

More active thermal control system technologies are being developed to accommodate volume and power restrictions of smaller spacecraft; cryocoolers are being designed to fit within 0.5U volumes, which will allow small spacecraft to use optical sensors and imaging spectrometers.

For feedback solicitation, please email: arc-sst-soa@mail.nasa.gov. Please include a valid business email.

References

(1) A. Anvari, F. Farhani, and K. S. Niaki. "Comparative Study on Space Qualified Paints Used for Thermal Control of a Small Satellite." 2009.

(2) Sheldahl, A Flex Company. "The Red Book." Jan 24, 2020 REV E. Available at: https://www.sheldahl.com/sites/default/files/2020-02/RedBook_0.pdf

(3) Thermal Management Technologies. "Products, Thermal Components: Flexible Thermal Straps." Accessed 2018. [Online] Available at: https://www.tmt-ipe.com/thermal-components

(4) Boyd Corporation. "Flexible Thermal Conductors -- Thermal Straps & Strap Assemblies." Datasheet. 2020. [Online] Accessed 2022. Available at: https://info.boydcorp.com/hubfs/Thermal/Conduction-Cooling/Boyd-Thermal-Straps-Technical-Datasheet.pdf

(5) Technology Applications, Inc. "Graphite Fiber Thermal Straps (GFTS)." 2022. [Online] Available at: https://www.techapps.com/graphite-fiber-thermal-straps

(6) Thermotive. "Products: Thermal Straps." 2019. [Online] Available at: http://www.thermotive.com/thermalstraps.html

(7) D., Gilmore. "*Spacecraft Thermal Control Handbook, Volume I, Fundamental Technologies, Chapter 8: Mountings and Interfaces."* 2002.

(8) Laird Technologies. Tflex HD80000 Series Thermal Gap Filler. Laird Technologies. Datasheet. [Online] Available at: https://www.laird.com/sites/default/files/tflex-hd80000-datasheet.pdf

(9) Laird Technolgies. "Tgon 800 Series Electrically and Thermally Conductive Interface Pad." Datasheet. [Online] Available at: https://www.laird.com/sites/default/files/tgon-800-datasheet.pdf

(10) Henkel Corporation, Bergquist. "Thermal Interface Materials Selection Guide. Bergquist." 2019. [Online] Available at: https://dm.henkel-dam.com/is/content/henkel/lt-8116-brochure-thermal-interface-materials-selection-guidepdf

(11) Thermal Management Technologies. "Thermally Efficient Deployable Radiators." Datasheet. 2021. [Online] Available at: https://www.tmt-ipe.com/product-sheets

(12) E. Urquiza, B.X. Zhang, M.P. Thelen, J.I. Rodriguez, and S. Pellegrino. "Folding Elastic Thermal Surface - FETS." June 1, 2013. [Online] Available at: https://www.techbriefs.com/component/content/article/tb/pub/techbriefs/mechanics-and-machinery/16598

(13) H.J. Kramer. "BIRD (Bi-Spectral Infrared Detection)." May 25, 2012. [Online] Available at: https://directory.eoportal.org/web/eoportal/satellite-missions/b/bird

(14) Y. Nakamura et al. "Small Demonstration Satellite-4 (SDS-4): Development, Flight Results, and Lessons Learned in JAXA's Microsatellite Project." 27th Annual AIAA/USU Conference on Small Satellites, Logan, UT. 2013.
(15) Thermal Management Technologies. "Thermal Storage Units." Datasheet. 2021. [Online] Available at: https://www.tmt-ipe.com/product-sheets
(16) Redwire Space. "Thermal Energy Storage Panel: Q Store." 2022. [Online] Available at: https://redwirespace.com/products/qstore/?rdws=nnn.szex.tfd&rdwj=43870
(17) D. Gilmore. Spacecraft Thermal Control Handbook, Volume I, Fundamental Technologies, Chapter 10: Heat Switches. 2002.
(18) NASA. NASA Technology Taxonomy and the NASA Strategic Technology Integration Framework, TX 14: Thermal Management Systems. July 2020. [Online] Available at: https://www.nasa.gov/sites/default/files/atoms/files/2020_nasa_technology_taxonomy_lowres.pdf
(19) Thermal Management Technologies. "Products: Small Spacecraft Structures. Thermal Management Technologies." 2019. [Online] Available at: https://www.tmt-ipe.com/small-spacecraft-structures
(20) K. Hogstrom. "State-of-the-Art Thermal Analysis Methods and Validations for Small Spacecraft," Ae241 Literature Survey. March 4, 2013.
(21) D. Hengeveld, J. Braun, E. Groll, and A. Williams. "Review of Modern Spacecraft Thermal Control Technologies and Their Application to Next-Generation Buildings." 2010. International High Performance Buildings Conference. Paper 40.
(22) R. Radebaugh. "Refrigeration for superconductors." 2004, IEEE, pp. 1719 - 1734.
(23) R. Hon, C. Kesler, and D. Sigurdson. "Integrated Testing of a Complete Low-Cost Space Cryocooler System." 2009.
(24) B. K. Malphrus et al. "The Lunar IceCube EM-1 Mission: Prospecting the Moon for Water Ice." Institute of Electrical and Electronics Engineers A&E Systems Magazine. April 2019.
(25) D., Gilmore. "Spacecraft Thermal Control Handbook, Volume I, Fundamental Technologies, Chapter 13: Thermoelectric Coolers." 2002.
(26) P. Champagne, J.R. Olsen, T. Nast, E. Roth, A. Collaco, G. Kaldas, E. Saito, V. Loung. "*Development of a J-T Micro Compressor.*" IOP Conf. Series: Materials Science and Engineering 101 (2015) 012009.



Table of Contents

Glossary ii
8.0 Small Spacecraft Avionics 219
8.1 Introduction 219
8.1.1 Chapter Organization and Disclaimers 220
8.2 State-of-the-Art: Onboard Computing 220
8.2.1 Radiation Mitigation and Tolerance Schemes 221
8.2.2 Computing Form Factors 222
8.2.3 Processor Architectures 223
8.2.4 Memory, Electronic Function Blocks, and Components 223
8.2.5 Bus Electrical Interfaces 224
8.2.6 Information Processing and AI 225
8.2.7 Highly Integrated Onboard Computing Products 228
8.3 State-of-the-Art: Flight Software 236
8.3.1 Implication of Onboard Computing on FSW 236
8.3.2 Frameworks 236
8.3.3 Operating Systems 239
8.4 On the Horizon: Avionics 239
8.5 Summary 240
References 241

Glossary

(AI/ML)	Artificial Intelligence/Machine Learning
(ASICs)	Application-specific Integrated Circuits
(CDH)	Command and Data Handling
(CMOS)	Complementary Metal-Oxide-Semiconductor
(ConOps)	Concept of Operations
(COTS)	Commercial-off-the-shelf
(CRAM)	Chalcogenide RAM
(DDD)	Displacement Damage Dose
(DRAM)	Dynamic RAM
(EPS)	Electrical Power System
(FERAM)	Ferro-Electric RAM
(FPGAs)	Field Programmable Gate Arrays
(FSW)	Flight Software
(I/O)	Input & Output
(LEO)	Low-Earth Orbit
(MRAM)	Magnetoresistive RAM
(OBC)	Onboard Computer
(PCM)	Phase Change Memory
(PSA)	Payload and Subsystems Avionics
(Rad-hard)	Radiation-hardened
(SDRs)	Software-defined Radios
(SEEs)	Single-event Effects
(SEL)	Single-event Latch-up
(SEUs)	Single-event Upsets
(SoCs)	System-on-chip
(SRAM)	Static Random-Access Memory
(SSA)	Small Spacecraft Avionics
(SWaP)	Size, Weight, and Power
(SWaP-C)	Size, Weight, Power, and Cost
(TID)	Total Ionizing Dose

8.0 Small Spacecraft Avionics

8.1 Introduction

Spacecraft avionics encompasses all electronic subsystems, components, instruments, and functional elements that enable a spacecraft to operate and fulfill its mission. This includes the primary flight sub-elements command and data handling (CDH), flight software (FSW), and the payload and subsystems avionics. These elements are configured according to specific mission architectures, operating concepts, development environments, and applicable standards. Collectively, the avionics system forms the foundational infrastructure upon which all spacecraft functions depend— the “brain and nervous system” of the spacecraft. It provides command, control, data management, and communication interfaces to every subsystem in some manner, whether in a direct point-to-point, distributed, integrated, or hybrid computing mode.

At its core, the CDH system is the FSW running on the onboard computer (OBC) responsible for managing spacecraft operations. CDH avionics are responsible for command and telemetry processing, real-time control using sensor inputs, network management, and data storage required to meet mission requirements. The onboard computing hardware within the CDH avionics includes the OBC along with the specialized integrated circuit (IC) chips on the OBC that support critical spacecraft functions e.g., memory devices, interface controllers, or data processing components. FSW consists of programs or algorithms running on the CDH avionics and all software running on the various subsystems and payload(s). FSW provides the instructions, operating environment, and autonomy logic that allow the spacecraft to execute both routine and mission-critical functions, manage subsystem operations, and generate and transmit telemetry.

Fundamentally, the principal avionics functions do not differ greatly between large and small spacecraft since mission objectives directly influence the avionics architecture. In both traditional spacecraft and SmallSats, the avionics system can be either centralized or distributed, single-string or redundant, and modular or monolithic. What matters is the required computational performance, data bandwidth, environmental robustness, and risk tolerance. Traditional large spacecraft are typically a high-size, weight, power, and cost (SWaP-C), flagship system with high-SWaP-C avionics design to reduce risk and address higher reliability requirements. Conversely, SmallSats—especially CubeSats—are low-SWaP-C systems built with more limited margins but greater tolerance for risk due to lower cost. While this approach is straightforward and reduces mission cost, it decreases redundancy that could introduce single points of failure and does not scale well for missions with high-rate payloads or advanced processing needs such as sophisticated autonomy, data handling, or fault-tolerant features.

Advances in electronics and semiconductor engineering, and miniaturized computing have transformed spacecraft avionics primarily for the smaller class of spacecraft that were previously limited by the low SWaP-C envelope, and accordingly low complexity and redundancy. As missions have grown more ambitious, increasing demands for onboard processing, modularity, and reliability have driven a shift toward more capable processors, distributed computing architectures, and flexible FSW frameworks. These developments now enable system-, board-, and chip-level designs for small spacecraft, including CubeSats, that can achieve functional parity with larger spacecraft through distributed architectures, system-level redundancy across nodes, and collaborative data processing.

As missions venture into more dynamic or distant environments, advanced fault-tolerant designs to enhance autonomy and resilience have become major drivers in avionics development. These farther distances imply that increased computational capability onboard will have high sensitivity to radiation. Mitigation strategies—such as watchdog timers, selective power cycling, and

software-based fault isolation—can improve robustness. Modern CDH avionics employ radiation-hardened-by-design (RHBD) techniques, fault tolerant architectures, and error mitigation approaches implemented at the software, hardware, and circuit levels.

Other notable trends include the use of high-speed data interfaces for large payloads (1), onboard AI/ML accelerators for real-time decision-making, and increased focus on cybersecurity to protect command and data links (2). Additional trends include the use of commercial off-the-shelf RFSoCs to interface with radio links and attitude and control systems that require hard real-time constraints (3). Further developments include onboard AI/ML-enabled autonomy and FSW middleware designed for SmallSats constellations, supporting resource management, scheduling and task assignment, and fault tolerance.

8.1.1 Chapter Organization and Disclaimers

Given the distributed and integrated nature of modern spacecraft avionics, this chapter examines onboard computing and FSW separately to clearly outline capabilities. Additionally, technology readiness for avionics can be muddled because all spacecraft avionics designs will differ per mission. Applying NASA's traditional TRL scale to onboard computing and FSW is challenging because avionics hardware and software evolve continuously often through incremental updates, reuse of components, and mission-specific customization rather than discrete, testable prototypes. Therefore, Section 8.2 describes the current state of the art of onboard computing, including components like memory, form factors, interfaces, and information processing, and radiation mitigation. Commercial products are listed in Table 8-4 under Section 8.2.7. The FSW environment is provided in Section 8.3, while Section 8.4 presents what is on the horizon for avionics development.

The information described below is not intended to be exhaustive; rather it provides an overview of current state-of-the-art technologies and their development status for small satellite subsystems. The list of organizations and companies in this chapter is not all-encompassing and does not constitute an endorsement from NASA. There is no intention of prioritizing certain companies or omit others based on their technologies or relationship with NASA. The information is provided for awareness and guidance only. The performance advertised may differ from actual performance because the information has not been independently verified by NASA subject matter experts and relies on information provided directly by manufacturers or from publicly available sources. It should be noted that TRL designations may vary depending on specific payload, mission requirements, reliability considerations, and the environment in which performance was demonstrated. Readers are highly encouraged to consult companies directly for further information regarding performance and TRL of the technology described.

8.2 State-of-the-Art: Onboard Computing

The capability of onboard computing is determined by the OBC hardware, including the IC chips responsible for executing instructions and performing calculations reliably in the harsh environment of space. The OBC hardware—board design and form factor, processor choice, memory architecture, power conditioning, radiation tolerance—forms the foundation of the spacecraft's command and data handling functions. Tertiary IC chips may be integrated into the OBC, including processors for computation, memory components such as RAM and Flash for data storage, and Field-Programmable Gate Arrays (FPGAs) for flexible logic operations. These components enable the OBC to communicate with subsystems, store data, and interface with sensors, however all primary computing functions are executed by the processor within the OBC. Collectively, these capabilities enable real-time control, command execution, telemetry generation, data storage, and subsystem coordination. These functions can be implemented in several ways, and advances in avionics now enable more options for low-SWaP-C SmallSat missions.

The way the OBC is used defines the avionics architecture; specifically, how control, decision-making, and data handling are distributed. This distribution may occur through a single, centralized control authority or through subsystems with their own processors or microcontrollers performing meaningful functions. If the primary OBC is responsible for all commanding—including control loops, subsystem commanding, data handling and routing, timekeeping and scheduling, and fault detection— the avionics architecture is centralized, since a single source is performing all the meaningful functions. Conversely, if the primary OBC communicates with additional support components that can operate without commands from the OBC, the architecture is distributed at the subsystem level. Architectures where information processing is distributed across multiple nodes can almost eliminate the single-point-of-failure issues, as the system does not rely on a single computing element.

Current trends in SmallSat onboard computing generally mirror those of larger-scale systems, emphasizing greater computational power and efficiency. Centralized avionics designs remain common due to their simplicity, lower cost, and straightforward integration using a single-board OBC. However, more complex SmallSat and CubeSat missions now have feasible solutions to employ higher-performance components or distributed avionics architectures. Factors to consider when selecting onboard computing solutions include the computing form factors (how the OBC is formed), information processing enhancements, radiation mitigation and tolerance schemes, memory, and bus electrical interfaces.

Cost and availability are likely primary factors in selecting a CDH subsystem design from a given manufacturer, although many groups develop custom CDH platforms. The ability to spread nonrecurring engineering costs over multiple missions and reduce software development through reuse are both desirable in a competitive market. Heritage designs work well for customers looking to select components with proven reliability for their mission provided key components are still in production.

8.2.1 Radiation Mitigation and Tolerance Schemes

While on-orbit, space radiation is a major factor to consider when designing the avionics system, and the effects of radiation on electronic devices can vary broadly (4). Radiation effects are often categorized into long-term cumulative effects and transient single-event effects (SEEs). Long-term effects are measured by total ionizing dose (TID) and displacement damage dose (DDD). TID, measured in krad, is the ionizing radiation absorbed by the device material over time, causing parametric or functional degradation of the device. DDD is the nonionizing damage caused by particle collisions with the device structure over time. SEEs occur when a single radiation particle strike deposits enough charge to cause an effect. SEEs can be destructive or nondestructive. Single-event upsets (SEUs) are nondestructive SEEs that can affect the logic state of a memory cell. Single-event latch-ups (SELs) are destructive SEEs that manifest as parasitic structures in complementary metal-oxide-semiconductor (CMOS) logic or bipolar transistor structures, potentially causing a high-current state.

Traveling into planetary space or longer LEO missions compel developers to consider reliability requirements and incorporate radiation-mitigation strategies into their respective spacecraft designs. For missions in harsher environments, spaceflight heritage and demonstrated radiation performance become primary differentiators when selecting electronics, especially compared to designs that rely heavily on commercial-off-the-shelf (COTS) parts. In contrast, experimental, high-risk missions typically focus on low-cost, easy-to-develop systems that take advantage of open-source software and hardware to provide an easy entry into space systems development, especially for hobbyists or those who lack specific spacecraft expertise. CubeSats are often either composed of only COTS components or a hybrid combination of COTS, rad-hard, and radiation-tolerant components. A default approach in SmallSat avionics has traditionally been COTS

components first (e.g., processor and memory), combined with rad-hardened supporting electronics such as ECC, watchdog timers, scrubbing, and redundancy to maximize the benefits of both technologies. These designs may also incorporate radiation-mitigation techniques to further enhance overall system reliability.

COTS components typically offer superior performance, energy efficiency, and affordability compared to their rad-hard alternatives; however, COTS devices tend to be highly susceptible to radiation. The miniaturization of electronics, sensors, and instruments has enabled spacecraft manufacturers to use more space-qualified parts. Advantages of COTS components have enabled low-cost CDH development, while also allowing developers to leverage start-of-the-art technologies in their designs.

An emerging trend is the adoption of radiation-hardened by design (RHBD) techniques within commercial semiconductor processes. In RHBD approaches, companies are modifying the transistors, gates, and physical layouts inside the silicon so the chip is inherently more resistant to radiation. These methods include specialized circuit topologies, hardened standard-cell libraries, and radiation-aware layout practices that provide protection against SEUs, SET-induced logic glitches, functional upsets, and latch-up. High-performance processors increasingly use selective hardening for the most vulnerable blocks, while applying architectural redundancy only where necessary to avoid excessive power or area overhead.

8.2.2 Computing Form Factors

The underlying platform for onboard computing systems is a printed circuit board (PCB) with chip(s) soldered on, which mechanically connect and communicate depending on the PCB layout. Modular form factors use standardized physical and electrical interfaces that allow components to interoperate or be swapped. Conversely, monolithic architectures often require significant non-recurring engineering because components are custom-designed and tightly coupled.

Standard CubeSat CDH designs are PCBs that can be stacked vertically using board-to-board connectors, often without a backplane and sometimes without a formal chassis (e.g., PC/104, CubeSat card stacks). This form factor is compact and lightweight, but limited in bandwidth compared to modern formats (5). The backplane-based plug-in card (PIC) systems use cards that slide into slots and connect with a common backplane (e.g., CompactPCI, SpaceVPX). This setup supports high-bandwidth, provides rigid mechanical alignment, and allows for hot swaps in some standards, although a chassis is required (6). Some vendors have made modifications to stackable interface connectors to address reliability and throughput concerns. Many vendors use mezzanine stackable "daughter" boards to enhance modularity between subsystem elements and payloads that must adhere to form factor constraints. Mezzanine modules are small add-on cards that are mounted onto a host board (e.g., PMC, XMC). This modular package allows users to select from a variety of computational processors. NASA’s R5 Realizing Rapid, Reduced-cost high-Risk Research project moved away from rigid PC/104 stacking to adopt flexible, modular frameworks that accommodate late-stage payload changes (7)(8).

Cable-connected topologies connect boards or modules through dedicated wiring harnesses rather than through stacked connectors or a backplane. In this approach, modules are linked using interfaces such as SpaceWire, Ethernet, CAN, or flexible flat-cable (FFC/flat-flex) connections. These cabling-based networks allow subsystems to be physically separated within the spacecraft while still supporting high-speed data transfer and deterministic communication paths. They also provide design flexibility, as each module can be independently located, thermally isolated, or shielded as needed.

It is also common for modern spacecraft to use a hybrid of architectures rather than committing to a single topology. For example, a central OBC might use an internal backplane for power and

housekeeping functions, while payload processors or interface modules connect via SpaceWire or Ethernet harnesses. This mixed approach enables designers to balance mass, integration simplicity, fault isolation, and performance, allowing each subsystem to be optimized for its specific role.

8.2.3 Processor Architectures

The choice of processor architecture is key in the spacecraft CDH layout, and mission complexity is often reflected directly in the processing hardware selected. While avionics technology continues to evolve rapidly—especially for SmallSat platforms—there is no single "best" processor type for all missions. Instead, the diversity of mission needs, data-handling requirements, autonomy levels, and power constraints leads engineers to select among several processor classes, each offering distinct advantages.

Traditional radiation-hardened processors have long formed the backbone of spacecraft computing, valued for their reliability, radiation tolerance, and predictable real-time behavior. These devices, including rad-hard microcontrollers (MCU) and radiation-tolerant ARM-based MCUs, typically provide modest processing capability, but extremely high robustness. They are well suited for deterministic tasks such as spacecraft housekeeping, sensor interfacing, and closed-loop control. Their architectural simplicity and flight heritage make them a dependable choice for missions prioritizing longevity, safety, and stable operation over raw compute throughput.

Modern high-performance processors, including advanced microprocessors and radiation-tolerant multicore devices, offer significantly greater compute capacity, throughput, and energy efficiency than earlier designs. These processors can support demanding onboard computing, including high-rate data handling, image processing, compression, and real-time decision-making. Their ability to run more capable operating systems and support complex software stacks makes them increasingly attractive for missions requiring autonomy, rapid onboard data reduction, or support for advanced payloads. As a result, these processors can easily satisfy the processing needs of most current spacecraft subsystems and are expected to remain viable for future spacecraft bus architectures.

One of the most significant architectural shifts in recent years is the emergence of System-on-Chip (SoC) platforms. Engineers can now integrate multiple computing elements—including CPUs, hardware accelerators, memory controllers, and programmable logic—onto a single piece of silicon. SoCs dramatically reduce size, mass, and power requirements compared to earlier discrete avionics designs, while providing substantially greater computational capability. Their high level of integration also simplifies board design and can reduce interconnect complexity, making them well suited for next-generation spacecraft that require both compact hardware and extensive onboard processing.

8.2.4 Memory, Electronic Function Blocks, and Components

The range of onboard memory for small spacecraft varies widely—typically from hundreds of KB to several GB—and scales upward with technological improvements. For CDH functions, onboard memory requires high reliability. A diverse suite of memory technologies are available for specific traits, including: volatile memory types for real-time processing, buffers, and temporary data handling (e.g., Static Random-Access Memory (SRAM) and Dynamic RAM (DRAM)); and non-volatile storage options for telemetry logs, subsystem data, and temporary payload storage (e.g., Magnetoresistive RAM (MRAM), Ferro-Electric RAM (FERAM), and Phase Change Memory (PCM)). SRAM remains a common choice due to its cost-effectiveness, maturity, and availability; typical space-grade SRAM is available in densities from 4 Mb to 32 Mb (0.5–4 MB), with some QSPI and NOR flash reaching higher.

Semiconductor manufacturers describe a memory chip's organization to indicate how the chip is structured internally. This typically includes its total storage capacity and the width of its data bus (such as 8-bit, 16-bit, or 32-bit). These details determine how many identical memory chips must be combined to match the processor's data-bus width. For a processor to access memory at full speed, the combined width of all memory chips must equal the CPU's bus width. If it does not, the system may need extra cycles to read or write data or require a memory controller to bridge the mismatch. Package can refer to the physical dimensions of the device, but it can also describe how the memory capacity is organized internally—such as how many bits the chip presents on its data bus.

Flash memory excels in delivering high-density storage, but has limited write cycles and slower operations. In contrast, ferroelectric RAM offers smaller capacity, yet boasts rapid write speed, low power, and ultra-high endurance—ideal for frequent data logging or sustaining mission-critical parameters. Sampler memory (SRAM/DRAM) sits in between, supporting runtime responsiveness rather than long-term data retention. Numerous manufacturers offer space-qualified, radiation-hardened memory and components certified to ESCC/QML and military standards. A chart comparing the various memory types and their performance is shown in Table 8-1.

Table 8-1: Comparison of Memory Types

Feature	SRAM	DRAM	Flash	MRAM	FERAM	PCM
Non-volatile	No	No	Yes	Yes	Yes	Yes
Operating Voltage	3.5 – 5 V	1.35-3.3 V	3.3 & 5 V	3.3 V	3.3 V	3.3 V
Data Retention (70°C)	N/A	N/A	>100 years	10 years	10 years	10 years
Endurance (Erase/Write cycles)	Unlimited	Unlimited	1E5	1E13	1E13	1E13
Access Time	10-25 ns	25 ns	50 ns	300 ns	300 ns	100 ns
Power	500 mW	300 mW	30 mW	900 mW	270 mW	Unk

8.2.5 Bus Electrical Interfaces

CubeSat class spacecraft continue to use interfaces that are common in the microcontroller or embedded systems world. Highly integrated systems will typically provide several interfaces to accommodate a wide range of users, and to ease the task of interfacing with peripheral devices and other controllers. FPGAs are commonly used for these interfaces because of their flexibility and ability to change interfaces as needed. Some of the most common bus electrical interfaces are listed below, along with applicable interface standards.

Table 8-2: Common bus electrical interfaces

Electrical Interfaces	Interface Standards
Serial Communication Interfaces (SCI)	RS-232, RS-422, RS-485 etc.
Synchronous Serial Communication Interface	I2C, SPI, SSC and Enhanced Synchronous Serial Interface (ESSI)
Networks	Ethernet, LonWorks, etc.
Fieldbuses	CAN Bus, LIN-Bus, PROFIBUS, etc.
Timers	PLL(s), Capture/Compare and Time Processing Units

Discrete IO	General Purpose Input/Output (GPIO)
A/D, D/A	Analog to Digital/Digital to Analog (ADC/DAC)
Debugging	JTAG, ISP, ICSP, BDM Port, BITP, etc.
SpaceWire/SpaceFibre	a standard for high-speed serial links and networks
High-speed data	RapidIO, XAUI, SerDes and MGT protocols are common in routing large quantities of mission data in the gigabit per second speeds

8.2.6 Information Processing and AI

Advances in on-orbit spacecraft information processing have garnered significant attention in recent years, particularly for Earth observation missions. A spacecraft's ability to collect, process, store, and transmit data efficiently within tight constraints is the core of information processing. While on-orbit, a spacecraft (large or small) collects significant volumes of raw data, stores it temporarily, and later transmits it to Earth for post-processing and analysis. Ideally, a spacecraft would process and compute the data in real time and downlink only distilled, useful information rather than vast amounts of unfiltered raw data. Advances in onboard electronics now enable computation on the "edge" of the spacecraft—or within the CDH avionics—where incoming data can be filtered, analyzed, and interpreted directly on orbit.

This shift from basic data logging to autonomous decision-making is driving the adoption of edge computing, Machine Learning (ML), and Artificial Intelligence (AI). Edge computing focuses specifically on where and how data is processed—moving high-value computation as close as possible to the source of the data. ML refers to the techniques that allow models to identify patterns or make predictions based on onboard sensor and payload data. AI encompasses higher-level logic and decision-making processes that manage how information is interpreted, prioritized, and acted upon within the spacecraft.

Spacecraft autonomy can be considered part of management, direction, and control for all spacecraft subsystems and functions. These subsystems may also have a degree of autonomy depending on the complexity of its local "smart subsystems" processor. NASA examines autonomous systems as a cross-domain capability that enables the spacecraft to operate in a dynamic environment independent of external control, including situational and self-awareness, reasoning and acting, collaboration and interaction, and engineering and integrity. SmallSat designers have particular interest in autonomous systems applications, and studies like Whitney & Melville's 2025 work on reinforcement learning for attitude control demonstrate that even 3U CubeSats are being equipped with trusted, autonomous onboard decision-making systems (9). Another example of autonomous spacecraft operations is the ASTREA (Agentic System for Thermal Regulation and Embedded Adaptation) AI system, which uses large language model (LLM)-guided control for in-flight thermal management, demonstrating semantically aware and adaptive decision-making. In 2025, ASTREA was integrated onboard the International Space Station (ISS), and was able to understand current limitations of agentic LLM-based systems in real flight environments (10).

AI Space Applications

As a field of research, AI is more than any single technique, such as a neural-network or LLM. Instead, AI encompasses numerous approaches for planning, reasoning, search, reinforcement learning, optimization, robotics, and more. Around 2015, researchers began running AI workloads on graphics processing units (GPUs), leading to massive performance gains and paved the way for modern GPUs and neural processing units (NPUs). To achieve the robust autonomous capabilities on-orbit, researchers can employ a heterogeneous architecture—combining multiple

processors like CPUs, GPUs, NPUs, or FPGAs, with increased emphasis on memory bandwidth, interconnect efficiency, and power-optimized system design (11).

These advancements have enabled onboard neural networks for autonomous station-keeping, orbit planning, and near real-time payload processing. In July 2023, D-Orbit's ION SCV004 CubeSat successfully ran the RaVAEn (Relational and Analogical Visual rEasoNing) VAE neural network onboard, demonstrating image compression and on-chip few-shot training (12).



Table 8-3: Examples of AI Space Applications		
AI Space Application	**Description**	**Example(s)**
Spacecraft image analysis	AI-driven computer vision greatly accelerates the interpretation of satellite imagery.	(13)
Autonomous Navigation & Robotics	Spacecraft can navigate and make decisions w/o human command.	NASA's Starling mission of four CubeSats formation flying
Space Debris Tracking & Collision Avoidance	Machine learning can improve the tracking and predictive modeling of objects in orbit, helping identify high-risk conjunctions.	LeoLabs and Neuraspace similarly use AI to sift sensor data and predict close approaches, issuing automated "conjunction" warnings (14)(15).
Space weather forecasting	Predicts solar storms or other events that could harm spacecraft or power grids.	National Aeronautics and Space Administration (NASA) and National Oceanic and Atmospheric Association (NOAA).
Mission Planning and Optimization		
Communications and Data Transmission	Cognitive communications research aims to mitigate the increasing communication complexity for mission users by increasing the autonomy of links, networks, and service scheduling.	Cognitive Communications project at NASA Glenn Research Center (GRC) aims to develop decentralized space networks with artificial intelligence (AI) agents optimizing communication link throughput, data routing, and system-wide asset management to mitigate this challenge (16).
Satellite Health Monitoring & Predictive Maintenance		DAGGER (Deep Learning Geomagnetic Perturbation) that analyzes satellite measurements of the solar wind to predict the impact of solar storms on Earth with 30 minutes of advance warning; accurate global predictions and inform decisions in the event of a solar storm (17).

8.2.7 Highly Integrated Onboard Computing Products

The demand for on-board computing capabilities, autonomous systems, and machine learning implementation has driven the commercial sector to emphasize high-performance products. Commercial-grade, highly integrated computing products—such as advanced System-on-Chip (SoC) modules and rugged compute boards—are transforming mission- and edge-critical environments. Modern data processing units that support higher-level capabilities such as autonomy, onboard information processing, and edge-computing algorithms are now widely implemented across SmallSat missions.

A variety of vendors develop highly integrated, modular, onboard computing systems for small spacecraft and CubeSats. These CDH packages combine processors and/or FPGAs with various memory banks and a variety of standard interfaces for other subsystems onboard.

System developers are gravitating toward ready-to-use hardware and software development platforms that can provide seamless migration to higher performance architectures. As with non-space applications, there is a reluctance to change controller architectures due to the cost of retraining and code migration. Following the lead of microprocessor and FPGA vendors, CubeSat avionics vendors are now providing simplified tool sets and basic, cost-effective evaluation boards.

FPGAs and software-defined architectures also give designers a level of flexibility to upload modifications and adapt to new requirements and interfaces. Emerging CubeSat avionics are increasingly integrating FPGA-based SDRs, enabling software-defined communications adaptable to multiple protocols.

Table 8-4 provides an overview of the current state-of-the-art for some of these components. It should be noted that while some products have achieved TRL 9 by virtue of a space-based demonstration, what is relevant in one application may not be relevant to another, and different space environments and/or reliability considerations may result in lower TRL assessments. Some larger, more sophisticated computing systems have significantly more processing capability than what is traditionally used in SmallSat onboard computing; however, the increase in processing power may be a useful tradeoff if payload processing and CDH functions can be combined. Overall throughput should be analyzed to ensure proper functionality under the most stressful operating conditions.

Table 8-4: Sample of Highly Integrated Onboard Computing Systems

Manufacturer Headquarters	Product	Processor/ SoC/ FPGA	Radiation Hardness Assurance (RHA)	Board Dimension (cm)	Power Consumption (W)	Orbits Flown
AAC Clyde Space Sweden	Kryten-M3	Smart Fusion 2 SoC including an ARM Cortex-M3 processor delivering 62.5 DMIPS	TID 20 krad (system level)	9.59x9.02x0.55	0.4	LEO
	Sirius OBC & TCM	32-bit LEON3FT (IEEE-1754 SPARC v8) fault-tolerant processor	TID 20 krad (system level)	9.59x9.02x1.72	1.3	LEO, lunar lander
Alén Space Spain	DARA OBC	ARM 32-bit Cortex-M7 with FPU	N/A	8.93x9.33x1.2	Max: 0.280	LEO, 2024
Aitech Systems Inc. USA	SP0-S	Power PC 1020, Alcatel RTAX	100 krad TID, SEL/LET 40 Mev-cm2/mg (without enclosure)	3U cPCI: 10.06x16x20.3	12	LEO, MEO, GEO, Lunar, Deep Space*
	SP1-S	64-bit Arm® Cortex®-A72 cores @ 1.8 GHz	100 krad TID (Target)	3U Space VPX: 10.06 x16x20.3	<25	TBD
	S-A1760	Pascal™ Architecture GPU w/256 CUDA® cores NVIDIA Denver 2 Dual-Core ARM® CPU + Cortex® A57 Quad-Core ARM® CPU	1.05 krad TID, < 1 type 2 SEFI update in 158 days (without enclosure)	12.7 x12.7x5.2	Configurable ≤ 5 Idle, 8-10 under typical CUDA load,<20 when System on Module is fully utilized	LEO*
	S-C8780	Intel® Pentium-D or Xeon-D, discrete 2D GPU, Xilinx UltraScale+ FPGA w/Dual-core ARM® CPU	TBD	3U Open VPX: 10.06 x16x20.3	Configurable 25-55	TBD
	S-C8500	Intel® Tiger Lake UP3 SoC, 4 cores/8 threads, integrated GPGPU with 96 Execution Units, Xilinx UltraScale+ FPGA w/Dual-Core ARM® CPU is Optional	1 krad TID, SEL/LET TBD (without enclosure)	3U Open VPX: 10.06 x16x20.3	CPU Configurable from 12-28, Total system 22-42 configs.	TBD
Aerospacelab Belgium	OBC	Xilinx Zynq-7045 ARM dual-core Cortex A9 running at 667MHz Kintex-7 FPGA with 350k Programmable Logic Cells, 218,600 Look-up tables (LUT) and 437,200 flip-flops (FF) Linux and FreeRTOS compatible	Radiation hardened supervisor MCU Radiation hardened watchdog Heavy ions (62.5 MeV) No destructive event	187x84.1x116.6 mm³ L x W x H Mass 1.325 kg	<4	LEO

Table 8-4: Sample of Highly Integrated Onboard Computing Systems

Manufacturer Headquarters	Product	Processor/ SoC/ FPGA	Radiation Hardness Assurance (RHA)	Board Dimension (cm)	Power Consumption (W)	Orbits Flown
Andes Aerospace Chile	Andes OBC	2x ARM 32-bit Cortex-M7 with FPU @ up to 550MHz	Estimated TID: 30krad (not tested) OBC+MRAM+NAND full cold redundancy	10x10x1.4	Depends on configuration. Active: ~0.1	LEO
Argotec Italy	OBC FERMI	Dual-Core LEON3FT SPARC V8 Processor with fault-tolerant memory controller +Microchip RTG4	Rad-hard	10.24x10x4.49	5 (depending on load)	Deep Space, Lunar Orbit, LEO
Berlin Space Technologies GmbH Germany	CDH-110	STM32F103	TID 30kRad (PCB level)	17.6x9.4x6.9	< 2	LEO
Bradford Space Netherlands	Stellar OBC + PDHS	Dual Polarfire SoC	30 krad (Si) + functional SEE resilience through SW EDAC and internal cold redundancy	13.3x11.5	< 25W Full Load / < 3 Typical / < 1 Idle	TBD
C3S Electronics Development LLC Hungary	OBC	32-bit ARM Cortex-M7	Continuous integrity check on the program memory, multi-level watchdog system, MRAM storage	9.2x8.95 x1.36 w/ daughterboard, 9.2x8.95x1.23 w/o	0.46 (measured in test mode, using eMMC as mass storage)	LEO
CesiumAstro USA	SBC-1461	1.4 GHz ARM Cortex	Rad Tolerant	5x8.4x1.3	8 typ.	LEO
	RDP-23FV	Xilinx Versal	Rad Tolerant to Rad Hard	16x10x2.54	50	LEO
Emxys Spain	ODALISS OBC	Dual 32-bit STM32 processor unit, ARM, Cortex-M7 + Cortex-M4, at 480MHz	Rad Tolerant TID of 20Krad	8.7x8.7x1	0.65	LEO
	ODALISS DIPP	Xilinx Zynq-7000 SoC Dual 667MHz 32-bit ARM Cortex-A9	Rad Tolerant TID of 20Krad	8.7x8.7x1	1.65	LEO
EnduroSat Bulgaria	OBC I	ARM Cortex M7	Tested at 40 krad TID	8.9x9.4x2.3 (with integrated GNSS)	1.5 Peak 0.2 Idle	400-600 km SSO, equatorial
	OBC II	ARM Cortex M7	40 krad TID (to be tested)	8.9 x 94 x 2.3 (with integrated GNSS)	6 W Peak < 1 W Idle	LEO



Table 8-4: Sample of Highly Integrated Onboard Computing Systems

Manufacturer Headquarters	Product	Processor/ SoC/ FPGA	Radiation Hardness Assurance (RHA)	Board Dimension (cm)	Power Consumption (W)	Orbits Flown
	EnduroSat GPC	NVIDIA Jetson Orin	40 krad TID (to be tested)	22x13.5x5	130 W Peak < 15 W Idle	LEO
GomSpace Denmark	NanoMind HP MK3	Xilinx Zynq 7030/7045	>20 krad	9.5x9.5x3.15	Dependent on customer application	LEO
Ibeos USA	EDGE-1100 (3U SpaceVPX)	AMD Ryzen SOC	TID: 30 krad SEE: >37 MeV	3U SpaceVPX; 16x10x2.5(pitch)	6-35	LEO & GEO
	EDGE-1100 Genie	AMD Ryzen SOC	TID: 30 krad SEE: >37 MeV	14.8x10.8x 3.4 – Stand-alone box	8-35	LEO & GEO
	Core-250	High Performance Space Computer Processor (HPSC), 8 x RISC-V cores, 3U SpaceVPX	--	16x10x2.5(Pitch)	<25	LEO, GEO
Innoflight USA	CFC-400XS	Defense Grade Xilinx UltraScale+ MPSoC	TID: 30 krad	8.2x8.2x2.7	6-25	LEO & GEO
	CFC-400XP	Defense Grade Xilinx UltraScale+ MPSoC	TID: 30 krad	17.2x10x2.5	4-30	LEO
	CFC-510P	AMD Ryzen GPGPU	TID: 30 krad	17.2x10x2.5	12-40	LEO
KP Labs Poland	Antelope OBC and DPU	OBC – RM57 Herkules microcontroller (Dual 300 MHz ARM Cortex-R5F with FPU in lock-step) DPU – AMD Xilinx Zynq UltraScale+ MPSoC (ZU2EG, ZU3EG, ZU4EG, ZU5EG), Quad ARM Cortex-A53 CPU, Dual ARM Cortex-R5 in lock-step	COTS with SEE mitigation	Motherboard – 1x1x1 Daughterboard - 7x4x2	From less than 0.5 (DPU is off) to 6 (DPU processes the data)	LEO
	Leopard DPU	AMD Xilinx Zynq UltraScale+ MPSoC (ZU6EG, ZU9EG, ZU15EG); Quad ARM Cortex-A53 CPU; Dual ARM Cortex-R5 in lock-step	COTS with SEE mitigation	Non-redundant: 9x9.5x5 Redundant: 9x9.5x7.8	7 static; up to 10 for deep learning inference	LEO
	Lion DPU	AMD Xilinx Kintex Ultrascale FPGA (KU035, KU060, KU095)	COTS with SEE mitigation	16x10x5	<15 for KU035 version	TBD
Laboratory for Atmospheric and	LASP Generic Small-sat FPGA Board	Kintex-7	25 krad	8.763x8.763	1	LEO

Table 8-4: Sample of Highly Integrated Onboard Computing Systems

Manufacturer Headquarters	Product	Processor/ SoC/ FPGA	Radiation Hardness Assurance (RHA)	Board Dimension (cm)	Power Consumption (W)	Orbits Flown
Space Physics USA						
Micro Aerospace Solutions USA	MAS-SBC-107	Arm® Cortex®-M7	Total Ionizing Dose of 30 krad (Si)	9×9.6	<30	LEO
Nara Space Technology Busan	NSTOBC	Atmel ARM 9 based Microprocessor Unit	<24 krad	9x9x1.6	0.429 (Idle)	LEO
NOVI LLC USA	Gen 2 OBC	AMD/Xilinx Versal (AI Edge Series): Dual-core ARM® Cortex®-A72, Dual-core ARM® Cortex®-R5F, Programmable Logic (FPGA), AI Engines. Vorago ARM MCU: Low-power ARM® Cortex®-M4, Embedded rad-hard FRAM.	Radiation-hardened Vorago ARM MCU, SEL immune Xilinx processor, Optional radiation-hardened memory, Built in SEU/SEFI mitigation, ECC protected memory interfaces, Redundant storage for boot images.	9.3x9.3x2.5	<0.75W (Low Power Mode) 5-50W (High Performance Modes, Application Dependent)	LEO
Novo Space USA	SBC002AV	Zynq Ultrascale+	TID: 30 krad; Automotive parts with Rad-tolerant in high criticality parts; Rich telemetry with local event response; Board sectorization and power control; ECC in Volatile memories; CRC / Reed-Solomon / Interleaving in Non-Volatile memories; FPGA and fabric use selective TRM on critical functionality; Scrubbing on soft FPGAs.	16x10	application dependent active mode max: 15	TBD
	SBC003AV	SmartFusion2		16x10	application dependent active mode max: 8	TBD
	SBC004AF	Versal ACAP		16x10	Under development	TBD
	SBC005AF	Polarfire		16x10	application dependent active mode max: 8	TBD
	GPU001AF	Jetson TX2i		8.7x5	active mode: 9-15	TBD



Table 8-4: Sample of Highly Integrated Onboard Computing Systems						
Manufacturer Headquarters	**Product**	**Processor/ SoC/ FPGA**	**Radiation Hardness Assurance (RHA)**	**Board Dimension (cm)**	**Power Consumption (W)**	**Orbits Flown**
	GPU002AF	Jetson Orin Nano	TID: 30 krad	8.7x5	active mode:6 - 11	TBD
Pumpkin Space Systems USA	PPM A1	MCU+DSP	N/A	90x96	0.05	LEO
	PPM A2	MCU+DSP	N/A	90x96	0.05	LEO
	PPM A3	MCU+DSP	N/A	90x96	0.05	LEO
	PPM B1	MCU+DSP	N/A	90x96	0.05	LEO
	PPM D1	MCU	N/A	90x96	0.05	LEO
	PPM D2	MCU+DSP	N/A	90x96	0.05	LEO
	PPM E1	MCU	N/A	90x96	0.05	LEO
	PPM B1	MCU+DSP	N/A	90x96	0.05	LEO
	PPM D1	MCU	N/A	90x96	0.05	LEO
	MBM2 w/BBB	MCU	~5 krad	90x96	2	LEO
Ramon Space USA	NuPod	Space Grade Xilinx Versal ACAP, Cortex A72 4x / 16x Core ARM	TID: 30 krad SEL: 43 MeV·cm2/mg	28.7x21.5x7.5 Mounted enclosure	20-90	TBD
Resilient Computing USA	RadPC-SBC-001	RISC-V 32-Bit (AMD Artix 7)	COTS with SEE mitigation	10x10	1.5	LEO, Lunar
SatRev S.A. Poland	OBC	ARM Cortex-A72 v8, quad-core 1.5 GHz, 64-bit	N/A	9.95x9.6x2.15	2.8 W typical, 5 W peak	LEO
SENyT Argentina	Q-OBC	STM32	COTS w/watchdog latch-up protection	9.6x9.0x1.8 w/ enclosure	< 0.2	TBD
Sierra Space USA	UMCD	Microchip RTSX72	100kRad TID (Si)	11.4x11.4x4.4	7	LEO, GEO
SkyLabs Slovenia	NANOhpc-obc	4x RISC-V 64-bit / PolarFire / SoC	COTS w/ SEE mitigation	9.5x9.1x1.3	3	LEO
	NANOhpm-obc	32-bit RISC-V core / PolarFire	COTS w/ SEE mitigation	9.5x9.1x1.3	<5	LEO, MEO
	NANOhpc-AI	4x RISC-V 64-bit; 2x Hailo-8 AI accelerator	COTS w/ SEE mitigation	9.5x9.1x2.8	8	TBD
	NANOhpc-DPU	4x RISC-V 64-bit; Zynq™ UltraScale+™, MPSoC ZU7EV	COTS w/ SEE mitigation	9.5x9.1x2.8	11	TBD
	NANOobc-2	PicoSkyFT / IGLOO 2	COTS w/ SEE mitigation	9.5x9.1x1.1	<1 Peak, <0.9 Idle	LEO, MEO
Space Dynamics Laboratory USA	SDL-25	UT700 LEON3-FT + RT3P FPGA	10 krad	13x9	2-6	LEO, GEO
	LEON 4	GR740 LEON4 + RTG4	50 krad	SpaceVPX 6U	12	LEO, GEO
	OBC-P4	4x ARM Cortex-M7	TBD	9.3x9.3x0.875		LEO



Table 8-4: Sample of Highly Integrated Onboard Computing Systems

Manufacturer Headquarters	Product	Processor/ SoC/ FPGA	Radiation Hardness Assurance (RHA)	Board Dimension (cm)	Power Consumption (W)	Orbits Flown
Space Inventor Denmark	Z7000	Xilinx Zynq 7030	TBD	-	-	LEO, GEO
Spacemanic Czech Republic	DeepThought	SAMV71	-	6.7x4.2x0.7	0.06	LEO
	Eddie	MSP430	-	6.7x4.2x0.7	0.33	LEO
SPiN USA USA	MA61C CubeSat	GR712RC dual-core 32-bit LEON3 fault-tolerant, SPARC V8 processor	Processor is 300 krad	9.599x9.027	1-1.2	TBD
	MA61C smallsat	GR712RC dual-core 32-bit LEON3 fault-tolerant SPARC V8 processor	Processor is 300 krad	10.5x10.5	1-1.2	TBD
	MA61C cPCI serial space	GR712RC dual-core 32-bit LEON3 fault-tolerant SPARC V8 processor	Processor is 300 krad	16x10	1-1.2	TBD
Spiral Blue Australia	Space Edge One	Nvidia Jetson Xavier NX	N/A	10x10	7	LEO
Southwest Research Institute (SwRI) USA	Centaur SBC	GR712RC dual core LEON3-FT CPU, Xilinx Ultrascale or Microchip RT-ProAsic or RTG4 FPGA	TID: Up to 60 krad (Si), more with shielding SEL: Immune to >67eV/mg/cm2 SEU: < 1 error per 24-hour period	Available in 3U/6U cPCI form factors	Low power < 4 Operation	LEO
	HP-SBC	PowerPC based MPC8548e CPU, Microsemi RT-ProASIC FPGA, Optional: Microsemi RTG4 FPGA, Optional: Xilinx Ultrascale FPGA	TID: Up to 60 krad (Si), more with shielding SEL: Immune to >67eV/mg/cm2 SEU: < 1 error per 24-hour period	Available in 3U/6U cPCI form factors	12-20 depending on clock frequency and FPGA pairing	LEO and GEO
TelePIX Co., Ltd. South Korea	TetraPLEX OBP	1. Microchip PolarFire® SoC (MPFS250T) - 64-bit RV64GC Quad Application processing cores (667 MHz) - 64-bit RV64IMAC monitor processor core (667 MHz) 2. NVIDIA® Jetson ORIN NX 16GB System-on-Module - 64-bit Cortex A78AE Armv8.2 (Eight-core) with Ampere GPU (1024	N/A	10x10x10	36 (max)	LEO (SSO)



Table 8-4: Sample of Highly Integrated Onboard Computing Systems

Manufacturer Headquarters	Product	Processor/ SoC/ FPGA	Radiation Hardness Assurance (RHA)	Board Dimension (cm)	Power Consumption (W)	Orbits Flown
		NVIDIA® CUDA® cores 32 Tensor cores)				
Trident Space Electronic Systems USA	VDRT	Versal VC1902	30 krad / 50MeV LU	10x14.6x2.54	<60	LEO/ MEO
	UDRT	MPSoC ZU19	30 krad / 40MeV LU	10x14.6x2.54	<50	LEO
UARX Space Spain	OBC	SmartFusion2 FPGA w/Cortex M3 SoC	Mission specific RHA to be performed	10x16	5	LEO
Unibap Sweden	iX10-100A	AMD Ryzen V1000 (CPU and GPU), Intel Myriad-X (VPU)	Radiation Tolerant COTS with SEE mitigation	10x10x6	25-40	LEO
	iX5-106	AMD Steppe Eagle (CPU and GPU), Intel Myriad-X (VPU) Microchip SmartFusion2 (FPGA)	Radiation Tolerant COTS with SEE mitigation	10x10x5	15-25	
Xiphos Quebec	Q7S	AMD-Xilinx Zynq-7020 Dual-core ARM Cortex-A9	25 krad	7.8x4.3x0.9	2	LEO
	Q8S	AMD-Xilinx Zynq Ultrascale+ MPSOC Quad-core ARM Cortex-A53	30 krad	8x8x1.12	>5	LEO
	Q8Js	AMD-Xilinx Zynq Ultrascale+ MPSOC Quad-core ARM Cortex-A53	30 krad	8x8x1.12	>5	LEO
ZAITRA Czech Republic	SKAIDOCK	AMD-Xilinx Zynq Ultrascale+ MPSOC, Quad-core ARM Cortex-A53	30 krad	9.01x9.4x2.91	5-20	LEO

*Orbits flown are on larger spacecraft

8.3 State-of-the-Art: Flight Software

Complexity in FSW can come from the architecture (e.g., the topology of the subsystems, automation/autonomy, and fault management), as well as the operational concept. Since the verification effort scales with software complexity, this process—if not properly regarded—can drive up the cost and schedule for a program or mission. Designs that enhance reliability and fault tolerance come at a cost of complexity, which further increases development overhead, and changing requirements will compound these costs. It is recommended to engage software teams early in the planning process. Increased processor performance, proliferation of rad-tolerant components, and higher mission autonomy are driving demands on FSW, requiring earlier, more integrated planning, richer tool chains, and deeper verification processes (19).

While the majority of FSW advances are proprietary within private companies, there are many considerations when choosing a development environment and/or operating system for a space mission such as memory and processing requirements, cost and schedule, software heritage and maturity, and subsystem-specific availability (20). The OBC operating system can range from lightweight RTOS (FreeRTOS, Zephyr, RTEMS) to full Linux stacks, depending on resource availability, timing requirements, and FSW needs. Onboard computing and FSW have a symbiotic relationship, since all spacecraft operations must be performed in a reliable and predictable fashion throughout the lifetime of the mission. The needs of each mission can vary greatly, but basic deterministic and reliable processing is a fundamental requirement. Adding additional “nice to have” features can balloon the overall complexity of the FSW, reduce the efficacy of testing, and increase risk to the mission as a whole.

It is essential that mission-critical FSW be as simple as possible. Survey options and plan early in any FSW effort. Wherever possible, early development and testing should be performed. Efforts to add additional features should be evaluated critically from a default posture of sticking to the baselined plan. With good planning and careful execution, a favorable outcome can be achieved. It is becoming more common to update software after the hardware is delivered (or even launched), and there are many software frameworks such as cFS that have features to enable software updates after deployment.

8.3.1 Implication of Onboard Computing on FSW

The processor and memory available on the CDH can impose significant limitations on the FSW, particularly when considering whether the selected processor can support the required operating system and its board support package. For smaller or simpler missions, or to reduce electronic complexity, designers often use lower-capacity embedded processors—sometimes in distributed processing architectures—which may also rely on dedicated onboard memory. These processors may have limited threading capabilities (for example, single-threaded execution), which are simpler to program and test but can further restrict FSW design choices. In contrast, modern integrated space avionics increasingly adopt heterogeneous and mixed-criticality architectures. These advanced configurations support more capable operating systems, enable multithreaded software execution, and facilitate complex redundancy strategies such as multiple modular redundant systems at the cost of complexity. Collectively, these trends allow for more robust radiation tolerance, higher system reliability, and expanded operational flexibility for critical small spacecraft missions.

8.3.2 Frameworks

Software frameworks impose boundaries and constraints that shape how the system is designed. A framework constrains the system-level behaviors (messaging, scheduling, component interactions) through its own internal structure—including coding patterns, file structure, message formats, lifecycle methods, state machine boundaries, or timing structures. This also enables

infrastructure services such as command handling, telemetry routing, time synchronization, and others that are either too expensive or error-prone to be done ad hoc.

While frameworks provide a lot of structure, mission-specific algorithms, guidance/navigation logic, and autonomous decision-making procedures are still required. Factors to consider when selecting a framework include the required timing cadence, how to partition responsibilities across components, how to handle concurrency, and how to balance real-time constraints. As an example, NASA's Core Flight System (cFS) is geared toward homogeneous, single-node avionics architectures and is not optimized for extremely tight computational environments (21). F Prime (F') is more rigid than cFS, with much of the architecture baked-in at compile time, although it can be extended to distributed systems with additional effort (22)(23). GERICOS has less flight heritage, but offers greater architectural freedom and supports heterogeneous, distributed architectures (24).

The challenges of flight software are frequently discovered during integration with late-schedule implementations. The more complicated the FSW is, the more risk is introduced into the mission. To manage this complexity, teams should implement early FSW prototyping, version control, and continuous testing, especially when integrating custom or COTS hardware (25), and consider using mature frameworks to reduce the amount of new code to be verified.

Component-based design makes a framework modular by breaking software into small, self-contained units with well-defined interfaces. Each component can be developed, tested, reused, or replaced independently, which reduces coupling and improves maintainability. The CCSDS (Consultative Committee for Space Data Systems) is an important consideration when selecting a framework because its standards support modular and interoperable system design. By defining consistent interfaces for data exchange, commanding, and communication, CCSDS enables reusable parts to integrate cleanly, regardless of the underlying hardware or software implementation. Other helpful considerations are framework services such as OS system support, which describes how well a software framework integrates with—and depends on—the operating system's services and constraints across target platforms. A supporting test suite is a packaged set of tests that comes with the framework to verify that the framework is correctly built, correctly installed, and behaving as expected on supported platforms. There is a trade-off in evaluating frameworks by their date of last release: older software can be stable and battle-tested or outdated and unmaintained, while freshly released software could be responsive to user reports but lacking maturity and testing. The reader is recommended to verify the latest versions of all listed frameworks in Table 8-5.



Table 8-5: FSW comparison table						
Framework	**Primary purpose/ Scope**	**Core Language**	**Open-Source?**	**Modularity**	**CCSDS**	**Released Quarter**
cFS (core Flight System) (26)	Reusable flight software framework for spacecraft of all sizes (CubeSat to flagship).	C	GitHub cfs.gsfc.nasa.gov	Yes	Yes	Q1 2026
F' (F Prime)	Used to model embedded systems framework.	C++	github.com/nasa/fprime	Yes	No	Q3 2025
NanoSat Mission Operations Framework	Supports missions by facilitating the development, distribution, and deployment of Apps on satellite missions.	Java	nanosat-mo-framework.github.io	Yes	Yes	Q2 2025
Space ROS/ ROS 2 (Space Robot Operating System)	Reusable software framework based on ROS2 for robotics and autonomous space systems.	C++ 14	github.com/david-dorf/spaceros_gz_demos	Yes	With Bridge	Q1 2026
PyCubed	Open-source, radiation-tested CubeSat avionics platform.	Python	github.com/pycubed	Yes	Yes	Q1 2023
pysimCoder	Rapid Prototyping application, that can be used to generate realtime code for different targets.	Linux	www.robots5.com/pysimcoder-installation-tutorial github.com/robertobucher/pysimCoder	Yes	Not native	Q3 2022
Matrix Laboratory	Proprietary programming and numeric computing platform.	Matlab	www.mathworks.com/discovery/what-is-matlab.html	Yes	Yes	Q3 2025
GEneRIC Onboard Software (GERICOS)	Offers a set of generic, reusable and customizable software components for the rapid development of payload flight software.	C++	No	Yes	No	Unk
Realtime Object-Oriented Distributed Operating System (RODOS)	a real-time embedded operating system.	C, C++	github.com/SpaceTeam/rodos	Yes	Yes	Unk

8.3.3 Operating Systems

Operating systems, when used, sit between flight software and the OBC to manage computer hardware, software resources, and provide common services for computer programs. They are primarily selected based on software compatibility requirements and real-time responsiveness. The industry has largely moved toward real-time operating systems (RTOS) or lightweight Linux distributions to manage multitasking and hardware resource allocation. Examples of commonly used operating systems are listed in Table 8-6.

Table 8-6: Operating Systems

Name	Description	Real-time?	Implementation Language	Open-Source?
VxWorks	Deterministic, hard real-time operating system.	Yes	C, C++	No
RTEMS	Hard real-time OS designed for embedded and space systems.	Yes	C	Yes, RTEMS License
FreeRTO	Lightweight real-time kernel for microcontrollers.	Yes	C	Yes, MIT License
Linux	Free, open-source operating system kernel.	Not standard	C	Yes, GNU GPL
Zephyr OS	Real-time OS for embedded systems.	Yes	C	Yes, Apache 2.0 License

8.4 On the Horizon: Avionics

Emerging onboard computing trends reside in the improvement of computing capacity of embedded systems (via edge computing) and the implementation of AI/ML algorithms to enable autonomous operations. Many CDH systems will continue to follow trends set for embedded systems. Short-duration LEO missions will continue to take advantage of advances made by industry leaders who provide embedded systems, technologies, and components. In keeping with the low-cost, rapid development theme of CubeSat-based missions, many COTS solutions are available and have flight heritage.

An area of growing interest for expanding into interplanetary space is rendezvous, proximity, and docking operations (RPOD), and the technologies that support these capabilities. Several projects across the space community are actively developing autonomous docking capabilities using AI-based planning. For instance, a new system called Autonomous Rendezvous Transformer (ART) uses a Transformer neural network to generate optimal, safe RPOD trajectories autonomously (31); a Carleton University research team is developing AI-guided satellite docking using computer vision and autonomy to manage relative motion and control (32); and DARPA's AI Next initiative enables advanced autonomy, including docking capabilities.

Cybersecurity is also becoming a driving factor in FSW. This is mostly handled through the encryption of commands, but as space becomes more crowded, more sophisticated cybersecurity schemes may be required of SmallSats. SmallSats can also be a testbed for demonstrating new hardware and software for cybersecurity.

To significantly improve the capabilities of space qualified computing technology, NASA's High-Performance Spaceflight Computing project is developing a radiation-tolerant, multi-GFLOPS CPU with extremely low power consumption. It's designed to dramatically enhance onboard computational power for spacecraft and aviation systems. This next generation,

fault-tolerant, cache-coherent multicore SoCs with onboard Ethernet are designed for ≥100× performance over current spaceflight processors (33).

Neuromorphic computing has emerged as a promising solution to the amplified challenges of data throughput, energy efficiency, and memory bandwidth as a result of edge computing and real-time AI applications. To close the gap between terrestrial neuromorphic computing capabilities and embedded space computing, researchers have begun to focus heavily on radiation-tolerant neuromorphic architectures, which aim to preserve energy-efficient, low-latency processing even in harsh radiation environments. Recent work extends neuromorphic principles—such as spiking neural networks, event-driven computation, and in-memory processing—to aerospace tasks, highlighting their potential to significantly increase onboard compute efficiency for autonomous navigation, hazard detection, and real-time decision-making. This growing research direction can be viewed as a neuromorphic extension of traditional space computing, leveraging biologically inspired processing paradigms to deliver higher performance within the severe power, volume, and reliability constraints of spacecraft systems (34).

Advancements reflecting Industry 4.0 trends continue in spacecraft avionics, predominantly including autonomy and onboard intelligence. AI/ML & machine vision are integrated through onboard accelerators and neural inference engines (35)(36)(37)(12). Digital Twins are being applied such as digital-twin-driven ADCS design for CubeSats fitted with robotic manipulators (36). Finally, software-defined-everything continues advancing avionics flexibility alongside FPGA stacks, reconfigurable radios, and modular SBC designs.

Containerization for FSW is the idea of packaging flight software components inside standardized, isolated runtime environments—like Docker or OCI containers used on Earth—so the software becomes more portable, modular, testable, and maintainable across different embedded flight processors. While containerization is commonplace terrestrially, adapting it for spaceborne embedded computing introduces unique constraints and opportunities.

Some modern tools, technologies, and approaches that should be considered when developing and deploying next-generation small spacecraft avionic systems are:

- Robotics and automation
- Model-based systems engineering
- Cloud computing
- Augmented reality/ virtual reality / mixed reality
- Advanced manufacturing

8.5 Summary

Space applications now require considerable autonomy, precision, and robustness, and are refining technologies for such operations as on-orbit servicing, relative and absolute navigation, inter-satellite communication, and formation flying. An exciting trend is that small spacecraft missions are becoming more complex as these platforms are now being used for lunar and deep space science and exploration missions. Small spacecraft technology is expanding to meet the needs of increasing small spacecraft mission complexity. This has accelerated over the past few years to achieve the next-gen goals of using small spacecraft to collect important science in deep space, and mitigate risk for larger, more complex mission-critical situations. In parallel, spacecraft electronics have matured with higher performance and reliability, and with miniaturized components that meet the growing needs of these now very capable spacecraft.

Constellation networks and swarms, synchronized formations, and other multi-satellite cluster formations have opened new opportunities for avionics systems. NASA's Starling swarm of four CubeSats have advanced several technologies that enable a spacecraft to function in a

synchronized manner without ground support (39). The Starling CubeSats also communicate together about their relative position without external commands. These autonomous operations do impose new constraints on the avionics system—for both single satellites and multi-satellite configurations—as the overall mission performance is dependent on all the platform elements acting in a co-dependent fashion.

Beyond raw processing capability, edge computing has emerged as a key trend, particularly for Earth observation missions, enabling onboard data management and reducing reliance on ground-based processing. Multiple vendors offer components that can be readily integrated into space-rated systems. Processing needs for traditional CDH functions are relatively stable, though SmallSats flying increasingly data-heavy payloads (i.e., imaging systems) have significantly raised the demand for onboard data-intensive processing. High-performance processors used to be added as a separate payload processing element to the CDH, but modern distributed avionics architectures can integrate high-performance, FPGA-based SDRs into the primary CDH platform.

The Small Spacecraft Avionics chapter has been updated with a broader, interrelated framework, in which CDH, FSW, and smart payloads are not just independent space platform subsystems but are part of an integrated avionics ecosystem which includes all electronic elements of a space platform, now primarily digitally based or managed. Also, avionics should not be considered as an isolated spaceflight technology component, but rather as a core digital engineering technology emphasis area capable of integrating products, processes, and technologies from other disciplines. To continue to be relevant and efficient, avionics communities must remain cognizant and receptive of the continuously evolving nature of the digital-based Industry 4.0 technology revolution seen in other related or associated vertical disciplines and solutions.

For feedback solicitation, please email: arc-sst-soa@mail.nasa.gov. Please include a valid business email for further contact.

References

(1) European Space Agency, “SpaceFibre,” [Online] Accessed: February 7, 2026, Available at: https://www.esa.int/Enabling_Support/Space_Engineering_Technology/Onboard_Data_Processing/SpaceFibre

(2) Cybersecurity and Infrastructure Security Agency, “Recommendations to Space System Operators for Improving Cybersecurity,” April 2024.

(3) P. Fiedler, E. Meenzen, et al. “Porting a Real-Time Operating System – A Student Endeavour,” 2024 Deutsche Gesellschaft für Luft- und Raumfahrt - Lilienthal-Oberth e.V., https://doi.org/10.25967/630347.

(4) National Academies of Sciences, Engineering, and Medicine: “Testing at the Speed of Light: The State of U.S. Electronic Parts Space Radiation Testing Infrastructure.” Washington, DC: The National Academies Press. 2018.

(5) RTD Embedded Technologies, Inc. “What is PC104? Rugged, Compact, Stackable and Modular,” [Online] Accessed: February 7, 2026, Available at: https://www.rtd.com/PC104/

(6) Curitss-Wright. “What is VPX,” [Online] Accessed: February 7, 2026, Available at: https://defense-solutions.curtisswright.com/capabilities/open-architectures/other/vpx

(7) K. Knesek, M. Alexander and J. Wisbiski, "Avionics Design Architecture for Low-Cost CubeSat Missions and Lessons Learned from R5-S2 and R5-S4," 2025 IEEE Aerospace Conference, Big Sky, MT, USA, 2025, pp. 1-15, doi: 10.1109/AERO63441.2025.11068544.

(8) H. Zhang, J. Zhou, and G. Liu, “A Building Block Assembly Based Modular Microsatellite Scheme,” 2023, Proceedings of 2022 International Conference on Autonomous Unmanned Systems (ICAUS 2022), ICAUS 2022. Lecture Notes in Electrical Engineering, vol 1010. Springer, Singapore. https://doi.org/10.1007/978-981-99-0479-2_12

(9) C. Whitney and J. Melville, “Toward Trusted Onboard Artificial Intelligence (AI): Advancing Small Satellite Operations using Reinforcement Learning,” 2025, 39th Annual Small Satellite Conference, Salt Lake City, UT. https://arxiv.org/pdf/2507.22198
(10) A.D. Mousist, “ASTREA: Introducing Agentic Intelligence for Orbital Thermal Autonomy,” October 11, 2025. https://arxiv.org/pdf/2509.13380
(11) “The Edge AI Technology Report 2026: How Intelligence at the Edge Is Reshaping Electronics Design,” findchips.com Blog, March 11, 2026, [Online] Accessed: March 19, 2026, Available at: https://blog.findchips.com/the-edge-ai-technology-report-2026-how-intelligence-at-the-edge-is-reshaping-electronics-design/
(12) V. Růžička, G. Mateo-Garcia, et al. “Fast model inference and training on-board of Satellites,” Computer Science: Artificial Intelligence, July 17, 2023, https://arxiv.org/abs/2307.08700
(13) Z. Li, “Predictive ‘AIMS’ AI Tool Has Been Aiding Weather Satellite Operations for Years,” July 25, 2024, ASRC Federal, [Online] Accessed: February 7, 2026, Available at: https://www.asrcfederal.com/predictive-aims-ai-tool-has-been-aiding-weather-satellite-operations-for-years/
(14) LeoLabs, “Real-time conjunction alerts for safety of flight,” [Online] Accessed: February 7, 2026, Available at: https://leolabs.space/conjunction-alerts/
(15) Neuraspace, “Satellite Collision Avoidance with AI,” [Online] Accessed: February 7, 2026, Available at: https://content.neuraspace.com/product-launch
(16) National Aeronautics and Space Administration, “Cognitive Communications,” August 5, 2025, [Online] Accessed: February 7, 2026, Available at: https://www.nasa.gov/glenn/glenn-expertise-space-exploration/scan/cognitive-communications/
(17) V. Thomas, “NASA-enabled AI Predictions May Give Time to Prepare for Solar Storms,” March 30, 2023, [Online] Accessed: February 7, 2026, Available at: https://www.nasa.gov/science-research/heliophysics/nasa-enabled-ai-predictions-may-give-time-to-prepare-for-solar-storms/
(18) https://spacenews.com/the-stealth-strategy-pays-off-uarx-space-emerges-as-europes-high-reliability-powerhouse/?utm_source=linkedin&utm_medium=jetpack_social
(19) A. Prajapati, “Evolution of core Flight System (cFS),” NASA Technical Reports Server (NTRS), [Online] Accessed: February 7, 2026, Available at: https://ntrs.nasa.gov/api/citations/20240004389/downloads/cFSFSW2024v10.pdf
(20) Build a CubeSat, “Flight Software,” CubeSat Resources, [Online] Accessed: February 7, 2026, Available at: https://cubesat-resources.space/development/flight-software/
(21) J. Furgala, S. Jero, A. Lin, and R. Skowyra, “Porting NASA’s core Flight System to the Formally Verified seL4 Microkernel,” Workshop on Security of Space and Satellite Systems (SpaceSec), 23 February 2026, San Diego, CA.
(22) Jet Propulsion Laboratory, “F Prime,” [Online] Accessed: February 7, 2026, Available at: https://fprime.jpl.nasa.gov/
(23) R. L. Bocchino, J. W. Levison and M. D. Starch, "FPP: A Modeling Language for F Prime," 2022 IEEE Aerospace Conference (AERO), Big Sky, MT, USA, 2022, pp. 1-15, doi: 10.1109/AERO53065.2022.9843754.
(24) P. Plasson, G. Brusq, F. Singhoff, H.N. Tran, S. Rubini, and P. Dissaux, “PLATO N-DPU ON-BOARD SOFTWARE: AN IDEAL CANDIDATE FOR MULTICORE SCHEDULING ANALYSIS,” February 2022.
(25) J.M. Bellardo, “Software: The Overlooked Glue that Holds CubeSats Together,” June 26, 2020, [Online] Accessed: February 7, 2026, Available at: https://www.nasa.gov/wp-content/uploads/2019/05/cubesat_software.pdf

(26) National Aeronautics and Space Administration, “The core Flight System,” 2026, [Online] Accessed: February 7, 2026, Available at: https://etd.gsfc.nasa.gov/capabilities/core-flight-system/
(27) Jet Propulsion Laboratory, “Introduction To F´,” [Online] Accessed: February 7, 2026, Available at: https://fprime.jpl.nasa.gov/latest/docs/user-manual/overview/01-full-intro/#the-origins-of-f
(28) “NanoSat MO Framework,” https://github.com/esa/nanosat-mo-framework/tree/master
(29) “Space ROS,” [Online] Accessed: February 7, 2026, Available at: https://space.ros.org/
(30) Observatoire de Paris, “PLATO N-DPU Flight Software,” January 15, 2024, [Online] Accessed: February 7, 2026, Available at: https://lesia.obspm.fr/PLATO-N-DPU-Flight-Software.html
(31) Stanford University, “Project: Autonomous Rendezvous Transformer (ART),” Stanford Space Rendezvous Laboratory, [Online] Accessed: February 7, 2026, Available at: https://slab.stanford.edu/projects/art
(32) J. Careless, “Carleton University Team Demonstrates Autonomous Satellite Docking in Lab,” spaceq.com, February 8, 2024, [Online] Accessed: February 7, 2026, Available at: https://spaceq.ca/carleton-university-team-demonstrates-autonomous-satellite-docking-in-lab/
(33) W. Powell, “High Performance Spaceflight Computing (HPSC) for Lunar and Planetary Missions,” Planetary Science Conference, March 12, 2025.
(34) Y. Wu, R. Long, Y. Zhu, Q. Jiang, Y. Zhan, et al. “Radiation-tolerant hafnium-based ferroelectric memcapacitors for neuromorphic computing,” Materials Today Communications, Volume 48, 2025, 113567, ISSN 2352-4928, doi.org/10.1016/j.mtcomm.2025.113567.
(35) F. Ortiz, V. Monzon Baeza, L.M. Garces-Socarras, et al. “Onboard Processing in Satellite Communications Using AI Accelerators. Aerospace. 2023; 10(2):101. doi.org/10.3390/aerospace10020101
(36) Australian Space Agency, “Aussie SpIRIT completes first phase of its mission,” September 23, 2025, [Online] Accessed: February 7, 2026, Available at: https://www.space.gov.au/news-and-media/aussie-nanosatellite-spirit-completes-first-phase-of-its-mission-september-2025
(37) European Space Agency, “Φsat-2 begins science phase for AI Earth images,” July 15, 2025, [Online] Accessed: February 7, 2026, Available at: https://www.esa.int/Applications/Observing_the_Earth/Phsat-2/Phsat-2_begins_science_phase_for_AI_Earth_images
(38) B. Koszek and Roman Sanchez, “Design of an ADCS enabled by the development of a digital twin of CubeSat equipped with robotic manipulator,” Smallsat Europe 27th - 28th May 2025.
(39) National Aeronautics and Space Administration, “What is Starling?” March 19, 2026, [Online] Accessed: March 19, 2026, Available at: https://www.nasa.gov/smallspacecraft/what-is-starling

Table of Contents

Chapter Glossary ii
9.0 Communications 244
9.1 Introduction 244
9.2 State-of-the-art: Radio Frequency Communications 245
9.2.1 Frequency Bands 245
9.2.2 System Architecture 246
9.2.3 Major Components in SmallSat Communication Systems 247
9.2.4 Design Considerations 248
9.2.5 Policies and Licensing 248
9.2.6 Encryption 249
9.2.7 Antennas 249
9.2.8 Radios 250
9.3 State-of-the-art: Free Space Optical Communications 268
9.3.1 System Architecture 269
9.3.2 Optical Ground Stations 269
9.3.3 Design Considerations 270
9.3.4 Policies and Licensing 271
9.3.5 Mission Examples 272
9.4 Future Communications Technologies 275
9.5 Summary 276
9.6 References 277



Chapter Glossary

(ADCS)	Attitude Determination and Control System
(BPF)	BandPass Filters
(CDH)	Command and Data Handling
(COTS)	Commercial-off-the-Shelf
(DORA)	Deployable Optical Receiver Aperture
(DLR)	German Aerospace Center
(DSN)	Deep Space Network
(DSP)	Digital Signal Processing
(DVB-S2)	Digital Video Broadcast Satellite Second Generation
(FCC)	Federal Communications Commission
(FIPS)	Federal Information Processing Standard
(FPGAs)	Field Programmable Gate Arrays
(FSM)	Fine-steering Mirror
(FSO)	Free Space Optical
(IARU)	International Amateur Radio Union
(IEEE)	Institute of Electrical and Electronics Engineers
(ISARA)	Integrated Solar Array and Reflectarray Antenna
(ISM)	Industrial, Scientific, and Medical
(ISOC)	Inter-spacecraft Optical Communicator
(ISS)	International Space Station
(JAXA)	Japanese Aerospace Exploration Agency
(JPL)	Jet Propulsion Laboratory
(LADEE)	Lunar Atmosphere and Dust Environment Explorer
(Lasercom)	Laser Communications
(LCH)	Laser Clearing House
(LCT)	Laser Communication Terminals
(LDPC)	Low-Density Parity-check Code
(LLCD)	Lunar Laser Communications Demonstration
(LNA)	Low Noise Amplifier
(LSRB)	Laser Safety Review Board
(MA)	Multiple Access
(MarCO)	Mars Cube One
(MEMS)	Micro-Electro-Mechanical Systems

(MRR)	Modulating Retro-Reflector
(NEN)	Near Earth Network
(NICT)	National Institute of Information and Communications Technology
(NOAA)	National Oceanic and Atmospheric Administration
(NPR)	NASA Procedural Requirements
(NSN)	Near Space Network
(NTIA)	National Telecommunications and Information Administration
(OCSD)	Optical Communication and Sensor Demonstration
(OCTL)	Optical Communication Telescope Laboratory
(OSIRIS)	Optical Space Infrared Downlink System
(PAT)	Pointing, Acquisition, and Tracking
(RF)	Radio Frequency
(SBIR)	Small Business Innovative Research
(SCaN)	Space Communications and Navigation
(SDR)	Software Defined Radios
(SME)	Subject Matter Expert
(SNR)	Signal-to-Noise Ratio
(SOTA)	Small Optical Transponder
(SWaP)	Size, Weight, and Power
(SST)	NASA Small Spacecraft Technology Program
(TDRS)	Tracking and Data Relay Satellite
(TMA)	Technology Maturity Assessments
(TRL)	Technology Readiness Levels
(TT&C)	Tracking, Telemetry & Command
(USTP)	University SmallSat Technology Partnerships
(VSOTA)	Very Small Optical Transponder
(WFF)	Wallops Flight Facility

9.0 Communications

9.1 Introduction

For most missions, the communication system enables the spacecraft to transmit data and telemetry to Earth, receive commands from Earth, and relay information from one spacecraft to another. A communications system consists of the ground segment—one or more ground stations located on Earth—and the space segment—one or more spacecraft and their respective communication payloads. The three functions of a communications system are receiving commands from Earth (uplink) and transmitting data down to Earth (downlink), and transmitting or receiving information from another satellite (crosslink or inter-satellite link) (Figure 9.1). There are two types of communication systems: radio frequency (RF) and free space optical (FSO); FSO is also referred to as laser communications (lasercom).

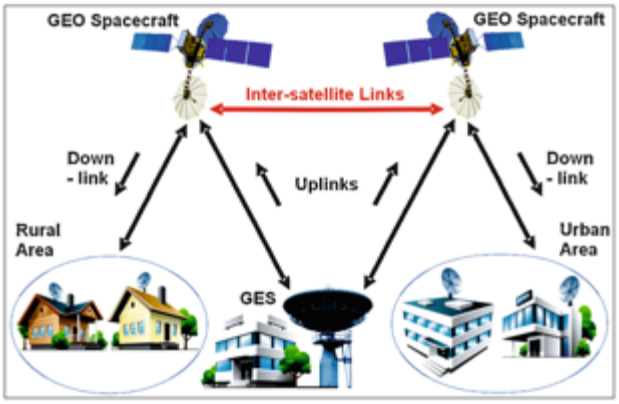


Figure 9.1: Satellite uplink, downlink, and crosslink. Credit: D. Stojce (2019).

Most spacecraft communications systems are radio-frequency-based. They typically operate within the designated Institute of Electrical and Electronics Engineers (IEEE) radio bands of 300 MHz to 40 GHz. RF systems communicate by sending data using electromagnetic waves to and from antennas. Information is modulated onto radio frequency electromagnetic waves and sent over a channel, through the atmosphere or space, to the receiving system where it is demodulated (Figure 9.2).

Although RF systems are typically used for low-rate space communication, recent developments in FSO communications have made FSO a compelling alternative to RF systems, particularly for high-rate communication. FSO systems consist of a transmitting terminal and receiving terminal. Like an RF system, information is modulated onto electromagnetic waves (at optical frequencies) and sent over a channel to the receiving system. FSO links operate at higher frequencies than RF links, generally in the near-infrared bands (e.g., 1064 nm or 1550 nm). Visible light is often

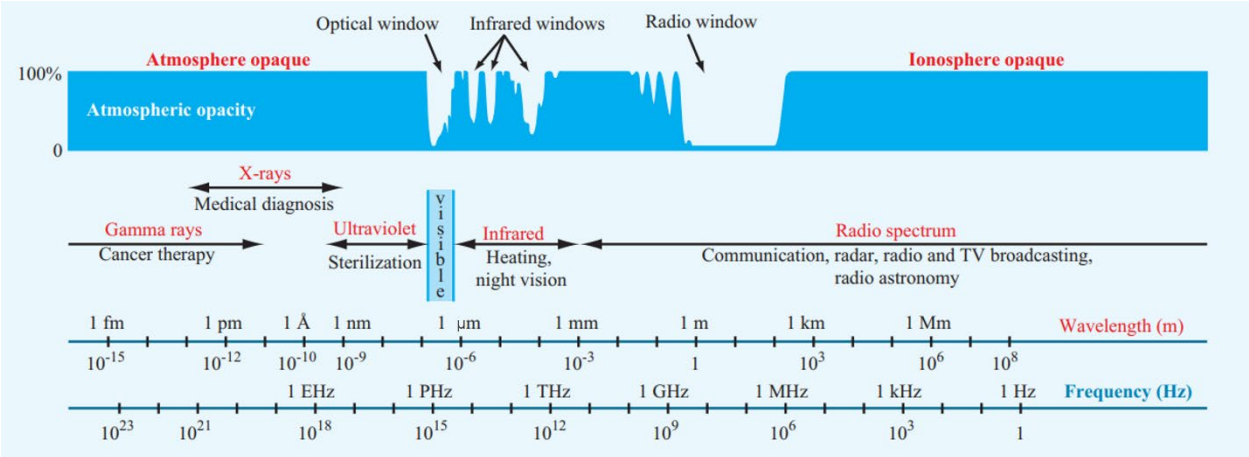


Figure 9.2: Atmospheric opacity of the electromagnetic wave spectrum with the infrared and radio windows used by spacecraft for communication. Credit: Microwave Radar and Radiometric Remote Sensing by Ulaby and Long.

not used due to eye safety concerns for technicians at the terminals. The use of higher frequencies and wider bandwidths can support higher data rates, but the shorter wavelengths also result in narrower beamwidths that require more accurate pointing towards the communication terminal with greater accurately and precisely.

This chapter organizes the state-of-the-art in small spacecraft communications technologies into two main categories: RF and FSO. Tables at the end of each section list hardware options for RF and developing FSO technologies for mission designers to consider.

The information described below is not intended to be exhaustive, but provides an overview of current state-of-the-art technologies and their development status for a particular small satellite subsystem. The list of organizations/companies in this chapter is not all-encompassing and does not constitute an endorsement from NASA. There is no intention of mentioning certain companies and omitting others based on their technologies or relationship with NASA. The information is for awareness and guidance only. The performance advertised may differ from actual performance since the information has not been independently verified by NASA subject matter experts and relies on information provided directly from the manufacturers or available public information. It should be noted that TRL designations may vary with changes specific to the payload, mission requirements, reliability considerations, and/or the environment in which performance was demonstrated. Readers are highly encouraged to reach out to companies for further information regarding the performance and TRL of the described technology.

9.2 State-of-the-art: Radio Frequency Communications

A radio communication system includes a radio transmitter, a free-space communication channel, and a radio receiver. At the top level, a radio transmitter system consists of a data interface, modulator, power amplifier, and an antenna. The transmitter system uses the modulator to encode digital data onto a high-frequency electromagnetic wave. The power amplifier then increases the output RF power of the transmitted signal to be sent through free space to the receiver using the transmit antenna.

The radio receiver system uses a receiving antenna, low-noise amplifier, and demodulator to produce digital data output from the received signal. The receiving antenna collects the electromagnetic waves and routes the signal to the receiver, which then demodulates the wave and converts the electrical signals back into the original digital message. Low-noise amplifiers are sometimes employed to minimize thermal noise in certain frequency bands and/or increase the received signal strength. In many cases, the functions of the modulator and demodulator are combined into a radio transceiver that can both send and receive RF signals.

Radio frequency communications for spacecraft are conducted between approximately 30 MHz and 60 GHz. The lower frequency bands (up to S-band) are typically more mature for SmallSat use; however, extensive use of these bands has led to crowding and challenges in acquiring licensing. Higher frequencies offer a better ratio of gain-to-aperture-size, but this is offset by the increased atmospheric attenuation at those frequencies and the higher free space loss that is directly proportional to the square of the frequency.

9.2.1 Frequency Bands

Satellite communications are conducted over a wide range of frequency bands. The typical bands considered for small satellites are UHF, S, X, and Ka. The most mature bands used for CubeSat communication are VHF and UHF frequencies. There has been a shift in recent years towards S and X, with Ka-band also being used for recent and future small satellite communications. The move to higher frequency bands has been driven by a need for higher data rates. At the higher frequencies, there is generally greater atmospheric and rain attenuation adding to increased free space loss. This needs to be compensated for with higher power transmission and/or higher gain

antennas with narrower beamwidths. Moving to higher-gain antennas increases the pointing accuracy required for closing the link. See Table 9-1 for a list of RF bands.

Table 9-1: Radio Frequency Bands	
Band	**Frequency**
VHF	30 to 300 MHz
UHF	300 to 1000 MHz
L	1 to 2 GHz
S	2 to 4 GHz
C	4 to 8 GHz
X	8 to 12 GHz
Ku	12 to 18 GHz
K	18 to 27 GHz
Ka	27 to 40 GHz
V	40 to 75 GHz

NASA spacecraft, which use the government bands of S-band, X-band, and Ka-band, may use the NASA Near Space Network (NSN). The primary frequency bands of S, X, and Ka are more advantageous than using the UHF band, which has a higher probability of local interference. Satellite Tracking, Telemetry & Command (TT&C) is typically conducted over S-band. Non-NASA spacecraft have access to a wide variety of ground system options ranging from do-it-yourself to pay-per-pass services.

In L-band, CubeSats can take advantage of legacy communications networks such as Globalstar and Iridium by using network-specific transponders to relay information to and from Earth. These networks reduce dependence on dedicated ground station equipment. However, they can only be used at orbital altitudes below the communication constellation and require experimental frequency authorization.

Ku-, K-, and Ka-band communication systems are the state-of-the-art for large spacecraft, especially in spacecraft-to-spacecraft communications, but they are still young technologies in the CubeSat world. They are becoming more attractive to SmallSat designers as the lower frequencies become more congested. At the higher frequencies, rain fade becomes a significant problem for communications between a spacecraft and Earth (1). Nonetheless, the benefits of operating at higher frequencies have justified further research by both industry and government alike. At JPL, the Integrated Solar Array and Reflectarray Antenna (ISARA) mission demonstrated high bandwidth Ka-band CubeSat communications with over 100 Mbps downlink rate (2). The back of the 3U CubeSat was fitted with a high gain reflectarray antenna integrated into an existing solar array. The successful demonstration of the reflectarray on ISARA became the basis for the Mars Cube One (MarCO) mission to Mars. The MarCO mission uses two twin CubeSats for a communications relay between the InSight lander and Earth. Using a X-band reflectarray they were able to successfully complete their mission (3). Another mission to use Ka-band for DTE communications was the Kepler telescope, launched in 2009. With future missions being increasingly data hungry, we are likely to see a shift towards Ka-band and, possibly, even higher frequencies.

CubeSats have also used the unlicensed Industrial, Scientific, and Medical (ISM) bands for communications. The Ames TechEdSat team has successfully demonstrated WiFi to downlink data at 1 Mbps. Notably, a group at Singapore's Nanyang Technological University used a 2.4 GHz ZigBee radio on its VELOX-I mission to demonstrate commercial-off-the-shelf (COTS) land-based wireless systems for inter-satellite communication (4). Similarly, current investigations are exploring the use of wireless COTS products, such as Bluetooth-compatible hardware, for inter-satellite communications (5).

9.2.2 System Architecture

A small satellite RF communications system consists of a transceiver comprised of a radio, an amplifier, and an antenna. Radios receive a message from the onboard computing subsystem, then produce and modulate an electromagnetic wave to create a signal. They are responsible for generating the signal and modulating or demodulating it. The radio is also where coding may be added to the signal. Channel coding is added to provide data error detection and correction capabilities, which ensures reliable communication under the conditions imposed by the satellite

transmission path. From Shannon's equation (6), it is known that the information capacity of a channel is related to its bandwidth and signal-to-noise ratio (SNR). The channel capacity (information flow) can be increased by increasing the SNR or the bandwidth, and many modulation and coding schemes make effective use of this tradeoff.

Radios offer some power amplification, but often the signals from small satellites require a greater boost. The power amplifier will take the signal from the radio and increase the RF output power before sending it to the transmit antenna. On the receive side, a low noise amplifier will take the weak signal from the receive antenna and amplify it while minimizing thermal noise. A bandpass filter might be used before the LNA to reject undesired frequencies. The radio will then be able to process the stronger signal with higher accuracy. In RF communications the role of the antenna is to increase and focus the strength of the signal in a specific direction. The digital message encoded on the RF carrier signal will be sent to and from the antennas of each system. See Figure 9.3 for an example transmit and receive block diagram.

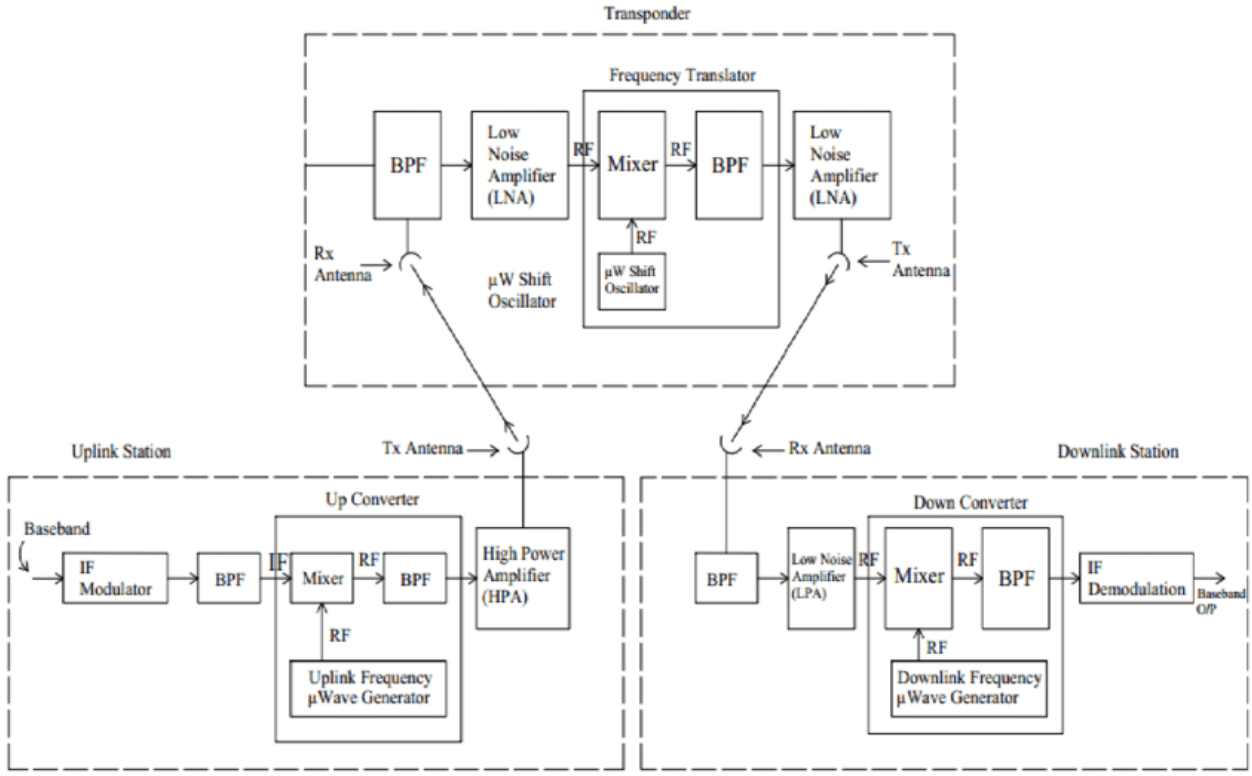


Figure 9.3: Transmit and receive block diagram. Credit: Karim et al. (2018). http://creativecommons.org/licenses/by/4.0/

9.2.3 Major Components in SmallSat Communication Systems

- Radio or Modulator/Demodulator: on the transmit side, it produces, modulates, codes, and amplifies an electromagnetic wave to create a signal. Adds modulation and coding as needed. As a receiver it decodes and demodulates received signals.
- Mixers: RF mixers are used in communications systems to change the frequency of the signal. If the frequency generated by the radio is not the desired transmit frequency, then an upconverter will convert the signal to a higher frequency for transmit. Similarly, the downconverter will downconvert a receive frequency to a lower one for processing.
- Filters: bandpass filters are used to reject undesired frequencies, typically before the LNA or downconverter.

- Amplifier: a power or gain amplifier is required for a transmit system. A low noise amplifier (LNA) is required for a receive system. LNAs, in addition to amplifying the (low power) received signal, serve to minimize the system noise temperature.
- Antenna: increases the strength of a signal in a specific direction, relative to the same signal strength without directionality. Transmits signals fed to it by a transmitter and receives signals propagated across free space. Antennas can be low-gain and omni-directional with a broad beam, or high-gain & directional with a narrow beam.
- Encryption: a cryptographic unit is an integrated encryptor/decryptor device that provides secure uplink, downlink, or crosslink for satellite communication links. Most small satellite designers will not require a cryptographic payload unit based on their threat level and may be able to use the communications radio for simple encryption schemes.
- Spread-spectrum communication applies a known frequency spreading function to the signal, which helps reduce interference from other transmitters, and provides more secure communications; as such, it is often used for multi-way communication networks. For example, the NASA Tracking and Data Relay Satellite (TDRS) multiple-access mode requires spread spectrum signals to support multiple simultaneous communication links.

9.2.4 Design Considerations

As with all spacecraft subsystems, there are power and mass constraints placed on the communications system. Based on these restrictions, several trade studies need to be performed to choose the optimal design. When designing an RF communications system, the first trades performed are for data rate, power consumption, and total mass. For example, a mission with high data rate needs would select a high frequency such as X-band for downlink and a directional high-gain antenna. Based on the ground station locations available, engineers would perform link budget analyses to determine the minimum power needed for a specific ground station antenna. This analysis would factor in rain and atmospheric attenuation, as well as modulation and coding. A few different link budget trades will be run, varying antenna size, RF output power and data rate. Each link will return a different margin of decibels, representing the reliability of the system. The engineers will proceed to calculate the final mass and power for each configuration. The mission designer will have a limit on mass and power constraints for the communications subsystem. Each configuration traded will compare data rate, power, and mass. A high data rate downlink may cost a high amount of mass for the antenna and power for the amplifier and radio. Conversely, a low-power, low-mass system may have a lower data rate.

Another factor that is considered in the design phase is pointing. Depending on the orbit of the satellite and whether the link is uplink/downlink, or crosslink, the system may have a specific pointing requirement. Large satellites frequently use gimbals—platforms that can pivot to point their antennas. The addition of a gimbal will increase the overall mass and power draws of the system. CubeSats frequently trade high-gain antennas for low-gain, omni-directional ones to maintain the link regardless of directionality. CubeSats may also change their attitude to point a body-mounted antenna, rather than use a gimbal.

9.2.5 Policies and Licensing

Any non-Federal U.S. spacecraft with a transmitter must be licensed by the Federal Communications Commission (FCC). The types of RF licenses used by small satellites are: Amateur (FCC Part 97) and Experimental (FCC Part 5) (7). An amateur license type of authorization is limited to hobbyists and non-profit use and comes with many FCC restrictions. Experimental Part 5 licenses are commonly used for university CubeSats and can be granted for a CubeSat operating in the amateur band (a SmallSat or SmallSat constellation can also apply under provisions of Part 25). A spacecraft with any sort of remote sensing capability must contact

the National Oceanic and Atmospheric Administration (NOAA) to find out if a NOAA license is required. A NOAA license is not an RF license and conveys no authority for the radiation of RF energy for communication. For government missions the National Telecommunications and Information Administration (NTIA) is the licensing authority.

For amateur licensing, there must be an FCC licensed amateur radio control operator. Downlink telemetry and communications cannot be obscured (encrypted). Use of science gathered via amateur radio downlink for profit (“pecuniary interest”) is prohibited. Frequency “assignment” in the amateur-satellite allocations requires coordination, a process administered by the International Amateur Radio Union (IARU) (8).

In 2018, the FCC adopted a Notice of Proposed Rulemaking to develop a new authorization process tailored specifically to small satellite operations, keeping in mind efficient use of spectrum and mitigation of orbital debris. Small satellites that would qualify for the new rules include those with 10 or lesser number of satellites under a single license. All individual satellites will have to be at least 10 cm or larger in the smallest dimension and weigh less than 180 kg. The maximum in-orbit lifetime of each individual satellite will be six years, including de-orbiting time, and they would have to be deployed under 600 km altitude. Each satellite will have a unique telemetry marker for tracking and will not release any debris (9).

9.2.6 Encryption

Encryption is the process of encoding information to conceal it from outside actors. Small satellites can use a cryptographic unit to encrypt or decrypt data prior to transmission. When data is being prepared for transmission, it is divided into packets. These packets are then scrambled according to the encryption scheme being used. An encryption scheme uses an encryption key generated by an algorithm to encode the data. The authorized receiver of the encrypted data will be able to decrypt the message using the appropriate key. Without the authorized key, decrypting the data will be extremely difficult.

With the increased proliferation of small satellites in low-Earth orbit comes an increase in vulnerabilities. Many SmallSats are comprised of COTS hardware and/or open-source software. While this strategy allows for a more flexible design approach, adversaries can gain insight into the design. Encryption of data in transit helps prevent other actors from commanding satellites or intercepting transmissions.

NASA requires any of its propulsive spacecraft within 2 million kilometers of Earth to protect their command uplink with encryption that is compliant with Level 1 of the Federal Information Processing Standard (FIPS) 140-3 (10). The FCC has also considered requiring encryption on the telemetry, tracking, and command communications as well as mission data for propulsive spacecraft, but decided not to incorporate a specific requirement at this time. A satellite with an amateur license cannot encrypt transmissions in any way and must consist of open information. The eligibility rules are listed in 47 CFR Part 97 (11).

9.2.7 Antennas

Antennas are used for propagating data through free space using electromagnetic waves. RF antennas are typically sized for their respective frequencies. This means that antennas are often chosen or designed specifically for their mission. COTS antennas are available for SmallSats and can be built to order. For missions that don’t have high data rate requirements, a simple patch or monopole antenna with low gain and efficiency will suffice. Due to their low directionality, these antennas can generally maintain a communication link even when the spacecraft is tumbling, which is advantageous for CubeSats lacking good attitude and accurate pointing control. New developments in antenna design have put technologies like the deployable reflector antenna,

reflectarray, and passive or active array antennas on the horizon for small satellites. Please see Table 9-2 for information on commercially available antennas for SmallSats/CubeSats.

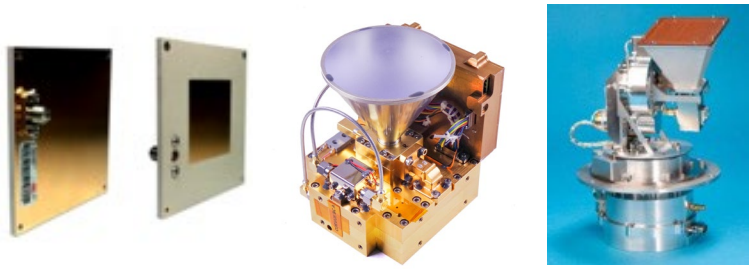


Figure 9.4: (from left to right) CubeSat-compatible S-band patch antenna (IQ Wireless), X-band high-gain antenna and pointing mechanism (Surrey Satellite Technology, Ltd.), and Ka-band transmitter with a horn antenna (Astro Digital).

There are two primary classifications of antenna: fixed or deployable. Fixed antennas do not require any power or triggering mechanisms. They remain stationary in the position that they are attached to the spacecraft. This includes patch antennas, array antennas, monopole antennas, omni-directional antennas, and horn antennas (see Figure 9.4). Deployable antennas require power to deploy and use mechanisms to configure into their final position. This includes whip antennas, parabolic reflectors, reflectarrays, helical and turnstile antennas (see Figure 9.5).

A communications link is often characterized by the frequency and data rate. The antenna is a key design decision for meeting data rate objectives by increasing link margin. Increasing the aperture or diameter of an antenna increases the link margin, which can allow designers to increase the data rate of the system or reduce the necessary transmit power.

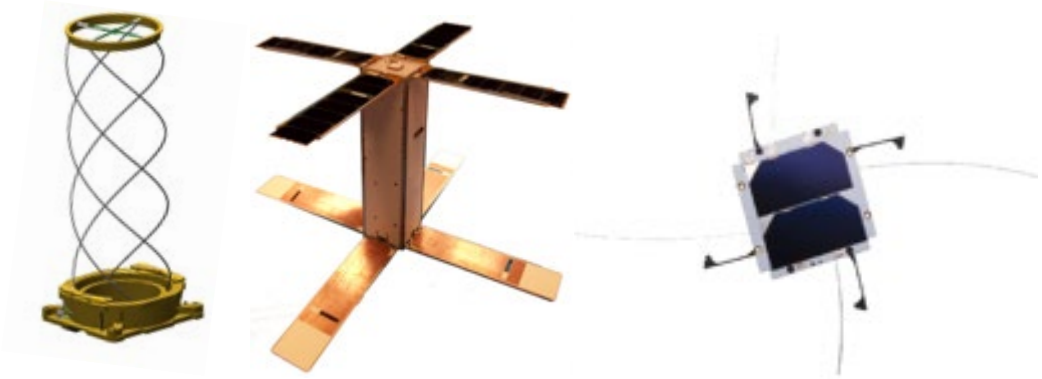


Figure 9.5: (from left to right) Example of deployable quadrifilar helical antenna (Helical Communication Technologies), SNaP spacecraft with Haigh-Farr's deployable UHF Crossed Dipole antenna (Space Missile and Defense Command), and EnduroSat UHF antenna with EnduroSat solar panels (EnduroSat).

9.2.8 Radios

Radios for SmallSat downlink are transceivers (transmitter and receiver in one). Transceivers convert digital information into an analog RF signal using a variety of modulation and coding schemes. Radios for TT&C are designed for low data rates, with high reliability and only need to transmit health data and receive commands. Traditional radios may be locked to a single frequency band and modulation/coding scheme based on their design and build. Software-defined radios (SDR) have some or all the radio's functions implemented in digital signal processing (DSP) software rather than hardware, Figure 9.6. Furthermore, spacecraft teams can change

such characteristics on-orbit by uploading new settings from the ground. By using Field Programmable Gate Arrays (FPGAs), SDRs have great flexibility that allows them to be used with multiple bands, filtering, adaptive modulation, and coding schemes, without much (if any) change to hardware (12). SDRs are especially attractive for use on CubeSats, as they are becoming increasingly small and efficient as electronics become smaller and require less power. NASA has been operating the Space Communications and Navigation (SCaN) Testbed on the International Space Station since 2012 for the purpose of SDR TRL advancement, among other things (13). Many radios can provide RF output power to the antenna directly. For higher power applications, an external RF amplifier or high gain antenna may be used. See Table 9-3 for information on commercially available radios for SmallSat/CubeSats.



Figure 9.6: Example of software defined radio, tunable in the range 70 MHz to 6 GHz. Credit: GomSpace.

This report recommends efficient modulation and coding schemes for spacecraft power and bandwidth to increase the data rate and meet bandwidth constraints with the limited power and mass for CubeSat spacecraft. Advanced coding, such as the Consultative Committee for Space Data Systems (CCSDS) low-density parity-check code (LDPC) family, with various code rates, is a powerful technique to provide bandwidth and power with high-order modulation to achieve high data rate requirements for CubeSat missions. Digital Video Broadcast Satellite Second Generation (DVB-S2), a significant satellite communications standard, is a family of modulations and codes for maximizing data rates and minimizing bandwidth use. DVB-S2 uses power and bandwidth efficient modulation and coding techniques to deliver performance approaching theoretical limits of RF channels. NASA's NSN has conducted testing at NASA Wallops Flight Facility (WFF) to successfully demonstrate DVB-S2 over a S-band 5 MHz channel achieving 15 Mbps with 16 APSK LDPC 9/10 code (14).

Table 9-2: Antennas									
Manufacturer	**Product**	**Type**	**Min Frequency**	**Frequency Band**	**Gain**	**Polarization**	**Mass**	**Dimensions**	**Flight Heritage**
---	**---**	**---**	**[MHz]**	**--**	**[dBi]**	**--**	**[g]**	**[cm]**	**---**
MMA Design	LAMBDA	Deployable Sinuous Antenna	100	UHF	>-1	Dual CP	4000	20x15x10 (stowed) 100x100 (deployed)	N
Oxford Space Systems	Helical antenna (high RF power handling)	Deployable	118-127/127-137	VHF	>2.5 (isoflux)	LHCP	<1400	40x35x34.5	Y
2NDSpace	CHORUS-01 LP	Dual Dipole	140 - 930	20	0	2x Linear	90	10x10x0.8	Y
2NDSpace	CHORUS-01 LP	Turnstile	140 - 930	20	0	Circular	90	10x10x0.8	Y
Oxford Space Systems	Yagi antenna	Deployable	156.5-162.5	VHF	>6.5	Dual Linear	<1000	92.5 x 50 (deployed)	Y
Spacemanic	Small Antenna Module	Dipole Cross Dipole	145 400 435	VHF, UHF	2.1	Linear/ RHCP	55	9.8X9.8X0.56	Y
Haigh-Farr, Inc.	Part Number: 17100	Crossed Dipole	307	VHF, UHF	--	RHCP	267	32x8x1	Y
Anteral	2211-301-01	Monopole antenna	400	UHF	--	Single linear polarized	--	--	Y
GomSpace	NanoCom ANT430	Omni Canted Turnstile	400-435	VHF, UHF	1.5	Circular	30	10x10	Y
Helical Communications Technologies	Helios Deployable Antenna	Helical	400-3000	VHF, S	3	Circular	180	10x10x3.5	Y
NanoAvionics	CubeSat UHF Antenna System 1x1U	Turnstile	400-500	UHF	1.37	--	33	10x10x0.7	Y
NanoAvionics	CubeSat UHF Antenna System 1x2U	Turnstile	400-500	UHF	2.31	--	50	20x10x0.7	Y

Table 9-2: Antennas									
Manufacturer	**Product**	**Type**	**Min Frequency**	**Frequency Band**	**Gain**	**Polarization**	**Mass**	**Dimensions**	**Flight Heritage**
---	**---**	**---**	**[MHz]**	**--**	**[dBi]**	**--**	**[g]**	**[cm]**	**---**
NanoAvionics	CubeSat UHF Antenna System 2x2U	Turnstile	400-500	UHF	3.4	--	65	20x20x0.7	Y
EnduroSat	UHF Antenna IU	Whip/Burn-wire	435-438, 400-403	UHF, VHF	> 0	RHCP	85	10x10	Y
EnduroSat	UHF Antenna 2U	Whip/Burn-wire	435-438, 400-403	UHF, VHF	> 0	Linear	210	22.5x9.9x 1.4	Y
SENyT	UHF antenna	Deployable turnstile	430-440	UHF	0	Circular	< 150	10x10x3 folded	N
ISISPACE	CubeSat Antenna System for 1U/3U	Tape	--	VHF, UHF	0	Circular, Linear	89	10x10x0.7	Y
Flexitech Aerospace	600MHz - 10GHz Spiral Antenna	Spiral	600-10000	UHF, L, S, C, X	3	Circular	1283	17x17x8.5	N
Oxford Space Systems	Helical antenna	Deployable	862–928	UHF	> 6.5-7.5	RHCP	<235	30 (deployed helical length)	Y
CesiumAstro	Vireo L-Band Phased Array	APA	960	L	22	Circular	49100	114x100x13.5	N
Anteral	2211-119-03 L2-Band DCP	2-port dual-circular-polarized (DCP) patch antenna	1200-1300	L	5.8	RHCP & LHCP	150	9.6x9.6x0.7 (excluding connector)	N
SENyT	Dual-band GNSS antenna	Patch	1215-1240 1560-1590	L	4.5	RHCP	< 100	10x10x0.35	N
EnduroSat	GNSS Patch Antenna L1+L2	Patch	1227.60 1575.42	L	3.3+	RHCP	114	8.3x9.8x0.8	N
Anteral	2211-119-02 L1-Band DCP	2-port DCP patch antenna	1550-1600	L	6	RHCP & LHCP	150	9.6x9.6x0.7 (excluding connector)	N
EnduroSat	GNSS Patch Antenna L1/E1	Patch	1559–1591	L	3.6+	RHCP	17	8.3 x 9.8 x 0.8	Y

Table 9-2: Antennas									
Manufacturer	**Product**	**Type**	**Min Frequency**	**Frequency Band**	**Gain**	**Polarization**	**Mass**	**Dimensions**	**Flight Heritage**
---	**---**	**---**	**[MHz]**	**--**	**[dBi]**	**--**	**[g]**	**[cm]**	**---**
SkyFox Labs	piPATCH-L1E1	Patch	1575.42	GPS-L1 GALILEO E1	--	--	50	9.8x9.8x1.3	Y
NAL Research Corporation	Antenna SYN7391-A/B/C (Iridium)	Flat Mount	1610-1626.5	L	4.9	RHCP	31	4.6x.4.3x1.0	Y
Oxford Space Systems	Helical antenna (high RF power handling)	Deployable	1980-2200	S	>4.0-4.5	RHCP	<1200	60 (deployed helical length)	Y
IQ Spacecom	S-Band Single Patch Antenna	Patch	1980-2500	S	6	Circular	49	7x7x0.34	Y
IQ Spacecom	S-Band Dual Patch Antenna	Patch	1980-2500	S	6	Circular	62	8x10x0.34	Y
IQ Spacecom	S-Band High Gain Patch Antenna	Patch	1980-2500	S	11.5	Circular	179	16x16x0.34	Y
Flexitech Aerospace	2-2.5GHz Turnstile Antenna	Turnstile	2000-2500	S	5	Circular	173	--	N
SkyLabs	S-band Patch Antenna	Patch	2025-2110	S	6	LHPC/RHPC	70	8.2x8.2x1.1	Y
Vulcan Wireless	ANT-S/S Unified S-Band Antenna	Patch	2025-2300	S	6.5	Circular	76	8x8x1	Y
EnduroSat	S-band Antenna Commercial	Patch	2025-2110	S	7	Selectable Circular	81	9.8x9.8x0.6	Y
Anteral	2211-114-02 Telecommand DCP	Patch	2000-2150	S	6	RHCP & LHCP	150	9.6x9.6x0.7 (excluding connector)	N
EnduroSat	S-band Antenna Wideband	Patch	2025-2110 2200-2290	S	5	RHCP	115	9.8x9.8x0.7	Y
SENyT	Dual-band S-band antenna	Patch	2050-2115 2215-2275	S	6.5	LHCP	< 100	10x10x0.35	N

Table 9-2: Antennas									
Manufacturer	**Product**	**Type**	**Min Frequency**	**Frequency Band**	**Gain**	**Polarization**	**Mass**	**Dimensions**	**Flight Heritage**
---	**---**	**---**	**[MHz]**	**--**	**[dBi]**	**--**	**[g]**	**[cm]**	**---**
ANYWAVES	S-Band TT&C Antenna	Patch	2025-2290	S	6.5	RHCP/LHCP	132	8x8x1.2	Y
Haigh-Farr, Inc.	P/N 21060	Waveguide	2020-2120	S	25	LHCP	667	10x10x4.1	N
ISISPACE	S-Band Patch Antenna	Patch	2200-2290	S	6.5	RHCP	50	8x8x1	N
CesiumAstro	Nightingale AAA-2SF1	Patch	2025 2200	S	5	RHCP LHCP	480	12x9.5x5	Y
AeroSpace Lab	SBA-TX	Patch	2200–2290	S	6.1 dBic	RHCP	118	9.5x9.5x2.4	Y
AeroSpace Lab	SBA - RX	Patch	2025–2110	S	6.1 dBic	CP	117	9.5x9.5x2.4	Y
Satlab	SAS-2	Patch	2025-2110 2200-2290	S	6.1	RHCP	107	10x8.0x0.68	Y
Anteral	2211-113-2 SCP	Patch	2042-2092 2220-2270	S	5.5	RHCP	129g	9.9x9.9x0.65 (excluding connector)	Y
Anteral	2211-114-01 TTC DCP	Patch	2025-2290	S	6	RHCP & LHCP	150	9.6x9.6x0.67 (excluding connector)	N
Anteral	2211-113-01 SCP	Patch	2000-2300	S	7	RHCP	196	9.7x9.7x3.6	Y
Anteral	2211-114-03 Telemetry DCP	Patch	2170-2320	S	6	RHCP & LHCP	150	9.6x9.6x0.7 (excluding connector)	N
Haigh-Farr, Inc.	S-band Patch Antenna	Patch	2245-2245	S	--	RHCP	48	4.8x6.5x6.5	Y
EnduroSat	S-band Antenna ISM	Patch	2400-2450	S	8.3	LHCP	64	9.8x9.8x0.6	Y
SENyT	S-band antenna	Patch	2400-2450	S	3.5	LHCP	<80	5x5x0.5	N
Anteral	2211-114-05 ISM DCP	Patch	2400-2450	S	6.5	RHCP & LHCP	150	9.6x9.6x0.7 (excluding connector)	N

Table 9-2: Antennas									
Manufacturer	**Product**	**Type**	**Min Frequency**	**Frequency Band**	**Gain**	**Polarization**	**Mass**	**Dimensions**	**Flight Heritage**
---	**---**	**---**	**[MHz]**	**--**	**[dBi]**	**--**	**[g]**	**[cm]**	**---**
Oxford Space Systems	Offset Reflector Antenna (muti feed)	Deployable	5030-5500	C	>41	Linear	<27200	350 (deployed reflector diameter, scalable to 600)	N
IQ Spacecom	X-Band Single Patch Antenna	Patch	7145-7250 8025-8400	X	6	Circular	10	3.5x3.5x0.18	Y
IQ Spacecom	X-Band High Gain Antenna	Patch	7145-7250 8025-8400	X	10	Circular	12	4x6x0.18	Y
Oxford Space Systems	"Hinged Rib" Cassegrain Antenna	Deployable	17500-20200 27500-30000	K/Ka	> 38/41	Dual Circular (2 channels for Tx & Rx)	< 2500	60 (deployed reflector diameter, scalable to 150)	N
Anteral	2211-128-22 X-Band SCP	Patch	7900-8500	X	12	RHCP/LHCP	100	5.5x5.5x0.65 (excluding connector)	N
Anteral	2211-128-44 X-Band SCP	Patch	7900-8500	X	>18	RHCP	127	9.9x9.9x0.65 (excluding connector)	Y
Anteral	2211-128-UPL-R-8x8-01 X-Band 8x8 Array	Patch	7900-8500	X	22	RHCP/LHCP	500	22x22x0.52 (excluding fixings and connector)	N
Anteral	2211-205-03 X band	Waveguide antenna	8000-10500	X	15-17	RHCP & LHCP	450	9.74x9.9x17.6	Y
PICOSATS	BEAMSAT X band 4 x 4 patch antenna	Patch	8000 - 8500	X	>16	RHCP	125	98x98x10.8	N
EnduroSat	X-band Patch Antenna	Patch	8025-8400	X	6	RHCP	2.2	2.4x2.4x0.2	Y

Table 9-2: Antennas									
Manufacturer	**Product**	**Type**	**Min Frequency**	**Frequency Band**	**Gain**	**Polarization**	**Mass**	**Dimensions**	**Flight Heritage**
---	**---**	**---**	**[MHz]**	**--**	**[dBi]**	**--**	**[g]**	**[cm]**	**---**
EnduroSat	X-band 2x2 Patch Antenna	Patch	8025-8400	X	12	RHCP	23.2	6.0x6.0x0.3	Y
EnduroSat	X-band 4x4 Patch Antenna	Patch	8025-8400	X	16	RHCP	53	9.8x8.3x0.3	Y
EnduroSat	X-Band 8x12 Patch Antenna	Patch	8025 - 8400	X	26	RHCP	490	25.4 x 17.2 x 0.7	N
ANYWAVES	X-band Payload Telemetry Antenna	Patch	8025-8400	X	11.5	Circular	65	7.3x7.3x11	Y
MMA Design	T-DaHGR	Deployable Reflectarray	8400 - 10000	X	29 – 42.5	Configurable	1300 to 11000	10x10x10 - 20x20x20 (stowed) Ø70-Ø200 (deployed)	N
MMA Design	NeuSAR	Deployable Reflectarray	10000	X	>45.5	V+H Linear	16550	52x52x25 (stowed) Ø300 deployed	Y
Anteral	2211-133-DWL-L-44-02 Ku-Downlink 4x4 Array	single-port right-handed-circular-polarized patch antenna	10700 - 11700	Ku	17	RHCP & LHCP	120	9.9 x 9.9 x 0.61 mm (excluding connector)	N
PICOSATS	BEAMSAT Ku band horn antenna	Horn antenna	10700-12750, 12750-14800	Ku	>15 >16	Linear	633	109.1x109.1x 205.3	N
Anteral	2211-212 Ku band	4-port DCP dual-band waveguide antenna	10700-12700 13750-14800	Ku	17	RHCP & LHCP	700	8.9 x 10.2 x 22.1	N

Table 9-2: Antennas									
Manufacturer	**Product**	**Type**	**Min Frequency**	**Frequency Band**	**Gain**	**Polarization**	**Mass**	**Dimensions**	**Flight Heritage**
---	**---**	**---**	**[MHz]**	**--**	**[dBi]**	**--**	**[g]**	**[cm]**	**---**
Anteral	2211-133-UPL-R-44-01 Ku-Uplink 4x4 Array	single-port right-handed-circular-polarized patch antenna	14000-14500	Ku	26	RHCP & LHCP	120	0.99x0.99x0.061 (excluding connector)	N
EnduroSat	K-band Patch Antenna	Patch	17700-20200	K	18	RHCP	76	6.5x6.5x1	N
PICOSATS	BEAMSAT K band 8 x 8 patch antenna	Patch antenna	17300 - 21200	K	>20	LHCP	135	94.5x94.5x14	N
Anteral	2211-138-8x8 - K-Band 8x8 Array	single-port right-handed-circular-polarized patch antenna	17800-20200	K	22.5	RHCP/LHCP	120	10x10x0.61 (excluding connector)	N
PICOSATS	BEAMSAT K/Ka band horn antenna	Horn antenna	17300 – 21200, 27000 - 31000	K/Ka	>19.6, >23.75	LHCP RHCP	570	88x88.8x218	Y
Anteral	2211-218	Waveguide antenna	17300 – 21200, 27000 - 31000	K/Ka	>21	LHCP & RHCP	620	10.2x10.2x19.7	Y
PICOSATS	BEAMSAT Ka band 8 x 8 patch antenna	Patch antenna	27000 - 31000	Ka	>20	RHCP	76	78x78x13.5	N
CesiumAstro	APA-1AT1	APA	24500	Ka	26.5	RHCP or LHCP	500	18x18x2	Y
CesiumAstro	Vireo Ka 288 Tx DRA	APA	20200	Ka	28	Circular, switchable on orbit	14500	27x23x16	N
CesiumAstro	Vireo Ka 576 Tx DRA	APA	17000	Ka	31	RHCP or LHCP,	26000 - 34000	40x 40x26.5	N

Table 9-2: Antennas									
Manufacturer	**Product**	**Type**	**Min Frequency**	**Frequency Band**	**Gain**	**Polarization**	**Mass**	**Dimensions**	**Flight Heritage**
---	**---**	**---**	**[MHz]**	**--**	**[dBi]**	**--**	**[g]**	**[cm]**	**---**
						switchable on orbit			
CesiumAstro	Vireo Ka 288 Rx DRA	APA	30000	Ka	28	Circular, switchable on orbit	7000	18x15.5x15.5	N
CesiumAstro	Vireo Ka 576 Rx DRA	APA	27000	Ka	31	RHCP or LHCP, switchable on orbit	23000 to 29500	40x40x26.5	N
Anteral	2211-250 EO	2-port DCP waveguide antenna	25500-27000	Ka	30	RHCP & LHCP	1000	20x20x20	N
Anteral	DCPCRS-500-40-EO	2-port dual-DCP cassegrain reflector antenna	31500-32500	Ka	40	RHCP & LHCP	2500	52.4 x52.4 x 25.5	N
PICOSATS	BEAMSAT horn antenna	Horn antenna	37500 - 43500	Q	>20	RHCP & LHCP	150	49x49x110	N
PICOSATS	BEAMSAT horn antenna	Horn antenna	37500 – 43500, 47500 - 52500	QV	>30	RHCP & LHCP	250	119x119x65	N
Anteral	2211-229	Waveguide antenna	37500-52400	QV	30.5	RHCP & LHCP	280	10x10x15.77	N
PICOSATS	BEAMSAT ADE antenna	ADE antenna	59000 - 71000	V	>30	RHCP & LHCP	83	79.5x79.5x43.4	N
EnduroSat	W-band Patch Antenna	Patch	71000-75000	W	23-29	RHCP	37	8.7x8.1x2.0	N
Anteral	2211-236	Waveguide antenna	71000-86000	E	31.5	RHCP & LHCP	152	7.5x7.5x9	N

Table 9-3: Radios									
Manufacturer	**Product**	**Type**	**Min Frequency**	**Frequency Band**	**Data Rate**	**Tx Power**	**Mass**	**Dimensions**	**Flight Heritage**
---	**---**	**---**	**[MHz]**	**--**	**[kbps]**	**--**	**[g]**	**[cm]**	**---**
Aerospace Lab	SSDR	SDR	6	S	1840	29 dBm RMS	575	12.6x11.1x5.3	Y
Vulcan Wireless	NSR-SDR	Radio	20.100-21200, 30000-31000	K/Ka	200,000	5W	615	18.3x9.2x3.6	N
Aerospacelab	XSDR	SDR	58	X	206,000	29 dBm RMS	555	12.6x11.1x5.3	Y
Space Micro	MicroSDR-C	SDR	70-3000	VHF, UHF, L, S, C	42,000	0	750	10x10x8	Y
Rincon Research	ASTROSDR	SDR	70-6000	VHF, UHF, L, S, C	--	5 dBm	95	9.0x9.0x1.613	Y
GomSpace	NanoCom SDR	SDR	70-6000	VHF, UHF, L, S, X	--	--	271	9x9x6.6	Y
NI Ettus Research	B205mini	SDR	70-6000	VHF, UHF, L, S, X	--	10 dBm	24	8.3x5.1x8	Y
Alén Space	TOTEM	SDR	70 - 6000	VHF, UHF, L, S	–	7 dBm	130	9.33x8.93x1.36	Y
Alén Space	TREVO	SDR	70 - 6000	VHF, UHF, L, S	–	7 dBm	<714	9.33x8.93x27.88	Y
Vulcan Wireless	NSR-SDR-MUOS	Transceiver	300-320, 360-380	UHF	64	8W	450	10x10x5.6	N
AAC Clyde Space	PULSAR-VUTRX	SDR	--	VHF, UHF	9.6	1.5 W	100	9.6x9x1.6	Y
SkyLabs	NANOcomm-2	Transceiver	130-470	VHF, UHF	< 25	31 dBm	110	9.5x9.1x1.2	Y
AstroDev	Helium-100	Transceiver	120-150, 400-450	VHF, UHF	38.4	3 W	78	9.6x9x1.6	Y
AstroDev	Lithium-1	Transceiver	130-450	VHF, UHF	9.6	0.25-4 W	48	1.0x3.3x6.5	Y
AstroDev	Beryllium-2	Transceiver	130-450	VHF, UHF	9.6	0.25-4 W	52	1x3.3x6.5	Y
GomSpace	NanoCom AX100	Transceiver	143-150, 430-440	VHF, UHF	0.1-38.4	30 dBm	24.5	6.5x4x7	Y
Spacemanic	Murgas	Transceiver	145 400 435	VHF, UHF	0.1 - 38.4 9.6	30dBm	25	6.7x4.2x0.7	Y
LY3H	SatCOM TP0	FM Repeater	144-146, 430-440	VHF, UHF	--	217 mW	59	--	Y

Table 9-3: Radios									
Manufacturer	**Product**	**Type**	**Min Frequency**	**Frequency Band**	**Data Rate**	**Tx Power**	**Mass**	**Dimensions**	**Flight Heritage**
---	**---**	**---**	**[MHz]**	**--**	**[kbps]**	**--**	**[g]**	**[cm]**	**---**
ISISPACE	TRXVU	Transceiver	145.8-150.05, 400.15-440	VHF, UHF	9.6	27 dBm	75	9x9.5x1.5	Y
Needronix	Cormorant	Transceiver, DNxD-capable digipeater, Morse beacon	145 - 220 or 390 - 500	VHF or UHF	9.6	30	22	4x7x0.65	Y
Emxys	ODALISS TTC	Transceiver	200	VHF, UHF	1.2	1 W (31 dBm)	<50	8.7x8.7x0.93	N
CesiumAstro	SDR-1001	SDR	300	UHF, L, S, C		-5 to 6	110	5x8.4x1.35	
CesiumAstro	SDR-2104	SDR	600	L, S, C, X		-5 to 6	900	16x10x2.54	
CesiumAstro	Nightingale RFPU	SDR	300, 24500	UHF, L, S, C, Ka		-5 to 6	3500	20x14.85x13.4	
CeisumAstro	SDR-1001	SDR	300 – 6000	UHF, L, S, C	< 62,500	-	100	5x8.4x1.3	N
AAC Clyde Space	TRX-U	Transceiver	390-450	UHF	19.2	2	140	8.3x5.7x1.6	Y
NanoAvionics	SatCOM UHF	Transceiver	395-440	VHF, UHF	2.4-38.4	3 W	7.5	5.6x3.3x6.6	Y
EnduroSat	UHF Transceiver Type II	Transceiver	400-403, 430-440	UHF	≤ 9.6	30 - 33 dBm	94	9.6x9.6x1.1	Y
SatRev S.A.	UHF Radio	Transceiver with AES128 encryption	400-405	UHF	0.45	<2W	158	9.6x9.95x1.565	Y
SENyT	Q-COMM	Transceiver	410-475 2400-2480	UHF, S	500	27 dBm	< 150	9.6x9.0x1.5 w/ enclosure	N
L3 Communications Inc. /SDL	Cadet	SDR	450	VHF, UHF	3,000	--	200	6.9x7.4x1.34	Y
CesiumAstro	Vireo RPU	SDR	600	L, S, C, X		-5 to 6	5000	25x15x20.3	N
sci_Zone, Inc.	LinkStar-STX3	Transmitter	1610-1625	L	0.009	--	48	8.6x5.3x2.9	Y
Qualcomm	GSP-1720	Transmitter	1610-1626.5, 2483.5-2500	L, S	9.6	31 dBm	60	11.9x6.5x1.5	Y



Table 9-3: Radios									
Manufacturer	**Product**	**Type**	**Min Frequency**	**Frequency Band**	**Data Rate**	**Tx Power**	**Mass**	**Dimensions**	**Flight Heritage**
---	**---**	**---**	**[MHz]**	**--**	**[kbps]**	**--**	**[g]**	**[cm]**	**---**
NAL Research Corporation	NAL Iridium 9602-LP	Iridium Satellite Tracker	1616-1626.5	L	--	1 W	136	6.9x5.5x2.4	Y
Near Space Launch	EyeStar-S4 Iridium	Transceiver	1618.75	L	0.1	31.96 dBm	29	6x3x2.1	Y
L3Harris	CXS-1000	Transponder	1700-2100	L, S	20,000	1-5 W	1360	10x10x11	Y
Tethers Unlimited	SWIFT-SLX	SDR	1700-2500	S	6,000	33 dBm	300	9x9.8x3.6	Y
Tethers Unlimited	SWIFT-XTS S Transceiver X Transmitter	SDR	1700-2500, 7000-8500	S, X	6,000-25,000	34 dBm	800	9x9.8x6	Y
AAC Clyde Space	TX-2400	Transmitter	2000-2300	S	6,000	2.5	70	6.8x3.5x1.5	Y
Syrlinks	EWC27 + OPT27-SRX	Transceiver	2025-2110	S	100,000	27-33 dBm	400	9x9.6x3.9	Y
Dragonfly Aerospace	CTRS	Transceiver	2200-2290	S	150 400	up to 0.5W	460	120x160x35	Y
Vulcan Wireless	NSR-SDR-S/S	Transceiver/Transponder	2025-2115, 2200-2300	S	4,000	4W	375	9.2x9.5x3.4	Y
Dragonfly Aerospace	CTRS	Transceiver	2025-2115, 2200-2300	S	512	up to 2W	1000	16x12x3.5	N
Vulcan Wireless	NSR-SDR-X/S	Transceiver/Transponder	2025-2115, 8000-8500	S, X	10,000	5W	375	9.2x9.5x3.4	N
Vulcan Wireless	NSR-SDR-X/S HP	Transceiver/Transponder	2025-2115, 8000-8500	S, X	10,000	10 W	615	18.3x9.2x3.6	N
Orion Space Solutions	Triton-XST	Transmitter	2200, 8000	S, X	<670 Mbps	25-50 W	500g	10x10x10	N
CesiumAstro	Vireo RPU	SDR	17000 27000	Ka	--	-5 to 6	7400	25x22.6x20.3	N
IQ Technologies for Earth and Space GmbH	HISPICO	Transmitter	2100-2500	S	1,000	27 dBm	100	9.5x4.6x1.5	Y



Table 9-3: Radios									
Manufacturer	**Product**	**Type**	**Min Frequency**	**Frequency Band**	**Data Rate**	**Tx Power**	**Mass**	**Dimensions**	**Flight Heritage**
---	**---**	**---**	**[MHz]**	**--**	**[kbps]**	**--**	**[g]**	**[cm]**	**---**
Innoflight, Inc.	SCR-104	SDR with AES-256 Encryption	2200-2290 1760-1840 2025-2110	S L/S	>4,500 1000	--	250 - 290	8.2x8.2x2.5 9.8x8.2x3.3	Y
CUBECOM	STXG2	Transmitter	2200-2290 2400-2480	S	25,000	--	137	9.6x9.0x13	N
Emhiser Research, Inc.	ETT-01EBA102-00	Transmitter	2200-2400	S	--	1 W	57	3x8.6x0.8	Y
Quasonix	NanoTX	Transmitter	2200.5-2394.5	S	50	1-10 W	--	3.3x8.6x0.8	Y
IQ Technologies for Earth and Space GmbH	SLINK-PHY	Transceiver	2200-2290, 2025-2110	S	64-4000	30 dBm	275	6.5x6.5x13.7	Y
ISISPACE	TXS	Transceiver	2200-2290	S	4.3	27-33 dBm	132	9.8x9.3x1.4	Y
Space Inventor	STTC-P3	SDR	2200-2290	S, X	9 – 10,000	33 dBm	230	9.1x9.4x1.7	Y
Satlab	SRS-3	Transceiver	2200-2290	S	512	30 dbM	190	8.7x9.3x1.7	Y
Satlab	SRS-4	Transceiver	2200-2290	S	-	33 dbM	253	9.3x8.7x1.75	Y
Syrlinks	S-band Transponder	Transponder	2200–2290	S	8-2000	27-33 dBm	--	--	Y
Syrlinks	EWC15-NG	Transceiver	2025-2110 2200-2290	S	512 2,000	33 dBm	1280	17.2x12x6.7	N
Syrlinks	EWC31	Transceiver	2025-2110 2200-2290	S	256 2,000	33 dBm	405	9.5x9.5x5.3	Y
Syrlinks	EWC31-NG	Transceiver	2025-2110 2200-2290	S	512 2,000	33 dBm	360	9.5x9x3.2	N
EnduroSat	S-band Transceiver II	Transceiver	2200 – 2290, 2025 - 2110	S	< 125	27-33 dBm	246	9.4x8.8x2.3	Y
EnduroSat	S-Band Transceiver III	Transceiver	2200 - 2290, 2025 – 2110,	S	≤ 3000	27 - 33 dBm	340	9.6x9.6x2.5	N
EnduroSat	S-band Transmitter	Transmitter	2200-2290, 2400-2450	S	≤ 20000	27 - 33 dBm	250	9.6 x 9.6 x 1.5	Y
General Dynamics	S-Band TDRSS/DSN	Transponder	2200-2300 2025-2220	S	12,000	0.03 W	4900	19x23x15	Y

Table 9-3: Radios									
Manufacturer	**Product**	**Type**	**Min Frequency**	**Frequency Band**	**Data Rate**	**Tx Power**	**Mass**	**Dimensions**	**Flight Heritage**
---	**---**	**---**	**[MHz]**	**--**	**[kbps]**	**--**	**[g]**	**[cm]**	**---**
SkyLabs	NANOlink-S base Gen2	Transceiver	2200-2300	S	< 4000	30 dBm	126	9.5x9.1x1.2	Y
SkyLabs	NANOlink-S boost Gen2	Transceiver	2200-2300	S	< 4000	37 dBm	250	9.5x9.1x2.2	Y
SkyLabs	NANOlink-S boost-dp Gen2	Transceiver	2200-2300	S	< 4000	31.5 dBm	391	9.5x9.1x3.2	Y
Microhard	Nano N2420	Modem	2400-2483.5	S	230	0.1-1 W	210	5x3x0.6	Y
Paradigma Technologies	PFES-1 ISL S Band TDD Front End	Transceiver	2400-2500	S	-	25 dBm	150	5.0x3.0x 1.0	N
Tethers Unlimited	SWIFT-XTX X Transmitter	SDR	7000-8500	X	25,000	33 dBm	300	9x9.8x6	N
General Dynamics	X-Band Small Deep Space	Transponder	7145-7230, 8400-8500	X	100,000	0.06	3200	18x17x11	Y
Space Dynamics Laboratory	IRIS V2.2	SDR Transponder	7145–7235 GHz 8400–8500 GHz	X, Ka, S, or UHF	0.1 - 10000	36	875	10.1x10.1x5.6	Y
Paradigma Technologies	PTX-1	Transmitter	7700 - 8500	X	-	43.5 dBm	800	12.5x10x3.0	N
Innoflight, Inc.	SCR-106	SDR with AES-256 Encryption	7800-8500 760-1840 2025-2110	X L/S	20,000 1,000	0.02-2.5 W	250 - 290	8.2x8.2x2.5 9.8x8.2x2.8	Y
Innoflight, Inc.	SCR-108	SDR with AES-256 Encryption	19200-21200 29000- 31000	Ka Ka	1 Gbps 20,000	0.02-3 W	404	9.8x8.7x3.9	Y
EnduroSat	X-band Transmitter	Transmitter	7900-8400	X	≤1.5 Gbps	27-33 dBm	270	9.6x9.6x2.6	Y
Dragonfly Aerospace	HDRTX-1.5	Transmitter	8025-8400	X	1.5 Gbps	< 4W	1600	17.5 × 14.5 × 5.5	Y
Dragonfly Aerospace	HDRTx-3	Transmitter	8025-8400	X	3 Gbps	up to 4W	1600	17.5×14.5×5.5	N
SkyLabs	NANOcast	Transmitter	8025-8500	X	<1 Gbps	37 dBm	164	9.5x9.1x1.3	N
CUBECOM	XTXG2	Transmitter	8025-8400	X	2.5 Gbps	--	137	9.6x9.0x1.3	N

Table 9-3: Radios									
Manufacturer	**Product**	**Type**	**Min Frequency**	**Frequency Band**	**Data Rate**	**Tx Power**	**Mass**	**Dimensions**	**Flight Heritage**
---	**---**	**---**	**[MHz]**	**--**	**[kbps]**	**--**	**[g]**	**[cm]**	**---**
CUBECOM	µHDTRX-X	Transmitter	8025-8400	X	1.5 Gbps	--	250	9.6x9.0x2.0	Y
CUBECOM	HDRTX	Transmitter	8025-8400	X	1 Gbps	--	250	9.6x9.0x2.0	Y
Satlab	SRX-8	Transmitter	8024-8400	X	<1 Gbps	33 dBm	300	9.3x8.7x2.2	Y
IQ Technologies for Earth and Space GmbH	XLINK	Transceiver	8025-8500, 7145-7250	X	64-25,000	30 dBm	--	<1 U	Y
SkyLabs	NANOcast	Transmitter	8025-8500	X	< 1 Gbps	37 dBm	164	9.5x9.1x1.3	N
Syrlinks	EWC27	Transmitter	8025-8500	X	1.4 Gbps	27-33 dBm	235	9x9.6x2.6	Y
Syrlinks	EWC27 + OPT27-SRX	Transceiver	2025-2110 8025-8500	S, X	256 1 Gbps	33 dBm	320	9.6x9x3.9	Y
Syrlinks	N-XONOS	Transmitter	2025-2110 8025-8400	S, X	256 4 Gbps	33 dBm	385	9.5x9x3.1	Y
Syrlinks	XONOS	Transmitter	2025-2110 8025-8500	S, X	256 6.3 Gbps	40 dBm	2400	20.6x15.2x6.9	N
Argotec	UST-Lite	Transponder	2025-2120 2200-2300 7145-7235 8400-8500 22550-23550 25500-27500	S, X, K, Ka	< 1 Gbps (higher possible with NRE)	8 dBm (input to SSPA)	<4000 (quad-band)	19.9x14.1x12.1 (quad-band)	N
Tethers Unlimited	SWIFT-KTX Ka Transmitter	SDR	20200-21200 24000-27000	Ka	25,000	33 dBm	300	9x9.8x4	N
Tethers Unlimited	SWIFT-KTRX Ka Transmitter	SDR	24000-27000	Ka	---	35 dBm	1,000	16x9.6x6	N
SpaceMicro	microKaTx-300	Transmitter	25250-27250	K	1 Gbps	2 W	1000	10x10x8	Y
AAC Clyde Space	PULSAR-DATA XTX X-Band Transmitter	SDR	--	X	50,000	2 W	130	9.6x9x1.1	Y
EnduroSat	X-band SDR	Transmitter	8000 - 8400	X	≤ 6 Gbps	27 - 33 dBm	<2500	9.2 x10x11.5	Y
Paradigma Technologies	PTRKU-1	Transponder / Transceiver	10700-12700 12750-14000	Ku	-	33 dBm	350	9.4x9.4x2.2	N

Table 9-3: Radios									
Manufacturer	**Product**	**Type**	**Min Frequency**	**Frequency Band**	**Data Rate**	**Tx Power**	**Mass**	**Dimensions**	**Flight Heritage**
---	---	---	**[MHz]**	--	**[kbps]**	--	**[g]**	**[cm]**	---
EnduroSat	K-band SDR	Transmitter	25500-27000	K	≤ 2 Gbps	27 - 33 dBm	<5000	9.2x10x15	N
AAC Clyde Space	PULSAR-DATA STX	SDR	--	S	7,500	1 W	100	9.6x9x1.7	Y
Honeywell	STC-MS03	Transceiver	--	S	6,250	3.16 W	1000	16x11x4.4	Y
Innoflight, Inc.	SCR-106HDR	SDR with AES-256 Encryption	7800-8500 1760-1840 2025-2110	X L S	1 Gbps 20,000	-	250 - 290	8.2x8.2x2.5 9.8x8.2x2.8	Y
EnduroSat	Versatile Wideband SDR (VW-SDR)	Transceiver	75 - 6000	VHF, UHF, L, S, C	982,000	-10 dBm	<1500	9.8x9.8x7.5	Y
Trident	RDRT	SDR – RF System on Chip (RFSoC)	100	L/S	8-channels 250MHz, 6554MH, 8-channels 250MHz, 4096MHz	-1 dBm Full-scale	571	10x14.6x2.54	N
Trident	ADCM	SDR – MPSoC Basecard and -SP converters - RX only	100	L, S, C	6.4GSPS single channel, 3.2 GSPS dual-channel	2.8dBm Full scale input	690	10x14.6x2.54	N
Space Dynamics Laboratory	Iris Radio V3	SDR Transponder	Various	Simultaneous Multiband: X, Ka, S	0.1 - 10000	34	720	10.1x10.1x3.8	N
PICOSATS	RADIOSAT	Transponder	17300 - 21200 27000 - 31000	K/Ka	-	5	690	93.5x114.15x45.6	Y



Table 9-3: Radios									
Manufacturer	**Product**	**Type**	**Min Frequency**	**Frequency Band**	**Data Rate**	**Tx Power**	**Mass**	**Dimensions**	**Flight Heritage**
---	**---**	**---**	**[MHz]**	**--**	**[kbps]**	**--**	**[g]**	**[cm]**	**---**
PICOSATS	RADIOSAT	Transponder	10700 -12750 12750 -13250 13750 -14800	Ku	-	5	< 1000	93.5x 114.2x62.1	N
PICOSATS	RADIOSAT	Transceiver	17300 - 21200 27000 - 31000	K/Ka	4 Gbps 1 Gbps	5	900	83.50 x 114.15 x 53	N
PICOSATS	BEAMSAT	Transceiver	10700 -12750 12750 -13250 13750 -14800	Ku	4 Gbps 1 Gbps	5	1000	93.5x114.2x7 0.6	N
PICOSATS	RADIOSAT SDR	Modem/Trans ceiver (SDR)	300 - 7000	UHF, L, S, C	4 Gbps 1 Gbps	0,001	< 500	83.5x96x25	N
Paradigma Technologies	PEWR-1 Wideband Receiver	Receiver	100 - 22000	VHF to Ka	-	0 dBm	550	20x10x1.5	N
Paradigma Technologies	PTRKA-1	Transponder / Transceiver	17200 - 21200 27000 - 31000	K/Ka	-	33 dBm	350	9.4x9.4x2.2	Y
PICOSATS	BEAMSAT	Transmitter	25500 - 27000	Ka	4 Gbps	5	900	83.5x114.15x 53	N
Paradigma Technologies	PTRQV-1	Transponder / Transceiver	37500 - 42500 47200 - 52400	K/Ka	-	30 dBm	350	9.4x9.4x2.2	N
Paradigma Technologies	PTQ-1	Transmitter	37500 - 42500	Q	-	22 dBm	350	9.4x9.4x2.2	Y
Paradigma Technologies	PTRQV-1	Transponder / Transceiver	37500 - 42500 47200 - 52400	QV	-	30 dBm	350	9.4x9.4x2.2	N

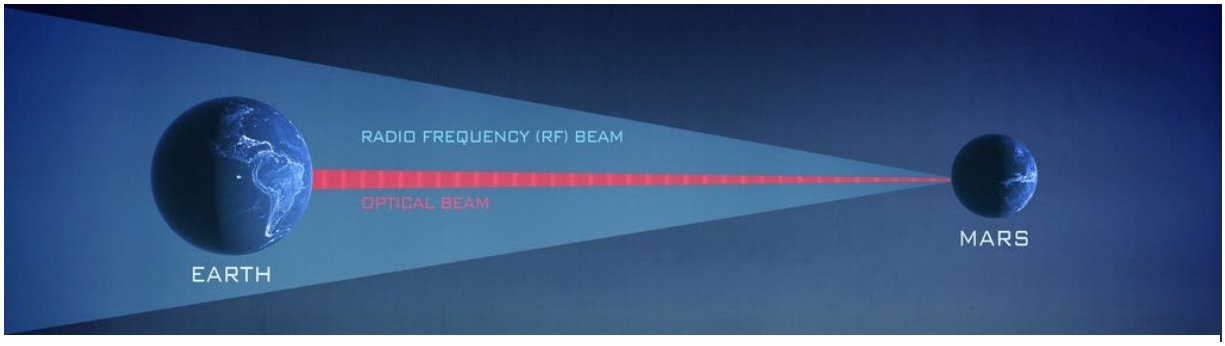


Figure 9.7: Laser vs RF link and data downlink. Credit: NASA

9.3 State-of-the-art: Free Space Optical Communications

Free space optical communications, or lasercom, uses optical wavelengths of electromagnetic radiation to transmit messages wirelessly between user terminals. While few small satellite optical communications terminals have flown, availability is improving, and optical communication is becoming a more common wireless communication technology for small satellites.

Due to the higher frequencies of electromagnetic energy used in lasercom, the amount of bandwidth available for communicating is much larger than that available for RF. This increase in bandwidth over RF enables much higher data rates. The beam width of a lasercom link is also typically much narrower than that of the RF link (displayed in Figure 9.7). The amount that a transmitted beam spreads as a function of its propagation distance is called its divergence. The divergence of a beam is proportional to the wavelength of the electromagnetic wave transmitted divided by the transmitted beam diameter. The high frequencies used in lasercom mean that the wavelength of the transmitted energy is orders of magnitude smaller than RF systems. These small wavelengths mean that the transmitter diameters and beam divergence of lasercom systems can also be much smaller, which enables the size, weight, and power (SWaP) of lasercom systems to be lower than those of similarly performing RF systems. Laser communications have a low probability of intercept, are difficult to jam, and encounter very little interference because of the narrow beamwidth. At present, optical frequencies are unregulated, unlike RF systems that require a licensing process to be able to communicate with a spacecraft.

Lasercom is not without its disadvantages, which include the required beam pointing accuracy and the impact that weather has on the signal. The small beam divergence of lasercom transmit beams means that the acceptable pointing error of the narrow beam is much smaller than that of typical RF systems. The frequencies used in lasercom systems are also susceptible to large amounts of attenuation due to moisture in clouds. This attenuation prohibits communication while there is cloud cover and incentivizes operators to build their optical ground stations in areas with infrequent cloud cover. While larger missions such as the Geosynchronous Lightweight Technology Experiment (GeoLITE), Near Field Infrared Experiment (NFIRE), and Lunar Laser Communication Demonstration (LLCD) demonstrated laser communications downlinks and crosslinks decades ago, SmallSats and CubeSats have successfully demonstrated laser communication downlinks from space. For example, The Aerospace Corporation, in cooperation with

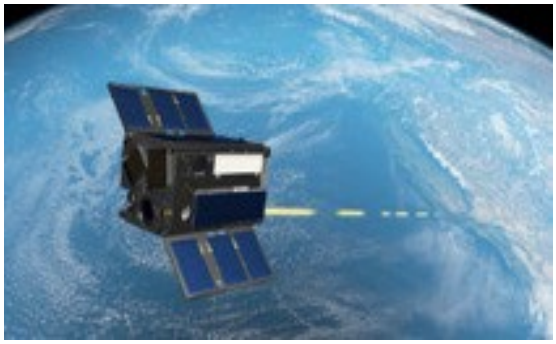


Figure 9.8: An artist rendering of laser communications for the OCSD. Credit: NASA.

NASA ARC, launched three CubeSats in its AeroCube Optical Communication and Sensor Demonstration (OCSD) series (Figure 9.8). OCSD-B and C demonstrated a 200 Mbps downlink from a 1.5U CubeSat to a 40 cm ground station (16). The Aerospace Corporation transmitter has also successfully flown on follow-on missions that were able to use lasercom systems to downlink science data (17).

9.3.1 System Architecture

An optical modem, optical amplifier, and optical head typically comprise a lasercom terminal (LCT) (see Figure 9.9 for an example system diagram of an optical head). As with radio terminals, component locations in optical terminals can vary; for example, the modulator may not be located near the optical front end. Also, the pointing mechanism might differ from the one shown in Figure 9.9.

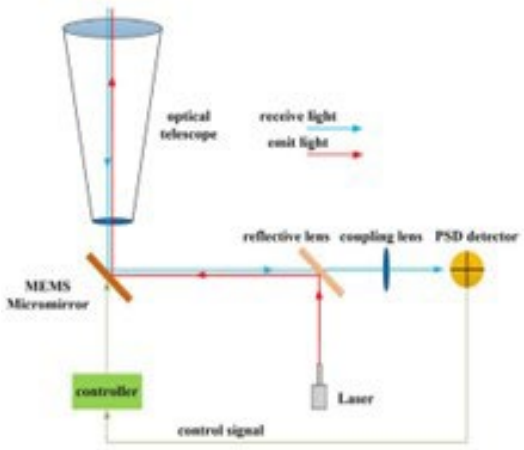


Figure 9.9: Optical head architecture diagram. Credit: Wang et al. 2023.

The key parameters of an optical communication system are frequency, modulation, aperture size, and range. Successful optical communications links require high pointing accuracy. The optical communication terminal on a spacecraft typically has a two-stage pointing system, with a coarse-pointing stage and a fine-pointing stage. The optical communication system often relies heavily on the spacecraft attitude determination and control system (ADCS) for coarse pointing and may use a second pointing mechanism such as a gimbal as additional support for coarse pointing. Fine pointing is often implemented with additional mirrors in the payload. However, pointing that is solely dependent on spacecraft attitude control has also been demonstrated. On transmit, energy passing through the optical aperture forms a very narrow beam. The larger the aperture, the narrower the beam; this creates higher power density at a receiver for a given range, but comes at the expense of more demanding pointing requirements for the transmit beam.

For two communication terminals to locate each other, they may shine higher-power and broader-beam “beacon” lasers to find each other before engaging the narrower and higher data rate link. Other strategies are possible, for example, scanning the direction of the data beam until acquisition is achieved. The beacon itself may also be modulated. Optical modems may be software-defined and can support multiple modulation and coding schemes, similar to RF.

9.3.2 Optical Ground Stations

The ground stations for optical communications understandably differ significantly from RF ground stations due to the need for the receiving aperture (typically a mirrored telescope) to maintain an optical-quality surface to focus the collected optical energy onto a receiver. Optical ground stations are often located at or near astronomical telescope sites, as they are located in favorable “seeing” environments, that is, locations with a low chance of cloud cover and calm, non-turbulent air. Optical ground stations are typically mounted inside protected domes or other structures to cover them during bad weather. These structures typically need to be opened for clear access to the sky. Since optical ground stations often have beacons, it is important to consider laser safety and their proximity to airports. Typical ground-to-space beacons are on the order of tens of watts of optical power for low-Earth orbit missions. Most optical ground stations are experimental facilities used for campaigns with specific research missions, although there have been recent developments in commercial optical ground stations. For a more detailed descriptions of existing optical ground stations, refer to the *Ground Data Systems and Mission Operations* chapter.

9.3.3 Design Considerations

Lasercom terminals can offer a smaller footprint and lower power draw compared to those of an RF terminal. However, lasercom pointing requirements are significantly more demanding. One of the largest challenges to widespread implementation is the pointing accuracy required for the LCT. To manage the pointing challenges, there are different types of system implementation and components that can be used, depending on resource constraints, performance requirements, and mission lifetime. The LCTs that have been designed, built, and operated on small satellite and CubeSat platforms have some significant differences from LCTs designed for larger spacecraft. Given the size, weight, and power constraints for SmallSat LCTs, mechanical gimbals are typically not used. SmallSat lasercom systems may rely entirely on the body pointing of the satellite to point the LCT at the ground station, or they may use an internal fine pointing mechanism to achieve the required fine-pointing performance.

On SmallSat platforms, the limited volume and tight packaging is often a major challenge in the design of low-SWaP LCTs. There are thermal management challenges during operation, as it is difficult to radiate enough heat given the limited surface area for radiators. There are also power constraints due to limited surface area for solar arrays and secondary battery systems. In addition, not all SmallSat platforms can achieve the pointing requirements necessary for laser communications. Typically, both precise three-axis reaction wheels for actuation and attitude determination sensing from at least one star tracker are necessary.

While RF bands with high frequency and bandwidth are also affected by clouds and rain, cloud cover can prove difficult or even insurmountable for optical communications systems due to the high levels of attenuation. If the cloud coverage is too great at a specific ground station, the transmission may be held for a later time or passed off to a different ground station. With advances in intersatellite networking and the development of extensive networks of optical communication ground stations, routing data around weather may become more feasible.

The atmosphere is also a source of aberrations for optical communication systems, particularly for terminals with larger apertures and more complex receivers designed to support higher data rates. For example, some high-rate optical downlink terminals that require coupling the received light into fiber receivers must use adaptive optics to correct atmospheric effects on the incident wavefront. Without correction of the wavefront, there would be a lack of received signal power to couple into the receive optical fiber due to the perturbed wavefront of the received light. Adaptive optics systems take a sample of the incident wavefront before it reaches the receiver and measure the aberrations of the wavefront to provide input to the control of the adaptive optics system that acts on the received light and counters the aberrations.

Lasercom crosslinks can provide a high bandwidth connection between two satellites, as well as perform ranging between the satellites, potentially with high ranging precision. Connecting two satellites across different orbit planes can help with data routing and can reduce how long it takes to route data to the end user. Lasercom crosslink systems are now in use for both commercial and government missions. Lasercom crosslink demonstrations have been performed from GEO-LEO, LEO-GEO, LEO-LEO, and are operational as part of the European Data Relay Service (43)(44), but these LCTs were developed for much larger spacecraft (20)(21). Crosslinks also have the challenge of both terminals being resource-constrained onboard a spacecraft. Space-to-ground links have an advantage in that the ground station apertures can be large with essentially unconstrained resources relative to what is available on a satellite. The challenges facing inter-satellite optical communications also center on pointing, acquisition, and tracking (PAT) requirements. Satellites in different orbital planes can have high relative velocities and performing pointing, acquisition, and tracking of the terminal can be a challenge. An advanced

opto-mechanical system may be needed to surmount this challenge, and special consideration may be needed in the design of the receive optics to manage high Doppler shifts.

9.3.4 Policies and Licensing

Given the early stages of implementation for satellite optical communication systems, both policy and regulatory approaches are still evolving. In the policy realm, there is an initial draft of the CCSDS Pink Book in process (CCSDS 141.0-P-1.1) with a goal to facilitate interoperability and cross-support between different communication systems. There is also an optical communications working group with NASA and ESA participation. The U.S. government Space Development Agency has also recently released its Optical Communications Terminal (OCT) Standard Version 4.0.0 (28th June 2024), which is a widely used design reference for space lasercom terminals, although not yet targeted specifically to small satellite terminals.

Regarding licensing and regulation, the situation is very different from the radio frequency domain. Currently there are no licensing requirements for laser communications. In the radio frequency spectrum, the main goal for licensing is to prevent interference between transmitters.

Lasercom interference is not currently coordinated by a regulatory body (like the ITU or NTIA in RF), although there have been historical ITU World Radiocommunication Conference resolutions that have considered implementing regulations. There is currently no regulation for two major reasons:

1) Laser communications is highly directional, which makes interference unlikely, due to the narrow divergence of the transmitting beam and corresponding small beam footprint at the receiver.
2) The small number of organizations that deploy laser communication systems doesn't warrant a complex coordination body like the ITU.

However, in the U.S. there are three regulatory entities that are concerned with aspects of outdoor laser operations: the FAA, the DoD Laser Clearing House (for DoD missions) and the NASA Laser Safety Review Board (for NASA missions).

FAA coordination is required if potentially harmful laser irradiance is transmitted through navigable airspace. This includes prevention of injury as well as potential distraction of pilots by visible lasers. The FAA will most likely only be concerned about transmitters at ground stations because transmitters on spacecraft are hundreds of miles above the highest-flying aircraft and beam dispersion is large enough that there are usually no safety implications. Missions should coordinate with their local FAA service center to get approval, documented with a "letter of non-objection."

The DoD Laser Clearinghouse (LCH) works to ensure that DoD and DoD-sponsored outdoor laser use does not impact orbiting spacecraft or their sensors. That includes both US DoD and foreign assets. LCH and mission operators might enter close cooperation where LCH permits specific laser engagements. The process of coordinating with LCH to get to that point can take many months and should be started as early as possible. However, currently LCH will only engage DoD and DOD-sponsored missions.

NASA's Laser Safety Review Board (LSRB) is focused on personnel safety for all outdoor laser operations. NASA missions prepare safety documentation and submit to LSRB for review before launch. The LSRB will also verify FAA concurrence. Further information on regulations can be found in ANSI Z136.6, American National Standard for Safe Use of Lasers Outdoors, and in (45).

9.3.5 Mission Examples

SmallSat and CubeSat missions using lasercom terminals have shown viable pathways for overcoming the challenges associated with lasercom to enable high-bandwidth communications. Please refer to Table 9-4 for more information on lasercom missions. These efforts promote research toward practical applications of space optical communication technologies in the future.

The Small Optical Transponder (SOTA) project led by the National Institute of Information and Communications Technology (NICT) in Japan successfully demonstrated a laser space-to-ground link from a 50 kg microsatellite multiple times between 2014 and 2016 (22). This LCT was capable of up to 10 Mbps; the Very Small Optical Transponder (VSOTA) LCT, also developed by NICT, is capable of 1 Mbps. VSOTA was integrated into the Rapid International Scientific Experiment Satellite (RISESAT) from Tohoku University and launched in 2019 (23). Planned for 2027 is the demonstration of several technologies to enable optical communication constellations.

The German Aerospace Center (DLR) develops LCTs under its Optical Space Infrared Downlink System (OSIRIS) program to support laser downlinks from small satellites, using reference beacons for fine pointing. OSIRISv1 launched in 2017 on the University of Stuttgart's Flying Laptop satellite, demonstrated 200 Mbps downlinks using a body-pointing-only approach and continues to support testing of DLR's optical ground stations. The OSIRISv2 LCT, launched in 2016 on DLR's BiROS satellite, provided 1 Gbps and employed closed-loop body pointing with a beacon reference; portions of the terminal have been commissioned to date (24)(25)(26). The OSIRIS4 CubeSat transmitter, demonstrated in 2021, achieved an optical downlink in a 0.3U package using a MEMs fast-steering mirror for fine pointing. Designed to be compatible with a 60 cm optical receiver, this terminal has been commercialized through TESAT with the product name CubeLCT (28). A modified version, CubeISL by DLR, adds a receive optical path and fiber amplifier to support 100 Mbps crosslinks at distances up to 1000 km and 1 Gbps downlinks. The terminal has a mass below 1 kg, a volume of 1U, and an operating power of about 30 W (35). A dedicated on-orbit demonstration of these terminals is planned for 2026 using two 6U CubeSats as host platforms (36).

The Aerospace Corporation completed the first demonstration of optical communications from a 1.5U CubeSat platform with the NASA-sponsored Optical Communication and Sensor Demonstration (OCSD) mission. The terminals achieved a 200 Mbps downlink data rate to a 40 cm ground station and did not use a beacon for a pointing reference (16). This transmitter has been flown since on multiple missions such as R3 (17) and the Rogue Alpha and Beta CubeSats (18). An updated version was later demonstrated on the Slingshot mission, achieving downlink rates at 250 Mbps (19). In 2025, The Aerospace Corporation also demonstrated an optical crosslink between two 6U CubeSats at distances of roughly 560 km using its Flashlight Laser Crosslink Terminal. This terminal occupies approximately two units of volume and supports bidirectional data rates of 312.5 Mbps (46).

MIT Lincoln Laboratory developed the TeraByte InfraRed Delivery (TBIRD) terminal, which achieved 200 Gbps downlinks. The transmitter uses commercial fiber telecommunication transceivers and amplifiers to support very high data rate downlinks. This project used NASA JPL's Optical Communication Telescope Laboratory (OCTL), which hosts a 1 m telescope with the adaptive optics necessary to couple the received light back into an optical fiber connected to a transceiver for demodulation. This terminal development was sponsored by NASA and was launched on the PDT-3 6U CubeSat mission in June of 2022 (33). It has thus far achieved the transmission of 4.8 Tb in a single pass and has demonstrated the value of implementing an automatic repeat request protocol in the use of lasercom downlinks (31)(32).

As part of NASA's CLICK mission, MIT developed the 1.2U CLICK-A terminal. The first phase of the mission flew the CLICK-A downlink terminal on a 3U CubeSat to demonstrate an optical

design that uses a secondary fine pointing micro-electromechanical systems (MEMS) fine-steering mirror (FSM) to achieve the necessary pointing requirements for optical communication without imposing those requirements on spacecraft body pointing or needing large gimbals. This LCT uses closed-loop fine pointing with a beacon reference and is designed to close its link with a 28 cm ground station. The terminal was integrated into a Blue Canyon Technology's XB1 spacecraft bus and was launched to and deployed from the ISS in 2022. The mission successfully demonstrated improved pointing with the MEMS FSM compared to body-only pointing. CLICK-A ultimately served as a risk-reduction phase for the CLICK-B and C mission operations (27).

The CLICK-B/C phase of the CLICK mission is developing a 1.5U crosslink LCT. The CLICK-B/C crosslink LCT is designed to establish a 20 Mbps link at separations from 25 to 580 km. CLICK-B and C will each be integrated into their own 3U Blue Canyon Technologies XB1 spacecraft. The LCTs are designed to be capable of precision ranging up to a precision of 50 cm relative to each other. The spacecraft will be launched to and deployed from the ISS in late 2026 and will fly in the same orbital plane (27).

The Laser Crosslink Experiment (LaCE) by Los Alamos National Laboratory consisted of two 6U CubeSats that demonstrated the Skylight Laser Communication Terminal crosslink as their primary objective. The Skylight LCT was designed to actively steer the laser communication payload to establish an optical link between the two CubeSats which it successfully did in 2024 (47)(48). At a distance of 7.4 km between each CubeSat, 2 Tbit/s was achieved in an urban environment with atmospheric turbulence. Future efforts aim to miniaturize the terminals while supporting data rates of up to 10 Gbit/s between a LEO spacecraft and the ground in 2026, and between a satellite and a high-altitude balloon in 2027.



Table 9-4: LCT Technologies								
Vendor/Developer	**Terminal**	**Platform**	**Data Rate**	**Mass**	**Power**	**Wavelength**	**Modulation**	**Launch Date**
---	**---**	**---**	**[Mbps]**	**[kg]**	**[W]**	**[nm]**	**---**	**---**
NICT	SOTA	SOCRATES	10	5.9	16	976/800/1549	OOK	May 2014
DLR	OSIRISv2	BiROS	1000	1.65	37	1550	OOK	June 2016
DLR	OSIRISv1	Flying Laptop	200	1.3	26	1550	OOK	July 2017
Aerospace Corporation	OCSD-B&C	AeroCube-7	200	<2.3	20	1064	OOK	December 2017
NICT	VSOTA	RISESAT	1	<1	4.33	980/1550	OOK/PPM	January 2019
Sony/JAXA	SOLISS	ISS	100	9.8	36	1550	OOK	July 2019
DLR	OSIRIS4CubeSat	PIXL-1	100	0.4	10	1550	OOK	January 2021
MIT Lincoln Labs	TBIRD	PDT-3	200,000	<3	100	1550	QPSK	May 2022
MIT	CLICK-A	CLICK	10	1.2	15	1550	PPM	July 2022
AAC Clyde Space	CubeCat	NorSat-TD	1000	<1.33	15	1550	OOK	April 2023
MIT	CLICK-B/C	CLICK	20	1.5	30	1537/1563	PPM	Est. 2026
DLR	CubeISL	CubeISL	100	1	30	1537/1553	OOK	2025
CACI	Skylight		100	1.6	35	1536/1553	PPM	May 2024
Emxys	ODALCOM	Optical transceiver	200	<1	2.6	1550	Unipolar NRZ	Est. 2026

9.4 Future Communications Technologies

As SmallSat missions become more complex, there is a greater need for higher data rates that drive the development of higher frequency communication systems—such as Ku-band, Ka-band, and W-band—for SmallSats. These bands enable higher-speed and higher-capacity data transmission and help alleviate the already overcrowded RF spectrum in lower frequency bands. Both RF congestion and interference risks have resulted from the rapid growth in the aerospace, commercial spacecraft, and 5G telecommunications sectors. Traditionally used for military radar and space communications, S-band allocations now face intense competition as commercial operators seek access to bands that were once reserved for more specialized applications. S-band remains widely used for higher-rate telemetry (up to ~10 Mbps), and many academic and commercial missions still rely on S-band transceivers.

Deployable Ka-band mesh reflectors have demonstrated gains above 40 dBi on 6U platforms (50). NASA's Investigation of Convective Updrafts (INCUS) mission aims to track the vertical dynamics of tropical convective storms, and each of the three identical ~100 kg SmallSats will carry active Ka-band radar and a deployable Ka-band mesh reflector antenna (51). Once fully deployed, the Ka-band reflector has a 1.6 m aperture on-orbit that will provide high-sensitivity Ka-band radar observations. At Ku-band, microstrip and dual-band shared-aperture phased arrays offer wide bandwidth, circular polarization, and up to ±55° electronic steering in low-profile formats suitable for CubeSats (52).

NEC Corporation is progressing with a technology demonstration of millimeter-wave Q/V-band transceiver equipment in orbit on a ~200-kg class spacecraft (53). This payload is designed to operate in the Q-band (approximately 33–50 GHz) and V-band (40–75 GHz), enabling high-capacity satellite downlinks and experiments to measure radio-wave propagation characteristics in these bands (54).

The other solution to the congested RF spectrum is to employ optical terminals for space-to-ground and space-to-space communication. Ongoing efforts are improving current optical communication in LEO for future SmallSat mission generations. While free space optical communication technology continues to progress toward fielding operational systems, other avenues of research have also been explored. Quantum key distribution is a protocol that shares a secret cryptographic key using entangled photons. Sources and optical front ends have been in development for transmitting these keys from small satellite spaceborne platforms (38)(39).

Another approach to expanding the communication windows for SmallSats in LEO is to form an intersatellite link to geosynchronous orbit. NICT is developing the CubeSat Small Optical Transponder (CubeSOTA) which aims to validate laser communication links between a 6U LEO CubeSat and a GEO satellite at data rates up to 10 Gbps (55). For larger spacecraft, one example is DLR's European Data Relay System (EDRS), which aims to enable near-real-time data relay between LEO and ground stations via GEO satellites equipped with laser communication terminals and Ka-band. Other terminals for larger SmallSats have been developed by Tesat, Mynaric (27), SpaceMicro (28), and SA Photonics in response to the development of the Space Development Agency's Proliferated Warfighter Space Architecture constellation and the use of LCTs in that architecture. Beyond this, DARPA has funded the Space-BACN program, which seeks to develop a reconfigurable multi-protocol inter-satellite LCT that can be supported on small satellites.

As SmallSats employ more autonomous onboard systems, multi-spacecraft missions will ultimately exchange navigation data directly between spacecraft, which will reduce reliance on ground control. Recent generations of CubeSat deep-space transceivers have integrated radiometric ranging capabilities in which timing codes embedded in the RF waveform provide

one-way or two-way ranging measurements. When combined with directional information from ground antennas, these radiometric observables enable accurate trajectory reconstruction for spacecraft operating beyond LEO.

Inter-spacecraft relay capabilities are gaining interest because they will enhance crosslink communication to extend the effective coverage of limited ground station networks. As SmallSats venture farther into space, transponders may offer a more efficient pathway for high-rate communications back to Earth. The limitations in RF power and antenna aperture further motivate the need for cooperative networks in which small spacecraft relay data through a larger, more capable mothership. Although transponders are common in traditional spacecraft, networked SmallSat swarms with fully operational RF crosslinks in deep space have not yet flown.

As of 2026, several CubeSats—including the MarCO pair, CAPSTONE, BioSentinel, ArgoMoon, and LunaH-Map—have operated beyond low-Earth orbit using the Iris deep-space transponder. The MarCO spacecraft employed deployable X-band reflectarray high-gain antennas and full-duplex UHF/X-band radios, enabling near-real-time relay of telemetry during the InSight lander's descent and landing on Mars. Following the success of these missions, the deployment of additional SmallSats to cislunar and interplanetary destinations is anticipated. In the longer term, crosslink-enabled relay architectures, in which clusters of CubeSats provide communication hops for larger spacecraft, are expected to play an increasingly critical role in deep-space exploration.

Through NASA's Small Spacecraft & Distributed Systems (SSDS) capability, the University SmallSat Technology Partnerships (USTP) initiative has begun advancing RF and optical communication systems. Listed below in Table 9-5 are USTP projects focused on SmallSat communications technology advancement. Further information can be found at the USTP website:

https://www.nasa.gov/smallspacecraft/university-smallsat-technology-partnership-initiative/

Table 9-5: USTP Initiative Communication Projects

Project	University	Current Status	Reference
*FIGARO, 5G arrays for lunar relay operations	San Diego State	Still in development	USTP Technology Expo presentation
*A Small Satellite Lunar Communications and Navigation System	University of Colorado, Boulder	Still in development	USTP Technology Expo presentation

9.5 Summary

There is already strong flight heritage for many UHF/VHF and S-band communication systems for CubeSats. Less common, but with growing flight heritage, are X-band systems. Higher RF frequencies already have CubeSat flight heritage, and the performance is improving. Although there are limited Ka-band systems for CubeSats today, high-rate transmitters such as the Astro Digital AS-10075 demonstrated 320 Mbps in the Landmapper-BC 3 v2 mission. While laser communication has been demonstrated on multiple CubeSat platforms, it is still not yet considered to be an established technology for SmallSats, however, this will likely change in the near future. More demonstrations are in development, with some already launched and operating, to demonstrate higher data rates and increased pointing performance. Since optical

communications uplink and downlink can be blocked by clouds, RF is considered complementary to maintain contact under all conditions. There is growing interest among the NASA science community in using constellations of CubeSats to enhance observations for Earth and space science.

For feedback solicitation, please email: arc-sst-soa@mail.nasa.gov. Please include a valid business email for further contact.

9.6 References

(1) J.N Pelton. "The Basics of Satellite Communications." s.l.: Professional Education International, Inc., 2006.

(2) National Aeronautics and Space Administration, “Integrated Solar Array and Reflectarray Antenna (ISARA) for High Bandwidth CubeSats.” July 26, 2016. [Online] Available at: https://www.nasa.gov/sites/default/files/atoms/files/isara_fact_sheet-26july2016.pdf

(3) National Aeronautics and Space Administration, “Mars Cube One (MarCO),” Jet Propulsion Laboratory California Institute of Technology | CubeSat. [Online] Available at: https://www.jpl.nasa.gov/cubesat/missions/marco.php

(4) S. Xie et al., "Wireless Sensor Network for Satellite Applications: A Survey and Case Study." Unmanned Systems, Vol. 2, pp. 261-277, 2014.

(5) R. Schoemaker and J. Bouwmeester, "Evaluation of Bluetooth Low Energy Wireless Internal Data Communication for Nanosatellites." Small Satellites Systems and Services Symposium. pp. 1-15, 2014.

(6) P.G. Farrell and A.P. Clark, "Modulation and coding." International Journal of Satellite Communications, 1984.

(7) A. Datta, “New FCC rules make small satellite licensing easier, faster, and cheaper. Geospatial World | Advancing Knowledge for Sustainability.” August 22, 2020. [Online] Available at: https://www.geospatialworld.net/blogs/new-fcc-rules-make-small-satellite-licensing-easier-faster-and-cheaper/

(8) J. Buxton and D. Glasbrenner, “Amateur Radio and Experimental Licensing for CubeSats.”

(9) CalPoly. “CubeSat Licensing Support.” [Online] Available at: https://www.cubesat.org/cubesatlicensingsupport

(10) National Institute of Standards and Technology. "Security Requirements for Cryptographic Modules, Federal Information Processing Standard (FIPS).” ISO/IEC 19790:2012; ISO/IEC 24759:2014

(11) 47 CFR Part 97, “Amateur Radio Service,” [Online] Available at: https://www.law.cornell.edu/cfr/text/47/part-97

(12) J.R. Wertz, D.F. Everett, and J.J. Puschell, "Space Mission Engineering: The New SMAD." Microcosm Press, Hawthorne, CA, 2015.

(13) S.K. Johnson, R.C. Reinhart, and T.J. Kacpura, "CoNNeCT's Approach for the Development of Three Software Defined Radios for Space Application." IEEE Aerospace Conference. pp. 1-13, Big Sky, MT, 2012.

(14) Y. Wong et al., "NASA Near Earth Network (NEN) DVB-S2 Demonstration Testing for Enhancing Data Rates for CubeSats." 31st Annual AIAA/USU Conference on Small Satellites, Logan, UT, 2019.

(15) National Aeronautics and Space Administration, "Iris V2 CubeSat Deep-Space Transponder (IRIS)," [Online] Available at: https://www.jpl.nasa.gov/cubesat/missions/iris.php

(16) T.S. Rose, D.W. Rowen, S.D. LaLumondiere, N.I. Werner, R. Linares, A.C. Faler, J.M. Wicker, C.M. Coffman, G.A. Maul, D.H. Chien, A.C. Utter, R.P. Welle, and S.W. Janson, “Optical Communications Downlink from a Low-Earth Orbiting 1.5U CubeSat.” Opt. Express 27, 24382-24392, 2019.

(17) D.W. Pack, G. Kinum, P.D. Johnson, T.S. Wilkinson, C.M Coffman, J.C. Mauerhan, B.S. Hardy, R. Russell, and K. Mercy, “Landsat Imagery from a CubeSat: Results and Operational Lessons from the R3 Satellite’s First 18 Months in Space.” Small Satellite Conference, Logan UT, 2020.

(18) D.W Pack, B.S Hardy, J.R. Santiago, D. Pietrowski, J.C. Mauerhan, P.F. Zittel, D.W. Rowen, C.R. Purcell, P. Thiyanaratnam, L.J. Gelinas, P.K. Su, J. Gussy, and J.M. Santiago, “Flight Operations of Two Rapidly Assembled CubeSats with Commercial Infrared Cameras: The Rogue-Alpha,Beta Program.” Small Satellite Conference, Logan UT, 2021.

(19) Aerospace Corporation “Aerospace’s SLINGSHOT 1 Demonstrates Pathway To Accelerating Space Innovation” Article 2024. [Online] Available at: https://aerospace.org/article/aerospaces-slingshot-1-demonstrates-pathway-accelerating-space-innovation

(20) T. Jono, Y. Takayama, N. Kura, K. Ohinata, Y. Koyama, K. Shiratama, Z. Sodnik, B. Demelenne, A. Bird, and K. Arai, “OICETS On-orbit Laser Communication Experiments. Page 610503, San Jose, CA, February 2006.

(21) R. Fields, D. Kozlowski, H. Yura, R Wong, J Wicker, C. Lunde, M. Gregory, B Wandernoth, and F. Heine, “5.625 Gbps Bidirectional Laser Communications Measurements Between the NFIRE Satellite and an Optical Ground Station.” International Conference on Space Optical Systems and Applications (ICSOS), pages 44–53, Santa Monica, CA, USA, May 2011. IEEE.

(22) H. Takenaka, Y. Koyama, M Akioka, D. Kolev, N. Iwakiri, H. Kunimori, A. Carrasco-Casado, Y. Munemasa, E. Okamoto, M. Toyoshima, “In-orbit Verification of Small Optical Transponder (SOTA): Evaluation of Satellite-to-ground Laser Communication Links.” Proc. SPIE 9739, Free-Space Laser Communication and Atmospheric Propagation XXVIII, 973903, March 15, 2016.

(23) H. Tomio, T. Kuwahara, S. Fujita, Y. Sato, M. Sakal, H. Kunimori, T. Kubooka, H. Takenaka, Y. Saito, M. Toyoshima, “Assembly and Integration of Optical Downlink Terminal VSOTA on Microsatellite RISESAT.” Proc. SPIE 11180, International Conference on Space Optics — ICSO 2018, 111805Z, July 12, 2019.

(24) C. Schmidt, C. Fuchs, “The OSIRIS Program at DLR," Proc. SPIE 10524, Free-Space Laser Communication and Atmospheric Propagation XXX, 105240R, 5 February 15, 2018.

(25) C. Fuchs, C. Schmidt, J. Keim, F. Moll, B. Rödiger, M. Lengowski, S. Gaißer, and D. Giggenbach, “Update on DLR''s OSIRIS Program and First results of OSIRISv1 on Flying Laptop.” Proc. SPIE 10910, Free-Space Laser Communications XXXI, 109100S, March 4, 2019.

(26) D. Giggenbach, C. Fuchs, C. Schmidt, B. Rödiger, S. Gaißer, S. Klinkner, D. Phung, J. Chabé, C. Courde, N. Maurice, H. Mariey, E. Samain, and G. Artaud, “Downlink Communication Experiments with OSIRISv1 Laser Terminal Onboard Flying Laptop Satellite.” Appl. Opt. 61, 1938-1946, 2022.

(27) W. Kammerer, P. Grenfell, L. Hyest, P. Serra, H. Tomio, N. Belsten, C. Lindsay, O. Čierny, K. Cahoy, M. Clark, D. Coogan, J. Conklin, D. Mayer, J. Stupl, J. Hanson, “CLICK Mission Flight Terminal Optomechanical Integration and Testing.” International Conference on Space Optics — ICSO, 2022.

(28) Tesat. “SMallest Laser Communication Transmitter Worldwide.” Technical Datasheet. 2022. [Online] Available at: https://www.tesat.de/images/tesat/products/220607_DataSheet_CubeLCT100M_A4.pdf

(29) K. Iwamoto, H. Komatsu, S. Ohta, Y. Kubo, T. Nakao, H. Yamazoe, T. Kamata, Y. Munemasa, H. Kunimori, M. Toyoshima, D. Koda, H. Sawada, T. Ikeda, “Experimental Results on In-orbit Technology Demonstration of SOLISS.” Proc. SPIE 11678, Free-Space Laser Communications XXXIII, 116780D, March 5, 2021.

(30) H. Komatsu, S. Ohta, H. Yamazoe, Y. Kubo, T. Nakao, T. Ito, D. Koda, H. Sawada, T. Ikeda, Y. Munemasa, H. Kunimori, T. Kubooka, M. Toyoshima, K. Iwamoto, “The Pointing Performance of the Optical Communication Terminal, SOLISS in the Experimentation of Bidirectional Laser Communication with an Optical Ground Station.” Proc. SPIE 11678, Free-Space Laser Communications XXXIII, 116780F, March 5, 2021.

(31) K. Riesing, et al., “Operations and Results from the 200 Gbps TBIRD Laser Communication Mission” Small Satellite Conference, Small Satellite Conference, Logan UT, 2023.

(32) C. M. Schieler et al., "Recent On-Orbit Results and ARQ Performance Analysis for the TBIRD 200-Gbps Mission." 2023 IEEE International Conference on Space Optical Systems and Applications (ICSOS), Vancouver, BC, Canada, 2023, pp. 49-55, doi: 10.1109/ICSOS59710.2023.10490285.

(33) Curt M. Schieler, Kathleen M. Riesing, Andrew J. Horvath, Bryan C. Bilyeu, Jesse S. Chang, Ajay S. Garg, Jade P. Wang, Bryan S. Robinson, "200 Gbps TBIRD CubeSat Downlink: Pre-flight Test Results." Proc. SPIE 11993, Free-Space Laser Communications XXXIV, 119930P, March 4, 2022.

(34) AAC Clyde Space. “AAC Clyde Space Succeeds with Laser Communication Terminal in Space. Press Release. 2024. [Online] Available at: https://cdn.bequoted.com/media/1/0ed1510b-9c33-4686-8547-55c3212c4737/AAC-Clyde-Space-Press-release-2024-01-24.pdf

(35) B. Rödiger, “DLRs Solutions for Optical Communications on CubeSats.” Small Spacecraft Systems Virtual Institute’s (S3VI) Monthly Webinar, 2023.

(36) J. Nonay, et al., "Horizontal Free-space Optical Link with CubeISL Over 143 km." J. Opt. Commun. Netw. 16, 593-601, 2024.

(37) AAC Clyde Space. “Laser Communications CUBECAT.” Technical Datasheet. 2022. [Online] Available at: https://www.aac-clyde.space/wp-content/uploads/2021/10/CUBECAT.pdf

(38) R. Bedington, J.M. Arrazola, and A. Ling, “Progress in Satellite Quantum Key Distribution.” Npj Quantum Information Vol. 3, 30, 2017.

(39) P. Serra, O. Čierny, W. Kammerer, E.S. Douglas, D.W. Kim, J.N. Ashcraft, G. Smith, C. Guthery, T. Vergoossen, A. Lohrmann, R. Bedington, C. Perumangatt, A. Ling, K. Cahoy, “Optical Front-end for a Quantum Key Distribution CubeSat.” Proc. SPIE 11852, International Conference on Space Optics, 118523C, June 11, 2021.

(40) D. Jacobs, J. Bowman, M. Patterson, M. Horn, C. McCormick and M. Adkins, “Plan for On-Orbit Demonstration of the Deployable Optical Receiver Array.” IEEE Aerospace Conference (AERO), pp. 1-8, 2022.

(41) J.E. Velazco and J.S. de la Vega. “Q4 – A CubeSat Mission to Demonstrate Omnidirectional Optical Communications.” IEEE Aerospace Conference, pp. 1-6, 2020.

(42) A. Carrasco-Casado et al., "Intersatellite-Link Demonstration Mission Between CubeSOTA (LEO CubeSat) and ETS9-HICALI (GEO Satellite).” IEEE International Conference on Space Optical Systems and Applications (ICSOS), pp. 1-5, 2019.

(43) European Space Agency. “European Data Relay Service.” [Online] Available at: https://www.esa.int/Applications/Telecommunications_Integrated_Applications/EDRS

(44) F. Heine, P. Martin-Pimentel, N. Höpcke, D. Hasler, C. Rochow, and H. Zech, "Status of Tesat Lasercomms Activities." Free-Space Laser Communications XXXIII, vol. 11678, pp. 45-50. SPIE, 2021.

(45) R. Lafon, J. Wu, B. Edwards, “Regulatory Considerations: Laser Safety and the Emerging Technology of Laser Communication.” Commercial Laser Communications Interoperability and Regulatory Workshop, Washington, DC, June 12, 2017.

(46) The Aerospace Corporation, “Aerospace Performs Optical Crosslinks Between CubeSats for the First Time,” February 27, 2025, [Online] Accessed: February 7, 2026, Available at:

https://aerospace.org/press-release/aerospace-corporation-performs-optical-crosslinks-between-cubesats-first-time

(47) S. Stanko, D. Frey, J. Ruvalcaba, S. Burk, et al. “Laser Crosslink Experiment: A Mission Overview,” 38th Annual Small Satellite Conference, 2024, Logan Utah.

(48) National Institute of Information and Communications Technology, “World's First Successful 2 Tbit/s Free-Space Optical Communication Using Small Optical Terminals Mountable on Satellites and HAPS,” December 16, 2025, Press release, [Online] Accessed: February 7, 2026, Available at: https://www.nict.go.jp/en/press/2025/12/16-1.html

(49) D. Wilson, “Nanosatellite Mission Yields Key Insights for Warfighter Capabilities,” June 23, 2025, Press releases, [Online] Accessed: February 7, 2026, Available at: https://www.niwcpacific.navy.mil/Media/Press-Releases/Article-Display/Article/4223309/nanosatellite-mission-yields-key-insights-for-warfighter-capabilities/

(50) Gurbet, Y.S., Doğu, S. Comprehensive Review of Ku, K, and Ka Band Antenna Designs: Applications in CubeSats. *Int. J. Aeronaut. Space Sci.* **27**, 447–496 (2026). https://doi.org/10.1007/s42405-025-00989-5

(51) Gupta G, Mancini A, Focardi P (2025) Feed assembly development for INCUS 1.6 m mesh reflector antenna. International Journal of Microwave and Wireless Technologies 17(5), 784–793. https:// doi.org/10.1017/S1759078725000364

(52) Wenxuan Xie et al., *“Hybrid-Decoupling-Based Shared-Aperture Phased Array Antenna for Ku/Ka-Band”*, Scientific Reports, 2025

(53) A. Carrasco-Casado, K. Shiratama, D. Kolev, H. Tsuji and M. Toyoshima, “Development and environmental validation of a compact EDFA with integrated LNA+HPA for satellite optical communications,” 2025, Front. Phys. 13:1542043, doi: 10.3389/fphy.2025.1542043.

(54) Photonics Media, “NEC Designs Payload for Optical Communications Satellite,” March 24, 2026, photonics.com [Online] Accessed: March 30, 2026, Available at: https://www.photonics.com/Articles/NEC-Designs-Payload-for-Optical-Communications/a72075

(55) Carrasco-Casado A, Shiratama K, Kolev D, Tsuji H and Toyoshima M (2025) Development and environmental validation of a compact EDFA with integrated LNA+HPA for satellite optical communications,” Front. Phys. 13:1542043, doi: 10.3389/fphy.2025.1542043.

Table of Contents

Chapter Glossary ii
10 Integration, Launch, Deployment, and Orbital Transport 281
10.1 Introduction 281
10.2 State-of-the-Art – Launch Integration Role 282
10.2.1 Launch Brokers and Launch Integrators 283
10.3 Launch Paradigms 283
10.3.1 Dedicated Launches 285
10.3.2 Rideshare Launches 286
10.4 Launch and Integration Hardware 286
10.4.1 Primary Structural Interfaces 286
10.4.2 Dispensers for Canisterized SmallSats 287
10.4.3 Separation Systems 289
10.5 Orbital Transfer / Maneuvering Vehicles (OTV/OMV) 291
10.5.1 Commercial Development/Services 292
10.6 International Space Station Options 298
10.6.1 Deployment from ISS 298
10.6.2 Deployment Above ISS 299
10.7 Summary 300
References 300

Chapter Glossary

(ACDS)	Attitude Determination and Control System
(CLIN)	Contract Line Item Number
(COTS)	Commercial-Off-the-Shelf
(CSLI)	CubeSat Launch Initiative
(CSO)	Client Space Object
(DPAF)	Dual Payload Attach Fitting
(EGSE)	Electrical Ground Support Equipment
(ESA)	European Space Agency
(ESPA)	EELV Secondary Payload Adapter
(FAA)	Federal Aviation Administration
(GEO)	Geostationary Earth Orbit
(GSE)	Ground Support Equipment
(ISS)	International Space Station
(JAXA)	Japan Aerospace Exploration Agency
(JEM)	Japanese Experimental Module
(JEMRMS)	Japanese Experimental Module Remote Manipulator System
(LEO)	Low-Earth Orbit
(LSP)	Launch Services Program
(MGSE)	Mechanical Ground Support Equipment
(MPAF)	Multi-Payload Attach Fitting
(MPEP)	Multi-Purpose Experiment Platform
(NASA)	National Aeronautics and Space Administration
(NICL)	Nanoracks Interchangeable CubeSat Launcher
(NOAA)	National Oceanic and Atmospheric Administration
(NRCSD)	Nanoracks CubeSat Deployer
(OMV)	Orbital Maneuvering Vehicle
(OTV)	Orbital Transfer Vehicle
(PCBM)	Passive Common Berthing Mechanism
(RCS)	Reaction Control System
(RUG)	Rideshare User Guide
(SLV)	Small Launch Vehicle
(SSMS)	Small Spacecraft Mission Service
(SSO)	Sun-Synchronous Orbit
(TRL)	Technology Readiness Level
(ULA)	United Launch Alliance
(USTP)	University SmallSat Technology Partnerships
(VADR)	Venture Class Acquisition of Dedicated and Rideshare

10 Integration, Launch, Deployment, and Orbital Transport

10.1 Introduction

The number of spacecraft launched in 2025 reached a new heigh, increasing by nearly 60% compared to 2024, totaling 4,577. A surge in Starlink constellation launches was largely responsible for this increase, accounting for approximately 70% of all spacecraft launched in 2025. Excluding Starlink, 45% of the remaining spacecraft launched in 2025 had a mass of 200 kg or less. While this represents a general decline in the < 200 kg class over the past five years, 2025 experienced a ~10% increase in launches of SmallSats between 11 – 600 kg, indicating a greater demand for larger platforms. While the average SmallSat mission still typically involves a spacecraft < 200 kg, the rise of larger next-generation spacecraft in constellations (i.e., Starlink, Iridium, Planet SkySat, Capella Acadia, etc.) will play a major role in the demand for fewer platforms that are bigger.

To address the growing demand for SmallSat launches, the “rideshare” launch market has emerged as a popular means for SmallSats to access space. This trend has been fueled by an increase in launch providers and improved launch capabilities, as well as the development of adapters and dispensers specifically designed for SmallSat and CubeSat missions. Rideshare launches are typically multi-manifest missions that either consist of 1) a large primary spacecraft that determines all the mission requirements (e.g., orbit, schedule, concept of operations, etc.), where secondary payloads are manifested to take advantage of the launch vehicle’s surplus mass, volume, and other performance margins, or 2) a single launch vehicle consisting entirely of SmallSats, also known as a “dedicated rideshare.” It should be noted that the term “payload(s)” in this chapter refers to the entire free-flying spacecraft deployed from a launch vehicle and is defined differently in Chapter 2 *Complete Spacecraft Platforms,* as instruments and technologies on spacecraft.

In support of making ridesharing a feasible option, orbital transport vehicles (OTVs) and orbital maneuvering vehicles (OMVs) provide “last mile” delivery services to their intended orbits for small satellites. These vehicles are becoming more common for microsatellite deployment and operational logistics. While historically referred to as “space tugs,” this term is being phased out by many in the commercial industry. The terms OTV and OMV are also falling out of favor, with many commercial offerings simply referring to the available systems as vehicles capable of in-space transportation services. For the purposes of this report, the terms OTV and OMV describe systems with onboard propulsion that can be launched to an approximate orbit and then propel themselves to one or more target orbits. There they can either deploy small spacecraft or serve as an integral part of a hosted payload. This chapter focuses on the use of these vehicles as deployers, while more information about hosted payload services is found in Chapter 2, *Complete Spacecraft Platforms*, Section 2.2.1. Some OTVs/OMVs are based on traditional rocket kick stages and are intended to work with specific launch vehicles. Several commercial companies have successfully flown OTVs/OMVs and are booking future launch manifests.

In 2022, NASA’s Launch Services Program introduced a new Indefinite Delivery/Indefinite Quantity (IDIQ) mechanism called the Venture Class Acquisition of Dedicated and Rideshare (VADR) launch services contract. The VADR contract was created to support more risk-tolerant NASA-sponsored missions with FAA-licensed commercial launch services using selected commercial providers. This approach enables unique launch capabilities for Class D or higher risk-tolerant payloads, including SmallSats and CubeSats, and since commercial services use a lower level of mission assurance for payloads with higher risk tolerance, this collaboration contributes to NASA’s science and research development efforts as an ideal mechanism for technical development. This contract mechanism supports both traditional and dedicated rideshare opportunities, offering lower-cost access to space with reduced NASA oversight and

mission assurance requirements. Initially awarded to 12 companies, the IDIQ VADR contract has since expanded through its on-ramp provision, with three additional vendors added in 2024. In 2025, Rocket Lab's Neutron was also included, broadening the contract's capabilities to medium-lift missions (1).

Educational SmallISat missions also have several avenues for accessing these opportunities. NASA's CubeSat Launch Initiative (CSLI) for example, has provided rides to a significant number of schools, nonprofit organizations, and NASA centers. The European Space Agency (ESA) "Fly Your Satellite" program is a similar program which provides launch opportunities to university CubeSat teams from ESA Member States, Canada, and Slovenia (3). NASA's University SmallSat Technology Partnerships (USTP) provides up to two years of funding and a collaborative partnership with NASA to advance university-led small satellite technologies (4).

The list of organizations/companies in this chapter is not all-encompassing and does not constitute an endorsement from NASA. There is no intention of mentioning certain companies and omitting others based on their technologies or relationship with NASA. The information is for awareness and guidance only. The performance advertised may differ from actual performance since the information has not been independently verified by NASA subject matter experts and relies on information provided directly from the manufacturers or from publicly available information. It should be noted that TRL designations may vary with changes specific to payload, mission requirements, reliability considerations, and/or the environment in which performance was demonstrated. Readers are highly encouraged to reach out to companies for further information regarding the performance and TRL of the described technologies.

10.2 State-of-the-Art – Launch Integration Role

Launch options for SmallSats include dedicated launches or rideshare launches. Regardless of the approach, integration with the launch vehicle is a complex and critical portion of the mission. The launch integration effort for a primary spacecraft typically includes the launch service provider, the spacecraft manufacturer, the spacecraft customer, the launch range, and sometimes a launch broker or integrator (2). When launching on a rideshare mission, the launch integration may become complex due to its multi-customer, multi-mission nature.

There are several options for identifying and booking a launch for a SmallSat. For rideshares, the spacecraft customer may choose to use a launch broker or launch integrator to facilitate the launch manifesting process or work directly with the launch service provider. A launch broker matches a spacecraft mission with a launch opportunity, whereas an integrator provides additional services related to multi-mission manifesting and/or integration.

Whether a spacecraft customer chooses to use a launch integrator or not, it is the responsibility of the spacecraft owner/operator to obtain the appropriate licensing for their spacecraft. These licenses may include: radio frequency licensing, remote sensing licensing, and laser usage approval (5)(6). The launch integrator or the launch service provider will require proof of licensure before integrating and/or launching the satellite. They will also require additional safety-related analyses and supporting data and documentation prior to launch, which typically includes orbital debris information, materials and venting data, and spacecraft-specific models (7).

For rideshare launches, many satellites are subject to a "do no harm" approach to protect the other spacecraft on the launch vehicle. A list of "do no harm" requirements is imposed on the rideshare satellites by the launch provider, launch integrator, or primary mission owner. These requirements vary by launch provider and launch integrator, but usually include restrictions on transmitters, post separation mechanical deployments, and hazardous materials. A comprehensive list of typical "do no harm" requirements is provided in the NASA Rideshare User Guide (RUG) (8).

10.2.1 Launch Brokers and Launch Integrators

A launch broker for small satellites is an individual or organization that matches a spacecraft with a launch opportunity, usually as a rideshare spacecraft. Typically, a launch broker does not provide any additional launch integration services beyond coordinating the relationship between the spacecraft manufacturer or customer and the launch service provider. Their purpose is to fill excess capacity on a launch, and they can also support negotiations between the launch provider and payload for scheduling, integration, safety testing, and cost (9).

Launch integrators work with the satellite customer and the launch vehicle provider to ensure that the customer's spacecraft is compatible with the launch vehicle by performing analyses and physical integration services. The launch integrator may provide the CubeSat dispenser, separation system, or other hardware required for integration, or these may be provided by the spacecraft customer.

10.3 Launch Paradigms

In the last decade, small spacecraft have accomplished some of the most prominent advances in the aerospace industry. The wide range of small spacecraft missions has reshaped the space industry, enabled academic research and commercial services, and strengthened scientific exploration and defense applications in both Earth orbit and deep space. The early SmallSat market grew rapidly from 2013 to 2020, by approximately 40%. This growth was driven by the widespread adoption of CubeSats. The "little platform that could" ignited academia's participation in space research and development, broadened commercial space services, and enabled numerous government research programs.

Three major trends emerged in the space industry after the adoption of CubeSats: the rise of CubeSat constellations, the evolution towards larger CubeSat platforms, and the use of CubeSat pathfinder demonstration missions. The first trend, CubeSat constellations, began with Planet Labs' Doves 3U high-frequency Earth observation constellation in 2013. Today, numerous commercial constellations deliver a variety of services, and as technology advances, upgraded satellites continually replace their predecessors. For example, Spire Global's Low Earth Multi-Use Receive (LEMUR) 3U constellation performs remote sensing for weather forecasting, and ship and aircraft tracking, with 65 active satellites (10). Hawkeye 360 operates a 3U CubeSat constellation to map radio frequency signals for geoanalytics with 30 active satellites (11), while Swarm Technologies introduced picosatellite Spacebees for low-bandwidth Internet of Things (IoT) connectivity. The second trend was the evolution of the CubeSat structure. The original 1U structure quickly expanded to 3U, then doubled in volume by 2014 with the 6U platform, and again in 2016 with the 12U platform (12). CubeSat deployers that were once constrained to one- to three-cubed canisters now offer up to 12U+ volume (see Section 10.4.1).

Finally, CubeSat-based pathfinder missions have demonstrated the viability of novel technologies. NASA's MarCO mission was the first-deep space CubeSat pathfinder to validate the survival of CubeSat avionics in deep space and demonstrate the capability to communicate with Earth (ref). NASA's Pathfinder Technology Demonstrator (PTD) series, based on a 6U bus developed by Terran Orbital Corporation, showcased advanced technologies that enabled direct infusion into a wider range of future science and exploration missions (13). Cislunar Autonomous Positioning System Technology Operations and Navigation Experiment (CAPSTONE) is a 12U spacecraft pathfinder mission to characterize near-rectilinear halo orbits for NASA's Artemis architecture and validating new navigation technology for the Lunar Gateway (14). CubeSat pathfinder missions are the foundation for modern SmallSat paradigms.

By 2020, the spacecraft market underwent another transformation with the deployment of Starlink's broadband *mega-constellation*. While commonly characterized by a numerical value of

satellites, NASA defines a mega-constellation as numerous satellites in close proximity with rapid separation velocities, creating elevated collision risks in LEO (15). Starlink alone accounted for 65% of all launched spacecraft that year in 2020, and this trend persisted through 2025. During this period, the platform's mass grew significantly—from less than 300 kg to about 800 kg within four years, with the upcoming v3 platform estimated at 1,500-2,000 kg. This surge in high-volume, larger spacecraft reshaped industry standards. To support this, in 2023, the FAA's Annual Compendium of Commercial Space Transportation raised its mass limit for small spacecraft from 600 kg to 1,200 kg (16).

When examining non-Starlink launch statistics, the average SmallSat mission is getting heavier as they become more capable. In 2025, more companies launched pathfinder constellations that will eventually join mega-constellation status such as Amazon LEO broadband network and the Guowang project for China's Satellite Network Group. Another new focus is on-orbit data centers, which could significantly increase computational power, storage, and raw data processing. China's Three-Body Computing Constellation launched the first group of 12 spacecraft in summer 2025, and Starlink is exploring data center applications with its mega-constellation (17).

Of the total non-Starlink spacecraft launched in 2025: microsatellites (11 – 200 kg) accounted for 17%; minisatellites (200 – 600 kg) represented 24%; and nanosatellites (including pico- and femtosatellites) accounted for about 15%. There continues to be an upward trend in the use of spacecraft platforms < 200 kg, as illustrated in Figure 10.1 below.

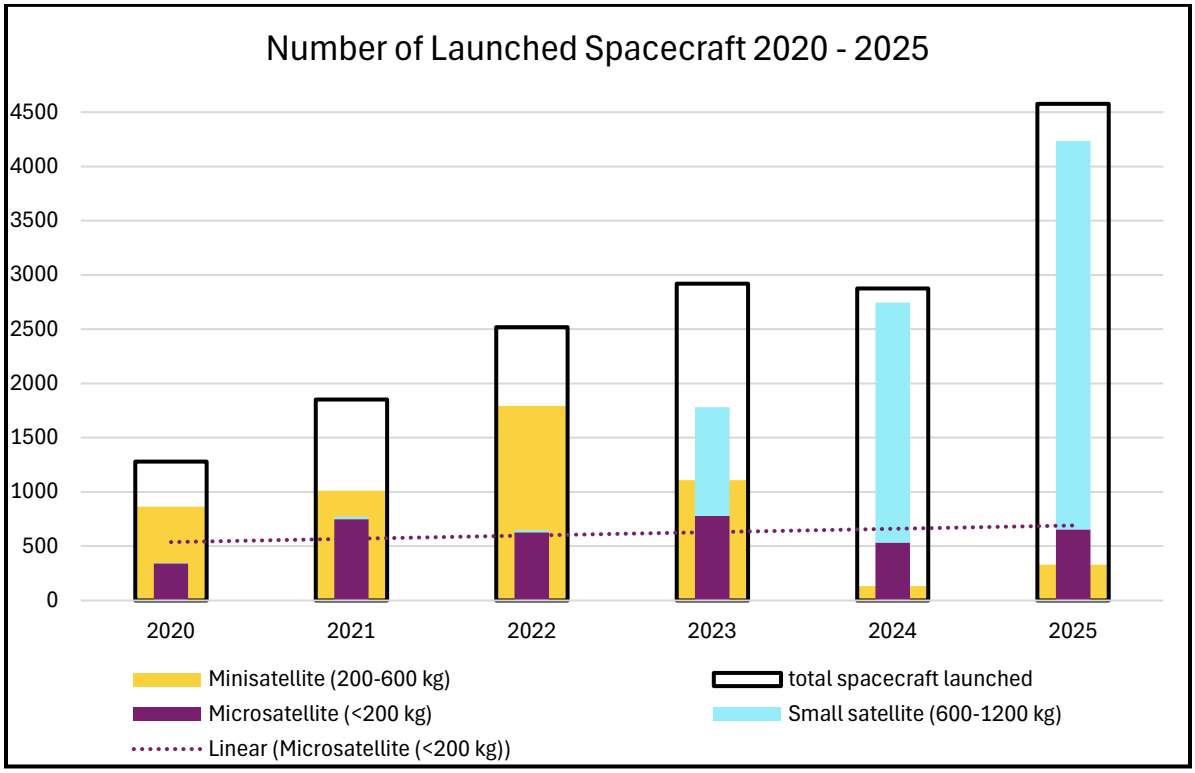


Figure 10.1: Number of spacecraft launched per year 2020-2025 in different mass categories.

The high volume of small spacecraft launches is expected to remain as SmallSat mission capabilities steadily expand. Companies are increasingly offering new or upgraded launch platforms focused on small satellites, including in-space services, rideshare programs, testing and integration, and mission support. Constellations, or multi-satellite missions, are broadening the applications of small spacecraft, while technical advances are enhancing broadband networks

and improving remote sensing applications. Today's SmallSat launch market includes dedicated vehicles for CubeSats and SmallSats, as well as rideshare programs that significantly improve access to space.

10.3.1 Dedicated Launches

Previously, small spacecraft were limited to secondary launch opportunities on large rockets, where the primary payload dictated the orbital parameters and launch readiness. Since it is not feasible for small spacecraft missions to use larger rockets due to the high per-kilogram cost, dedicated small launch vehicles (SLVs) are now an option, offering tailored access to space. SLV rides can be scheduled faster and can accommodate multiple destination requirements using an altitude control (or multi-ignition) system in the final stage. They also allow specific accommodations—such as a nitrogen purge or late battery charges— that are generally unavailable on rideshare missions (sometimes included as standard, or at additional cost). The trade-off is higher cost: dedicated launches have smaller manifests, lower launch frequency, and significantly higher price points compared to rideshare options.

Several small launchers are exploring options for satellite recovery and rocket reusability. Table 10-1 below highlights some of the current small launchers that have dedicated and tailored ride options for small spacecraft missions. Currently, Rocket Lab's Electron is the most widely used small vehicle as of April 2026. Several dedicated rocket companies across the globe have been in development for years and have either recently launched their maiden flights or are planning to do so soon.

Table 10-1: Commercial dedicated small launch vehicles

Manufacturer **Headquarters**	**Vehicle**	**Performance to LEO (kg)**	**Number of Stages**	**Propellant Type**	**Recent Flight**
Rocket Lab USA	Electron	200	2	Kerosene	February 2026
Galactic Energy China	Ceres-1	420	4	Solid, Hydrazine	January 2026
Indian Space Research Organisation (ISRO) India	SSLV	500	3	Solid	August 2024
Firefly USA	Alpha	630	2	Kerosene, LOX	TBD
Northrop Grumman USA	Minotaur-1	580	4	Solid,	June 2024
Upcoming, in development					
Astra USA	Rocket 4	750	2	RP-1/ LOX	TBD
Innospace South Korea	Hanbit-Nano HyPER	90	2	Hybrid, Paraffin	December 2025
Isar Aerospace Germany	Spectrum	1000	2	LOX/ Propane	*March 2026*
Gilmour Space Australia	Eris	215	3	Hybrid	*2026*
Space One Japan	KAIROS	150	4	Solid, Liquid	December 2024

Planned Launches

The expansion of small satellite capabilities will drive demand for dedicated launchers. Flying a spacecraft as a dedicated payload is the best method of ascent for missions that need a specific orbit, near full utilization of available launch vehicle performance, interplanetary trajectories, precisely timed rendezvous, or special environmental considerations. Technology developers and

the scientific community can take advantage of the rapid iteration cycles and low capital cost of small spacecraft to enable new advances in space capabilities and scientific understanding.

10.3.2 Rideshare Launches

Rideshare arrangements provide cost-effective access to space using proven launch vehicles with scheduled flights throughout the year. Large launchers typically have excess mass and volume margins, enabling small spacecraft to fly as secondary payloads alongside primary missions. Ridesharing opportunities have expanded significantly—with more vehicles, orbits, services, and deployment methods now available. Modern rideshare mechanisms now exist that offer a variety of options for small spacecraft missions: commercial rideshare programs, purpose-built dispenser platforms attached to larger vehicles, and government launch services.

SpaceX's Transporter rideshare program offers Falcon 9 rides starting at $350k for ~50 kg, with a high launch cadence (18). Rocket Lab has increased rideshare availability, completing 10 Electron rideshare missions in 2025 with planned launches in 2026. Other commercial rideshare options include orbital maneuvering and transfer vehicles are further discussed in Section 10.5. NASA's VADR launch services contract includes Standard Launch Services (CLIN 1) and Streamlined CubeSat Launch Services (CLIN 2), covering dedicated launches, anchor payload rideshares, and traditional rideshare options. Additionally, NASA's Science Mission Directorate Rideshare Office (SRO) coordinates rideshare opportunities across compatible payloads and government missions (19).

Future ridesharing will include lunar orbit services and high-energy orbits, as well as offering a larger variety of precise LEO orbits for multiple missions on a single launch. Ridesharing via orbital vehicles is discussed below in Section 10.5.

10.4 Launch and Integration Hardware

This section describes the hardware required to mount, protect, connect, and release a spacecraft from the launch vehicle. The method by which SmallSats are deployed into orbit is a critical part of the launch process and depends on the satellite's form factor. CubeSats benefit from their adherence to standardized deployer designs which enable integration across multiple launch configurations. Spacecraft that do not conform to a canisterized configuration require different hardware, typically bolted directly to the launch vehicle. Hardware that attaches the spacecraft, protects it during ascent, and ultimately releases it includes primary structural interfaces (non-separating), dispensers, and separation systems.

The exact configuration and standards vary by launch vehicle, and selecting an appropriate and reliable launch option is part of the launch qualification process (9). With the rise of CubeSat constellations, integration hardware capable of launching multiple SmallSats simultaneously and consecutively has become standard. This section highlights examples of integration flight hardware for both SmallSats and CubeSats, though readers are encouraged to explore additional services. Other integration hardware such as fairings, umbilicals, isolation mounts, harnesses, sequencing systems, and MGSE/EGSE are essential but beyond the scope of this report.

10.4.1 Primary Structural Interfaces

Primary structural interfaces such as adapter rings and platforms provide the mechanical connection between the spacecraft and the launch vehicle, ensuring proper load transfer and alignment. While they may host separation hardware, they are not inherently separation systems. These interfaces must meet strict requirements for bolt patterns, center-of-gravity limits, stiffness, and height to maintain structural integrity during ascent. The ESPA ring (Figure 10.2, top) exemplifies this concept as a multi-payload adapter originally developed by Moog Space and

Defense Group, featuring six 38 cm (15″) ports that can each support up to 257 kg. Similar designs are now offered by multiple providers in various configurations (21).

Many launch vehicles also incorporate Dual or Multi-Payload Attach Fittings (DPAF/MPAF) for co-manifested missions, though these are typically vehicle-specific and not covered here. ESA's Small Spacecraft Mission Service (SSMS) dispenser for Vega demonstrates the trend toward modularity, allowing flexible arrangements to accommodate diverse payloads (20). These structural interfaces are critical for rideshare missions, as they enable efficient stacking and integration of multiple spacecraft while maintaining compliance with dynamic and environmental constraints.



Figure 10.2: {top} ESPA Ring {lower} ESPA Grande Ring. Credit: Moog, Inc.

10.4.2 Dispensers for Canisterized SmallSats

The purpose of this hardware is to eject the spacecraft safely into orbit, and most services offer different features, interfaces, connections, and designs for small spacecraft specifications. The most recent CubeSat Design Specification document is found at http://www.cubesat.org, a website maintained and operated by California Polytechnic State University, San Luis Obispo, the creators of the CubeSat form factor.

The CubeSat form lends itself to container-based integration systems, or dispensers, which serve as an interface between the CubeSat and the launch vehicle. It is a rectangular box with a hinged door and spring mechanism. Once the door is commanded to open, the spring deploys the CubeSat. Many companies currently manufacture dispensers for the CubeSat form factor which follow one of two constraint systems: the rail-type dispenser, and the tab-type dispenser. Due to the large number of dispenser manufacturers, the different companies are not listed here. Instead, a brief overview of the two types of dispensers is provided.

A rail-type dispenser (Figure 10.3) supports CubeSats that have rails, which extend the length of the CubeSat on four parallel edges. The rails on the CubeSat prevent it from rotating inside the dispenser. After the dispenser door opens, the rails slide along guides inside the dispenser and the CubeSat is deployed. As such, it is important that any rail-based CubeSat follow the current development specifications to ensure compliance. This type of dispenser is the most widely manufactured configuration, with more than fifteen manufacturers worldwide. Some rail-type dispensers use a clamping mechanism to securely hold the CubeSats in place during launch.

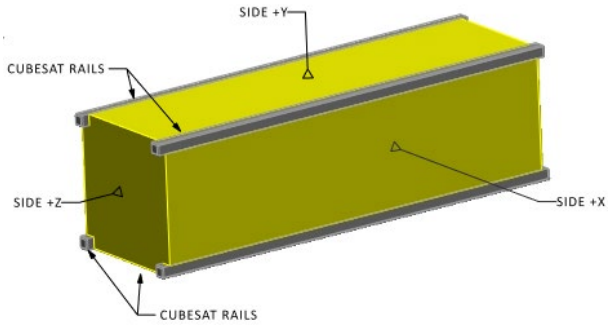


Figure 10.3: The Rail-type CubeSat. Credit: Cal Poly's CubeSat Program.

A tab-type dispenser (Figure 10.4) supports CubeSats with tabs which run the length of the CubeSat on two parallel edges. Typically, the dispenser grips the tabs to hold the CubeSat in place, only releasing it after the door has been commanded to open. More developers

are beginning to develop their own tab-based designs for CubeSat dispensers. Many are based on the original Planetary Systems Corporation standard, however some offer features such as built-in isolation to accommodate for the launch vehicle environment such as the Maverick tabbed dispenser. In addition, there are some tab-based dispensers that do not grip the tabs. Rather, they provide a slot to accommodate the tab, which slides freely within the slot. While use of tab-type dispensers is growing, they remain a minority among dispensers purchased and used by developers.

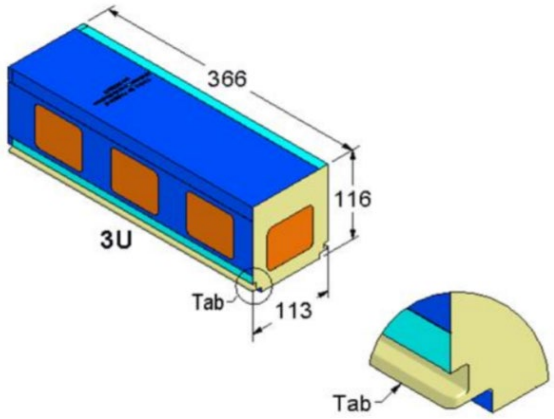


Figure 10.4: The Tab-type CubeSat. Credit: Planetary Systems Corporation.

While CubeSats generally design their spacecraft with considerations for either rail versus tab, the choice of the actual dispenser is commonly the launch vehicle provider or launch broker/integrator's. They determine which dispensers will be installed on the launch vehicle. As each dispenser manufacturer has slightly different volumes and requirements, it is beneficial to design the CubeSat for as wide a range of dispensers as possible to maximize launch opportunities. When selecting a dispenser, key considerations include size compatibility, deployment dynamics such as tip-off rates, initiator and door mechanisms, and compliance with safety and electrical inhibit requirements. Deployment profiles also differ between ISS-based and direct launch vehicle missions, and factors like reset capability and shock isolation can influence reliability and cost.

Additionally, some dispenser manufacturers have features that may violate the "do no harm" requirements set forth by the launch vehicle or launch integrator. Therefore, it is beneficial for the CubeSat to evaluate "do no harm" recommendations from a variety of organizations, as these requirements can vary from flight to flight on the same launch vehicle based on the risk posture of the primary payload and/or the mission "owner" (8).

Table 10-2 provides a non-comprehensive list of commercial dispensers that provide spacecraft physical and material requirements for integration. In response to the demand for larger CubeSats, dispensers for 12U and 16U CubeSats are now available through several launch service providers, including Voyager Space, United Launch Alliance (ULA) through the Atlas series, and a variety of European vendors.

Table 10-2: Commercial Small Spacecraft Dispensers / Deployers

Manufacturer Headquarters	Product	Volume Configurations	Type
Cal Poly USA	Dispenser	1U, 3U	Tab
COMAT France	Dispenser	3U, 6U, 12U	Rail
Dhruva Space India	DSOD	1U, 3U, 6U, 12U, 16U	Rail
Exolaunch	EXOtube, EXOpod Nova Cubesat Deployer	0.25U, 1U, 2U, 3U, 6U, 6U XL, 8U, 12U, 16U	Rail
Gran Systems Taiwan	MyPOD and Test PODs	3U, 6U, 12U, 16U	Rail
ISISPACE The Netherlands	DuoPack, QuadPack	1U, 2U, 3U, 4U, 6U, 8U, 12U, 6UXL, 12UXL, 16U	Rail
Maverick Space Systems USA	Mercury series	3U, 6U, 6T, 12U, 12T, 16U	Rail, Tab

NPC Spacemind Italy	SMPOD	1U,2U,3U,4U,6U,6U XL, 8U, 12U, 12U XL, 16U	Rail
Rocket Lab USA	Canisterized Satellite Dispenser (CSD), and Advanced Satellite Dispenser (ASD)	3U, 6U, 12U 6U, expandable to 3U–12U	Tab
Tyvak USA	Railpod III, 6U NLAS, 12U Deployer	3U, 6U, 12U	Rail
UARX Space Spain	RAMI	1U, 2U, 3U, 6U, 12U	Rail
Voyager Space USA	NanoRacks CubeSat Deployer (NRCSD)	1U, 2U, 3U, 6U	Rail
Xterra USA	CubeSat Dispenser (XCD)	1U, 2U, 3U or 6UXL	Rail

10.4.3 Separation Systems

Small satellite missions that do not meet the CubeSat form factor or use a CubeSat dispenser for integration into the launch vehicle require a different separation mechanism. Separation devices for SmallSats generally follow either a circular pattern or a multi-point (three or four- point) pattern bolted to the launch vehicle. Depending on the launch vehicle or integrator, separation systems may already be in place and available to secondary spacecraft. It should be noted that separation systems are often among the most complex hardware involved in spacecraft launch operations. Prior to launch vehicle selection, NASA LSP recommends that the spacecraft team explicitly define the requirements for their separation system and properly evaluate the launch provider feedback to ensure compatibility.

If a spacecraft is given the option to bring its own separation system to launch, great care should be taken in its selection, including the development maturity and flight heritage of any separation system. Engineers must ensure the system is properly sized for the spacecraft's flange and load requirements, meets stiffness and strength criteria, and uses a low-shock release method to protect sensitive instruments. Additional considerations include tip-off rates, redundancy in initiators, electrical inhibit compliance, and integration compatibility with the launch vehicle. These factors are critical for mission success and should be addressed early in the design process.

Circular separation systems use two rings held together by a clamping mechanism and are more commonly used in ESPA-class and larger microsatellite missions. One ring is attached to the launch vehicle, and the other ring is attached to the spacecraft. Once the clamping mechanism is released, the two rings separate and are pushed apart by springs. Clamp bands are separation systems that hold a spacecraft tightly to the launch vehicle and transmit launch loads—the mechanical forces the spacecraft experiences during ascent (vibration, shock, axial loads, lateral loads). General rules of thumb: clamp bands are sized to ensure they can safely carry these launch loads without slipping, damaging the spacecraft interface, or overstressing the structure. They remain locked during ascent and then release via a tensioned band mechanism or frangible device once the spacecraft reaches orbit.

Marman band separation systems use energy stored in a clamp band, often along with springs, to achieve separation. The Marman band is tensioned to hold the spacecraft in place. Some Marman bands use pyrotechnic devices to cut the clamping bolt; however, many companies offer a low-shock release mechanism which is potentially better for spacecraft sensitive to shock.

Modern multi-point systems are made with low-shock mechanisms to minimize structural damage to sensitive electronics or optical hardware on the spacecraft, and are popular for small/mid-size spacecraft due to lower shock and modularity. Several companies are now providing multi-point separation systems instead of circular band systems. Using a multi-point separation system may

result in mass savings over a circular separation system. However, some systems require additional simultaneous signals from the launch vehicle provider to ensure proper release, such as the PSM 3/8B low-shock separation nut developed by Beyond Gravity to fit OneWeb satellites. ISISPACE has the M3S Micro Satellite Separation System (see Figure 10.5), which is designed for satellites up to 100 kg, but can be configured for higher masses.

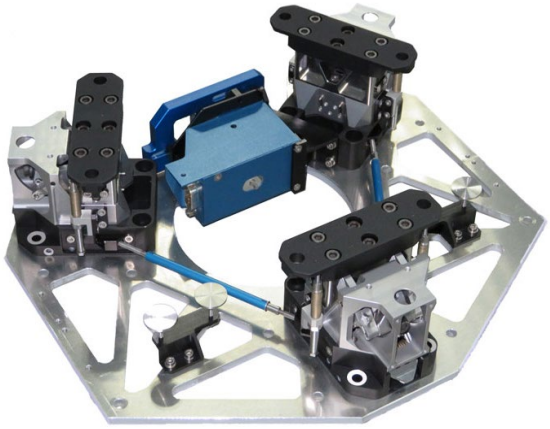


Figure 10.5: ISISPACE M3S Micro Satellite System. Credit: ISISPACE.

The separation system directly influences—or impacts—the spacecraft loads on the launch vehicle. Given the stiffness and fundamental frequency requirements of traditional rideshare missions, many companies are favoring 4-point separation systems for MicroSats and SmallSats as a viable alternative to traditional MLB or clamp band systems. These systems function in a similar way to the systems above and are typically rated for microsatellites (≤100 kg); however, offer less complexity than a traditional MLB or clamp band system. For example, EBAD's Payload Release Module has a 4-point spacecraft dispensing application and can accommodate lateral or axial separation.

The rapid acceptance of this launch solution is driven by the fundamental frequency requirements of traditional rideshare launches, with the goal that reduced stiffness at the interface will increase the compatibility of SmallSats and MicroSats for those types of launches. In addition to reduced complexity, many of these also result in cost savings, which can be passed on to both the integrator and the SmallSat manufacturer. Many integrators are exploring the addition of such systems into their portfolios to accommodate launches in the near future.

Cake Topper and Plate System for Rideshares

SpaceX has developed a system that differs from the SPA system for rideshare missions to SSO (Transporter Missions) and mid-inclination orbits (Bandwagon Missions). This system of plates rather than a ring is intended to allow more payloads to be included in the circumferential space for flight on their commercial rideshare missions. In addition, for larger spacecraft or spacecraft that cannot be horizontally mounted during flight, they also offer a cake topper option. Figure 10.6 shows these two options. The blue box shows the plate option, which has a specific set of rideshare loads for the mission's part of Transporter or Bandwagon missions. The green box denotes the cake topper option, which also has separate environments. User guides for both configurations are available on the launch provider's website. For missions that will fly under the VADR contract, please contact NASA's Launch Services Program (LSP) for additional guidance and applicable environmental constraints.

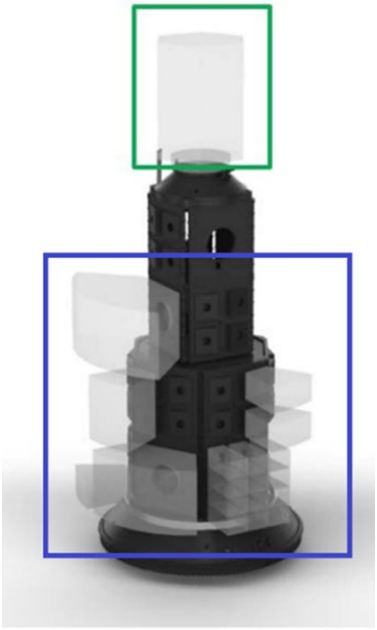


Figure 10.6: SpaceX cake topper (green) and Plate System (blue) configurations. Credit: SpaceX.

Table 10-3: SmallSat Separation Devices				
Manufacturer **Headquarters**	**Product**	**Max Payload capacity (kg)**	**Type**	**Key features / Compatibility**
Beyond Gravity Switzerland	PAS 381S, PSR 1575 mm (62”), PSM 3/8B	200	Clamp band Multi-point	Vega rocket Moog ESPA
Ensign Bickford Aerospace & Defense (EBAD) USA	Payload Release Ring (PRR)-8	70	Hold-Down & Release	Configurable, based on the SpaceX electrical interface
	PRR-15 Release Ring	250	Hold-Down & Release	
	Payload Release Module	1000	Hold-Down & Release	Compatible with SpaceX Transporter 9 and Transporter 12 Rideshare missions
Exolaunch Germany	CarboNIX series	500	Clamp band	Any launch vehicle
	Quadro Arrow	250	Spring Pusher System	Supports SpaceX Transporter rides
	Quadro Versa	1000	Multi-Point	Compatible with SpaceX rideshare interfaces
ISISPACE The Netherlands	M3S Micro Satellite Separation System	120	Hold-Down & Release	Configurable and compatible
Rocket Lab USA	Mark II Motorized Lightband	1000	Clamp band	Configurable and compatible
	Advanced Lightband (ALB)	1000	Clamp band	Configurable and compatible
SAB Aerospace Italy	Vampire	1500	Clamp Band	Vega and Vega-C
Sierra Space	QwkSep LPSS	300	Clamp Band	Moog ESPA grande
UARX Space Spain	SAU&RON-8	80	Clamp Band	ESPA compatible
	SAU&RON-15	350	Clamp Band	
	SAU&RON-24	800	Clamp Band	

10.5 Orbital Transfer / Maneuvering Vehicles (OTV/OMV)

One of the main disadvantages of riding as a rideshare is the inability to launch into the desired orbit. For rideshares with a primary spacecraft, the primary mission determines the orbital destination, so the secondary spacecraft orbit usually does not perfectly match the needs of the secondary payload. However, by using an OTV or OMV, secondary spacecraft can maneuver much closer to their desired orbits. OTVs are generally more coarsely propulsion capable, while OMVs may offer hosted systems more in terms of power, pointing, and communications. The OTV/OMV market is nascent, with many planned systems but few with existing flight heritage. This emerging technology is an area of interest in the near term for both SmallSats and CubeSats, as it offers a significant capability to reach destinations not previously achievable with systems of this scale. The ability for small spacecraft to reach new orbits could enable a much wider range of mission designs for destinations both near and far.

The distinction between OTV/OMVs and hosted payload providers is not always clear, with many OTV/OMVs offering both the deployment of free-flying spacecraft at secondary orbits from the vehicle and the hosting of instruments or technologies that stay attached to the vehicle. Similar

OTV/OMV systems can be used to service other spacecraft, including deorbiting or relocation to a graveyard orbit. For information regarding those capabilities, refer to Chapter 13 *Deorbit Systems*.

Commercial delivery and deployment system launches have increased in frequency since the early 2020s. The vehicles that flew successfully in 2025 all had their pathfinders launched in 2023. Figure 10.7 is a launch timeline of OTV/OMVs with commercial payload services as part of the vehicle's documented purpose. This cadence is expected to continue upward as more vehicles become space-qualified and as new companies emerge. The data is derived from publicly accessible data and only includes launches by the providers described in this report. There may be more launches than indicated herein, and the success of the launch/mission is not accounted for.

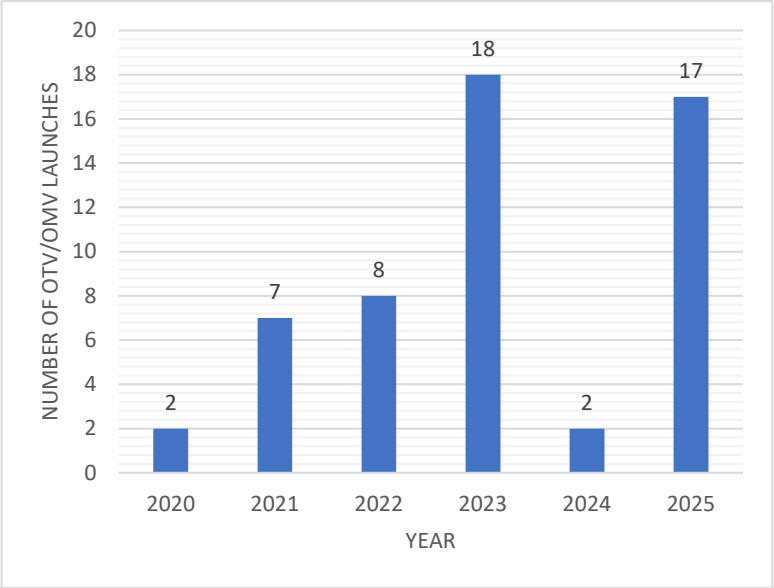


Figure 10.7: Number of OTV/OMV launches between 2020-2025. Credit: NASA

10.5.1 Commercial Development/Services

As discussed above, the ESPA ring provides a structure to which SmallSats or CubeSat dispensers are mounted. The idea of adding propulsion to an ESPA ring led to many of the early commercial OMV/OTV vehicle designs. Systems that were originally derived from the ESPA ring include the retired SHERPA vehicle by Firefly (previously Spaceflight Inc.) (28), the Northrop Grumman Space Systems (previous Orbital Sciences Corporation) ESPAStar Product Line, and the Moog METEOR. The ESPAStar product line has gone through multiple programs with multiple names. The ESPAStar line has significant flight heritage from the Long Duration Propulsive ESPA (LDPE) satellites, now known as the Rapid On-Orbit Space Technology Evaluation Ring (ROOSTER) program of the United States Space Force (USSF). While the SHERPA system is no longer commercially available, Firefly is now offering rides on its Elytra OTV/OMV product line, which appears to build upon the ESPA ring heritage for specific compatibility with Firefly's small- and medium-lift launch vehicles. Rocket Lab is another launch provider offering an OMV/OTV platform. The Photon system is an evolution of the Electron launch vehicle Kick Stage.

Other systems are being developed from the ground up by commercial entities to provide orbital transport, hosting, and deployment services. For example, Northrop Grumman, in addition to its ESPAStar series, has a proven Mission Extension Vehicle (MEV) that can host payloads, but is primarily developed to dock and extend the life of large GEO satellites. To date, the MEV has successfully extended the life of two Intelsat systems.

The current state-of-the-art OTV vehicle offerings tend to advertise thousands of km/s of delta-V, which enable the following services:

- Altitude change / planetary transfer – changing the altitude from where the vehicle was deployed by the launch vehicle. This could be an altitude raise or lowering operation, depending on the needs of the integrated payloads. In some cases, if escape velocity is

reached, this maneuver can be used to transfer to lunar orbits or beyond. A payload delivery and deployment vehicle could perform multiple altitude raises and lowers during a single mission.

- Inclination change – changing the angle of the orbit with respect to the angle at which the vehicle was initially deployed by the launch vehicle. This can be done during the same burn as an altitude change to increase efficiency, or as a standalone operation. This operation dramatically changes what is viewable on the ground swath of the orbiting spacecraft. It can also dramatically change the solar incidence of the orbit.
- Phasing – this refers to changing the position of a spacecraft within a given orbit. Assuming the same orbit of two spacecraft, the phasing of each of them would dictate at what time each of them is over a specific ground swath. This is typically achieved with a “slow-down” burn to achieve a smaller orbital period, and then a “recircularization” burn to return the spacecraft to its original orbit.
- Constellation deployment – this is the ability for a single payload delivery vehicle to drop multiple spacecraft into a constellation formation. This dramatically reduces the propulsive need of the individual small spacecraft and can enable constellations of small spacecraft to achieve much more than they could if they needed propulsion to deploy and phase themselves.

Many OTVs and OMVs are designed with a large excess propellant volume so that after the initial contracted services, the hosting vehicle can remain in orbit and be contracted for additional future services such as deorbiting via “pushing” another spacecraft or contracted inspection services. Some providers are developing systems specifically for these in-space services, including Astroscale, Starfish Space, and Turion Space. Technology gaps in the development of all these highly capable space vehicles include RF licensing challenges, ACDS component availability, reliable propulsion systems, and lack of standardization for payload interfacing.

The following sections contain an overview of commercial OTV/OMV vehicles and their development status, and Table 10-4 provides corresponding vehicle parameters.

Elytra

The Elytra vehicle line is a series of orbital vehicles offered by Firefly Aerospace. The smallest vehicle is the Elytra Dawn, optimized for intra-LEO mobility. The largest vehicle is the Elytra Dark, which offers payload transportation to lunar orbit and beyond. The Elytra line builds on Firefly’s previous Space Utility Vehicle design and experience, as well as the Spaceflight SHERPA (Firefly acquired Spaceflight in 2023). The first Elytra Mission 1 is planned to fly on Blue Origin’s New Glenn rocket no earlier than 2026 to demonstrate rapid payload reconfiguration prior to launch, Firefly in-house technologies, as well as two on-orbit deployments. For more information, visit https://fireflyspace.com.

Chimera

Epic Aerospace has a line of Chimera systems ranging from smaller LEO vehicles up to larger GEO-targeting vehicles. The LEO vehicles are intended to enable altitude changes from 450 km from the deployment location to larger, rapid and phasing maneuvers (3 hours of Local Time at Ascending Node (LTAN) change in less than 90 days is advertised). The GEO systems advertise capabilities beyond Earth, with trans-lunar injection from GTO/LEO as an option. The first LEO Chimera system was launched in January of 2023 and is currently operational, and the most recent launch was the Chimera GEO 1 in February 2025 as a rideshare payload. For more information, visit https://epic-aerospace-web.netlify.app.

ION

The ION Satellite Carrier system by D-Orbit provides distinct LEO environments to customers and even offers in-orbit testing to third-party payloads. Missions with the same orbital plane can be released into their specific ‘slots’ without phasing maneuvers. Additionally, this system provides on-orbit advanced storage and computational capabilities.

The ION Carrier was first used in 2020 to deploy Planet Labs’ constellation satellites and has been used 21 times as of December 2025 to deploy small satellites. The most recent flight occurred in November 2025, when two ION Carriers delivered eight missions to sun-synchronous orbit at an altitude of approximately 510 km. D-Orbit supported Europe’s first Capture-the-Flag (CTF) cybersecurity competition that also occurred in November 2025, where seven ION vehicles provided telemetry for the realistic mission scenarios to identify and exploit vulnerabilities in space systems. For more information, visit https://www.dorbit.space.

Photon

The Kick-Stage-derived Photon system is a flight-proven vehicle that deploys payloads to target orbits not otherwise achievable by the Electron launch vehicle. In addition, the system can be mounted on an ESPA port of other launch vehicles as a secondary payload. Rocket Lab advertises other vehicles alongside Photon that can be used for hosted payload services and orbital insertion services: the Explorer, Lightning, and Pioneer.

The Photon system has flown seven times as of March 2026; most recently in November 2025 with the ESCAPADE mission, which involved two spacecraft on modified versions of the Photon traveling to Mars to characterize the Martian atmosphere. For more information, visit www.rocketlabusa.com/.

Quark

The Quark vehicles by Atomos (now part Katalyst Space Technologies) aim to offer many in-space services to small spacecraft such as deployment and orbit changes (raising, phasing, and inclination), rendezvous, docking, and satellite life extension. The first version, Quark-LITE, launched in spring 2024, and despite communication and tumbling issues, it successfully showcased rendezvous, docking, and refueling capabilities—laying the groundwork for more advanced GEO missions (29). Upcoming Atomos GEO-1 and -2 missions were planned to implement the Quark-Alpha with payload delivery to GEO by 2026, though the status is unknown.

Vigoride

The Momentus Space Vigoride orbital service vehicle has flown three times with a maximum payload capacity of 750 kg to LEO, and can be launched from an ESPA Grande ring, SpaceX XL rideshare plate, or a dedicated launch vehicle. Propelled by a microwave electrothermal thruster, it enabled orbital maneuvers and payload deliveries. The first flight in May 2022 experienced a solar-array deployment anomaly, while two subsequent flights in 2023 were successful. Additional units like Vigoride-7 are slated for missions beginning in 2026. For more information, visit https://momentus.space/.

OSSIE

UARX Space developed the Orbit Solutions to Simplify Injection and Exploration (OSSIE) orbital transfer and hosted payload vehicle. This spacecraft is designed to be modular and scalable to satisfy customer requirements by using either electric or chemical propulsion. The vehicle is designed to transport payloads of up to 400 kg and incorporates green propellant thrusters for orbital maneuvering. UARX Space leads the system architecture, mission design, and operational concept, with selected European partners contributing to specific subsystems, including

guidance, navigation, and control. The first OSSIE qualification mission, planned for launch in 2026, will demonstrate multi-customer operations, supporting 12 payloads ranging from PocketQubes and CubeSats to hosted payloads (31). For more information, visit https://www.uarx.com/.

Mira

The Mira Orbital Transfer Vehicle by Impulse Space provides several specific services such as orbital transport, constellation deployment, payload hosting, deorbiting maneuvers, and others. Mira's first launch was in November 2023 (LEO Express 1) and has since then met all mission objectives over the course of nine months. LEO-Express-2 mission (also dubbed Remora) launched in January 2025 and involved Starfish Space's autonomous satellite guidance software that enabled the Mira vehicle to perform close-proximity maneuvers with another Mira vehicle (32). While the Mira vehicle was designed for payload hosting, deployment, and orbital adjustments, the Helios vehicle is a high-powered kick stage advertised to provide transportation services out to Cislunar environments. Helios uses a combination of liquid oxygen and liquid methane to transport more than 4,000 kg of payload from LEO to GEO in less than 24 hours. The first flight is planned for some time in 2026 (33). For more information, visit https://www.impulsespace.com.

Optimus

Space Machines Company developed the Optimus vehicle to carry hosted payloads and perform close inspections of Client Space Objects (CSOs) in LEO. Optimus first operated in 2024 with 8 hosted payloads from international customers and was powered by a bi-propellant chemical propulsion system (34). Optimus is getting 'upgraded' with a "Block-2" platform for more agility and maneuverability for carrying sensitive sensors for detailed inspection images to be taken of satellites from 10 km. Optimus Viper is planned for the next launches in 2026 and 2027 to LEO mid-inclination and SSO orbits. For more information, visit https://www.spacemachines.com.

Blue Origin

The Blue Ring space mobility vehicle by Blue Origin is advertised to provide in-space computing capability, hosting services, and delivery services for more than 3,000 kg of commercial and government payloads. Blue Ring aims to support missions in medium Earth orbit out to the cislunar region as a host spacecraft platform. It uses a combination of chemical and solar electric propulsion with rollout solar arrays. The maiden flight of Blue Origin's rocket New Glenn, DarkSky-1, launched in January 2025 with the Blue Ring pathfinder though a booster was lost during landing. In November 2025, New Glenn launched successfully a second time, including the reusable first stage, and will test Blue Ring's mission operation capabilities and core flight systems in space for the first time (36). Additionally, this launch carried and deployed NASA's Escape and Plasma Acceleration and Dynamics Explorers (ESCAPADE) mission of twin-minisatellites that will study Mars's space weather.

Laelaps

The Laelaps spacecraft by Kall Morris Inc. is designed for various on-orbit servicing capabilities that is built around a 15-inch ESPA-class satellite bus and equipped with a multi-armed, articulated robotic device called REACCH. By launching as a rideshare option on commercially available launch vehicles, Laelaps can relocate multiple objects in space with its onboard electric propulsion and REACCH. REACCH does not require any docking adaptor for a safe capture and release on-orbit and will maneuver functioning assets throughout LEO without affecting operability. For more information, visit https://www.kmi.space/laelaps.

Table 10-4: Commercial Orbital Transfer / Maneuvering Vehicles					
Company Headquarters	**Vehicle**	**Heritage**	**Operational Altitudes**	**Maximum Payload Capacity (kg)**	**Delta-V (m/s, max payload)**
Atomos Space USA	Quark	Flown	LEO	400	-
Blue Origin USA	Blue Ring	Upcoming	-	-	-
D-Orbit Italy	ION	Flown Successfully	-	-	-
Epic Aerospace Argentina	Chimera LEO Block 0	Flown Successfully	+/- 450 km from LEO deployment	300	200
	Chimera LEO Block 1	Upcoming	+/- 450 km from LEO deployment	300	950
	Chimera GEO Block 0	Upcoming	GTO to TLI	300	1800
	Chimera GEO Block 0 / Bus	Upcoming	GTO to TLI	290	1800
Exolaunch Germany	Reliant Standard	Upcoming	+/- 275 km from LEO(?) deployment	200	-
	Reliant Pro	Upcoming	+/- 275 km from LEO(?) deployment	260	-
Exotrail France	Spacevan LEO	Flown Successfully	LEO (~400-2000 km)	~200	~500
	Spacevan GEO	Upcoming	Above LEO (e.g., MEO, GEO, Cislunar >2000 km)	~150	~2200
Firefly USA	Elytra Dawn	Upcoming	LEO	-	-
	Elytra Dusk	Upcoming	LEO to GEO	-	-
	Elytra Dark	Upcoming	LEO to Lunar/Planetary	-	-
Gilmour Space Technologies Australia	ElaraSat bus	Flown Successfully	LEO	30	-
Impulse Space USA	Mira	Flown Successfully	LEO	300	500
	Helios	Upcoming	GEO	-	-
Intuitive Machines USA	Nebula	Flown	MEO, GEO, Lagrange Points, NRHO, LLO	-	-
Kall Morris Inc. USA	Laelaps	Upcoming	LEO	-	-
Moog USA	SL-OMV	Upcoming	400 - 700 km	6 x 12 (+ additional, if containerized)	< 200

Table 10-4: Commercial Orbital Transfer / Maneuvering Vehicles					
Company Headquarters	**Vehicle**	**Heritage**	**Operational Altitudes**	**Maximum Payload Capacity (kg)**	**Delta-V (m/s, max payload)**
	METEORITE	Upcoming	500 – 1200 km	100 (or more, with caveats)	>175
	METEOR	Upcoming	500 – 1200 km	750	>400
Momentus USA	Vigoride	Flown Successfully	250 - 2000 km (GEO and LLO also available)	800	< 2000
Rocket Lab USA	Photon	Flown Successfully	LEO, MEO, GEO, and beyond	-	-
Space Machines Company Australia	Optimus Viper	Flown	300 – 700 km	50	500
TransAstra USA	WorkerBee (multiple configurations)	Upcoming	LEO, MEO, GEO, HEO, Lunar/Planetary	200 – 2000	-
UARX Space Spain	OSSIE	Upcoming	350 – 1000 km	400	690
Quantum Space USA	RANGER	Upcoming	LEO, MEO, GEO, cislunar	6000	Up to 10 km/s

Information not disclosed or unknown is represented as -

10.6 International Space Station Options

The International Space Station (ISS) provides several methods for deploying CubeSats and SmallSats. The sections below discuss SmallSat deployment from the ISS as well as deployment above the ISS. The ISS also accommodates hosted payload instruments and experiments, but those accommodations are outside the scope of this chapter, as they are for individual instruments and experiments themselves and are not satellites.

10.6.1 Deployment from ISS

The ISS provides several options for deploying satellites. Generally, satellites are launched below the ISS to avoid potential contact with the ISS. Below are several options for launching from the ISS.

Nanoracks CubeSat Deployer (NRCSD)

Nanoracks CubeSat Deployer (NRCSD) (Figure 10.8) is a self-contained CubeSat dispenser system that mechanically and electrically isolates CubeSats from the ISS, cargo resupply vehicles, and ISS crew. The NRCSD is a rectangular tube that consists of anodized aluminum plates, base plate assembly, access panels, and deployer doors. The inside walls of the NRCSD are a smooth-bore design to minimize and/or preclude hang-up or jamming of CubeSat appendages during deployment, should they become released prematurely.

For deployment, the platform is moved outside via the Kibo Module's Airlock and slide table, which allows the Japanese Experimental Module Remote Manipulator System (JEMRMS) to move the dispensers to the correct orientation and provide command and control to the dispensers. Each NRCSD can hold six CubeSat units as large as a 6U (1 x 6U). The NRCSD DoubleWide can accommodate CubeSats up to 12U (2 x 6U) with Nanoracks being able to launch up to 48U per cycle. The CubeSats deploy at a 51.6° inclination, into a 400 – 420 km orbit 1 to 3 months after berthing at the station.



Figure 10.8: Nanoracks CubeSat Deployer. Credit: Nanoracks.

Nanoracks ISS MicroSatellite Deployment – Kaber Deployer Program

Nanoracks Kaber Microsat Deployer is a reusable system that provides command and control for satellite deployments into orbit from the Japanese Experimental Module Airlock Slide Table of the ISS. The Kaber supports satellites with a form factor of up to 24U and a mass of 82 kg and uses a Nanoracks separation system with a circular interface similar to the separation systems discussed above. Satellites are launched to the ISS on a pressurized launch vehicle, mounted to the Kaber deployer, and deployed outside the ISS (43).

JEM Small Satellite Orbital Deployer (J-SSOD)

The Japanese Experimental Module (JEM) Small Satellite Orbital Deployer (J-SSOD) is a Japanese Aerospace Exploration Agency (JAXA) developed CubeSat deployer used to launch CubeSats from the ISS. The J-SSOD can launch CubeSats up to the 6U form factor (2x3

configuration). The satellites, with their dispensers, are installed on the Multi-Purpose Experiment Platform prior to the Kibo's robotic arm Japanese Experiment Module Remote Manipulator System (JEMRMS) transferring the Multi-Purpose Experiment Platform (MPEP) to the release location. At that point, the CubeSats are deployed (44).

Bishop Nanoracks Airlock Module

A new airlock module, Bishop, was developed for the ISS by Nanoracks, Thales Alenia Space, and Boeing, and is the first commercial, privately developed module for the space station **Error! Reference source not found.**. Bishop provides more than five times the volume of the current Japanese Experimental Module (JEM) airlock, allowing for larger satellites and payload experiments. Bishop can host satellites and payloads, as well as deploy them, based on the needs of the mission. It has been attached to the exterior of the ISS since December 21, 2020, and has been instrumental in deploying CubeSats from the ISS (46).

10.6.2 Deployment Above ISS

Regular access to the ISS is very attractive for many satellite providers. However, the lower altitude of the ISS means the in-orbit lifetime for satellites is generally shorter. This section discusses the options that have been developed to deploy CubeSats above the ISS using a cargo resupply module.

Nanoracks Interchangeable CubeSat Launcher (previously E-NRCSD)

The Nanoracks Interchangeable CubeSat Launcher (NICL) is a system to deploy CubeSats into orbit above the ISS by using the Northrop Grumman Cygnus ISS Cargo Resupply vehicle. The first mission to use the ENRCSD was on the OA-6 mission in March 2016; the updated E-NRSD design (NICL) was scheduled to have its first flight in March 2023; however, the geopolitical situation between Ukraine and Russia has impacted the concept of operations that would have enabled this demonstration. Specifically, the ISS program currently will not allow the Cygnus mission to boost above the station to deploy CubeSats, so the NICL will be delayed until that changes.

In the past, up to 36U of CubeSats in any form factor up to 16U could be deployed above the ISS with each Cygnus mission. CubeSats are installed in the Nanoracks deployer and mounted externally to the Cygnus vehicle before launch. They remain external to the ISS for the duration of time that Cygnus is attached to the station, so the associated space environment should be taken into consideration when designing spacecraft (e.g., survival of spacecraft components in extreme temperatures, and unexpected behaviors or annealing of materials that undergo long durations of thermal cycling). The deployment altitude is dependent upon the propellant margins remaining in the Cygnus, but is typically 465-500 km, meeting a minimum of 45 km above the ISS altitude (47). It is hoped that this capability will return soon, allowing additional deployment options for CubeSats from the ISS.

SEOPS SlingShot

SEOPS SlingShot is a system to deploy CubeSats into orbit above the ISS using the Northrop Grumman Cygnus ISS Cargo Resupply Vehicle. The first mission to use the SlingShot was in 2019. SlingShot can fly up to 72U of CubeSats per Cygnus mission; the largest CubeSat form factor it can fly is 12U. This deployment method differs from the ENRCSD in that the satellites and their dispensers are flown to the ISS as pressurized cargo on a resupply mission. Astronauts remove the satellites and install the dispensers onto the Cygnus Passive Common Berthing Mechanism (PCBM) just prior to Cygnuss' departure from the station. Once Cygnus departs the ISS, it raises to an altitude of approximately 500 km and deploys the CubeSats (48). As these CubeSats are hosted in a different location and manner than the ENRCSD CubeSats, it is possible

for Cygnus to carry CubeSats in both locations on a single mission. Due to the geopolitical situation in Europe, this capability is also on hold with the hope that it will return in the future.

10.7 Summary

The spacecraft launch market has adjusted to the increasing accessibility of spaceflight. Advances in technology and reduced launch costs have laid the foundation for this booming industry. Spacecraft constellations, typically ranging from a few kilograms to over 300 kg in mass, are driving much of this demand. Starlink's mega-constellation of 800 kg platforms represents more than half of all spacecraft launched in 2025. This trend is expected to accelerate in 2026, with significant expansion in both platform size and constellation scale.

To support this growing demand, a wide variety of launch mechanisms now make space more accessible for smaller missions. NASA's VADR launch services contract offers dedicated launches, anchor payload rideshares, and traditional rideshare options. Commercial providers like Rocket Lab and SpaceX deliver low-cost access to space, while expanded ridesharing opportunities now include more vehicles, orbits, services, and capabilities. The rise of commercial OMV/OTV services has enhanced the value of smaller missions by enabling longer mission lifetimes, greater capabilities, and orbital maneuvering for smaller spacecraft. The number of available commercial OMV/OTVs continues to grow, with new pathfinder designs launching this year.

In parallel, government and commercial sectors are investing in research and development for in-space services, including hosted payload rideshares and deorbit/reentry services. This surge in LEO spacecraft has amplified the importance of space situational awareness to ensure effective tracking, collision avoidance, and debris removal. Constellations continue to dominate the launch demand, driven by broadband communication networks and high-resolution imaging enabled by advancements in miniaturized technology. Furthermore, autonomous swarms of microsatellites are showcasing modern hardware and software capabilities, opening new frontiers for future multi-spacecraft missions (49).

For feedback solicitation, please email: arc-sst-soa@mail.nasa.gov. Please include a valid business email.

References

(1) National Aeronautics and Space Administration. "13 Companies to Provide Venture Class Launch Services for NASA," Jan 26, 2022. [Online] Available at: https://www.nasa.gov/press-release/13-companies-to-provide-venture-class-launch-services-for-nasa

(2) AIAA. AIAA R-099-2001. Recommended Practice Space Launch Integration. American Institute of Aeronautics and Astronautics, Reston, VA, 2001.

(3) D. Hill. "NASA Announces 12th Round of Candidates for CubeSat Space Missions," April 7, 2021. [Online] Available at: https://www.nasa.gov/feature/nasa-announces-12th-round-of-candidates-for-cubesat-space-missions

(4) National Aeronautics and Space Administration. "What is the University SmallSat Technology Partnership Initiative?" [Online] Accessed: March 14, 2026. Available at: https://www.nasa.gov/smallspacecraft/university-smallsat-technology-partnership-initiative/

(5) E.M. Sims and B.M. Braun, "Navigating the Policy Compliance Roadmap for Small Satellites." s.l.: The Aerospace Corporation, November 2017.

(6) Department of Defense. DoD Instruction 3100.11: Management of Laser Illumination of Objects in Space. 2016.

(7) California Polytechnic State University, San Luis Obispo (Cal Poly) CubeSat Systems Engineer Lab. CubeSat 101 Basic Concepts and Processes for First-Time CubeSat Developers. s.l.: NASA CubeSat Launch Initiative, October 2017.
(8) National Aeronautics and Space Administration, Launch Vehicle Secondary Payload Adapter Rideshare Users Guide with Do No Harm (SMD SPA RUG with DNH) Rev3, 2023.
(9) E.S. Nightingale, L.M. Pratt, and A. Balakrishnan. "The CubeSat Ecosystem: Examining the Launch Niche (Paper and Presentation)." IDA Science and Technology Policy Institute. December 2015
(10) National Aeronautics and Space Administration, "CSDA Vendor – Spire," [Online] September 12, 2025. Accessed: March 14, 2026. Available at: https://science.nasa.gov/earth-science/csda/vendor-spire/
(11) HawkEye 360. "HawkEye 360 Successfully Launches Cluster 13 and Establishes Initial Communications," Press Release [Online] January 12, 2026. Accessed: March 14, 2026. Available at: https://www.he360.com/hawkeye-360-successfully-launches-cluster-13-and-establishes-initial-communications/
(12) C.B Burkhard and S.V. Weston, "Small Spacecraft Technologies: The Evolution of CubeSat Spacecraft Platforms," NATO Science and Technology Organization Specialist meeting. October 11-14, 2021.
(13) National Aeronautics and Space Administration, "Pathfinder Technology Demonstrator," [Online] Accessed: March 14, 2026. Available at: https://www.nasa.gov/smallspacecraft/pathfinder-technology-demonstrator/
(14) National Aeronautics and Space Administration. "CAPSTONE," [Online] Accessed: March 14, 2026. Available at: https://www.nasa.gov/mission/capstone/
(15) R. Hills, A. Alexander, et al. "Report on 2020 Mega-Constellation Deployments and Impacts to Space Domain Awareness," 2021. Advanced Maui Optical and Space Surveillance Technologies Conference (AMOS) – www.amostech.com.
(16) Federal Aviation Administration. "Additional Information," [Online] Accessed: March 14, 2026. Available at: https://www.faa.gov/space/additional_information
(17) E.B. Vucer. "China's three-body solution: The world's first supercomputer in space," May 22, 2025. [Online] Accessed: March 14, 2026. Available at: https://www.trtworld.com/article/c7feb363ff4e
(18) [Online] Accessed: March 14, 2026. Available at: https://www.spacex.com/rideshare
(19) A. Mendoza-Hill et al. "Rideshare on NASA Missions: Realities and Triumphs," Small Satellite Conference presentation, Salt Lake City, UT, 2025.
(20) European Space Agency. SSMS modular parts. [Online] Available at: https://www.esa.int/ESA_Multimedia/Images/2019/06/SSMS_modular_parts#.XuOX3YQCe7o.link
(21) Moog. "ESPA Overview." [Online] Available at: https://www.csaengineering.com/products-services/espa.html
(22) Puteaux, M and Najjar, A. "Analysis | Are smallsats entering the maturity stage?" August 6, 2019. [Online] Available at: https://spacenews.com/analysis-are-smallsats-entering-the-maturity-stage/
(23) D. Hill. "NASA Announces 12th Round of Candidates for CubeSat Space Missions," April 7, 2021. [Online] Available at: https://www.nasa.gov/feature/nasa-announces-12th-round-of-candidates-for-cubesat-space-missions
(24) European Space Agency. "New CubeSat Missions Selected for the Third Cycle of Fly Your Satellite," February 3, 2020. [Online] Available at: https://www.esa.int/Education/CubeSats_-_Fly_Your_Satellite/New_CubeSat_missions_selected_for_the_third_cycle_of_Fly_Your_Satellite

(25) Erwin, S. “Air Force CubeSat successful deployed from Atlas 5 upper stage,” August 8, 2019. [Online] Available at: https://spacenews.com/air-force-cubesat-successfully-deployed-from-atlas-5-upper-stage/
(26) The CubeSat Program, Cal Poly SLO. CubeSat Design Specification (CDS) Rev 14. San Luis Obispo, California, July 14, 2020.
(27) E. Marchand, “D-Orbit launches dual orbital transportation missions, passes 200-payload milestone,” December 8, 2025, [Online] Available at:https://www.copernical.com/news-public/item/55291-2025-12-08-05-55-11
(28) Andrews, J. “Spaceflight Secondary Payload System (SSPS) and SHERPA Tug - A New Business Model for Secondary and Hosted Payloads.” 26th Annual AIAA/USU Conference for Small Satellites (2012).
(29) Atomos Space’s First Mission On-orbit is a Trial by Fire. [Online] Available at: https://techcrunch.com/2024/03/22/atomos-spaces-first-mission-on-orbit-is-a-trial-by-fire/
(30) Momentus. Vigoride User's Guide V1.0. February 23, 2020. [Online] Available at: https://momentus.space/site/wp-content/uploads/2020/02/Momentus-Vigoride-Users-Guide.pdf
(31) UARX Space, “UARX and Sener have partnered to work on OSSIE Orbital transfer vehicle,” [Online] Accessed October 2nd, 2023. [Online] Available at: https://www.satelliteevolution.com/post/uarx-and-sener-have-partnered-to-work-on-ossie-orbital-transfer-vehicle
(32) Impulse Space, “Starfish Space Completes Autonomous Rendezvous and Proximity Mission in LEO with Impulse Space,” December 15, 2025. [Online] Available at: https://www.impulsespace.com/updates/starfish-space-completes-autonomous-rendezvous-and-proximity-mission-in-leo-with-impulse-space
(33) Impulse Space, “Impulse Space Unveils Design Specifications for New High Performance Kick Stage, Helios,” Press Release. January 17, 2024. https://www.impulsespace.com/updates/impulse-space-unveils-design-specifications-for-helios
(34) Space Machines Company, “Space Machines Company’s Optimus Satellite Successfully Launched.” March 5, 2024. [Online] Available at: https://www.australiandefence.com.au/news/news/space-machines-company-s-optimus-satellite-succesfully-launched
(35) Blue Origin. “New Glenn Launches NASA’s ESCAPADE, Lands Fully Reusable Booster,” November 13, 2025. [Online] Available at: https://www.blueorigin.com/news/new-glenn-launches-nasa-escapade-lands-fully-reusable-booster
(36) Blue Origin. “New Glenn Completes Second Stage Hotfire,” September 23, 2024. [Online] Available at: https://www.blueorigin.com/news/new-glenn-completes-second-stage-hotfire
(37) D. Werner. “D-Orbit Satellite Carrier Delivers Planet SuperDoves to Desired Orbits.” Spacenews.com October 28, 2020. [Online] Available at: https://spacenews.com/d-orbit-demonstrates-ion/
(38) D. Werner, “TransAstra Claims NASA Contract for Debris Capture Bag,” Spacenews.com August 29, 2023. [Online] Available at: https://spacenews.com/transastra-claims-nasa-contract-for-debris-capture-bag/
(39) D. Lentz. “SpaceX Launches Transporter-10 Rideshare from Vandenberg,” March 4, 2024. NASASpaceFlight. [Online] Available at: https://www.nasaspaceflight.com/2024/03/transporter-10/
(40) Space Machines Company. “Technology – Optimus.” [Online] Available at: https://www.spacemachines.com/technology

(41) J. Foust, “Exotrail Deploys First Satellite from Orbital Transfer Vehicle.” SpaceNews. [Online] Available at: https://spacenews.com/exotrail-deploys-first-satellite-from-orbital-transfer-vehicle/
(42) S. Erwin, “Exotrail Developing Space Tug to Carry Small Satellites to Geostationary Orbit,” SpaceNews. [Online] Available at: https://spacenews.com/exotrail-developing-space-tug-to-carry-small-satellites-to-geostationary-orbit/
(43) Nanoracks. Kaber Nanoracks ISS Microsatellite Deployment System. [Online] Available at: https://nanoracks.com/wp-content/uploads/NRMSD-overview.pdf.
(44) JAXA. JEM Small Satellite Orbital Deployer (J-SSOD). [Online] Available at: https://iss.jaxa.jp/en/kiboexp/jssod/.
(45) N. Natario. "Commercial Space Companies in Houston Looking Forward to SpaceX Launch.” May 26, 2020. [Online] Available at: https://abc13.com/society/commercial-space-companies-looking-forward-to-spacex-launch-/6213469/
(46) A. Thompson, "The International Space Station is now Home to the World's 1st Commercial Airlock." December 23, 2020. Accessed July 9, 2021. [Online] Available at: https://www.space.com/nanoracks-bishop-airlock-installed-space-station
(47) Nanoracks. External Cygnus Deployment. [Online] Available at: https://nanoracks.com/products/external-cygnus-deployment/
(48) National Aeronautics and Space Administration, “SlingShot,” [Online] Available at: https://www.nasa.gov/mission_pages/station/research/experiments/explorer/Facility.html?#id=7847
(49) R. Hunter, E. Agasid, et al., “NASA’s Starling Mission and Space Situational Awareness Implications,” 2025 Advanced Maui Optical and Space Surveillance Technologies Conference (AMOS) – www.amostech.com.



Table of Contents

Chapter Glossary 2
11.0 Ground Data Systems & Mission Operations 304
11.1 Introduction 304
11.2 Ground Systems Architecture 305
11.2.1 Types of Communication Infrastructures 306
11.3 Frequency Considerations 307
11.3.1 Frequency Selection: Link Budget 308
11.3.2 Frequency Licensing 308
11.4 Ground Segment Services 309
11.4.1 Ground Networks – NASA and Partners 310
11.4.2 Ground Segment as a Service (GSaaS) 317
11.4.3 Space Relay Network - NASA 324
11.4.4 Low Latency, Low Rate (Short Burst) Space Relay Providers 328
11.5 Ground Stations Components 329
11.5.1 Ground Station Operation 329
11.5.2 Component Hardware for Ground Systems (GS) 331
11.5.3 Ground Software 333
11.6 Mission and Science Operations Centers 338
11.6.1 Software for Mission Operations 340
11.7 End-to-End Communications and Compatibility Testing 341
11.7.1 End-to-End Hardware for Ground Systems 342
11.8 Cyber Security 348
11.9 State-of-the-Art – Ground Data and Supporting Systems 349
11.9.1 Technologies 349
11.9.2 Ground Aggregators 351
11.9.3 Scheduling and Mission Operations Software 352
11.10 On the Horizon 358
11.10.1 Free Space Optical Communications 359
11.10.2 Optical Ground Stations and Future Infrastructure Requirements 360
11.10.3 Techniques to Improve Optical Comm Reliability 366
11.10.4 Role of Optical Relays 366
11.11 Summary 367
References 368



Chapter Glossary

(API)	Application Programming Interface
(AWS)	Amazon Web Services
(C2)	Command & Control
(CCSDS)	Consultative Committee for Space Data Systems
(CFDP)	CCSDS File Delivery Protocol
(DSN)	Deep Space Network
(DTE)	Direct-to-Earth
(DVB-S2)	Digital Video Broadcast Satellite Second Generation
(EGSE)	Electrical Ground Support Equipment
(EIRP)	Effective Isotropic Radiated Power
(ESA)	European Space Agency
(ESOC)	European Space Operations Centre
(FCC)	Federal Communications Commission
(GEO)	Geosynchronous Equatorial Orbit
(GNSS)	Global Navigation Satellite System
(GPS)	Global Positioning System
(GSaaS)	Ground Segment as a Service
(GUI)	Graphic User Interface
(HEO)	Highly Elliptical Orbit
(HF)	High Frequency
(HPAs)	High-Power Amplifiers
(I&T)	Integration and Test
(IARU)	International Amateur Radio Union
(ITU)	International Telecommunications Union
(KSAT)	Kongsberg Satellite Services AS
(KSC)	Kennedy Space Center
(LEO)	Low Earth Orbit
(LNA)	Low-Noise Amplifier
(MEO)	Medium Earth Orbits
(MOC)	Mission Operations Center
(NEN)	Near Earth Network
(NSN)	Near Space Network
(NTIA)	National Telecommunications and Information Administration
(NORAD)	North American Aerospace Defense Command
(OGS)	Optical Ground Station
(PNT)	Position, Navigation, and Timing
(PPM)	Pulse Position Modulation
(RF)	Radio Frequency
(SDR)	Software Defined Radio

(SLE)	Space Link Extension
(SNSPD)	Superconducting Nanowire Single Photon Detector
(SOC)	Science Operations Center
(SWaP)	Size, Weight, and Power
(TDRS)	Tracking and Data Relay Satellites
(TDRSS)	Tracking and Data Relay Satellite System
(TLE)	Two-Line Element
(TT&C)	Telemetry, Tracking, and Control
(UHF)	Ultra-High Frequency
(USRP)	Universal Software Radio Peripheral
(VHF)	Very High Frequency
(VMs)	Virtual Machines
(XTCE)	XML Telemetric and Command Exchange

11.0 Ground Data Systems & Mission Operations

11.1 Introduction

The ground segment is a critical part of the end-to-end science data return, and includes all the ground-based elements used to collect and disseminate information from the satellite to the end user (Figure 11.1). The primary elements of a ground system are summarized in Table 11-1.

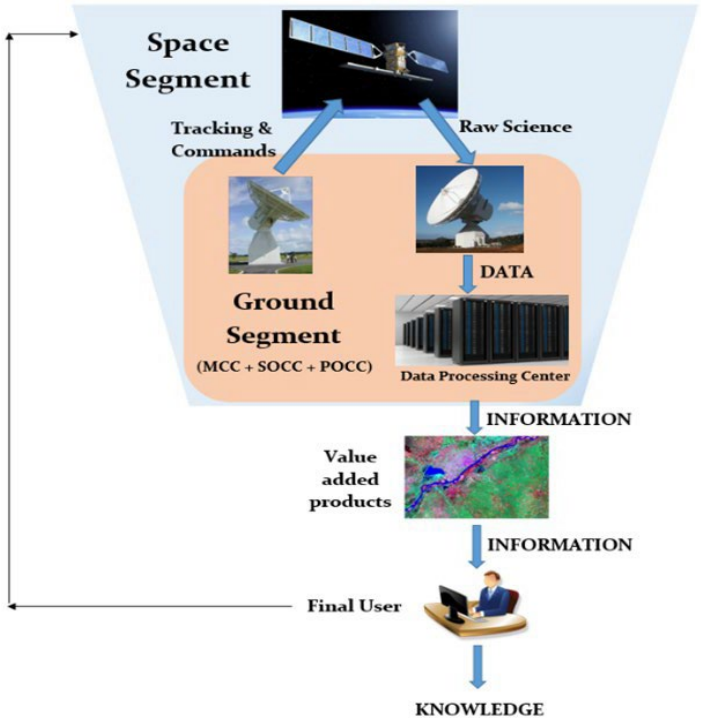


Figure 11.1: Functional relationship between the space segment, ground segment and final user for a small satellite mission. Credit: NASA.

Significant changes are occurring across government and commercial ground stations and services, along with evolving integration between these sectors. Since its inception in 1958, NASA has relied on internally developed systems to receive data from Earth-observing satellites and communicate with astronauts in orbit. Over time, commercial providers developed the capabilities to reliably and securely communicate with objects in low-Earth orbit (LEO), services that NASA is increasingly procuring as a near-Earth mission customer.

NASA combined the Near Earth Network (NEN) and the Space Network (SN) into the Near Space Network (NSN) in October of 2020. To support commercialization initiatives, NASA plans to increase reliance on industry-provided communications services for near-Earth missions by 2030 (1). As of 2026, commercial providers do not support missions at Sun-Earth Lagrange Points or in Deep Space; therefore, the Deep Space Network (DSN) and large NSN assets (≥18 m) continue to play a critical and needful role in returning science data from these regions for heliophysics, astrophysics and planetary science missions.

Table 11-1: Primary Elements of a Ground System

Element	Function
Ground Stations	Telemetry, tracking, and command interface with the spacecraft
Ground Networks	Connection between multiple ground elements
Control Centers	Management of the spacecraft operations
Remote Terminals	User interface to retrieve transmitted information for additional processing

The NSN provides Direct-to-Earth (DTE) services via a global system of commercial and NASA-owned ground stations that provide line of sight communications and tracking services to missions ranging from low-Earth orbit and extending to Sun-Earth Lagrange Points 1 & 2. These services are augmented by Space Relay services via relay satellites in geosynchronous orbit.

Ground segment design depends on several factors including, but not limited to:

- Data volume to satisfy mission requirements
- Location of ground assets relative to mission orbit parameters
- Budget limitations
- Distribution of the team
- Controlling organization (federal vs. non-federal users)
- Regulatory requirements
- Latency requirements

The ground system is responsible for collecting and distributing the mission's most valuable asset: data. Selecting an appropriate ground system is critical to mission success.

All small satellites rely on some form of a ground segment to communicate with the spacecraft, ranging from hand-held radios using amateur frequencies to large dish antennas operating on licensed federal or non-federal bands. The commercial marketplace for Telemetry, Tracking and Commanding (TT&C) services continues to expand and has matured to enable commercialization of DTE radio frequency communications. NASA is fostering a growing commercial market by leveraging industry capabilities to improve the efficiency and robustness of ground networks. In addition, NASA plans to enhance its communications capabilities to provide near-continuous communications support to Artemis lunar missions through relay and navigation services in lunar space.

11.2 Ground System Architecture

A typical small satellite mission ground system architecture includes the following elements:

- Ground Station Terminal: Transmitter and receiver or transceiver at the ground station to transmit and receive information, including related hardware such as antennas. These may be in Radio Frequency (RF) or optical wavelengths.
- Mission Operations Center (MOC):
  - Commands the spacecraft
  - Monitors spacecraft performance
  - Requests and retrieves data as necessary
- Science Operations Center (SOC):
  - Generates and disseminates science data products
  - Determines science operations to be relayed to the MOC
- Ground Station Data Storage and Network:
  - Provides real-time connectivity to the MOC for commands and telemetry
  - Temporarily stores data for retrieval by the MOC and/or SOC

Figure 11.2 illustrates a generic small satellite ground architecture that uses NASA's NSN for nominal ground passes and the NASA SN for low-latency communications.

In this architecture, the MOC is responsible for all communication to and from the spacecraft, while the SOC and engineering teams interface directly through the MOC to process commands. This is especially important during commissioning and troubleshooting, when engineering teams require direct access to the flight system. This architecture also provides a separate database of telemetry and housekeeping data that is generated from the MOC and accessible to stakeholders.

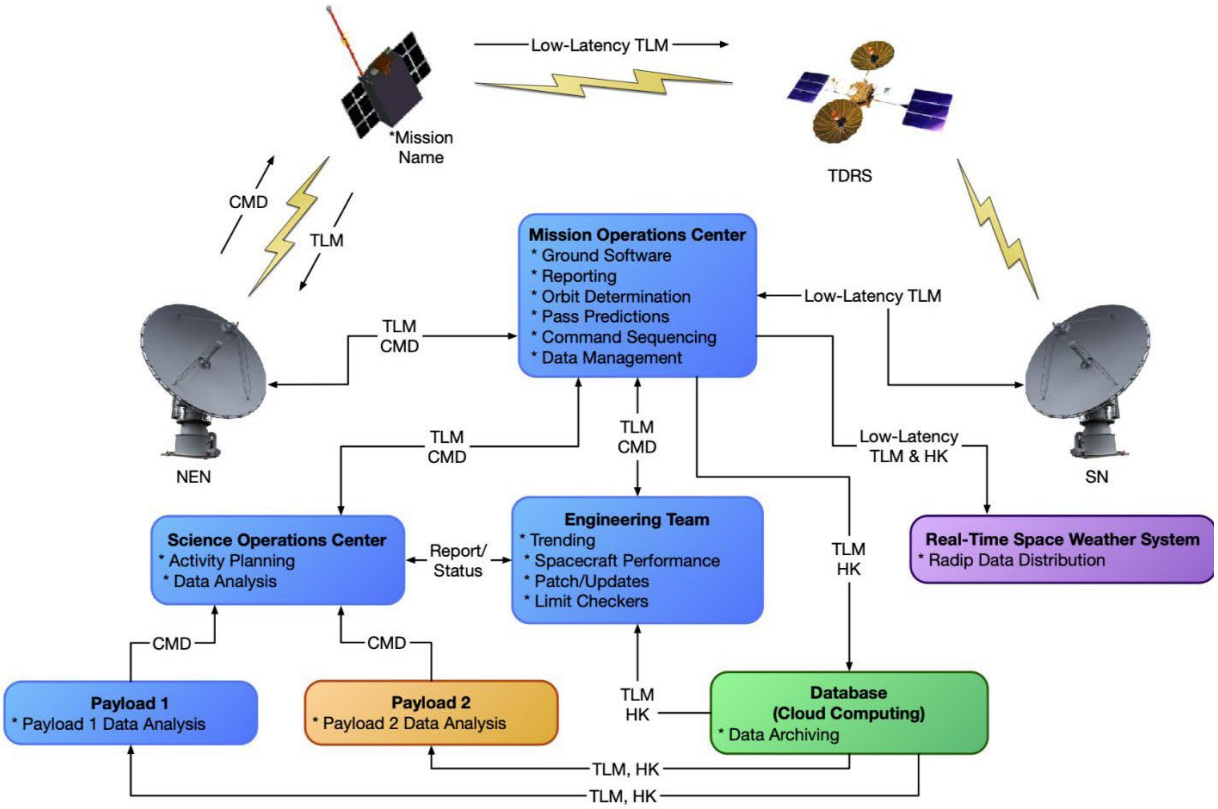


Figure 11.2: Example of a ground system architecture for a small satellite using NASA's Near Space Network. Credit: NASA.

11.2.1 Types of Communication Infrastructure

Communications services may be either DTE or augmented by space relay. DTE ground stations provide direct point-to-point access with antennas at ground stations which are strategically located and equipped with telemetry, command, and tracking services. DTE antennas for NASA small satellites are high gain parabolic dish antennas used to support S, X, and Ka bands, while some universities still use parabolic or UHF Yagi antennas. DTE ground stations could also incorporate phased array antenna systems or equipment for optical communications. The DTE services are especially effective for missions needing frequent, short-duration contacts with high data throughput. They are also capable of handling longer latency durations due to orbital dynamics and station visibility.

Space relay services involve an intermediate satellite that communicates with a ground station on the Earth's surface. Relay communication satellites for LEO spacecraft can be in Geosynchronous Equatorial Orbit (GEO), about 36,000 km from Earth, or in LEO. Relays are essential for providing communication and tracking when direct-to-ground communications are not feasible due to physical asset visibility constraints. It is common for a LEO spacecraft to only be in a DTE ground station's line of sight for a portion of the orbit. The addition of space-based relay assets can provide missions with full-time coverage and continuous access to communication and tracking services. They are most useful for missions that need continuous coverage, low latencies, and coverage of launch, critical events, or emergencies.

Communication with DTE ground stations can achieve much higher data rates than what is possible for space-based relays. When considering a GEO relay satellite, it can be ten times the distance from the low-Earth orbit spacecraft than the DTE ground station. With communication propagation losses being a function of the reciprocal of the distance squared, the same communications system can achieve orders of magnitude higher data rates with the DTE ground station. Achieving comparative data rates for a relay system would require a significant increase in power. The current LEO relays have hardware limitations that permit data rates of 9.6 kbps or less, which is low relative to SmallSats being able to achieve 3 Mbps or more with DTE ground stations.

11.3 Frequency Considerations

The spacecraft transceiver and ground station need to be on a coordinated frequency to communicate. Selecting transmit and receive frequencies are a critical part of the spacecraft communications system design process. Frequencies are divided into different bands as shown in Table 11-2. See a list of supported frequencies per ground station in their specific sections.

Typical bands considered for small satellites and therefore ground stations are Ultra High Frequency (UHF), S, X, and Ka. UHF was the band of choice for early small satellites, but in recent years, there has been a shift to S, X, and Ka. A ground station needs to maintain antennas and receivers such that the ground receive matches the space segment's transmit frequency and vice versa. Since Transmit (Tx) and Receive (Rx) have different key drivers and requirements, many ground stations are dual or tri-band.

Table 11-2: Frequency Bands

Band	Frequency
HF	3 to 30 MHz
VHF	30 to 300 MHz
UHF	300 to 1000 MHz
L	1 to 2 GHz
S	2 to 4 GHz
C	4 to 8 GHz
X	8 to 12 GHz
Ku	12 to 18 GHz
Ka	27 to 40 GHz
V	40 to 75 GHz
W	75 to 110 GHz
mm	110 to 300 GHz

Ground Station Receive (Spacecraft Return, Telemetry)

Ground station receive frequencies are mostly S and X band from a LEO/ GEO orbit, and X and Ka band from deep space. Ka band has been implemented for transmit and is NASA's desired band for future small satellite missions. This shift has been driven by higher data return demands and frequency control. The higher frequencies permit more data to be transmitted over a given period but require more stringent pointing. UHF is appealing to some universities, due to the lower cost of hardware for both the spacecraft and ground station, good link margins, and more omni-directional pattern capability with the spacecraft but yields lower data rates and has a higher probability for interference. Higher frequencies provide wider bandwidths, and the matching antennas have narrower beamwidths or are arrayed for a higher gain, thus more stringent pointing is required.

Ground Station Forward (Spacecraft Commanding)

The key driver for successfully commanding a satellite from the ground is the ability to establish and maintain a communication link. The most critical period occurs immediately after spacecraft separation from the launch vehicle, when the satellite may not yet have full control over its attitude; therefore, a wide beamwidth for the spacecraft receiving antenna(s) in the selected frequency is essential. For this reason, ground stations are designed with higher transmit power and Low-Noise Amplifiers (LNAs) to compensate for the low-gain, ideally omnidirectional single-patch receive antennas typically used in lower frequency bands.

11.3.1 Frequency Selection: Link Budget

Calculating the RF link budget is the first step when designing a telecommunications solution. It is a calculation of the end-to-end performance of the communications link with the constraint of maintaining a required link margin. Maintaining a 3 dB link margin is adequate for data return from a satellite in low-Earth orbit at a slant range of 1,500 km. Usually commanding to a Near-Earth orbit has plenty of margin because of the high power and aperture size of the ground station, and the lower required data rate on the account of the commands' low volume. When considering deep space communication, a 3 dB link margin is desired, but for distant spacecraft, such as New Horizons at 7 billion kilometers from Earth, 1 dB or less margin may be all that is practically feasible. The budget calculation adds and subtracts all the power gains and losses that a communication signal will experience within the system. Factors such as uplink amplifier gain and noise, transmit antenna gain, slant angles and corresponding free space loss, satellite transceiver noise levels and power gains, receive antenna and amplifier gains and noise, cable losses, and atmospheric attenuation are considered. There is a duality to frequency effects: free space loss over the same range is less for lower frequencies; however, the wavelength is much smaller for higher frequencies, thus a same size ground aperture provides a much higher gain over temperature (G/T). On the spacecraft end, a multi-element high-gain Ka-band antenna array for example fits in the palm of a hand. For high volume data return, which is where communications bottlenecks occur, higher frequencies are desirable – all the way up to optical wavelengths at 1550 nm (see Section 11.10.1, *Free Space Optical Communications*).

11.3.2 Frequency Licensing

RF communication frequencies are intentionally protected. Within each frequency band there are government and non-government designations amongst the frequencies. Some frequencies are government use only, others are non-government only, and some are shared. Government bodies that regulate the frequency usage in the United States are the Federal Communications Commission (FCC) and the National Telecommunications and Information Administration (NTIA). Other countries may have their own national governing bodies, and all national bodies around the world must coordinate with the International Telecommunications Union (ITU), which is the governing body at the international level. The FCC is responsible for issuing communications licenses to non-government users and the NTIA handles government users. Licenses are required for both the satellite and ground station to transmit on a designated frequency or frequencies. It is becoming more common for small satellites to use multiple bands. For example, some missions have used UHF for uplink and S- band for downlink, while others have used S-band for uplink and X-band for downlink. Some of the non-government frequencies are dedicated for amateur usage.

Early university small satellites relied heavily on the use of amateur frequency bands. In recent years, there has been movement by the International Amateur Radio Union (IARU) and the FCC to significantly limit the use of amateur frequencies for small satellites. Those interested in using these frequencies are expected to first communicate their intention with the IARU and obtain a coordination letter prior to applying with the FCC. It is recommended that missions with a new communication system design apply with the FCC or NTIA once an operations concept and a spacecraft design are defined, to verify a proper communications approach and associated hardware has been selected. Missions using a legacy communications approach can typically wait until they have been given a launch manifest. The licensing process can take several months and needs to be completed prior to launch. Some of the processing time is associated with the FCC and NTIA having to also coordinate with the ITU. Both the FCC and ITU are working to implement more streamlined small satellite licensing options. Such improvements will be necessary as constellations of small satellites become more prevalent.

11.4 Ground Segment Services

Ground segment services may include the four categories below. The NSN is a full-service ground station network and offers all four major service categories. Not all commercial services offer all services.

1) Mission Integration – this includes development of service agreements, interfaces, documentation, support of reviews, etc.
2) Mission Planning and Scheduling – this includes performing link and loading analyses, supporting service requests, and generating and implementing operational schedules.
3) User Mission Data Transfer – this primarily includes spacecraft forward command and return telemetry data.
4) Position, Navigation and Timing (PNT) – this includes navigation.

Position information is critical for commanding the spacecraft. Commanding may be scripted by the mission and is actuated through ground services. Challenges are usually associated with the initial satellite-to-ground station link closure. Typically, two-line elements (TLE) or state vectors are established and shared by the launch provider after deployment. This information can be used to create an initial orbit solution for ground station antenna pointing. Low-Earth orbit missions can use North American Aerospace Defense Command (NORAD) TLE data (see https://www.space-track.org) for satellite location. However, it could take up to a week or more for NORAD to add the new object to their tracking list. This process could be delayed further if multiple spacecraft are ejected in close proximity, and it may not be clear which NORAD element set corresponds to which spacecraft. It is not uncommon to spend weeks attempting contact with different NORAD-tracked objects until the correct one is found. The position prediction accuracy based on the NORAD TLE also diverges over time and a new TLE will be needed to maintain data link. This is typically not an issue since the TLE is updated regularly, but on-board Global Positioning System (GPS) data (if equipped) can help determine the orbital parameters for the ground station to define latest orbital parameters.

Another method is to locate the satellite as it rises from the horizon. Ground station operators can point a directional antenna 5-10 degrees above the horizon to detect the satellite and synchronize with the radio. Most antenna tracking software will commence automatic tracking after the initial acquisition is successful. A half-duplex or full-duplex system could make a difference as well. Program track instead of auto-track is used for half-duplex. With a full-duplex system, the ground antenna attempts to acquire the downlink first. Predicts (NORAD or state vectors) are still used to initially acquire the spacecraft. If the predicts are off, the antenna can initiate a mechanical scan to increase the search area. Once the downlink is acquired, the ground antenna can auto-track and automatically point at the satellite for the duration of the pass. Additional passes are scheduled during spacecraft and payload commissioning. Table 11-3 describes NSN's transport and tracking capabilities.

Table 11-3: NSN Interfaces and Capabilities

Interface/ Capability[1]	**Direct to Earth**	**Space Relay**
Terrestrial Link Data Transport Capabilities		
Data Storage [1]	Station Storage: 5-30 days Cloud-based: Mission-driven	7 days
Network Data Rate [1]	Mission-driven (up to 1.2 Gbps)	
SLE Protocols	F-CLTU, EF-CLTU (Forward) RAF, RCF, ROCF (Return)	
SLE Versions Supported [2]	CCSDS 910.4, CCSDS 911.1, CCSDS 911.2, CCSDS 911.5, CCSDS 912.1, CCSDS 912.11, CCSDS 912.3, CCSDS 913.1	

Offline-Data Transfer	CFDP, SFTP	
Security	Trusted Networks (Access Controls, Firewalls, Authentications, etc.)	
Spacecraft Navigation Tracking Capabilities		
Radiometric Tracking Services [1]	Tone Ranging 1-way or 2-way Doppler Antenna Angle Data	Spread Spectrum Ranging 1-way or 2-way Doppler Antenna Angle Data
Radiometric Measurement Accuracy [1]	Range: S-band: < 5 meters, 1σ Doppler (Range-Rate): S-band 1-way: ≤ 30 mm/s, 1σ S-band 2-way: ≤ 15 mm/s, 1σ X-band 1-way: ≤ 7 mm/s, 1σ Ka-band 1-way: ≤ 2 mm/s, 1σ Antenna Angles: S: 0.03°, X: 0.05° Ka: 0.01° (auto), 0.05° (program)	Range: ≤ 2.73 meters, 1σ Doppler (Range-Rate): 1-way ≤ 1.55 mm/s, 1σ 2-way ≤ 3.1 mm/s, 1σ Antenna Angles: ≤ 0.1°
Radar Tracking Service Bands	C-band (5.4-5.9 GHz) Single Object X-Band (10.499 GHz) Multi Object	N/A
Radar Tracking Loop Gain (dB)	C-Band: 212-245 (227 Typical) X-Band: 246 (nominal)	
Other [1]	Ground Antenna Slew Rate: Azimuth and Elevation: ≥ 10°/sec (10°/sec^2) * Train: ≥ 5°/sec (5°/sec^2) * WS1 18-m system ≥ 2°/sec (1°/sec^2)	Time Transfer Measurement: User Spacecraft Clock Calibration System: ≤ ±5 μs Return Channel Time Delay: ±25% of a bit period

[1] Services and performance (Data Rates, EIRP, G/T, etc.) are not uniform across assets.
[2] Additional capabilities above those listed could be supported as well.
[3] NASA may consider adding technologies not currently on its roadmap.
[4] 2nd and 3rd Generation TDRS only.

Another critical time in the life of a spacecraft is commissioning; either commissioning of the spacecraft bus, or commissioning of science instruments, including in-space calibration. During commissioning phases, additional time and support personnel are typically scheduled (1).

11.4.1 Ground Networks – NASA and Partners

The ground stations, MOC, SOC, and the supporting infrastructure connecting them together, make up a ground network. Ground station antenna dish diameters, LNAs, frequency feeds, station gain over temperature (G/T) requirements are carefully selected for each network and are optimized for targeted ranges. NASA's NSN ground network provides services to satellites up to 2 million km range from Earth; NASA owns and JPL maintains the DSN for missions beyond two million km, including planetary.

At NASA's Goddard Space Flight Center, the Exploration and Space Communications (ESC) projects division oversees the operations, maintenance and advancement of the Space Communications and Navigation (SCaN) program office's NSN. Operating at a high-level of reliability and proficiency, the NSN provides communications and navigation services for missions

within two million kilometers of our planet, bringing down an average of almost 30 Terabytes of critical data daily. Through space relays and ground-based assets, NSN provides data delivery and satellite tracking services, empowering new discoveries about the universe and our home planet. JPL is responsible for managing and maintaining the DSN.

NASA Near Space Network

"The newly established NSN is more than just an aggregation of the NEN's and SN's space-based technologies, ground stations and antennas; it's the network through which NASA and other space users will now arrange for support services for their near-Earth missions. Critically, those support services may be provisioned through government or commercial network assets in a way that is seamless to users—a cornerstone in SCaN's effort to incorporate increasing levels of commercial service while ensuring mission needs are met."

The NSN provides direct-to-earth telemetry, commanding, ground-based tracking, and data and communications services to a wide range of customers. The network consists of NASA, commercial, and partner S-band, X-band, and Ka-band ground stations supporting spacecraft in LEO, GEO, Highly Elliptical Orbit (HEO), Lunar orbit, and Lagrange point L1/L2 orbit up to one million miles from Earth. The NSN supports multiple robotic and launch vehicle missions with NASA-owned stations and through cooperative agreements with interagency, international, and commercial services. Table 11-4 shows the radio frequencies that the NSN supports via the NTIA.

Table 11-4: NSN Supported Radio Frequencies and Bandwidths

Band	Function	Frequency Band (MHz)
S Uplink	Earth to Space	2,025 – 2,110
X Uplink	Earth to Space	7,190 – 7,235 (Two NEN sites to 7,200)
S Downlink	Space to Earth	2,200 – 2,300
X Downlink	Space to Earth, Earth Exploration	8,025 – 8,400
X Downlink	Space to Earth, Space Research	8,450 – 8,500
Ka Downlink	Space to Earth	25,500 – 27,000

A comprehensive list of Forward and Return capabilities per frequency are in Table 11-5. Systems are compliant with most CCSDS recommendations. The NSN consists of geographically dispersed ground stations operated by NASA and its commercial partners (Figure 11.3).

Government

- NASA's Alaska Satellite Facility, Fairbanks — Supports: S/X Band — Assets: 11.3m, 11m, 9.1m
- NASA's Kennedy Uplink Station — Supports: S-band - Assets: 6.1m
- NASA's Ponce de Leon Station — Supports: S-band - Assets: 6.1m
- NASA's Wallops Ground Station (GS), Virginia — VHF, S/X Band — Assets: 11m/5m
- NASA's White Sands GS, New Mexico — Supports: VHF, S/Ka Band — Assets: 18.3m
- NASA's White Sand Complex, New Mexico — Supports VHF, S/Ka Band — Assets: 11m
- NASA's McMurdo Ground Station, Antarctica — Supports: S/X Band — Assets: 10m
- Fairbanks Command and Data Acquisition Station (NOAA partnership), Gilmore Creek, Alaska

Commercial

- KSAT Singapore — Supports: S/X Band — Assets: 9.1m
- KSAT Svalbard, Norway — Supports: S/X Band — Assets: 11.3m/11.3m/13m

- KSAT TrollSat, Antarctica — Supports: S/X Band — Assets: 7.3m/7.3m
- KSAT Punta Arenas – Supports: S/X Band — Assets: 11.5m
- KSAT Inuvik -- Supports: S/X Band — Assets: 13m
- SANSA Hartebeesthoek, South Africa — Supports: S/X Band — Assets: 12m/10m
- SSC Kiruna, Sweden — Supports: S/X Band — Assets: 13m/13m
- SSC Santiago, Chile — Supports: S Band — Assets: 9m/12m/13m
- SSC Space US North Pole, Alaska — Supports: S/X Band — Assets: 5m/7.3m/11m/13m
- SSC Space US Dongara, Australia — Supports: S/X Band — Assets: 13m
- SSC Space US South Point, Hawaii — Supports: S/X Band — Assets: 13m/13m



Figure 11.3: NSN Global Ground Station Locations. Credit: NASA

Table 11-5: NSN Direct to Earth Command and Telemetry Capabilities per Frequency		
Interface/ Capability[1]	**Direct to Earth**	**Space Relay**
Forward (Command) Communications		
Frequency Bands (Near-Earth Use)	S-band: 2025-2110 MHz X-band: 7190-7235 MHz	S-band: 2025-2110 MHz Ku-band: 13.775 GHz Ka-band: 22.55-23.55 GHz [4]
Maximum Bandwidth	S-band: 5 MHz X-band: 10 MHz	S-band: 6 MHz Ku-band: 50 MHz Ka-band: 50 MHz [4]
Forward Max Data Rate [1,2] (prior to encoding)	S-band: 5 Mbps X-band: 5 Mbps	S-band MA: 300 Kbps S-band SA: 4.2 Mbps Ku-band: 50 Mbps Ka-band SA: 50 Mbps [4]
Antenna System EIRP (dBW) [1]	S-band: 51-81 (56 Typical) X-band: 85-86	S-band MA: 42 [4] S-band SA: 48.5 [4] Ku-band SA: 48.5 [4] Ka-band SA: 63 [4]

Modulation [2,3]	PM, FM, PCM, PCM/PM, PCM/PSK/PM, BPSK, QPSK, OQPSK, UQPSK	Spread spectrum: BPSK or UQPSK Non-spread: BPSK, QPSK, OQPSK, PCM/PM, or PCM/PSK/PM
Encoding [2,3]	Uncoded, or LDPC ½ or 7/8	Uncoded, Rate ½ Conv., Reed-Solomon, Concatenated (½ Conv. + RS), LDPC ½ or 7/8
Polarization	Circular (LHC, RHC)	Circular (LHC, RHC) (LHC only for MA services)
Return (Telemetry) Communications		
Frequency Bands (Near-Earth Use)	S-band: 2200-2290 MHz X-band: 8025-8400 MHz X-band (SRS): 8450-8500 MHz Ka-band: 25.5 – 27 GHz [4]	S-band: 2200-2290 MHz Ku-band: 15.0034 GHz Ka-band: 25.25 – 27.5 GHz [4]
Maximum Bandwidth	S-band: 5 MHz X-band: 375 MHz X-band (SRS): 10 MHz Ka-band: 1500 MHz	S-band (MAR & SAR): 6 MHz Ku/Ka-band: 225 MHz [4] Ka-band (Wide): 650 MHz [4]
Return Max Data Rate [1,2] (prior to encoding)	Rates will vary – examples: S-band: 2.2 Mbps (PACE) X-band: 220 Mbps (ICESat-2) X-band (SRS): 13.1 Mbps (IRIS) Ka-band: 3.5 Gbps (NISAR)	S-band MA: 1 Mbps S-band SA: 14.1 Mbps Ku/Ka-band: 600 Mbps [4] Ka-band (Wide): 1200 Mbps [4]
Antenna System G/T (dBW) [1]	S-band: 19.1-29.6 (21 Typical) X-band: 30.5-37.8 (32 Typical) Ka-band: 38-45 (41.3 Typical)	S-band MA: 3.2 (for LEO) S-band SA: 9.5 (for LEO) Ku-band: 24.4 (for LEO) Ka-band: 26.5 (for LEO) [4]
Demodulation [2,3]	PM, FM, PCM, PCM/PM, PCM/PSK/PM, BPSK, QPSK, OQPSK, AQPSK, SQPN, 8PSK	Spread spectrum: BPSK or UQPSK Non-spread: BPSK, QPSK, OQPSK, PCM/PM, or PCM/PSK/PM
Decoding [2,3]	Uncoded, Rate ½ Conv. and/or Reed-Solomon, LDPC ½ or 7/8, or Turbo Rate ½	Uncoded, Rate ½ Conv., Reed-Solomon, Concatenated (½ Conv. + RS), LDPC ½ or 7/8, Rate 7/8 TPC
Polarization	Circular (LHC, RHC)	Circular (LHC, RHC) (LHC only for MA services)

[1] Services and performance (Data Rates, EIRP, G/T, etc.) are not uniform across assets.
[2] Additional capabilities above those listed could be supported as well.
[3] NASA may consider adding technologies not currently on its roadmap.
[4] 2nd and 3rd Generation TDRS only.

While NASA's NSN is often reserved for NASA-funded missions, other ground network options exist for non-government-funded satellite operators. One common option, especially amongst amateur operators, is to take advantage of the UHF and VHF amateur network around the world.

The NSN is exploring how to provide higher data rates for CubeSat missions with techniques such as Digital Video Broadcast Satellite Second Generation (DVB-S2). Higher data rates either increase science return or reduce the number of minutes per day of required ground station contacts. Higher data rates also enable mother-daughter small satellite constellations, where the mother spacecraft handles the communication with Earth for multiple daughter spacecraft. Functions such as Multiple Satellite per Aperture (MSPA) are planned to be implemented on the Lunar Exploration Ground Sites (LEGS) mission.

The NSN facilitates Commercial Services (CS) and negotiated a bulk-buy discount for all NASA missions. This allows for contacts on the NSN Contractor/University Operated and CS apertures to be at no-cost for NASA missions. The NSN does schedule CS in accordance with NASA mission-defined priority. The Networks Integration Management Office (NIMO) at NASA GSFC is the liaison for customers that wish to use NSN services. NIMO has a variety of services and capabilities available and can coordinate support from providers throughout NASA, other US agencies, US commercial entities, and foreign governments. Some of the services that NIMO can provide include:

- Requirements Development
- Communications Design Support & Guidance
- Optical Communications Analysis
- Network Feasibility Analysis
- Spectrum Management
- RF Compatibility Testing
- Launch Support

Network Feasibility Analysis includes determining NSN station loading as a function of the mission's priority and determining the availability of planned stations for the contacts requested. Prior to the mission deployment, the NSN commits to providing the requested stations and contact time as outlined in the network feasibility analysis.

For new customer mission service requests please fill out the NSN Service Inquiry Form at: http://go.nasa.gov/NSNServiceInquiry.

If interested in more information on using the Near Space Network (NSN), please also refer to https://esc.gsfc.nasa.gov/projects/NSN.

NASA Deep Space Network

The DSN is optimized to conduct telecommunication and tracking operations with space missions in GEO. This includes missions at lunar distances, the Sun-Earth LaGrange points, and in highly elliptical Earth orbits, as well as missions to other planets and beyond. The DSN has supported, or is currently supporting, missions to the Sun as well as every planet in the Solar System (including dwarf planet Pluto). Two missions (Voyager I and Voyager II) have reached interstellar space and still communicate with the DSN. The DSN offers services to a wide variety of mission customers, as shown in Table 11-6.

Table 11-6: DSN Customers, Mission Characteristics, Frequencies, and Services

Customers	Mission Phases
• NASA • Other Government Agencies • International Partners	• Launch and Early Orbit Phase (LEOP) • Cruise • Orbital • In-Situ
Mission Trajectories	**Frequency Bands –** Includes Near-Earth and Deep Space Bands, Uplink and Downlink, Command, Telemetry, and Tracking Services
• Geostationary or GEO • HEO • Lunar • LaGrange • Heliocentric	• S-Band (2 GHz) • X-Band (7, 8 GHz) • Ka-Band (26, 32 GHz)

• Planetary	

DSN services include:

- Command Services
- Telemetry Services
- Tracking Services
- Calibration and Modeling Services
- Standard Interfaces
- Radio Science, Radio Astronomy and Very Long Baseline Interferometry Services
- Radar Science Services
- Service Management

Custom and tailored DSN services can also be arranged for missions and customers. DSN-provided data services are accessed via well-defined, standard data and control interfaces:

- The CCSDS
- The Space Frequency Coordination Group (SFCG)
- The ITU
- The International Organization for Standardization (ISO)
- De facto standards widely applied within industry
- Common interfaces specifiedby the DSN

The use of data service interface standards enable interoperability with similar services from other providers.

Figure 11.4 shows the DSN antennas and their locations. As of 2021, each DSN ground station in California (United States), Madrid (Spain), and Canberra (Australia) operated four 34 m Beam Wave Guide antennas and one 70 m antenna. By the late 2020s, this is planned to increase to include one 70 m plus four 34 m antennas at each DSN site.

The DSN supports RF testing using the following facilities:

- Development and Test Facility (DTF-21), located near NASA Jet Propulsion Laboratory (JPL)
- Compatibility Test Trailer (CTT-22), able to come to the spacecraft site

For more information on DSN, please see:
https://www.nasa.gov/directorates/space-operations/space-communications-and-navigation-scan-program/scan-services-and-scheduling/
https://deepspace.jpl.nasa.gov/about/commitments-office/
https://deepspace.jpl.nasa.gov

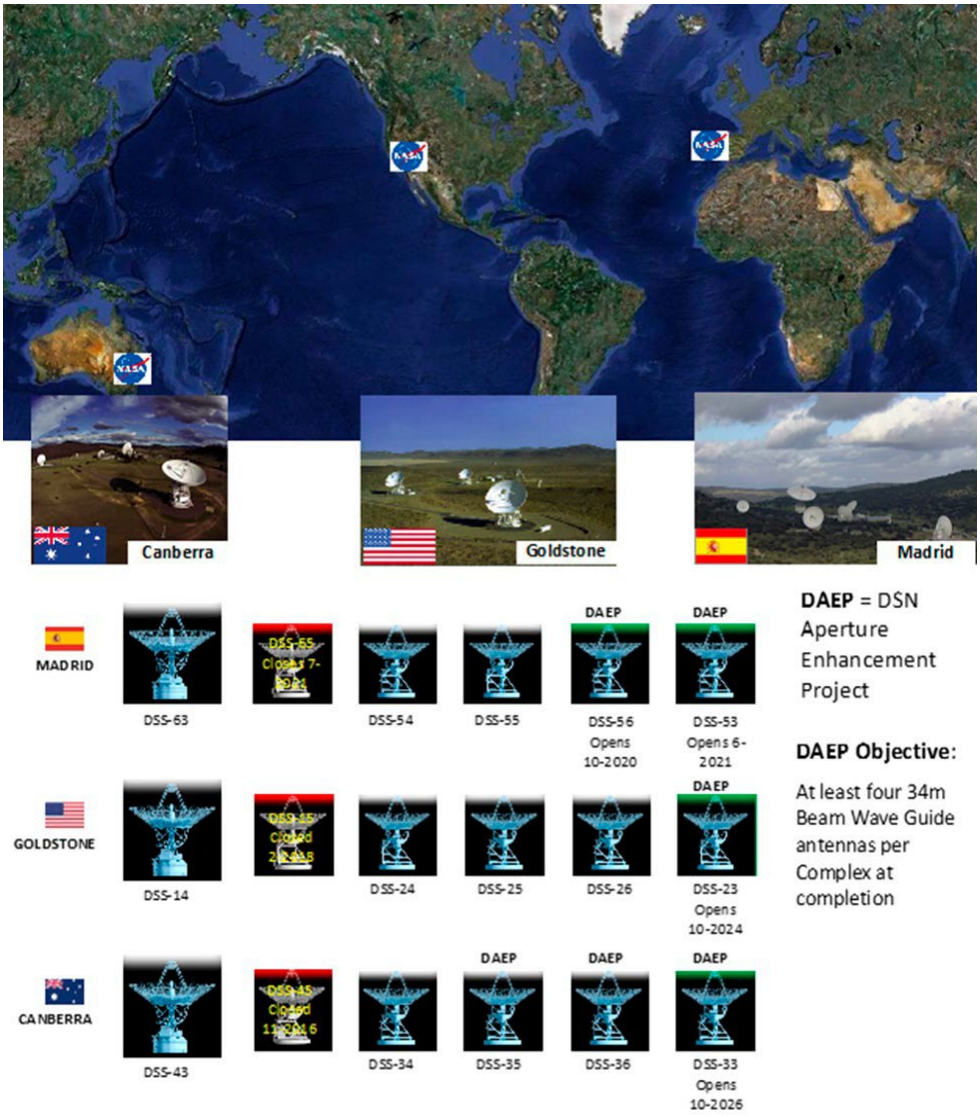


Figure 11.4: DSN antennas and their locations. Credit: NASA.

Swedish Space Corporation

Swedish Space Corporation (SSC) is a global provider of ground station services, including support to launch and early operations, on-orbit TT&C and data downlink, and even lunar services (see https://sscspace.com/). The SSC Infinity Network is specifically designed for constellations of small satellites in low-Earth orbits. The global network provides TT&C and data download and delivery services to SmallSat operators, and customer interfaces consist of web-based portals for pass scheduling on 5-meter and smaller antennas. SSC Infinity also uses standard configurations and standardized ground system hardware, limiting the number of mission configurations to help keep costs lower for satellite operators.

Using ground services will generally require some degree of pre-coordination (or “onboarding”) between the operator and provider, which is usually done before launch. This will vary between providers but may include contracting mechanisms; frequency licensing and coordination between the operator and the provider; compatibility testing; and the sharing of mission and vehicle-specific information to ensure the ground stations are properly configured for the operator to use. Once the

onboarding process is complete, satellite operators can schedule passes between their satellite(s) and desired ground station(s) in advance (the time window varies for each provider). The schedules for each ground station are deconflicted based on scheduling priority, and all frequency and modulation adjustments for the satellite are completed in advance of the pass by the service provider.

KSAT^{LITE}

The baseline of Kongsberg Satellite Services AS (KSAT)'s 3.7-meter KSAT^{LITE} antennas provide X-band and S-band for downlink and S-band for uplink. KSAT operates over 100 KSAT^{LITE} antennas at 15+ ground station sites across the globe, supporting over 1.5 million passes in 2023 alone. In addition, KSAT^{LITE} offers a global Ka-band network capable of supporting missions with higher data rates. KSAT^{LITE} is an extension of the existing KSAT ground station antenna network with lower costs, increased flexibility, and improved availability and pass selection. The KSAT



Figure 11.5: 2024 KSAT^{LITE} ground network map. Credit: KSAT.

network has uniquely located polar stations in the Arctic and Antarctic regions, providing 100% availability on passes for spacecraft in polar orbit. The network also includes mid-latitude ground stations, providing access for diverse orbits and mission profiles.

Additionally, KSAT has a network of large aperture antennas that are purpose built for supporting missions in cis-lunar space and beyond. In 2023 KSAT invested in a network of three 20m LEGS-class antennas that will be placed around the globe to provide full coverage of the Moon, which will be fully operational by Q1 of 2027. See Figure 11.5 for 2024 KSAT^{LITE} ground network map.

11.4.2 Ground Segment as a Service (GSaaS)

Ground Station as a Service (GSaaS) is a managed service which enables customers to communicate, downlink, and process data from their satellites/spacecrafts on as a pay-as-you go basis without needing them to build their own satellite ground stations. These services are usually scalable and use edge cloud services as an intermediate for customers data (3)(4).

AWS Ground Station

AWS Ground Station is a managed service (Figure 11.6.) that lets customers build ground segment architectures in the cloud to control their satellites, process satellite data, and scale satellite operations without having to worry about building or managing their own antenna infrastructure. Customers can stream satellite data from any of the AWS antennas to the Amazon Elastic Compute Cloud (EC2) for real-time processing or to directly store data in the Amazon Simple Storage Service (S3). Additionally, customers can easily integrate their space workloads with other AWS services in near real-time using Amazon's low-latency, high-bandwidth global network. For example, customers who downlink terabytes of data daily can easily access AWS services such as Amazon SageMaker to quickly derive useful information. Other AWS services include Amazon VPC, Amazon Rekognition, and Amazon Kinesis Data Streams. These services allow operators to reduce data processing and analysis times for use cases like weather prediction or natural disaster imagery from hours to minutes or seconds. This also enables operators to quickly create business rules and workflows to organize, structure, and route the satellite data before it can be analyzed and incorporated into key applications such as imaging analysis and weather forecasting. A map of the AWS Ground Station antenna regions is shown in Figure 11.7.

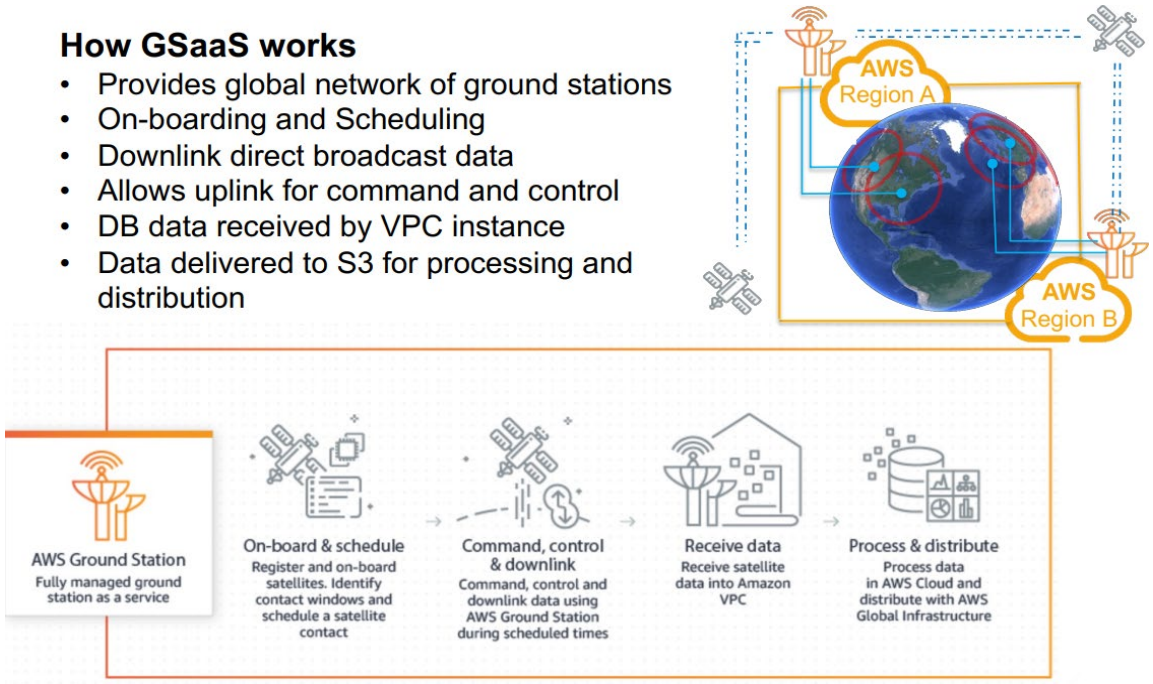


Figure 11.6. GSaaS Flow Chart. Credits: NASA/Amazon Web Services.

AWS Ground Station offers 5.4-meter apertures at each of the antenna regions. AWS Ground Station provides satellite antennas direct access to AWS services for faster, simpler, and more cost-effective storage and processing of downloaded data. Frequencies and link parameters are as follows:

- S-band uplink: 2025-2120 MHz
- S-band downlink: 2200-2300 MHz with G/T of 16 dB/K
- X-band downlink: 7750-8400 MHz with G/T of 30.5 dB/K

AWS Ground Station antennas are interconnected via Amazon's low-latency, highly reliable, scalable, and secure global network backbone. As of September 2024, the AWS Cloud spans 108 Availability Zones within 34 geographic regions around the world, with announced plans for 18 more Availability Zones and 6 more AWS Regions in Mexico, New Zealand, the Kingdom of Saudi Arabia, Thailand, Taiwan, and the AWS European Sovereign Cloud.

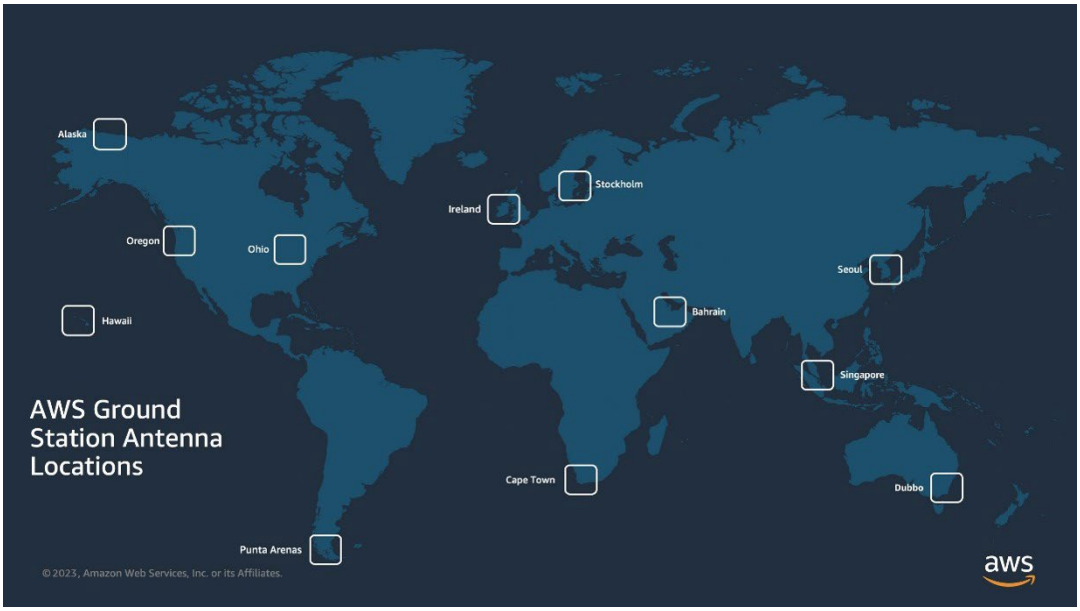


Figure 11.7. AWS Ground Station Locations (2026). Credit: Amazon Web Services

Customers have access to multiple billing structures including pay-as-you-go (PAYG) option, where customers pay only for what they use on a per minute basis; Dedicated Mission Support (DMS) option, where customers would receive schedule prioritization on one antenna for their constellation; or Dedicated Antenna Solution (DAS) option, where AWS collaborates with customers to design a custom solution tailored to specific mission requirements, including support for specific spectrum bands, antenna apertures, and/or locations. The PAYG, DMS, and DAS solutions can also be combined for additional capacity needs.

Scheduling: AWS Ground Station provides an easy-to-use graphical console that allows operators to reserve contacts and antenna time for their satellite communications. They can review, cancel, and reschedule contact reservations up to 15 minutes prior to scheduled antenna times. Access can be scheduled to AWS Ground Station antennas on a per-minute basis, so operators only pay for the scheduled time. They can access any antenna in the ground station network, and there are no long-term commitments. https://aws.amazon.com/ground-station.

Leaf Space

Leaf Space is a ground-segment-as-a-service provider, operating a globally distributed ground station network to support satellites of any size in LEO, MEO and GEO environments. Leaf Space's "Leaf Line" network (see Figure 11.8) enables TT&C and payload data transmissions to and from the satellite operators' mission control software and delivery endpoint of choice. Leaf does so via a simple API interface, a proprietary autonomous scheduling software, and global network coverage, supporting satellites in every LEO orbit – mid, high, equatorial-inclination. Leaf Line antennas are fully owned or fully managed, ensuring maximum availability, flexibility, and independence of operations. Leaf Line is powered and orchestrated by a secure cloud architecture designed to support multiple satellite missions and operators at the same time. The network's secure architecture allows seamless use of any antenna without requiring any further

resource overheads or worrying about varying performance over different ground stations. Leaf Space works closely with its customers to execute both routine operations and complex tasks such as LEOP or custom CONOPS.

Leaf Line consists of 3.7m and 3.9m diameter antennas and supports operations in S-band uplink (2025-2110 MHz, EIRP: 50 dBW), S-band downlink (2200-2290 MHz, G/T: 12.8 dB/K), X-band downlink (8025-8500 MHz, G/T: 25.4 dB/K), and Ka-band downlink (25.5-27 GHz, G/T: 30.0 dB/K). Leaf Space is constantly improving its network architecture in terms of sites, capacity, antenna performances and pass scheduling flexibility, in order to cater to a wide variety of customers. With an eye towards the future of the sector, Leaf Space is working to integrate larger-aperture antennas for GEO missions, optical ground systems as well as cislunar-oriented solutions to its existing network.

In addition to providing access to the Leaf Line network, Leaf Space procures, deploys, and operates dedicated and/or custom ground stations for its customers (a service offering called “Leaf Key”), enabling operators with non-standard frequencies, access, or data requirements to leverage Leaf Space’s cloud architecture and ground segment experience without compromising on antenna time. For more information, please contact sales@leaf.space or visit https://leaf.space.

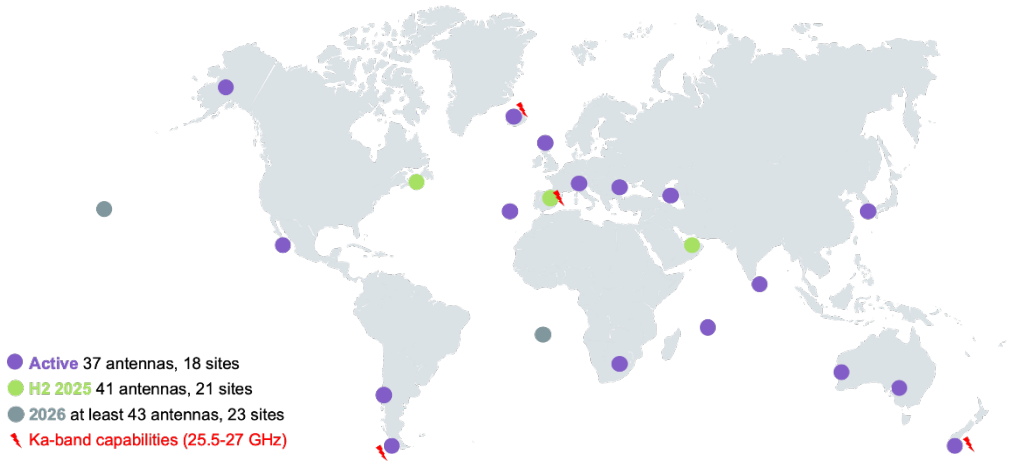


Figure 11.8: The Leaf Line network, October 2025. Credit: Leaf Space.

Laser Light Communications

Laser Light Communications operates a Global Network platform, delivering a first-of-a-kind 21st century data service that will transform the way high volume communications traffic is carried. Using a hybrid infrastructure spanning terrestrial, subsea, and space domains, an end-to-end software defined architecture provides up to 400 Gbps of all-optical connectivity and provisioning within minutes (see https://www.laserlightcomms.com/).

Network On Demand

- Pay-as-you-go: only pay for the duration you use the service with no upfront or fixed costs.
- Cost Effective: automation and end-to-end control yields significant operating cost savings.
- Secure: highly targeted, dynamic, laser links are extremely difficult to intercept and can be encrypted.
- High Capacity/ Performance: data delivery at up to 400 Gbps in the most direct route from origination to destination, automatically bypassing points of congestion.

Data Transport as a Service

- Pay-as-you-go: only pay for volume you use when you use it with no upfront or fixed costs.
- Cost Effective: automation and end-to-end control yield significant operating costs savings.
- Secure: highly targeted, dynamic, laser links are extremely difficult to intercept and can be encrypted.
- High Capacity/Performance: data delivery at optical speeds -- up to 400 Gbps directly from the point of origination to the point of destination, automatically bypassing points of congestion along the way.

Atlas Global Network

ATLAS Space Operations, Inc. provides satellite RF communication services to the government and commercial sectors through geographical dispersion and cloud services, offering GSaaS on a global network of 34 ground stations and 51 antennas, see Figure 11.9. (https://atlasspace.com/).



Figure 11.9: ATLAS Space Operations ground network map, September 2024. Credit: ATLAS Space Operations.

All ATLAS ground stations are built upon the Freedom™ Software Platform (Figure 11.10 below) within a cloud-based distributed operations center which facilitates dynamic demand and scalable growth. Through geographical dispersion of its ground stations and cloud services, ATLAS provides a resilient capability that delivers dependable low latency data. ATLAS bases its mission success model on its global network of operational and traditional RF parabolic ground stations that are integrated with network management and scheduling software. These platforms work together as a mission architecture to meet customer requirements for routine satellite-to-ground communications.

ATLAS' Global Antenna Network is fully integrated with the Freedom Software, providing users with a robust, low latency, and secure communications solution, including: automated network operations, set-and-forget scheduling, mixed modem capability, real-time metrics, and single secure VPN access. Once integrated into the ATLAS Network, a single secure VPN enables access and load balancing of network resources. Freedom Core Services advance operations beyond legacy constructs and enable users the freedom and flexibility to reliably schedule satellite passes with minimal human interaction via machine-to-machine capabilities. Entire data processing and forwarding workflows can be automated within the cloud to ensure spacecraft data is ready for use as soon as it arrives at the Mission Operations Center.

ATLAS supports deploying clusters and serverless instances onto AWS. ATLAS hardware parameters are highlighted below (ATLAS Enterprise Sites and Digital Partner Sites). In addition to S-band and X-band capabilities, ATLAS can provide VHF, UHF services in Japan and Guam. The existing and planned ATLAS antenna systems support RF connectivity for LEO, MEO, GEO, and L1 orbits. ATLAS is actively pursuing technology development for deep space capabilities. ATLAS' global federated network is also displayed below. A summary of government and commercial ground stations and antennas in Table 11-7 and shown in Figure 11.10 is ATLAS' Global Federated Network of ground stations.

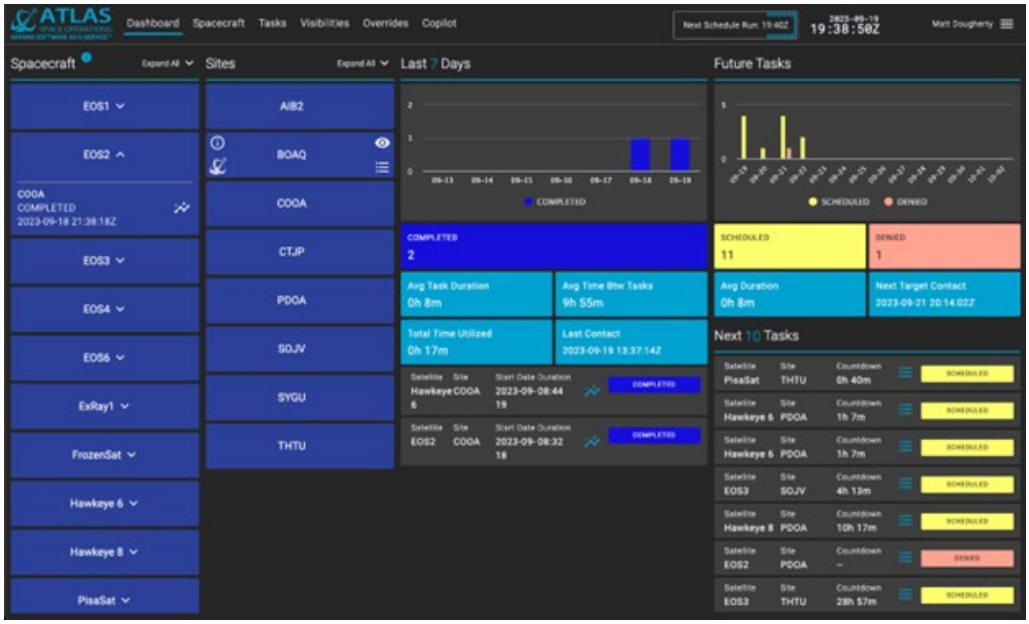


Figure 11.10. The Freedom™ Software Platform is a simple and scalable ground network management system. Credit: ATLAS Space.

Freedom Space Technologies, headquartered in Colorado Springs, CO, was established as a non-traditional small business and wholly-owned subsidiary of ATLAS Space Operations. Their purpose is to address and support the Department of Defense (DoD) and Intelligence Community (IC) mission requirements.

Table 11-7: ATLAS Federated Antenna Network

Location	Lat	Long	Antenna Size (m)	Rx Freq (MHz)	G/T Long (dB/K)	Tx Freq (MHz)	EIRP (dBW)	Polariza-tion
Utqiagvik (Barrow), AK, USA	71.27	-156.81	3.7	S: 2200-2300 X: 7900-8400	12.8 25.4	S: 2025-2120	60.0	R/LHCP
Dundee, Scotland	56.40	-3.18	3.7	S: 2200-2400 R/LHCP X: 7800-8400	13.6 26.5	S: 2025-2120	48.0	R/LHCP
Chitose, Japan	42.77	141.62	3.4	S: 2200-2300 X: 7900-8500	11.5 26.4	S: 2025-2120	52.0	R/LHCP
Mojave, CA, USA	35.05	-118.15	3.0	S: 2200-2300 X: 7900-8500	11.3 25.9	S: 2025-2110	54.4	R/LHCP
Dubai, United Arab	24.94	55.35	3.7	S: 2200-2300 X: 7900-8400	12.8 25.4	S: 2025-2120	50.0	R/LHCP

Table 11-7: ATLAS Federated Antenna Network								
Location	**Lat**	**Long**	**Antenna Size (m)**	**Rx Freq (MHz)**	**G/T Long (dB/K)**	**Tx Freq (MHz)**	**EIRP (dBW)**	**Polariza -tion**
Emirates								
Paumalu, Hawaii, USA	21.67	-158.03	7.3	S: 2200-2300 X: 7900-8500	20.7 31.0	S: 2025-2120	65.0	R/LHCP
Harmon, Guam	13.51	144.82	3.7	S: 2200-2300 X: 7900-8400	13.6 25.1	S: 2025-2110	52.4	R/LHCP
Sunyani, Ghana	7.34	-2.34	3.0	S: 2200-2300	12.4	S: 2025-2110	50.1	RHCP
Mwulire, Rwanda	-1.96	30.39	9.3	S: 2200-2300 X: 7900-8500	21.5 36.0	S: 2025-2120	60.0	R/LHCP
Tahiti, French Polynesia	-17.63	-149.60	3.7	S: 2200-2300 X: 7900-8400	13.9 27.4	S: 2025-2110	47.5	R/LHCP
Awarua, New Zealand	-46.52	168.38	3.7	S: 2200-2300 X: 8025-8500	13.7 27.0	S: 2025-2120	49.0	R/LHCP
Sodankylä, Finland*	67.36	26.63	7.3	S: 2200-2300 X: 7900-8500	19.8 32.1	S: 2025-2110	54.8	R/LHCP
Öjebyn, Sweden	65.33	21.42	7.3	S: 2200-2290 X: 8025-8400 Ka: 25500-27000	18.0 32.0 35.7	S: 2025-2110	55.2	R/LHCP
North Pole, Alaska, USA	64.79	-147.53	7.3	S: 2200-2300 X: 8000-8500 Ka: 25500-27000	19.0 32.0 35.7	S: 2025-2120	53.0	R/LHCP
Stockholm, Sweden*	-	-	5.4	S: 2200-2300 X: 7750-8400	16.0 30.5	S: 2025-2120	50.0	R/LHCP
Dublin, Ireland*	-	-	5.4	S: 2200-2300 X: 7750-8400	16.0 30.5	S: 2025-2120	50.0	R/LHCP
Guildford, United Kingdom	51.24	-0.61	5.4	S: 2200-2290 X: 8025-8400	17.0 30.0	S: 2025-2110	53.2	R/LHCP
Portland, Oregon, USA*	-	-	5.4	S: 2200-2300 X: 7750-8400	16.0 30.5	S: 2025-2120	50.0	R/LHCP
Obihiro, Japan	42.59	143.45	7.3	S: 2200-2290 X: 8025-8400 Ka: 25500-27000	17.9 31.5 35.0	S: 2025-2110	55.2	R/LHCP
Columbus, Ohio, USA*	-	-	5.4	S: 2200-2300 X: 7750-8400	16.0 30.5	S: 2025-2120	50.0	R/LHCP
Seoul, South Korea*	-	-	5.4	S: 2200-2300 X: 7750-8400	16.0 30.5	S: 2025-2120	50.0	R/LHCP
Pendergrass, Georgia, USA	34.17	-83.67	5.4	S: 2200-2290 X: 8025-8400	17.0 30.0	S: 2025-2110	53.2	R/LHCP
Deadhorse, Alaska, USA*	-	-	5.4	S: 2200-2300 X: 7750-8400	16.0 30.5	S: 2025-2120	50.0	R/LHCP
Zallaq, Bahrain*	-	-	5.4	S: 2200-2300 X: 7750-8400	16.0 30.5	S: 2025-2120	50.0	R/LHCP
Kapolei,	-	-	5.4	S: 2200-2300	16.0	S: 2025-	50.0	R/LHCP

Table 11-7: ATLAS Federated Antenna Network								
Location	**Lat**	**Long**	**Antenna Size (m)**	**Rx Freq (MHz)**	**G/T Long (dB/K)**	**Tx Freq (MHz)**	**EIRP (dBW)**	**Polariza -tion**
Hawaii, USA*				X: 7750-8400	30.5	2120		
Accra, Ghana	5.74	-0.30	7.3	S: 2200-2290 X: 8025-8400 Ka: 25500-27000	18.0 32.0 35.7	S: 2025-2110	65.0	R/LHCP
Singapore*	-	-	5.4	S: 2200-2300 X: 7750-8400	16.0 30.5	S: 2025-2120	50.0	R/LHCP
Alice Springs, Australia*	-23.75	133.88	7.3	S: 2200-2290 X: 8025-8400 Ka: 25500-27000	18.0 32.0 35.7	S: 2025-2110	65.0	R/LHCP
Pretoria, South Africa	-25.88	27.70	7.3	S: 2200-2290 X: 8025-8400 Ka: 25500-27000	18.0 32.0 35.7	S: 2025-2110	55.2	R/LHCP
Mingenew, Australia*	-29.01	115.34	5.0	S: 2200-2300 X: 8025-8500	14.0 29.5	S: 2025-2120	55.0	R/LHCP
Cordoba, Argentina	-31.52	-64.46	5.4	S: 2200-2290 X: 8025-8400	17.0 30.0	S: 2025-2110	53.2	R/LHCP
Cape Town, South Africa*	-	-	5.4	S: 2200-2300 X: 7750-8400	16.0 30.5	S: 2025-2120	50.0	R/LHCP
Dubbo, Australia*	-	-	5.4	S: 2200-2300 X: 7750-8400	16.0 30.5	S: 2025-2120	50.0	R/LHCP
Punta Arenas, Chile*	-	-	5.4	S: 2200-2300 X: 7750-8400	16.0 30.5	S: 2025-2120	50.0	R/LHCP
Ushuaia, Argentina	-54.51	-67.11	7.3	S: 2200-2290 X: 8025-8400 Ka: 25500-27000	17.9 32.0 33.0	S: 2025-2110	56.0	R/LHCP

Viasat

Viasat has delivered hundreds of ground antennas to NASA, other civilian space agencies, governments, and satellite industry partners throughout the world since the 1960s and has recently become a ground service provider. This move leverages decades of hardware engineering, with the global Real-Time Earth (RTE) network of ground terminals, complemented by a satellite relay network philosophy in GEO for low latency (near-real time) applications. A map of ground assets is shown in Figure 11.10. Viasat operates 7.3 m and 5.4 m antennas in 3 frequency bands (Table 11-8) and plans to include 13m class antennas in the near future. The RTE ground segment service enables communications for next-generation and legacy LEO satellites using S, X, and Ka-bands. RTE offers downlinks from low megabits per second to multiple gigabits per second powered by cutting edge software-defined radios at each site. The service includes high-speed connectivity for backhaul, real-time data streaming, and real-time monitoring of overhead passes. Following a contract award on the NASA NSN Service contract

and successful completion of the capability validation task order, Viasat RTE is now available to current and future NASA missions.

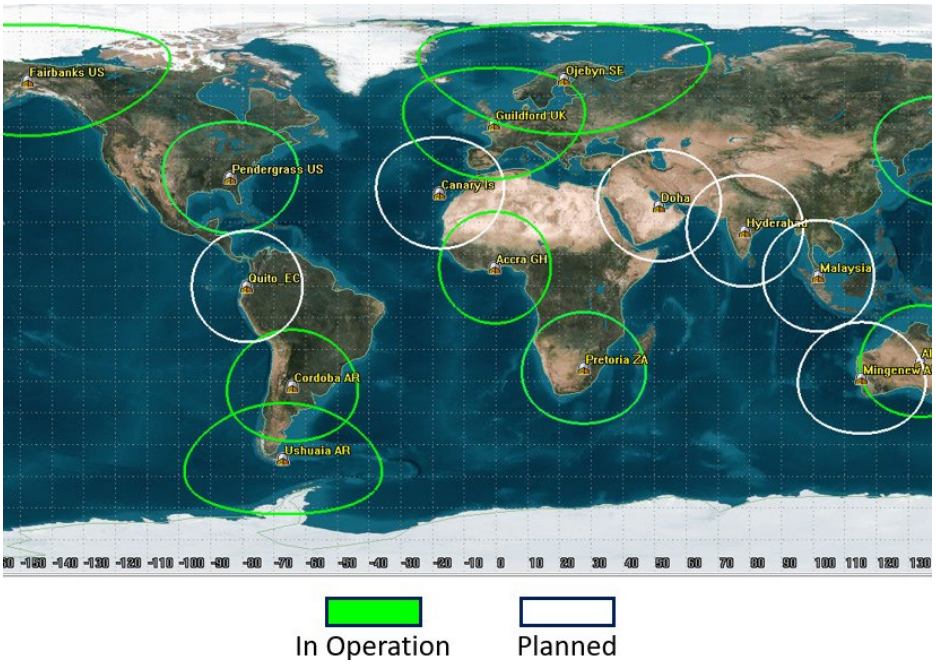


Figure 11.10: Viasat RTE global ground stations, December 2025. Credit: Viasat.

Viasat's HaloNet provides a turnkey launch and orbital communications solution with multi-band GEO-relay and Direct-to-Earth satellite links. It supports mission requirements including launch telemetry, TT&C, low- and high-data rate transmission, contingency operations, and science alerts. The system manages hardware, system integration, end-to-end transport, and service support, and communications are enabled through Viasat's space relay constellation and small terminals that connect directly to Viasat's GEO spacecraft. Data are delivered to the Mission Operations Center (MOC) via Viasat's secure, redundant global IP network. HaloNet ensures resilience through multiple transport paths and multi-waveform terminals. Services include continuous or on-demand L-band TT&C for Low Earth Orbit (LEO) spacecraft, high-throughput Ka-band links, and DTE solutions. Viasat's spectrum resources and orbital positions provide reliable and secure communications for launch and spacecraft operations. Visit https://www.viasat.com/ for more information.

Table 11-8: Viasat Ground Stations

Location	Antenna	L-band Uplink	S-band Uplink	S-band Downlink	X-band Downlink	Ka-band Downlink
Pendergrass, GA, USA (PGG)	5.4 m X-Y Full motion 5 °/sec max speed	N/A	2025-2110 MHz EIRP: 53.2 dBW Selectable RHCP or LHCP	2200-2290 MHz G/T: 17 dB/K Simultaneous RHCP and LHCP	8025-8400 MHz G/T: 30 dB/K Simultaneous RHCP and LHCP	N/A
Guildford, UK (GDD)	5.4 m X-Y Full motion 5 °/sec max speed	N/A	2025-2110 MHz EIRP: 53.2 dBW Selectable RHCP or LHCP	2200-2290 MHz G/T: 17 dB/K Simultaneous RHCP and LHCP	8025-8400 MHz G/T: 30 dB/K Simultaneous RHCP and LHCP	N/A

Table 11-8: Viasat Ground Stations						
Location	**Antenna**	**L-band Uplink**	**S-band Uplink**	**S-band Downlink**	**X-band Downlink**	**Ka-band Downlink**
Alice Springs, AU (ASP01, ASP02)	7.3 m X-Y Full motion 6 °/sec max speed quantity 2	1755-1850 MHz EIRP: 63.4 dBW	2025-2110 MHz EIRP: 65.0 dBW Selectable RHCP or LHCP	2200-2290 MHz G/T: 18 dB/K Simultaneous RHCP and LHCP	8025-8400 MHz G/T: 32 dB/K Simultaneous RHCP and LHCP	25500-27000 MHz G/T: 34.5 dB/K Simultaneous RHPC and LHCP
Accra, Ghana (ACC)	7.3 m X-Y Full motion 6 °/sec max speed	1755-1850 MHz EIRP: 63.4 dBW	2025-2110 MHz EIRP: 65.0 dBW Selectable RHCP or LHCP	2200-2290 MHz G/T: 18 dB/K Simultaneous RHCP and LHCP	8025-8400 MHz G/T: 32 dB/K Simultaneous RHCP and LHCP	25500-27000 MHz G/T: 34.5 dB/K Simultaneous RHCP and LHCP
Cordoba, AR (COR)	5.4 m X-Y Full motion 5 °/sec max speed	N/A	2025-2110 MHz EIRP: 53.2 dBW Selectable RHCP or LHCP	2200-2290 MHz G/T: 17 dB/K Simultaneous RHCP and LHCP	8025-8400 MHz G/T: 30 dB/K Simultaneous RHCP and LHCP	N/A
Öjebyn, Sweden (OJY)	7.3 m X-Y Full motion 6 °/sec max speed	N/A	2025-2110 MHz EIRP: 55.2 dBW Selectable RHCP or LHCP	2200-2290 MHz G/T: 18 dB/K Simultaneous RHCP and LHCP	8025-8400 MHz G/T: 32 dB/K Simultaneous RHCP and LHCP	25500-27000 MHz G/T: 34.5 dB/K Simultaneous RHCP and LHCP
Pretoria, South Africa (PRY)	7.3 m X-Y Full motion 6 °/sec max speed	N/A	2025-2110 MHz EIRP: 55.2 dBW Selectable RHCP or LHCP	2200-2290 MHz G/T: 18 dB/K Simultaneous RHCP and LHCP	8025-8400 MHz G/T: 32 dB/K Simultaneous RHCP and LHCP	25500-27000 MHz G/T: 34.5 dB/K Simultaneous RHCP and LHCP
Obihiro, Japan (OBO)	7.3 m X-Y Full motion 6 °/sec max speed	N/A	2025-2110 MHz EIRP: 55.2 dBW Selectable RHCP or LHCP	2200-2290 MHz G/T: 18 dB/K Simultaneous RHCP and LHCP	8025-8400 MHz G/T: 32 dB/K Simultaneous RHCP and LHCP	25500-27000 MHz G/T: 34.5 dB/K Simultaneous RHCP and LHCP
North Pole Alaska USA 7.3 m (NTP01)	7.3 m El-Az-Train El & Az: 15 °/s max speed Train 6 °/s max	N/A	2025 – 2120 MHz EIRP: 53 dBW Selectable RHCP or LHCP	2200–2300 MHz G/T: 19 dB/K Simultaneous RHCP and LHCP	8000–8500 MHz G/T: 32 dB/K Simultaneous RHCP or LHCP	N/A

Table 11-8: Viasat Ground Stations						
Location	**Antenna**	**L-band Uplink**	**S-band Uplink**	**S-band Downlink**	**X-band Downlink**	**Ka-band Downlink**
North Pole Alaska USA (9.1 m (NTP02)	9.1 m El-Az-Train	N/A	2042–2052 MHz EIRP 38 dBW Selectable RHCP or LHCP	N/A	8000–8500 MHz G/T: 34 dB/K RHCP	N/A
Tierra del Fuego, Argentina (USH)	7.3 m El-Az-Train El & Az: 15 °/s max speed Train 6 °/s max	N/A	2025-2110 MHz EIRP: 55.2 dBW Selectable RHCP or LHCP	2200-2290 MHz G/T: 17.9 dB/K Simultaneous RHCP and LHCP	8025-8400 MHz G/T: 32 dB/K Simultaneous RHCP and LHCP	25500-27000 MHz G/T: 34.7 dB/K Simultaneous RHCP and LHCP (Upgrade required)
Dubai, UAE	9.1 m El-Az-Train		2025-2110 MHz EIRP 38 dBW Selectable RHCP or LHCP	2200-2290 MHz G/T: 20 dB/K Simultaneous RHCP and LHCP	8025-8400 MHz G/T: 34 dB/K Simultaneous RHCP and LHCP	N/A

*Denotes antenna redundancy

11.4.3 Space Relay Networks - NASA

Unlike a traditional ground network that communicate directly from a “client” satellite to a ground station on the ground, space relay networks use intermediary communication satellites to relay data from the “client” satellite down to a ground station. Although some no longer consider it state-of-the-art, NASA’s Tracking and Data Relay Satellite System (TDRSS), shown in Figure 11.12, remains one of the most well-known space relay networks. TDRSS relays data from the International Space Station (ISS) and the Hubble Space Telescope to NASA ground stations around the world.

Space relay networks can be beneficial for small satellites in low-Earth orbit because those SmallSats are only in view of a ground station for a portion of their orbit. However, depending on the orbit of the relay satellites, a low-Earth orbit SmallSat may remain in view of a relay satellite for most of its orbit. This makes relay networks particularly beneficial for a SmallSat, especially immediately after deployment when ground stations are still attempting to acquire the satellite. The relay network can transmit satellite telemetry, tracking, and control data to the ground, enabling faster satellite identification. This capability is particularly valuable when satellites are deployed with multiple spacecraft during a rideshare mission. This data can also contain satellite health information to provide mission teams with insight while awaiting ground station acquisition or troubleshooting information prior to commissioning. Another benefit is the ability to obtain real-time event notifications without prior scheduling. Scientists are interested in using this technology to alert the scientific community when certain phenomenon are observed. Space relay networks often require specialized hardware or software that must be integrated into a satellite prior to launch. In general, a satellite operator will purchase a modem compatible with the relay network and integrate it into their spacecraft to access the network. It is common for network providers to license proprietary chipsets to developers who build modem hardware and act as service brokers.

Because of this added hardware requirement, the decision to leverage a space relay network must be made prior to launch.

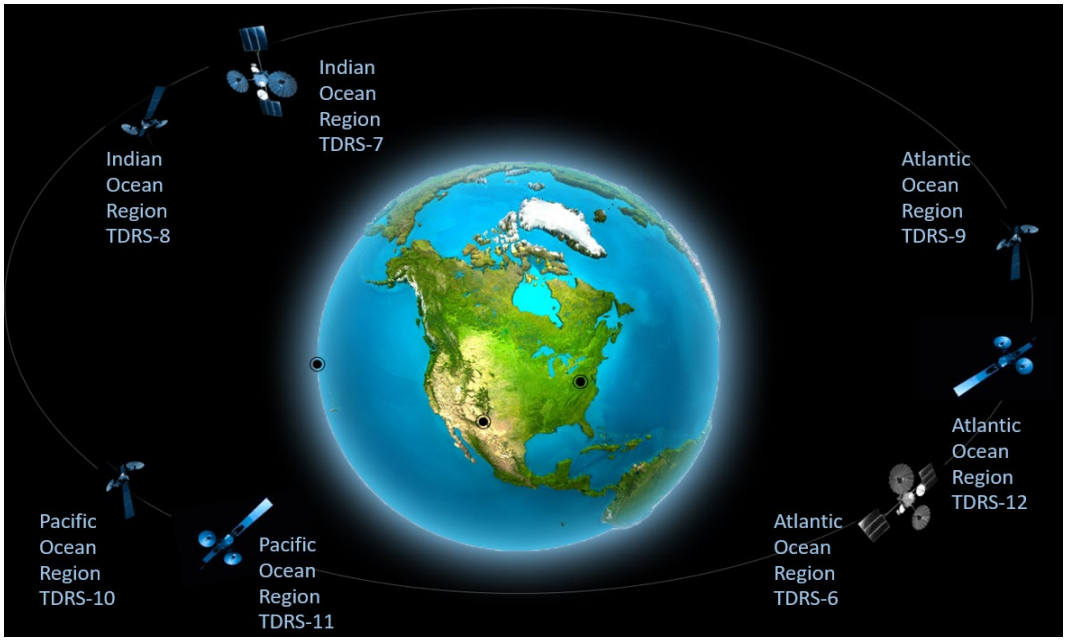


Figure 11.11: NASA's Tracking and Data Relay Satellite System. Credit: NASA.

11.4.4 Low-Latency, Low-Rate (Short Burst) Space Relay Providers

Space relay solutions are less common than traditional direct-to-Earth systems, but several options exist for small satellites (see Table 11-9). To access a space relay network, a satellite operator purchases a modem from the relay provider and integrates it onto their satellite to access relay services. In general, space relays are best suited for obtaining satellite TT&C data (health and safety of the vehicle) rather than supporting large data downlinks.

Table 11-9: Service Providers for Space Relay Networks

Product	Manufacturer	TRL	Specifications
Iridium Global Network	Iridium	9	LEO relay requiring 9600 series transceivers onboard the satellite
Fast Pixel Network	Analytical Space	6	Establish a data transport network in LEO

The Iridium network is one example that satellite operators can use for delivering low-latency messages. Iridium uses a combination of Frequency Division Multiple Access (FDMA) and Time Division Multiple Access (TDMA) for its communication waveforms. L-band (1616–1626.5 MHz) is used for uplink and downlink between the user spacecraft and the Iridium constellation. Inter-satellite communication links between Iridium satellites are accomplished through Ka-band (23.18–23.28 GHz). Operators install an Iridium transceiver (9600-series) onboard their spacecraft to communicate with the Iridium network. Messages are relayed through Iridium's Short Burst Data Service, which is hosted on Iridium's cloud platform for easy user operation. For each transceiver unit, a data plan must be selected and purchased, much like cellular phone data plans, and the plan details are linked to the unit's ID, which is referred to as International Mobile Equipment Identity (IMEI). The key feature of this system is the option for "IMEI-to-IMEI" transmission. When an Iridium IMEI is activated, up to five output destinations may be specified. Most vendors allow for a combination of email addresses, fixed IP addresses, or another device with an IMEI.

Iridium has announced the commercial availability of its Certus 100 “midband” service, providing 88 kbps connectivity via small antennas and battery-powered devices for basic data communications and Internet of Things (IoT) applications (5)

Analytical Space is another company to monitor for future services. Their recent contract will place a LEO relay in orbit to aggregate data from GEO satellites. Through the Fast Pixel Network, Analytical Space Inc. plans to establish a data transport network in low-Earth orbit to ingests data from geospatial intelligence satellites, transfer data between nodes via high-speed optical intersatellite links, and deliver it to military, intelligence and commercial customers (6). High-speed MEO and GEO commercial relays are not currently operational, but several are planned. These are listed in the State-of-the-Art Ground Data and Supporting Systems section (11.9).

11.5 Ground Stations Components

The hardware for ground stations consists of the tracking antenna, its feed, and the modem that converts the RF waveform into digital packets and vice versa.

11.5.1 Ground Station Operation

A DTE ground station is comprised of a system of hardware and software that work together to convert an RF signal from a satellite into digital data. The first key element of the system is the antenna. It is selected based on the frequency and gain required to communicate with the satellite. NASA uses parabolic reflector antennas for RF ground communications, while some universities use dish or Yagi antennas.

The dish antenna uses a parabolic reflector to collect signals from the spacecraft and focus them onto a feed antenna. The feed antenna is typically a horn antenna with a circular aperture. The size of a dish is at least several wavelengths in diameter at the frequency of operation and can be increased for higher gains. The distance between the feed antenna and the parabolic reflector can also be several wavelengths. For example, a Ka-band 34 m deep-space antenna with a feed distance of 15 m would be approximately 3,000 wavelengths for the dish diameter and 1,500 wavelengths for the feed distance, relative to a 1 cm Ka-band wavelength. The gain of a dish reflector (Figure 11.12) is frequency-dependent and directly proportional to the square of its diameter. Dish antennas are available in sizes ranging from 1 meter to 70 meters in diameter.

The antenna collects RF waves, and the antenna feed converts the electromagnetic waves into conducted RF electrical signals. The feed consists of a resonant pickup tuned to the transmit or receive frequency, a low-gain low-noise amplifier, a sharp filter, and a second LNA with higher gain than the first amplifier. These elements condition the signal. The signal then travels through a coaxial cable to a nearby location where a radio demodulates the RF signal into digital data. In the uplink direction, the radio modulates data bits onto an RF carrier, which is amplified to 10 W or more. The amplified RF signal is transmitted through the antenna feed, and the antenna radiates and focuses the electromagnetic waves towards the satellite.



Figure 11.12: Ground Antenna in Fairbanks, Alaska. Credit: NASA/ Clare Skelly.

It is desirable to have high antenna gain; however, as the gain increases, the beamwidth decreases. There is a practical trade-off in which the beamwidth may become so narrow that tracking is difficult, or the antenna becomes so large that it is difficult to procure or manage. A typical antenna radiation pattern is shown in Figure 11.13. There is a main lobe where most of the transmitted energy is concentrated. The remaining energy is distributed in the sidelobes on either side of the main lobe. The reduced sidelobes are intentional to minimize reception of ground noise from terrestrial emitters and to limit interference to other systems during transmission. The blue arrows in the Figure indicate the full-width half-max gain point at about ±6°, corresponding to an allowable antenna pointing error of less than 6° and an effective gain of approximately 16 dBi for link budget calculations. If higher gain is required, the antenna size will increase and the beamwidth will correspondingly decrease.

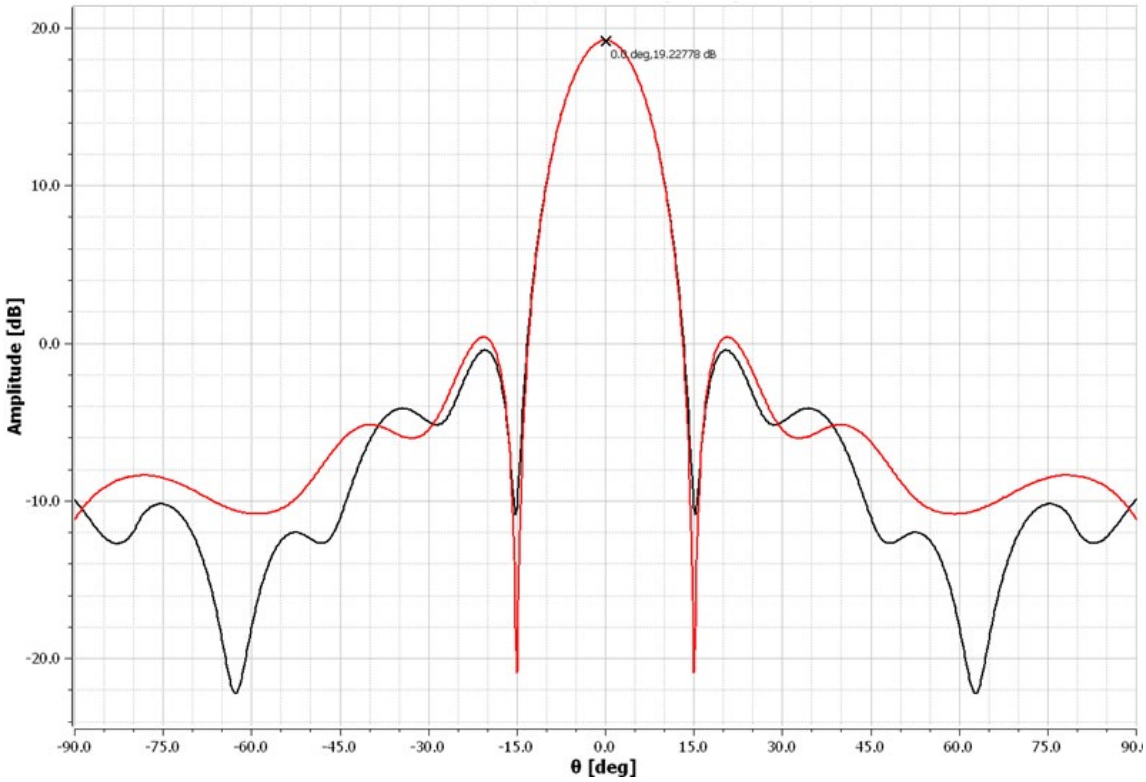


Figure 11.13: Antenna pattern from a 1.8-meter diameter parabolic dish operating at 915 Mhz with a high gain center lobe and diminished side lobes. Credit: NASA.

Directional antennas point toward the satellite as it moves over the ground station. Pointing adjustments are required in both the vertical (elevation) and horizontal (azimuth) directions. These movements are accomplished using motors and gear systems. Tracking software is used to predict the satellite's future position. The satellite position and time are processed through additional software that converts this information into commands for the antenna motor controller. Time is critical factor, and GPS time is used by the computer generating the satellite position estimate. A dedicated GPS receiver is connected to the computer for this purpose.

The cost of a DTE ground station is directly correlated with the aperture size, which drives the requirements for the ground station foundation, pedestal, motors, and gear systems. Yagi antennas are generally less expensive. They sustain lower wind loads and therefore can use smaller foundations for support. In contrast, dish antenna reflectors sustain comparatively high wind loading and therefore require stronger concrete foundations and larger motor and gearbox assemblies than Yagi antennas.

11.5.2 Component Hardware for Ground Systems (GS)

This section provides examples of GS components and supporting equipment. Table 11-10 lists representative products in each category. The antenna feed consists of the RF pickup, LNA, and mechanical filters located directly on the antenna. A radome is an RF-transparent enclosure that protects the antenna from environmental conditions.

Table 11-10: Ground System Components

Product	Manufacturer	Type of Product
Tracking Antenna	Viasat, Safran	Antennas for small satellites in and S, X and Ka-band frequencies
Antenna Feed	See End-to-End Hardware Section 11.7.2	RF pickup, mechanical filters, LNA
Radio, Software Defined	NI Ettus Research	USRP X410, up to 7.2 GHz with RFSOC advanced FPGA and meeting wide bandwidth requirements. USRP X310: DC-6 GHz with up to 160 MHz of baseband bandwidth, multiple high-speed interfaces
Data Receiver	Safran Data Systems	Cortex CRT (low data rate) and HDR (high data rate (previously by Zodiac)
Modem, for TT&C and Payload Reception	Safran Data Systems	Satcore, plug-and-play modem for TT&C and Payload Reception
Digital Processing	Kratos	SpectralNet: Digital IF product that converts analog signals at RF frequencies up to S-band into digital IF packets.
Radome	Infinite Technologies	Antenna radomes
Ground Station Dongle	GAUSS	A USB low-power board to simulate ground station in laboratory conditions. The USB dongle integrates both a low-power UHF transceiver and a TNC, thus miniaturizing common ground station rack systems
Integrated Testing Systems (EGSE) & Ground Station TT&C Modems	Celestia Satellite Test & Simulation	Hardware and software elements all operating within a single reference platform and environment
Tracking Antenna	SatRev S.A.	Antennas for small satellites in and UHF and S-band frequencies
Modem, for TT&C and Payload Reception	SatRev S.A.	UHF for TT&C and Payload Reception
Radome	SatRev S.A.	Antenna radomes

Cortex HDR

Several NSN, SSC, and NOAA stations use the Cortex HDR High Data Rate Receiver, which performs demodulation, decoding, and frame synchronization on the X-band data stream. Each virtual channel in the AOS frame received by the station's X-band receiving system is written into separate files. Files are separated into one-minute intervals for a single VCID, enabling faster turnaround time and smaller transmission units in case of transfer issues. File-based data is stored in a buffer (e.g., for 7 days) for retransmissions and failure recovery when necessary. At

the end of a pass, ground stations such as NSN sites perform an automatic secure file transfer protocol (SFTP)/secure copy protocol (SCP) push to the customer. If the customer wants to "replay" a dataset, they may use the self-service SFTP/SCP interface to pull their data to their site. Alternatively, the customer may choose to manually retrieve files instead of using automatic file transfer **Error! Reference source not found.**

USRP X310 and X410 Open-Source Software-Defined Radios for SatCom Applications

The NI Ettus Research brand includes the Universal Software Radio Peripheral (USRP) family of products. The USRP is one of the most widely used open platforms for small satellite communications, with options ranging from high-performance to low-cost to highly deployable configurations. One of the most widely used hardware units for satellite communication applications is the USRP X310 with the UBX RF daughterboard. The USRP X310 is a high-performance software-defined radio capable of transmitting and receiving modulated signals. With up to 160 MHz of instantaneous bandwidth and a frequency tuning range up to 6 GHz, the X310 with UBX provides the raw hardware performance required for many ground station satellite communication applications. The USRP family supports a wide range of software toolchains, from LabVIEW to GNU Radio, with many existing IP modules for modulation and demodulation. The USRP X310 is intended for laboratory environments; however, it can be configured for rugged, weatherproof applications. Many small satellite researchers use the USRP as ground station equipment due to its adaptability with open-source software and its embedded FPGA preprocessing capability. The USRP X310 offers two channels, 10 GigE, and PCIe intergace, whereas the NI Ettus USRP X410 is equipped with dual 100 GbE interfaces capable of significantly higher data throughput (13).

Kratos OpenSpace SpectralNet

OpenSpace SpectralNet eliminates the distance constraints in RF transport by digitizing RF signals into standard VITA-49 or DIFI IP packets for transmission over IP networks while preserving frequency and timing characteristics, and then reconstructing the RF signals at their destination. By eliminating distance constraints between antennas and signal processing equipment, this technology enables operators to deploy new ground architectures with several advantages, including mitigating rain fade effects for Ku/Ka satellites, reducing costs through centralizing operations, simplifying disaster recovery and system maintenance, optimizing antenna placement, and enabling migration from hardware-based ground systems to virtual ground systems. SpectralNet performs these functions while protecting the operator's existing investment in current equipment. In addition to removing distance constraints, digitizing RF signals into DIFI packets provides a pathway to virtualizing network functions such as modems and receivers that run on general-purpose computing platforms. For more information, see https://www.kratosspace.com/.

Integrated Testing Systems and Ground Station TT&C Modems

Celestia Satellite Test and Simulation (Celestia STS) provides ground-based solutions in satellite simulation, testing, communication, and data processing. Equipment is available in standard configurations or can be customized to meet specific mission requirements. These systems are typically deployed in AIT (Assembly, Integration, and Test) cleanroom environments or ground stations. Celestia EGSE solutions have been used in more than 80% of European Space Agency (ESA) missions.

Celestia STS develops ground-based satellite testing and communication systems and adapts its products to meet specific mission requirements. The company has extensive experience in ground segment engineering and is positioned to support evolving industry needs. Increasing demand for high-speed, secure data transmission is driving the adoption of optical communications for satellite-to-ground and inter-satellite links (7).

Infinite Technologies Radomes

A well-designed radome serves as a protective cover for an antenna while minimizing adverse effects on its electrical performance. Figure 11.14 illustrates an example of a radome supplied by Infinite Technologies. Radomes create a controlled environment for the antenna system, shielding sensitive equipment from environmental stresses such as wind, snow, ice, and salt spray. By protecting the antenna from these elements, a radome can extend its operational life and reduce maintenance costs.



Figure 11.14: Infinite Technologies small radome. Credit: Infinite Technologies.

Incorporating a radome early in the system design phase is important. Doing so allows the use of lighter and more cost-effective components, such as drive motors and foundations, because the radome eliminates wind loads on the antenna. Additionally, the controlled environment within the radome increases system availability, enabling the antenna to operate efficiently under harsh environmental conditions with minimal signal degradation. Maintenance personnel also benefit from the radome, as it provides protection from weather during antenna maintenance activities.

For a radome to be effective, it must be tailored to the specific requirements of the system it protects. A carefully selected and well-designed radome can enhance system performance and reliability by:

- Enabling operation in severe weather conditions by shielding the antenna from wind, rain, snow, hail, sand, salt spray, insects, animals, UV exposure, windblown debris, and extreme temperature fluctuations.
- Creating a controlled environment that minimizes downtime, extends component and system life, and supports more economical choices in antenna pedestals, foundations, and drive systems.
- Providing security and protection for the antenna system against observation, vandalism, and other threats.

11.5.3 Ground Software

Ground software visualizes and calculates the satellite location in orbit and controls the tracking antenna. Command and control software manages command scripts sent to the satellite and can display and analyze telemetry. Many software options are open-source and free. Other software

may be purchased from companies with a long history in ground segment solutions that have previously provided hardware products to perform these tasks (Table 11-11).

Table 11-11: Software for Ground Systems

Product	Manufacturer	TRL	Type of Product
softFEP	ARKA AMERGINT	9	Software commands and telemetry data processor handling formatting and interface conversion. Full support for NSA Type 1 crypto, AES encryption/decryption and CCSDS data links.
OpenSpace quantumFEP	Kratos	9	Software that performs data formatting and interface conversion for commands and telemetry, with full support for NSA Type 1 and AES encryption/decryption devices.
Gpredict	Alexandru Csete	9	Open-source software that tracks satellites and provides orbit prediction in real-time. Radio and antenna rotator control for autonomous tracking.
GNU Radio	GNU Project	9	Free software development toolkit that provides signal processing blocks to implement software-defined radios and signal processing systems.
HWCNTRL	DeWitt & Associates	9	Ground station control program with an automation software package.
Expedite	Remos Space Systems, AB	9	CPU-based software modem for telemetry, telecommand, and payload data over UHF–L-band links, featuring integrated mission scheduling and transmission sequence control.

softFEP

ARKA AMERGINT softFEP applications are deployed virtually on cloud architectures or hosted on dedicated servers. The applications perform control center data formatting and interface conversion for commands and telemetry, with support for NSA Type 1 and AES encryption/decryption devices. SoftFEP applications are built on a proven library of more than 1,000 software components. This allows each softFEP application to be tailored to the specific requirements of the ground system. Processing chains configured via Python scripts move satellite downlink data from ground receipt for processing and route uplink data to the radiating site. Deployment of softFEP on multiple virtual machines (VMs) or within the cloud is inherent in the product architecture. Virtualized softFEP deployments support a wide range of ground system architectures while leveraging cloud-computing benefits. When applications are deployed in VMs, they can be hosted locally or run remotely in the cloud and interoperate across network connections. Customers have deployed softFEP applications as independent network gateways, black front-end processors, red front-end processors, and data recorders, flowing data between the VMs as a satellite contact is processed. Visit https://arka.org/ for more information.

quantumFEP

Kratos developed OpenSpace quantumFEP (qFEP) is a virtual front-end processor for TT&C. The system is designed to match the requirements, schedules, and budgets of quick-turn programs. qFEP connects C2 systems to RF signal processing equipment, handling command and telemetry stream formatting, encryption/decryption, CCSDS processing, and network interfaces to either quantumRadio (qRADIO) or third-party ground antenna networks. Supported deployment options include generic compute servers, virtual machine environments, bare-metal installations, or orchestration through Kratos OpenSpace Platform,

and qFEP's small memory footprint allows for more efficient use of system resources. In addition, the product achieves hardware independence by eliminating custom drivers, firmware, and hardware cards. Figure 11.15 illustrates the qFEP system architecture. For more information, see https://www.kratosspace.com/.

Key features of quantumFEP are:

- Pure software implementation for signal processing functions
- Support for CCSDS TC, TM, and AOS frame protocols, as well as Cadet, AX.25 and Reed=Solomon Encoding
- Suitable for a wide range of satellite programs
- Compatibility tested with widely used ground-station modems
- Built-in test functions reduce integration and test (I&T) effort and cost
- Configurable as mission requirements change or as new missions come online
- Commercial AES encryption/decryption standard feature with built-in AES key manager
- Standard TCP/IP, GEMS, REST, and VITA-49 interfaces support seamless integration
- Access and control from anywhere through the web, with no client software to install or maintain

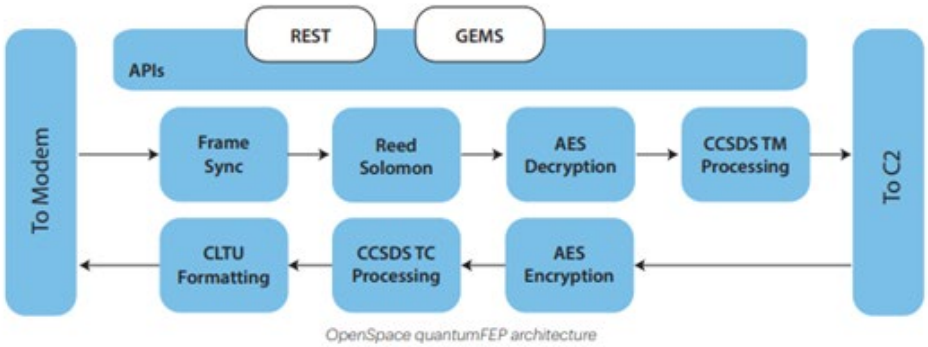


Figure 11.15: Kratos qFEP system architecture. Credit: Kratos.

Gpredict

Gpredict is a real-time satellite tracking and orbit prediction application. It can track a large number of satellites and display their positions and other data in lists, tables, maps, and polar plots (radar view), as shown in Figure 11.16. It can also predict future passes and provide detailed information about each pass. Gpredict differs from other satellite tracking programs in that it allows satellites to be grouped into visualization modules. Each of these modules can be configured independently, allowing unlimited flexibility in the look and feel of the modules. It also allows satellite tracking relative to multiple observer locations simultaneously. http://gpredict.oz9aec.net/

The following are key features of the software:

- Fast, accurate real-time satellite tracking using the NORAD SGP4/SDP4 algorithms
- No software limit on the number of satellites or ground stations
- Appealing visual presentation of the satellite data using maps, tables, and polar plots (radar views)
- Allows satellites to be grouped into modules, each with its own visual layout and independently confirgurable; multiple modules can be used simultaneously
- Radio and antenna rotator control for autonomous tracking

- Efficient, detailed prediction of future satellite passes, with user-configurable parameters to support both general and specialized predictions
- Context-sensitive pop-up menus allow future passes to be quickly predicted by selecting any satellite
- Extensive configuration options that allow advanced users to customize both the functionality and look and feel of the program
- Automatic updates of Keplerian Elements from the web via HTTP or FTP, or from local files
- With a robust design and multi-platform implementation, Gpredict can be integrated into modern computer desktop environments, including Linux, BSD, Windows, and MacOS X
- As free software licensed under the GNU General Public License, it can be freely used, studied, modified, and redistributed

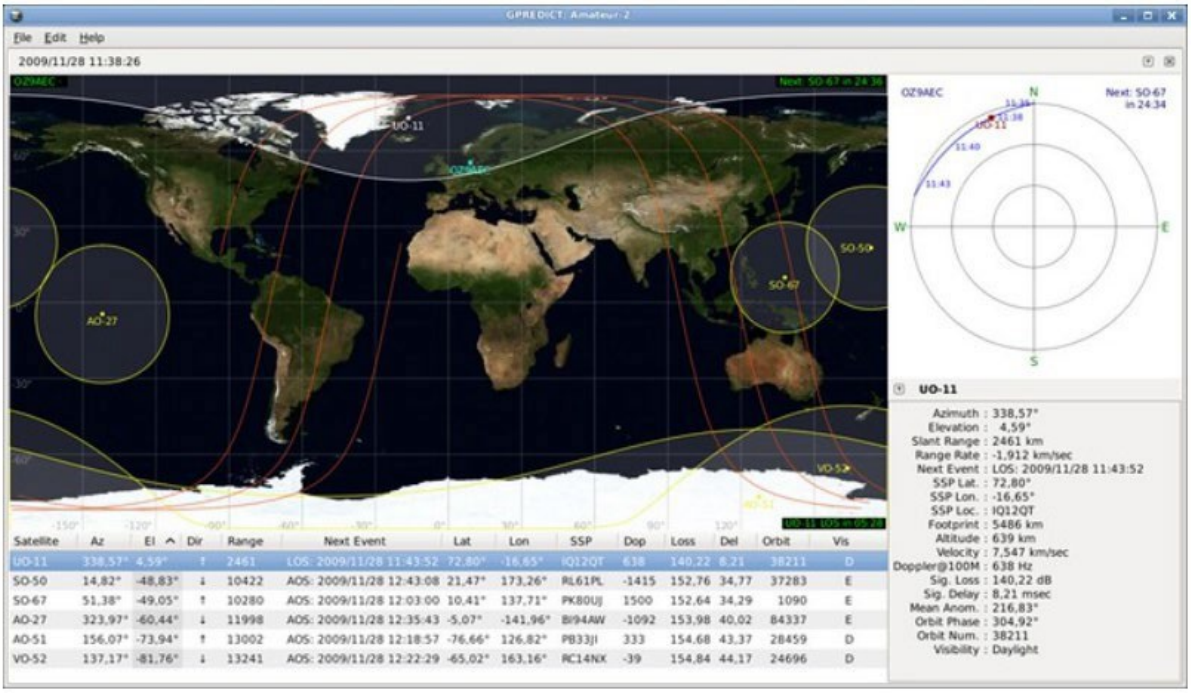


Figure 11.16: Gpredict graphical display with multiple satellites. Credit: Gpredict.

GNU Radio

GNU Radio is a free and open-source software development toolkit for developing radio systems in software rather than entirely in hardware. It can be used with readily available, low-cost external RF hardware and runs on most modern computers to create software-defined radios. It can also be used without hardware in a simulation environment.

GNU Radio performs signal processing and can be used to develop applications that receive data from digital streams or to transmit data into digital streams, which are then sent using hardware. GNU Radio includes filters, channel codes, synchronization elements, equalizers, demodulators, vocoders, decoders, and other elements (referred to as blocks) typically found in radio systems. It also provides a method for connecting these blocks and managing how data is passed between them. Blocks can be implemented in C++ or Python.

As GNU Radio is software-based, it handles only digital data. It operates on digitally sampled

waveforms that can correspond to RF signals with digital or analog modulation. Typically, complex baseband samples are the input data type for receivers and the output data type for transmitters. Analog hardware is then used to shift the signal to the desired center frequency. Aside from this requirement, any data type can be passed between blocks, including bits, bytes, vectors, bursts, or more complex data types. GNU Radio supports heterogeneous computing, where some blocks run on an FPGA or GPU. These acceleration techniques are particularly important for processing large bandwidths or data rates, especially in embedded platforms where size and power consumption are usually constrained. Execution scheduling and data movement in heterogeneous environments are active areas of development and research in the GNU Radio runtime. GNU Radio can be used on embedded systems, such as ARM SoCs running Linux, as well as on more powerful desktop or server systems. GNU Radio is frequently used as part of ground stations, both for standard protocols such as CCSDS and for custom modems. Some commercial ground-station-as-a-service solutions that support GNU Radio modems include Azure Orbital Ground Station and AWS Ground Station. Another example is the open-source, community-driven SatNOGS network. GNU Radio is also useful for prototyping and laboratory testing. Additionally, some small satellites run GNU Radio on-board, typically as part of a flexible SDR payload. Figure 11.17 shows an example of a GNU Radio block diagram. For more information, visit wiki.gnuradio.org/index.php/Main_Page.

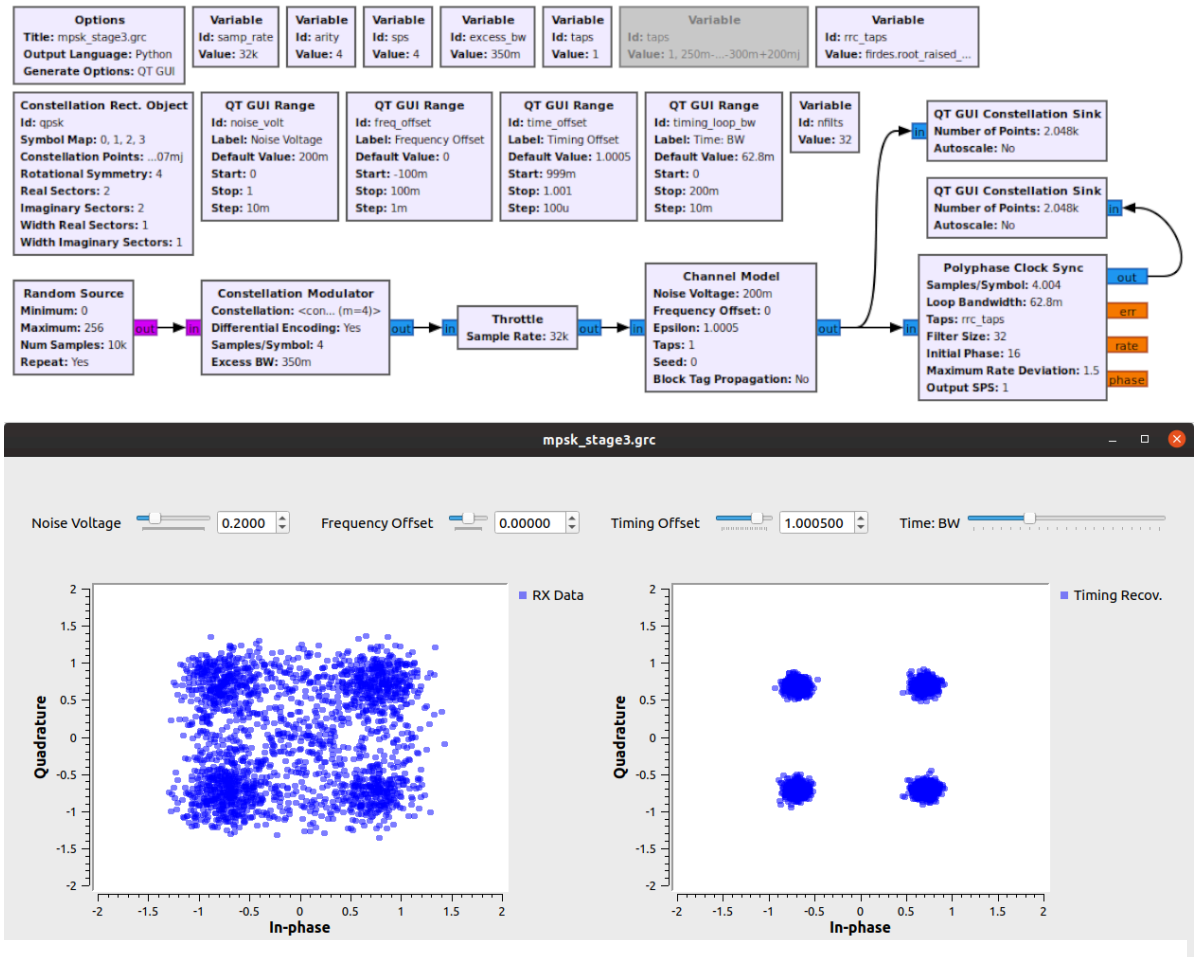


Figure 11.17: GNU Radio block diagram example for a 2-meter NBFM receiver. Credit: GNU Radio.

HWCNTRL

HWCNTRL is a satellite ground station control program installed on more than 30 sites worldwide. This automation software package supports multiple antennas and instruments simultaneously. Satellite passes are generated upon user request based on the ephemeris set, and users can select specific passes to add to the schedule. Scheduled events can be single-use or recurring on a daily or weekly basis. A control/status screen is available for each instrument in the system, and users can view and modify instrument settings through these screens. For more information, visit https://www.dewitt-assoc.com/groundStation.html.

Expedite

The Expedite software modem by Remos Space Systems performs real-time demodulation, decoding, encoding, and frame synchronization in compliance with CCSDS standards, and supports data exchange through TCP/IP, REST, WebSocket, and FTP interfaces. As the central control unit, Expedite directly manages the sequencer, which coordinates signal routing, timing, and safety interlocks. The sequencer controls high-power amplifiers (HPAs), low-noise amplifiers (LNAs), and RF switches to support both half- and full-duplex communication modes, ensuring safe and synchronized operation during transmit and receive transitions. Expedite is compatible with widely used small satellite transponders including GomSpace AX100 and X2150, Clyde Space, EnduroSat, and ISIS, and is used across government, commercial, and academic ground stations worldwide. For more information on Remos Space Systems, please reach out to info@remosspace.com.

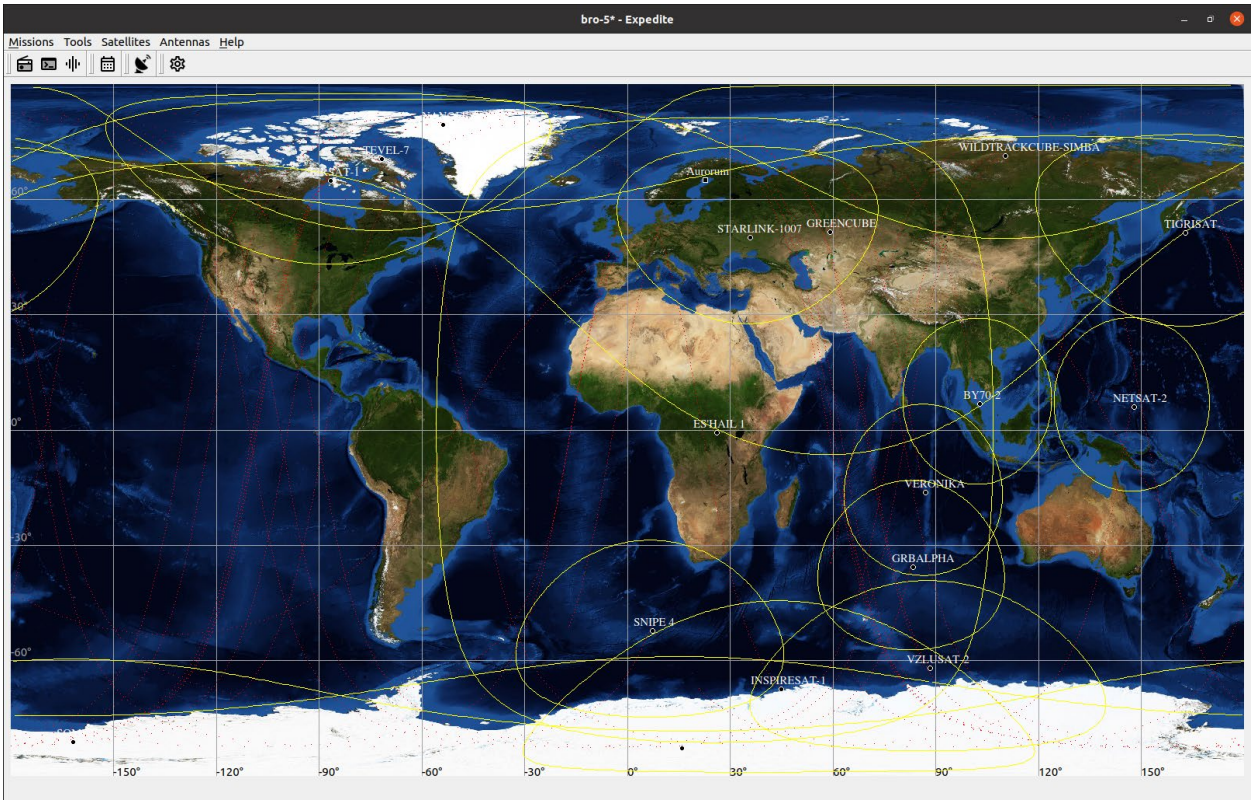


Figure 11.18: Expedite Main GUI showing tracked satellites. Credit: Remos Space Systems, AB.

11.6 Mission and Science Operations Centers

The Mission Operations Center (MOC) is where satellite commanding is generated, ground station control is managed, and telemetry is archived. It is typically a physical location where the resources required to operate the satellite is located. It is often located in a secure room with controlled access to protect the satellite operating equipment and prevent unauthorized control. The room typically contains several terminals, allowing multiple subsystem experts to review telemetry or run analysis programs concurrently. An example of a MOC with multiple terminals is shown in Figure 11.19.



Figure 11.19: Mission Operation Center at NASA Ames Research Center. Credit: NASA

The size of the MOC is determined by mission complexity. More personnel are present during critical events or when resolving anomalies. For a SmallSat mission, complexity is typically lower, and the MOC is correspondingly smaller. In addition to the terminals and telemetry analysis software, other resources are used to manage the satellite. These may include physical models of the satellite used to study anomalous telemetry. In the case of CubeSats, a functioning spacecraft engineering model may be used to test commands and reproduce anomalies.

All tasking requests for future satellite operations are managed by the mission operations team. The team generates command plans, simulates satellite response to verify those plans, and, if confidence in the simulations is insufficient, executes the commands on engineering model hardware prior to approval for upload. The MOC team also manages downloads. They determine the availability of ground resources. If the MOC does not own its own ground stations, a contact request is submitted to the ground station provider. The MOC submits data required for satellite commanding, including commands and payload parameter settings, a schedule of events for the flight computer, and ephemeris and pointing tables for the attitude control system, along with a mission timeline. After contact, data are returned to the MOC by the ground station.

Prior to launch, rehearsals are conducted with all personnel at their stations, using simulated telemetry with inserted anomalies to test the team. This ensures readiness with the appropriate analysis software and integration test data to quickly diagnose issues and propose corrective actions. At the time of launch, the MOC is fully staffed, as this is a critical event. Telemetry must be interpreted and acted upon quickly.

The Science Operations Center (SOC) is the focal point for all mission science data. The science team uses it to store and analyze data. From this analysis, the science team generates satellite

tasking requests that are sent to the mission operations team. External requests for additional data collection are first evaluated by the science team to assess feasibility before tasking requests are submitted to the operations team.

The SOC is typically separate from the MOC. The payload developer typically maintains a separate operations center at their facility with access to supporting resources. Before cloud-based storage, the SOC was a physical location where data servers resided to archive mission science data. Prior to secure network solutions, dedicated computers within the SOC ran programs specifically designed to analyze science data. If the mission was secure and the data classified, the physical SOC was protected with restricted access. Missions that do not produce classified data can take advantage of a virtual SOC, where science data and analysis tools reside in the cloud. A virtual SOC allows scientists to access data remotely without requiring a physical location. As cyber security techniques improve, more secure missions may adopt virtual SOC architectures, with only highly classified missions maintaining secure physical SOCs.

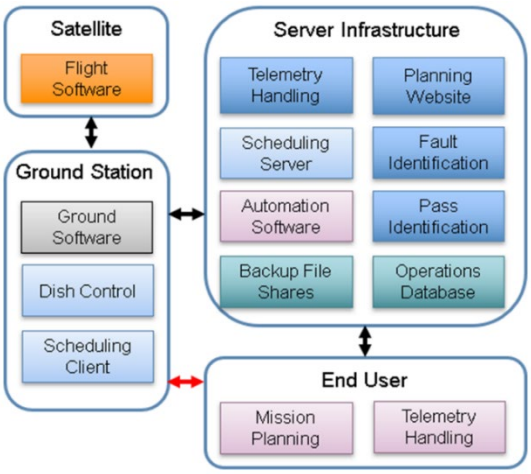


Figure 11.20a: Software functions for elements within the ground segment. Credit: NASA.

11.6.1 Software for Mission Operations

Mission operations rely on software across all elements of the ground segment. Figure 11.20a outlines software functions for each element. Satellite flight software manages state-of-health telemetry, payload data, and interfaces with ground segment software. Figure 11.20b provides an example of command and telemetry data flow for a mission using DTE and relay services. Transmission can begin autonomously by programming the satellite to recognize when it is over a ground station or within view of a relay

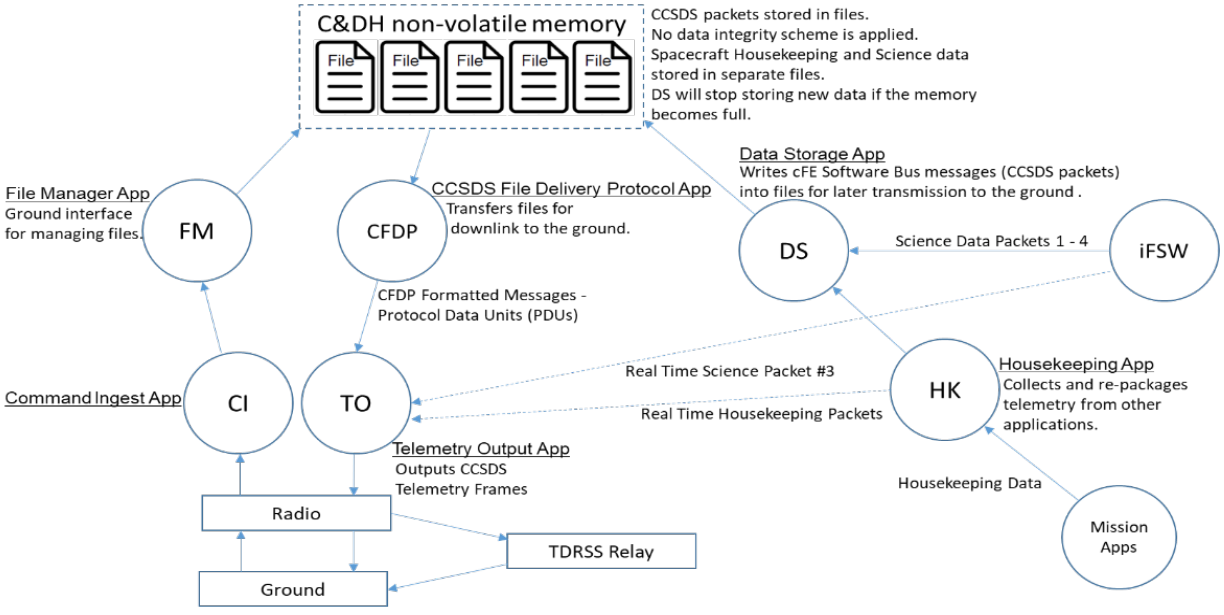


Figure 11.20b: Command and telemetry data flow for a SmallSat mission using DTE and relay services. Credit: NASA.

satellite. Transmission can also be triggered by a command from a ground station or relay satellite. When a communications link is established, the radio enters a higher-power transmit mode and sends the data. The flight software manages data flow into and out of the radio, ensuring buffers do not overflow. It formats housekeeping and science data into packetized formats compatible with ground station requirements. Ground networks use established data protocol standards. For example, NASA's NSN incorporates standards proposed by the CCSDS. The flight software unpacks received packets to retrieve uploaded commands and data.

Software supporting the ground segment exists onboard the satellite, at the physical ground stations, and within the MOC (including server infrastructure and end-user applications). Ground stations use software for antenna control, command generation, signal formatting and encoding, pass scheduling, and MOC interfacing. One software computes pointing direction using Two-Line Element (TLE) data, a mount model, and GPS time. It generates time-based motor control commands. The motor controller executes these commands to track the satellite during a pass. During the pass, another software suite monitors the link, processes and encodes commands, handles signal formatting or encryption, and demodulates and decodes received transmissions. This software also manages the network connection with the MOC, including TLE updates, data uploads, and data retrieval requests. After contact, received data are transferred back to the MOC. The ground station may also generate its own telemetry for contact. This data is used to trend system performance. Performance trending provides insight into degradation for both the satellite and the ground station. Ground stations may also use scheduling software when supporting multiple missions. This software uses orbit simulation and current TLE data to determine expected contact times. It identifies conflicts between contact opportunities and assists with schedule optimization. A schedule is generated for a given period and is programmed into the ground station control system for execution. This process can be automated, but an operator typically monitors the system.

Mission planning software in the MOC is required for missions involving complex satellite behavior, such as target pointing during science data collection. The software includes models of satellite dynamics and component capabilities. Events are planned as sequences of actions executed in a defined order with estimated timing. The software simulates satellite response, and actions and timing are iteratively adjusted to optimize performance and avoid fault conditions. The output includes all commands and databases required by the satellite. This output is submitted to ground station ingest software for upload prior to the planned event.

The SOC uses software to handle the receipt, unpacking, reconstruction and post-processing of mission science data. Using an ISS payload as an example, science data are downlinked via TDRSS to NASA Marshall Space Flight Center (MSFC), where they are separated into science streams and routed to the appropriate payload SOCs. At the SOC, a computer outside the company firewall continually operates to receive data from MSFC. On this computer, NASA-provided TReK software manages data transfer by interfacing with MSFC systems. The science team retrieves the data and transfers it securely through the corporate firewall into the SOC. The science team develops parsing software to unpack data stored in CCSDS format. Additional software reconstructs the original payload data products (e.g., images). Further processing software generates post-processed data products that are archived and distributed to users. Common programming languages for these applications include Interactive Data Language (IDL) and Python.

11.7 End-to-End Communications and Compatibility Testing

A SmallSat undergoes various tests throughout its development cycle to verify proper functionality. For the communication subsystem, end-to-end communication and compatibility testing with the selected ground network is the most critical test. Compatibility testing verifies that the ground

station can properly communicate with the satellite on the uplink and downlink RF channels. Ideally, compatibility would be validated by testing the flight spacecraft with the actual ground station that will be supporting the mission. This may not be practical for larger or high-cost satellites, due to logistics associated with shipping and risk of damage. Two alternatives to shipping the satellite are typically used. One option is to include sending a replicate set of ground station hardware to the satellite facility for testing. A second option is to test with only the flight radio or an ETU radio (also common to include the flight computer) at the ground station or at a test lab configured with the ground station hardware. Drawbacks to these alternatives include not testing the exact command path or determining whether ground sensitivity is sufficient.

For CubeSats, it is commonly feasible to bring the CubeSat to the ground station for testing. If that is not feasible, then at a minimum, the radio and flight processor (or Engineering Development Units (EDUs) should be used. Testing at the ground station allows for the entire equipment chain to be part of the test, including the low-noise amplifier (LNA) and transmit/receive switch, if used. It is desirable to initially test in a closed-loop configuration, where the satellite is connected to the ground system at the antenna port via a cable (with appropriate attenuators in line). If the satellite is fully integrated, disconnecting the flight antenna may not be feasible. In this case, a small monopole antenna located indoors near the CubeSat can be connected to the ground system. The monopole antenna connection to the ground system may vary depending on the ground antenna configuration but should include as much of the ground system electronics as practical.

Some missions include an outdoor open-loop test with the CubeSat and ground antenna. This method allows for the entire ground system, including the ground antenna, to be included in the test. However, the ground antenna typically cannot point directly at the CubeSat due to mechanical limitations or to limit the received signal so ground system RF components are not overdriven. Off-pointing and reflections from the ground and local structures can also make it difficult to achieve a valid test.

End-to-end network testing primarily validates the ground station to MOC interface. This test verifies that the MOC can properly receive downlink data from the ground station and that the ground station can receive and process uplink command data. Initial end-to-end testing will validate network connectivity, showing that network connections can be established and firewall rules at the ground station and MOC are in place. Once network connectivity is established, the MOC can transmit commands to the ground station for capture. The ground station can then transmit simulated or recorded data to the MOC for validation.

It is preferable to conduct initial end-to-end network testing prior to compatibility testing. In cases where the satellite can be brought to the ground station, a full end-to-end test can be performed. Command transmissions from the MOC, through the network and ground system to the satellite can be validated. A complete end-to-end telemetry dataflow from the satellite to the control center can also be validated.

11.7.1 End-to-End Hardware for Ground Systems

A complete ground system can be provided as a kit with all the necessary components bundled together and set up to work seamlessly. These end-to-end solutions include the antenna, its controller, and the RF feed with all the necessary filtering and low-noise amplification for the particular frequency of interest. They use a software-defined radio or a dedicated transceiver to convert between digital packets and RF waveforms. Software is included to process the satellite position and direct the antenna to track it. Additional software is used to archive and display the information within the digital packets. Three vendors, GAUSS, Innovative Solutions In Space (ISISPACE) and GomSpace, listed in Table 11-12 provide solutions for the low-cost CubeSat and small satellite market. One vendor, Surrey Satellite Technology Limited, offers a higher-end system, installation services, and personnel support. The final vendor listed, Kratos, offers a

different end-to-end solution that begins with a digitized RF waveform. The Kratos Quantum software then demodulates, filters, unpacks, parses, displays, and archives the data **Error! Reference source not found.**.

Table 11-12: End-to-End Hardware for Ground Systems		
Product	**Manufacturer**	**Type of Product**
Complete Ground Solution	GAUSS	Small satellite provider offering a complete ground solution. UHV, VHF, and S-band
Complete Ground Solution	ISISPACE	Small satellite provider offering a complete ground solution. UHV, VHF, and S-band
Complete Ground Solution	GomSpace	Small satellite provider offering a complete ground solution. UHV, VHF, and S-band
Surrey Ground Segment	Surrey Satellite Technology Ltd.	Major contractor offering a complete ground solution. S-band uplink/downlink and X-Band downlink capability
Quantum	Kratos	Major contractor with a complete ground solution
Expedite Turnkey Ground Station	Remos Space Systems, AB	Integrated ground station solution combining software-defined modem, automation sequencer, and multi-band antenna system for end-to-end satellite telemetry, telecommand, and payload data operations across UHF, VHF, S-, and L-band links.
Complete Ground Solution	SatRev S.A.	Small satellite provider offering a complete ground solution. UHV, VHF, and S-band

GAUSS Ground Station Kit

The GAUSS ground station is a turnkey solution. It can be configured with UHF, VHF and S-band on the same pointing system. An example of the associated hardware is shown in Figure 11.21.

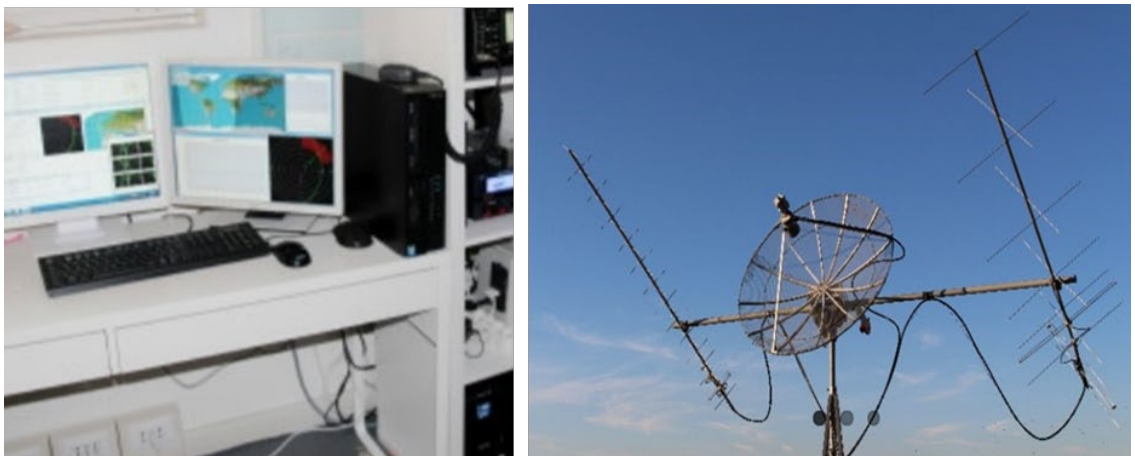


Figure 11.21: (left) GAUSS ground station hardware, transceiver and (right) tracking antenna. Credit: GAUSS Srl.

Hardware features of the systems offered include:

- High gain Yagi-Uda VHF and UHF antennas (>16 dBi for UHF)
- Low-noise amplifiers and band-pass filters for VHF and UHF bands
- Low-loss RF coaxial cables
- 1.5-meter parabolic dish for higher frequencies downlink (up to 6 GHz, default feed is for S-band)

- VHF: uplink and downlink up to 100 W using radio and Terminal Node Controller (TNC), software-defined radio (SDR) optional
- UHF: uplink and downlink up to 70 W, using radio and TNC, SDR optional
- TX using ICOM-9100 hardware, RX recording and decoding via SDR
- Several RF and electrical fuses for lightning protection
- S-Band: downlink using SDR for recording and post-processing of I/Q RF data
- Az/El rotor for high-torque maneuvering
- Hardware components power switch on/off to minimize power consumption
- Full HD camera for instant antenna monitoring and picture logging

The features of the software that accompanies the system include:

- Automatic TLE download from publicly available repositories
- SGP4 propagator as suggested by USAF NORAD's Space-Track
- Rotor control (compatibility with several rotor controllers, e.g. Yaesu, RF Hamdesign)
- Assisted rotor pointing calibration and verification using Sun position
- Fully compatible with ICOM-9100 satellite radio and GAUSS USB ground dongle
- Separated Doppler shift corrections for uplink and downlink frequencies
- DUPLEX TX/RX mode
- Instant weather check and logging to operate the ground station safely
- Lightning detection for safe antenna operation
- Instant logging of all subsystems operation
- Ground map with live Earth clouds
- Compatible with several TNCs (Kantronics, Symek, Paccomm, Kenwood)
- Email report to ground station operators
- Instant email alerts for non-nominal conditions of the satellite or GS hardware components
- Session programming for weeks of unattended ground station operations
- GUI command recording for easy session programming
- One button programming to include a whole set of commands in the session
- Manual override during pass for last-minute command addition
- Control and handling of multiple satellites using configurable priorities
- Satellite TLM decoding, graphing, and archiving into a database accessible by web
- Integrated satellite payload data handling and decoding (e.g., for image file processing)
- TCP/IP connections for remote ground station and TNC operations

For more information, visit www.gaussteam.com/services/ground-station/.

Innovative Solutions In-Space Ground Station Kit

The ISISPACE small satellite ground station is a low-cost, turnkey solution that is designed to communicate with satellites in low-Earth orbit that operate in either amateur frequency bands or commercial bands. The frequency bands covered are S-band, UHF, and VHF. The ground station consists of an antenna and a 19-inch rack which houses the transceiver, rotor control and computer which make the system very compact. Examples of these components are shown in Figure 11.22. The transceiver makes use of an SDR that provides flexibility to swiftly reconfigure modulation/coding/data-rate in real time. Most commonly used modulation schemes and coding methods are already implemented, and any customization requests can also be handled. For more information, visit www.isispace.nl.



Figure 11.22: (left) ISIS ground station hardware, transceiver rack and tracking antenna (right). Credit: ISISPACE.

GomSpace Ground Station Solutions

GomSpace offers two products (A) NanoGround, and (B) Hands-off Operations Platform (HOOP) that can be used as ground segment building blocks for a wide variety of missions.

A. NanoGround provides a communication gateway for spacecraft using GomSpace AX2150 and NanoCom Link S/SX S-band and X-band radios. NanoGround provides a TMTC link over S-band as well as IP networking over S and X-bands and is designed to be easily integrated with commercial ground station service providers. As of September 2024, NanoGround offers built-in integration for KSAT's ground station network. AWS Ground Station and LeafSpace ground station network support will be available in the near term. Other ground station networks are being considered and can be discussed based on client need. https://gomspace.com/product/nanoground/

B. HOOP is GomSpace's Mission Control software solution, providing autonomous "hands-off" satellite operations for single spacecraft and constellations. HOOP can either be operated by GomSpace's Mission Operations Team for client missions or it can be purchased by clients on a subscription basis to manage their own missions. HOOP comes pre-built with integration for GomSpace NanoGround, providing an out-of-the-box solution to operate missions flying GomSpace satellites. HOOP's capabilities will be expanded in the near term with an upcoming release to support CCSDS communication protocols. This expanded capability will allow HOOP's application domain to include third-party satellites. HOOP has been in operation since 2020 and currently manages LEO missions. As of September 2024, five additional HOOP missions are in development and planned for near-term execution. https://gomspace.com/hoop.aspx

Surrey Satellite Technology Ltd. Ground Station Kit

Surrey can provide complete turnkey ground segment solutions for a range of space platforms, including all the hardware and software necessary to operate, maintain, process and archive data. Services provided by Surrey include:

- S- and X-band ground stations with full motion antenna systems from 2.4 meters to 7.3 meter in diameter, with radome options available for harsh climates
- SSTL Pilot Satellite Control Software
- Mission planning systems
- Radiometric and geometric image processing
- Data storage solutions
- Site surveys, ground segment installation and training
- Technical and maintenance support packages

In addition, Surrey can work with customers to integrate their ground segment solutions with existing ground infrastructure or with third-party ground station networks. For more information on Surrey Satellite Technology, visit https://www.sstl.co.uk/contact-us.

Kratos Ground Station Solutions

Kratos virtual ground solutions begin with the OpenSpace SpectralNet digitizer converting analog signals at RF frequencies up to S-band into digital IF VITA-49 or DIFI IP packets. Kratos Quantum virtualized network functions (VNFs) such as quantumReceiver (qRX) or quantumRadio (qRadio) then process the digitized RF waveform. Kratos virtualized network functions run on general-purpose compute and can be dynamically instantiated for different mission directives like mission data downlink and TT&C at the click of a button. Figure 11.23 provides a visualization for the system concept.

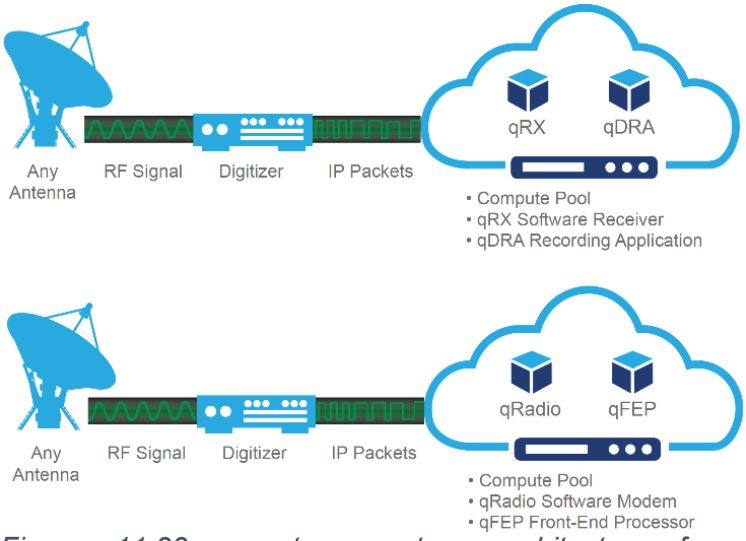


Figure 11.23: quantum system architecture for wideband satellite signal processing for mission data downlink (top) and narrowband satellite signal processing for TT&C and narrowband payloads (bottom). Credit: Kratos.

All components are available separately to support an existing C2 solution or third-party ground network with existing signal processing and antenna resources. The quantum products include:

1) quantumCommand (qCMD), COTS software application for command and control (C2) of small spacecraft;
2) quantumFEP (qFEP), connects C2 systems to RF signal processing equipment: handling command and telemetry stream formatting, encryption/decryption devices, CCSDS processing, and network interfaces to either qRADIO or third-party ground antenna networks;
3) quantumRadio (qRadio), the software modem for RF signal processing on-premise or in the cloud;
4) quantumDRA (qDRA), a data recording and archiving application supporting CCSDS/non-CCSDS header and channel data routing with IP-based interfaces;
5) quantumRX (qRX), a fully virtualized wideband software receiver, specifically tuned to streaming Earth observations in near-real time with 500 MHz bandwidth using Digital IF digitizers;
6) quantumTX (qTX), a fully virtualized wideband software transmitter, specifically tuned for Earth observation and remote sensing satellites with over 1 Gbps throughput for uplinks.

In 2021, Kratos introduced a virtual, software-defined architecture solution called the OpenSpace Platform. As an enterprise level end-to-end system, it provides satellite operators and service providers the flexibility to scale on-demand as their operations grow in size and capability. By leveraging Digital IF over IP with time-deterministic latency and software defined networks, the platform allows virtualized functions such as modems, channelizers, recorders and combiners to be orchestrated on generic servers in a ground station or public or private cloud environment. The virtual architecture lends itself to upgrades and/or updates automatically, ensuring ongoing

reliability and security. In addition, the ability to test software releases in real time allows ground equipment functions to be included in continuous integration and continuous delivery cycles. Software-defined architectures are more agile, programmable, and automated, enabling the ground system to work in tandem with dynamic satellite payloads. By shifting from RF signals and analog equipment to a virtualized, IP-based infrastructure, orchestration can occur dynamically. Figure 11.24 illustrates the OpenSpace architecture concept. For more information on Kratos' solutions, visit https://www.kratosdefense.com/contact.

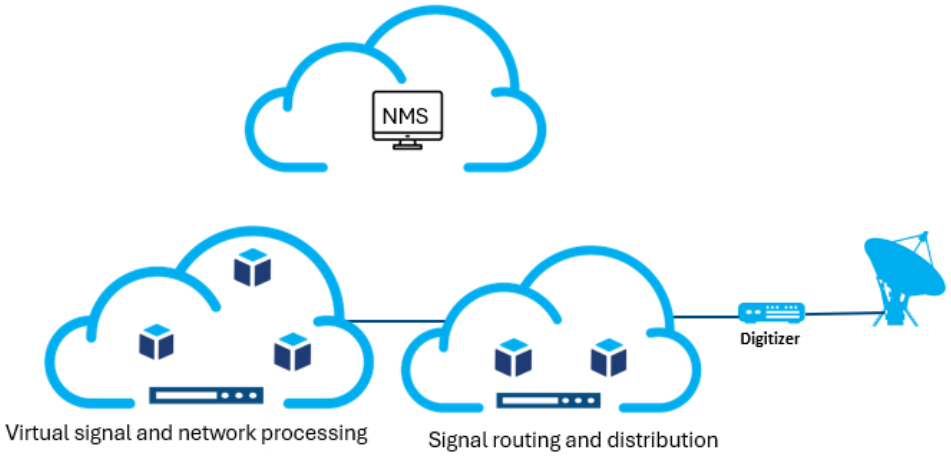


Figure 11.24: Kratos OpenSpace architecture concept keeps most of the RF ground equipment remote from the ground station. Credit: Kratos.

Remos Space Systems

The Expedite Turnkey Ground Station by Remos Space Systems is an integrated ground segment solution for UHF, VHF, S-, and L-band satellite communications. It combines the Expedite software modem (in Section 11.5.3), a sequencer, and a multi-band antenna system to provide a complete platform for telemetry, telecommand (TM/TC), and payload data operations. The system is intended for small satellite missions, academic institutions, and government programs requiring

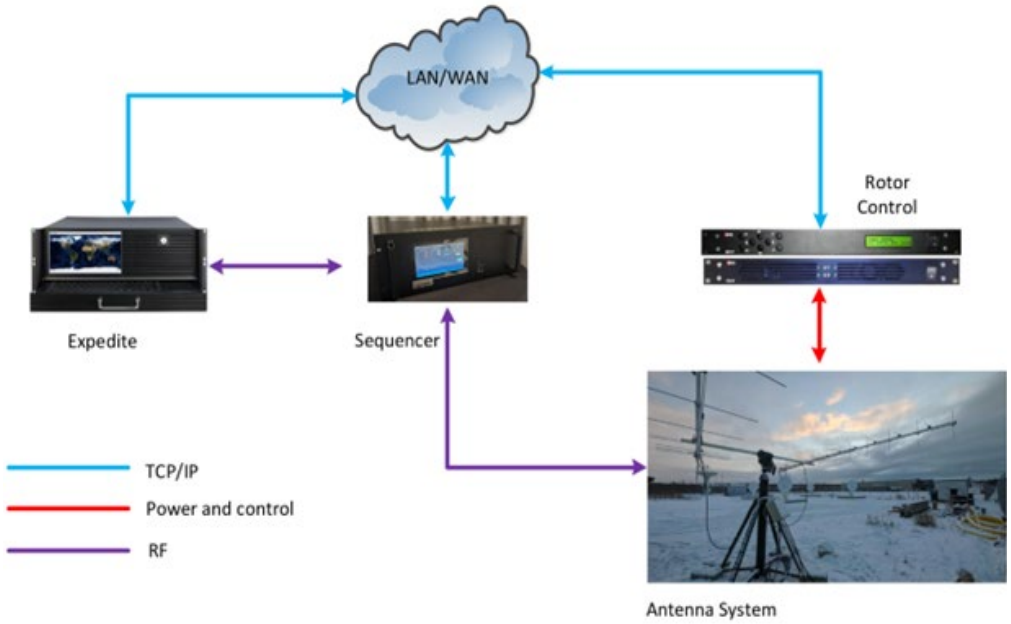


Figure 11.25: Expedite turnkey ground station. Credit: Remos Space Systems

a compact and deployable ground station. Figure 11.25 below illustrates the Expedite turnkey solution.

The turnkey configuration allows rapid installation and operation with minimal infrastructure. It includes mission scheduling, automated antenna tracking, and remote control capabilities. The system can function as a standalone unit or integrate within GSaaS networks. Typical applications include commercial and research satellite operations, academic training programs, and demonstration missions for emerging space nations. For more information on Remos Space Systems, please reach out to info@remosspace.com.

11.8 Cyber Security

Security for a space system must address all mission elements—the flight platform, payloads, ground segment, and supporting services—because attackers can target any portion of the system-of-systems. The most accessible path for a remote adversary is typically the end-to-end command path, whether by injecting signals over the RF uplink/downlink, subverting transport networks (space or ground), or compromising command authority (e.g., operations centers). External dependencies (e.g., GNSS/PNT services, ground stations, external data providers) can also be manipulated to create mission impact. Jamming and denial of service against command/telemetry flows, as well as exploitation of vulnerabilities in any subsystem or component, can lead to system-level effects. These risks require early, risk-based, cybersecurity informed engineering carried from pre-Phase A through mission termination, consistent with U.S. policy and NASA requirements.

11.8.1 Minimum Protections for Command Authority

NASA missions shall protect command authority using authenticated encryption from the point of command generation to the spacecraft. At a minimum, cryptographic modules shall meet FIPS 140-3, Level 1 (or successor) and use FIPS validated algorithms and authenticated modes (e.g., AES-GCM) consistent with NASA-STD-1006A Space System Protection Requirements (SSPR 1). Where backup command links are used, authentication shall be enforced at minimum on those backups (SSPR 2). Projects shall treat command link CPI as CUI and protect it per NASA policy (SSPR 3).

Implementation note (non normative): CCSDS guidance documents provide protocol level security options for protecting telecommand and telemetry (e.g., integrity, authentication, confidentiality) and should be applied commensurate with mission risk. See CCSDS 350.0 G 3 The Application of Security to CCSDS Protocols and CCSDS 350.7 G 2 Security Guide for Mission Planners.

11.8.2 Resilience to External Dependencies (GNSS/PNT and Ground Infrastructure)

Space systems shall be resilient to the complete loss or temporary interference of external PNT sources (e.g., GNSS) consistent with SSPR 4. Recommended practices include multi-constellation GNSS, autonomous fallback navigation modes, and filtering and anomaly rejection in flight/ground software (e.g., Kalman filtering; rejection of out-of-family position/velocity/time changes; ignoring GNSS in known jamming zones; automatic receiver reset/recovery). Ground segments should capture GNSS quality metrics (e.g., C/N_0, DSA, PRNs tracked/available) and jamming/spoofing indicators in telemetry and operations logs to support detection and triage activities.

11.8.3 Defense in Depth (On Board and Ground)

Because external protections can be bypassed, projects should adopt defense-in-depth measures across flight and ground segments, including:

- Secure boot and runtime integrity checks; cryptographic verification of onboard software/firmware; compartmentalization/segmentation of critical functions to limit lateral movement.
- Onboard intrusion detection/response proportional to platform SWaP and risk.
- Ground operations security controls: unique user logons, least privilege access, segmentation/isolation of critical networks, strict command database protections (no hardware/backdoor/firecode commands that bypass authentication/encryption), and validation gates for critical commanding (time-based checks, user approvals, execution delays, pre-execution re-validation, comprehensive logging).

Reference practice: Align system security engineering with NIST SP 800-160 design principles (Appendix F) and integrate them in the systems engineering lifecycle, ensuring threats are addressed through architecture, design, implementation, verification, and operations.

11.8.4 Supply Chain Risk Management (SCRM)

Projects shall implement supply chain assurance commensurate with risk, covering hardware, software, and services. Recommended additions include:

- SBOMs for all flight/ground software and third-party components; continuous vulnerability monitoring.
- Verification of cryptographic module validation (FIPS 140-3) or documented equivalence for space-qualified implementations; secure firmware update processes with authenticity checks.
- Vendor sourcing/manufacturing transparency and repeatable, deterministic processes; added scrutiny of tiers and integrators.

11.8.5 Continuous Monitoring, Detection, and Incident Response

Ground systems should deploy real-time anomaly detection for command, telemetry, and network traffic with SIEM integration and mission-specific playbooks. Projects, spectrum managers, and operations centers shall report unexplained or suspicious interference (RF or cyber) per NASA-STD-1006A (SSPR 5/6) to the Agency focal point (MRPP) and other designated organizations, enabling enterprise-wide triage and response (9).

11.8.6 Policy and Standards Context

U.S. policy calls for risk-based, cybersecurity informed engineering and capabilities to retain positive control of space vehicles. Projects should leverage widely adopted best practices and norms (e.g., NIST CSF, CCSDS security guidance) and integrate security early in mission planning (10)(11)(12)(13)(14).

11.9 State-of-the-Art – Ground Data and Supporting Systems

11.9.1 Technologies

Multiple Spacecraft Per Aperture

The Annual Small Satellite Conference on the grounds of Utah State University is the premier event amongst small satellite stakeholders, and its themes reflect the trends of the times. As scientists are increasingly interested in characterizing fields (going beyond single-point measurements) requiring swarms of satellites, as well as the emergence of Distributed Satellite Missions (multiple satellites working in concert towards one common goal), MSPA is a critical enabler. While it is not a new concept, few ground stations have invested in such upgrade. The DSN has the capability to track multiple spacecraft per antenna (MSPA) (up to four) if they are all within the scheduled antenna's beamwidth. The 34 m antennas at each complex can be combined into an array, with or without the co-located 70 m antenna. The combined G/T depends on several

factors but is approximately increased by the sum of the antenna areas from the arrayed apertures minus approximately 0.3 dB of combining loss. For instance, arraying four 34-meter antennas results in an increase of 5.72 dB.

Automation and Modeling

The MOC of the future will include a "lights out" or fully automated option. This requires software on the ground station side to run the antenna automatically. Automation software will receive a list of times that the antenna should track the satellite and manage that list. It will send TLEs and data to the antenna with no one present, receive downlinked telemetry, and archive the data. Software automatically parses the telemetry, compares key watch items to defined limits, and alerts the team via email or phone text message. FreeFlyer by AI solutions combine astrodynamics/ spacecraft propagation, coverage and contact analysis (including swarms), attitude and maneuver modeling, and orbit determination (20).

Large Ground Antennas: to the Moon and Beyond

For years there has been a gap between NSN's largest 18m and DSN's 34/70m antennas, and such large antennas were not available from commercial ground providers. This gap has now been filled.

In 2022 Viasat introduced new 19/24m aperture antennas (Figure 11.26) at their Antenna Systems campus in Duluth, GA supporting several ongoing programs. The size and architecture of these larger apertures support current programs while offering the flexibility and scalability to support future and forward planning missions (18).

NASA Lunar Exploration Ground Sites

SCaN has announced Lunar Exploration Ground Sites (LEGS) to provide direct-to-earth communication and navigation services for missions operating from 36,000 kilometers (km) in the GEO to cis Lunar and other orbits out to 2 million km. To fully support distant orbits there will be three LEGS sites evenly spaced around the Earth. The Ground sites use CCSDS Modulation and coding schemes for forward and return data. Specialized/unique Mod-Cods are optional. User Local Equipment on-site is optional. The 18m assets are listed as White Sands, USA: 32.544863, -106.612504 Matjiesfontein, South Africa: -33.231224, 20.58163 (TBD) and Pacific Region TBD. MSPA is planned for up to 4 simultaneous return services per aperture (Max 3 for Ka). Use of LEGS for other than Artemis support is TBD. See Table 11-13 for projected performance of LEGS assets.



Figure 11.26: Viasat's new large-aperture space-to-ground communication antennas are ready to support lunar, cislunar, deep space and DoD missions. Credit: Viasat.

Table 11-13: Projected Performance of LEGS Assets Pending Finalization

RF Performance Criterion	Radio Frequency Performance (Return)		
	S-Band	X-Band	Ka-Band
G/T (minimum)	28 dB/K	39 dB/K	47.5 dB/K

11.9.2 Ground Aggregators

Table 11-14 lists those Ground Service providers who own and/or operate their own brand of ground assets. Irrespective of the nature of ownership, satellite operators are reliant on the limited ground stations they have access to. Satellite operators have well defined windows for exchanging information with their satellites. To meet evolving demand from within the fast-growing segment of the space industry, multiple aggregator models have emerged from private market participants. Services from companies such as RBC Signals, Infostellar, Amazon Web Services, and Spaceit are offered through specialist ground station capacity aggregator platforms. These are digital solutions enabling ground station operators to provide their excess capacity to a global user base. Since this is very similar to the business model of Uber, these aggregator services represent the ongoing "Uber-ization" of ground station services within the space industry. The downstream service markets are observing new players with new products and services. With increasing competition, the differentiating factors are shrinking in number. When the upstream capabilities start resembling each other, the key differentiators will include the ability to communicate with the satellites on-demand (19).

RBC Signals

RBC Signals is a provider of global satellite data communication products and solutions. It offers secure space communication solutions in every major frequency band using a worldwide network of company-owned and partner-owned ground systems. RBC Signals delivers dynamic solutions offering affordability, flexibility, and resiliency. Its diverse products and services offer complete end-to-end solutions for best-in-class multi-network solutions (see https://rbcsignals.com).

RBC Signals has aggregated a growing network of over 90 antennas in nearly 60 locations worldwide offering extensive capabilities. A map of these locations is shown in Figure 11.27. As of 2025, RBC Signals owns about 30% of the ground stations, and the rest are partner stations. For those needing turnkey access to existing antennas, RBC Signals offers ground station antenna-as-a-service with the flexibility to secure unlimited satellite passes ("core") or 'pay-by-the-pass/minute/GB'. This is made possible through a combination of their own network of highly capable systems and the unique "sharing economy" model, wherein they leverage the unused excess capacity of dozens of partner-owned antennas worldwide. RBC Signals provides turnkey bring-your-own-antenna hosting solutions, enabling customers to pair their own equipment with robust, high-end ground infrastructure virtually anywhere in the world. The company uses a distributed compute architecture where most processing is handled in the cloud or at a data center and some processing occurs either on the satellite or at the terrestrial edge near the ground station. It also supports on-premise cloud infrastructure from providers like AWS and Microsoft, along with virtual server hosting at the ground level. Expanding its offerings, RBC Signals recently introduced Go.BIC, a new intersatellite link service developed in partnership with IQ SpaceCom and Viasat (20). RBC Signals entered into a global agreement with Viasat to enable dynamic leasing of L-

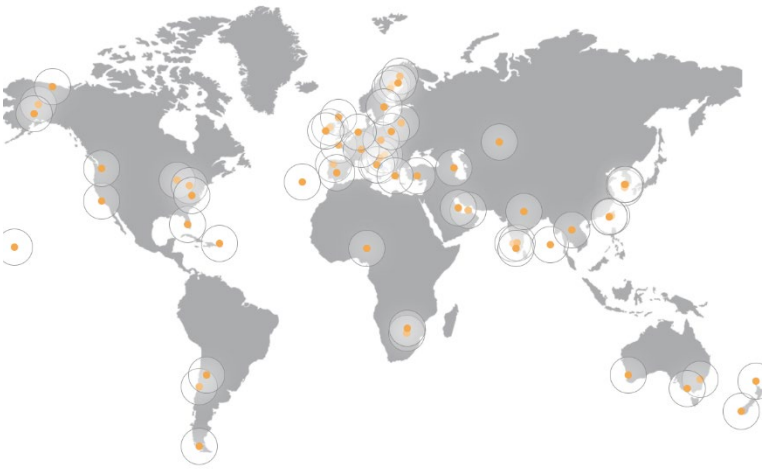


Figure 11.27: RBC Signals ground network map October 2025. Credit: RBC Signals.

and Ka-band spectrum, supporting downlink from spacecraft in GEO to LEO space for emerging IoT applications. The company is also funded by the ESA under the STORM (Spectrum Trading and Operations for Radio-frequency Management) program to advance spectrum trading, sharing, and dynamic allocation technologies that optimize space-to-ground communications.

Table 11-14: Service Providers for DTE Ground System Network

Product	Dish Sizes (m)	Services	MSPA
ATLAS Global Network	Various partners with other stations	S-band, X-band, UHF (Ka-band in 2017) Built on AWS cloud infrastructure	Partner dependent
KSAT and KSAT^{LITE} by Konsberg Sat. Services	> 10 part of NSN or 3.7 (KSAT^{LITE})	X-band and S-band D/L and S-band U/L. VHF, UHF, Ka-band D/L. KSAT^{LITE} designed specifically for SmallSats	No
SSC Infinity by Swedish Space Corporation	13, 7.3 NSN partner	Designed specifically for SmallSats; Uses standardized HW	Not found
AWS Ground Station by Amazon	5.4	Built on AWS cloud infrastructure	Not found
Viasat	7.3, 5.4	Global network operating in S, X, and Ka-bands that can reach LEO, MEO, GEO, and HEO orbits	Mission Dependent
Leaf Space	3.7	Standardized global network accessible through UHF, S, X and Ka-band	Yes
NASA, Near Space Network	9 to 11, & 5	Global network operating in S, X, and Ka- bands that can reach LEO, GEO, HEO, and Lunar orbits; up to 2 mil km	Legacy: NoLEGS (18m): planned, Yes
NASA/ JPL, Deep Space Network	34, 70	Operating at S, X, K, Ka bands. Includes Morehead State 21m in X-band. 8 m optical receive aperture planned for 2030s	Yes
NASA UHF Ground Station	18	Operates in UHF (400 – 470 MHz)	No
RBC Signals Global Ground Station Network	24 to 33	VHF, UHF, S, C, X, Ku, and Ka-bands	Partner Dependent

11.9.3 Scheduling and Mission Operations Software

With the growing number of ground operators and aggregators, to take advantage of the plethora of assets, scheduling is emerging as the single most important enabler. As individual providers may have their own scheduling formats, for seamless operations, a common scheduler is critical, and this is true for NASA's commercialization efforts as well.

Mission operations and ground support suites must also use software and systems for testing, and to monitor, command, control, and communicate with the spacecraft, as well as display status and disseminate data across all aspects of a space mission (including spacecraft performance and procedures, systems health, science and technology data handling and management, and telemetry tracking and control functions). For smaller spacecraft and missions, it is usually best

to use the same ground support software for mission operations, integration and testing, and development and testing activities. There are numerous open-source and proprietary tools and programs available for these activities.

Scheduling: InfoStellar

InfoStellar offers communication services in the VHF, UHF, S, X, and Ka bands. Table 11-15 lists the frequency bands offered by InfoStellar which can be filtered by the tool available on their website. Figure 11.28 shows all 34 antennas on the platform that are either live or for which integration is planned or underway. With multiple commercial small-satellite operators in the market, the need for enhanced mission operations is now much more than an industry-wide requirement.

Table 11-15: Select Frequency Bands by InfoStellar

Downlink		Uplink	
X Band 8 – 12GHz	S Band 2 – 4GHz	S Band 2 – 4GHz	UHF Band 300MHz – 1GHz
Ka Band 27GHz – 40GHz	None No Uplink Channel	VHF Band 30 – 300MHz	None No Uplink Channel

The following section provides an overview of mission operations and scheduling software products that can be integrated into a MOC (see Table 11-16). While the specific aspects of each of these products are discussed below, they all have some common features. In general, these software applications cover functions related to mission scheduling and tasking, commanding and telemetry, and monitoring and control. Many of them also have automation features that enable "lights-out" operations or reduced staffing requirements.

All these products are highly customizable. They can not only adapt to multiple missions, satellites, and ground stations, but they also allow for customized visualizations, analyses, and user interface views. Additionally, many of these products are cloud-based or have a web interface to enable easier access for an operator from virtually anywhere. https://www.infostellar.net/

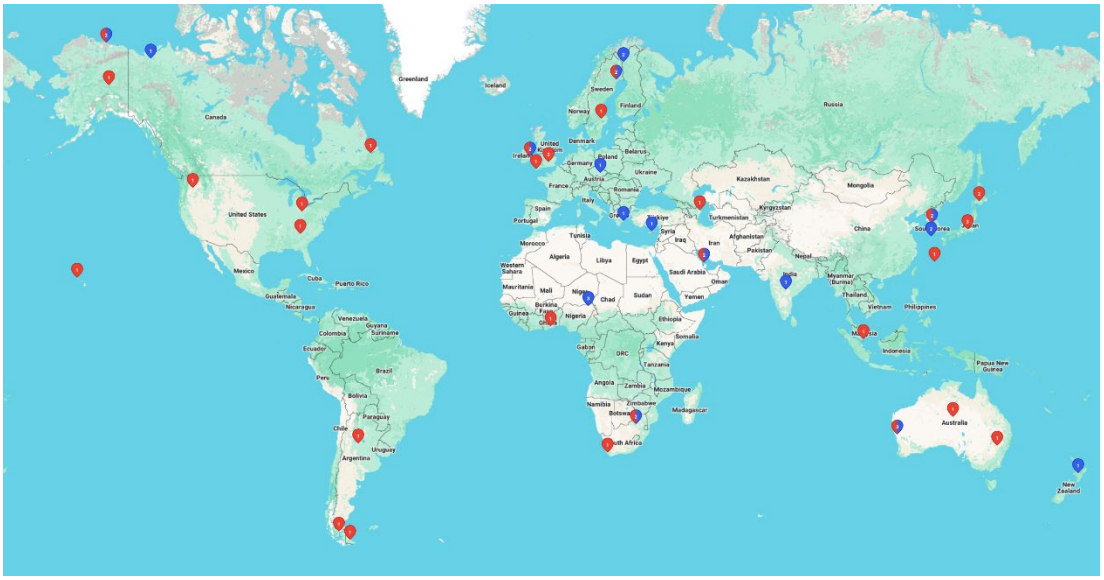


Figure 11.28: All 52 antennas on the StellarStation platform that are active or for which integration is planned. (31 active {red}, 21 planned {blue}. Credit: InfoStellar.

Table 11-16: Mission Operations and Scheduling Software		
Product	**Manufacturer**	**Type of Product**
COSMOS	OpenC3	Open-source command and control system that can be used in all phases of testing and operations
Galaxy	The Hammers Company	Command and telemetry system that has been available since 2000
Mercury	The Hammers Company	Automation for the flow of data files through a mission operations center or other facilities
Stars	The Hammers Company	Cloud compatible, spacecraft fleet trending and data access system
SECRYT	The Hammers Company	Software uplink command encryption, telemetry decryption
tACT	The Hammers Company	Web-Based Team Activity Scheduling System
Auria Family of Products	Auria	Group of mission planning and scheduling products for both aerial and satellite imaging applications
Yamcs	Space Applications Services	Open-source command and control system
ACE Premier Family of Products	Braxton Technologies	Group of hardware and software components for end-to-end Satellite Operations Center (SOC)
Mission Control Software	Bright Ascension	Monitoring and control interface with “lights- out” automation features built-in
Major Tom	Xplore	Cloud-based command and telemetry system that can interface with some COTS flight software

OpenC3 COSMOS

OpenC3 COSMOS is a free, open-source, open-architecture, command, control and communications system providing commanding, scripting, and data visualization capabilities for embedded systems and systems of systems. COSMOS is now a fully containerized, microservice-based architecture with a web-based frontend. COSMOS is intended for use during all phases of testing (board, box, and integrated system) and during operations. OpenC3 COSMOS is made up of a set of applications that can be grouped into four categories: real-time commanding and scripting; telemetry visualization; offline analysis; and utilities. Figure 11.29 shows how data flows through the microservices and is made available to users through an API and from a web-based interface. Any embedded system that provides a communication interface can be connected to COSMOS. All real-time communications of both commands and telemetry are logged in a cloud-native data store, which can use local hardware, or cloud-based storage for potentially infinite storage.

Additionally, program-specific tools can be written using the open-source OpenC3 COSMOS libraries, and these tools can interact with the commands and telemetry of all targets connected to the system. A paid enterprise edition of COSMOS is also available that adds important scaling and security features including: user accounts, Role-Based Access Control (RBAC), Kubernetes support with Helm charts, calendar and automation capabilities, and a library of pre-built plugins for common devices and protocols like SCPI devices and CFDP.

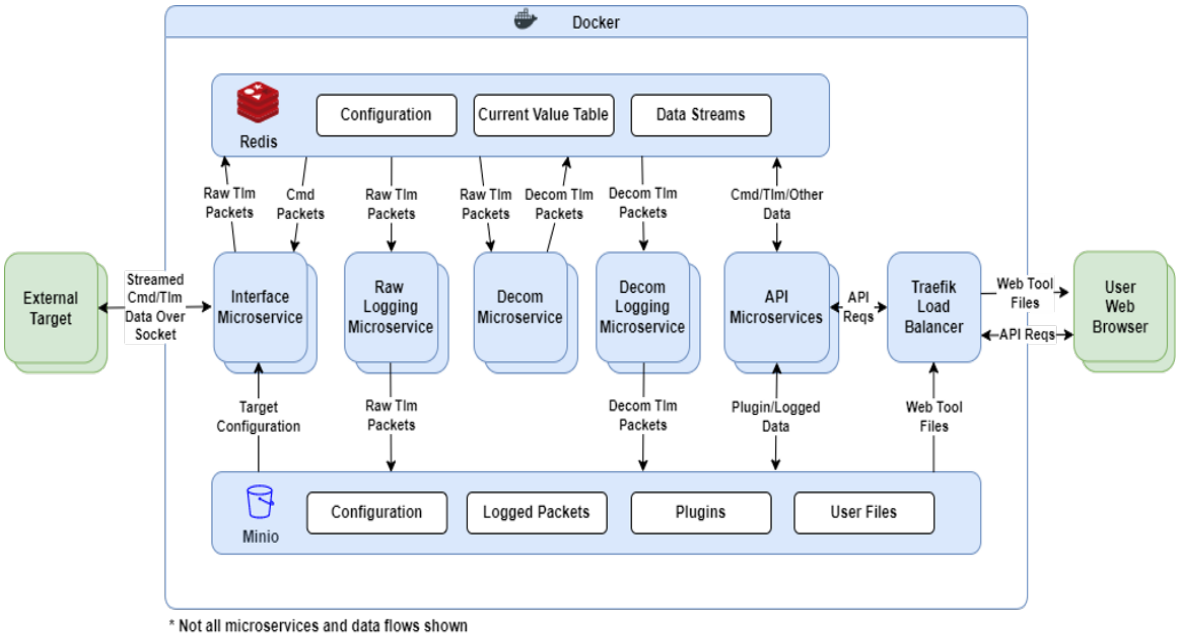


Figure 11.29: COSMOS5 architecture and context diagram. Credit: OpenC3, Inc. https://openc3.com/

The Hammers Company

The Hammers Company offers a suite of ground data software and system solutions designed to support the entire spacecraft lifecycle; from instrument and/or component development, including flight software, through mission operations. Their commercial real-time command and telemetry system, Galaxy, has heritage on missions ranging from stratospheric balloons, CYGNSS (Cyclone Global Navigation Satellite System) and Landsat observation satellites in Earth orbit and Lunar Reconnaissance Orbiter (LRO). Galaxy is designed to handle spacecraft fleet operations by accepting telemetry from, and sending commands to, multiple spacecraft and ground stations simultaneously. See Table 11-14 for more Hammers Company ground data software and https://hammers.com/.

Major Tom

Xplore's Major Tom® is a scalable, cloud-based mission control platform that provides satellite mission operations and planning tools for ground station scheduling, satellite tasking and telemetry monitoring. It provides satellite operators the ability to integrate and control ground segment applications and services, and further de-risks mission operations with features such as built-in ground network integrations, advanced analytics, interactive dashboards, and a customizable commanding API. Major Tom's gateway API architecture, definitions, and protocols can integrate with custom ground station providers. This software is compatible with a heterogenous network of ground station providers and supports both constellation and individual mission operations with flexibility in satellite communication and commanding. New ground station network locations and providers can be added and it works with a unified data model for constant functionality across the entire network. Figure 11.30 provides a screenshot of the dashboard.

For more information, visit https://www.xplore.com/services/operations-as-a-service/major-tom.html.

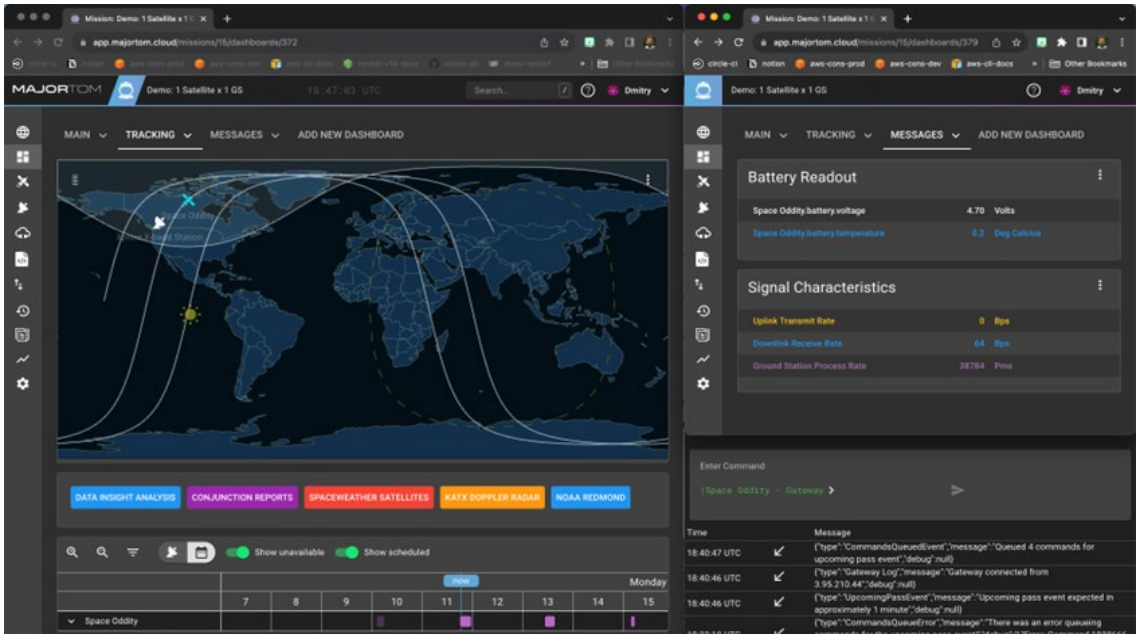


Figure 11.30: Major Tom's configurable dashboards allow operators to oversee and interact with the mission in the way they are most comfortable. Credit: Xplore.

Auria Family of Products

Auria specializes in mission planning, scheduling, and space situational awareness software. The software suite consists of multiple applications that support analysis and operations for aerial and satellite imaging and space-to-ground networking. The mobile, web, desktop, and onboard scheduling applications have a variety of features, including: configurable systems, constraints, and goals; high-performance algorithms; deconflicted scheduling plans; visualizations and animations on the user interface, and flexible process flows and automation. Figure 11.31 shows Auria's Collection Planning and Analysis Workstation (CPAW). For more information, visit https://www.auria.space/

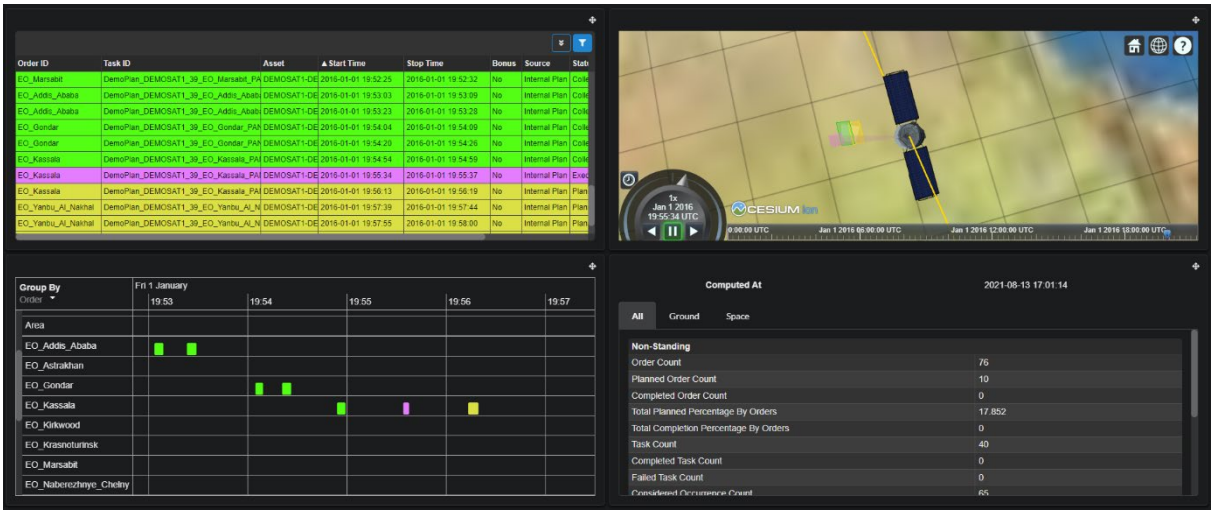


Figure 11.31: Auria CPAW dashboard. Credit: Auria.

ACE CrtlPoint

The ACE CrtlPoint from Parsons (acquired Braxton Technologies in January 2021) is an automated space vehicle and ground station command and control (C2) application with a plug-in architecture that provides nearly “lights-out” TT&C operations. ACE CrtlPoint includes the hardware and software components necessary for a satellite MOC. Key applications include: integration with antenna scheduling; ground station control and status; data forwarding for analysis; command plan execution; anomaly detection; and a turnkey TT&C system. COTS capabilities plug into standardized environments, allowing the product to be ready for deployment immediately within a range of mission architectures. https://www.parsons.com/products/ace-ctrlpoint/

Bright Ascension HELIX

Bright Ascension rebuilt its original mission control software into a modern suite called HELIX, a highly integrated, end-to-end software platform for the entire mission lifecycle from flight software development, testing and simulation, to ground operations and end user insights and analytics. The HELIX suite includes the HELIX Groundkit, an advanced ground software development platform that assembles complete and bespoke ground software systems; HELIX Ops, the mission control environment designed to scale from single CubeSat missions to large multi-platform constellations; and HELIX Flightkit, a modular flight software development environment, designed to create mission-specific flight software using configurable and pre-validated components. Flightkit can reuse and adapt software packages developed for one mission for another mission with different platforms or subsystems. This flexibility allows teams to respond rapidly to changing requirements by easily swapping functional elements in and out of the system. Flightkit includes a library of pre-validated, ready-to-use components, along with the ability to develop custom modules to meet mission-specific functionality. Figure 11.32 is HELIX main screen. https://brightascension.com/helix/



Figure 11.32: HELIX main screen. Credit: Bright Ascension.

Yamcs Mission Control

Yamcs is a mission control software developed by Space Applications Services that is publicly available under the GNU Affero GPL license. It is designed for the command and control of the

spacecraft, payload, ground station, and ground equipment, and supports telemetry reception, archiving, telecommand sending, alarm generation, and replay processing. Yamcs features a comprehensive web interface. The backend can be extended or customized using Java (though some plugins are only available to customers) and can be deployed in the cloud or on premises. The platform also supports industry standards like Consultative Committee for Space Data Systems (CCSDS), CCSDS File Delivery Protocol (CFDP), CubeSat Space Protocol (CSP), and XML Telemetric and Command Exchange (XTCE). The extensive API includes both REST and WebSocket. A desktop tool is available for authoring operator displays. Plugins for popular open-source visualization frameworks, such as Grafana and OpenMCT, are also available. A companion tool, the Yamcs Gateway, enables the development of Electrical Ground Support Equipment (EGSE) for spacecraft and payload development, supporting low-level interfaces like CAN bus, MIL-1553, SpaceWire and RS422. Figure 11.33 is a screenshot of the web GUI. In addition to the public AGPL releases, Space Applications Services offers commercial licenses and enterprise Support for Yamcs. For more information, see https://yamcs.org/.

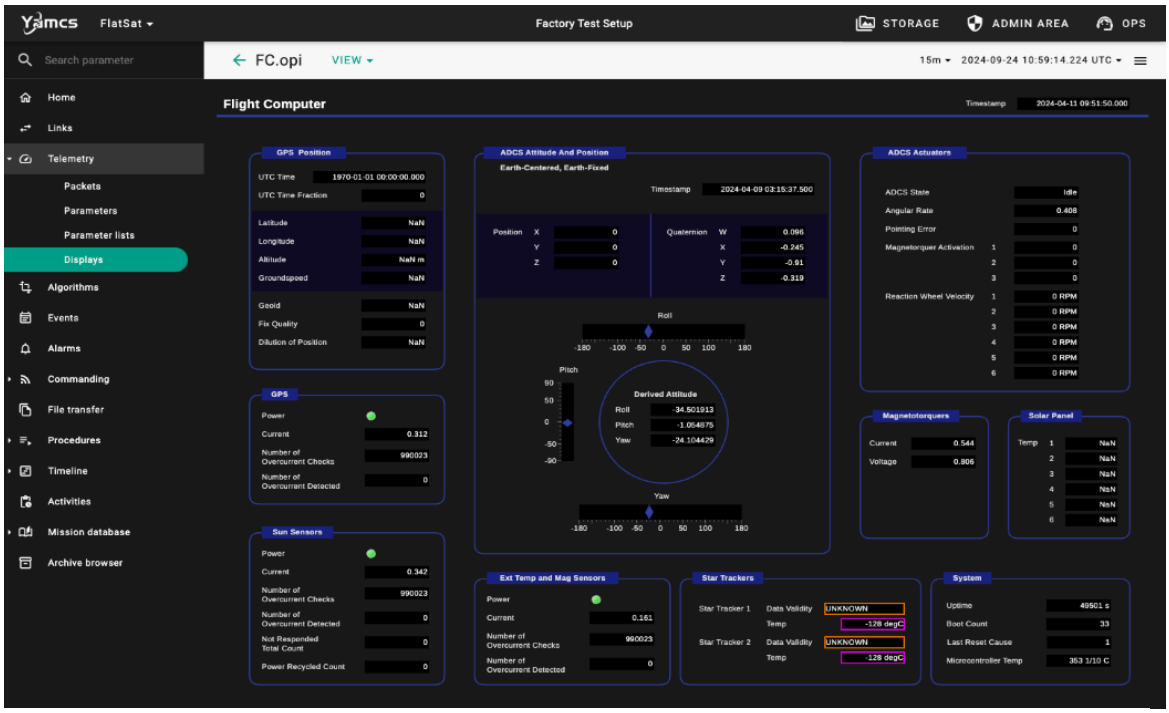


Figure 11.33: Screenshot of Yamcs web GUI. Credit: Yamcs.

11.10 On the Horizon

Ground data systems must continue to evolve to keep up with the rapid pace of small satellite technology. Advancements in onboard processing and data storage will demand more capability in getting data to the ground. Mass production of small satellites is quickly becoming a reality and large constellations are now starting to be deployed to orbit. This will require ground system technology that can communicate with multiple satellites simultaneously. Free Space Optical communications and phased array ground systems are emerging solutions to these needs. While both technologies have seen years of investment, they are now just starting to be integrated into ground networks. While it may still be years before they become a staple for these networks, the following sections provide insight into the state of these technologies and where they are headed in the future.

11.10.1 Free Space Optical Communications

Increasing demand for data from NASA missions has led to a migration over the past few decades to increasingly higher RF bands (X, K, and Ka) and ultimately to the optical and near-infrared regimes. Free Space Optical (FSO) communications are expected to increase data rates by two orders of magnitude over traditional RF links (see the *Communications* chapter for more on FSO communications). The next generation systems will incorporate optical communications, and several early flight demonstrations and uses of optical communications in the coming decade are expected to be transformative for NASA and other space organizations. Whereas Ka-band frequencies go up to 40 GHz, the optical signal reaches up to 200,000 GHz. Higher frequencies have the potential for significant increases in data rates, theoretically proportional to frequency-squared if all other factors are equal. At optical wavelengths, other factors, such as atmospheric losses, receiver sensitivity, aperture, and power, must also be considered, but nonetheless, optical communications offer the potential for orders of magnitude improvement in data throughput.

For space applications, lasers are being used as the light source. Laser systems with dynamic systems such as fast-steering mirrors are used to accurately point the laser on the spacecraft to the ground terminal. Other methods using laser arrays for beam pointing are also being developed to reduce the need for complex dynamic pointing systems. Data is transmitted in the form of hundreds of millions of short pulses of laser light every second. The light is made of photons and the optical ground terminals are set up to collect the light at the photon level. In fact, the ground terminals are designed for an environment where relatively few photons may be received from the transmitter spacecraft, especially from deep space. Direct photon detection with Pulse Position Modulation (PPM) is used instead of the common RF technique of direct carrier coherent modulation to convey information. PPM modulation uses a time interval that is divided into several possible pulse locations, but only a single pulse is placed in one of the possible positions, determined by the information being transmitted. To detect extremely faint optical signals with relatively few photons through the atmosphere, optical ground stations can use a superconducting nanowire single-photon detector (SNSPD), which, to increase the sensitivity of the nanowires, uses a 1-Kelvin cryocooler. A real-time signal processing receiver uses time-stamped photon arrivals to synchronize, demodulate, decode, and de-interleave signals to extract information codewords. Hence, while the specific technologies employed differ in some respects from those used in radio frequency ground terminals, the higher-level functions performed by the optical communication ground terminal are similar.

Optical communication is attractive for mission designers using small, resource-constrained spacecraft because it offers a path to relatively high data rates with relatively small, low-power spacecraft equipment. The same volume and power savings can be experienced on the ground terminal side as well. This is driven by the size of the wavelengths involved. Because RF wavelengths are longer, the size of their transmission beam covers a wider area; therefore, the capture antennas for RF data transmissions must be very large. Laser wavelengths are orders of magnitude shorter, allowing data to be transmitted across narrower, tighter beams. This results in the ability to deliver the same amount of signal power to much smaller collecting areas. The reduction in antenna size applies for ground and space receivers, which allows for size and mass reductions on the spacecraft side.

NASA made great strides with its optical communication demonstration on the Lunar Atmosphere and Dust Environment Explorer (LADEE) mission. The pivotal NASA Lunar Laser Communications Demonstration (LLCD) was able to achieve 622 Mbps from lunar distance. NASA has several ongoing and planned optical communications demonstrations, including O2O, Illuma-T, T-Bird, and the Laser Communications Relay Demonstration (LCRD). LCRD is supported by Optical Ground

Station (OGS)-1 at OCTL, and OGS-2 in Hawaii (51).

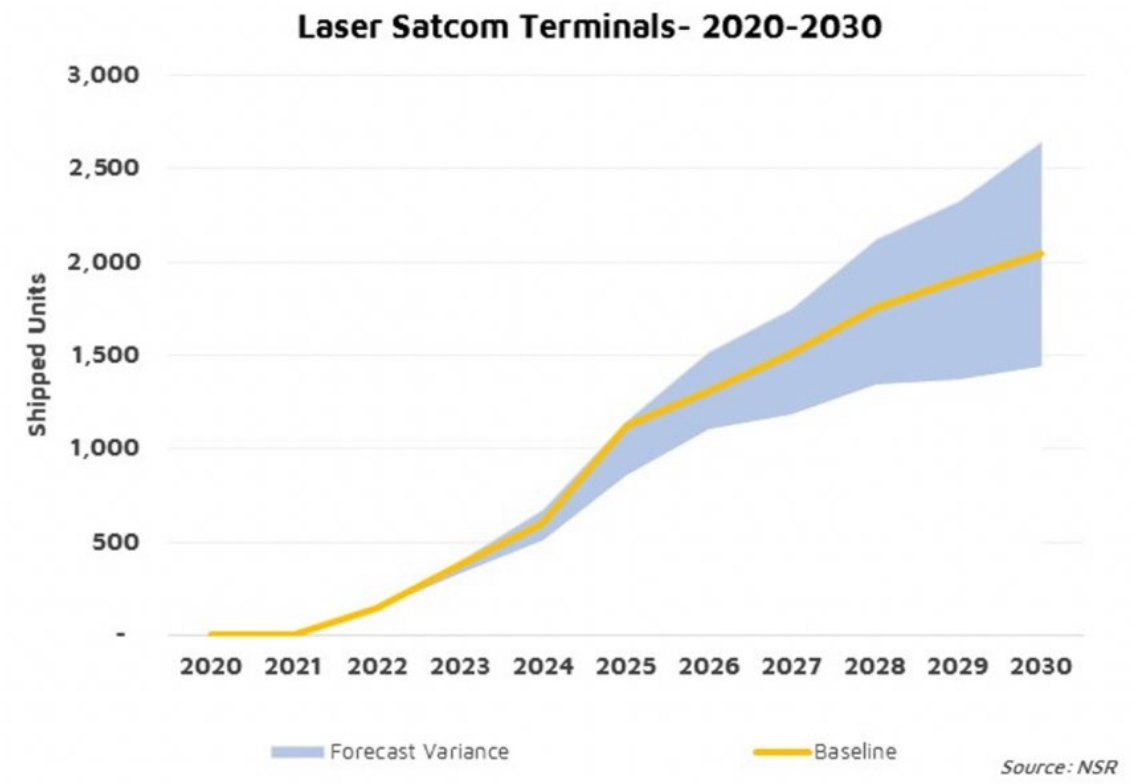


Figure 11.34: Laser terminals future forecast. Credit: Northern Sky Research.

Northern Sky Research (NSR) predicts growth for optical communications, which needs to be matched by OGS (Figure 11.34). “The demand now is not for just one gigabit per second, not 10 gigabits per second, but tens if not hundreds of gigabits per second. And it’s growing exponentially. The only way to achieve that is by starting to use optical communications or laser communications to augment or to complement RF communications” (Barry Matsumori, CEO of BridgeComm, 2022) (22).

11.10.2 Optical Ground Stations and Future Infrastructure Requirements

OGS contain notably different equipment than RF stations, including an optics assembly, photon counter assembly (usually involving a photon-counting nanowire detector and cryostat), and signal processing assembly with a time-to-digital converter. Since optical communications use a frequency higher than RF (e.g., 1,550 nm downlink and 1,065 nm uplink wavelengths), the optical dishes can be smaller than RF antennas. To receive optical signals from a low-Earth orbit, 40–60 cm telescopes are sufficient. For successful deep space optical communications, calculations show that 3 m, 4 m, or even 8 m diameter ground apertures are required, depending on the distance from Earth. For these size apertures, when a 3–8 m OGS is not available, partnerships can be formed with large astronomy telescopes. For example, JPL-designed OGS equipment has been integrated at the Palomar Observatory (Hale 5-m telescope) for future use by the Deep Space Optical Communications (DSOC) demonstration. Note that OGS for LEO and deep space require different types of modems. It is also important for OGS to have spatial diversity. Weather,

atmospheric conditions, turbulence, and aerosols in the air can degrade laser propagation. Because certain types and depth of cloud covers can cause signal loss, probability of link success increases with multiple diverse locations.

For interoperability between SmallSats and public and private optical ground stations, a common communications standard is key. The Consultative Committee for Space Data Systems (CCSDS) and Space Development Agency (SDA) provide recommendations for communications standards, including optical communications. Adhering to these standards by both SmallSats and ground stations allows for multi-mission optical ground stations.

JPL is operating the Optical Communications Telescope Laboratory (OCTL) at Table Mountain, CA, with a 1 m telescope, as shown in Figure 11.5 This dish was used for the LADEE mission and offered strong performance from a lunar distance (21). Most notably, JPL operates the DSN, supporting two-way RF communications and ranging services. Given the existing infrastructure, it is advantageous to augment a DSN RF antenna by installing optical segments at its center, making it a dual-purpose, RF-optical hybrid antenna**.** The installation is being implemented in two phases.

In 2022 a small prototype RF-Optical system, including the mirror, cameras, and backend has been installed at DSS-13 (Figure 11.36) at the Goldstone Deep Space Communications Complex. DSS-13 is the R&D 34 m BWG antenna at Goldstone. The combination of seven small (0.5 m) mirrors comprises a synthesized prototype optical aperture of about 1.3 m diameter. Since late 2023, DSS-13 has been continuously performing active laser downlinks. Control was verified to maintain segment position to <1 microradian, with first light successfully received from natural light sources. 1550 nm light was measured through the 100-meter fiber at the pedestal. JPL was able to track multiple sources across the sky from 20-80 degrees elevation.

A JPL designed communications detector and optical receiver have been installed and tested over the air on DSS-13 as well.



Figure 11.35: JPL's OCTL showing a 1-meter optical aperture. Credit: NASA JPL.

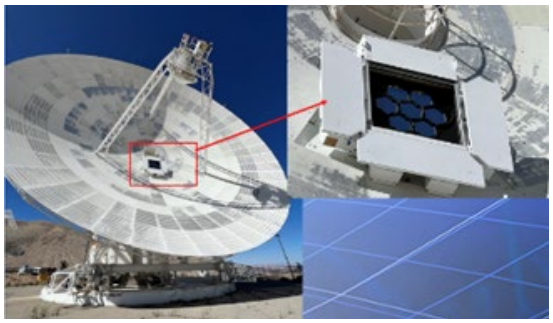


Figure 11.36: JPL's DSS-13, a 34m RF antenna, showing a 1.3-meter optical aperture in its center. Credit: NASA JPL.



Figure 11.37: Artist overlay of built DSN RF antenna and planned 8m optical segments at its center. Credit: NASA.

The operational RF-Optical hybrid will ultimately include 64 mirrors each of 1 m diameter, installed as a segmented 8 m optical receive aperture/mirror physically inside one of the new DSN 34 m radio frequency ground terminals

(DSS-23, in California). The final phase includes completion of the full 64- segment aperture on DSS-23, as illustrated in Figure 11.37, including a full year of field tests. This 8 m equivalent optical ground aperture will be operational in the early 2030s.

DSS-23 will be capable of a full set of RF services with the 34 m antenna in addition to high-rate optical communications with its 8 m optical assembly. Before the full operational readiness dates for optical communications, the 1.3 m partial optical systems will be usable at various times for best effort demonstration optical communications passes in the near-Earth or lunar regimes, as well as for deep space missions.

The DSS-23 optical receiver is the same design that JPL is delivering to the Palomar Observatory for use with the DSOC optical communications technology demonstration on the NASA Psyche mission. This receiver is also installed in ground terminals at White Sands and other locations for near- and deep-space missions, as well as Artemis. One exciting implication of this 8m equivalent optical aperture is that it meets the 230 Mbps downlink data rate requirement for human exploration of Mars.

Looking at the broader optical communications landscape, over the past decade the community has been confronted with a chicken-and-egg problem: due to the lack of a ground segment, the FSO space segment has been slow to develop, and additional investments have not been made due to the low number of satellites flying an FSO ground segment.

Europe

The European Optical Nucleus Network was formed between ESA ESOC, the Germany Aerospace Centre (DLR), Global Security Operations Center (GSOC), and KSAT. Parties agreed to have an interoperable, multi-mission approach based on the Consultative Committee for Space Data Systems (CCSDS) standards. Starting locations and characteristics are summarized in Table 11-17. The Nemea OGS (Figure 11.38) has been operational since 2022 after initial investments in the first commercial OGS, with the other stations expected to follow. The goal is to bring all building blocks together into an automated, cost-efficient, operational, multi-mission optical ground station service. This OGS uses modified COTS components to reduce cost and could also serve as a blueprint for future stations. KSAT co-located its first OGS with KSAT RF antennas in the mid-latitudes at Nemea, due to the temperate, weather, and the ability to shae existing infrastructure. The OGS is compliant with the Optical On-Off Keying (CCSDS 141b1) draft standard and is designed to be cost competitive to the KSAT^{LITE} service that KSAT is currently offering in the RF domain. The telescope is mounted more than 3 m above the ground to avoid ground layer turbulence. The dome is a one-part, completely retractable structure with UV-resistant plastic fabric. It is not connected to the telescope foundation to avoid coupling of vibrations caused by wind to the telescope system.



Figure 11.38: KSAT's low-complexity optical ground station in Nemea (2021).

- KSAT co-located its first OGS with KSAT RF antennas in the mid-latitudes at Nemea, due to the temperate weather and sharing the existing infrastructure,
- The OGS is compliant with the Optical On-Off Keying (CCSDS 141b1) draft standard and is designed to become cost competitive with the KSAT^{LITE} service, which KSAT currently offers in the RF domain.
- The goal was to bring all building blocks together into an automated, cost-efficient, operational,

multi-mission optical ground station service.

- For cost reduction modified COTS components have been selected.
- The telescope is mounted more than three meters above the ground to avoid ground layer turbulence.
- The dome is a one-part completely retractable structure with UV resistant plastic fabric. It is not connected to the telescope foundation to avoid coupling of vibrations caused by wind to the telescope system.

The First Data Link Between Commercial Optical Terminals has been validated through a temporary Sony optical terminal placed on the ISS, with a channel data-rate of 150 Mbit/s with BER varying from 1e3 and <1e-6.

Table 11-17: European Optical Nucleus Network OGS Key Parameters

	Nemea	Almeria	Tenerife
Downlink wavelength support range	*1529-1569nm*	*1529-1569nm*	*1529.5-1568 nm*
Telescope main aperture diameter	*50 cm*	*60 cm*	*80 cm*
Elevation angle support range	*20° to 90°*	*10° to 85°*	*10° to 87° (LEO)* *10° to 89° (GEO)*
Max. operation wind speed	*15 m/s* *(18 m/s gust)*	*15 m/s* *(18 m/s gust)*	*14m/s*
Operational min. sun-distance	*20°*	*20°*	*TBC*
Tracking modes	*Program-track* *Auto-track*	*Program-track* *Auto-track*	*Program-track* *Auto-track*
Temperature operational range	*-15°C to 40°C*	*-5°C to 35°C*	*TBC*
Acquisition Beacon Source	*1589.3nm, 5W (peak)*	*1589 – 1591nm, 5W (peak) TBC*	*1591.26 nm, 5 W* *1590.4 nm, 8 W*
Acquisition beacon divergence angle *(1/e² full-angle)*	*632 µrad*	*1000 µrad* *TBC*	*500 µrad*
FoV of auto-track system	*8.5x6.8 arcmin*	*15x12 arcmin* *TBC*	*8.6 arcmin* *(diameter)*
Absolute pointing error*	*< 5 arcsec*	*< 10 arcsec*	*< +- 103 arcsec* *(99% confidence)*
Auto-track accuracy	*1 arcsec RMS* *max. error 3 arcsec*	*1 arcsec RMS*	*0.41 arcsec RMS*
Site (mean) clear-sky probability	*Summer: 80-95%* *Winter <60%*	*Summer: >75%* *Winter: >55%*	*81%*
Site long term average seeing	*Day: 2.7 arcsec* *Night: 3.6 arcsec*	*TBD*	*Day: 2.2 arcsec* *Night: 1.8 arcsec*
Site WAN connectivity	*10 Gbps*	*10 Gbps*	*10 Gbps*
Location coordinates	*Lat. 37°50'42.5"N* *Long. 22°37'24.0"E* *278.7 m above sea level*	*Lat. 37°5'36.3''N* *Long. 2°21'31,1''W* *498 m above sea level*	*Lat. 28°17'58.7"N* *Long 16°30'38.5"W* *2382 m above sea level*

Japan

The National Institute of Information and Communications Technology (NICT) optical ground station in Japan also received transmissions from the SOLISS system by Sony CSL installed on

the Kibo's exposed facility on the ISS (25). In 2021, NICT also reported that the 1 m optical ground station in Koganei, Tokyo received via optical communication images taken by the satellite's camera using the SOTA optical communications device mounted on a 50 kg-class microsatellite.

Germany

The DLR German Aerospace Center is another organization active in optical communications. About 25 km west of Munich, Germany, is their Optical Ground Station Oberpfaffenhofen (OGS-OP) that houses a 40 cm Cassegrain telescope (26). The German Aerospace Center has also developed a transportable optical ground station (TOGS). It has a 60 cm deployable telescope in a Ritchey- Chretien-Cassegrain configuration with a focal ratio of f/2.5. The telescope is supported by an alt-azimuth mount on a structure with four adjustable legs for leveling the mount and compensating for rough terrain. It has been successfully used to track the OPALS instrument on the ISS and serves as the primary ground station for the OSIRIS payload on the BiROS satellite. The German Aerospace Center OGS-OP and TOGS are shown in Figure 11.39.



Figure 11.39: (left) OGS-OP and (right) TOGS. Credit: German Aerospace Center. https://creativecommons.org/licenses/by/3.0/de/legalcode.

WORK Microwave is a system integrator and provides satellite communication technologies, including turnkey OGS tailored to mission requirements. In collaboration with KSAT and Astelco Systems, WORK Microwave contributed to the establishment of the first commercial ground station for ESA at Nemea, Greece, which became operational in 2021 (25). This station, designed with a half-meter aperture telescope from Astelco and a baseband modem developed by WORK Microwave, supports data rates up to 3 Gbps and was validated through tracking of sun-illuminated spacecraft. Separately, WORK Microwave developed a fully SDA Tranche 1 and 2 compliant Digital Optical Ground (DOG) suite that enables system configuration, monitoring, and control, and communication (30). This includes the DOG-M1 multi-mission modem, DOG-DA optical detector, DOG-CA electro-optical converter, and DOG-A1 amplifiers. The DOG suite supports bi-directional optical communication at rates up to 10 Gbps and is compatible with both SDA and CCSDS standards. While the Nemea station incorporates components from WORK Microwave, the fully SDA-compliant DOG suite represents a more recent and comprehensive system architecture, intended for broader deployment across LEO, MEO, GEO, and deep space missions. Figure 11.40 shows the OGS DOG schematics, with telescope control from WORK Microwave's partners. More info on https://work-microwave.com/digital-optical-groundstation/.

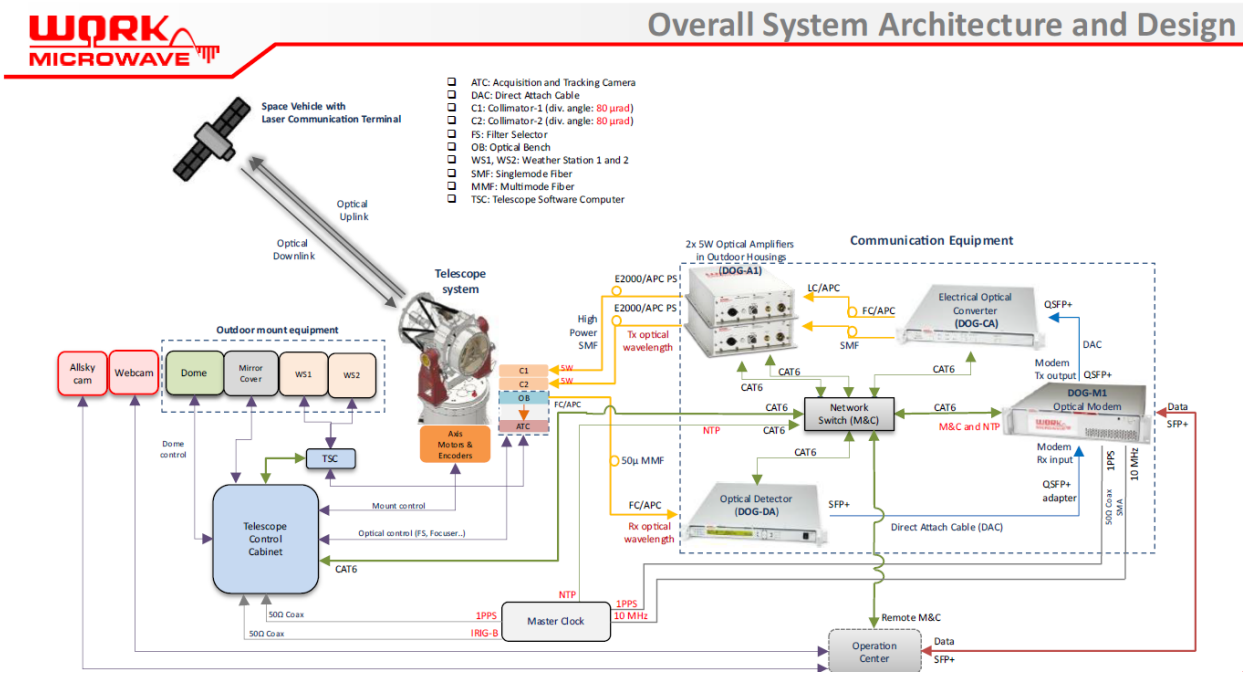


Figure 11.40: Schematics of the OGS with the Digital Optical Ground (DOG) station suite. Credit: WORK Microwave Inc.

Australia – New Zealand

The Australian Optical Ground Station Network (AOGSN) will eventually be made up of four ground stations in Western Australia, South Australia, the Australian National University (Australian Capital Territory), and New Zealand. The plan is to tie these stations together to produce a communication network that can support optical, RF, and future quantum communications. In spring 2021, Thales Australia signed a research extension with the SmartSat Cooperative Centre (CRC) for the development of advanced optical communications technologies (27).

Sascha Schediwy, head of the research group responsible for designing and building the WA Optical Ground Station (Figure 11.41), believes lasers will play a crucial role in future human missions to the Moon. "It's likely to be how we'll see high-definition footage of the first woman to walk on the Moon," Dr. Schediwy said (abc.net.au).



Figure 11.41 The 70 cm Western Australian Optical Ground Station (WAOGS) is installed on a rooftop at the University of Western Australia. Credit: The International Centre for Radio Astronomy Research.

United States

In the U.S., The Aerospace Corporation is a player in the optical communication arena. Their manned OGS 40 cm telescope, located in El Segundo, CA, demonstrated 200 Mbps from 725 km. It is operating at a 1,064 nm wavelength; thus, it is not compatible with other optical

ground stations or most COTS optical space terminals.

11.10.3 Techniques to Improve Optical Comm Reliability

Laser communication is essential for future telecom networks to supplement RF communications and enable:

- Very high throughput links (> 10 Gb/s and up to Tb/s)
- Communication without frequency band limitation
- Highly secure, stealthy, and non-interceptable links

It is essential for operational use cases:

- Multispectral observation of Earth from space (very bandwidth intensive)
- Securing sovereign communication
- Telecommunication constellations that rely on very broad bandwidth links

Cailabs

Cailabs develops, manufactures, and delivers turnkey Optical Ground Stations for laser communication, enabling high-speed satellite-to-ground links. With its standard TILBA-OGS-L10 design, Cailabs provides secure, robust, and spectrum-license-free bidirectional connections exceeding 10 Gbps for LEO-to-ground communications. TILBA-OGS integrates several key building blocks, based on proprietary Multi-Plane Light Conversion (MPLC) technology: TILBA-ATMO (downlink injection into a single mode fiber), TILBA-IBC (uplink incoherent beam combining), and TILBA-CBC (coherent beam combining). These sub-systems enable TILBA-OGS to effectively mitigate atmospheric turbulence on both the receiver (Rx) and transmitter (Tx) sides of the link without the hassles and complexity of adaptive optics or co-aligned multiple apertures. This turbulence-mitigation technology ensures scalability to meet future terabit-per-second (Tbps) feeder link requirements and beyond.

Using TILBA-OGS-L10, Cailabs has performed successful space-to-ground laser communications with several spacecraft constellations. In 2025, Cailabs announced robust and repeatable bidirectional communication links with Kepler Pathfinder following SDA OCT standard v3.0.1, demonstrating the first commercial realization of SDA-compliant satellite-to-ground optical communications. TILBA-OGS is fully compatible with CCSDS and SDA standards (all tranches) and supports integration with a wide range of ground modems.

As of October 2025, TILBA-OGS is installed in France (operated by Cailabs) and in Western Australia (operated by Swedish Space Corporation), with 10+ additional units under production for governmental and commercial OGS programs. Cailabs is ready to meet the growing market demand with its new assembly and validation platform, capable of building up to five TILBA-OGS units in parallel. Following its recent $67 million fundraising, Cailabs is scaling its production capacity to 50 Optical Ground Stations per year by 2027, paving the way for the rapid deployment of a global optical ground station network (28). (https://www.cailabs.com/en/)

11.10.4 Role of Optical Relays

Optical inter-satellite links are “critical to the success of the Space Development Agency’s low Earth orbit constellation” known as the Transport Layer. SDA-Funded laser terminal technology could connect to multiple satellites simultaneously. Each satellite in the Pentagon’s “planned mesh network of communications satellites could have as many as many as four laser links so they can talk to other satellites, airplanes, ships, and ground stations.” BridgeComm, which recently received an SDA contract, “developed a so-called ‘one-to-many’ optical communications technology for point-to-multipoint transmissions” which could “help reduce the cost of building constellations by requiring fewer terminals,” Michael Abad-Santos, senior vice president of business development and strategy at BridgeComm] said. BridgeComm first demonstrated “point

to multipoint optical communications in 2019 in a project with Boeing, and has since continued to mature the technology," Abad-Santos said (29).

Warpspace is a private Japanese company developing an inter-satellite communication system based on laser communication (Figure 11.43). The WarpHub InterSat link relays will enable low latency data delivery from MEO, and in the future they will connect to the Lunar Gateway or planetary deep space via optical communications (see https://warpspace.jp/).

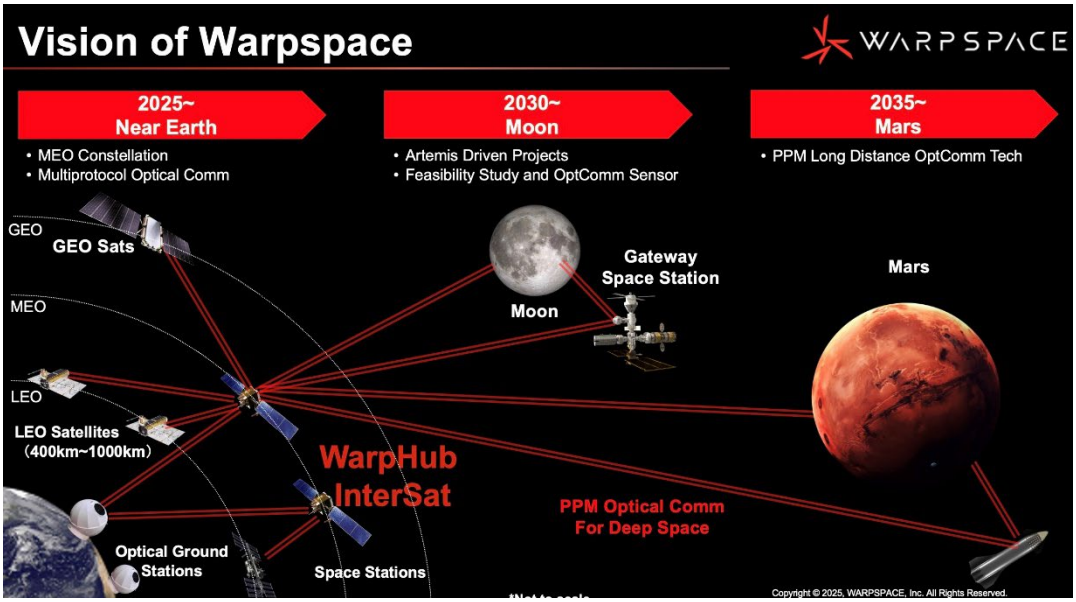


Figure 11.43: Warpspace plans a satellite network in MEO with optical communications hardware to be reached by LEO. Credit: Warpspace.

11.11 Summary

The ground segment serves as the gateway to getting valuable data collected by the satellite into the hands of the user. It is a critical component of the satellite system that requires attention at the earliest stages of mission planning. Understanding what ground solution best meets the needs of the mission has a direct impact on the spacecraft design, concept of operations, launch schedule, mission operations cost, and expected data volume for processing. Much effort also goes into preparing for the interaction between the satellite and ground network. Developing software and simulations, drafting operations manuals, conducting operations rehearsals, and performing compatibility tests are all part of standard practice. Post- launch, the ground station also plays a key role in locating and commissioning the spacecraft.

In looking forward to the future of ground systems, the clear objective is how to bring the data down more efficiently. Great strides are being made with optical communications where it is possible to have increases in data per pass that are orders of magnitude above what can be achieved with RF communications. Optical communication technology is now being infused into ground system architectures, and flight hardware is becoming miniaturized enough to fit within small satellites. The ability of these systems to quickly change beam directions and acquire multiple targets will be critical for communicating with constellations of small satellites.

While the tried-and-true RF ground system solution remains the workhorse for small satellites, the innovative nature of the small satellite platform will soon challenge the community to adapt to systems capable of handling hundreds of satellites and high data volumes. Efforts are ongoing

to keep pace, but only time will tell whether ground systems will continue to advance or potentially impede the small satellite revolution.

For feedback solicitation, please e-mail: arc-sst-soa@mail.nasa.gov. Please include a valid business e-mail so someone may contact you further.

References

(1) K. Schauer, "NASA to Commercialize Near-Earth Communications Services." October 26, 2020. [Online] Available at: https://www.nasa.gov/feature/Goddard/2020/nasa-to-commercialize-near-earth-communications-services

(2) National Aeronautics and Space Administration, "Space Communications and Navigation." [Online] 2021 Available at: https://www.nasa.gov/directorates/heo/scan/services/networks/near_space_network

(3) Uppal, Rajesh. "Satellite Ground Segment as a Service (GSaaS) driven by New Space requirements." [Online] Available at: https://idstch.com/space/satellite-ground-segment-as-a-service-gsaas-driven-by-new-space-requirements/

(4) Nguyen, Louis. "Ground Stations as a Service (GSaaS) for Near Real-time Direct Broadcast Earth Science Satellite Data." [Online] Available at: https://esto.nasa.gov/forums/estf2021/Presentations/June10/Nguyen_GSON_ESTF2021.pdf

(5) R. O'Dwyer. "Iridium 88kbps service commercially available." November 11, 2021. [Online] Available at: https://smartmaritimenetwork.com/2021/11/11/iridium-88kbps-service-commercially-available/

(6) D. Werner. "Analytical Space wins $26.4 million to establish optical network." February 10, 2021. [Online] Available at: https://spacenews.com/analytical-space-wins-26-4-million-to-establish-optical-network/

(7) Celestia ST, "TNO and Celestia STS sign agreement to commercialize Optical Modem." June 30, 2021. [Online] Available at: https://celestia-sts.com/2021/tno- and-celestia-sts-sign-agreement-to-commercialise-optical-modem/

(8) DeWitt, Henry. Satellite Ground Station Control. DeWitt & Associates. Accessed: July 2022. [Online] Available at: http://www.dewitt-assoc.com/groundStation.html

(9) National Aeronautics and Space Administration, "Space System Protection Standard" NASA-STD-1006A. July 15, 2022. [Online] Available at: https://standards.nasa.gov/sites/default/files/standards/NASA/A/0/2022-07-15-NASA-STD-1006A-Approved.pdf

(10) National Institute of Standards and Technology, "Security Requirements for Cryptographic Modules," FIPS PUB 140-3, March 22, 2019. [Online] Available at: https://doi.org/10.6028/NIST.FIPS.140-3

(11) National Institute of Standards and Technology, "Engineering Trustworthy Secure Systems," November 2022, [Online] Available at: https://doi.org/10.6028/NIST.SP.800-160v1r1

(12) Consultative Committee for Space Data Systems, "Application of Security to CCSDS Protocols," Informational Report, Issue 3, March 2019, [Online] Available at: https://ccsds.org/Pubs/350x0g3.pdf

(13) Consultative Committee for Space Data Systems, "Security Guide for Mission Planners," Informational Report, Issue 2, April 2019, [Online] Available at: https://ccsds.org/Pubs/350x7g2.pdf

(14) Cybersecurity and Infrastructure Security Agency, Space Policy Directive 5, Cybersecurity Principles for Space Systems, September 04, 2020, [Online] Available at:

https://www.cisa.gov/resources-tools/resources/space-policy-directive-5

(15) National Aeronautics and Space Administration, “NASA’s Commercial Communications Services.” [Online] Available at: https://www.nasa.gov/directorates/heo/scan/services/nasas_commercial_communications_services

(16) R. Ross, V. Pillitteri, R. Graubart, D. Bodeau, R. McQuaid, “Developing Cyber Resilient Systems: A Systems Security Engineering Approach.” SP 800-160 Vol. 2. November 2019.

(17) R. Ross, M. McEvilley, J. Oren, “Systems Security Engineering: Considerations for a Multidisciplinary Approach in the Engineering of Trustworthy Secure Systems.” NIST SP 800-160 Vol. 1, November 2016 (Updated March 21, 2018), [Online] Available at: https://csrc.nist.gov/publications/detail/sp/800-160/vol-1/final

(18) R. Jewett, “Viasat Releases New Large-Aperture Space-to-Ground Communication Antennas,” ViaSatellite, January 20, 2022. [Online] Available at: https://www.satellitetoday.com/ground-systems/2022/01/20/viasat-releases-new-large-aperture-space-to-ground-communication-antennas/

(19) Sampathkumar, Arun Kumar. Uber-ization of Ground Stations. “The Small Satellite Market’s Enabling Aggregator Wave.” [Online] Available at: https://interactive.satellitetoday.com/via/august-2021/uber-ization-of-ground-stations-the-small-satellite-markets-enabling-aggregator-wave/

(20) IO Spacecom. “Launching Go.BIC at SmallSat Conference 2024.” Press Release. August 5, 2024. [Online] Available at: https://www.iq-spacecom.com/news/highlights/iq-spacecom-and-rbc-signals-launch-the-go-bic-service

(21) National Aeronautics and Space Administration, “LLCD: 2013-2014,” July 15, 2018 [Online] Available at: https://www.nasa.gov/directorates/heo/scan/opticalcommunications/llcd/

(22) Waterman, S. “Space Lasers Come of Age: Optical Communications for Satellites Are Ready for Prime Time.” February 22, 2022. [Online] Available at: https://interactive.satellitetoday.com/via/march-2022/space-lasers-come-of-age-optical-communications-for-satellites-are-ready-for-prime-time/_fragment.html

(23) National Aeronautics and Space Administration, “Lunar Laser Communication Demonstration: NASA’s First Space Laser Communication System Demonstration Fact Sheet.” [Online] Available at: https://www.nasa.gov/sites/default/files/llcdfactsheet.final_.web_.pdf

(24) Krynitz, Martin and Heese, Clemens and Knopp, Marcus Thomas and Schulz, Klaus-Jürgen and Henniger, Hennes, “The European Optical Nucleus Network,” 16th International Conference on Space Operations (SpaceOps 2021), 03.-05. May 2021.

(25) National Institute of Information and Communications Technology, “Small Optical Link for International Space Station (SOLISS) Succeeds in Bidirectional Laser Communication Between Space and Ground Station.” April 30, 2020. [Online] Available at: https://www.nict.go.jp/en/press/2020/04/30-1.html

(26) Florian Moll, Amita Shrestha, Christian Fuchs, “Ground Stations for Aeronautical and Space Laser Communications at German Aerospace Center.” Proc. SPIE 9647, Advanced Free-Space Optical Communication Techniques and Applications. https://core.ac.uk/reader/31021696

(27) Thales, “Beam me up! Thales & Goonhilly Earth Station Collaborate on Research into Laser Beams as Data Pipes.” June 8, 2021. [Online] Available at: https://www.thalesgroup.com/en/australia/press-release/beam-me-thales-goonhilly-

earth-station-collaborate-research-laser-beams

(28) Swedish Space Corporation. “SSC awarded 2.26M€ for NODES.” Press Release. May 15, 2023. [Online] Available at: https://sscspace.com/ssc-awarded-2-26me-for-nodes/

(29) S. Erwin, “DoD Space Agency Funds Development of Laser Terminal that Connects to Multiple Satellites at Once.” March 10, 2022. [Online] Available at: https://spacenews.com/dod-space-agency-funds-development-of-laser-terminal-that-connects-to-multiple-satellite-at-once/

(30) “World´s 1st SDA T1 & T2 compliant digital optical ground station comms package,” March 6, 2024. Satnews. [Online] Available at: https://news.satnews.com/2024/03/06/worlds-1st-sda-t1-t2-compliant-digital-optical-ground-station-comms-package/



Chapter Contents

Chapter Glossary ii
12.0 Identification and Tracking Systems 373
12.1 Introduction 373
12.2 Identification and Tracking Ground Systems 375
12.3 Tracking Aids 377
12.4 Devices that Communicate Position and ID via Radio 378
12.5 Devices that Use Coded Light Signals 380
12.5.1 Van Atta Arrays and RF Interrogation Receivers 381
12.5.2 Laser-Interrogated Corner Cube Reflectors 382
12.5.3 Passive Increase in Albedo 382
12.6 Future Efforts 383
12.7 Summary 383
References 383

Chapter Glossary

(18 SDS)	U.S. Space Force 18th Space Defense Squadron
(19 SDS)	U.S. Space Force 19th Space Defense Squadron
(CA)	Conjunction Assessment
(CARA)	NASA's Conjunction Assessment Risk Analysis program
(CAESAR)	Conjunction Analysis and Evaluation Service, Alerts and Recommendations
(CCR)	Corner Cube Reflectors
(CNES)	Centre National d'Etudes Spatiales (French Space Agency)
(COTS)	Commercial-off-the-Shelf
(CUBIT)	CubeSat Identification Tag
(D/T/I)	Detection, Tracking and Identification
(EGTN)	ExoAnalytic Global Telescope Network
(ELROI)	Extremely Low Resource Optical Identifier
(EUSST)	European Union Space Surveillance and Tracking program
(FCC)	Federal Communications Commission
(GEO)	Geostationary Equatorial Orbit
(GNSS)	Global Navigation Satellite System
(GPS)	Global Positioning System
(GUI)	Graphical User Interface
(HEO)	Highly Elliptical Orbit
(HUSIR)	Haystack Ultrawideband Satellite Imaging Radar
(ILRS)	International Laser Ranging Service
(LEDs)	Light Emitting Diodes
(MEO)	Medium Earth Orbit
(NPR)	NASA Procedural Requirements
(NTE)	Nanosatellite Tracking Experiment
(NTIA)	National Telecommunications and Information Administration
(OCAP)	Orbital Conjunction Assessment Plan
(OD)	Orbital Determination
(OEM)	Orbit Ephemeris Message
(O/Os)	Owner/Operators
(OSAs)	Orbital Safety Analysts
(PNT)	Position, Navigation, and Timing
(RF)	Radio Frequency
(RFID)	Radio Frequency Identification
(SRI)	Stanford Research Institute
(SSA)	Space Situational Awareness
(SSN)	Space Surveillance Network
(SWaP)	Size, Weight, and Power
(TLE)	Two-Line Element
(TraCSS)	Traffic Coordination System for Space

12.0 Identification and Tracking Systems

12.1 Introduction

In the past, most launches involved a single, large satellite launching on a dedicated launch vehicle. Small satellites as secondary payloads were sometimes “dropped off” along the way to the primary payload’s orbit or rode along to the final orbit with the primary payload. In either case, it typically was not that difficult for tracking radars to distinguish between primary and secondary payloads based on size and operational parameters.

Recently, however, multi-manifest or “rideshare” launches have become more common, and providers (1)(2)(3) are launching multiple CubeSats, or bundling CubeSats and other smaller payloads with larger payloads to fill up the excess capacity of almost any given launch vehicle. For technical and cost reasons, such launches generally deploy small satellites and CubeSats into very similar orbits over a short time window. “Batch” launches with a lack of separation between satellites can prevent effective tracking and create “CubeSat confusion” (4). When CubeSats are deployed close together in space and time, they can be difficult to distinguish from each other by tracking radars, making it difficult to determine which orbits correlate to which spacecraft, preventing a unique orbital state for each object from being added to the catalog of on-orbit objects (5)(6). Even when successful, these objects frequently remain unidentified for a lengthy period of time. It is not unusual for the process to take weeks to months to sort out which object is which, while some may never be positively identified at all. If the orbital states cannot be determined and the spacecraft cannot be added to the catalog of on-orbit objects, neighboring satellites may be unaware of close approaches, thereby hindering their ability to mitigate risks of collision. Furthermore, if identification is not resolved then conjunction warnings may not be sent to the responsible party or – even worse – they may be erroneously sent to an incorrect party if a mis-identification occurs.

Due to their standardized shape and size, CubeSats look very similar to one another, especially when they are in orbit hundreds of kilometers away. If there are unidentified objects from a launch, then the possible number of associations of object identifications (IDs) to tracked objects scales as n! (n-factorial, where n is the number of unidentified space objects from the launch). For example, if there are just two objects, say a payload and an upper stage, there are two ways in which you can associate the IDs with the tracked objects, and even that can be a challenge (7). However, if there are ten unidentified objects, there are 3,628,800 possible combinations; with 20 this rises to 2.4×10^{18} combinations. The magnitude of the problem becomes large very quickly. Annually, several multi-manifest deployments already deliver over 100+ objects per launch. As new launch vehicles come to market, this capacity is anticipated to increase to several hundred objects per launch, meaning that an already acute problem will only intensify.

Small satellites can improve their chances of being identified and tracked through good coordination with tracking agencies pre-launch, through community sharing of position/velocity, maneuvering, and covariance data in clearly defined, consistent, standardized formats (ex: Orbit Comprehensive Message (OCM)), and through careful selection of deployment direction and timing (8). Good spacecraft design choices can also improve the chances of small satellites surviving launch and early orbit (9), and can even make use of in-space commercial radio networks as a “back-up” method of communicating, should primary systems fail (10). However, despite improvements in both design and coordination, many small satellites still go unidentified. This has led to the introduction of tracking aids – independent systems that help owners and trackers identify small satellites and CubeSats, in some cases even if the satellite is malfunctioning.

Even if a small satellite is trackable (or rendered trackable through one of the enhancements discussed below), it is important that this position information be combined with satellite planned

maneuver information and packaged into a predicted ephemeris that can be sent regularly (at least daily) to a conjunction assessment (CA) screening authority. The only way that CA screenings can be meaningful is if a satellite's future position is used by the screening authority in the screening process. Non-cooperative tracking, even if it is well and frequently performed, cannot anticipate satellite maneuvers, and this information is essential to a robust conjunction assessment system. Maneuverable satellites (which include satellites that employ non-propulsive trajectory modification methods, such as differential drag) must assemble and furnish durable predicted ephemerides to the screening authority, either through indigenous means (i.e., unaided tracking and their own flight dynamics system's production of a predicted ephemeris) or via one of the position determination approaches to be described in order to ensure the operators are aware of close approaches with them. Non-maneuverable spacecraft need only ensure that they are trackable, although the CA best practices documents (12) all stress the importance of owner/operators (O/Os) taking responsibility for ensuring that screening authorities possess timely and accurate predicted position information for their spacecraft.

O/Os need not perform ephemeris generation themselves; there are several commercial companies that will perform this function on their behalf, and it is plausible that government systems will have a similar capability in the near future. O/Os can furnish a third-party provider with their on-board Global Navigation Satellite System (GNSS) data and their maneuver plans, enabling the provider to produce a predicted ephemeris with a realistic covariance regularly (i.e., at least daily in LEO, three times daily for orbits with perigees below 500 km) and furnish it to the appropriate screening authority. It is important that quality orbit determination be performed in such cases, which means both accurate predicted state estimates and, perhaps even more important for orbital safety, realistic covariance matrices accompanying each ephemeris point. Because satellite collision likelihood calculations require a statement of the state prediction uncertainty in order to compute the probability of collision, it is very important that realistic covariance estimates be produced and included with the ephemeris; this is not always a routine flight dynamics product, so it is necessary that ephemeris "vendors" be queried about their abilities to tune their organization development process to produce realistic covariances and their methodologies for verifying covariance realism. The NASA Conjunction Assessment Risk Analysis (CARA) repository, (search for "NASA CARA Analysis Tools") contains covariance realism evaluation code and associated theoretical and technical documentation. Small missions or university research CubeSat endeavors are offered special rates by some firms for ephemeris generation, so such O/Os should ask about special pricing structures that may make ephemeris data quite affordable.

While the thrust of the above comments pertains to routine satellite identification and tracking once a satellite is firmly established in its final orbit and placed into the space catalogue, a particular problem occurs directly after satellite injection but before cataloguing—the collision avoidance "COLA Gap." During large launch deployments, it is often difficult to reliably distinguish multiple spacecraft, and it can take days or even weeks for enough spacecraft separation and regular tracking to occur to allow durable cataloguing. Because only catalogued objects are accommodated by the conjunction assessment enterprise, spacecraft caught in the COLA Gap are not included, thus creating a collision danger both to other satellites and to themselves. Producing an ephemeris from on-board GNSS information or using one of the beacon or tracking aid devices enumerated below can allow a deployed satellite's current position, and therefore predicted position ephemeris, to be assembled rapidly. This ephemeris can be forwarded as a special submission to the CA screening process, thus closing the COLA Gap.

Finally, it should be recognized that regular predicted orbit information is required until spacecraft demise, not just during active operations. Operators should consider this obligation when selecting a deployment orbit. If a satellite is not regularly trackable by non-cooperative sources

such as the United States Space Force Delta 2, this problem must be addressed through other means, such as processing of on-board GNSS information to produce a predicted ephemeris. This mechanism needs to persist fully through spacecraft re-entry or placement in a disposal orbit. This requirement is one reason that independently powered GNSS beacons are an attractive solution for satellites that are not easily trackable and will not pursue active deorbit at the end of their main mission. GNSS beacons also offer more precision than traditional, non-cooperative sources which has advantages in congested regions of space. Tracking is also important for spacecraft in cislunar space, where non-cooperative tracking is limited and GNSS solutions may not be technically feasible.

The information described below is not intended to be exhaustive but provides an overview of current state-of-the-art technologies and their development status for a particular small spacecraft subsystem. It should be noted that Technology Readiness Level (TRL) designations may vary with changes specific to payload, mission requirements, reliability considerations, and/or the environment in which performance was demonstrated. Readers are highly encouraged to reach out to companies for further information regarding the performance and TRL of the described technology. NASA does not endorse any of the companies or technologies described. Finally, there is no intention of mentioning certain companies and omitting others based on their technologies or relationship with NASA.

12.2 Identification and Tracking Ground Systems

The United States Space Force Delta 2 is responsible for performing space surveillance and providing foundational Space Situational Awareness (SSA) for the US Department of Defense as well as for other agencies and space entities. Delta 2's 18th Space Defense Squadron (18 SDS), located at Vandenburg Space Force Base in California, performs all catalog maintenance functions, including detection, tracking, and identification (D/T/I) of artificial objects in Earth orbit, and maintaining the space catalog which is publicly available on Space-Track.org. As part of their activities, they provide launch support, re-entry assessment, and other SSA functions. Orbital safety activities, such as conjunction assessment (which identifies close approaches between launch and other catalogued in-orbit objects) are provided by Delta 2's 19th Space Defense Squadron (19 SDS) at the Naval Support Facility at Dahlgren, VA. Maintaining the catalog is achieved via the US Space Surveillance Network (SSN), which is formed by a suite of sensors around the world (15). 18 SDS is currently tracking more than 50,000 objects in Earth orbit and can provide data for pieces as small as 10 cm in characteristic length. They issue two-line elements (TLEs) that are updated on a regular basis and can be used to compute predicted orbit positions for spacecraft communications acquisition and other purposes. They also produce precision vectors with covariance that can be used to perform conjunction analyses. TLEs are not accurate enough to be used for conjunction assessment, and do not include covariances that are needed to compute a probability of collision.

The US Space Force next generation SSA sensor, known as the Space Fence, was declared operational in March 2020 and can track objects below the previous 10 cm limit. It is located on Kwajalein Atoll, in the Republic of the Marshall Islands, and consists of a S-band radar system to track objects primarily in low-Earth orbit, although it can track objects in medium-Earth orbit (MEO) and geostationary equatorial orbit (GEO) as well. The 20th Space Surveillance Squadron based in Huntsville, Alabama, manages the Space Fence and provides data to 18 SDS to augment the space catalogue (16). Another important sensor in the SSN is the Haystack Ultrawideband Satellite Imaging Radar (HUSIR), which is the highest-resolution, long-range sensor in the world. HUSIR simultaneously generates X- and W-band images that can provide valuable information about the size, shape and orientation of Earth orbiting objects (17). These are just two examples of sensors that make up the SSN, many having specific unique capabilities that support the SSN's various functions, including conjunction assessment.

The NASA CARA program acts as the intermediary between 18/19 SDS and NASA satellite missions. CARA gathers orbit ephemeris and covariance files from the NASA spacecraft operations teams and provides this data to NASA's Orbital Safety Analysts (OSAs) at Vandenberg for screening and close approach prediction. CARA provides risk assessment of these predicted close approaches to NASA missions beyond the 19 SDS support provided to non-NASA users, including operations concept development, specialized probability of collision computation, high interest event notification, and conjunction geometry analysis, among other functions (14). The French Space Agency (CNES) created a conjunction risk assessment team called Conjunction Analysis and Evaluation Service, Alerts and Recommendations (CAESAR) that provides risk assessment services to their missions as part of the European Union Space Surveillance and Tracking (EUSST) program (18).

In 2023, NASA released Revision 1 to their best practices handbook entitled "Spacecraft Conjunction Assessment and Collision Avoidance Best Practices Handbook," which is a great reference for satellite operators with respect to collision avoidance topics (12). NASA Procedural Requirements (NPR) 8079.1 codifies those best practices as requirements for NASA space flight programs, projects, and vehicles to protect the space environment and reduce the risk of collision (13).

Besides USSF Delta 2, several commercial entities are providing tracking capabilities that can be purchased by stakeholders. ExoAnalytic and Slingshot Aerospace each operate global telescope networks consisting of dozens of observatories and hundreds of telescopes tracking orbiting objects in GEO, highly elliptical orbit (HEO), and MEO. The Exoanalytic Global Telescope Network (EGTN) can collect angles and brightness measurements. They each maintain a proprietary catalog of satellites and space debris that are regularly tracked and cataloged (19).

LeoLabs is another commercial entity providing spacecraft tracking and support services. They use a group of distributed Earth-based, phased-array radars to make a commercial-off-the-shelf (COTS) satellite tracking service targeted to the specific requirements of SmallSat operators in low-Earth orbit. They currently have radar locations in New Zealand, Costa Rica, the Azores, Poker Flat, AK, Midland, TX, Arizona, Western Australia, and Argentina. There are currently seven functioning radar sites as of 2024, with plans for more radars strategically located around the world to track objects down to size levels approaching those tracked by the DoD. The predicted performance also includes a revisit time of over 10 observations per day for specific objects. Through their LeoTrack platform, they can use their radar data to perform precision tracking and curate orbit information products for satellites as small as 1U. Their system includes an open-source graphical user interface capable of displaying all the catalog in real time, as well as fundamental orbit information about each individual object. They also offer a commercial launch and early orbit service, with SpaceX as one of their historic customers (20).

Catalogs provided by these commercial entities are different from the one maintained by 18 SDS in accuracy and objects included. Spacecraft owner/operators should be aware of the differences before choosing to use a particular service for a particular purpose. For conjunction assessment purposes, having multiple differing solutions can be confusing. The Department of Commerce was charged in Space Policy Directive-3 with creating a space traffic coordination system that enables commercial capabilities for conjunction assessment. In the future they may offer a conjunction assessment service that merges data from multiple sources in one solution as they work to transition the service currently provided by 19 SDS. Initial capability of the Traffic Coordination System for Space (TraCSS) is planned for 2026. Lessons learned from NASA's Starling (launched July 2023) and Starlink constellations are being fed into the design of TraCSS.

NASA's Starling 1.5 mission extension, using the four-CubeSat Starling swarm of spacecraft, was built on the Starling primary mission demonstration of autonomous maneuver planning and

execution. Partnering with SpaceX and their Starlink constellation, Starling 1.5 demonstrated an advanced space traffic coordination solution for co-located groups of autonomous spacecraft from different owner/operators. The onboard autonomous maneuvering software for the original Starling mission, consisting of Emergent Space Technologies (acquired by York Space Systems) Navigator and Autopilot products, can perform probability of collision calculations and propose risk mitigation maneuvers for conjunctions with co-located vehicles. A space traffic coordination hub on the ground will be able to receive maneuver responsibility claims from an operator, indicating that they intend to maneuver to reduce the conjunction risk, receive and screen proposed new trajectories in near-real-time, and provide operators conjunction data messages with screening results. This will enable highly automated operations, including conjunction risk assessment and mitigation between satellite owner/operators.

12.3 Tracking Aids

For spacecraft that cannot be routinely tracked by the SSN, it is important to ensure trackability by another means to enable other owner/operators to know where your spacecraft is to prevent debris-producing collisions. This is especially important for SmallSats that have orbital lifetimes that exceed operational lifetimes, as the risk to orbital neighbors remains after tracking activities have stopped. For NASA spacecraft, trackability until demise is required in NPR 8079.1 and assessed as part of the required Orbital Conjunction Assessment Plan (OCAP) written during design.

Tracking aids come in several categories, each with benefits and drawbacks (21). Table 12-1 summarizes the broad categories available, with representative examples discussed below. Size, weight, and cost vary for each of the examples, but all can be considered compatible with a CubeSat mission; see the references for detailed information on size, weight, and power (SWaP) and cost, all of which become more favorable each year with technology improvements and economies of scale. Once the augmented tracking data is collected, ephemeris data is made available to CARA/19 SDS for screening.

Several commercial companies offer services that will process the data produced by tracking aids and produce predicted orbit ephemeris data that can be used to perform conjunction assessment. These include SpaceNav, COMSPOC, and Kayhan Space, with Kayhan Space focusing specifically on small spacecraft support.

Table 12-1: Types of Tracking Aids

Technology Scheme	Description and Reference Mission	TRL	Citation
CubeSat position and ID via radio	A position, navigation, and timing (PNT) receiver is attached to a CubeSat, along with a radio to transmit the information via a LEO communications provider (or directly to the ground); example: BlackBox, Blinker.	7-9	(22) (23)
Coded light signals from light source on exterior of CubeSat	Exterior-mounted LEDs with large-aperture telescopes to receive the signal or diffused LED lasers with ground-based photon-counting cameras.	6-7	(24) (25)
Radio Frequency interrogation of an exterior Van Atta array	For example, exterior mounted radio frequency identification (RFID) tag & commensurate radar.	7-9	(26)

Laser interrogated corner cube reflectors (CCR)	One or several small CCRs can be attached to CubeSat exterior; ground-based laser and receiver telescope needed to distinguish number of CCRs.	7-9	(27)
Passive augmentations to visibility	Use of high-albedo paint or tape, improving overall conductance of the exterior of the satellite or other methods to increase visibility.	7-9	
Orbital Whereabout Locator (OWL)	A tuna can mounted plug and play device equipped with a battery that helps identify and keep track of a satellite with a GNSS based tracker, monitors key parameters of a satellite and downloads data using an omnidirectional antenna in any orientation.	7-9	

12.4 Devices that Communicate Position and ID via Radio

The most comprehensive (but also potentially the most complex and SWaP-intensive) option involves equipping a small satellite with an independent positioning, navigation, and timing (PNT) receiver and a separate radio capable of transmitting data to an independent communications provider. An example technology is the Black Box system by NearSpace Launch, Inc. that comes in several form factors for mounting internally or externally to a small satellite or CubeSat. The patch antenna shown in the first image is approximately 10 x 8 cm and can weigh as little as 22 grams; larger systems such as the one shown in the third image of Figure 12.1 have flown and are considered TRL 9. Another example often used for CubeSats is the NovAtel OEM7700. JAXA offers a strap-on tracking device called mini-Mt. Fuji; they can provide sensor tracking, or operators can track it themselves. These systems combine a low-power GPS receiver with a low-power radio capable of communicating with a low-Earth orbit communication provider (in the case of Black Box, the Iridium network), and operate independently from the spacecraft's regular command and telemetry links. Externally mounted versions often include solar cells for independent power generation. A Black Box system is currently flying on Spaceflight Sherpa-FX orbital transfer vehicle, launched on January 24, 2021, and returned GPS fixes to the developer which were analyzed and presented at the October 2021 and October 2022 International Astronautical Congress (28). As a further service, NearSpace Launch can generate a low- or high-precision ephemeris for one's satellite and furnish this to the O/O, who can then submit it to a CA screening authority.

The advantages to such a system are that it provides complete data on a satellite's position and requires no specialized ground equipment (other than the equipment used by the communications provider). Some such systems are independently powered and can provide data even if the host satellite never powers up, though others are dependent on spacecraft power to function. These systems are the most complex of the tracking aids described, however, and despite their relatively small size, are still the most SWaP-intensive of the options examined. Systems that rely on power from the host vehicle are also useless if the host vehicle suffers a power anomaly or failure. Having an additional onboard radio that communicates with other space assets necessitates additional oversight by the Federal Communications Commission (FCC) (or National Telecommunications and Information Administration (NTIA) for US Government missions licensing and coordination).

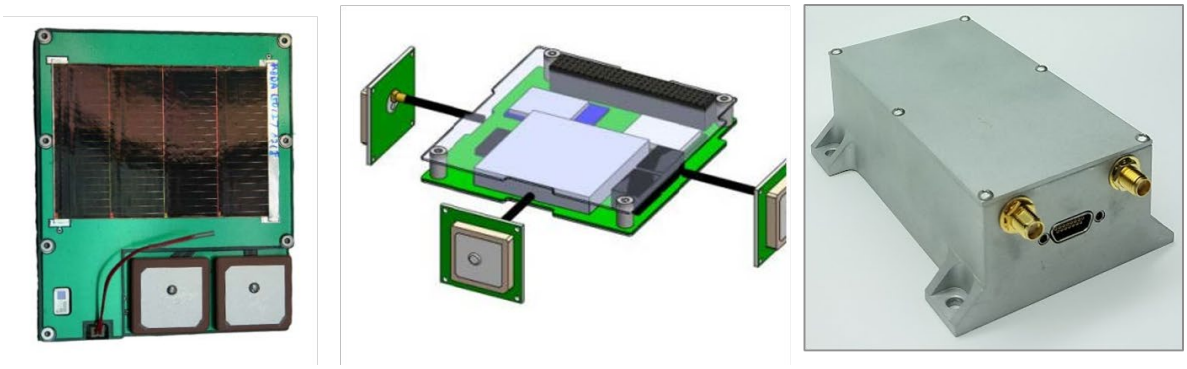


Figure 12.1: (left) Thin Patch or Stamp Black Box for side mounting. (Middle) PC104 Black Box for internal stack mounting. (Right) Standard Black Box for larger satellites. TRL 9: flown on spaceflight launch. Solar array and antennas not shown. Credit: NearSpace Launch, Inc.

In choosing such systems, it is important to choose one that is spac- rated, otherwise pre-launch testing must be performed via simulation. The system should also provide fast convergence after launch to allow rapid computation of an orbit determination solution to provide to 18/19 SDS for conjunction assessment screening as soon as possible after separation; this allows solution of the "COLA Gap" problem, namely providing orbital safety information and capabilities between payload injection and the time of the satellite's cataloging, which could be as long as several weeks. Other available features, like multi-frequency, multi-GNSS, and availability of pseudoranges are nice-to-have, but the benefit for conjunction assessment is marginal vs. just having a receiver. If flying a GPS system, it is important to ensure that the GPS data be available in the download stream and not just internally available to the spacecraft computer for onboard use.

Overall, when selecting such a system, the following considerations apply:

- Independent power of the device to ensure that it continues to function in the presence of internal spacecraft faults and be able to issue position information all the way until spacecraft demise;
- An ephemeris generation capability, either as a service from the device manufacturer, an indigenous capability of the O/O, or a service provided by a third-party provider. These ephemerides need to be submitted at least daily to the CA screening authority;
- The inclusion of planned satellite maneuvers in the predicted ephemeris to be furnished; and
- The existence of a ground network and communications path to allow the regular receipt of the broadcast data to achieve the requirements stated above.

It is also important to note that this approach can truly operate without *a priori* orbit state knowledge. That is to say, it does not require prior knowledge of an object's location in space to provide a tip or cue for initial or subsequent interrogation. Such data is often necessary with other approaches described below (to varying degrees) but is not required for this family of devices, because the radios are either omnidirectional or the receiver network is sufficiently proliferated that broadcasts can be received from any orbit without such prior knowledge.

12.5 Devices that Use Coded Light Signals

Identification systems and devices that make use of light emitting diodes (LEDs) and coded light signals have the advantage of being relatively simple and capable of uniquely identifying satellites. However, all systems flown to date have required power from the host satellite, leading to issues with detection (29) if the host satellite fails to power up. Current implementations are also relatively large, though future systems are expected to be much smaller and may include independent power. Devices such as the Extremely Low Resource Optical Identifier (ELROI) beacon (Figure 12.2), under development by Los Alamos National Lab (29), use exterior-mounted LEDs or diode lasers that blink in a prescribed sequence to uniquely identify satellites. The ELROI system is designed to be independently powered by a small solar cell and battery and is packaged into a system as small as a Scrabble tile, though only larger systems – with power provided by the host satellite – have flown.

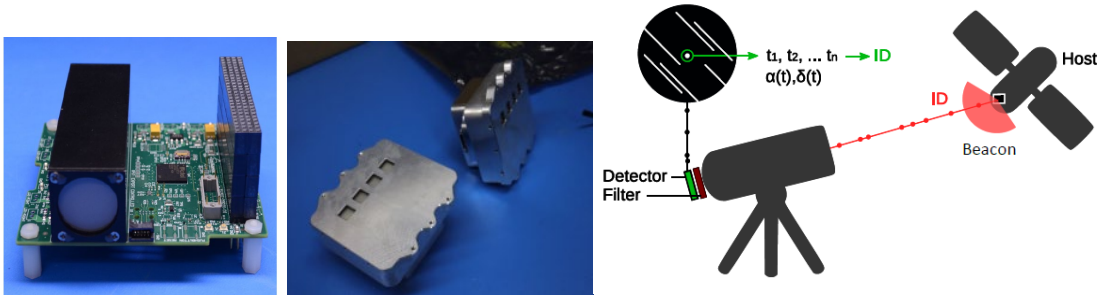


Figure 12.2: (left) ELROI PC104 beacon unit that was installed on NMTSat.d; (middle) Two ELROI beacon units delivered for a launch in 2021; (right) ELROI Optical Detection System. Credit: Los Alamos National Laboratory.

The emitters on such devices can be regular LEDs or diffused diode lasers but require specialized ground equipment – either a large-aperture telescope or a photon-counting camera – to track and identify the object as it passes overhead. Figure 12.2 (right) shows how the ELROI system works: a photon-counting camera attached to a telescope tracks the signal from a diode laser and decodes the ID of the host satellite from the on/off pattern of flashes. ELROI successfully demonstrated definitive identification on two CubeSats, LaCE-1 and R5-S4 in 2024 and 2025.

LED-based systems require relatively clear night-time skies for identification and dedicated ground equipment (telescope and sensor). The light sources are too faint to allow blind searching of the sky for the satellite; orbital information from a SSA provider is also required to find and track the CubeSat, although the process of tracking the satellite via an optical telescope allows the orbital ephemeris to be updated. Therefore, this tracking enhancement alone cannot be used to identify and catalogue the spacecraft. Issues with attitude control on the host satellite can also complicate the identification process. In addition, using LEDs or other light sources on a satellite while in Earth's shadow should be done carefully to minimize interference with astronomical observations **Error! Reference source not found.**. The SatCon1 report (37) **Error! Reference source not found.**on page 6 lists several recommendations to be followed: 1) assure the light source is fainter than apparent magnitude of V ~7 (and the fainter the better), and 2) provide advance notice of any illumination times, including accurate orbital elements.

12.5.1 Van Atta Arrays and RF Interrogation Receivers

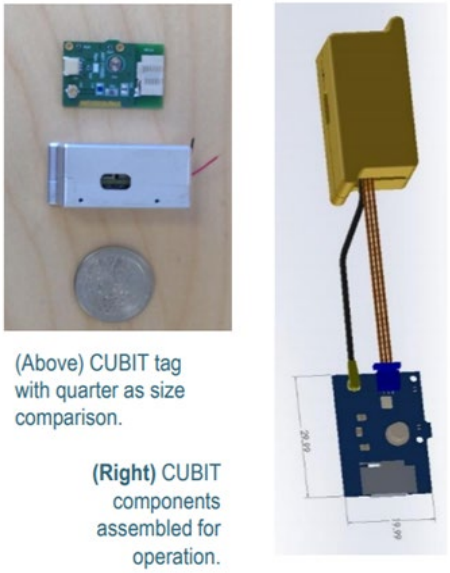


Figure 12.4: CUBIT. Credit: SRI International.

Another method for increasing the ability to track and identify small satellites involves devices that respond when interrogated by a radio frequency (RF) signal of appropriate wavelength. One such system, the CubeSat Identification Tag (CUBIT) shown in Figure 12.4, is like the RFID devices used in proximity badges (26). Built by SRI International and partnered with NASA Ames, CUBIT responds with a short burst of information when interrogated by a radio signal of the correct frequency. CUBIT is relatively small and designed to be independent of host vehicle power. The implementations that have flown contain a small battery suitable for 30 days of in-orbit life, which covers the most critical early orbit identification period. It could therefore be coupled with a coded light emitter to overcome the inability of that system to allow object identification. The device is separated into an internally mounted electronics unit attached to an exterior antenna to minimize the exterior footprint of the unit. Two units have flown and were successfully demonstrated in space onboard TechEdSat-6 in 2017 and TechEdSat-7 in 2020. A relatively large ground architecture (in CUBIT's case, a 30 m antenna and an array of antennas) is required to interrogate the system and successfully acquire the low-power response. CUBIT is patent-pending, and SRI has reached commercialization agreements with potential vendors. Future research will continue with a recently awarded AFWERX Phase 1 study.

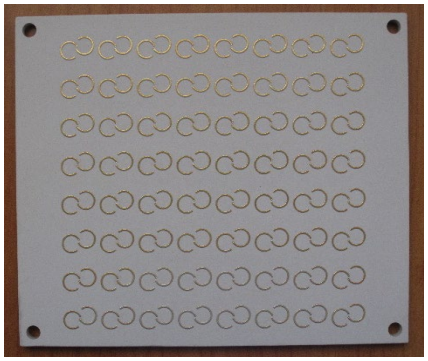


Figure 12.5: NTE Van Atta array retro-reflector in the Ku-band, fits standard 1U panel, tuned to HAX RADAR frequency. Credit: Naval Information Warfare Center.

Another example of an RF-interrogated device is a Van Atta array, a passive device that re-radiates RF energy back to its source (30). One such device, the Nanosatellite Tracking Experiment (NTE) consists of a 64-element Van Atta array of tiny, paired antennas tuned to a Ku-band RF frequency, as shown in Figure 12.5 (31). When interrogated at the proper frequency range, the incident RF field received by each antenna is fed to a corresponding antenna via a passive transmission line, where it is re-radiated. This significantly increases the radar cross-section of the object, allowing it to be more easily tracked. Unique identification is difficult, however, and requires specialized ground stations that tend to be expensive to operate. A satellite carrying a Van Atta array device will be distinguishable from one not carrying such a device, or from one carrying a device tuned to a different frequency band, but two satellites carrying identical Van Atta array will return the same signature. The RF interrogation also requires a ground source of the appropriate frequency. However, Van Atta array devices are entirely passive and extremely low SWaP, making them easy to include on small satellites and CubeSats. NTE devices have flown in space but results from those flight experiments have not yet been published.

No capability currently exists at the SSN to process Van Atta array data, so it would be incumbent on the spacecraft operator to produce its own orbit determination solution from the data to provide an ephemeris to 18/19 SDS for CA screening.

12.5.2 Laser-Interrogated Corner Cube Reflectors

Corner cube reflectors (CCRs), long used in the space industry, are special mirrors designed to reflect laser light back in the direction from which it originated. They require no internal energy source. When illuminated by a laser, they provide a return signal that can be detected on the ground by a fast camera, as seen in Figure 12.6. Putting a different number of CCRs on a set of CubeSats allows the ground station to differentiate between the CubeSats (i.e., a CubeSat with one CCR will produce a different return signal from another with two CCRs or three CCRs, etc.). One can use a laser and telescope system like those employed by the International Laser Ranging Service (ILRS) (32), which are high-TRL systems that have been operating for decades. Precise *a priori* orbital information is required to lase the CubeSat and receive a return signal, and the number of satellites that can be uniquely identified is limited by the number of corner cube reflectors that can be attached.

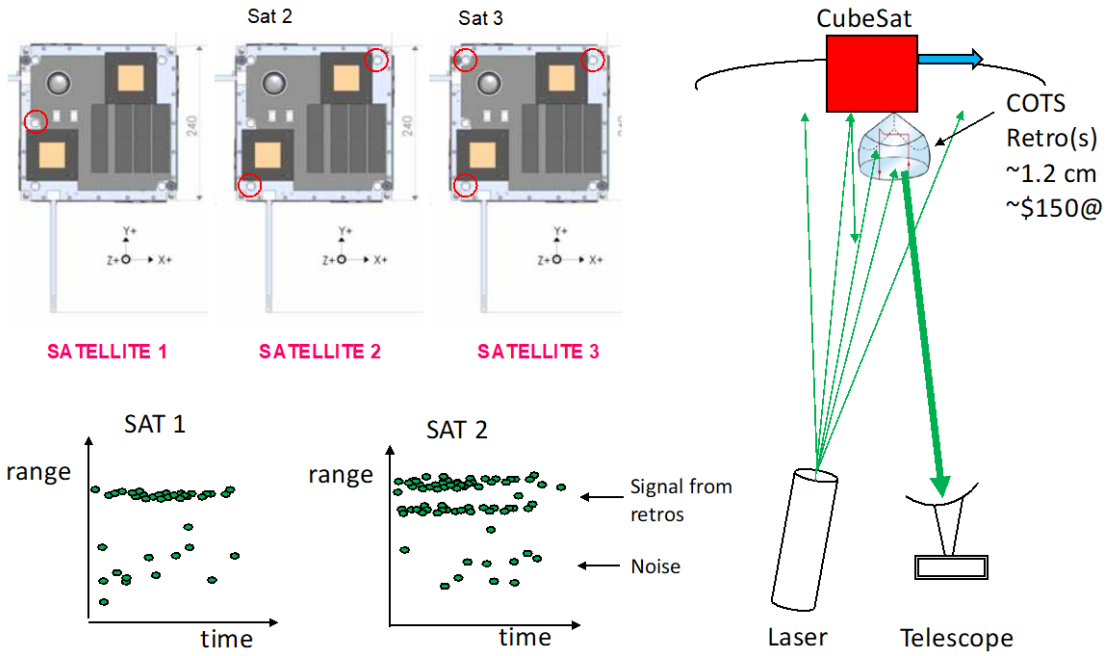


Figure 12.6: Corner Cube Reflectors. Credit: The Aerospace Corporation.

12.5.3 Passive Increase in Albedo

The simplest method of increasing satellite trackability involves using high-albedo paint, special tape, or other simple methods to increase the optical or radar visibility of a small satellite, allowing it to be more easily detected by ground-based systems (33). White-colored thermal paint has been used for years to increase the ability of satellites to reject heat, which also improves their visibility and trackability. Additionally, CubeSats often deploy a mission-specific configuration of wire antennas and/or cylindrical boom structures which can serve as unique identifiers using ground-based optical or radar characterization, while also increasing radar cross-section or photometric return to improve trackability (34). Such approaches are simple, require little to no SWaP, and are readily available, but do not uniquely identify the satellite, and are limited in their effectiveness. Wires and booms also have the added complexity of deployment considerations.

12.6 Future Efforts

Many in the community are aware of the "CubeSat confusion" issue, and there is a growing effort to mitigate this problem (35)(36). Numerous commercial providers have endorsed the Space Safety Coalition to promote responsible space safety guidelines across the community. Through this adoption of relevant international standards for space mission design, the development of more effective space safety guidelines and best practices can establish a more cohesive space environment (41).

On the horizon, High Earth Robotics plans to create the Argus constellation – twelve optical 6U HERO-1 nanosatellites with space telescope payloads in GEO that can identify objects, take high-resolution images of damaged satellites, and help identify solutions to avoid further degradation. The constellation is intended to be resilient to interference and communications link interruption (39). Vantor is another commercial company that operates in LEO and offers a “Non-Earth Imaging” (NEI) service that can identify satellites when properly cued and tasked (11).

Finally, government agencies and industry organizations are looking to standardize many of the approaches, data products, and technologies discussed in this document. Such an effort would ensure interoperability and place a “stamp of approval” that will reassure operators that their efforts are accepted as a best practice.

12.7 Summary

Small satellites and CubeSats are likely to continue increasing in popularity, and multi-manifest launches provide a very cost-effective way to get large numbers of satellites into space. Improving the ability to identify and track small satellites in space – especially those deployed in batches from a single launch vehicle – can help both small satellite owners and the entire space enterprise avoid the pitfalls of “CubeSat confusion.” Tracking SmallSats from launch through demise is critical to avoid collisions and preserve the space environment from orbital debris. It is important that the end-to-end cost and resulting capability are evaluated when choosing a tracking option to ensure that the needed functionality is provided.

For feedback solicitation, please email: arc-sst-soa@mail.nasa.gov. Please include a business email so someone may contact you further.

References

(1) Spaceflight. [Online] 2021. Accessed March 3, 2021. Available at: https://spaceflight.com

(2) Nanoracks. “Nanoracks Books CubeSat Rideshare and Habitat Building Demonstration in Single SpaceX Falcon 9 Launch”. [Online] 2019. Accessed March 3, 2020. Available at: https://nanoracks.com/rideshare-habitat-building-demonstration/

(3) Kirtland Airforce Base. “Space Test Program”. [Online] 2007. Accessed April 8, 2020. Available at: https://www.kirtland.af.mil/About-Us/Fact-Sheets/Display/Article/826059/space-test-program/

(4) M.A. Skinner. "CubeSat Confusion: how to avoid ‘dead on arrival’." International Astronomical Congress 71st meeting, October 12-14, 2020.

(5) I. Klotz. "SpaceX Rideshare Mission Spawns 12 Orphan CubeSats." Aerospace Daily and Defense Report, August 12, 2019.

(6) L. Grush. "Why the Air Force Still Cannot Identify more than a Dozen Satellites from One December Launch: The case of the unknown satellites." [Online] 2019. Available at: https://www.theverge.com/2019/4/2/18277344/space-situational-awareness-air-force-tracking-sso-a-spaceflight-CubeSats

(7) J. Bloch et al. "The ALEXIS Mission Recovery." 17th annual American Astronomical Society (AAS) guidance and control conference, Keystone, CO, 1994.
(8) B. Braun and S. Herrin. "The More, the Messier: ORS-3 lessons for multi-payload mission deployments." 1-10. 10.1109/AERO.2016.7500582. 2016.
(9) C.C. Venturini. "Improving Mission Success of CubeSats." [Online] Aerospace Report number TOR-2017-01689. June 12, 2017. Accessed May 15, 2019. Available at: https://www.nasa.gov/sites/default/files/atoms/files/improving_mission_success_of_CubeSats_-_tor-2017-01689.pdf
(10) H.D. Voss et al.: "Globalstar Communica0on Link for CubeSats: TSAT, GEARRS1, and GEARRS2." 29th AIAA/USU Conference on Small Satellites, Logan UT, August 9, 2015.
(11) Vantor, "WorldView Space," 2026, [Online] Accessed February 24, 2026, Available at: https://vantor.com/product/worldview/space/.
(12) NASA Spacecraft Conjunction Assessment and Collision Avoidance Best Practices Handbook, Rev 1, Feb 2023, https://nasa.gov/cara.
(13) NASA, "NASA Spacecraft Conjunction Analysis and Collision Avoidance for Space Environment Protection," June 27, 2023, https://nodis3.gsfc.nasa.gov/
(14) NASA, "Conjunction Assessment Risk Analysis," 2022, [Online] Available at: https://cms.nasa.gov/conjunction-assessment.
(15) Launch Conjunction Assessment Handbook. LAUNCH CONJUNCTION ASSESSMENT HANDBOOK VERSION 1.0, DECEMBER 2018. 18 SPCS Process for Launch Conjunction Assessment, JFSCC, 18th Space Control Squadron Combined Space Operations Center (CSpOC)Vandenberg Air Force Base, California, www.s p a c e-track.org.
(16) S. Erwin. "Space Fence surveillance radar site declared operational". [Online] Accessed September 29, 2020. Available at: https://spacenews.com/space-fence-surveillance-radar-site-declared-operational/
(17) Massachusetts Institute of Technology, Lincoln Labs. "Haystack Ultrawideband Satellite Imaging Radar." [Online] 2022. Accessed July 2022. Available at: https://www.ll.mit.edu/r-d/projects/haystack-ultrawideband-satellite-imaging-radar
(18) French Space Agency, "Space Surveillance And Tracking," January 15, 2025, [Online] Available at: https://cnes.fr/en/projects/sst.
(19) ExoAnalytics Solutions. "Space Domain Awareness (SDA)." [Online] 2020. Accessed March 18, 2020. Available at: https://exoanalytic.com/space-domain-awareness
(20) LeoLabs. "LeoLabs Partners with SpaceX to Track Starlink Satellite Deployments," October 27, 2020. [Online] Available at: https://leolabs-space.medium.com/leolabs-partners-with-spacex-to-track-starlink-satellite-deployments-4e579052546f
(21) M.A. Skinner. "Making Small Satellites Visible: Nanosat tracking and identification techniques and technologies." International Astronomical Congress 70th meeting, Washington DC, October 21-25, 2019.
(22) H.D. Voss, J.F. Dailey, M.B. Orvis. "Black Box' Beacon for Mission Success, Insurance, and Debris Mitigation." 32nd Annual AIAA/USU Conference on Small Satellites, Logan UT. 2018.
(23) A.J. Abraham. "*GPS Transponders for Space Traffic Management*." Center for Space Policy & Strategy, Aerospace Corporation, April 2018.
(24) J. Cutler, P. Seitzer, C.H. Lee *et al*. "Improved Orbit Determination of LEO CubeSats: Project LEDsat." AMOS Technologies Conference, Maui, Hawai`i. September 2017.
(25) D.M. Palmer R.M. Holmes. "*ELROI: A License Plate for Your Satellite*." Journal of Spacecraft and Rockets, Vol. 55, No. 4, pp. 1014-1023, 2018.
(26) S. Phan. "'Spaceflight Industries' SSO-A Flight Launches with SRI International's CUBIT Technology Onboard, Developed to Track and Identify Low Earth Orbit Satellites." [Online]

Accessed October 30, 2019. Available at: https://www.sri.com/blog/spaceflight-industries-sso-flight-launches-sri-internationals-cubit-technology-onboard

(27) G. Kirchner, L. Grunwaldt, R. Neubert, F. Koidl, M. Barschke, Z. Yoon, H. Fiedler, C. Hollenstein, "Laser Ranging to Nano- Satellites in LEO Orbits: Plans, Issues, Simulations." 18th International Workshop on Laser Ranging, Fujiyoshida, Japan. 2013.

(28) H.D. Voss et. al., "'Black Box' RF Sat-Link for Space Debris, Mission Success and Risk Mitigation," International Astronautical Congress, 2022.

(29) D.M. Palmer et. al., "Progress Towards the ELROI Satellite License Plate." 34th Annual Conference on Small Satellites, Logan, UT. 2020.

(30) D. Bird. "Design and Manufacture of a Low-Profile Radar Retro-Reflector." RTO SCI Symposium on "Sensors and Sensor Denial by Camouflage, Concealment and Deception", Brussels, Belgium, April 19-20, 2004, and published in RTO-MP-SCI-145.

(31) D. Lane et. al. "Nanosatellite Tracking using Passive Retro-Reflectors." SSC20-WKIV-04, 34th Annual Conference on Small Satellites, Logan, UT, 2020.

(32) NASA. "ILRS Overview," [Online] May 9, 2016. Accessed July 2022. Available at: https://ilrs.gsfc.nasa.gov/about/Overview.html

(33) D. Hall. "Optical CubeSat Discrimination." AMOS Technical Conference, September 2008.

(34) C. Chong and M. Shozo. "Metrics for feature-aided track association." 9th International Conference on Information Fusion, IEEE, 2006.

(35) US Federal Communications Commission, "Orbital Debris in the New Space Age, Report and Order and Further Notice of Proposed Rulemaking." FCC-20-54, paragraph 62, April 24, 2020.

(36) M. Skinner, A. Goodyear, et al., "CUBESAT CONFUSION: CUBESAT ID VIA GROUND-BASED OBSERVATIONS OF A PULSED LED BEACON," 21st IAA SYMPOSIUM ON SPACE DEBRIS, 74th International Astronautical Congress 2023.

(37) AAS and NSF NOIRLab, "SATCON1 Report: Dark and Quiet Skies Technical Workshop on Satellite Constellations," 2020, p. 6. [Online] Available at: https://satcon1.aas.org.

(38) M. Skinner, M. Coletti, M.C. Voss, T. Svitek, J.C. Lee, K. Auman, H. Patel, E.J. Moyer. "Mitigating CubeSat Confusion: results of in-flight technical demonstrations of candidate tracking and identification technologies." 72nd International Astronautical Congress (IAC), Dubai, United Arab Emirates, 25-29 October 2021.

(39) M. Skinner, K. Auman, E.J. Moyer, M.C. Voss, J.C. Lee, R. Olcott, H.E. Weiher, A.M. Goodyear, D.A. Hinkley. "Mitigating CubeSat Confusion: further results of in-flight technical demonstrations of candidate tracking and identification technologies," 73rd International Astronautical Congress (IAC), Paris, France, 18-22 September 2022.

(40) Abraham, Andrew et. al. "*A Prototype GPS Transponder of Space Traffic Coordination*." Journal of Space Safety Engineering, Vol. 12, No. 4, pp. 792-810, 2025.

(41) Space Safety Coalition, "Best Practices for the Sustainability of Space Operations," January 2026, V 2.40



Chapter Glossary ii
13 Deorbit Systems 384
13.1 Introduction 384
Definitions 385
13.2 Orbital Debris Regulations 386
13.2.1 Considerations for Orbital Lifetime Requirements in LEO 387
13.3 State-of-the-Art – Passive Deorbit Systems 388
13.3.1 High TRL Drag Sails 388
13.3.2 Deployable Booms 396
13.3.3 Electromagnetic Tethers 396
13.3.4 Natural Deorbiting Highways 397
13.4 State-of-the-Art – Active Deorbit Systems 397
13.4.1 Active Debris Removal Hardware 397
13.4.2 Active Debris Removal / Spacecraft Reentry Services 399
13.5 Summary 402
References 402

Chapter Glossary

(ACS3)	Advanced Composite Solar Sail System
(ADCS)	Attitude Determination and Control System
(ADE)	Aerodynamic Deorbit Experiment
(ADR)	Active Debris Removal
(AFRL)	Air Force Research Laboratory
(BC)	Ballistic Coefficient
(CLEAR)	Clearing of the LEO Environment with Active Removal
(COPUOS)	Committee on the Peaceful Uses of Outer Space
(COSMIC)	Cleaning Outer Space Mission through Innovative Capture
(CRD2)	Commercial Removal of Debris Demonstration
(CSTT)	CubeSat Terminator Tape
(D3)	Drag Deorbit Device / D-Orbit Decommissioning Device
(DLR)	German Aerospace Center
(DOM)	Deorbit Mechanism
(EOL)	End-of-Life
(ESA)	European Space Agency
(ESEO)	European Student Earth Orbiter
(FAA)	Federal Aviation Administration
(FCC)	Federal Communications Commission
(GCD)	Game Changing Development
(GTO)	Geostationary Transfer Orbit
(HPS)	High Performance Space Structure Systems
(IADC)	Inter-Agency Space Debris Coordination Committee
(ISS)	International Space Station
(JAXA)	Japan Aerospace Exploration Agency
(LEO)	Low-Earth Orbit
(MSFC)	Marshall Space Flight Center
(NSTT)	NanoSat Terminator Tape

(ODMSP)	Orbital Debris Mitigation Standard Practices
(RPO)	Rendezvous and Proximity Operations
(SBIR)	Small Business Innovation Research
(SSO)	Sun-synchronous Orbit
(SSR)	Space Sustainability Rating
(SSTL)	Surrey Satellite Technology Ltd.
(STMD)	Space Technology Mission Directorate
(TES-n)	Technology Educational Satellite series
(TRL)	Technology Readiness Level
(TTP)	Thermosphere Test Probe
(UN)	United Nations
(UTIAS-SFL)	University of Toronto Institute for Aerospace Studies Space Flight Laboratory
(WEF)	World Economic Forum

13 Deorbit Systems

13.1 Introduction

Space debris, also known as orbital debris or space pollution, are derelict artificial objects left in space on purpose or accidentally that include larger nonfunctional spacecraft and rocket bodies, and smaller disintegrated mission-related objects such as lens caps, ejected bolts, or even paint flakes. Additionally, larger space debris are commonly broken up into even smaller fragments due to collisions, erosion, or expelled particles from spacecraft or rocket bodies. This presents a major problem in the space environment as spacecraft can be damaged or destroyed by space debris collisions due to the very high velocities of the debris objects, which then produces even more space debris.

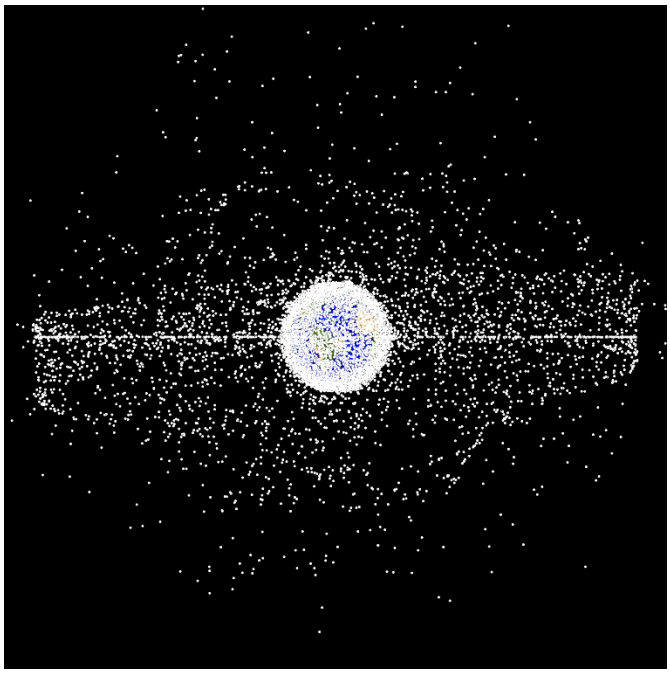


Figure 13.1: Orbital debris around Earth. Credit: NASA.

While space debris is present throughout space, there is a large accumulation around Earth, particularly in low-Earth orbit (LEO), where most space operations take place. This is also attributed to the increased launch cadence of small spacecraft and the recent surge in constellations over the past decade. Improved access to space has made LEO accessible and less expensive for more countries, organizations, and institutions to launch small spacecraft, which adds to the associated risks and threats of space debris. Estimates of the accumulation of orbital debris suggest approximately 1,100,000 objects with a diameter 1–10 cm, and over 36,500 pieces with diameters >10 cm, are in orbit between geostationary, equatorial, and LEO altitudes (1). Figure 13.1 shows a representation of the orbital debris around Earth. Additionally, the orbital lifetime of space debris can be extremely long since atmospheric drag is only effective at altitudes below ~250 km (2).

Due to the inherent problem of space debris, there are ongoing policy measures to establish the importance of mitigating and removing space debris. The general guideline is that spacecraft in LEO must deorbit, also known as decay, or be placed in a graveyard orbit within a maximum of 25 years after the completion of their mission (3). This standard spacecraft lifetime regulation has been recently updated to direct NASA and other national agencies to reassess current mitigation policies, especially regarding the potential advantages and cost implications resulting from limits on the orbital debris lifetime limits (4). These regulations have incorporated spacecraft decay capabilities into mission design.

The rate of spacecraft decay in LEO depends on several factors, including initial orbit parameters, the ballistic coefficient of the spacecraft, and solar weather conditions, all of which play a fundamental role in compliance with decommissioning regulations. Small spacecraft designers have examined various strategies for complying with decommissioning regulations to accelerate spacecraft decay post mission: spacecraft may be launched into lower orbits to enable natural decay within a few years, or equipped with deorbit systems to accelerate altitude decay and eventual reentry into Earth's atmosphere. Natural decay in <5 years can be achieved for most

SmallSats at altitudes <400 km, however several SmallSat missions must be in orbits beyond 400 km requiring the use of deorbit methods.

Spacecraft deorbit methods are either passive or active. Passive deorbit methods have gained maturity since the last iteration of this report, and there are more devices with high Technology Readiness Levels (TRL≥8) capable of satisfying current lifetime requirements. Traditionally, passive systems were the main option for deorbiting due to their increased simplicity, however recently active methods are gaining traction. Common active deorbiting approaches require attitude control and, in some cases, surplus propellant post-mission, such as a steered drag sail that relies on a functioning attitude control system, or on actuators for pointing the sail. Propulsion devices for deorbiting techniques are considered risky due to potential failure or malfunction of either the spacecraft, throughout its operational life, or the propulsive technology itself. Adequate attitude control and navigation capabilities after the mission for a controlled reentry are never a guarantee. Some of the new active deorbiting solutions include a separate spacecraft that can attach to the defunct satellite to bring it down to lower orbits where the satellites can complete deorbit using atmospheric drag.

The influx of small spacecraft in LEO has driven the development of space situational awareness and space traffic management data. For more information, please see the *Identification and Tracking Systems* chapter.

Chapter Organization

This chapter is organized as follows:

- Orbital Debris Regulations (13.2)
- State-of-the-Art – Passive Deorbit Systems (13.3)
- State-of-the-Art – Active Deorbit Systems (13.4)

Orbital space debris has been a known issue, and there has been ongoing research in this field. It is now a hot topic item, and the Orbital Debris Regulations section provides an overview of current policies for deorbit mitigations, their origins, and the organizations responsible for implementing orbital debris regulations. The Passive and Active Deorbit System sections contain technology descriptions, summary tables of devices, and previous, current, and planned missions. This chapter provides a comprehensive guide to existing commercial technologies and technology demonstrations for both methods, and the authors have attempted to highlight technology gaps and the current development status of each deorbit method.

The information described below is not intended to be exhaustive but provides an overview of current state-of-the-art technologies and their development status as discussed in open literature. Companies mentioned in this chapter are presented as informational only and do not represent an endorsement by NASA. There is no intention of mentioning certain companies and omitting others based on their technologies or relationship with NASA. It should be noted that TRL designations may vary with changes specific to payload, mission requirements, reliability considerations, and/or the environment in which performance was demonstrated. Readers are highly encouraged to reach out to companies for further information regarding the performance and TRL of the technologies described.

Definitions

- *Disposal* refers to removal of spacecraft from the orbital environment.
- *Deorbit* refers to lowering spacecraft's orbital altitude, also referred to as *decay.*
- *Decay* refers to a gradual decrease of the distance between a spacecraft and the Earth.
- *Atmospheric Drag* refers to molecular collisions with the spacecraft body.
- *Drag Area* refers to the spacecraft surface area experiencing atmospheric resistance.

- *Orbital Lifetime* refers to the total time a spacecraft remains in orbit.

13.2 Orbital Debris Regulations

Space debris has been a concern for several decades, but with visible sightings of reentry fragments of spacecraft and rocket bodies, the urgency to address space debris has grown. NASA's Orbital Debris Program Office[1] was created in 1979, and the Air Force Space Debris Research Program was initiated in the 1980s. NASA was among the first organizations to implement plans for mitigation and remediation of space debris in the early 1990s, and in 1993 the Inter-Agency Space Debris Coordination Committee (IADC) was founded as an international body.

NASA collaborated with the Department of Defense in 1997 to develop the U.S. Government Orbital Debris Mitigation Standard Practices (ODMSP) (5). The agency's most recent orbital debris guidelines can be found in NASA NPR 8715.6B "NASA Procedural Requirements for Limiting Orbital Debris and Evaluating the Meteoroid and Orbital Debris Environments" (6) and NASA Standard 8719.14C "Process for Limiting Orbital Debris" (3). These technical documents describe the processes and requirements to limit orbital debris for all NASA spacecraft missions. The guidelines, among other considerations, include a limit on the risk of potential human casualties caused by reentering debris, which shall not exceed 1 in 10,000 (5). Of the three spacecraft disposal methods identified – direct retrieval, atmospheric re-entry, and maneuvering into a storage orbit – atmospheric reentry was deemed the most feasible for most spacecraft missions. Therefore, a maximum 25-year post-mission orbital lifetime (no longer than 30 years after launch or relocation to a graveyard orbit for safe storage) was established for all U.S. spacecraft. The rationale for this specific orbital lifetime was based on the minimum propellant required to maneuver to a lower orbit, as predicted by orbital debris models (7).

The IADC is an entity formed by national and multi-national space agencies, including NASA, ESA, JAXA, and several others, and is widely recognized by the international community as the technical authority on space debris. In 2002, the IADC established the Space Debris Mitigation Guidelines to address orbital debris. Their findings and procedures are submitted to the United Nations (UN), as space debris has been one of the main interests of the UN Committee on the Peaceful Uses of Outer Space (COPUOS). In 2007, mitigation guidelines based on the IADC procedures were accepted by the COPUOS and endorsed by the UN (5). The IADC adopted the 25-year orbital lifetime guideline for space objects in LEO.

The U.S. Federal Communications Commission (FCC) regulates all radio communication across the U.S. and all U.S. spacecraft must be licensed for space communications. Since the early 2000s, the FCC has deliberated over how best to mitigate orbital debris from FCC-authorized space activities and formally adopted debris mitigation regulations (2) in 2004. These FCC regulations include orbital debris mitigation plans as part of license applications, and require applicants to disclose "the design and operational strategies that they will use, if any, to mitigate orbital debris," and to "identify particular methods by which a proposed satellite system will mitigate orbital debris" (2). The FCC adopted the ODMSP 25-year lifetime guideline as well and commented that the 25-year "rule" should be tightened, as this no longer adequately addresses current orbital debris issues arising from the launch of large constellations and the expected increase in future LEO space activity. In September 2022, the FCC adopted a new rule for all FCC-licensed satellites within the LEO region (<2000 km) to reduce the lifetime requirement to 5 years post-launch (8). There are ongoing discussions at the agency and federal level to determine the final policies.

[1] https://www.orbitaldebris.jsc.nasa.gov/

Since this updated “5-year lifetime rule” by the FCC, there has been increased focus on space debris removal activities. In April 2023, the FCC created a new Space Bureau responsible for the regulation of satellites and space debris (9). The World Economic Forum (WEF) released the “Space Industry Debris Mitigation Recommendations” document in June 2023 to standardize a series of recommended behaviors for satellite operations. One of these listed recommendations is to target five years or less after end-of-life for spacecraft removal. The document was signed by several companies including Airbus, The Aerospace Corporation, SES, and Planet. The WEF collaborated with ESA, the MIT Media Lab, and other stakeholders to establish a Space Sustainability Rating (SSR) system to provide a measurable score to characterize spacecraft mission compliance with international space debris mitigation guidelines (10)(11).

The Federal Aviation Administration (FAA) announced in September 2023 a proposal to create a new rule to limit the growth of debris from commercial launch vehicles to reduce collision risk and limit space debris in populated LEO environments (12). The new regulation will give commercial launch operators specific options for orbital debris countermeasures, requiring disposal of their rocket upper stages by performing a controlled reentry within 30 days after mission completion, moving them to a less congested or graveyard orbit (within 30 days), placing them in an Earth escape trajectory (within 30 days), retrieving them with active debris removal within five years after launch, or performing an uncontrolled atmospheric disposal within 25 years.

13.2.1 Considerations for Orbital Lifetime Requirements in LEO

Small spacecraft launched at or around 400 km altitude naturally decay in under five years, however at orbital altitudes beyond 500 km, there is no guarantee the spacecraft will deorbit within that timeframe, and some may not deorbit within 25 years. This is due to low atmospheric density and its effect on ballistic coefficient, as seen in Figure 13.2. This graph displays various cases of SmallSats with distinct masses, drag areas, and initial orbits, under atmospheric density conditions corresponding to solar cycle maximum and minimum over the 11-year solar cycle.

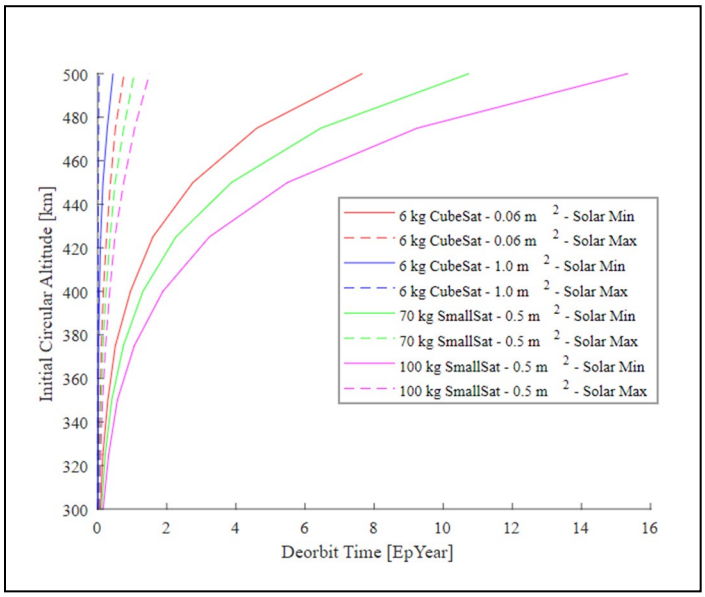


Figure 13.2: Initial orbit altitudes yield different lifetimes depending on the ballistic coefficient of the spacecraft. Three representative area-to-mass ratios are shown. Note that the propagation stops at 16 years, but the initial altitudes yield even longer times. Credit: NASA.

The varying solar weather conditions can affect the deorbit performance for a given altitude and can have a significant impact on orbital lifetimes. The atmospheric drag force that satellites experience is increased during solar maximum, resulting in a faster decay. In this situation, the Sun emits extra energy into the atmosphere and creates higher density layers in LEO that produce stronger drag forces on satellites (13). It is common for some missions to plan their launch periods around the solar cycle; if the stricter 5-year orbital lifetime requirement becomes widely accepted, more operators may consider this approach, as the deorbit time can be reduced by more than 10 years as seen in Figure 13.2.

Another important factor that affects orbit propagation in LEO is the spacecraft's ballistic coefficient (BC). Spacecraft BC is defined in this chapter as the mass to area ratio multiplied by the inverse of the drag coefficient, assumed to be 2.2. By this definition, a spacecraft with a lower ballistic coefficient will decay faster due to lower mass-to-area ratio. As shown in Figure 13.2, a 6U spacecraft with an area of 0.06 m^2 and an assumed mass of 6 kg has a ballistic coefficient of 45, which is significantly lower than that of a 100 kg spacecraft with an area of 0.5 m^2 and a BC of 90.

Since timing the launch for a particular solar weather scenario may not be feasible, another strategy for satellite operators to comply with orbital lifetime requirements is to decrease their spacecraft ballistic coefficient or mass to area ratio. Deorbit technologies such as drag devices can effectively increase the spacecraft's drag area and may play an increasingly important role in LEO operations.

13.3 State-of-the-Art – Passive Deorbit Systems

Passive deorbit methods require no further active control after deployment, relying only on natural perturbations and forces to deorbit the spacecraft. They are popular for their minimal mass, power, and cost constraints, and high reliability characteristics. Passive methods consist of a deployed structure, such as a drag sail, boom, or electromagnetic tether, to reduce the spacecraft's ballistic coefficient. This raises atmospheric drag on the spacecraft, accelerating the reentry process. These techniques have greatly matured in the last ten years, and recent developments have made passive deorbit technology well understood and space-ready.

This section provides information on drag sails, deployable booms, and electromagnetic tethers. In the last decade, there have been several SmallSat missions that have demonstrated passive deorbit capabilities with a deployed sail, boom, or tether. Some notable deorbit missions led by academic programs, research institutions and government organizations, and commercial entities are described under *Missions* for each deployed structure.

13.3.1 High TRL Drag Sails

Drag devices are the most common deorbit technology for satellites orbiting in LEO. They are advantageous due to simplicity and small stowed volumes. For certain area-to-mass ratios in altitudes equal to or lower than 800 km, drag devices can be deployed to increase the drag area for faster deorbiting to meet emerging 5-year requirements. This technology has been implemented in several small spacecraft missions, and several companies and institutions are developing prototypes that are increasingly more mature, providing solutions for missions that lack the resources for active deorbit systems.

Many mission designers are discovering that drag sails do not need to be complicated in material or shape to be effective. It is important to note that some missions described below are better documented due to publicly available data. Table 13-1, located at the end of this section, summarizes state-of-the-art passive deorbit systems. Solar sail technology development and mission information are found in the *In-Space Propulsion* chapter.

Missions

In January 2011, the NanoSail-D2 mission successfully demonstrated a drag sail to deorbit the spacecraft from a 650 km altitude and 72° inclined orbit. NanoSail-D2 was deployed from the minisatellite FASTSat–HSV to demonstrate the deorbit capability of a low-mass, high surface area sail. The 3U spacecraft, developed at NASA Marshall Space Flight Center (MSFC) and Ames Research Center (ARC), reentered Earth's atmosphere in September 2011.

CanX-7 started at an initial ~700 km Sun-synchronous orbit (SSO), deployed a drag sail in May 2017 and re-entered April 2022. The thin film sail—developed and tested at University of Toronto Institute for Aerospace Studies Space Flight Laboratory (UTIAS-SFL)—consists of four modules, each providing 1 m^2 of drag area (see Figure 13.3). Each sail section deployed mechanically with spring booms, preserving geometry and incorporating separate electronics for individual telemetry and command to mitigate risk of single-point failures. This is useful for custom adaptability to various spacecraft geometries and ballistic coefficient requirements for other missions (14).

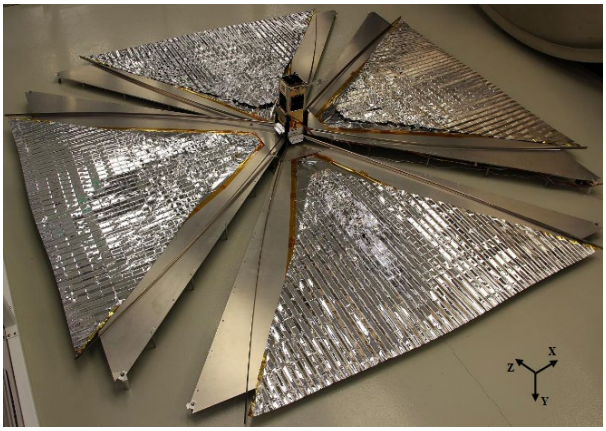


Figure 13.3: CanX-7 deployed drag sail during testing. Credit: Cotten et al. (2017).

The Surrey Space Centre, based in the United Kingdom, developed DragSail technology that was implemented in a family of missions. Funded by the European Commission QB50 program and the DEPLOYTECH partnership that included the German Aerospace Centre (DLR) and NASA Marshall Space Flight Center, among others, the Inflatesail 3U CubeSat first demonstrated the DragSail in 2017 and included a mast/drag-sail technology that successfully deorbited the satellite in just 72 days. This achievement was the first time a spacecraft has deorbited using European inflatable and drag-sail methods (15).

The RemoveDebris mission, developed under the European Commission FP7 program by a consortium of several institutions such as Airbus and the Surrey Space Centre, consisted of a 100 kg spacecraft, deployed from the ISS in 2018. One of the experiments it carried was a passive drag augmentation device consisting of a sail. The sail was deployed in March 2019, however, trajectory data indicated only partial deployment, as no significant altitude change was observed. The lessons learned from this incident were implemented in another version for the Space Flight Industries' SSO-A mission that incorporated two of these sails. In that case, the assembly did not include an inflatable boom (15).

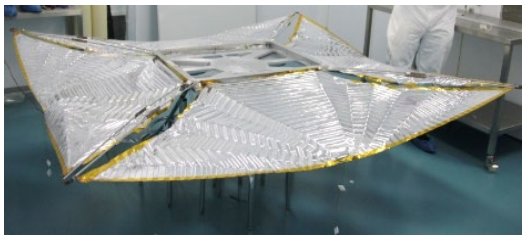


Figure 13.4: Icarus-3 drag sail implemented in the Carbonite-1 mission. Credit: Cranfield Aerospace Solutions.

As part of the ESA CleanSat program, Cranfield Aerospace Solutions developed a variety of drag augmentation systems called Icarus which are similar to other drag devices where drag is increased by deploying a membrane sustained by rigid booms. The first demonstration was the Icarus-1 sail that flew on the TechDemoSat-1 mission from SSTL launched in 2014 and re-entered May 2019. Another version also flew on the Carbonite-1 spacecraft, also built by SSTL and launched in 2015. The Icarus sail is a thin aluminum structure located around the satellite side panel that contains four stowed Kapton trapezoidal sails and booms. The Icarus-1 sail system had a mass of 3.5 kg for about 5 m^2 of sail area, and the Icarus-3 sail had a mass of 2.3 kg for 2 m^2 sail area (Figure 13.4). Another technology developed by Cranfield Aerospace Solutions is a de-orbit mechanism (DOM) device like the Icarus drag sail but in a smaller cuboid outline. The mechanical system varies from Icarus since the sails are triangular and the booms work as tape springs themselves. This system flew on the European Student Earth Orbiter (ESEO) that was a

45 kg satellite with several student payloads launched in March 2018. The DOM module has a mass of 0.5 kg and will deploy a sail with an area of 0.5 m^2 to deorbit ESEO after decommissioning (16).

The Spinnaker product line of drag sails that focus on low size, weight, power, and cost (SWaP-C) and a reliable approach to meeting FCC deorbit requirements by Applied Aerospace & Defense (acquired Vestigo Aerospace in 2026). Launched in March 2025, the Sphinx mission consisted of a 32 kg Astro Digital Corvus-Micro microsatellite and deployed an 18.8 m^2 Spinnaker 3 drag sail intended to dramatically shorten orbital lifetime and generate engineering telemetry and imagery of deployment (17). This demonstration is to support upcoming tests of deorbiting upper rocket stages.

MMA Design LLC patented the dragNET de-orbit system, which is a 2.8 kg module (Figure 13.5 [top]) featuring four stowed thin membranes that deploy through a single heater-powered actuator. The sail has an area of 14 m^2 that can effectively deorbit a 180 kg spacecraft at an altitude of 850 km within 10 years (18). The dragNET was a part of the ORS-3 Minotaur Upper Stage and facilitated its deorbit 2.1 years after launch in November 2013. In October 2022, the dragNET deorbit system was launched as part of the General Atomics GAzelle satellite, as seen in the lower image of Figure 13.5, and is still operational (19).

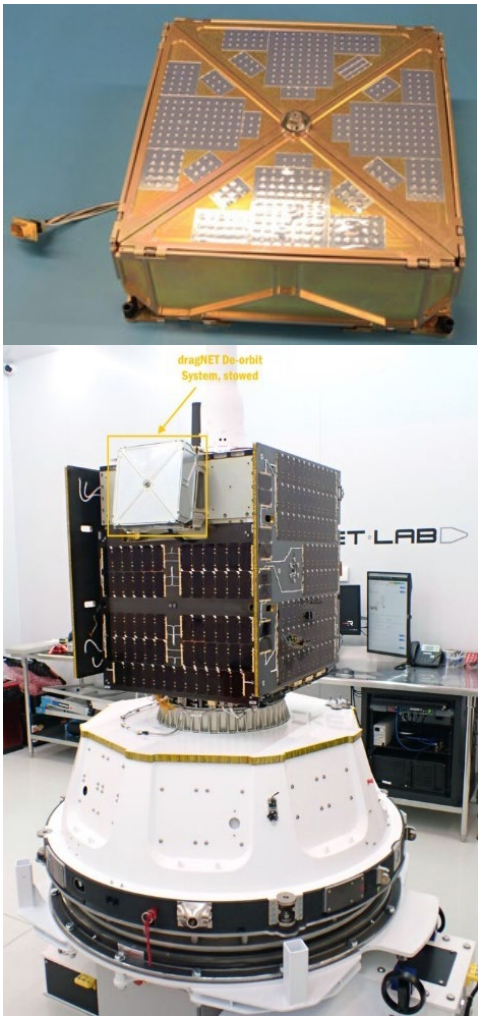


Figure 13.5: [top] The dragNET module. [bottom] dragNET module attached to the GAzelle satellite prior to launch. Credits: MMA design.

NPC Spacemind developed and launched a series of CubeSat missions that demonstrated their ARTICA deorbit system, which consists of a deployable 2.1 m^2 drag sail. The total size of the deorbiting system is 0.3 U which makes it suitable for CubeSats as small as 1U (20). In November 2022 and in January 2023, the DanteSat 3U CubeSat, and the Future-SM3 6U CubeSat, Futura-SM3, were respectively launched and successfully operated with an ARTICA system onboard. These two new missions extend the ARTICA flight heritage after the earlier UrsaMaior, 1-Kuns, and Alpha missions, launched in 2017, 2018 and 2020 respectively (21).

The Planetary Society's LightSail-2 was a 3U CubeSat mission with a solar sail launched in June 2019 and deployed from the Prox-1 satellite once in orbit. The mission demonstrated that solar sail technology can be used in LEO by modifying its orbital altitude over the course of the mission. The 32 m^2 sail was able to extend the mission lifetime by reducing orbital decay and on some occasions, it was also able to overcome drag entirely. In late November 2022, the mission successfully re-entered the atmosphere according to orbital predictions (22).

The Drag Augmentation Deorbiting System (ADEO) is a scalable drag sail developed by High Performance Space Structure Systems (HPS). There are various configurations of the ADEO sail: the ADEO-N series is tailored for small satellite missions of 20-250 kg, while the ADEO-M and ADEO-L target larger sizes, 100-700 kg and 500-1500 kg respectively. The ADEO-N series corresponds to sail sizes of 5±2 m^2, while ADEO-M covers areas within 15 ± 5 m^2. There are other smaller versions as well for picosatellites (ADEO-P) and CubeSats (ADEO-C) in particular, and the option to configure the sail size according to customer needs. Various configurations of the ADEO-N product family have been tested already (23). The NABEO-1, launched in 2018, attached to the center of a Rocket Lab Electron rocket Kick Stage and the sail was deployed 90 minutes after launch (24). In late December 2022, the ADEO-2 sail was deployed with a 10x10x10 cm package from the D-orbit ION-2 satellite carrier (Figure 13.6). For more information, contact ADEO@hps-gmbh.com.

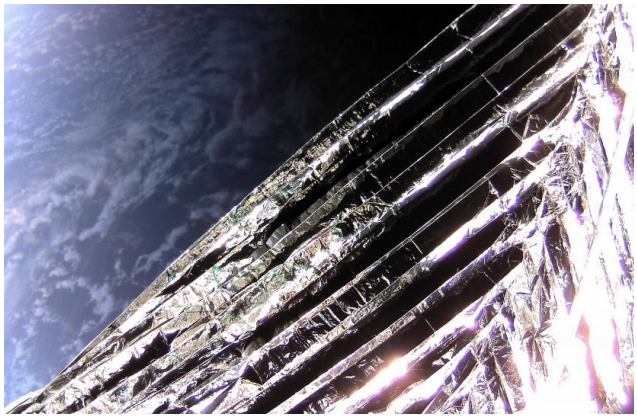


Figure 13.6: The ADEO-2 system deployed in LEO in December 2022, picture captured by the D-orbit's ION spacecraft carrier. Credits: HPS GmbH, Germany (www.hps-gmbh.com).

Gama launched its first spacecraft mission, a 6U CubeSat named Gama Alpha, in January 2023 into a ~550 km LEO and is currently still in orbit. This first technology demonstration mission aims to test the deployment and control of their 73.3 m^2 solar sail, and the final phase of the mission will use the sail to rapidly deorbit the satellite (25).

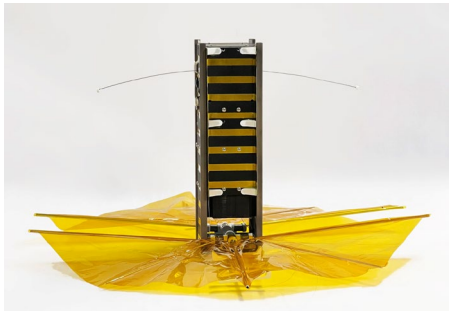


Figure 13.7: SBUDNIC CubeSat with drag sail made from Kapton polyimide film. Credit: Brown Univ.

SBUDNIC, shown in Figure 13.7, and designed and built by Brown University students with support from D-Orbit, AMSAT-Italy, La Sapienza-University of Rome, and NASA Rhode Island Space Grant, demonstrated a practical, low-cost method to cut down on space debris. Rather than taking debris out of orbit after it becomes a problem, this $30 drag device made from Kapton polyimide can be added onto satellites to radically reduce how long they're in space. SBUDNIC was launched on a SpaceX rocket May 2022 as part of the Transporter 5 ridesharing mission. The plastic drag sail was deployed at about 520 kilometers and the satellite re-entered August 2023, about five years ahead of schedule (26).

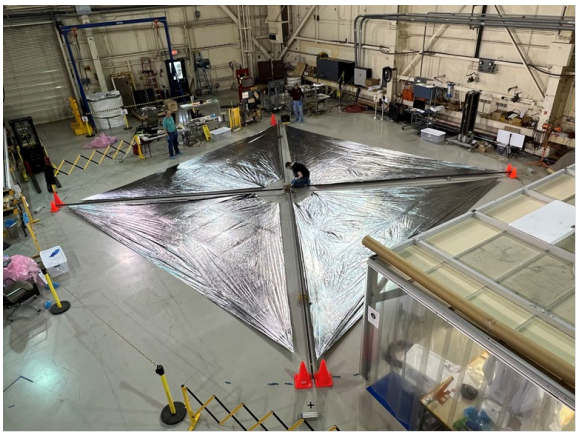


Figure 13.8: The ACS3 sail fully deployed during its pre-integration fit test. Credits: NASA Langley.

The Advanced Composite Solar Sail System (ACS3) was a mission developed at NASA Langley and NASA Ames that consisted of a

spacecraft that deployed an 81 m^2 solar sail in a 1000 km sun-synchronous orbit (see Figure 13.8). The sail, composed of a combination of composite materials with distinct properties, was deployed using lightweight booms from a 12U CubeSat bus, developed by NanoAvionics. ACS3 launched in April 2024 (27). Although the main objective of the mission to show the propulsive capabilities of the solar sail were not achieved, the sail was successfully deployed prior to decommissioning in 2026.

TechEdSat (Passive) Exo-Brake Series



Figure 13.9: TechEdSat-10 aft-imaging captures Exo-Brake deployment July 2020 (29). Credit: NASA.

The Technology Educational Satellite program, also known as TechEdSat-n (TES-n), at NASA Ames Research Center (ARC) has contributed significantly to the development of drag devices. It consists of a series of nanosatellite technology demonstrations in collaboration with several universities including San Jose State University and the University of Idaho (28). One of the main goals of the program is to test and improve deorbiting techniques and develop a unique targeting capability with their own drag device design known as the Exo-Brake. Being used as both a passive and a controlled active deorbit system, the Exo-Brake is an atmospheric braking system that is distinguished from other drag devices with its parachute qualities rather than solar-sail behavior due to its tension-based structural elements (see Figure 13.9). This is fundamental for accurate deorbit targeting since the device must retain its shape without collapsing during those critical reentry moments near the atmosphere interface (~100 km altitude), known as the Von Karman line (32). Development of the Exo-Brake is funded by the Entry Systems Modeling project within the NASA Space Technology Mission Directorate's (STMD) Game Changing Development (GCD) program.

The Exo-Brake was first implemented as a passive deorbit device on TES-3 and TES-4, and then on TES-5 and TES-7. In comparison to other objects without a disposal device, the TES-7 flight is shown with other objects deployed from the same carrier, as seen in Figure 13.10. With a low ballistic coefficient induced by the deployed Exo-Brake, TES-7 re-entered in approximately 1.3 years from an initial 500 km orbit. This design incorporated a compact, low volume gas-generator cartridge to inflate the Exo-Brake struts.

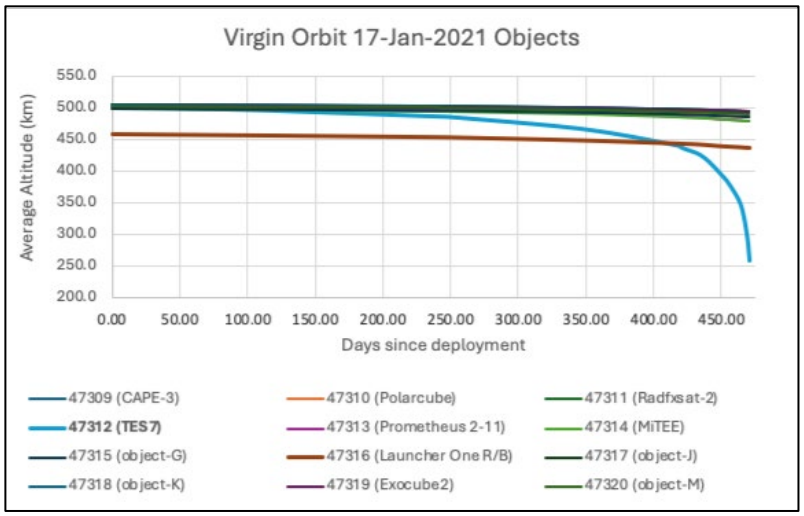


Figure 13.10: TES-7 deorbit compared to other deployed objects from the same carrier. Credit: NASA/Virgin Galactic

More recently, a simpler mechanical deployment scheme was developed (patent pending) that improves packaging performance by increasing the deployed-drag-area-to-stowage-volume ratio, as applied to TES-11. This has been further miniaturized for TES-22 which was launched in January 2025 as a test for a proposed future Thermosphere Test Probe (TTP) to be part of a small cohort during

solar coronal events. The passive Exo-brake (not drag-modulated for deorbit targeting) has advanced recently for disposal activities to meet the new 5-year deorbit lifetime requirement. Table 13-1 provides a comprehensive overview of TES-n missions with passive Exo-Braking capability.

Table 13-1: Passive TechEdSat-N Spacecraft

TES-n mission (Volume)	Deployment (month, year)	Deorbit Duration Reentry Year	Nominal Drag Area (m^2)	Deployed Orbit Alt. & Inc.	Technology Tested Notes (ref)
TES-1 (1U)	October 2012	May 2013	NA	412 km, 51.7°	(33)
TES-2 (1U)	April 2013	April 2013	NA	223 km, 51.6°	First test of Iridium (34)
TES-3 (3U)	November 2013	January 2014	0.35	413 km, 51.6°	Original Passive Exo-Brake
TES-4 (3U)	March 2015	April 2015	0.35	398 km, 51.6°	Upgraded Exo-Brake design
TES-5 (3.5U)	March 2017	July 2017	0.35	403 km, 51.6°	Two-state Drag Modulated Exo-Brake for targeted re-entry (35)
TES-6 (3.5U)	November 2017	May 2018	0.564	402 km, 51.7°	Variable Exo-Brake settings (36)
TES-7 (2U)	January 2021	May 2022	1.2	499 km, 60.7°	High Packing Density Exo-Brake (37)
TES-9 (3U)	Planned	TBD	-	-	Automatic deorbiting using the Exo-Brake system
TES-11 (6U-W)	July 2024	February 2026	0.790	508 km, 97.4°	Advanced disposal Exo-Brake mechanism

Table 13-2: Drag Sail Missions							
Product / Mission	**Manufacturer**	**Mission host and launch mass**	**Device mass (kg)**	**Initial orbit (alt and inc.)**	**Launch Year**	**Deployment Year**	**Drag Area (m^2)**
NanoSail-D2	NASA MSFC/ARC	FASTSAT (4.2 kg)	N/A	650 km 72 deg	2010	2011	10
Drag-Net	MMA Design	ORS-3 Deployed a Minotaur Upper Stage (100 kg)	2.8	N/A	2016	2016	14
Drag-Net	MMA Design	General Atomics GAzelle Satellite	2.8	N/A	2022	TBC	14
Icarus-1	Cranfield Aerospace Solutions	SSTL TechDemoSat-1 (157 kg)	3.5	635 km	2014	2019	6.7
Icarus-3	Cranfield Aerospace Solutions	Carbonite-1 (80 kg)	2.3	650 km 98 deg	2015	2018	2
DOM	Cranfield Aerospace Solutions	ESEO (45 kg)	0.5	572 × 588 km 97.77 deg	2018	2020	0.5
Terminator Tape	Tethers Unlimited, Inc.	Prox-1 (71 kg)	0.808	717 km 24 deg	2019	2019	10.5
DragSail	Surrey Space Centre	InflateSail (3.2 kg)	N/A	505 km 97.44 deg	2017	2017	10
Exo-Brake	NASA	TechEdSat 5 (3.4 kg)	N/A	405 km 51.5 deg	2014	2015	0.35
Exo-Brake	NASA	TechEdSat 7 (3 kg)	N/A	485 x 513 km 60.7 deg	2021	2021	1.2
Exo-Brake	NASA	TechEdSat 13 (4 kg)	N/A	499 x 509 km 45 deg	2022	2022	0.083
Exo-Brake	NASA	TechEdSat 15 (4.5 kg)	N/A	215 x 285 km 137 deg	2022	2022	0.087
removeDebris	Surrey Space Centre	removeDebris (100 kg)	N/A	405 km 51.5 deg	2018	2019	16
CanX-7	UTIAS-SFL	3U CubeSat (3.6 kg)	0.8 (4 modules of 0.200)	688 km 98 deg	2016	2017	4
NABEO-1	HPS	1U CubeSat (attached to Rocket Lab Kick Stage)	0.85	500 km	2018	2018	2.5
ADEO-2	HPS	1U CubeSat (attached to the D-orbit ION carrier)	3.4	N/A	2021	2022	3.6

Table 13-2: Drag Sail Missions							
Product / Mission	**Manufacturer**	**Mission host and launch mass**	**Device mass (kg)**	**Initial orbit (alt and inc.)**	**Launch Year**	**Deployment Year**	**Drag Area (m^2)**
ADEO-Cube series	HPS	1-50 kg	0.5	LEO	N/A	N/A	2
ADEO-N series	HPS	20-250 kg	0.8	LEO	N/A	N/A	5±2
ADEO-M series	HPS	100-700 kg	4	LEO	N/A	N/A	15±5
ADEO-L series	HPS	500-1500 kg	9.5	LEO	N/A	N/A	20±100
ARTICA (ALPHA)	NPC Spacemind	1U CubeSat	0.285 (0.3U)	5865 Km, 70.16 deg	2020	2020	2.2
ARTICA (FUTURA SM 3)	NPC Spacemind	6U CubeSat	0.285 (0.3U)	N/A	2023	N/A	2.2
ARTICA (DANTESAT)	NPC Spacemind	3U CubeSat	0.285 (0.3U)	415 km	2022	2022	2.2
ARTICA (URSA MAIOR)	NPC Spacemind	3U CubeSat	0.285 (0.3U)	450 km, 97.1 deg	2017	2019	2.2
ARTICA (1KUNS)	NPC Spacemind	1U CubeSat	0.285 (0.3U)	N/A	2018	2019	2.2
LightSail – 2	The Planetary Society	3U CubeSat	N/A	720 km	2019	2022	32
ACS3	NASA	12U CubeSat	1 (6U)	1000 km SSO	2024	2024	81
Gama ALPHA	Gama	6U CubeSat	N/A	550 km	2023	N/A	73.3
NANO dragsail (28)	Frond Space Systems	2U-12U CubeSat	0.25	<650 km	2025	N/A	1
MICRO dragsail (29)	Frond Space Systems	50-100 kg spacecraft	<1600	<650 km	2025	N/A	10

13.3.2 Deployable Booms

Deployable booms, while not strictly a deorbit device themselves, are a vital component of many deorbit systems. They are structural components that can be stowed during launch, then deployed once in space to provide the support structure required for various drag sail designs. More specific information regarding deployable booms can be found in the *Structures, Materials, and Mechanisms* chapter.

Missions

The University of Florida developed the Drag Deorbit Device (D3) and De-Orbit Control System 2U CubeSat that provides both attitude stabilization and modulation of the satellite drag area at the same time, making the overall solution an alternative to regular ADCS units. This technology was licensed exclusively to Orbotic Systems who have changed and Trademarked the product title “D3 De-Orbit Drag Device". Four 3.7 m long tape-spring booms form the D3, which can deorbit a 15 kg satellite from an altitude of 700 km. A final design has already been tested and simulated, including thermal-vacuum and fatigue testing (38). Figure 13.11 shows two images of the final design. The mission was selected by NASA through the CubeSat Launch Initiative, and on September 6, 2022, D3 was successfully placed in orbit (39).

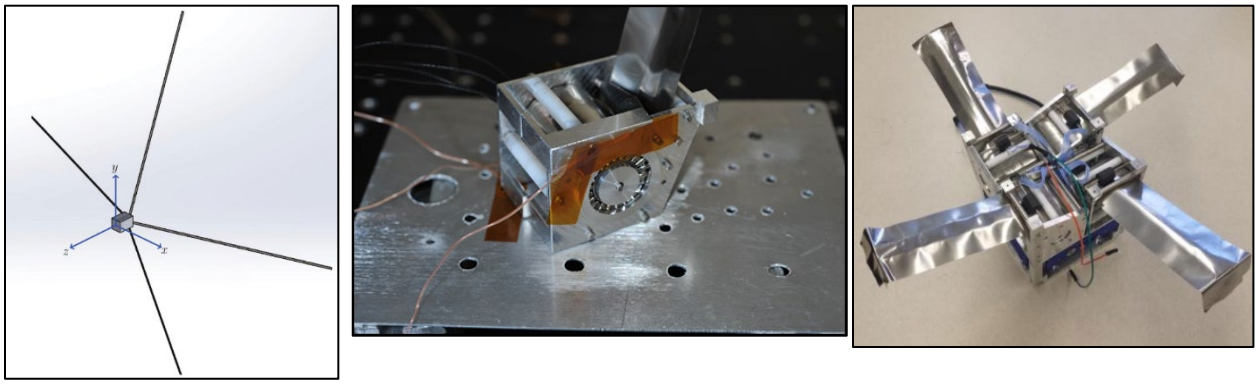


Figure 13.11: D3 CAD design (left), boom inside thermal vacuum chamber (center), and prototype design (right). Credit: Omar et al., 2019, and Martin et al., 2019.

13.3.3 Electromagnetic Tethers

In addition to drag sails, electromagnetic tethers have proven to be an effective deorbit method. This technology uses a conductive tether to generate an electromagnetic force as the tether system moves relative to Earth’s magnetic field.

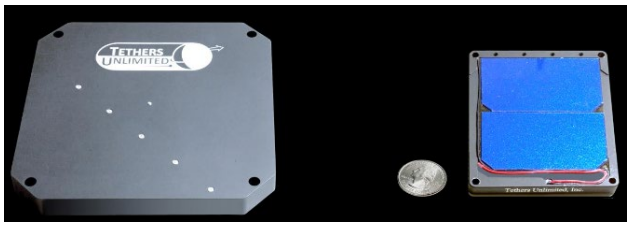


Figure 13.12: Image of the NSTT (left) and the CSTT modules. Credit: Tethers Unlimited.

Missions

Tethers Unlimited (now Amergint Technologies) developed Terminator Tape that uses a burn-wire release mechanism to actuate the ejection of the terminator’s cover, deploying a 70 m long conductive tape at the conclusion of the small spacecraft mission. There are currently two main modules. The first, NSTT for NanoSats, has a mass of 0.808 kg. The second, CSTT, is made for CubeSats and has a mass of 0.083 kg. Figure 13.12 shows an image of both systems. The 70 m long NSTT has been implemented in the 71 kg Prox-1 satellite, launched in mid-2019 by AFRL (40). DragRacer, an experiment jointly developed by Tethers Unlimited, Millennium Space Systems, RocketLab, and TriSept Corp., consisted of one satellite (Alchemy) equipped with

Terminator Tape and another (Augury) without it, to characterize the tape performance. Alchemy reentered in July 2021 while Augury is still in orbit (41).

13.3.4 Natural Deorbiting Highways

Finally, analysis has shown that there exists a natural network of what may be called “deorbiting highways or corridors” (42). Judicious injection into specific orbits in LEO may result in relatively rapid natural orbital decay. There exist dynamical resonances associated with solar radiation pressure, lunisolar perturbations and Earth's gravitational harmonics. In turn, these dynamical resonances are associated with natural deorbiting corridors; furthermore, their effectiveness is proportional to the spacecraft’s area-to-mass ratio. These LEO dynamical resonances are expressed as a network of specific orbital initial conditions. For example, for a nearly circular initial orbit at an altitude of 700 km, and assuming a typical value of the area-to-mass ratio, a spacecraft with an initial inclination of approximately 41 degrees will have a shorter lifetime in orbit than an identical spacecraft with an initial inclination of 20 degrees. The former example is an example of leveraging a natural deorbit corridor associated with these dynamical resonances. The downside of using this approach is that small satellites (a) often go as “piggyback” payloads to larger missions and do not have the luxury of picking an orbit, and (b) often go to sun-synchronous orbits which for typical area-to-mass ratio values are not dynamically close to these natural deorbiting corridors.

13.4 State-of-the-Art – Active Deorbit Systems

While it is still less common to design an active deorbiting system on a spacecraft directly due to mass, size, and power constraints, other methods enable active decommissioning. Several companies, such as Astroscale and ClearSpace, offer active spacecraft-based deorbit services and have already started initial technology demonstration missions to advance their deorbit systems. These deorbit systems consist of separate, dedicated spacecraft that attach to decommissioned satellites to place them into decaying or graveyard orbits. This niche is quite appropriate for the growing number of constellations that are planned to launch over the next few years.

The NASA STD-8719.14C document stipulates that all NASA-sponsored spacecraft using controlled reentry must have a designed trajectory to ensure that any remaining debris does not impact landmasses. Specifically, debris with a kinetic energy exceeding 15 Joules must stay at least 370 km away from any foreign landmass, or within 50 km from any territory of the United States or the permanent ice pack of Antarctica (3). This requirement implies that spacecraft must be equipped with improved active deorbit capabilities. There have been advances on deorbit technologies that can either be used on a specific mission or provided through commercial services.

This section highlights some of the main stakeholders that are working towards the implementation of active space debris removal services, and some promising technologies that can potentially be used for actively deorbiting spacecraft in the future.

13.4.1 Active Debris Removal Hardware

This section focuses on efforts to develop technologies for active debris removal. These include the active control of the Exo-Brake on the TechEdSat series for targeted re-entry, as well as potential and upcoming missions dedicated to actively removing orbital debris using drag sails, deployable booms, and electromagnetic tethers. In addition, some upcoming missions include orbiting vehicles to execute active operations to remove small satellites at end of life.

TechEdSat (Active) Exo-Brake Series

The Exo-Brake design has evolved from a fully passive device to one with active control capability that can target a specific reentry location by adjusting the drag device for the optimal ballistic coefficient based on the satellite's orbital determination. The TES-6 mission first implemented this technology with a 3.5U CubeSat and deployed the Exo-Brake from the rear and targeted reentry over NASA Wallops Flight Facility. Although the target area was overshot, analysis shows that a low 4–5 kg/m^2 ballistic coefficient configuration would have yielded suitable results if placed at 300 km (see Figure 13.13). TES-6 successfully demonstrated the reentry experiment and the command/control capability by overflying Wallops right before reentering.

The Exo-Brake targeting technology has been demonstrated on TES-6 and TES-10 missions and was going to be implemented on TES-8 except a power system failure occurred after Exo-Brake deployment but before targeting. The Exo-Brake on TES-10 was an improved version of the previous TES-5 and TES-6 devices with a wider ballistic coefficient range (6–18 kg m^2) to enable better control authority for a targeted deorbit flight test over Wallops (37). TES-13 and TES-15 used variations of the TES-7 design for active, controlled mission deorbiting (43). Table 13-3 provides a comprehensive overview of the different TES-n missions.

Table 13-3: Active TechEdSat-N Spacecraft

TES-n mission (Volume)	Deployment (month, year)	Reentry (month, year)	Nominal Drag Area (m^2)	Deployed Orbit Alt. & Inc.	Technology Tested Notes
TES-8 (6U)	January 2019	April 2020	0.5	406 km, 51.6°	Hot Exo-Brake; improved version of TES-5 and -6 designed for continued operation in high temperature environment
TES-10 (6U)	July 2020	March 2021	0.564	416 km, 51.6°	largest iteration Exo-Brake and performed targeting experiment
TES-13 (3U)	January 2022	July 2024	0.087	504 km 45°	Autonomous navigation and targeted reentry;
TES-15 (3U)	October 2022	October 2022	0.087	250 km, 137°	Hot Exo-Brake re-entry test; unable to complete full test
TES-22 (1U)	January 2025	TBD	2.00	~500 km	Rapid Disposal (Exo-Brake/Heliophysics Test Probe)
TES-23 (3U)	March 2026	TBD	-	-	Rapid Disposal (Exo- Brake), RADSET

RemoveDebris Consortium Partners

The RemoveDebris mission focused on testing several active debris removal experiments with different technologies on mock targets in LEO. In total, the RemoveDebris spacecraft carried two 2U CubeSats, a net, harpoon, laser ranging instrument, and a drag sail. One experiment deployed a 5 m net toward simulated space debris using one of the CubeSats, DebrisSat 1, and a balloon. Both DebrisSat 1 and the balloon were captured at ~11 m and maneuvered to a lower altitude, re-entering in March 2019 (44). Another active debris technology used a harpoon and a deployable target where the target platform attached to a 1.5 m boom was deployed from the main spacecraft, and a tethered harpoon was fired at 19 m/s to strike the center of the platform. Once that occurred, the boom that connected both harpoon and target platform joined the harpoon and target platform at one end. However, a tether secured the target in place, avoiding the

creation of new debris. This resulted in the first space demonstration of harpoon-based debris—with a dry mass of 4.3 kg—capture technology.

13.4.2 Active Debris Removal / Spacecraft Reentry Services

This section focuses on commercial efforts to provide space debris removal services. This commonly involves a "servicer" spacecraft released from a host spacecraft that rendezvous with an object, captures it via attachment or docking method, and releases it in a lower altitude for reentry. Several core technologies, such as autonomous navigation, rendezvous and proximity operations (RPO), and robotics, are being developed by NASA and international space agencies, academics and researchers, and the commercial industry to boost the active debris removal service. Some deorbit removal services require the spacecraft to be fitted with a deorbit fixture for their servicer spacecraft to attach to. In response to the surge of small spacecraft constellations, deorbit fixtures are now being integrated into several new spacecraft constellations.

Some companies, like Momentus, are more focused on in-orbit servicing capabilities as a whole that include deorbit and removal applications. Those companies with a deeper affiliation with in-orbit servicing are featured in the Orbital Transfer / Maneuvering Vehicles (OTV/OMV) section of the *Integrated, Launch, Deployment, and Orbital Transfer* chapter.

Astroscale Holdings Inc.

Astroscale aims to provide services that will address the end-of-life (EOL) scenario of newly launched satellites and be proactively engaged in active debris removal. They are involved in collaborations with a variety of governmental and international organizations (such as the US government, ESA, the European Union, or the United Nations) that aim to address space debris removal. Since 2022, they are responsible for the Cleaning Outer Space Mission through Innovative Capture (COSMIC) mission design as part of the Active Debris Removal (ADR) mission with the UK Space Agency that will remove two defunct British spacecraft in 2028 (45).

Astroscale is collaborating with other efforts to implement their Generation 2 Docking Plate on future spacecraft for future removal activities or to remove critical debris such as rocket upper stages or defunct satellites (46). As part of JAXA's Commercial Removal of Debris Demonstration (CRD2) initiative—which focuses on the removal of large Japanese-made space debris in two mission phases—Astroscale developed the capture mechanism that enables close proximity operations on-orbit. Phase I consisted of a 150-kg Active Debris Removal by Astroscale-Japan (ADRAS-J) satellite that identified and characterized a rocket upper stage on-orbit. It was launched in July 2024 and maintained a constant distance of 50 m and began its decommissioning in early 2026 (47).

As part of their EOL campaign, the End-of-Life Services by Astroscale demonstration (ELSA-d) mission launched on March 22, 2021 and has successfully demonstrated EOL technologies in LEO with Astroscale's docking plate (48). ELSA-d consisted of two spacecraft: a "servicer" and "client" where the client spacecraft represented a piece of space debris that the servicer rendezvoused with and eventually attached to. With respective launch masses ~175 and ~17 kg, the servicer and client spacecraft repeatedly performed several complex demonstrations including magnetic capture and rendezvous operations of both tumbling and non-tumbling cases. In January 2022, the servicer spacecraft successfully released the client counterpart and initiated autonomous relative navigation over the course of multiple orbits as part of the mission plan. As of 2024, the servicer spacecraft is expected to re-enter in 3.5 years.

Planned for launch in 2026, the ELSA-M demonstration mission will leverage lessons learned for magnetic docking and autonomous navigation technologies demonstrated in the precursor ELSA-d mission. ELSA-M will dock with and remove a OneWeb spacecraft using Astroscale's compatible magnetic capture mechanism (49). OneWeb plans to have Astroscale's docking plate

on their future spacecraft for this continued deorbit service (50). An important note is that several science missions are undertaking extensive efforts to make their spacecraft magnetically neutral, which may be a concern for magnetic docking methods.

ClearSpace

Another company that is solely focused on the design and execution of space debris removal is ClearSpace. By advancing robotics to support in-orbit servicing applications such as disposal, transport, inspection, assembly, manufacturing, repair, and recycling, ClearSpace aims to help establish a market for in-orbit servicing and debris removal. Collaborating with ESA, ClearSpace-1 is a space debris removal mission designed to locate and capture a non-cooperative, tumbling object via a four-armed robotic device (51). The object to be removed was originally a 100 kg VEGA upper stage, however in August 2023, it collided with another piece of space debris (52). The mission will now rendezvous with Project for On-Board Autonomy (PROBA)-1 —ESA's first spacecraft with fully autonomous technologies, launched 20 years ago—capture it with a group of robotic arms, and then both spacecraft will be deorbited together to a lower orbit for final disintegration in the atmosphere.

ClearSpace entered the preliminary design review in October 2023 of the Clearing of the LEO Environment with Active Removal (CLEAR) mission currently projected to launch in the second half of 2026. This study is designed to remove at least two UK non-operational satellites that have been in orbit for more than 10 years in a ~700 km orbit and have a natural deorbit time longer than 100 years (51). The CLEAR spacecraft features unfolding arms used to capture and release target objects.

D-Orbit

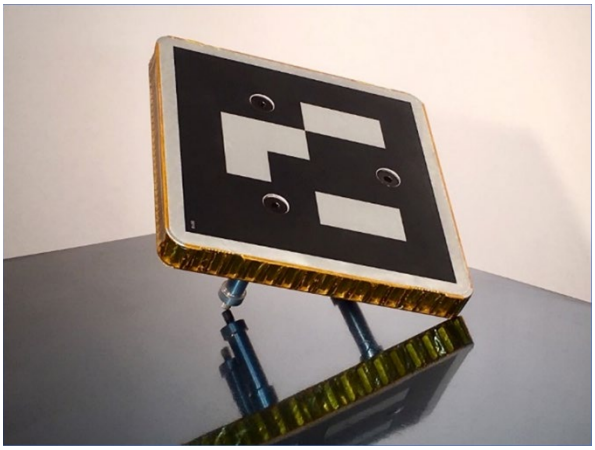
Known for their transportation services onboard their ION CubeSat carrier platform, D-Orbit also provides an external solid motor booster specifically for deorbiting purposes. This independent module, known as D-Orbit Decommissioning Device (D3), shown in Figure 13.13, is a solution that is optimized for end-of-life maneuvers and was first demonstrated in 2017 (53). This technology would need to be added prior to launch and is activated from the ground or host spacecraft. More information on the ION is in *Chapter 10: Launch, Integration, Deployment, and Orbital Transport*.



Figure 13.13: D-Orbit D3 module. Credit: D-orbit.

Voyager Space

The main objective of Voyager Space is advancing humanity's presence in space and on Earth. They focus on space exploration and infrastructure, microgravity research, and technological innovations that will contribute to a sustainable space economy and enhance humanity's future. As part of their in-space servicing and assembly, they developed the DogTag, which is an inexpensive, lightweight, versatile, and advanced grappling interface. This fixture enables small spacecraft to be captured by various mechanisms such as magnetic grapples, mechanical arms, electrostatic or gecko adhesive, and even harpoons. This interface allows for spacecraft servicing or decommissioning and is compatible with other techniques to accommodate different mission needs (54). Figure 13.14 includes an image of the flight DogTags and a table of its main features. Since 2021, OneWeb includes the DogTags grappling fixture on their launched satellites to make space more sustainable (55). In total, over 500 DogTags have already been launched to space.



Bounding Volume	150mm x150mm x 65mm
Total Mass	250g
Mounting Interface	3x M5x0.8 threaded inserts on an 84.5mm bolt-hole circle
Compatible Gripping Methods	Magnetic Capture Adhesive Capture - Electrostatic - Gecko - Hot-Melt - Chemical Mechanical Capture - Pinch-Grasp - Snare Penetrating Capture (Harpoon)

Figure 13.14: DogTag prototype. Credit: Voyager Space.

Kall Morris Inc.

Another orbital debris research and solution development company with a focus on active debris removal techniques is Kall Morris Inc (KMI). They are developing a commercially viable system designed to capture and detumble an object— whether a client satellite at end-of-life or uncooperating debris object—and release it into a deorbit altitude (56). Their Laelaps spacecraft will rendezvous with and attach itself to a target object using a multi-armed, articulated robotic device called REACCH. As depicted in Figure 13.15 {left}, REACCH will capture, move, and release the object in a deorbit altitude. Gecko adhesion is incorporated on the REACCH tentacles in order to attach to the debris object and easily release the object when the tentacles retract.

With the assistance of the University of Southern California, by May of 2025 REACCH completed Astrobee-enabled International Space Station (ISS) testing sponsored through the Center for the Advancement of Science in Space (CASIS) 2025 (57). Laelaps in-space testing is anticipated in Q4 2027, with component ground testing leading up to that time. Figure 13.15 {right} is an image of REACCH on the ISS.

In 2027, the Space Machines Company's orbital transport vehicle will enter lunar orbit to rendezvous with and capture debris in lunar orbit. The Australian-built Optimus orbital transport vehicle (OTV) will rendezvous with, capture, and return hazardous debris from lunar orbit to Earth. Along the way, it will carry Australian payloads to lunar orbit for testing and development of lunar exploration communications and situational awareness infrastructure before returning them to Earth.



Figure 13.15: {left} REACCH interpretation and {right} REACCH during ISS Capture testing with Astrobee. Credit: Kall Morris Inc. Credits: Kall Morris Inc.

TransAstra was awarded a Phase 2 Small Business Innovation Research contract from NASA to continue developing their inflatable capture bag technology for space debris remediation. This device will be capable of enveloping and subsequently removing a non-cooperative object in orbit. A collaboration with ThinkOrbital, a company based in Colorado, includes the transport of the removed debris to an on-orbit processing plant.

13.5 Summary

Space debris regulations are becoming more stringent. Consequently, several deorbit technologies have matured significantly in recent years. Traditionally passive systems have been more common, have flown on various missions, and have reached TRL 9 following successful demonstrations. Drag sails are the main technology for passive systems, and several companies have already commercialized and brought these products to market. Other systems such as electromagnetic tethers, deployable booms, or the NASA TechEdSat series Exo-Brake have also been prototyped and demonstrated in space, now with navigation capabilities and increased reliability. The investment in active systems has also grown significantly. Several companies are offering transfer vehicles to remove debris or deorbit spacecraft at the end of their mission, and compatible systems for spacecraft rendezvous and removal are being developed in parallel. As an example, the RemoveDebris mission has successfully tested two different active methods: a net and a harpoon for potential future implementation in active debris removal operations. Companies such as Astroscale and ClearSpace are developing missions to remove defunct satellites and are launching precursor technology demonstration spacecraft in the initial stages of their roadmaps. In conclusion, the various deorbit technologies have seen a significant TRL increase since the last iteration of this report, and their robustness is expected to continue improving as demand for deorbiting services increases with additional launches and evolving regulations.

For feedback solicitation, please email: arc-sst-soa@mail.nasa.gov. Please include a business email so someone may contact you further.

References

(1) European Space Agency. “Space Debris by the Numbers,” December 6, 2023. [Online] Available at: https://www.esa.int/Space_Safety/Space_Debris/Space_debris_by_the_numbers

(2) Federal Communications Commission. “Mitigation of Orbital Debris: Second Report and Order,” June 21, 2004. Available at: https://docs.fcc.gov/public/attachments/FCC-04-130A1.pdf

(3) NASA. “Process for Limiting Orbital Debris,” NASA-STD-8719.14C. November 5, 2021.

(4) National Orbital Debris Implementation Plan, of the Orbital Debris Interagency Working Group, National Science and Security Council, July 2022.

(5) Liou, J., NASA. Orbital Debris Briefing, Executive Office of the President/Office of Science and Technology Policy (EOP/OSTP) Briefing, Washington D.C., December 8, 2017. Available at: https://ntrs.nasa.gov/api/citations/20170011662/downloads/20170011662.pdf

(6) NASA. “NASA Procedural Requirements for Limiting Orbital Debris and Evaluating the Meteoroid and Orbital Debris Environments,” NPR 8715.6B. February 16, 2017-2024. [Online] Available at: https://nodis3.gsfc.nasa.gov/displayDir.cfm?t=NPR&c=8715&s=6B

(7) National Academies of Sciences, Engineering, and Medicine. 2011. Limiting Future Collision Risk to Spacecraft: An Assessment of NASA's Meteoroid and Orbital Debris Programs. Washington, DC: The National Academies Press. https://doi.org/10.17226/13244.

(8) Federal Communications Commission. “Space Innovation; Mitigation of Orbital Debris in the New Space Age,” FCC-Fact Sheet. September 8, 2022. Available at: https://docs.fcc.gov/public/attachments/DOC-387024A1.pdf
(9) Khlystov, N. and Schrogl, K. “Space Industry Debris Mitigation Recommendations,” Future of Space Network - Sustainable Space Initiative, Centre for the Fourth Industrial Revolution, World Economic Forum document, June 2023.
(10) World Economic Forum. “Space Sustainability Rating,” [Online] Available at: https://www.weforum.org/projects/space-sustainability-rating/
(11) Foust, J. “U.N. opens “window of opportunity” to improve space governance” spacenews.com. June 14, 2023.]Online] Available at: https://spacenews.com/u-n-opens-window-of-opportunity-to-improve-space-governance/
(12) Federal Aviation Administration. “FAA Proposed Rule Would Reduce the Growth of Debris from Commercial Space Vehicles,” September 20, 2023. [Online] Available at: https://www.faa.gov/newsroom/faa-proposed-rule-would-reduce-growth-debris-commercial-space-vehicles
(13) National Oceanic and Atmospheric Administration. “Satellite Drag,” [Online] Available at: https://www.swpc.noaa.gov/impacts/satellite-drag
(14) Cotten, B., Bennett, I. and Zee, R. E. “On-Orbit Results from the CanX-7 Drag Sail Deorbit Mission,” 10th Annual Small Satellite Conference, August 2006, Logan Utah.
(15) Underwood, C. et al. “InflateSail de-orbit flight demonstration results and follow-on drag-sail applications,” Acta Astronautica, 2019, Vol. 162, pages 344-358. ISSN: 0094-5765
(16) Palla, C., Kingston, H, and Hobbs, S. Damstadt: "Development of Commercial Drag-Augmentation for Small Satellites." ESA Space debris Office, Ed. T. Flohrer & F. Schimtz, 2017.
(17) Applied Aerospace and Defense, “Applied Invests in Deorbit Systems with Acquisition,” February 24, 2026, [Online] Available at: https://appliedaero.space/applied-invests-in-deorbit-systems-with-acquisition
(18) MMA Design. “dragNET™ De-Orbit System,” MMA Design: Products. 2020 [Online] Available at: https://mmadesignllc.com/product/dragnet-de-orbit-system/
(19) MMA Design. “Another MMA dragNET De-orbit Systems Launches with GAzelle Satellite.” [Online] Available at: https://mmadesignllc.com/2022/10/dragnet-deorbit-launches-with-gazelle-satellite/
(20) NPC Spacemind. “Artica.” [Online] Available at: https://indico.esa.int/event/234/contributions/3929/attachments/3014/3634/Clean_Space_ARTICA_Present.pdf
(21) Cowing, K. “Spacemind Successfully Launches Three Italian Nanosatellites Into Orbit From The International Space Station.” Press Release, Spacemind. February 2, 2023. [Online] Available at: https://spaceref.com/space-commerce/spacemind-successfully-launches-three-italian-nanosatellites-into-orbit-from-the-international-space-station/
(22) Davis, J. “LightSail 2 completes mission with atmospheric reentry.” The Planetary Society. November 17, 2022. [Online] Available at: https://www.planetary.org/articles/lightsail-2-completes-mission
(23) Laube, P. et al. “ADEO-N – Deployable Passive De-Orbit Sail Subsystem Enabling Space Debris Mitigation for CubeSats, SmallSats and Constellations,” DLR German Aerospace Center, D-Orbit S.p.A, European Space Agency.
(24) Sinn, T., Garcia Hemme, H., Gehly, S., and Le May, S. “The NABEO-1 CubeSat dragsail launched onboard Rocket Lab’s “It’s Business Time: Design, Testing, Launch and De-Orbit Mission,” 33rd Annual Small Satellite Conference Presentation, August 2019, Logan Utah.
(25) “Gama’s revolutionary propulsion Gama Alpha Solar Sail mission launches.” satenews.com. January 4, 2023. [Online] Available at:

https://news.satnews.com/2023/01/04/gamas-revolutionary-propulsion-gama-alpha-solar-sail-mission-launches
(26) “Satellite built by Brown students and launched by SpaceX shows a low-cost way to reduce space junk.” News from Brown. March 15, 2023. [Online] Available at: https://www.brown.edu/news/2023-03-15/sbudnic
(27) Wilkie, K. “The NASA Advanced Composite Solar Sail System (ACS3) Flight Demonstration: A Technology Pathfinder for Practical Smallsat Solar Sailing.” 35th Annual Small Satellite Conference, August 2021, Logan, Utah.
(28) B. Taylor, V. Lewis, S. Shore, S. Schaffler, A. Tresoldi, M. Longato, S. Luo, and G. Aglietti. “Te Pūnaha Ātea -1 (TPA-1), a Capability Development and Validation Mission From New Zealand.” Technical Poster Session 3. 37th Annual Small Satellite Conference, August 2023, Logan, Utah.
(29) Frond Space Systems. “MICRO Dragsail: Effect deorbiting for Microsatellites in LEO.” [Online] Available at: https://frond.space/products/micro-sail/
(30) NASA. “What are NASA’s Technology Educational Satellites?” September 20, 2022. [Online] Available at: https://www.nasa.gov/ames/techedsat
(31) Tavares, F. “TechEDsat-10 Deploys from the Space Station,” NASA.gov. August 5, 2020. [Online] Available at: https://www.nasa.gov/image-feature/ames/techedsat-10-deploys
(32) M. Murbach et al. “The Exo-Brake as an Inexpensive Means of Achieving Sample Return from Low Earth Orbit – Recent Flight Tests.” Washington, D.C.: 70th International Astronautical Congress (IAC), 2019.
(33) M. Murbach et al. "The TechEdSat-N Series: A Collaborative Technology Development Platform in the Nano-Satellite Form Factor." Meeting: International Space Station Research & Development Conference. July 23-26, 2018. NASA HQ.
(34) M. Murbach et al. "The TechEdSat-N and ETC Series." October 23, 2017.
(35) M. Murbach et al. "TechEdSat 5 / PhoneSat 5 (T5/P5)," 30th Annual Small Satellite Conference, August 2016, Logan, Utah. [Online] Available at: https://digitalcommons.usu.edu/cgi/viewcontent.cgi?article=3490&context=smallsat
(36) M. Murbach et al. "Successes with Exo-Brake Development and Targeting for Future Sample Return Capability TES-6, 7, 8, Flight Experiments." June 9, 2019.
(37) M. Mooney-Rivkin et al. "TechEdSat 7, 10, 13, 15: Exo-Brake Experiments on the ISS, First Virgin Orbit, and First Firefly-Alpha Test Flights." CubeSat Developers Workshop, 2023. Available at: http://mstl.atl.calpoly.edu/~workshop/archive/2023/presentations/2023_Day1_Session1_Brock_MooneyRivki_TechEdSat.pdf
(38) Martin, T., Omar, S., and Bevilacqua, R. “Controlled Spacecraft Re-Entry of a Drag De-Orbit Device (D3),” Journal of Undergraduate Research, 2019, Vol. 21.
(39) Satellite Evolution. “De-orbit Drag Device (D3) successfully placed in orbit by NanoRacks.” September 14, 2022. [Online] Available at: https://www.satelliteevolution.com/post/de-orbit-drag-device-d3-successfully-placed-in-orbit-by-nanoracks
(40) Stankey, H. C. and Hoyt, R. P. “In-Flight Performance of the Terminator Tape End-of-Life Deorbit Module,” 35th Annual Small Satellite Conference, August 2021, Logan Utah.
(41) S. Bilén, “Space tethers demonstrate deorbit capability,” Aerospace America, December 1, 2021, [Online] Available at: https://aerospaceamerica.aiaa.org/year-in-review/space-tethers-demonstrate-deorbit-capability/
(42) Alessi, E. M., Schettino, G., Rossi, A. and Valsecchi, G. B “Natural Highways for End-of-Life Solutions in the LEO region.”, 2018. arXiv: 1805.05726v1.
(43) M. Murbach et al. "BrainStack: A Platform for Artificial Intelligence & Machine Learning Collaborative Experiments on a Nano-Satellite," 2023. 37th Annual Small Satellite Conference, Logan Utah.

(44) Aglietti, G. et al. “The active space debris removal mission RemoveDebris. Part 2: in orbit operations,” Acta Astronautica, Elsevier, 2020, Vol. 168, pp. 310-322.
(45) Astroscale. “Astroscale's UK National ADR Mission COSMIC Achieves Significant Progress in Space Cleanup Efforts.” April 22, 2024. [Online] Available at: https://astroscale.com/astroscales-uk-national-adr-mission-cosmic-achieves-significant-progress-in-space-cleanup-efforts/
(46) Astroscale. “Astro Digital Embraces Responsible Satellite Operations with Astroscale’s Simple and Innovative Docking Plate Integration.” Press Release. July 31, 2023. [Online] Available at: https://astroscale.com/astro-digital-embraces-responsible-satellite-operations-with-astroscales-simple-and-innovative-docking-plate-integration/
(47) Astroscale. “Astroscale’s ADRAS-J Mission Completes Operations, Begins Deorbit.” Mission Updates, March 25, 2026. [Online] Available at: https://www.astroscale.com/en/news/astroscales-adras-j-mission-completes-operations-begins-deorbit
(48) Astroscale. “Astroscale’s ELSA-d Finalizes De-Orbit Operations Marking Successful Mission Conclusion.” [Online] Available at: https://astroscale.com/astroscales-elsa-d-finalizes-de-orbit-operations-marking-successful-mission-conclusion/
(49) Astroscale. “ELSA-M.” [Online] Available at: https://www.space.com/astroscale-elsa-m-space-debris-removal-funding
(50) Astroscale. "Astroscale UK Signs £2.5 Million Agreement to Develop Space Debris Removal Technology Innovations with OneWeb." Press Release. May 24, 2021 [Online] Available at: https://astroscale.com/astroscale-uk-signs-2-5-million-agreement-to-develop-space-debris-removal-technology-innovations-with-oneweb/
(51) European Space Agency. “ClearSpace-1.” [Online] Available at: https://www.esa.int/Space_Safety/ClearSpace-1
(52) ClearSpace. “ClearSpace-1 Mission Changes in Response to Space Debris Collision to Go Leaner, Faster and Safer.” space.com. April 24, 2024. [Online] Available at: https://clearspace.today/clearspace-1-mission-changes-in-response-to-space-debris-collision-to-go-leaner-faster-and-safer
(53) D. Werner. “D-Orbit charts ambitious course for space logistics business,” Spacenews, June 15, 2022. [Online] Available at: https://spacenews.com/d-orbit-ambitions/
(54) Voyager Space. "DogTags: Universal Grapple Fixture." [Online] Available at: https://voyagerspace.com/innovate/in-space-servicing-assembly/
(55) Maclay, T., Goff, J., Sheehan, J.P., and Han, E. “The development of commercially viable ADR services: Introduction of a small-satellite grappling interface,” 2020, Journal of Space Safety Engineering, Volume 7, Issue 3, pages 364 – 368.
(56) Kall Morris Inc. “Technologies: REACCH,” August 2024 [Online] Available at: https://www.kallmorris.com/reacch
(57) Northern Michigan University, “Alumni Company Captures Space Objects on the ISS,” Northern Today, July 15, 2025, [Online] Available at: https://news.nmu.edu/alumni-system-completes-first-commercial-capture

Summary

This report provides an extensive overview and assessment of the state-of-the-art (SoA) for small spacecraft technologies publicly available as of April 2026. The reader should be aware that the pace of SmallSat technology advancement overall is rapidly accelerating and varies per subsystem chapter. Recent developments in small satellite technologies reflect a broader shift from experimental, low-cost platforms toward highly capable, mission-flexible systems that can operate across increasingly demanding environments. Advances in materials science, power systems, avionics, and communications are collectively enabling this transition, while market dynamics are pushing both emerging startups and established players to differentiate through cost efficiency, performance, and service-based models.

One of the most critical enabling areas is energy storage and power management. Ongoing research into solid electrolyte materials is driving the next generation of batteries, offering improved safety, energy density, and thermal stability compared to traditional lithium-ion designs. These advances are particularly important for CubeSats and other small spacecraft, where tight volume and mass constraints demand highly efficient energy solutions. At the same time, improvements in maximum power point tracking (MPPT) algorithms are allowing satellites to extract more usable energy from solar arrays under varying orbital conditions. Coupled with this is a growing emphasis on thermal management: as silicon-based power devices approach their operating temperature limits, advanced cooling solutions and materials with enhanced thermal conductivity are becoming essential to maintain performance and reliability.

Thermal and power challenges are closely linked to the increasing computational and operational demands placed on small satellites. A major trend in spacecraft technology is the push toward high-performance avionics capable of supporting autonomy, edge processing, and machine learning. These capabilities are particularly valuable for missions in dynamic or remote environments, where real-time decision-making reduces reliance on ground control. As Earth observation missions, for example, generate ever larger volumes of data, onboard processing helps mitigate constraints in downlink bandwidth and power availability for high-rate transmissions. Edge computing thus becomes not just an enhancement, but a necessity for maintaining mission efficiency.

Communications technology is also evolving rapidly. Optical communication systems, once considered impractical for small spacecraft, are now becoming feasible for microsatellite missions. These systems offer significantly higher data rates compared to traditional radio frequency links, helping address the growing bottleneck in data transmission. However, regulatory constraints—such as limits on power flux density set by bodies like the ITU and NTIA—continue to shape system design, requiring careful balancing of transmission power, bandwidth, and interference considerations.

Another notable shift is in platform design and mission architecture. Traditional CubeSat constellations are increasingly being replaced or supplemented by more capable clusters of spacecraft and larger small-satellite platforms. The acceptable mass threshold for minisatellites and small satellites has expanded, reflecting demand for systems that can carry more sophisticated payloads and support longer, more complex missions. This trend is evident in both commercial and government sectors, where customers are seeking platforms with greater autonomy and versatility, including the ability to operate beyond low Earth orbit (LEO). Indeed, small satellites are no longer confined to LEO science missions; they are emerging as viable candidates for deep-space exploration and lunar applications, as demonstrated by initiatives like NASA's Commercial Lunar Payload Services (CLPS) program [1], which aims to deliver scientific instruments to the Moon at reduced cost.

The evolving ecosystem is also reshaping the satellite supply chain and business models. The integration of hardware components—such as satellite buses and deployment systems—has become increasingly interconnected, with growth in one segment driving expansion in the other. At the same time, startups are introducing innovative service-based approaches. For example, some companies offer power control and distribution unit (PCDU) functionality as a service, charging customers based on mission duration or power usage rather than requiring upfront hardware investment. This reflects a broader trend toward modularity and commercialization, making advanced capabilities more accessible to a wider range of operators.

Finally, industry dynamics reveal a divergence in strategic priorities. Emerging companies tend to focus on cost reduction, scalability, and localization of production, aiming to capture market share through affordability and flexibility. In contrast, established players emphasize performance, reliability, and heritage, catering to high-stakes missions where risk tolerance is low. Despite these differences, both segments are responding to the same overarching demand: a need for more capable, adaptable small satellite platforms that can support increasingly complex and data-intensive missions.

In summary, small satellite technologies are undergoing a significant transformation driven by advances in materials, power systems, avionics, and communications, alongside evolving market demands. These developments are enabling a new class of spacecraft that bridge the gap between traditional CubeSats and larger satellites, opening the door to more ambitious missions in Earth orbit and beyond.

This report will be updated annually as emerging technologies mature and become state of the art. Any current technologies that were inadvertently overlooked in this version may be included in subsequent editions. Updates to technologies listed in this report could be also modified in subsequent revisions. This report is also available online at: https://www.nasa.gov/smallsat-institute/sst-soa. Technology inputs, updates, or corrections can be made by reaching out to the editor of this report at arc-sst-soa@mail.nasa.gov.

References

(1) NASA, “Commercial Lunar Payload Services.” 2026, [Online] Available at: https://www.nasa.gov/commercial-lunar-payload-services/.

NASA Procedural Requirements

NPR 7123.1D
Effective Date: July 05, 2023
Expiration Date: July 05, 2028

COMPLIANCE IS MANDATORY FOR NASA EMPLOYEES

Printable Format (PDF)

Subject: NASA Systems Engineering Processes and Requirements Updated w/Change 2

Responsible Office: Office of the Chief Engineer

| TOC | ChangeLog | Preface | Chapter1 | Chapter2 | Chapter3 | Chapter4 | Chapter5 | Chapter6 | AppendixA | AppendixB | AppendixC | AppendixD | AppendixE | AppendixF | AppendixG | AppendixH | AppendixI | AppendixJ | AppendixK | ALL |

Appendix E. Technology Readiness Levels

TRL	Definition	Hardware Description	Software Description	Success criteria
1	Basic principles observed and reported.	Scientific knowledge generated underpinning hardware technology concepts/applications.	Scientific knowledge generated underpinning basic properties of software architecture and mathematical formulation.	Peer reviewed documentation of research underlying the proposed concept/application.
	Examples: a. Initial Paper published providing representative examples of phenomenon as well as supporting equations for a concept. b. Conference presentations on concepts and basic observations presented within the scientific community.			
2	Technology concept and/or application formulated.	Invention begins, practical application is identified but is speculative, no experimental proof or detailed analysis is available to support the conjecture.	Practical application is identified but is speculative; no experimental proof or detailed analysis is available to support the conjecture. Basic properties of algorithms, representations, and concepts defined. Basic principles coded.	Documented description of the application/concept that addresses feasibility and benefit.

This document does not bind the public, except as authorized by law or as incorporated into a contract. This document is uncontrolled when printed. Check the NASA Online Directives Information System (NODIS) Library to verify that this is the correct version before use: https://nodis3.gsfc.nasa.gov.

			Experiments performed with synthetic data.	
	Example: Carbon nanotube composites were created for lightweight, high-strength structural materials for space structures.			

TRL	Definition	Hardware Description	Software Description	Success criteria
3	Analytical and experimental proof-of-concept of critical function and/or characteristics.	Research and development are initiated, including analytical and laboratory studies to validate predictions regarding the technology.	Development of limited functionality to validate critical properties and predictions using non-integrated software components.	Documented analytical/experimental results validating predictions of key parameters.
	Examples: a. High efficiency Gallium Arsenide solar panels for space application is conceived for use over a wide temperature range. The concept critically relies on improved welding technology for the cell assembly. Samples of solar cell assemblies are manufactured and submitted to a preliminary thermal environment test at ambient pressure for demonstrating the concept viability. b. A fiber optic laser gyroscope is envisioned using optical fibers for the light propagation and Sagnac Effect. The overall concept is modeled including the laser source, the optical fiber loop, and the phase shift measurement. The laser injection in the optical fiber and the detection principles are supported by dedicated experiments. c. In Situ Resource Utilization: Demonstrated the application of a cryofreezer for CO2 acquisition and microwave processor for water extraction from soils.			

TRL	Definition	Hardware Description	Software Description	Success criteria
	Component and/or breadboard validation in a laboratory environment.	A low fidelity system/component breadboard is built and operated to demonstrate basic functionality in a laboratory environment.	Key, functionality critical software components are integrated and functionally validated to establish interoperability and begin architecture development. Relevant environments defined and performance in the environment predicted.	Documented test performance demonstrating agreement with analytical predictions. Documented definition of potentially relevant environment.

This document does not bind the public, except as authorized by law or as incorporated into a contract. This document is uncontrolled when printed. Check the NASA Online Directives Information System (NODIS) Library to verify that this is the correct version before use: https://nodis3.gsfc.nasa.gov.

4	**Examples:** a. Fiber optic laser gyroscope: A breadboard model is built including the proposed laser diode, optical fiber and detection system. The angular velocity measurement performance is demonstrated in the laboratory for one axis rotation. b. Bi-liquid chemical propulsion engine: A breadboard of the engine is built and thrust performance is demonstrated at ambient pressure. Calculations are done to estimate the theoretical performance in the expected environment (e.g., pressure, temperature). c. A new fuzzy logic approach to avionics is validated in a lab environment by testing the algorithms in a partially computer-based, partially bench-top component (with fiber optic gyros) demonstration in a controls lab using simulated vehicle inputs. d. Variable Specific Impulse Magnetosphere Rocket (VASIMR): 100 kW magnetoplasma engine operated 10 hours cumulative (up to 3 minutes continuous) in a laboratory vacuum chamber.			
TRL	**Definition**	**Hardware Description**	**Software Description**	**Success criteria**
5	Component and/or brassboard validated in a relevant environment.	A medium-fidelity component and/or brassboard, with realistic support elements, is built and operated for validation in a relevant environment so as to demonstrate overall performance in critical areas.	End-to-end software elements implemented and interfaced with existing systems/simulations conforming to target environment. End-to-end software system tested in relevant environment, meeting predicted performance. Operational environment performance predicted. Implementations.	Documented test performance demonstrating agreement with analytical predictions. Documented definition of scaling requirements. Performance predictions are made for subsequent development phases.
	Examples: a. A 6.0-meter deployable space telescope comprised of multiple petals is proposed for near infrared astronomy operating at 30K. Optical performance of individual petals in a cold environment is a critical function and is driven by material selection. A series of 1m mirrors (corresponding to a single petal) were fabricated from different materials and tested at 30K to evaluate performance and to select the final material for the telescope. Performance was extrapolated to the full-sized mirror. b. For a launch vehicle, TRL 5 is the level demonstrating the availability of the technology at subscale level (e.g., the fuel management is a critical function for a re-ignitable upper stage). The demonstration of the management of the propellant is achieved on the ground at a subscale level.			

This document does not bind the public, except as authorized by law or as incorporated into a contract. This document is uncontrolled when printed. Check the NASA Online Directives Information System (NODIS) Library to verify that this is the correct version before use: https://nodis3.gsfc.nasa.gov.

c. ISS Additive Manufacturing Facility: Characterization tests compare parts and material properties of polymer specimens printed on ISS to copies printed on the ground.

TRL	Definition	Hardware Description	Software Description	Success criteria
6	System/sub-system model or prototype demonstration in a relevant environment.	A high-fidelity prototype of the system/subsystems that adequately addresses all critical scaling issues is built and tested in a relevant environment to demonstrate performance under critical environmental conditions.	Prototype implementations of the software demonstrated on full-scale, realistic problems. Partially integrated with existing hardware/software systems. Limited documentation available. Engineering feasibility fully demonstrated.	Documented test performance demonstrating agreement with analytical predictions.

Examples:

a. A remote sensing camera includes a large 3-meter telescope, a detection assembly, a cooling cabin for the detector cooling, and an electronics control unit. All elements have been demonstrated at TRL 6 except for the mirror assembly and its optical performance in orbit, which is driven by the distance between the primary and secondary mirrors needing to be stable within a fraction of a micrometer. The corresponding critical part includes the two mirrors and their supporting structure. A full-scale prototype consisting of the two mirrors and the supporting structure is built and tested in the relevant environment (e.g., including thermo-elastic distortions and launch vibrations) for demonstrating the required stability can effectively be met with the proposed design.

b. Vacuum Pressure Integrated Suit Test (VPIST): Demonstrated the integrated performance of the Orion suit loop when integrated with human-suited test subjects in a vacuum chamber.

TRL	Definition	Hardware Description	Software Description	Success criteria
	System prototype demonstration in an operational environment.	A high-fidelity prototype or engineering unit that adequately addresses all critical scaling issues is built and functions in the actual operational environment and platform (ground, airborne, or space).	Prototype software exists having all key functionality available for demonstration and test. Well integrated with operational hardware/software systems demonstrating operational feasibility. Most	Documented test performance demonstrating agreement with analytical predictions.

This document does not bind the public, except as authorized by law or as incorporated into a contract. This document is uncontrolled when printed. Check the NASA Online Directives Information System (NODIS) Library to verify that this is the correct version before use: https://nodis3.gsfc.nasa.gov.

7			software bugs removed. Limited documentation available.	

Examples:

a. Mars Pathfinder Rover flight and operation on Mars as a technology demonstration for future micro-rovers based on that system design.

b. First flight test of a new launch vehicle, which is a performance demonstration in the operational environment. Design changes could follow as a result of the flight test.

c. In-space demonstration missions for technology (e.g., autonomous robotics and deep space atomic clock). Successful flight demonstration could result in use of the technology in a future operational mission

d. Robotic External Leak Locator (RELL): Originally flown as a technology demonstrator, the test article was subsequently put to use to help operators locate the likely spot where ammonia was leaking from the International Space Station (ISS) External Active Thermal Control System Loop B.

TRL	Definition	Hardware Description	Software Description	Success criteria
8	Actual system completed and "flight qualified" through test and demonstration.	The final product in its final configuration is successfully demonstrated through test and analysis for its intended operational environment and platform (ground, airborne, or space). If necessary*, life testing has been completed.	All software has been thoroughly debugged and fully integrated with all operational hardware and software systems. All user documentation, training documentation, and maintenance documentation completed. All functionality successfully demonstrated in simulated operational scenarios. Verification and Validation completed.	Documented test performance verifying analytical predictions.

Note:
*"If necessary" refers to the need to life test either for worn out mechanisms, for temperature stability over time, and for performance over time in extreme environments. An evaluation on a case-by-case basis should be made to determine the system/systems that warrant life testing and the tests begun early in the technology development process to enable completion by TRL 8. It is preferable to have the technology life test initiated and

This document does not bind the public, except as authorized by law or as incorporated into a contract. This document is uncontrolled when printed. Check the NASA Online Directives Information System (NODIS) Library to verify that this is the correct version before use: https://nodis3.gsfc.nasa.gov.

	completed at the earliest possible stage in development. Some components may require life testing on or after TRL 5. **Examples:** a. The level is reached when the final product is qualified for the operational environment through test and analysis. Examples are when Cassini and Galileo were qualified, but not yet flown. b. Interim Cryo Propulsion Stage (ICPS): A Delta Cryogenic Second Stage modified to meet Space Launch System requirements for Exploration Mission-1 (EM-1). Qualified and accepted by NASA for flight on EM-1.

TRL	Definition	Hardware Description	Software Description	Success criteria
9	Actual system flight proven through successful mission operations.	The final product is successfully operated in an actual mission.	All software has been thoroughly debugged and fully integrated with all operational hardware and software systems. All documentation has been completed. Sustaining software support is in place. System has been successfully operated in the operational environment.	Documented mission operational results.
	Examples: a. Flown spacecraft (e.g., Cassini, Hubble Space telescope). b. Technologies flown in an operational environment. c. Nanoracks CubeSat Deployer: Commercially developed and operated small satellite deployer on-board the ISS.			

Note: In cases of conflict between NASA directives concerning TRL definitions, NPR 7123.1 will take precedence.

| TOC | ChangeLog | Preface | Chapter1 | Chapter2 | Chapter3 | Chapter4 | Chapter5 | Chapter6 | AppendixA | AppendixB | AppendixC | AppendixD | AppendixE | AppendixF | AppendixG | AppendixH | AppendixI | AppendixJ | AppendixK | ALL |

| NODIS Library | Program Formulation(7000s) | Search |

This document does not bind the public, except as authorized by law or as incorporated into a contract. This document is uncontrolled when printed. Check the NASA Online Directives Information System (NODIS) Library to verify that this is the correct version before use: https://nodis3.gsfc.nasa.gov.

DISTRIBUTION:
NODIS

This document does not bind the public, except as authorized by law or as incorporated into a contract. This document is uncontrolled when printed. Check the NASA Online Directives Information System (NODIS) Library to verify that this is the correct version before use: https://nodis3.gsfc.nasa.gov.

This document does not bind the public, except as authorized by law or as incorporated into a contract. This document is uncontrolled when printed. Check the NASA Online Directives Information System (NODIS) Library to verify that this is the correct version before use: https://nodis3.gsfc.nasa.gov.